27/0023/V.3

NUREG/CP-0023
Vol. 3

Proceedings of the U.S. Nuclear Regulatory Commission

Eighth Water Reactor Safety Research Information Meeting

NEWARK PUBLIC LIBRARY
APR 2 1982
U. S. GOVT. PUBS.
DEPOSITORY 376

Held at
National Bureau of Standards
Gaithersburg, Maryland
October 27-31, 1980

U.S. Nuclear Regulatory Commission

Office of Nuclear Regulatory Research

Y 3. N88:

The views expressed in these proceedings are not necessarily those of the U. S. Nuclear Regulatory Commission.

The submitted manuscript has been authored by a contractor of the U.S. Government under contract. Accordingly the U.S. Government retains a nonexclusive, royalty-free license to publish or reproduce the published form of this contribution, or allow others to do so, for U.S. Government purposes.

Available from

GPO Sales Program
Division of Technical Information and Document Control
U.S. Nuclear Regulatory Commission
Washington, DC 20555

Printed copy price: $14.00

and

National Technical Information Service
Springfield, VA 22161

NUREG/CP-0023
Vol. 3

Proceedings of the U.S. Nuclear Regulatory Commission

Eighth Water Reactor Safety Research Information Meeting

Held at
National Bureau of Standards
Gaithersburg, Maryland
October 27-31, 1980

Date Published: March 1982

Office of Nuclear Regulatory Research
U.S. Nuclear Regulatory Commission
Washington, D.C. 20555

FINAL AGENDA

EIGHTH WATER REACTOR SAFETY RESEARCH INFORMATION MEETING

AT THE

NATIONAL BUREAU OF STANDARDS
ADMINISTRATION BUILDING 101
GAITHERSBURG, MARYLAND

October 27-31, 1980

TABLE OF CONTENTS

MONDAY, OCTOBER 27, 1980

9:15 am	Introductory Remarks	Commissioner
9:30 am	Reactor Safety Research Program	T. E. Murley, NRC
10:00 am	Highlights of WRSR Achievement in FY 80 and Status of LOCA Safety Evaluation	L. S. Tong, NRC

LOFT PROGRAM

Chairman: G. D. McPherson, NRC

11:20 am	Results of LOFT Small Break Experiments L3-1, L3-2, L3-5/5a, and L3-7.	J. H. Linebarger, INEL
12:10 pm	LOFT: A Nuclear Plant Providing Realistic Answers to PWR Licensing Issues	C. W. Solbrig, INEL
12:30 pm	Results of Anticipated Transient Experiments	C. W. Solbrig, INEL
2:00 pm	Flow Measurement Techniques in LOFT Small Break Experiments	D. J. Hanson, INEL
2:35 pm	LOFT Program Overview	N. C. Kaufman, INEL

SEMISCALE PROGRAM

Chairman: W. C. Lyons, NRC

3:30 pm	Key Results of Semiscale	L. P. Leach, INEL

MONDAY, OCTOBER 27, 1980

SEMISCALE PROGRAM Cont'd

4:15 pm -	Results of Semiscale Pumps On/Off Experiments	G. W. Johnsen, INEL

FUEL BEHAVIOR RESEARCH

Chairman: M. L. Picklesimer, NRC

9:15 am - 10:20 am -	Introduction Research Highlights	- See Page 1 of the Agenda
11:00 am -	FRAPCON-2 Steady State Fuel Code	C. Mohr, PNL
11:30 am -	Recent PNL Studies on GAP Conductance and Fuel Stored Energy	D. D. Lanning, PNL
12:00 pm-	Status of Multi-Rod Burst Test Program	R. Chapman, ORNL
12:30 pm -	Clad Embrittlement Criteria-Application To An Assessment of of the Margin of Performance of ECCS in LWRs	T. F. Kassner H. M. Chung, ANL

Severe Fuel Damage and Core Melt Research

Chairman: R. R. Sherry, NRC

2:00 pm -	An Assessment of the Influence of Surface Thermocouples on the Behavior of Nuclear Fuel Rods During a Large Break LOCA	T. R. Yackle, INEL
2:25 pm -	Response of Preirradiated Fuel Rod Bundle During Reactivity Initiated Accident Test 1-4	P. E. MacDonald, INEL
3:55 pm -	Flooding Experiments in Blocked Arrays (FEBA): Recent Results and Future Plans	P. Ihle, KfK, FRG
4:40 pm -	FG Release from Irradiated Fuel	S. Gehl, ANL
5:00 pm -	Measured Release of Radioactive Xenon, Krypton, and Iodine from UO_2 During Nuclear Operation and a Comparison with Release Models	A. D. Appelhans, INEL

TUESDAY, OCTOBER 28, 1980

ANALYSIS DEVELOPMENT PROGRAM

Chairman: S. Fabic, NRC

(A) Development of Detailed Advanced Codes for Systems Analysis

9:15 am -	TRAC-PD2 Description and Application	R. Pryor, LASL
10:30 am -	TRAC-BD1, Transient Reactor Analysis Code for Boiling Water Systems	F. Aguilar, INEL

(B) Development of Fast Running, Simplified Geometry Advanced Codes for Systems Analyses

11:00 am -	TRAC-PFO and PF1	D. Liles, LASL
11:30 am -	RELAP-5 - An Advanced Fast Running LWR Transient Analysis Code	

(C) Development and Application of Component Codes

12:30 pm -	Some Recent Applications of the K-FIX Code	B. J. Daly, LASL

(D) System Code Assessment and Application

2:00 pm -	Code Assessment for Nuclear Reactor Accident Analysis Programs	S. Fabic, NRC
2:20 pm -	Code Assessment Results at LASL	T. Knight, LASL
2:50 pm -	Assessment of TRAC-PIA Using Calculations for Integral Facilities	A. C. Peterson, INEL
3:30 pm -	Code (JRAC-PIA) Assessment Results at BNL	P. Saha, BNL

SEPARATE EFFECTS PROGRAM

Thermalhydraulic Modeling

Chairman: L. H. Sullivan, NRC

4:00 pm -	Overview of Thermalhydraulic Modeling	L. H. Sullivan, NRC
4:05 pm -	Steam-Generator Flow Patterns and Modeling	P. Griffith, MIT
4:25 pm -	Upper Plenum Dump	Y. Sudo, JAERI

TUESDAY, October 28, 1980
SEPARATE EFFECTS PROGRAM
Thermalhydraulic Modeling Cont'd

4:40 pm	Summary of Condensation Studies	S. G. Bankoff, NWU
5:05 pm	RPI Research in the Area of Phase Distribution and Separation Phenomena and LWR Instability Phenomena	R. T. Lahey, Jr. RPI

RISK AND SEVERE ACCIDENT SEQUENCE ANALYSIS

Chairman: Gordon E. Edison, NRC

9:45 am	Auxiliary Feedwater Reliability in PWRs	G. E. Edison, NRC
10:30 am	Analysis of Pressurized Water Reactor Station Blackout	B. F. Saffell, INEL
11:00 am	Loss-of-Feedwater Transients in PWRs	R. D. Burns, III, LASL
11:30 am	Severe Core Damage Accident Progression: Best Estimate and Uncertainties	W. B. Murfin J. B. Rivard M. L. Corradini, Sandia
12:00 pm	Severe Accident Sequence Assessment in BWRs	M. H. Fontana, ORNL

ADVANCED INSTRUMENTATION

Chairmen: Y. Y. Hsu and N. N. Kondic, NRC

2:00 pm	Overview	Y. Y. Hsu, NRC
2:10 pm	Pulsed Neutron Activation Techniques in Water Reactor Safety Research	P. Kehler, ANL
2:25 pm	A Pulsed Neutron Generator for Use With Pulsed Neutron Activation Techniques	G. E. Rochau, Sandia
2:40 pm	Liquid Level Detection Techniques	K. G. Turnage G. N. Miller, ORNL
3:25 pm	2D/3D Instrumentation Overview - ORNL	B. Eads, ORNL
3:55 pm	Overview of 2D/3D Instrumentation Developed at EG&G Idaho, Inc.	R. E. Rice, INEL

TUESDAY, OCTOBER 28, 1980
ADVANCED INSTRUMENTATION cont'd

4:05 pm -	Low Energy Sodium Iodide Gamma Densitometer for 2D/3D Program	J. B. Colson, INEL
4:20 pm -	An Optical Liquid Level Detector for High Temperature/Pressure Water Environment	B. L. Watson, INEL
4:35 pm -	Advanced Instrumentation Project	W. H. Roach, INEL
4:45 pm -	Laser Doppler Anemometry Instrumentation of Two-Phase Flows	M. L. Wilson, INEL
5:00 pm -	Steam Generator Instrumentation	J. R. Wolf, INEL
5:20 pm -	Non-intrusive Density Profile Determination Gamma Beam Densitometer, Tomography and Scattering	N. N. Kondic, NRC

WEDNESDAY, OCTOBER 29, 1980

2D/3D RESEARCH PROGRAM

Chairman, W. S. Farmer, NRC

9:30 am -	Results of PKL Small Break Experiments	D. Hein F. Winkler, KWU, FRG
10:25 am -	The German 2D/3D-UPTF Program	E. F. Hicken K. Hofmann, GRS, FRG
10:50 am -	Results of CCTF Core 1 Tests	Y. Murao, JAERI
11:30 am -	TRAC Analysis Support for the 2D/3D Program	K. A. Williams, LASL
12:10 pm -	Measurement of Two-phase Flow at the Core Upper Plenum Interface Under Simulated Reflood Conditions	D. G. Thomas, ORNL

SEPARATE EFFECTS PROGRAM

Chairman: W. D. Beckner, NRC

2:00 pm -	THTF Heat Transfer Data	J. D. White, ORNL

READEX FICHE best copy available

WEDNESDAY, OCTOBER 29, 1980
SEPARATE EFFECTS PROGRAM Cont'd

2:45 pm -	BWR Blowdown/Emergency Core Cooling Integral Program (TLTA Large and Small Break)	G. L. Sozzi, GE
3:30 pm -	BWR Refill-Reflood Program: Overview and Experimental Results	G. W. Burnette, GE
4:00 pm -	BWR Refill-Reflood Program Model Development for TRAC-BD	J. G. M. Andersen, GE
4:30 pm -	FLECHT-SEASET (1) Unblocked Channel Data (2) Blocked 21-Rod Bundle Tests	L. E. Hochreiter, W

REACTOR OPERATIONAL SAFETY PROGRAM

Chairman: R. Feit, NRC

10:45 am -	Status of the Fire Protection Program	L. J. Klamerus, Sandia
11:30 am -	Fire Protection System Modeling: The Fire Resistance of Walls Penetrated by Electric Cables	L. W. Hunter S. Favin, APL

REACTOR OPERATIONAL SAFETY: OPERATOR-MACHINE INTERFACE

Chairman: W. S. Farmer, NRC

2:00 pm -	Advances in Noise Analysis for Nuclear Plant Surveillance and Diagnostics	D. N. Fry, ORNL
2:30 pm -	The Safety-Related Operator Actions Program at ORNL	P. M. Haas, ORNL
3:30 pm -	Simulators and Thier Use in Training Operators	D. W. Jones, MSU/CNS
4:00 pm -	Defining the Role of the Operating Crew	R. A. Kisner, ORNL
4:30 pm -	Advanced Display and Diagnostic at LOFT	O. R. Meyer, INEL

WEDNESDAY, OCTOBER 29, 1980

EPRI REACTOR SAFETY RESEARCH PROGRAM

2:00 pm - Safety Research at EPRI-An Update	W.B. Loewenstein, EPRI
3:30 pm - Recent Missile Tests	G. Sliter, EPRI
4:00 pm - BWR IGSCC Research Program	K. Stahlkopf, EPRI
4:30 pm - Analysis of Small-Break Heat Removal Tests	R. Duffey, EPRI
5:00 pm - Validating Risk Analysis; Selected Aspects	G. Lellouche, EPRI

THURSDAY, OCTOBER 30, 1980

APPLIED MECHANICS AND SITE TECHNOLOGY

Seismic Safety Margins Research Program

9:50 am - Introduction	J. Richardson, NRC
10:00 am - Overview of SSMRP Program	P. Smith, LLL
10:40 am - Systems Model and Methodology	G. Cummings, LLL
11:20 am - Seismic Input	D. Bernreuter, LLL
12:00 pm - Soil-Structure Interaction	J. Johnson, LLL

Seismic Safety Margins Research Program

Chairman: C. W. Burger, NRC

2:00 pm - Structural Response	J. Johnson, LLL
2:40 pm - Subsystem Response	T. Y. Chuong, LLL
3:30 pm - Component Fragility	M. Bohn, LLL
4:30 pm - Best Estimate vs Evaluation Model	J. Johnson, LLL

THURSDAY, OCTOBER 30, 1980

SITE SAFETY RESEARCH PROGRAM

Meteorology

Chairman: R. F. Abbey, NRC

9:50 am -	Overview of NRC Meteorology Research Program	R. F. Abbey, NRC
10:45 am -	Near-Ground Tornado Wind Fields	J. R. McDonald, Texas Tech. U
11:15 am -	Measured Pressure Loads on Model Structures in Simulated Tornado-Like Flow	M.C. Jischke, U of Oklahoma
11:45 am -	Automobile Impact Studies	R. Chiapetta, Chiapetta-Welch & Assoc.
12:15 pm -	Atmospheric Dispersion Field Experiments to 80 km	I. Van der Hoven, NOAA Air Resources Laboratory

Seismic Hazard

Chairman: J. Harbour, NRC

2:00 pm -	Overview of NRC Programs in Seismology and Geology	J. Harbour, NRC
3:00 pm -	Reservoir-Induced Seismicity	A. Murphy, NRC
3:45 pm -	Northeastern U.S. Seismic Network	P. Pomeroy, NRC Consultant
4:30 pm -	Tectonic Features in the Vicinity of the Charleston 1886 Earthquake	J. Behrendt, USGS

METALLURGY AND MATERIALS RESEARCH PROGRAMS

9:15 am -	Welcome and Introduction	L. C. Shao, NRC
10:00 am -	Introduction	C. Z. Serpan, NRC

Irradiation Effects and Neutron Dosimetry

Chairman: C. Z. Serpan, NRC

10:30 am -	LWR Dosimetry Improvement Program Overview	W. N. McElroy, HEDL
11:00 am -	Reactor Calculation "Benchmark" PCA Blind Tests Results	F.B.K. Kam, ORNL

THURSDAY, OCTOBER 30, 1980
METALLURGY AND MATERIALS RESEARCH PROGRAMS
Irradiation Effects and Neutron Dosimetry Cont'd

11:30 pm -	Neutron Characterization of HSST Irradiation Facility and of Simulated RPV Dosimetry - Embrittlement Experiment	A. Fabry, ORNL/CEN/SCK

Fracture Mechanics

Chairman: M. Vagins, NRC

12:00 pm -	Experimental Verification of the Behavior of Surface Flaws in Thick-Walled Steel Cylinders During Severe Thermal Shock (TSE-5 and TSE-5A)	R. Cheverton, ORNL
12:30 pm -	Crack Stability Analysis for Vessel Tests in the Upper Shelf Temperature Range	J. Merkle, ORNL
2:00 pm -	Validation of "Key Curve" Analysis of Elastic-Plastic Fracture Toughness	J. Joyce, USNA
2:30 pm -	Toughness and Ductile Shelf Properties of Irradiated Low-Shelf Weld Metals	F. J. Loss, NRL
3:20 pm -	Cyclic Irradiation - Annealing - Reirradiation of RPV Steels and Welds	J. R. Hawthorne, NRL
3:50 pm -	Crack Growth Rate of Irradiated Vessel and of Piping Steels in PWR Environments	H. Watson/ W. Cullen, NRL
4:20 pm -	Crack Arrest Methodology and and Standard Test Methods for RPV Evaluations	G. Irwin/W. Fourney, UMD
4:50 pm -	Validation of Tearing Instability on Degraded LWR Piping	J. P. Gudas, NSRDC

FRIDAY, OCTOBER 31, 1980
Pipe Failure Model and Effects

Chairman: M. Vagins, NRC

9:15 am -	Probability Models for Piping Failure	D. Harris, SAI

FRIDAY, OCTOBER 31, 1980
METALLURGY AND MATERIALS RESEARCH PROGRAMS
Pipe Failure Models and Effects Cont'd

9:55 am	Experimental Program for Pipe to Pipe Impact Effects	M. C. C. Bampton, PNL
10:30 am	Verification of Two Phase Jet	D. Tomasko, Sandia
11:00 am	Pipe Whip Code Development	G. Powell, Un. of CA/ Berkeley

Environmentally Assisted Cracking and Steam Generator Integrity

Chairman: J. Muscara, NRC

11:30 am	Program for Environmental-Assisted Cracking in LWRs	W. J. Shack, ANL
12:10 am	Progress and Plans for Steam Generator Integrity Research	R. Clark, PNL
12:40 am	Stress-Corrosion Cracking of Steam Generator Tubes	D. VanRooyen, BNL

Nondestructive Evaluation

Chairman: J. Muscara, NRC

2:00 pm	Improved Eddy Current Inspection of Steam Generator Tubes	C. V. Dodd, ORNL
2:25 pm	Reliability of Flaw Detection	F. L. Becker, PNL
3:20 pm	SAFT-UT for Flaw Imaging and Display Techniques	G. Ganapathy, U Mich
3:55 pm	ISI Application of SAFT-UT	J. Jackson, SWRI
4:25 pm	Models for A/E Monitoring of Reactors	P. H. Hutton, PNL
4:55 pm	Detection of IGSCC Initiation	L. Yeager, DAI

STRUCTURAL ENGINEERING RESEARCH PROGRAMS

Chairman: G. Bagchi, NRC

9:15 am	Introduction	G. Bagchi, NRC
9:30 am	Category I Structures (Safety Margin at Ultimate Load)	C. A. Anderson, LASL

FRIDAY, OCTOBER 31, 1980

STRUCTURAL ENGINEERING RESEARCH PROGRAMS Cont'd

10:30 am - Hydrogen Explosion	M. Fardis, MIT
11:15 am - Containment Safety Margin	W. VonRiesemann, Sandia
12:00 pm - Evaluation of Dynamic Testing of NPP Structures	C. A. Kot, M. G. Srinivasan, ANL

STRUCTURAL ENGINEERING RESEARCH BRANCH

Chairman: G. Bagchi, NRC

2:00 pm - Codes and Standards With Relation to Containment Safety Margins	R. N. White, Cornell
2:40 pm - Large Scale Testing of Containment Elements	H. G. Russell, PCA
3:30 pm - Analytical Approach for Evaluation of Codes, Standards and the Inherent Safety Margin in Safety-Related Structures	J. J. Connor, MIT
4:15 pm - Load Combinations	B. Ellingswood, NBS

MECHANICAL ENGINEERING RESEARCH PROGRAM

Load Combinations

Chairman: J. O'Brien, NRC

9:15 am - Introduction	J. A. O'Brien, NRC
9:25 am - General Description of Load Combination Program	C. K. Chou, LLNL

Event Decoupling (LOCA Plus Earthquake)

9:45 am - Probabilistic Model and Computational Procedure	L. L. George, LLNL
10:20 am - Fracture Mechanics Evaluation	R. D. Streit, LLNL
10:50 am - Results and Conclusion	S. C. Lu, LLNL

FRIDAY, OCTOBER 31, 1980

MECHANICAL ENGINEERING RESEARCH PROGRAMS
Load Combinations Cont'd

Load Combination Methodology

11:25 am	Load Combination Methodology	C. A. Cornell, MIT
11:55 am	Load Combination Methodology	M. W. Schwartz, LLNL
12:15 pm	Application to Nuclear Systems of the Load Combination Methodology	M. K. Ravindra, S&L

Chairman: D. Reiff, NRC

2:00 pm	Nonlinear System Modeling	S. Masri, USC
2:30 pm	Piping Benchmarks	M. Reich, BNL
3:15 pm	Snubber Research and Testing	A. Onesto, ETEC
3:45 pm	Experimental and Preliminary Analytical Results of Coupled Fluid-Structure Interactions During Blowdown of the HDR Vessel	U. Schumann, KfK (FRG)
4:10 pm	Earthquake Simulation Experiments Performed at the HDR Facility	G. Katzemeier, KfK (FRG)
4:30 pm	HDR Dynamic Tests of Late 1979	G. Howard, ANCO
5:00 pm	Predictions of Recirculation Loop Response at HDR to Simulated Blast Excitation	R. Guenzler, INEL

Advances in Noise Analysis for Nuclear Plant Surveillance and Diagnostics*

D. N. Fry N. E. Clapp, Jr. W. H. Sides, Jr.
J. T. Mihalczo, W T. King

Oak Ridge National Laboratory
Oak Ridge, Tennessee

INTRODUCTION

We are currently demonstrating an automated surveillance system at Sequoyah-1. The need for such a system was discussed at last year's Water Reactor Safety Research Information Meeting,[1] where we reported our application of noise analysis to a variety of safety-related problems in nuclear plants, including loose-parts monitoring, stability monitoring, bulk coolant boiling detection and postaccident monitoring and diagnosis. It was evident to the Nuclear Regulatory Commission (NRC) from these as well as previous diagnostic tasks[2,3,4] that "baseline" data are invaluable in assessing the significance of safety-related events in nuclear plants. Therefore, the NRC has asked us to install and demonstrate an automated surveillance and baseline noise signature acquisition system at the Tennessee Valley Authority's Sequoyah-1 pressurized-water reactor plant.

We are also developing a non-perturbing method that can be used to monitor subcritical reactivity during initial core loading in LWRs, in fuel storage and processing facilities, and potentially during postaccident recovery operations such as TMI-2.

AUTOMATED SURVEILLANCE SYSTEM

ORNL noise analysts, under Department of Energy (DOE) funding, previously developed a surveillance system to monitor nuclear plant signals for changes in their statistical properties that may be indicative of anomalous conditions or an approaching component failure.[5] The system employs pattern recognition techniques in conjunction with consistency checks (to maintain a low false alarm rate) and is designed to operate on-line and continuously, with only infrequent need for human attention.

---

*Research sponsored by the Office of Nuclear Regulatory Research, U. S. Nuclear Regulatory Commission under Interagency Agreement DOE 40-544-75 with the U. S. Department of Energy and contract W-7405-eng-26 with the Union Carbide Corporation.

The system begins operation in a "learning" mode, during which a sufficient number of power spectral densities (PSDs) of each signal are measured to determine the baseline PSD and its statistical variations. The length of the learning period, selected by the noise analyst, is usually 10-24 hours.

After the learning period, the system begins the surveillance mode, in which recently acquired PSDs are statistically compared with previously learned (baseline) PSDs to determine whether the current values are within expected statistical variations. If they are not, the PSDs are stored for later study by a noise analyst. Current PSDs are also compared with a "trend" PSD, which is the average of all acceptable PSDs accumulated since the baseline was established. This trend comparison permits slow variations in the PSD to be accepted by the system as normal.

SEQUOYAH DEMONSTRATION

The automated surveillance and baseline signature acquisition installed at Sequoyah-1 has access to power-range neutron flux, pressure, flow, temperature, vibration, and pressurizer level signals (a total of 23) by means of a patch panel. The system can monitor simultaneously any 16 of these signals, as selected by the analyst. At present only four channels are capable of performing noise analysis - - the other 12 signals are used to provide a plant status label for each noise signature that is stored on the magnetic disk. An expanded system, to be installed next year, will have the capability to perform noise monitoring on all 16 channels. One of these systems will be operational at Sequoyah for ∿ 18 months or until the first refueling.

Hopefully, this demonstration will show that a means is now available to obtain - - on-line and without a need for human attention - - the long-term characteristics of plant sensor noise signals, properly documented in a concise, easily retrieved form.

SUBCRITICAL REACTIVITY MONITORING

We are also developing a method to determine the reactivity of a far-subcritical system from neutron noise spectral density measurements performed with a special ^{252}Cf source/detector.[6,7] The advantage of this method of reactivity determination over alternative methods is that it determines the reactivity at the subcritical state of interest without requiring a calibration at the delayed critical condition. Thus it is well suited for applications such as initial core loading, fuel storage facility monitoring, and postaccident core condition measurements.

We have performed calculations to estimate the detector efficiency and the length of time required for performing Cf-driven measurements during fuel loading operations in a boiling-water reactor. Our next step is to investigate the influence of spatial harmonics on the interpretability of such measurements by performing time-dependent, two-dimensional diffusion theory calculations of a large LWR core.

OTHER ADVANCES IN NOISE ANALYSIS

In addition to the studies outlined above, we have made advances in assessment of other surveillance and diagnostic methods as reported in references 8-22.

References

1. D. N. Fry, "Application of Noise Analysis to Safety-Related Diagnostics and Assessments," Seventh Water Reactor Safety Research Information Meeting at the National Bureau of Standards, Washington, D.C., November 5-9, 1979.

2. D. N. Fry, R. C. Kryter, and J. C. Robinson, "Analysis of Neutron-Density Oscillations Resulting from Core Barrel Motion in a PWR Nuclear Power Plant," Annals of Nucl. Energy, 2, 341-351 (1975).

3. D. N. Fry, et al., "Use of Neutron Noise to Detect BWR-4 In-Core Instrument Tube Vibrations and Impacting," Nucl. Technol, 43, 42-54 (April 1979).

4. R. C. Kryter, et al., "TMI-2 On-Site Monitoring and Diagnostic Measurements Using Noise Analysis," unpublished summary report prepared for the President's Commission on the Accident at Three Mile Island (August 1979).

5. W. H. Sides, Jr. and K. R. Piety, "Automated Pattern Recognition System for Noise Analysis," Trans. Am. Nucl. Soc., 34, 720-722 (June 1980).

6. J. T. Mihalczo, V. K. Paré, G. L. Ragan, M. V. Mathis and G. C. Tillet, "Determination of Reactivity from Power Spectral Density Measurements with Californium-252", Nucl. Sci. Eng. 66 29-59 (1977).

7. W. T. King, "Feasibility of ^{252}Cf Source Driven Neutron Noise Measurements in Water Moderated Reactors," Ph.D. dissertation, The University of Tennessee (1980).

8. F. J. Sweeney, "Modeling the Local Component of In-Core Neutron Detector Noise in a BWR," Trans. Amer. Nucl. Soc. 33, 854 (November 1979).

9. F. J. Sweeney, "Sensitivity of Detecting BWR Control Rod Vibrations Using Neutron Noise," Trans. Amer. Nucl. Soc. 33, 793 (November 1979)

10. B. R. Upadhyaya and M. Kitamura, "Monitoring BWR Stability Using Time Series Analysis of Neutron Noise," Trans. Amer. Nucl. Soc. 33, 342 (November 1979).

11. M. Kitamura, "Detection of Sensor Failures in Nuclear Plants Using Analytic Redundancy," Trans. Amer. Nucl. Soc. (June 1980).

12. F. J. Sweeney and J. C. Robinson, "Relative Importance of Attenuation and Reactivity Effects in Explaining Local and Global BWR Neutron Noise," Trans. Amer. Nucl. Soc. (June 1980).

13. J. E. Stoneking and R. C. Kryter, "Screening Procedures for Vibrational Qualification of Nuclear Plant Piping," Proc. Fourth National Congress on Pressure Vessel and Piping Technology, San Francisco, August 1980.

14. F. Sweeney, "A Theoretical Model of Boiling Water Reactor Neutron Noise," Ph.D. dissertation, The University of Tennessee (1980).

15. B. R. Upadhyaya and M. Kitamura, "Stability Monitoring of Boiling Water Reactors Using Time Series Analysis of Neutron Noise," submitted for publication in Nuclear Science and Engineering.

16. R. C. Kryter et al., "Application of Noise Analysis to Safety-Related Assessment and Reactor Diagnostics," Proc. International Meeting on Thermal Reactor Safety, Conf-800403, Knoxville, April 1980.

17. F. Shahrokhi, "Metallic Loose-Parts Detection and Characterization," Ph.D. dissertation, The University of Tennessee (1980).

18. M. Kitamura and B. R. Upadhyaya, "An Improved Time Series Modeling Approach for Diagnosis and Surveillance of Reactors," Proc. International Meeting on Thermal Reactor Safety, Conf-800403, Knoxville, April 1980.

19. J. C. Robinson and D. N. Fry, "Diagnostics at TMI Using Noise Analysis," Proc. International Meeting on Thermal Reactor Safety, Conf-800403, April 1980.

20. F. J. Sweeney et al., "Stochastic Modeling of BWR Neutron Noise," 13th Informal meeting on Reactor Noise, Cadarach, France, May (1980).

21. W. H. Sides, Jr., "An Automated Noise Analysis System for Improving Plant Performance," NRC-IEEE Conference on Advanced Electrotechnology Applications to Nuclear Power Plants, Washington, DC, January 1980.

22. R. C. Gonzalez, "Application of Pattern Recognition Technique to Nuclear Reactor Surveillance," Proc. IEEE Conf. Decision and Control, Vol. 2, p 1069-1071, December, 1979.

D. N. FRY -- SURVEILLANCE & DIAGNOSTIC METHODS GROUP
INSTRUMENTATION & CONTROLS DIVISION -- ORNL

ADVANCES IN NOISE ANALYSIS FOR NUCLEAR PLANT SURVEILLANCE AND DIAGNOSTICS

Presented at the Eighth Water Reactor Safety Research
Information Meeting at the National Bureau of Standards
October 29, 1980

ORNL HAS THREE INTEGRATED PROGRAMS TO STUDY AND DEVELOP SURVEILLANCE AND DIAGNOSTIC METHODS FOR IMPROVING REACTOR SAFETY

(1) CONTINUOUS, ON-LINE REACTOR SURVEILLANCE SYSTEM
(2) SUBCRITICAL REACTIVITY MONITORING BY THE ^{252}CF-SOURCE-DRIVEN NEUTRON NOISE METHOD
(3) NOISE DIAGNOSTICS FOR SAFETY ASSESSMENT

THESE TOPICS ARE DESCRIBED IN GREATER DETAIL, ONE BY ONE, IN LATER SLIDES

(1) CONTINUOUS, ON-LINE REACTOR SURVEILLANCE SYSTEM

-- LICENSING AND SAFETY ISSUES --

o NOISE ANALYSIS TECHNIQUES HAVE BEEN USED WITH SUCCESS TO DETECT AND DIAGNOSE ANOMALOUS BEHAVIOR IN REACTORS OF ALL TYPES THROUGHOUT THE WORLD

o EARLY DETECTION AND DIAGNOSIS OF ANOMALOUS TRENDS, FOLLOWED BY CORRECTIVE ACTION, WILL ENHANCE REACTOR SAFETY BY REDUCING CHALLENGES TO ENGINEERED SAFEGUARDS SYSTEMS

CONTINUOUS, ON-LINE REACTOR SURVEILLANCE SYSTEM

-- SCOPE --

- DEMONSTRATE AN AUTOMATED NOISE SURVEILLANCE AND BASELINE SIGNATURE ACQUISITION SYSTEM AT SEQUOYAH-1
- OBTAIN CONTINUOUS DATA TO STUDY THE BEHAVIOR OF THE NOISE ON SELECTED PLANT SIGNALS THROUGHOUT A FUEL CYCLE
- GENERATE SIGNALS CHARACTERISTIC OF ANOMALOUS CONDITIONS, USING OUT-OF-PILE TEST FACILITIES

IN-PLANT EXPERIENCE AND OUT-OF-PILE TESTS ARE ESSENTIAL TO THE DEVELOPMENT AND DEMONSTRATION OF A WORKABLE IN-PLANT SURVEILLANCE AND DIAGNOSTICS TOOL

- MUST DEMONSTRATE CAPABILITY OF ANALYSIS SYSTEM TO FUNCTION IN PLANT ENVIRONMENT AND ITS COMPATIBILITY WITH PLANT INSTRUMENTATION SYSTEMS
- MUST OBTAIN CHARACTERISTICS (E.G., STATIONARITY) OF NOISE SIGNALS UNDER NORMAL PLANT OPERATING CONDITIONS
- HOPE TO OBTAIN (FROM TEST FACILITIES) CHARACTERISTICS OF SIGNALS REPRESENTING ANOMALOUS CONDITIONS
- MUST DEFINE AREAS IN WHICH NOISE ANALYSIS CAN PROVIDE UNAMBIGUOUS DIAGNOSIS OF SAFETY PROBLEMS

IMPORTANT PARTS OF AN INTEGRATED PROGRAM ARE ADVANCED NOISE ANALYSIS METHODOLOGY AND COMPUTER TECHNIQUES FOR AUTOMATING NOISE MONITORING

- DATA COMPACTION AND DIMENSIONAL REDUCTION TO MINIMIZE DATA STORAGE REQUIREMENTS
- CATALOGING OF NOISE SIGNATURES THROUGH APPLICATION OF STATE VARIABLE METHODOLOGY
- FUNCTIONALLY REDUNDANT INPUT SIGNALS TO MINIMIZE FALSE ALARMS
- ADVANCED PATTERN RECOGNITION AND TREND ANALYSES TO IMPROVE DETECTION SENSITIVITY AND RELIABILITY
- CONDITIONING AND PRE-ANALYSIS OF NOISE SIGNALS USING DISTRIBUTED MICROPROCESSORS TO INCREASE SPEED AND REDUCE COST

THE ORNL/NRC SYSTEM WILL REPRESENT AN ADVANCEMENT IN THE ART OF AUTOMATED NOISE ANALYSIS

- OBTAINS PSDs OF FOUR SIGNALS
- AUTOMATICALLY LEARNS STATISTICAL DESCRIPTION OF NOISE SIGNALS
- MONITORS FOR CHANGES IN SIGNAL STATISTICS
- STORES ANY UNUSUAL SIGNATURES FOR LATER DISPLAY AND STUDY BY A NOISE ANALYST
- LABELS STORED SIGNATURES WITH A PLANT STATUS LABEL CONSISTING OF UP TO 16 QUANTITIES PRESELECTED BY THE ANALYST

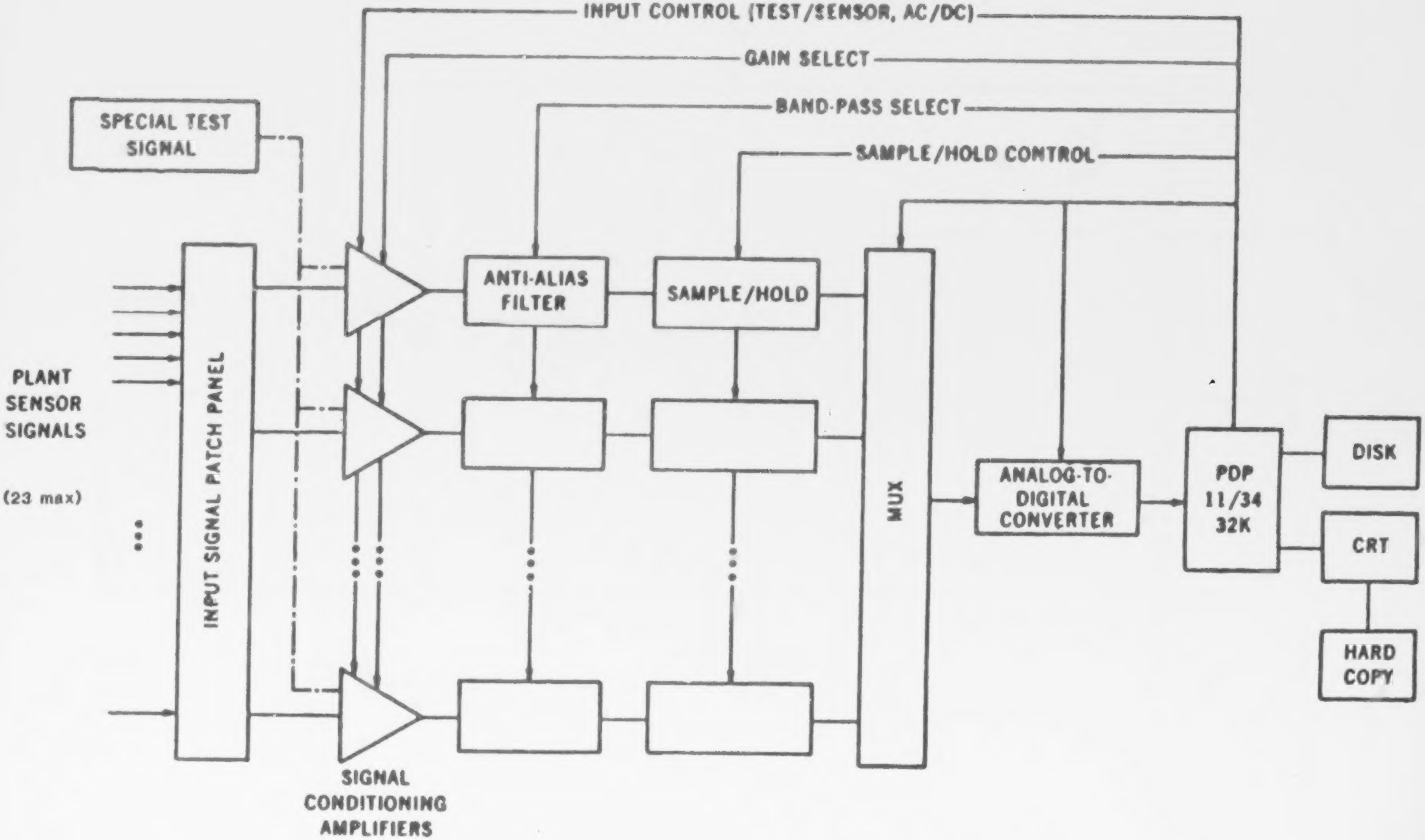
THIS SYSTEM HAS BEEN INSTALLED AT SEQUOYAH-1

INPUT CONTROL (TEST/SENSOR, AC/DC)
GAIN SELECT
BAND-PASS SELECT
SAMPLE/HOLD CONTROL
SPECIAL TEST SIGNAL
PLANT SENSOR SIGNALS
(23 max)
INPUT SIGNAL PATCH PANEL
SIGNAL CONDITIONING AMPLIFIERS
ANTI-ALIAS FILTER
SAMPLE/HOLD
MUX
ANALOG-TO-DIGITAL CONVERTER
PDP 11/34 32K
DISK
CRT
HARD COPY

The software logic:

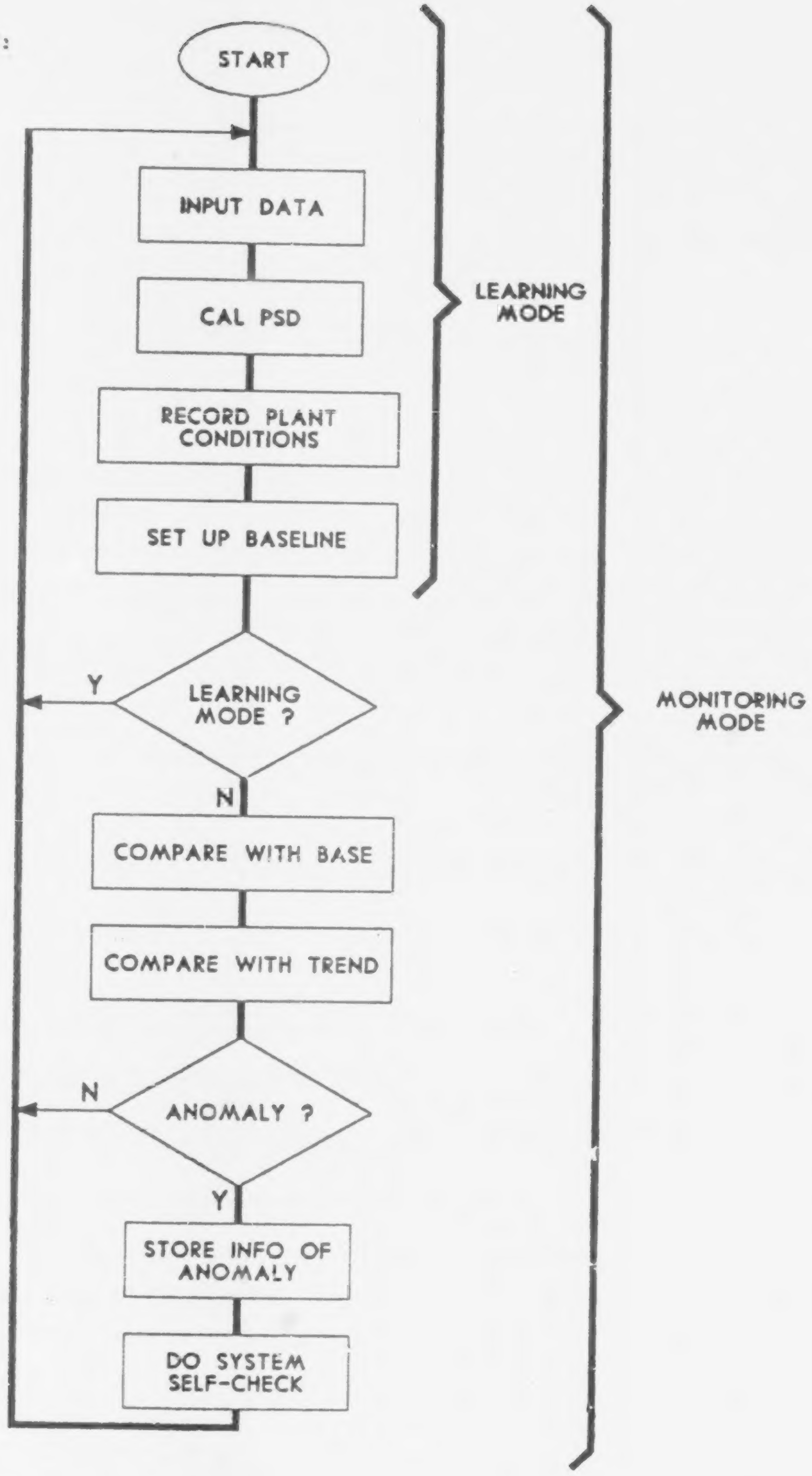
START
INPUT DATA
CAL PSD
RECORD PLANT CONDITIONS
SET UP BASELINE
LEARNING MODE
Y
LEARNING MODE ?
N
COMPARE WITH BASE
COMPARE WITH TREND
N
ANOMALY ?
Y
STORE INFO OF ANOMALY
DO SYSTEM SELF-CHECK
MONITORING MODE

SURVEILLANCE SYSTEM HAS ACCESS TO TWENTY-THREE SIGNALS AT SEQUOYAH-1

- POWER-RANGE NEUTRON FLUX (6)
- INTERMEDIATE-RANGE NEUTRON FLUX
- CORE-EXIT TEMPERATURE (4)
- REACTOR COOLANT SYSTEM PRESSURE
- REACTOR COOLANT SYSTEM FLOW
- HOT-LEG TEMPERATURE
- COLD-LEG TEMPERATURE
- PRESSURIZER WATER LEVEL STEAM GENERATOR
- STEAM FLOW
- STEAM GENERATOR FEEDWATER FLOW
- STEAM GENERATOR WATER LEVEL
- STEAM GENERATOR STEAM PRESSURE
- STEAM GENERATOR FEEDWATER TEMPERATURE
- REACTOR PRESSURE VESSEL VIBRATION
- CONTROL ROD DRIVE MOVEMENT (DATA ACQUISITION INHIBIT)

THE NEXT GENERATION SURVEILLANCE SYSTEM SHOULD HAVE ON-LINE DIAGNOSTIC CAPABILITY

- TO DIAGNOSE AND PROVIDE ALARMS FOR THOSE MALFUNCTIONS THAT CAN BE UNAMBIGUOUSLY IDENTIFIED USING NOISE ANALYSIS
- TO PROVIDE PLANT OPERATORS WITH CONFIRMATORY INFORMATION FOR TESTING AND DIAGNOSING SUSPECTED ANOMALIES
- TO PROVIDE NOISE ANALYSTS WITH SUPPLEMENTAL INFORMATION TO AID IN UNDERSTANDING THE CAUSES OF ABNORMAL NOISE SIGNATURES
- TO PROVIDE NOISE ANALYSTS WITH READILY ACCESSIBLE DATA ACQUISITION AND PROCESSING CAPABILITY FOR POSTACCIDENT DIAGNOSTICS

-- PRESENT STATUS --

- THE ORNL/NRC SYSTEM IS OPERATING AT SEQUOYAH-1 AND WILL REMAIN THERE FOR ~18 MONTHS OR UNTIL THE END OF THE FIRST FUEL CYCLE

- OUT-OF-PILE DATA HAS ALSO BEEN OBTAINED FROM THE THERMAL-HYDRAULIC TEST FACILITY AT ORNL FOR THE PURPOSES OF STUDYING

  - TEMPERATURE NOISE CAUSED BY SUBCOOLED AND BULK BOILING OF COOLANT

  - PRESSURE AND FLOW NOISE ACCOMPANYING COOLANT BOILING

(2) SUBCRITICAL REACTIVITY MONITORING

-- Licensing and Safety Issues --

- IMPROVED METHODS TO MONITOR REACTIVITY WOULD INCREASE SAFETY DURING REACTOR FUEL LOADING OPERATIONS AND IN FUEL STORAGE AND FABRICATION FACILITIES
- IMPROVED METHODS WOULD ALLOW SUBCRITICALITY TO BE MONITORED FOLLOWING INCIDENTS SUCH AS TMI-2, WHERE FIXED OR SOLUBLE CONTROL MATERIALS MAY BE LOST

SUBCRITICAL REACTIVITY MONITORING

- - SCOPE - -

- ASSESS THE FEASIBILITY OF SUBCRITICAL REACTIVITY MONITORING IN FULL-SIZE LWR CORES USING THE ^{252}Cf-SOURCE-DRIVEN NEUTRON NOISE METHOD
- CALCULATE DETECTION EFFICIENCIES AND SO THE ABILITY TO MEASURE SUBCRITICALITY IN BWRs
- EVALUATE THE EFFECTS OF SPATIAL HARMONICS ON INTERPRETABILITY OF THE MEASUREMENTS

ADVANTAGES OF THE ^{252}CF-SOURCE-DRIVEN
NEUTRON NOISE METHOD OF
SUBCRITICALITY DETERMINATION ARE:

- DOES NOT NEED A REFERENCE MEASUREMENT AT OR NEAR CRITICAL
- SUBCRITICALITY INFERENCE DOES NOT DEPEND ON RELATIVE OR ABSOLUTE VALUES OF INHERENT SOURCE STRENGTH OR DETECTION EFFICIENCY

THE METHOD REQUIRES PLACEMENT OF
THREE DETECTORS IN OR VERY NEAR THE
CORE TO BE MEASURED:

- A DETECTOR CONTAINING A ^{252}CF SOURCE, PLUS TWO CONVENTIONAL NEUTRON DETECTORS

- REACTIVITY IS OBTAINED FROM

$$\frac{\Delta K}{K} = C \cdot \frac{G_{s1}\, G_{s2}}{G_{ss}\, G_{12}}$$

WHERE

G_{s1} IS CPSD* OF SOURCE AND CONVENTIONAL DETECTOR # 1

G_{s2} IS CPSD OF SOURCE AND CONVENTIONAL DETECTOR # 2

G_{ss} IS PSD OF SOURCE DETECTOR

G_{12} IS CPSD OF CONVENTIONAL DETECTORS # 1 & # 2

AND C IS A CONSTANT COMPOSED OF KNOWN OR EASILY MEASURED CORE PHYSICS PROPERTIES

- - PRESENT STATUS - -

SO FAR IN THE PROGRAM, IT HAS BEEN DETERMINED
(FROM STATIC DIFFUSION CALCULATIONS)
THAT

- DETECTION EFFICIENCY FOR A GAMMA-TOLERANT 5-GRAM FISSION COUNTER PLACED IN THE CENTER OF A BWR-4 IS $\sim 10^{-4}$ COUNTS/FISSION; THIS IS ADEQUATE TO PERFORM SUBCRITICALITY MEASUREMENTS IN REASONABLE DATA AQUISITION TIMES

- HOWEVER, MEASUREMENT COULD BE MADE IN LESS THAN ONE HOUR IF HIGH-SENSITIVITY LITHIUM-LOADED GLASS SCINTILLATOR DETECTORS WERE USED; THIS WOULD BE PRACTICAL FOR INITIAL LOADING OF BWRs, WHERE GAMMA FLUX WOULD BE LOW

(3) NOISE DIAGNOSTICS FOR SAFETY ASSESSMENT

- - LICENSING AND SAFETY ISSUES - -

- MONITORING FOR LOOSE PARTS IN THE PRIMARY SYSTEM
- ASSURING ADEQUATE CORE STABILITY IN BWRs
- DETECTING COOLANT BOILING IN PWRs
- DETECTING EXCESSIVE VIBRATIONS OF IN-CORE INSTRUMENT TUBES, FUEL ELEMENTS AND CORE SUPPORT BARREL
- DETERMINING POSTACCIDENT CONDITIONS

NOISE DIAGNOSTICS FOR SAFETY ASSESSMENT

- - SCOPE - -

- PROVIDE EXPERIMENTAL AND ANALYTICAL ASSESSMENTS, USING NOISE DIAGNOSTICS, AS REQUESTED BY NRC
- ASSIST NRC IN DEVELOPING CRITERIA FOR ASSESSMENT OF LOOSE PARTS MONITORING SYSTEMS

- - PRESENT STATUS - -

WE HAVE COMPLETED

- A STUDY OF TECHNIQUES USED BY THE UTILITY INDUSTRY TO DETECT, LOCATE, AND CHARACTERIZE LOOSE PARTS IN REACTOR COOLANT SYSTEMS
- A FEASIBILITY STUDY ON THE USE OF NEUTRON NOISE TO MONITOR CHANGES IN BWR STABILITY
- DEVELOPMENT AND TESTING OF A STOCHASTIC CODE FOR MODELING NOISE SOURCES AND CALCULATING THEIR SIGNATURES IN BWRs

AND ARE CONTINUING TO

- ACQUIRE BASELINE NOISE SIGNATURES FROM OPERATING PLANTS FOR POTENTIAL USE BY NRC IN SAFETY ASSESSMENTS
- EVALUATE NEW TECHNIQUES FOR DIAGNOSIS OF SAFETY-RELATED PROBLEMS

IN CONCLUSION,

WE EXPECT THAT SUCCESSFUL COMPLETION OF THESE THREE PROGRAMS WILL BROADEN AND STRENGTHEN NRC's PLANT SAFETY DATA AND SKILL BASE BY PROVIDING

- A PROVEN ON-LINE REACTOR SURVEILLANCE SYSTEM FOR DETECTING AND DIAGNOSING ANOMALOUS OPERATIONAL TRENDS

- A METHOD FOR MONITORING REACTIVITY DURING FUEL LOADING OPERATIONS, IN FUEL STORAGE FACILITIES, AND IN REACTORS FOLLOWING CORE DISRUPTIVE ACCIDENTS

- DIAGNOSTIC TECHNIQUES THAT CAN BE USED TO ASSESS THE SAFETY OF PLANTS WITH SUSPECTED ANOMALIES, OR FOLLOWING ACCIDENTS SUCH AS TMI-2

*U.S. GOVERNMENT PRINTING OFFICE : 1980 O-341-742/478

THE SAFETY-RELATED OPERATOR ACTIONS PROGRAM AT ORNL

by

P. M. Haas
Engineering Physics Division
Oak Ridge National Laboratory

Presented At The

Eighth Water Reactor Safety Research Information Meeting
Gaithersburg, Maryland
October 29, 1980

The Safety-Related Operator Actions Program at ORNL

P. M. Haas
Engineering Physics Division
Oak Ridge National Laboratory

ABSTRACT

A program of simulator exercises and field data collection is being conducted at Oak Ridge National Laboratory to collect and assess data on nuclear power plant operator performance during accident events. The data can be used to support development of standards and regulatory guides, design decisions, risk assessments and other research and development or analyses related to operational safety. The near-term goal is to provide data to support a design criteria for automation of safety-related actions. This paper describes the planned program and presents preliminary results that have been obtained.

The Safety-Related Operator Actions Program at ORNL

P. M. Haas
Engineering Physics Division
Oak Ridge National Laboratory

INTRODUCTION

Program Purpose

The Safety-Related Operator Actions Program at Oak Ridge National Laboratory is intended to provide the U. S. Nuclear Regulatory Commission (USNRC) with quantitative and qualitative data on the performance of nuclear power plant operators during accident events. The data base is necessary to support licensing decisions, development of design standards, and safety/risk assessment studies related to the fundamental issues of operator reliability and the need or desirability of automating key safety-related actions. Information from this program will supplement results of ongoing and planned studies in a number of areas related to operational safety, such as emergency operating procedures, operator training and qualification and control room design.

Program Background, History

The program was initiated in late 1978, in response to an immediate need for an assessment of available data to support development of an American National Standards Institute standard (ANSI/ANS-N660),which is intended to provide design criteria for determining whether key safety-related actions should be automated. The approach taken to establishing the N660 criteria was to specify certain time limits for operator performance of safety-related actions, and a primary concern of the standards writing group (now designated ANS 58.8) and NRC was the lack of data from actual operating experience to support quantitative criteria. ORNL was asked to determine the availability and accessibility of field data, and develop a program of collection and assessment of useful data.

The study involved a review of Licensee Event Reports (LERs) and associated docket material, a comprehensive search of site documents - log books, internal reports, computer output, etc. - at five operating reactor sites (10 units), and structured survey of operators to extract quantitative and qualitative data from "expert opinion". It was concluded that each of the individual sources was of limited use, but that careful extraction and compilation of data from all sources could produce useful results for selected events. However, there simply are not enough field data to provide an adequate "statistical" data base. A program of controlled exercises, or "experiments", on full-scope nuclear plant simulators was proposed. In order to address the fundamental problem of extrapolation of results from the simulator to the real environment, it was proposed to "calibrate" the simulator experiments to field data by comparing results from both sources for selected exercises.

This preliminary study was nearing completion in March 1979 at the time of the TMI-2 occurrence, and the summary report[1] was completed by June 1979. At that time, NRC had an immediate need for an independent assessment of nuclear plant simulators and their use in operator training. ORNL agreed to perform that assessment through its subcontractor, Memphis State University Center for Nuclear Studies (CNS), and data collection for the safety-related operator action was delayed. A report[2] has been issued sumarizing the CNS study, and that work is the subject of a separate paper in this session by D. W. Jones of CNS. In March of 1980, the proposed program of simulator and field data collection was reinitiated. This paper describes the work in progress and some of the initial results. A related study, which will provide information to support development of a Reg. Guide endorsing ANSI/ANS 3.5 "Nuclear Plant Simulators for Use in Operator Training" was initiated in September 1980, but will not be discussed in this paper.

CURRENT PROGRAM

The current program consists primarily of three tasks: (1) collection and assessment of data from controlled simulator exercises; (2) collection and assessment of field data; and (3) calibration of simulator to field data. By the end of FY 1981, it is planned to have the bulk of the "historic" field data collection completed and to have an initial data base from both PWR and BWR simulator exercises that is "calibrated" to field data. An important part of the initial work is to identify the performance shaping factors that have the most significant impact on operator performance. Subsequent simulator experiments can help to quantify the effects of those performance shaping factors and evaluate the improvement in performance realized from modifications or proposed modifications to control room design, procedures, training, etc.

Simulator Exercises

The simulator exercises are currently being conducted by General Physics Corporation (GPC) at the Tennessee Valley Authority (TVA) Training Center near Soddy-Daisy, Tennessee. Licensed nuclear plant operators from different utilities perform a controlled series of exercises that involves a number of transient events (typically 6 to 10 during an eight-hour period) with periods of "normal operation" in between. The operators are informed that data are being recorded as part of a study for ORNL sponsored by NRC, and the instructor is not permitted to "interfere" with the exercise after it is initiated. Other than these two factors, the experiments are conducted as routine training exercises. There is no attempt to create a "more realistic environment" by introducing additional simulated "stress" or other artificial factors. The fact that some difference exists between the environment of a training simulator and an actual plant under accident conditions is recognized and is, in fact, the reason for the intended calibration of simulator data to field data. Future simulator exercises will be conducted under similar conditions.

Performance Monitoring System. The key to precise collection of quantitative data in the simulator exercises is the Performance Monitoring System (PMS) which is incorporated into the simulator software. The PMS was developed by GPC under contract to EPRI. It is installed on both the PWR (Sequoyah) and BWR (Browns Ferry) simulators at the TVA Training Center. During the conduct of an exercise, all digital and analog input and output to and from the control panel instruments is recorded on-line at one-second intervals and is stored on magnetic tape. Processing of the raw data takes place off-line. Identification of the specific control panel response that provides an indication of the operator's actions of interest is made by experienced operators. Then a computer code is written that extracts from the raw data tapes whether or not those actions were performed and, if so, the precise time at which they were performed. The automatic on-line data collection provided by the PMS overcomes much of the inherent problems of lack of accuracy, precision, objectivity and transparency when using human observers to record personnel performance.

Subjective Data. Despite the capabilities of the PMS, it cannot record valuable subjective data such as "potential" problems or possible problems of inter-operator interaction. Therefore in these experiments, a qualified instructor is used as an observer. His comments are incorporated with the data record. In addition, debriefing interviews with the operators are carried out in a structured manner. The interviewer questions the operators about the symptoms of the events, any apparent difficulties in responding, or any factors that may have affected performance. Transcripts of these recorded debriefings provide qualitative information on key performance shaping factors. Thus the simulator data consists of interpreted output from the PMS, comments from the observers, and a structured debriefing interview with the operators. In addition, background information on the operators, such as previous training and experience, are collected in order to evaluate possible effects of such individual factors.

Field Data Collection

The field data collection is being carried out by CNS. The primary effort is directed toward extraction of quantitative data, in particular response-time data, from records of accident events that have occurred. LER summaries and summaries of safety-related occurrences produced by the Nuclear Safety Information Center at ORNL are used as an indicator to identify applicable events that have occurred. However, these sources usually provide little quantitative data. Consequently, a team consisting of at least one qualified operator and one psychologist conducts a site visit during which all available records - control room logs, supervisor logs, computer output, plant upset records, etc. - that relate to the event are examined, and when possible, copied for further review. As much as possible, an attempt is made to review the details of the event with site personnel, especially any available who were involved with the event of interest. However, constraints on the availability of site personnel have made this extremely difficult.

To supplement the data acquired on specific events at a particular site, a structured written questionnaire is being administered to operators on a voluntary basis. The questionnaire addresses various factors that could affect performance, including control room indications of the event, procedures, training, control room design, and "psychological stress". Since the questionnaires are administered on a voluntary basis, and availability of site personnel time is limited, the amount of data collected during this initial data collection period is not likely to be great; but the subjective input from experienced operators should provide valuable information about key performance shaping factors.

Calibration of Simulator Data

The concept of "field-calibrated simulation" was suggested by Swain[3] for application in a somewhat different context. Conceptually, the approach is simular to that which might be used for any engineering correlation:

1) Identify the relevent variables and their likely influence.
2) Determine which variables should be subject to experimentation and which should be held constant or uncontrolled, and define the quantitative measures of those parameters.
3) Concurrently determine which variables can be measured, manipulated and controlled in the real situation and how they are quantified.
4) Perform the experiment and the "field-data" collection.
5) Develop a mathematical model that provides a consistent functional relationship between the two sets of data for the variables identified.
6) Use the model to predict future results; perform confirmatory experiments or data collection; and refine the model to extend its predictive capabilities.

For the field data collection, it is clear at the onset that it will be extremely difficult to quantify the many potentially significant variables, and that data available will be relatively few and often subjective. Therefore the "mathematical model" can be expected to be simplistic, and the calibration somewhat crude. However, it does appear to be feasible to establish whether there are at least consistent relationships between simulator and field data (e.g., actions requiring more time than others in the simulator also require more time than the same actions in the field data). If such a consistency is demonstrated and key performance shaping factors are identified in this early work, further analysis and experiments can provide the data to support a more comprehensive predictive model.

Results to Date

The initial series of ten "experimental runs" on the PWR simulator was completed in late August. Analysis of the results is not complete at this time, but some initial quantitative and qualitative data are available. Collection of field data is still in progress, and statistical analysis cannot yet be completed. However, some typical results are available that illustrate the kind of information it is possible to extract.

Simulator Data. The initial PWR exercises consisted of seven transient events grouped into five "modules". The debriefing interview was held at the end of each module. For each accident event, key operator actions were identified as "milestones" to provide a time-line for evaluating the operator response and to provide a comparison for results of field data. The seven events and the key operator actions are listed in Table 1. The events were selected because they have a range of accident severity (and, therefore, presumably, frequency of occurrence and "psychological stress") and significantly different symptoms, because preliminary LER searches indicated there should be enough occurrences in operating experience to provide data for calibration of simulator results, and because they are practical training exercises acceptable to the utilities voluntarily participating in the study. Although very severe events such as a large LOCA are of interest, the emphasis on field data collection precluded

Table 1. Accident Events Used in the Initial PWR Exercises

Event	Symptoms	Operator Action Milestones
RTD Failure	Automatic Rod Motion High Temp. Alarms/Annunciator High Meter Reading	1. Shift to manual rod control 2. Defeat failed channel 3. Manually adjust tave 4. Return to automatic rod control
Nuclear Instrument Failure (Power Range)	Automatic Rod Motion High Power Alarms/Annunciator High Meter Reading	1. Shift to manual rod control 2. Defeat failed channel 3. Manually adjust tave 4. Return to automatic rod control
Dropped Rod	Rod Bottom Light Automatic Rod Motion Rod on Bottom Alarm/Annunciator	1. Reduce turbine power 2. Shift to manual group rod control 3. Pull rod to bank position 4. Shift to automatic rod control
Flux Tilt (Due to FW Pump Trip)	MFP Trip Annunciator System Runback Annunciator Automatic rod motion	1. Align for automatic boration 2. Flush boration line 3. Return to normal valve lineup
Small LOCA - Leak in Letdown Line	Ice-Condensor Door Annunciator Humidity Increase on Recorder Ice-Condensor Door Position Indicator Pressurizer Pressure Low - Annunciator Pressurizer & VCT Level Low	1. Start charging pump 2. Establish excess letdown 3. Isolate leak
SG Tube Leak	Blowdown Stream Radioactivity Alarm Pressurizer Pressure Low Pressurizer & VCT Level Low	1. Start charging pump(s) 2. Commence shutdown 3. Close MF reg. valve 4. Complete shutdown to hot SB 5. Isolate SG
Inadvertent S.I. at Power	Rx Trip - Numerous Annunciators Equipment Running Lights on S.I. Pumps, RHR Pumps	1. Stop centrifugal charging pumps 2. Reset S.I. 3. Re-establish letdown 4. Restore normal charge & pump seal water 5. Secure S.I. & RHR pumps

selection of such events at this time. Also, two other studies[4,5] have included simulator exercises on the large LOCA, and data from these will be available for comparison to results from this program.

Typical data on time to perform the key actions are illustrated by the results for the event "Dropped Rod" shown in Table 2. There are eight runs from Utility "A" and two from Utility "C". Note that performance is recorded for the team of operators. It is not possible to distinguish individual actions. The data most readily collected by the PMS are the times to correctly perform the required action. Errors of omission are readily identified. Errors of commission are more difficult to extract, simply because of the difficulty of identifying in advance all the possible errors. The raw data tape, of course, provides a record of all control panel actions, and errors of commission could be extracted. This has not been attempted for these data. The N660 standard, in fact, does not attempt to deal directly with errors of commission, but instead sets criteria on the basis of time for correct performance as presented here.

The N660 criteria focus primarily on two "time tests". Time Test 1 deals with the time required for the operator to recover from any initial "shock", diagnose the event, verify automatic actions, and plan his subsequent actions and initiate the first manual action. These actions might generally be referred to as "decision tasks".[6] Time Test 2 addresses the time required to perform discreet manual actions. Interpretation of the data shown in Table 2 for use to support Time Test 2 will require careful analysis of each event and its specific required actions. In most cases, the time for performance is a function of the equipment response as well as operator capability. Also, the milestone tasks listed may often include several discreet actions.

The data presented for the time to perform the initial action is more directly interpretable in terms of the N660 criteria, Time Test 1. For the case of the dropped rod, initiating reduction in turbine power requires several discreet control manipulations which are performed very nearly simultaneously. The time reported is a reasonably precise measurement of the performance of the "decision tasks" referred to above. A summary

Table 2.

Initial Simulator Data (Response Times in Seconds) for DROPPED ROD

Shift	Action 1 Reduce turbine power	Action 2 Shift to manual group rod control	Action 3 Pull rod to bank position	Action 4 Shift to automatic rod control
A1	32	1375	2394	2801
A4	41	1104	1512	1605
A3	48	1529	1821	1928
C1	49	611	921	1052
C2	57	951	1329	1350
A8	71	489	--	1369
A6	97	1241	2104	2195
A2	202	1005	1620	1760
A7	223	862	1503	1533
A5	1170	1119	1423	1508

Time to initiate first action: Mean = 199 seconds = 3.3 min.
(N = 10) Std. Dev. = 347 seconds = 5.8 min.

of the time to initiate the first manual action in each of the seven events is presented in Table 3. Since these are very preliminary data presented without supporting analysis, there is no attempt to draw conclusions at this time. There do appear some obvious and expected differences in response times between events such as RTD Failure which has specific, clearly delineated symptoms, and small LOCA, for which the early symptoms are relatively non-specific and not well annunciated.

Field Data, Comparison to Simulator Data. For obvious reasons, data collected from historic records are less precise and often more subjectively derived. Usually log-book entries will be recorded no more precisely than one-minute intervals, and often there are discrepancies between different log books or other documents which can be resolved only by judgement of the data analyst. Computer logs, when available, offer more precise and objective data, but are often very difficult to interpret, even with the assistance of site personnel. Extraction of meaningful field data is an extremely tedious, labor-intensive task. However, some success has been achieved.

Table 4 illustrates the kind of data that are being extracted. These are preliminary data for the rod-drop event. At this time it has been possible to extract quantitative data for 20 occurrences. As indicated in the table, the best information available for many of the occurrences does not make it possible to distinguish between the time of the event alarm and the time of the initial action. Log book entries typically list one time and indicate an "immediate" response. It is difficult to treat these data quantitatively in a statistical analysis. For purposes of initial comparison of these preliminary results to the simulator exercises it is simply assumed that any entry indicating a response within a minute or less can be treated quantitatively as a response time of one minute. Then the data indicate that in 16 of the 20 occurrences the first manual action was initiated at t = 1 minute, and in four occurrences the time required was 2 minutes. For this crude treatment, the mean and standard deviation of the response time are 1.2 and 1.0 minutes, respectively. For the ten simulator runs, the mean and standard deviation were 3.3 and 5.8 minutes, respectively.

Table 3.

Initial Simulator Data - PWR

Time (Seconds) to Initiate First Manual Action

	Event						
Shift	Rod Drop	SGTR	RTD Failure	MFP Trip Flux Tilt	NI Failure	Small LOCA	Inadv. S.I.
A1	32	100	10	875	9	802	505
A2	202	-51*	7	114	14	194	208
A3	48	84	7	556	8	835	317
A4	41	102	14	299	9	852	149
A5	1170	34	6	35	7	588	---
A6	97	53	10	54	14	464	197
A7	223	---	19	505	13	---	---
A8	71	170	33	137	23	2038	1023
C1	49	30	10	456	6	547	186
C2	57	37	9	408	5	---	274
MEAN	199	67.8	12.5	344	10.8	790	357
(Std. Dev.)	(347)	(51.5)	(8.2)	(268)	(5.4)	(551)	(291)

---

*The times listed are referenced to the time of the specific event alarm (Blowdown Stream Radioactivity). In this case, the operators performed the initial action (start charging pump) prior to the alarm.

Table 4. Typical Field Data: Dropped Rod

		Clock Time							
	Event	Action 1		Action 2		Action 3		Action 4	
Shift	Alarm	T_i	T_c	T_i	T_c	T_i	T_c	T_i	T_c
A1	1933	1933	1947	--	--	1947	2002	--	--
A3	0420	0420	0446	--	--	0448	0509	--	--
A4	1319	1320	1349	--	--	1349	1410	--	--
A5	1346	1346	1417	--	--	1435	1458	--	--
A6	0957	0959	1020	--	--	1036	1107	--	--
A11	1254	1315	--	--	--	--	--	--	--
A13	0958	0958	1057	--	--	1100	1111	--	--
A15	1226	1226	1256	--	--	1315	1328	--	--
A19	1930	1930	2005	--	--	2008	2032	--	--
A20	0234	0234	0246	--	--	0247	0305	--	--
A22	0349	0349	--	--	--	0455	0507	--	--
A23	1725	1725	1739	--	--	--	1739	--	--
A24	1735	1737	1813	--	--	1820	1833	--	--
A25	2237	2237	2248	--	--	--	2314	--	--
A26	0821	0821	0850	--	--	0913	0927	--	--
A27	0825	0827	0855	--	--	--	0910	--	--
A28	0120	0120	0148	--	--	0150	0223	--	--
A29	1735	1737	1813	--	--	1820	1833	--	--
A31	1245	1245	1330	--	--	1418	1430	--	--
C1	1052	1052	1105	--	--	--	--	--	--

T_i = Time action initiated.

T_c = Time action completed.

Action 1 = Reduce turbine power.
Action 2 = Shift to manual group rod control.
Action 3 = Pull rod to bank position.
Action 4 = Shift to automatic rod control.

A similar comparison is available for the event "Inadvertent Safety Injection". In this event, the problem for the operator is to determine that the safety injection is indeed inadvertent and take action to stop the injection and assure that the reactor system has been brought to a safe shutdown condition. The symptoms, "decision tasks" or cognitive process, and presumed "psychological stress" would appear to be quite different for this event than for the dropped rod. Field data collected during the preliminary study in 1978-79 for 42 occurrences of this event are illustrated in Fig. 1. The figure is a cumulative probability plot of time to perform the first manual action, i.e., reset the safety injection signal. For these data a log-normal distribution was assumed and appropriate parameters estimated from the plot. At this time, there has been no analysis done to justify the use of a log-normal distribution for the simulator data. However, for the sake of comparison, one might compare the logarithmic means of the two data sets:

$$\bar{T} = \left(\prod_{i=1}^{n} T_i \right)^{1/n}$$

where n = number of data points

T_i = ith response time.

The values of $\bar{T}$ are 4.8 minutes and 1.9 minutes, respectively for the simulator and the field data. If no distribution is assumed, the simple arithmetic means are 6.0 minutes for the simulator data and 3.4 minutes for the field data.

It is generally assumed that performance under simulator conditions will be "better" than in the "real environment" for a number of reasons - anticipation of the event occurrence and "reduced stress levels" in the simulator environment, etc. It is interesting to note that if "time to respond" is an appropriate measure of performance, these few data for the two events examined do not support that assumption. The mean times are greater in the simulator environment. There are a number of obvious factors - familiarity of the test subjects with the Sequoyah site-specific procedures and control room, current state of training, etc. - which could dominate or distort the results, and the data are certainly too few to support general conclusions. However, the assumption

ORNL-DWG 80-9794

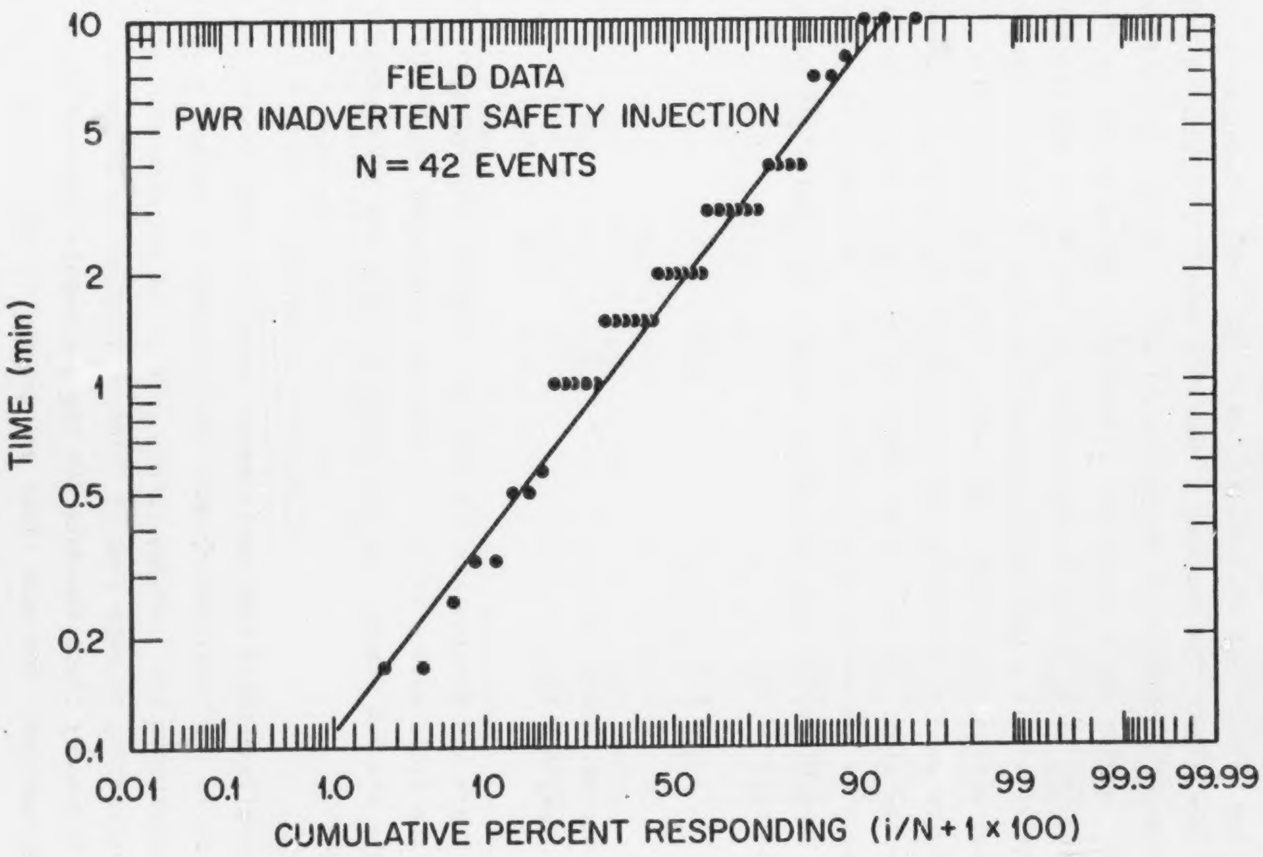

Fig. 1. Probability (Frequency) Plot of Response Time for the PWR Event "Inadvertent Safety Injection".

that performance in the real situation will necessarily be "worse" than in the simulator environment is clearly questionable.

It is encouraging, but equally inconclusive, that the data comparison for these two events tend to support the suggestion of "consistency" between the two data sets. That is, the event requiring more time for response in the simulator (inadvertent safety injection) also requires more time in the field. As performance data are accumulated for different tasks in the two environments one would hope to establish this kind of consistency if a correlation does exist between the two sets of data.

CONCLUSION

The current program of simulator experiments and field data collection should be viewed as one necessary element in NRC's overall approach to improving operational safety of nuclear power plants. It will provide specific information on operator response times useful for the near-term needs for the N660 Standard and will form the basis for development of a realistic data base on operator performance necessary for a broad range of analysis and assessments currently in progress or planned. The results and analysis of data completed at this time are very preliminary and should not be used to form general conclusions. However, they do demonstrate that the approach to development of a data base from field-calibrated simulator results should be successful.

During this early work the program will serve not only to quantify operator performance but to identify problems - key performance shaping factors that could be modified to improve performance. As more data are accumulated and analyzed in this and other ongoing programs, modifications to current designs and regulatory or operational practices will be made. Many modifications in practice and some to design have already been made since the TMI-2 event, and the majority of these directly relate to operator performance. A continued program of data collection and assessment will be necessary to quantitatively assess the impact of these modifications and assure that the result is improved safety. Much of this quantitative evaluation can be made by using full-scope simulators where it is impractical to collect data from operating reactors, particularly if simulator results can be calibrated to operational data.

REFERENCES

1. P. M. Haas and T. F. Bott, "Criteria for Safety-Related Operator Actions: A Preliminary Assessment of Available Data," NUREG/CR-0901, ORNL/NUREG/TM-330 (1979).

2. D. W. Jones, D. K. Baer and C. C. Francis, "Nuclear Power Plant Simulators: Their Use in Operator Training and Requalification," NUREG/CR-1482, ORNL/NUREG/TM-395 (1980).

3. A. D. Swain, "Field Calibrated Simulation," SC-R-67-1045, Sandia Corporation (1967).

4. E. J. Kozinsky and T. B. Sheridan, "Operator Response Times on Training Simulators," (draft) GP-R-632, Research Project 769-2, Prepared for Electric Power Research Institute (May, 1980).

5. M. A. Haley, "Westinghouse Operator Action Program: Preliminary Recommendations to ANS 58.8 Working Group on Criteria for Safety-Related Operator Actions," Attachment 3 Westinghouse Class 3 Document (May, 1980).

6. *ibid*, p. 1.

*U.S. GOVERNMENT PRINTING OFFICE : 1980 O-341-742/478

SIMULATORS AND THEIR USE IN TRAINING OPERATORS

D.W. JONES, PH.D.

Nuclear power plant simulators may be described in terms of key parameters such as the number of systems simulated, preprogrammed malfunctions, preprogrammed initial conditions, and training features. Comparing existing simulators on this basis shows little change in the number of initial conditions and systems simulated over the past decade. The number of preprogrammed malfunctions has, however, increased significantly. The number and sophistication of training features has also shown considerable improvement.

Nineteen nuclear power plant simulators are scheduled to be in service by the end of 1981. Those simulators in operation have, to date, accumulated approximately 61 simulator years of operating experience. Of these simulators, three were constructed by NSSS Vendors for their own use. The remaining simulators were constructed by only two commercial simulator vendors, and only one type computer is used in modern simulators. The limited market has not created significant competition in the past decade, although current market expansion now offers greater opportunity for competition.

Key issues in the construction of simulators include the accuracy and scope of simulation; the time to which the response of the plant is followed into an accident; the extent to which the interaction of systems is simulated; and the extent to which accidents involving phenomena such as two-phase flow are simulated. Although there has been some improvement in the extent to which simulators address these issues since the accident at three Mile Island, opportunity for improvement remains in many issues. A limiting factor in simulation is the combination of speed and memory size compatiable with real-time simulation. It appears that modern simulators provide an efficient use of state of the art techniques in computer simulation, although improvements in mathematical modeling of plant systems and transients may allow advances in power plant simulation to be made. A major advance in state of the art simulation depends upon improvements in both computer technology and mathematical modeling of systems and transient states. There is also need to develop and refine a methodology to validate simulator performance in the case of plant transients on which actual data has not been accumulated by operational experience.

Historically, training programs and excercises for operators on simulators were limited to about 14 days of simulator time. Of this, approximately 40% was devoted to accident drills while the remainder was devoted to learning to operate the plant under normal conditions. There is little evidence that training exercises were based upon a formal analysis of the needs of the operator in training but more on a subjective opinion of training needs. An attempt is currently being made to develop a programmatic methodology for planing training programs which would be based upon a task analysis of the operator's job. This trend promises to improve the quality of simulator training.

The selection of malfunctions for simulation has heretofore been based largely upon subjective opinions of the needs of operators. Often the selection of malfunctions appears to be based upon a simple extension of those included in the last simulator of that type constructed. The selection of a malfunction for simulation should be based upon the importance of the particular malfunction to the safety and reliability of plant operations and the need for that malfunction in the training of operators. An attempt was made to develop a methodology for selection of malfunctions which includes the ranking of malfunctions on the basis of safety criteria.

Application of the resulting criteria to a selected list of malfunctions indicated that many malfunctions not currently simulated were important to the safe and reliable operation of the plant. Other malfunctions currently simulated on most power plant simulators were found to be less important that some which were not simulated. The application of this methodology, however, requires extensive refinement. Specific criteria should be developed for the simulator applicable to the plant simulated, the purpose of the simulator, and the training needs of the facility. The results of the trial application show that further investigation of methodology for selecting malfunctions is warrented.

The ability of the operator to respond rapidly and correctly in time of emergency must be one of the principal objectives of training programs. There is, however, no evidence that many issues involving human factors considerations have been formally addressed in the development of present day simulator training. The development of a formal methodology for inclusion of such human factor considerations as the response of an operator during periods of high stress in the development of training programs may offer an opportunity for significant improvement of simulator training.

In general, industry is making important steps forward in considering factors which can improve training and in attempting to utilize technology developed for non-nuclear operator training in other industries to improve training of nuclear plant operators. The encouragement of these attempts to improve the quality of nuclear operator training offers a recognizable potential for improvement in the safety and reliability of nuclear plant operation.

SLIDES

1. BWR SIMULATORS IN THE UNITED STATES
2. PWR SIMULATORS IN THE UNITED STATES
3. SUMMARY OF SIMULATOR CHARACTERISTICS
4. TYPICAL SIMULATOR TRAINING PROGRAM
5. SIMULATOR TRAINING ISSUES
6. SIMULATOR TRAINING ISSUES
7. SIMULATOR TRAINING ISSUES
8. CRITERIA FOR SELECTION OF MALFUNCTIONS
9. ANALYSIS OF PWR MALFUNCTIONS
10. ANALYSIS OF BWR MALFUNCTIONS
11. HIGH PRIORITY EVENTS NOT SIMULATED
12. HIGH PRIORITY EVENTS NOT SIMULATED, CONT.
13. LOW PRIORITY EVENTS SIMULATED
14. LOW PRIORITY EVENTS SIMULATED, CONT.
15. RECOMMENDATIONS

BWR SIMULATORS IN THE UNITED STATES

PLANT SIMULATED	NSSS VENDOR	NPPS VENDOR	TRAINING FEATURES	INITIAL CONDITIONS	SYSTEMS SIMULATED	PREPROGRAMMED MALFUNCTIONS	COMPUTER	SERVICE DATE
Dresden-2 (BWR/3)	GE	GE	3	21	33	107	GEP 4020	1968
Browns Ferry (BWR/4)	GE	S	9	18	47	149	SEL 85	1976
Susquehanna (BWR/4)	GE	S	6	26	34	100	SEL 32/55	1979
Black Fox (BWR/6)	GE	S	6	26	27	142	SEL 32/55	1980
Perry (BWR/6)	GE	S	NA*	NA	25	NA	SEL 32/55	1980
Limerick (BWR/6)	GE	S	NA	NA	31	NA	SEL 32/55	1980
Hartsville	GE	S	6	26	27	142	SEL 32/55	1980

*NA: No information available

PWR SIMULATORS IN THE UNITED STATES

PLANT SIMULATED	NSSS VENDOR	NPPS VENDOR	TRAINING FEATURES	INITIAL CONDITIONS	SYSTEMS SIMULATED	PREPROGRAMMED MALFUNCTIONS	COMPUTER	SERVICE DATE
Rancho Seco	B&W	S	NA*	NA	27	73	GP 4B	1970
Zion-1	W	W	3	16	NA	99	PDP 11/35	1972
Calvert Cliffs	CE	S	NA	20	22	100	GP 4B	1972
Indian Point-2	W	S	NA	NA	26	NA	PDP 11/45	1975
McGuire	W	S	NA	19	22	256	PDP 11/45	1976
Sequoyah	W	S	9	21	29	140	SEL 85	1976
Shearon Harris	W	S	NA	NA	23	NA	SEL 32/77	1978
WNP 1,4	B&W	S	NA	NA	25	NA	SEL 32/55	1979
Surry-1	W	EAI	9	21	19	231	SEL 32/55	1978
Palo Verde	CE	EAI	9	21	28	214	SEL 32/55	1980
Snupps	W	EAI	NA	NA	NA	NA	NA	1979
Seabrook	W	S	NA	NA	24	152	SEL 32/55	1981
Vogtle	W	S	NA	NA	NA	NA	NA	NA

*NA: No information available

SUMMARY OF SIMULATOR CHARACTERISTICS

TRAINING FEATURES	3 to 9
INITIAL CONDITIONS	16 to 26
SYSTEMS SIMULATED	19 to 47
PREPROGRAMMED MALFUNCTION	73 to 256
TYPICAL COMPUTER	SEL 32/55
COMMERCIAL VENDORS	2
EXPERIENCE BY 1980	61 Simulator Years

CHARACTERISTICS OF SIMULATOR TRAINING

PRE - TMI

(1) 3 TO 4 OPERATORS PER GROUP

(2) APPROXIMATELY 14 DAYS SIMULATOR TIME FOR EACH PERSON

(3) ABOUT 40% OF TIME SPENT IN EMERGENCY DRILLS

(4) 1 WEEK OF QUALIFICATION TRAINING EACH 2 YEARS

SIMULATOR TRAINING ISSUES

1. ACCURACY TO WHICH SIMULATION REPRODUCES PLANT RESPONSE IN NORMAL OPERATION.
2. ACCURACY TO WHICH SIMULATION REPRODUCES PLANT RESPONSE DURING ACCIDENTS.
3. EXTENT TO WHICH SIMULATION REPRODUCES TOTAL SYSTEM RESPONSE.
4. TIME TO WHICH SIMULATION FOLLOWS PLANT RESPONSE INTO AN ACCIDENT.
5. EXTENT TO WHICH SIMULATION TAKES ACCOUNT OF SYSTEM INTERACTION DURING ACCIDENT.
6. NUMBER OF TRAINING FEATURES INCORPORATED INTO SIMULATOR.
7. NUMBER OF INITIAL CONDITIONS PREPROGRAMMED.
8. NUMBER OF MALFUNCTIONS PREPROGRAMMED.
9. SELECTION OF MALFUNCTIONS FOR SIMULATION.
10. AMOUNT OF TIME FOR EACH TRAINEE SPENT ON THE SIMULATOR.
11. TRAINING FOR ACCIDENT RESPONSE.
12. BASIS FOR TRAINING PROGRAM AND SIMULATOR EXERCISES.
13. INCLUSION OF HUMAN FACTORS CONSIDERATIONS IN TRAINING.
14. INCLUSION OF TRAINING OF OPERATORS TO RESPOND UNDER STRESS.

CRITERIA FOR SELECTION OF MALFUNCTIONS

A. IMPORTANCE TO SAFETY	0 - 15
B. FREQUENT OCCURRENCE	0 - 4
C. PRECURSOR TO SAFETY EVENT	0, 5
D. RESULTS IN PLANT OUTAGE	0, 3

ANALYSIS OF PWR MALFUNCTIONS

System	Importance Factor						
	0-4	5-8	9-12	13-16	17-20	21-24	25-28
Emergency Diesel Generator			2	5	3	9	
Service Water		1	2	2		2	
Plant Ventilation			1	6		3	
Circulating Water		1	1	7			
Emergency Plan		1		4	1		
Electrical Distribution		1	6		2	4	
Component Cooling Water	1		3	5	5	2	
Reactor Protection					2	2	
Rod Control		5	3	8	4	7	
Residual Heat Removal		2	2	3	1	3	
Emergency Core Cooling				9	3	14	
Feedwater		2	1	14			
Auxiliary Feedwater			2	5	1	2	
Chemical and Volume Control			3	6		4	
Radiation Monitoring		1		14		1	
Main Steam and Turbine	2			8	3	2	
Containment		1	1	5		8	1
Nuclear Instrumentation		1		14			
Reactor Coolant System	2		1	6	3	12	
Fire	2	1	1	4	7	4	
Condensate		1	2	5		1	0
Mode Status Requirements					3	3	
Total for All Systems	7	18	31	140	38	83	1
Number of Malfunctions simulated by 50% or more of simulators	0	7	7	37	4	15	0

ANALYSIS OF BWR MALFUNCTIONS

System	Importance Factors			
	0-4	5-8	9-11	12-23
Condensate and Feedwater	1		1	1
Containment	1	4	2	3
Diesel Generator	1	4		
ECCS - Core Spray			2	1
ECCS - HPCI	1	2	3	2
ECCS - Isolation Condensor		1	1	
ECCS - LPCI			2	
ECCS - RCIC		1	4	
ECCS - RHR			1	2
Electrical		1		2
Fire Protection			2	
Main Steam & Turbine		1	2	2
Nuclear Instrumentation	6	1	3	
Off Gas/Standby Gas Tr.		1		3
Reactor Controls		1	1	4
Reactor Coolant	1	0	3	5
Standby Liquid Control		1	2	1
Total for All Systems	11	18	31	26
Number of Malfunctions simulated by 50% or more of simulators	0	2	8	2

HIGH PRIORITY EVENTS NOT SIMULATED

NO.	PWR SYSTEM, MALFUNCTION (EVENT)*	FREQUENCY OF OCCURRENCE	CURRENTLY SIMULATED	ANALYSIS REQUIRED	JUSTIFICATION				IMPORTANCE FACTOR
					A	B	C	D	
1	REACTOR COOLANT (All Modes)								
	Average temperature (T_{avg}) high limit exceeded, large deviation at full power	.26	0/7	X	12	1	5	3	21
	All pressurizer safety valves inoperable	.04	0/7	X	15	1	5	3	24
2	CHEMICAL AND VOLUME CONTROL (All Modes)								
	Charging pump suction piping crack or break	.09	0/7	X	15	1	5	3	24
3	CONDENSATE (All Modes)								
	Condensate storage tank level below limit for power operation	.48	0/7	X	15	1	5	3	24
4	RESIDUAL HEAT REMOVAL (Modes 4-6)								
	RHR system leakage or pipe rupture	.09	0/7	X	15	1	5	3	24
5	PLANT VENTILATION (All Modes)								
	Containment hydrogen control (skimmer) fans failure	.09	0/7	X	15	1	5	3	24
6	REACTOR PROTECTION (Modes 1-3)								
	Reactor trip breakers failure to trip	.04	0/7	X	15	1	5	3	24
7	CONTAINMENT (All Modes)								
	Containment isolation actuation channel failure to isolate, first phase	.04	0/7	X	15	1	5	3	24
	Containment isolation main steam and feedwater systems rupture capability failure	.04	0/7	X	15	1	5	3	24

HIGH PRIORITY EVENTS NOT SIMULATED

NO.	BWR SYSTEM, MALFUNCTION (EVENT)*	FREQUENCY OF OCCURRENCE	CURRENTLY SIMULATED	ANALYSIS REQUIRED	JUSTIFICATION				IMPORTANCE FACTOR
					A	B	C	D	
1	REACTOR COOLANT (Any Mode) Reactor Water level instrument failure	0.9	0/4	X	12	1	5	3	21
2	REACTOR CONTROLS (Any Mode) Control rod drive piping leaks/ruptured	.34	0/4	X	12	1	5	3	21
3	ELECTRICAL (Any Mode) Loss of off-site power	.28	0/4	X	12	1		3	16
4	CONDENSATE AND FEEDWATER (All Modes) Feedwater leak/ruptured	.07	0/4	X	12	1	5	3	21
5	CONTAINMENT (All Modes) Excess drywell leakage-various packing/seal leaks	.28	0/4	X	12	1	5	3	21

LOW PRIORITY EVENTS WHICH ARE SIMULATED

NO.	PWR SYSTEM, MALFUNCTION (EVENT)*	FREQUENCY OF OCCURRENCE	CURRENTLY SIMULATED	ANALYSIS REQUIRED	JUSTIFICATION				IMPORTANCE FACTOR
					A	B	C	D	
1	REACTOR COOLANT (All Modes)								
	Channel T_{avg} failure high	0	6/7	X	5		5	3	13
	Pressurizer heaters failure, SCR failure	0	5/7	X	7		5	3	15
2	CHEMICAL AND VOLUME CONTROL (All Modes)								
	Charging pump failure to start	.04	7/7	X	5	1	5	3	14
	Charging line pipe crack or break failure in containment	0	3/7	X	7		5	3	15
	Letdown to VCT failure	0	5/7		7			3	10
	Loss of letdown	0	4/7		7			3	10
3	ELECTRICAL DISTRIBUTION (All Modes)								
	Reactor coolant pump bus overload on pump start	0	4/7	X	5			3	8
4	CONDENSATE (All Modes)								
	Condensate booster pump failure	0	5/7		5		5		10
	Heater drain pump failure	0	4/7		5			3	8
5	FEEDWATER (Modes 1-3)								
	HP heater drain pump failure	0	4/7	X	5			3	8

LOW PRIORITY EVENTS WHICH ARE SIMULATED

NO.	BWR SYSTEM, MALFUNCTION (EVENT)*	FREQUENCY OF OCCURRENCE	CURRENTLY SIMULATED	ANALYSIS REQUIRED	JUSTIFICATION				IMPORTANCE FACTOR
					A	B	C	D	
1	REACTOR CONTROLS (Any Mode)								
	Pattern control system failure	.14	1/4	X		1	5		6
2	MAIN STEAM AND TURBINE (Any Mode)								
	Valve response time out of spec	.34	1/4			1	5		6
3	EMERGENCY CORE COOLANT - REACTOR CORE ISOLATION COOLING (Mode: Above Required Pressure Set Point)								
	RCIC Speed erratic	.28	2/4	X	5	1			6

RECOMMENDATIONS

1. ALL TRAINING SHOULD BE BASED UPON A TASK ANALYSIS WHICH IDENTIFIES TRAINING OBJECTIVES. FORMAL PROGRAM DEVELOPMENT ENCOURAGED.

2. SIMULATORS SHOULD BE DESIGNED TO SUPPORT TRAINING NEEDS RATHER THAN TRAINING BASED ON WHAT THE SIMULATOR WILL AFFORD.

3. RESEARCH SHOULD BE PERFORMED TO OPTIMIZE EFFECTIVENESS OF TRAINING TO PREPARE OPERATIONS TO COPE WITH EMERGENCY SITUATIONS.

4. STANDARDS AND OTHER GUIDELINES SHOULD REFLECT CONTINUOUS IMPROVEMENT OF PROGRAMS AND FACILITIES TO MEET STATE OF THE ART CAPABILITY RATHER THAN MINIMUM REQUIREMENTS.

U.S. GOVERNMENT PRINTING OFFICE : 1980 O-341-742/478

Defining the Role of the Operating Crew

R. A. Kisner G. F. Flanagan
Oak Ridge National Laboratory
September 1980

The safe operation of a nuclear power plant depends on the correct, precise interaction of many systems and components within the plant. Supervision of these systems and their interactive effects is the responsibility of the plant operating crew. The crew has potential for either initiating or mitigating disturbances in plant operation. Recent events have shown the need for enhancing the capabilities of the operating crew, especially in preventing and limiting hazardous conditions and equipment damage. One area, in particular, where improvements can be introduced is the control room.

Most problems encountered with control room design can be segregated into two general problem classes. The first relates to readability and ambiguity of information display and control commands. The second class relates to the relevance and adequacy of information and control options that support the operators actions. The latter category deals with assisting the operator in problem analysis and decision making. Significant improvements in operator performance will require solving the major problems of both categories. A carefully reasoned, holistic approach will assure both designers and regulators that old problems are not replaced with new problems of a potentially more dangerous or unpredictable nature. This implies a systems engineering approach to control room modification and operational aids development.

One of the first steps of a systems approach is to define functional requirements. Since we are concerned with a human-machine system, an important step is to define the role of the operating crew. A description of the operating crew's role would provide a basis from which to judge the adequacy of information and control options.

Nuclear power plant operating crews in the United States are composed of teams of individuals representing several levels of training, experience, and responsibilities. The primary responsibility for safe plant operation rests on the shift supervisor. The assignment of duties to individual reactor operators is done at the discretion of the shift supervisor. The members of the crew are not specialized in specific areas but, rather, are expected to be proficient operators of all plant systems and, therefore, are interchangeable. The current structure of the operating crew has no separation of responsibility by function or reactor system. Description of the role should be as general as possible so that it will not become plant specific and still be meaningful.

The role of the operating crew has many perspectives depending on the state of the plant and the objective of the next phase of operation. In addition, each organization involved with nuclear power production and regulation describes the role with a different emphasis. Sources of role descriptions of interest to this project are (1) emergency operating instructions (EOIs), (2) power plant designers, (3) operator examiners, (4) operator trainers, (5) utility management, and (6) regulators. These role descriptions will represent views of the functions currently performed at power plants using existing procedures and equipment. Some differences in descriptions are expected since the charters of these organizations are diverse and they would naturally place different requirements on the objectives of operations; however, because consistent design criteria and objectives were not applied to control rooms and crew functions, additional discrepancies in descriptions were present. By evaluating this collection of role descriptions regarding human behavioral factors, ergonomic factors, and the experiences of aerospace and defense industries, we will identify deficiencies in each approach and develop guidelines for improvement.

One description of the operators' role has been completed. The description provides a characterization of an operating crew's function under emergency conditions using the emergency operating instructions (EOIs) of a typical pressurized water reactor (TVA Sequoyah nuclear power plant). The operators' role was determined to be task oriented. EOIs limit the operator to specific responses during defined emergency conditions. To carry out the role, four basic functions are defined by the EOIs for the operator to perform as follows: (1) observe the symptoms of an emergency condition, (2) verify the response of automatic systems, (3) stabilize emergency conditions, and (4) initiate recovery actions. These functions occur sequentially.

Defining the present role of the operating crew and critically appraising it will suggest possible improvements in function and structure. Applying a systems approach will help develop a well-defined, optimum crew role by matching human and machine capabilities to the functional requirements of the plant system. A well-defined role will become the basis for developing design requirements and review criteria for potential operational aids. The systems approach will also lead to an improved crew structure with improved response to abnormal and emergency situations (i.e., reduced errors, fast response time, and increased diagnostic capabilities) as well as to normal operating situations and with improved interaction with maintenance activities.

References

1. Oh, C. B. et al., A Characterization of the Nuclear Power Plant Operator's Role, Technology for Energy Corporation, R-80-022 (August 1, 1980).

2. El-Bassioni, A. A., Hedrick, R. A., and Starostecki, R. W., Review of Standards and Requirements Affecting Human Factors in Nuclear Power Plant Control Rooms, Science Applications, Inc., SAI 1-245-08-124-00 (Draft) (September 1980).

3. Sides, W. H. Jr., Oh, C. B., and Knight, P. F., A Survey of Proposed Functional Requirements for a Disturbance Analysis and Surveillance System, ORNL/NUREG/TM-396 (February 1980).

DEFINING THE ROLE OF THE OPERATING CREW

R. A. KISNER G. F. FLANAGAN
OAK RIDGE NATIONAL LABORATORY

Presented At The
Eighth Water Reactor Safety Research Information Meeting
U. S. Nuclear Regulatory Commission
Gaithersburg, Maryland
October 27-31, 1980

OUR PRIME CONCERN IS FOR THE SAFE OPERATION OF THE NUCLEAR POWER PLANT

1. PUBLIC SAFETY
2. ENVIRONMENT PROTECTION
3. PLANT SAFETY
4. SYSTEMS INTEGRITY
5. COMPONENTS AND PARTS INTEGRITY
6. ADHERENCE TO TECH SPEC
7. OPTIMUM OPERATION OR PERFORMANCE

THE SAFETY OF A NUCLEAR POWER PLANT IS DEPENDENT ON THE HARMONIOUS INTERACTION OF MANY ELEMENTS

1. Component reliability
2. Plant design
3. Control system functioning
4. Safety system functioning
5. Maintenance
6. Operation

THE NUCLEAR POWER PLANT OPERATING CREW HAVE THE POTENTIAL OF STABILIZING OR DESTABILIZING PLANT DISTURBANCES, WHETHER EQUIPMENT INDUCED OR CREW INDUCED.

*STABLE → OPERATOR → STABLE
STABLE → OPERATOR → UNSTABLE
*UNSTABLE → OPERATOR → STABLE
UNSTABLE → OPERATOR → UNSTABLE

OUR OBJECTIVE IS TO PROVIDE THE TECHNICAL BASIS FOR DEVELOPING DESIGN REQUIREMENTS, DEVELOPING REVIEW CRITERIA, AND ASSESSING THE INPACT ON SAFETY FOR METHODS TO ENHANCE THE CAPABILITY OF THE REACTOR OPERATING CREW.

1. Operator roles
2. Functional requirement of Operational Aids
3. Safety designs requirements of Operational Aids
4. Develop methods to characterize Operational Aids
5. Monitor and assess the development of DASS

THE PROGRAM WILL DESCRIBE THE ROLE OF THE OPERATOR

1. GUIDED BY SYSTEM CONCEPT
2. USE OF PROCEDURES
3. DEFINE EQUIPMENT INTERACTION
4. INTERFACE WITH OTHER PERSONNEL
5. TRAINING REQUIREMENTS
6. LEGAL RESTRICTIONS
7. DIFFERENCES IN ROLE BETWEEN TYPE OF REACTOR AND OPERATION MODE
8. REGULATIONS, STANDARDS, CODES,...

THE ROLE OF THE OPERATING CREW COULD BE DESCRIBED BY MANY ORGANIZATIONS, EACH WOULD EMPHASIZE A DIFFERENT PERSPECTIVE

1. Trainers (Task)
2. Operators
3. Designers
4. Regulatory (Safety)
5. Research Organizations
6. Utility Management (Power Production)

OBSERVE SYMPTOMS

- MONITOR PHYSICAL SIGNS
- IDENTIFY EMERGENCY EVENT
- CONFIRM EVENT

VERIFY AUTOMATIC RESPONSE

- DEFINE REQUIRED SYSTEMS
- ACTUATE NONFUNCTIONING SYSTEMS
- TERMINATE INAPPROPRIATE RESPONSES

STABILIZE CONDITIONS

- VERIFY & REGULATE EQUIPMENT & SYSTEMS
- IDENTIFY SOURCE OF EMERGENCY EVENT
- RESET SYSTEMS & COMPONENTS

INITIATE RECOVERY ACTIONS

- STABILIZE SYSTEM PROCESS VARIABLES
- RESET & START COMPONENTS OF SECONDARY IMPORTANCE
- SUSTAIN CRUCIAL REACTOR SYSTEMS
- RESOLVE PROBLEM WITH OTHER PERSONNEL

THE OPERATOR'S ROLE
DURING EMERGENCY CONDITIONS

SEVERAL APPROACHES MUST BE TAKEN TO DEFINE THE OPTIMUM ROLE OF THE OPERATOR

SYSTEM REQUIREMENTS

WHAT FUNCTIONS ARE REQUIRED TO ACHIEVE THE OBJECTIVE?

HUMAN CAPABILITY

WHAT ARE THE LIMITATIONS OF THE HUMAN?

WHAT ARE THE EXCELLENCES OF THE HUMAN?

CONSTRAINTS

WHAT ARE THE BOUNDARIES IMPOSED BY EXTERNAL FORCES?

CODES? REGULATIONS?

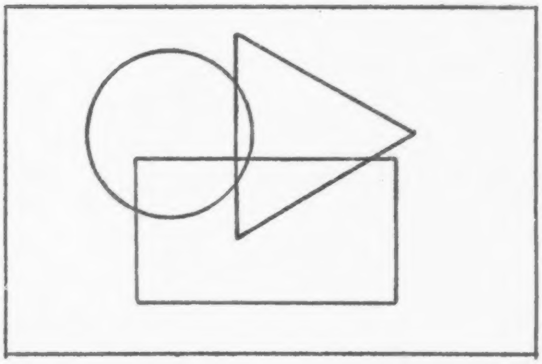

ANY INTERFACE OR INTERACTION POINT WITH THE OPERATING CREW MUST BE IDENTIFIED AND EXPLORED.

1. INSTRUMENT (PHYSICAL DISPLAYS AND CONTROLS)
2. FUNCTIONAL (CHARACTERISTICS OF INSTR, CONTROLS, & PROCESS)
3. MANAGEMENT (OPERATING PHILOSOPHY)
4. MAINTENANCE (PERSONNEL COMMUNICATION)
5. OPERATION (PERSONNEL COMMUNICATION)
6. INSTRUCTIONAL (WRITTEN PROCEDURES)
7. NRC (REGULATING PHILOSOPHY)

THE NUCLEAR PLANT OPERATING CREW INTERFACE IS NOT LIMITED TO THE CONTROL CONSOLE

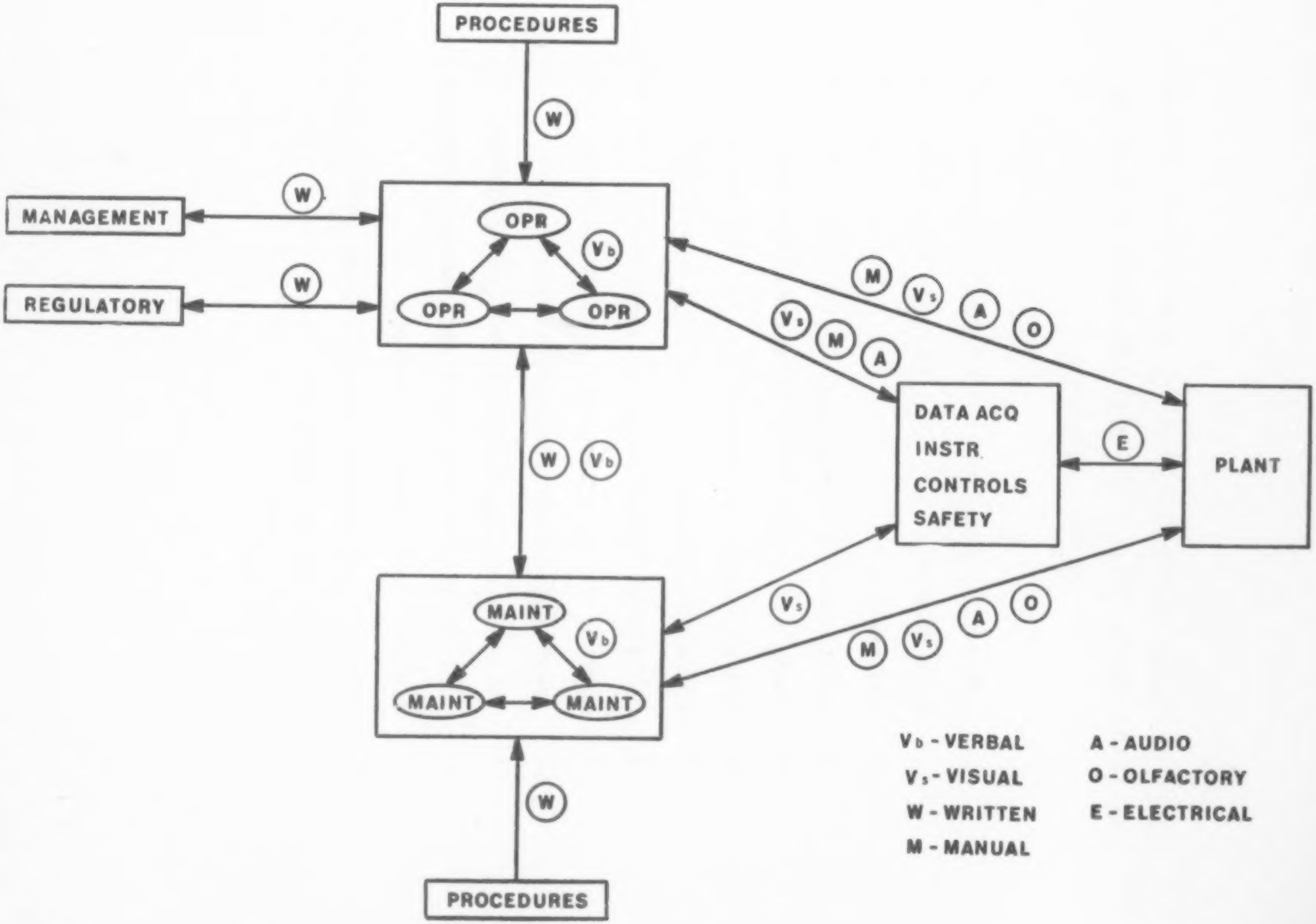
PROCEDURES
W
MANAGEMENT
W
REGULATORY
W
OPR
OPR
OPR
V_b
M
V_s
A
O
V_s
M
A
DATA ACQ
INSTR
CONTROLS
SAFETY
E
PLANT
W
V_b
V_s
M
V_s
A
O
MAINT
MAINT
MAINT
V_b
W
PROCEDURES
V_b - VERBAL
V_s - VISUAL
W - WRITTEN
M - MANUAL
A - AUDIO
O - OLFACTORY
E - ELECTRICAL

THE CHARACTERISTICS OF THE HUMAN CAN OFFER HELPFUL OR HARMFUL SERVICES

1. LOW PREDICTABILITY
2. SLOW RESPONSE
3. LOW PRECISION
4. SINGLE CHANNEL/TASK
5. LARGE BUT OFTEN UNACCESSIBLE MEMORY
6. MEMORY CANNOT BE ERASED
7. INDUCTIVE REASONING
8. PATTERN RECOGNITION
9. COMPLEX VALUE JUDGMENTS
10. IMPROVISING/SELF-PROGRAMMING
11. PROGRAMMING INFLUENCED BY WORK ENVIRONMENT
12. SUSCEPTABLE TO GOAL SHIFT/NOT DEVOTED TO WORK
13. PERFORMS EVEN WHEN OVERLOADED
14. REPAIR OFTEN BEYOND CAPABILITY OF LOCAL FACILITY
15. DOES NOT BECOME OBSOLETE

AUTOMATED SYSTEMS HAVE HELPFUL OR HARMFUL CHARACTERISTICS

1. HIGH PREDICTABILITY
2. FAST RESPONSE
3. ROUTINE, REPETITIVE, & PRECISE
4. HIGH DATA THROUGH PUT
5. MULTITASK
6. LARGE ACCESSIBLE MEMORY
7. ERASABLE MEMORY
8. DEDUCTIVE CAPABILITY
9. SEMI-FIXED PROGRAMMING
10. NOT SUSCEPTIBLE TO GOAL SHIFT/DEVOTED TO WORK
11. NO OVERLOAD CAPABILITY
12. CANNOT OPERATE BEYOND DESIGN SCOPE
13. REPAIR OFTEN PERFORMED LOCALLY
14. PRONE TO OBSOLESCENCE

WE WANT TO FIT THE OPERATIONAL AID TO THE OPERATOR SO THAT THE RESULTING COMBINATION IS MORE EFFECTIVE THAN EITHER ELEMENT TAKEN SEPARATELY

CHARACTERISTIC	OPERATOR	MACHINE
SPEED	SLOW	FAST
WORK NATURE	REQUIRES VARIETY	ROUTINE & REPETITIVE WITH PRECISION
EFFICIENCY	SINGLE CHANNEL/TASK	MULTI CHANNEL/TASK
MEMORY	LARGE MEMORY WHICH REQUIRES ASSISTANCE FOR RECALL	RELATIVELY EASY MEMORY ACCESS
ADAPTABILITY	SELF-PROGRAMMING IMPROVISING PATTERN RECOGNITION COMPLEX VALUE JUDGMENTS	INFLEXIBLE PROGRAMMING (CANNOT OPERATE BEYOND DESIGN SCOPE) DATA REDUCTION FIXED, SPECIFIC ALGORITHM
OVERLOAD CAPACITY	PERFORMS WHEN OVERLOADED BY LOAD SHEDDING	NO OVERLOAD CAPABILITY
RELIABILITY	PRIORITY MAY BE STRESS RELATED	PREDICTABLE

best copy available

UNDER HIGH STRESS, MANY OF THE FEATURES THAT MAKE HUMAN OPERATORS SO EFFECTIVE, CEASE FUNCTIONING

1. Loss of cognitive ability
    - access to process image
    - inductive reasoning
    - inventiveness

2. Inability to sort out seemingly contradictory information

3. Limitation of decision making ability

4. Jumps to preprogrammed task

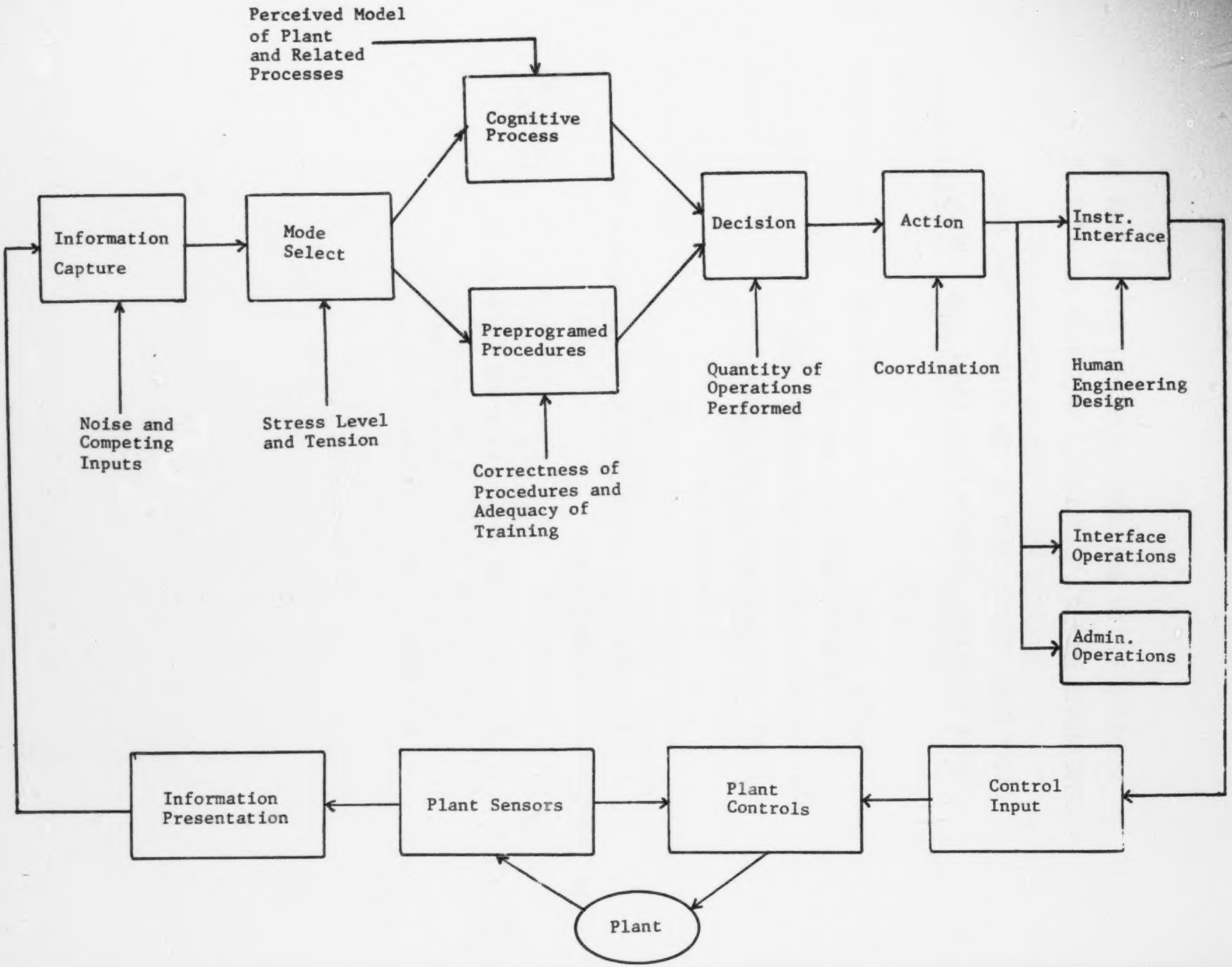
Perceived Model of Plant and Related Processes
Information Capture
Mode Select
Cognitive Process
Preprogramed Procedures
Decision
Action
Instr. Interface
Noise and Competing Inputs
Stress Level and Tension
Correctness of Procedures and Adequacy of Training
Quantity of Operations Performed
Coordination
Human Engineering Design
Interface Operations
Admin. Operations
Information Presentation
Plant Sensors
Plant Controls
Control Input
Plant

GIVEN THAT AN OPTIMUM STRUCTURE AND ROLE CAN BE DESCRIBED FOR THE OPERATING CREW, THEN THE TYPE OF OPERATOR ASSISTANCE NEEDED AND THE METHOD OF INTERACTION WITH THE CREW CAN BE IDENTIFIED

1. Operations Structure
2. Information Flow Requirements
3. Operator Capability
4. Machine Capability
5. Systems Requirements
6. Implementation Constraints

WHAT ARE THE MOST BASIC JOB FUNCTION CATEGORIES THAT THE OPERATING CREW SHOULD PERFORM?

1. ADMINISTRATION
   - o RECORD KEEPING
   - o BUILDING SECURITY
   - o FEEDBACK
   - o PERSONNEL SUPERVISION

2. SYSTEMS SUPERVISION
   - o PROBLEM SOLVING
   - o PROBLEM ANTICIPATING
   - o SYSTEM OPTIMIZING

BASIC JOB FUNCTION CATEGORIES CONT'D:

3. EQUIPMENT SUBSTITUTION
    - FAILED EQUIPMENT
    - OVERLOADED EQUIPMENT
    - DESIGN DEFICIENCY

4. COMMUNICATIONS COORDINATION
    - ONSITE
    - OFFSITE

CREW FUNCTIONS DURING ABNORMAL CONDITIONS

1. Surveillance
2. Detection
3. Analysis
4. Diagnosis
5. Correction (short-term)
6. Restoration (long-term)

THESE ARE THE STEPS OR PROCEDURES THAT THE OPERATING CREW SHOULD PERFORM TO RESPOND TO A PLANT UPSET CONDITION

1. ESTABLISH THAT A DEVIATION HAS OCCURRED
2. ACQUIRE PROCESS AND SUPPORT SYSTEMS INFORMATION
3. VALIDATE THIS INFORMATION
4. IDENTIFY THE STATUS OF THE PLANT

GENERAL SET OF PROCEDURES CONT'D:

5. DETERMINE A PRIMARY COURSE OF ACTION AND CONTINGENCY PLANS
6. BEGIN EXECUTING THE PLAN
7. VALIDATE THE EFFECTIVENESS OF EACH STEP OF THE PLAN
8. ESTABLISH THAT THE DEVIATION HAS BEEN CORRECTED AND THE SYSTEM IS STABLE.

IN A GENERAL SENSE, THE OPTIMUM ROLE OF THE NUCLEAR POWER PLANT OPERATING CREW CAN BE DESCRIBED.

1. THE OPTIMUM ROLE CAN BE FOUND BY MATCHING HUMAN CAPABILITY AND MACHINE CAPABILITY TO THE FUNCTIONAL REQUIREMENTS OF THE PLANT SYSTEM.

2. BY APPLYING THE CONSTRAINTS IMPOSED BY EXTERNAL FORCE, E.G., REGULATORY, ECONOMIC, UNION, ... , A REASONABLE DEFINITION OF THE CREW ROLE CAN BE DEVELOPED.

3. THE OPTIMUM ROLE CAN BE COMPARED WITH THE INTENDED AND ACTUAL ROLES OF THE OPERATING
ING IMPROVEMENTS TO BE
MA SYSTEMS, EQUIPMENT
TRAINING, PROCEDURES, ...

*U.S. GOVERNMENT PRINTING OFFICE : 1980 0-341-742/478

NUCLEAR REGULATORY COMMISSION
EIGHTH WATER REACTOR SAFETY RESEARCH INFORMATION MEETING
October 27-31, 1980

DISTURBANCE ANALYSIS AND SURVEILLANCE SYSTEMS (DASS)
AND
RELATED STUDIES

Presented by

R. M. Kanazawa
Nuclear Safety and Analysis Department

Richard M. Kanazawa October 24, 1980

DISTURBANCE ANALYSIS AND SURVEILLANCE SYSTEMS (DASS) AND RELATED STUDIES

The Electric Power Research Institute has undertaken research in the area of operator aids for nuclear power plants since 1976. The early work focused on improvement on plant availability through better disturbance detection and diagnosis capability tools for use by nuclear plant operators. Subsequent to the TMI-2 accident, increased attention has been given to disturbance analysis and surveillance system research and development, primarily for the improvement of plant safety. Currently EPRI has in a place a program comprised of several research projects, at the center of which is DASS development, which is aimed at improving the performance of the oeprating crew in nuclear power plants. Research goals are to identify operator aids and support systems with proven safety and availability benefits and to facilitate their implementation in operating reactors in the near-term, such that additional benefits (i.e., DASS) can be realized.

As a way to introduce and put into perspective the research results to be described, let us examine the current operational situation for U.S. nuclear power plants. Conventional nuclear plant control and operation is by means of a combination of manual and automatic controls activated in the control room. An operational crew, comprised of shift supervisor, reactor operators and shift technical advisor, operate the plant systems by utilizing information provided to them by means of measured process variable and alarms. Engineered safeguards which are implemented as control logic to actuate trips and control rod system scram occur automatically when key sensed variables are outside of allowable limits. Outside of these minimal automatic operations related to plant shutdown and safety systems, the operating crew is responsible for manually controlling the nuclear power plant systems. This is done by the operator utilizing the information available to him in the control room and making decisions on the actions which he believes to be appropriate to the situation.

While the current operating process (utilization of existing control board information, automatic safety function actuations, manual controls exercised by operating crew) may be successful, the TMI accident has challenged the industry to improve the control of nuclear power plants and further reduce the small probability of control failures and operator errors.

In order to provide insights into possible improvements to nuclear plant control processes, we have examined those factors which effect the performance of the key decision-making element in the control process: the human operator. The major categories in which improvements lie are:

PLANT PROCESSES - The factors affecting operator performance may include: 1) system engineering in terms of degree of controllability or type of behavior possessed by the system; 2) instrumentation systems adequacy in terms of quality and quantity of measured system variables; and 3) system interaction and complexity in terms of operator understanding of system behavior.

INFORMATION - Factors affecting operator decision-making are embodied in the main control room in the form of: 1) control board displays and recorders; 2) alarm annunciator system; and 3) plant process computer.

ANALYSIS - The operator processes information in order to decide upon the action he will take. The decision-making process, while complex, would at the least appear to be affected by the operator's: 1) training; 2) discussions/interactions with others on the operating staff; and 3) operating procedures.

MANAGEMENT - This category includes factors which effect every individual's performance, such as: 1) qualifications of the individual; 2) work conditions or physical environment; and 3) organizational atmosphere.

We now briefly examine some of the near-term requirements faced by the industry relevant to improvement of reactor systems control and operation, keeping in mind the previous discussion of factors which affect nuclear plant operator decision-making.

NUREG 0696 (Emergency Response Facilities) - Requires installation of the following:

- Safety Parameter Display System which is to provide continuous display of key variables required to assess the plant state.
- Technical Support Center which, when activated, provides on-site accommodation of outside technical consultants, utility management and NRC representatives.
- Emergency Operations Facility provides staging area for emergency work crews and facilitates news media briefings.
- Nuclear Data Link provides periodic scan of plant operating data for transmission to NRC.

REGULATORY GUIDE 1.47 (Safety Status Monitoring) - Requires means for determining the status of safety systems such as valve lineups and system component operational condition.

REGULATORY GUIDE 1.97 (Post-Accident Monitoring) - Requires means for measuring and recording plant variables which reflect the state and performance of safety systems and radiological release in post-accident condition.

NUREG 0660 (Action Plan) - Includes various items related to operator training, porcedures, staffing and control room reviews.

From the preceding examination of near-term requirements, it would appear that pieces of the factors involved in operator decision-making are addressed, but that integration of the pieces into an overall problem solution are lacking. Results from EPRI research projects can be presented to show how an integrated approach to the improvement of operator decision-making can be facilitated by a DASS concept.

The following research projects have been completed, or are in progress:

DISTURBANCE ANALYSIS

- Disturbance Analysis System (DAS)
- Disturbance Analysis and Surveillence System (DASS)
- Augmented DASS

RELATED ACTIVITIES

- Safety Functions Concept Evaluation
- Analysis of Operator Decision-Making
- Process Computer Interface Guidelines
- Signal Validation and Sub-System Diagnosis

First, work related to DASS research and development is described briefly and then the various phases of DASS are described. Current work is described to present what we believe to be an integrated approach to improving the decision-making of nuclear plant operators.

DASS-RELATED ACTIVITIES

- Process Computer Interface Guidelines - In conjunction with the Nuclear Power Division, the Nuclear Safety and Analysis Center (NSAC) supported work which documents the technical and administrative issues associated with nuclear plant computer system upgrades. The key guidelines included in the final report are that computer upgrades must be implemented on a plant-specific basis, but that the generic strategy should be evolution to a flexible, distributed processing network which would allow for changing near-term requirements and efficient future expansions, such as implementation of DASS.

- Signal Validation and Sub-System Diagnosis - Work is underway to develop and refine techniques involving analytic redundancy and consistancy checks to verify measurements in the steam generator and feedwater control systems of a nuclear plant. The developed and demonstrated techniques may be applied to other plant systems to provide signal validation and sub-loop diagnostic methodology. The work is directly aimed at establishment of a validated data base upon which DASS functional modules operate.

- Analysis of Operator Decision-Making - Four recent transients at four different nuclear power plants were analyzed in order to assess the potential improvement to operator decision-making from various improvements to training, procedures, staffing, operator aids, and control room enhancements. A descriptive model of decision-making was utilized in a detailed analysis of seventeen key decisions. The preliminary results of the analysis which utilized a panel of experts in human factors, system engineering and plant operations are:

    - All stages of decision-making (alert, data gathering, information processing, procedure selection and performance) can be improved by improving operator's knowledge of plant behavior.

    - Addition of shift technical advisor judged to have beneficial effect on information processing stage

    - Control board control improvements appear to have potential only to improve procedure execution stage.

- Improvements in procedures were judged to be of small help in improving decision-making stages.
- DASS functions judged to provide potential aid to the operator in alert and information processing stages.

- Safety Function Concepts Evaluation - Two concepts based upon important plant function monitoring are being evaluated by means of operator performance measurements in a nuclear plant training simulator. A safety panel comprised of six individual CRT displays of plant variable time histories grouped according to plant functions such as reactivity control, core heat removal, etc., is one concept which is being evaluated with respect to the existing simulator control boards. The other concept is a hierarchical, retroactive, information display system which is also being evaluated with respect to the existing control boards. Both quantitative and qualitative measurements of operator actions are being made to determine the relative benefits of each operator aid. Crews undergoing retraining are currently providing operator performance data with and without an operator aid.

DISTURBANCE ANALYSIS

- Disturbance Analysis System - Results from an early availability-oriented DAS evaluation have been presented by A. B. Long at the Seventh Water Reactor Safety Research Meeting, held last year. A prototype system based upon cause-consequence trees for the feedwater and component cooling water systems to provide disturbance detection identification, correction and prediction was evaluated with operators at a training simulator. The following are the key findings from the operator evaluations:

  Proof of principle and feasibility were demonstrated by the design, assembly and demonstration of a prototype DAS.

  The project experience supported findings from similar projects that engineering and validation of plant-specific models are the most expensive tasks involved in disturbance detection and analysis.

  The operator performance measurements and analysis showed:

a. DAS provided earlier warning of a disturbance than the conventional alarm/annunciator system.
b. The more precise information from the DAS computor resulted in smaller plant deviations from the nominal.
c. The time after disturbance detection until operators initiated control actions was unaffected by DAS.
d. Human engineering and human factors improvements were needed in the DAS CRT displays to allow more effective and correct use by operators.

- Disturbance Analysis and Surveillance System - Identical, parallel efforts supported and managed by EPRI and DOE to define the goals and functions for a plant-wide DASS. Two independent teams were formed comprised of a nuclear reactor vendor, elective utility, architect/engineer and engineering consultant. Babcock & Wilcox, Duke Power, Burns & Roe and General Physics comprised one team and Westinghouse, Commonwealth Edison, Sargeant & Lundy and Systems Control made up the other team. Both teams performed engineering design and cost/benefits studies to determine the scope and feasibility of a DASS and applied the engineering methods and cost/benefits analysis to a single example of a DASS function. A technical advisory group provided project review and guidance for both teams during the parallel but independent studies. The advisory group, constituted of experts from utilities, other reactor vendors, NRC, national labs, NASA and similar domestic and foreign projects, critiqued the final design results of both teams and have issued a summary report containing evaluations, conclusions and recommendations.

  Among the conclusions and recommendations which were made are the following:
  - Only the high priority DASS functions should be included in a modest, first version of DASS for operator evaluation.
    Critical safety and availability functions monitoring
    Disturbance detection
    System status monitoring
    Technical specification monitoring
  - Important to understand and meet the needs of operating crew.
  - DASS must be flexible to allow for plant-specific installation and integration into operating procedures and plant engineering.

  - Reliability and accuracy must be system design requirements in order to facilitate validation and verification process.
  - DASS must be modular in design and implemented to readily allow expansion and changes to be made.

- Augmented DASS - Utilizing the results of the scoping and feasibility studies, EPRI and DOE plan to continue research in DASS by means of operator and engineering evaluations of prototype systems and utilization of both training simulators and selected operating plants. The approach being taken recognizes that DASS must attempt to alleviate problems of human operator decision-making compounded by near-term industry requirements and the diversity of nuclear power plants. Therefore, the project approach has been deisgned to meet three primary needs:
  - an understanding of the operator's role
  - coordination with near-term requirements
  - development of generic design methods

The approach to be taken has the following specific aspects which are designed to meet the above-stated needs:

- Evaluation of prototype systems using operator performance measures
- Build upon cirtical safety function monitoring with disturbance detection and diagnosis functions.
- Demonstrate the phased implementation concept by an augmentation of prototypes using design tools to build plant-specific models

The design framework for DASS functional capabilities utilizes the design results from the scoping and feasibility studies. The framework incorporates safety and availability goals and requirements as the means for a top-down design to prioritize information and the establishment of "target" states in order to detect disturbances. Measurements of plant variables are used to determine the subsystem measured states and to determine the mode of the plant (startup, refueling, power generation, etc.) so that appropriate target states can be calculated by plant models for comparison with measured states. Discrepancies between measured and target states are processed in the hierarchy of priority of disturbance significance according to threats to critical requirements for safety and availability. Within this framework for prioritization of disturbance significance, functions to aid the operator, such as verification of safety control actuations, technical specification monitoring and configuration monitoring can be implemented as additions to the sub-system and component state target versus actual comparisons.

Functions such as input data validation, output display formatting and data archiving, are included in DASS as overhead-type functions.

It is planned to begin evaluation of a modest DASS, built upon critical function monitoring by the end of 1981 and to augment the prototype system with additional functions built from the use of system design tools derived from dynamic systems modeling and probabilistic risk analysis by the end of 1982.

In summary, DASS intends to approach the problem of improving nuclear plant control by focussing on operator decision-making. Firstly, plant processes are to be presented to the operator from a safety-related and availability-related critical requirements perspective thereby improving the operator's understanding of the systems and their dynamic inter-relationships. Secondly, the information from the measured plant process variables is to be processed and refined in order to provide a higher level of information relevant to the safety and availability status of the nuclear plant processes, thereby aiding operator's information processing. Thirdly, DASS will allow the operator to make decisions using disturbance analysis information which is prioritized according to safety and availability goals thereby improving the operator's control actions. In addition, DASS is to incorporate in its development, operator training, plant operating procedures and support of maintenance/engineering operations. The near-term requirements for critical safety function monitoring are to be utilized by DASS in order to begin implementation of an integrated solution to aiding nuclear plant operator decision-making.

CONTROL OF NUCLEAR POWER PLANTS

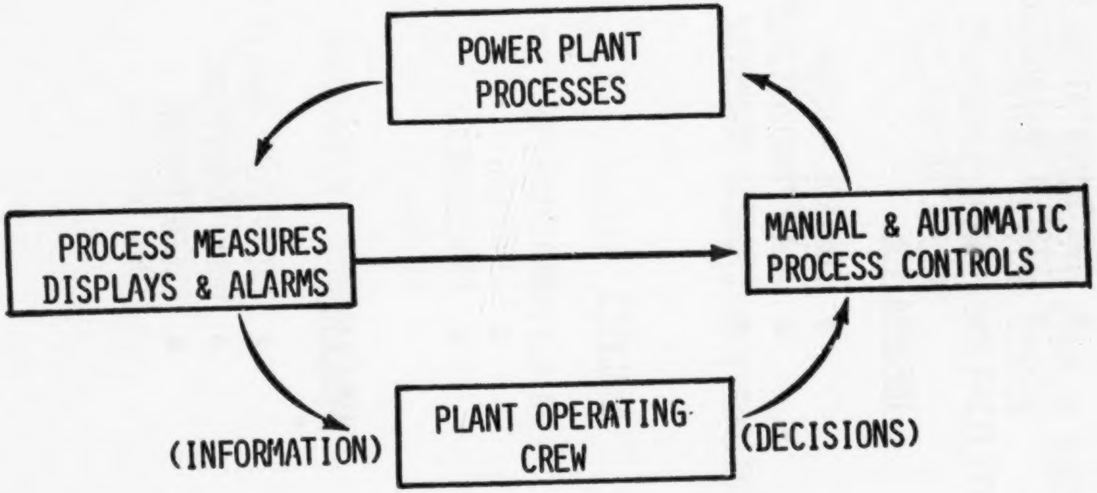
POWER PLANT PROCESSES
PROCESS MEASURES DISPLAYS & ALARMS
MANUAL & AUTOMATIC PROCESS CONTROLS
(INFORMATION)
PLANT OPERATING CREW
(DECISIONS)

FACTORS IN OPERATOR DECISION-MAKING

PLANT PROCESSES

- SYSTEM ENGINEERING
- INSTRUMENTATION SYSTEMS
- SYSTEM INTERACTIONS/COMPLEXITY

INFORMATION

- CONTROL BOARDS
- ALARM/ANNUNCIATOR SYSTEM
- PROCESS COMPUTER

ANALYSIS

- TRAINING
- STAFFING
- PROCEDURES

MANAGEMENT

- INDIVIDUAL QUALIFICATIONS
- WORK CONDITIONS
- ORGANIZATION

ABL/HT 10/80

NEAR-TERM REQUIREMENTS

NUREG 0696 (1/82)

- SAFETY PARAMETER DISPLAY SYSTEM
- TECHNICAL SUPPORT CENTER
- EMERGENCY OPERATIONS FACILITY
- NUCLEAR DATA LINK

REG. GUIDE 1.47 (1/82)

- SAFETY SYSTEMS STATUS MONITORING

REG. GUIDE 1.97 (6/82)

- POST-ACCIDENT MONITORING

NUREG 0660 (VARIES)

- REQUIREMENTS RELATED TO:
  - STAFFING
  - TRAINING
  - PROCEDURES
  - CONTROL ROOM

ABL/HT 10/80

DISTURBANCE ANALYSIS

PHASE I (1976 - 1979)

- DISTURBANCE ANALYSIS SYSTEM (DAS)
  - LIMITED SCOPE
  - SIMULATOR EVALUATION

PHASE II (1979 - 1981)

- DISTURBANCE ANALYSIS & SURVEILLANCE SYSTEM (DASS)
  - SCOPING AND FEASIBILITY
  - PARALLEL PROJECTS FUNDED BY DOE & EPRI

PHASE III (1981)

- DASS -- STAGE ONE
  - MODEST SCOPE
  - CONVENTIONAL ENGINEERING
- DASS -- STAGE TWO
  - AUGMENTED SCOPE
  - IMPROVED ENGINEERING

ABL/HT 10/80

RELATED WORK

SAFETY FUNCTION MONITORING

- SAFETY FUNCTION MONITORING CONCEPTS- PANEL/CONSOLE
- OPERATOR PERFORMANCE MEASUREMENT

ANALYSIS OF OPERATOR DECISION-MAKING

- TIME LINE ANALYSES OF FOUR RECENT EVENTS
- EXPERTS' JUDGING OF POTENTIAL IMPROVEMENTS

PROCESS COMPUTER INTERFACE GUIDELINES

- HARDWARE & SOFTWARE REQUIREMENTS
- ADDITION/EXPANSION ISSUES

SIGNAL VALIDATION AND SUB-SYSTEM DIAGNOSTICS

- EXISTING INSTRUMENTATION
- REDUNDANCY AND CONSISTENCY CALCULATIONS

SAFETY FUNCTION MONITORING EVALUATION

OBJECTIVE: EVALUATE OPERATOR PERFORMANCE WITH DIFFERENT SFM CONCEPTS DURING SIMULATED PLANT DISTURBANCES

CONCEPTS:

1. EXISTING CONTROL BOARDS
2. SAFETY PANEL
3. SAFETY CONSOLE

- EVALUATIONS RELATIVE TO EXISTING CONTROL BOARDS
- REQUIRES DEVELOPMENT OF APPROPRIATE TRAINING AND PROCEDURES IN USE OF CONCEPTS
- OPERATOR PERFORMANCE MEASUREMENTS NEEDED FOR EVALUATION OF OPERATOR AIDS (DASS)

DESCRIPTION OF TEST:

- DESIGN AND BUILD CONCEPTS
- PERFORM HUMAN FACTORS REVIEWS
- INSTALL AND CHECK IN TRAINING SIMULATOR
- EVALUATIONS INVOLVE:

  8 OPERATOR CREWS
  9 TRANSIENTS/CREW/EXISTING CONTROL BOARDS
  9 TRANSIENTS/CREW/SAFETY PANEL OR CONSOLE

- PRELIMINARY RESULTS BY 12/31/80

ABL/HT 10/80

DISTINGUISHING FEATURES

	SAFETY PANEL	SAFETY CONSOLE
GOAL:	VERIFY STATUS OF IMPORTANT SAFETY FUNCTIONS	DETECT AND MITIGATE THREATS TO SAFETY FUNCTIONS
SCOPE:	20 VARIABLES	200-300 VARIABLES
USAGE:	SECONDARY TO EXISTING CONTROL BOARDS, POST-DECISION. CONFIRMATION/ VERIFICATION	SUPERVISORY OVERVIEW OF PLANT. DIAGNOSTIC AID FOR DECISIONS.
FUNCTION:	NON-INTERACTIVE. SINGLE LEVEL TREND INFORMATION	HIERARCHICAL, INTERACTIVE INFORMATION SYSTEM WITH ALARM CAPABILITY.

ABL/HT 10/80

OPERATOR DECISION ANALYSIS

OBJECTIVE: DEVELOP DESCRIPTIVE MODEL CHARACTERIZING FACTORS INFLUENCING OPERATOR DECISION MAKING

- PRIORITIZE MODIFICATIONS
- INTERPRET SIMULATOR EVALUATIONS
- DIRECT FURTHER R&D ACTIVITIES

METHOD: DETAILED ANALYSIS & OPERATOR INTERVIEWS

FOUR RECENT INCIDENTS:

1) OYSTER CREEK (5/79) ----LOSS OF RECIRC. FLOW
2) NORTH ANNA (9/79) ------EXCESSIVE COOLDOWN & VCT OVERFLOW
3) PRAIRIE ISLAND (10/79) -STEAM GENERATOR TUBE RUPTURE
4) OCONEE (11/79) ---------LOSS OF ICS POWER & EXCESSIVE COOLDOWN

IDENTIFICATION & CRITIQUE OF KEY DECISIONS

JUDGES' REVIEW OF CANDIDATE IMPROVEMENTS

CANDIDATE IMPROVEMENTS TO DECISION ANALYSIS

AVAILABILITY OF ADDITIONAL PERSONNEL
STAFFING - PRIOR DEFINITION OF OPERATOR RESPONSIBILITIES
ADDITION OF SHIFT TECHNICAL ADVISOR

SKILL TRAINING
UNDERSTANDING OF STANDARD AND EMERGENCY PROCEDURES
TRAINING - KNOWLEDGE OF SPECIFIC PLANT CHARACTERISTICS
KNOWLEDGE OF POWER PLANT FUNDAMENTALS
TRAINING IN DECISION SKILLS

MONITORING BASIC SAFETY AND AVAILABILITY FUNCTIONS
DISTURBANCE DETECTION AND CLASSIFICATION
DASS - INFORMATION INTEGRATION
ACTION IDENTIFICATION
PREDICTIVE SIMULATION

PROCEDURES - PROCEDURE ACCESSIBILITY AND ACCURACY

DISPLAY IMPROVEMENT
CONTROL BOARD - CONTROL IMPROVEMENT
CONTROL/DISPLAY INTEGRATION
WORKSPACE LAYOUT

STAGES OF DECISION-MAKING

INFORMATION	- ACTIVATION/DETECTION OBSERVATION/DATA COLLECTION
ANALYSIS	- IDENTIFICATION INTERPRETATION EVALUATION
ACTION	- TASK DEFINITION PROCEDURE FORMULATION PROCEDURE EXECUTION

PRELIMINARY RESULTS OF DECISION ANALYSIS

- OPERATOR'S KNOWLEDGE OF PLANT BEHAVIOR APPEARS TO HAVE BROAD POTENTIAL TO IMPROVE DECISION, I.E., AFFECTS ALL STAGES OF DECISION-MAKING.

- ADDITION OF SHIFT TECHNICAL ADVISOR JUDGED TO HAVE BENEFICIAL IMPACT IN INFORMATION INTEGRATION PHASE OF DECISION-MAKING.

- CONTROL-BOARD IMPROVEMENTS ONLY APPEAR TO HAVE BENEFITS IN IMPROVING PROCEDURE EXECUTION STAGE.

- PROCEDURES IMPROVEMENTS WERE JUDGED TO BE OF SMALL HELP IN DECISION IMPROVEMENTS.

- DASS JUDGED TO PROVIDE PRIMARY BENEFITS TO OPERATOR IN ALERT AND INFORMATION ANALYSIS STAGES.

PHASE I - DAS (NP-1379)

DESCRIPTION

- AVAILABILITY - ORIENTED PROTOTYPE SYSTEM (DISTURBANCE DETECTION, IDENTIFICATION, CORRECTION. PREDICTION)
- PRE-ANALYZED CAUSE-CONSEQUENCE PATTERNS FOR FEEDWATER & COMPONENT COOLING WATER SYSTEMS
- EVALUATED WITH OPERATORS AT TRAINING SIMULATOR

RESULTS

- PROOF OF FEASIBILITY OF CONCEPT
- ENGINEERING AND VALIDATION OF PLANT-SPECIFIC MODELS MOST EXPENSIVE TASK
- OPERATOR PERFORMANCE MEASUREMENTS SHOWED:
    1. DAS PROVIDED EARLIER DISTURBANCE ALARM THAN CONVENTIONAL ALARM
    2. MORE PRECISE INFORMATION RESULTED IN SMALLER PLANT DEVIATION FROM NOMINAL
    3. TIME AFTER DETECTION UNTIL OPERATOR CONTROL ACTION INITIATED UNAFFECTED BY DAS
    4. IMPROVEMENTS NEEDED IN DAS FOR MORE EFFECTIVE USE BY OPERATORS

PHASE II - DASS

- IDENTICAL, INDEPENDENT SCOPING AND FEASIBILITY STUDIES
  - TEAMS

    BABCOCK & WILCOX
    DUKE POWER
    BURNS & ROE
    GENERAL PHYSICS
    WESTINGHOUSE
    COMMONWEALTH EDISON
    SARGEANT & LUNDY
    SYSTEMS CONTROL
  - DEFINE GOALS AND FUNCTIONS FOR PLANT-WIDE DASS
  - PROVIDE EXAMPLE APPLICATION OF ENGINEERING METHODS AND COST/BENEFITS ANALYSIS

- TECHNICAL ADVISORY GROUP (TAG)
  - EXPERTS FROM UTILITIES, VENDORS, NRC, NATIONAL LABS, LOFT, NASA, CANDU, HALDEN, EPRI, DOE
  - PROVIDE REVIEW AND GUIDANCE TO BOTH STUDIES
  - ENDORSEMENT OF CONTINUED RESEARCH BY MEANS OF EVALUATIONS, CONCLUSIONS, RECOMMENDATIONS

- REPORTS:
  DOE - PROJECT 42-6770
  EPRI - PROJECT NP-891-3
  TAG - SUMMARY AND EVALUATION REPORT

PHASE III - DASS

PROBLEM:

- HUMAN OPERATOR
- INDUSTRY PRESSURE
- DIVERSITY OF NUCLEAR PLANTS

NEEDS:

- UNDERSTAND OPERATOR ROLE
- RESPONSIVENESS
- GENERIC SOLUTION

APPROACH:

- BUILD UPON CRITICAL SAFETY FUNCTION
  - MONITORING:
    - TECHNICAL SPECIFICATION MONITORING
    - SYSTEM STATUS MONITORING
    - DISTURBANCE DETECTION
    - VERIFY CONTROL AND SAFETY ACTIONS
- EVALUATE PROTOTYPE DASS USING SIMULATOR, OPERATING PLANT
- ESTABLISH STANDARD FRAMEWORK AND INTERFACES FOR PHASED IMPLEMENTATION
- CREATE PLANT DATA BASE AND DEVELOP ENGINEERING DESIGN TOOLS TO FACILITATE RAPID VALIDATION & VERIFICATION OF PLANT SPECIFIC MODELS

DASS FUNCTIONAL/CONCEPTUAL DESIGN

DEFENSE IN DEPTH

PREVENT	OPERATOR ACTIONS WHICH COULD INITIATE A DISTURBANCE
TERMINATE	PLANT DISTURBANCES CAUSED BY OPERATOR ACTION & EQUIPMENT FAILURE
MITIGATE	THE CONSEQUENCES OF UNSAFE CONDITIONS

GOALS

AVAILABILITY: IMPROVE PLANT CAPACITY FACTORS	SAFETY: MAINTAIN BARRIERS TO RADIOACTIVE RELEASE

PROCESS MEASUREMENTS

CRITICAL AVAILABILITY REQUIREMENTS	CRITICAL SAFETY REQUIREMENTS

FUNCTIONAL REQUIREMENTS

CAPABILITIES WHICH ENSURE MEETING CRITICAL REQUIREMENTS

SYSTEM REQUIREMENTS

SYSTEMS DESIGNED TO PRESERVE REQUIRED FUNCTIONAL CAPABILITIES
SUPPORT SYSTEMS/SUB-SYSTEMS NECESSARY FOR VITAL SYSTEMS

ABL/HT 10-80

PLANT SUBSYSTEMS

1. REACTOR
2. PRESSURIZER
3. REACTOR COOLANT SYSTEM
4. MU/LD. PURIFICATION
5. CHEM. ADD. AND SAMPLING
6. DECAY HEAT REMOVAL
7. ECCS
8. STEAM SUPPLY
9. TURBINE/GENERATOR
10. CONDENSER
11. FEEDWATER TRAIN
12. AUXILIARY FEEDWATER SYS.
13. COMPONENT COOLING
14. RECIRC. COOLING WATER
15. AUXILIARY SERVICE WATER
16. LP SERVICE WATER
17. COOLANT STORAGE
18. COOLANT TREATMENT
19. ELECTRIC PWR DIST.
20. CONTROL AREA VENTILATION
21. AUX. BUILDING VENTILATION
22. REACTOR BUILDING COOLING
23. EXTERNAL ENVIRONMENT

PLANT STATE ELEMENTS

- SUBSYSTEM FUNCTIONS
  1. ENERGY GEN/TRANSFER
  2. TRANSPORT
  3. STORAGE
  4. CONTROL
     - TEMPERATURE
     - PRESSURE
     - LEVEL
     - REACTIVITY
     - CHEMISTRY
     - PARTICULATES
     - MASS

- SUBSYSTEM PHYSICAL STATES
  5. FLUID STATE
  6. FLUID INVENTORY
  7. CONFIGURATION
  8. INTEGRITY
  9. STABILITY
  10. CHEMICAL STATE
  11. RADIOACTIVITY LEVEL

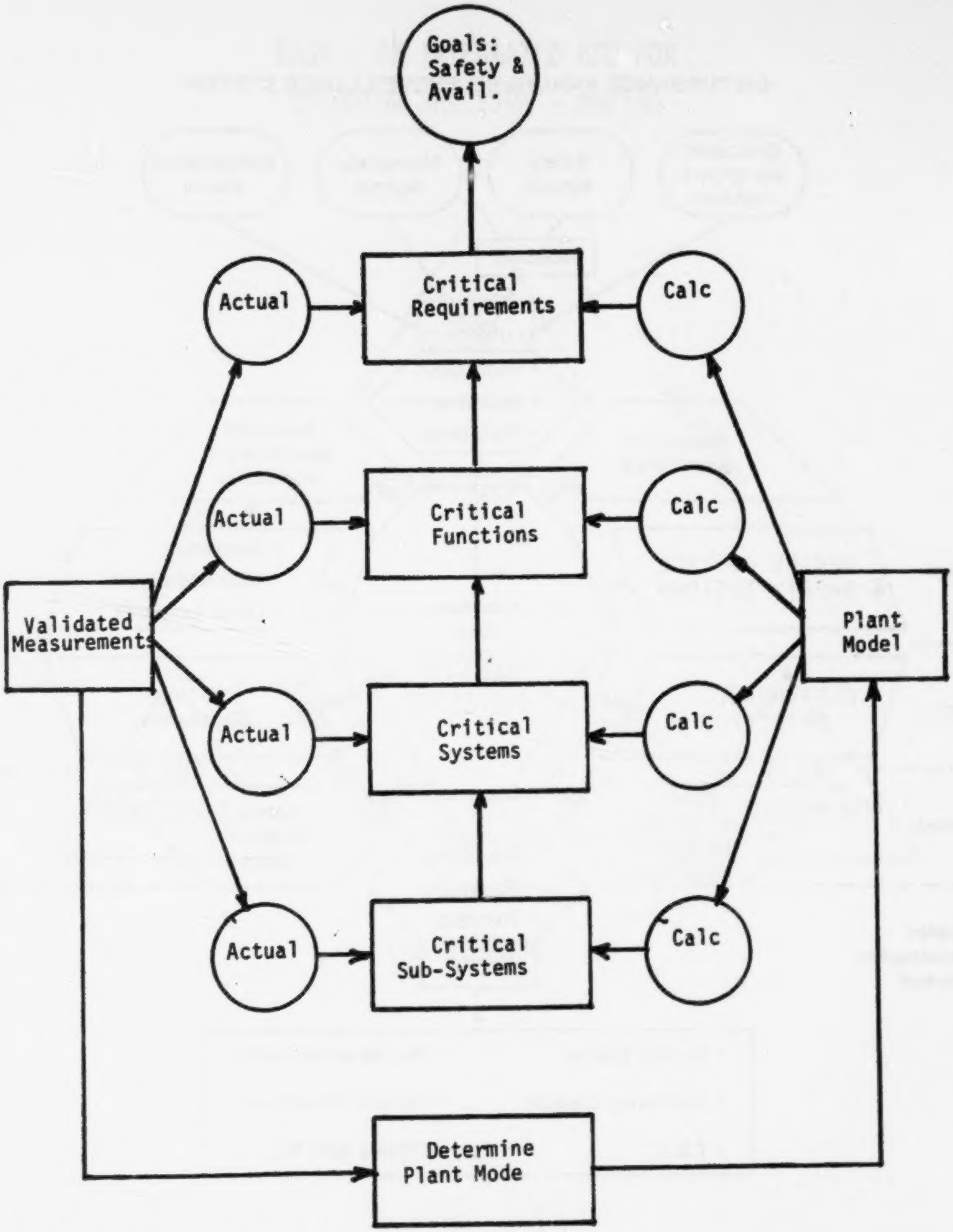
Goals: Safety & Avail.
Actual
Critical Requirements
Calc
Actual
Critical Functions
Calc
Validated Measurements
Plant Model
Actual
Critical Systems
Calc
Actual
Critical Sub-Systems
Calc
Determine Plant Mode

DISTURBANCE ANALYSIS & SURVEILLANCE SYSTEM

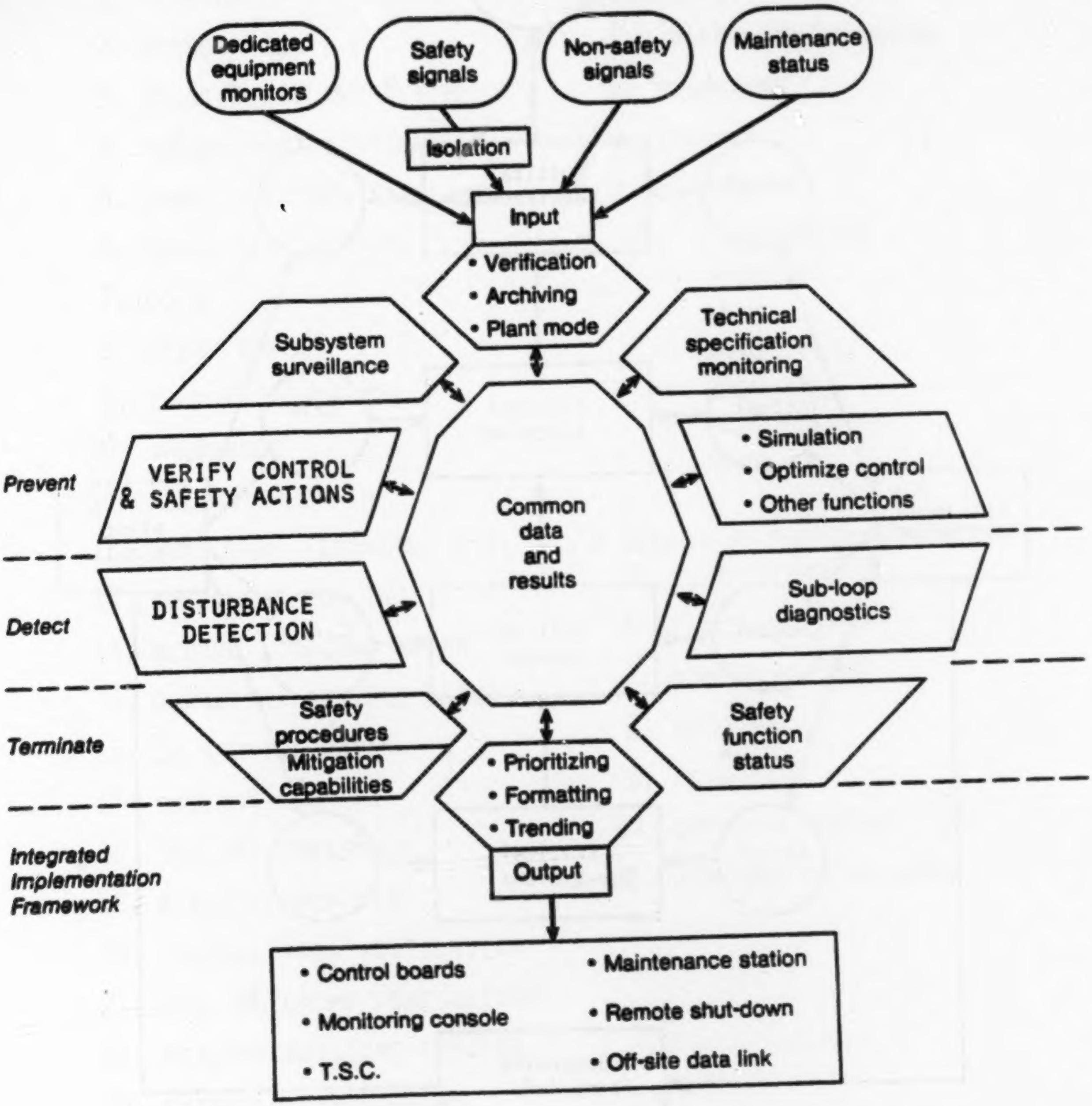
Dedicated equipment monitors
Safety signals
Non-safety signals
Maintenance status
Isolation
Input
• Verification
• Archiving
• Plant mode
Subsystem surveillance
Technical specification monitoring
Prevent
VERIFY CONTROL & SAFETY ACTIONS
• Simulation
• Optimize control
• Other functions
Common data and results
Detect
DISTURBANCE DETECTION
Sub-loop diagnostics
Terminate
Safety procedures
Mitigation capabilities
Safety function status
• Prioritizing
• Formatting
• Trending
Integrated Implementation Framework
Output
• Control boards
• Monitoring console
• T.S.C.
• Maintenance station
• Remote shut-down
• Off-site data link

DASS - AN INTEGRATED AID FOR OPERATOR DECISION - MAKING

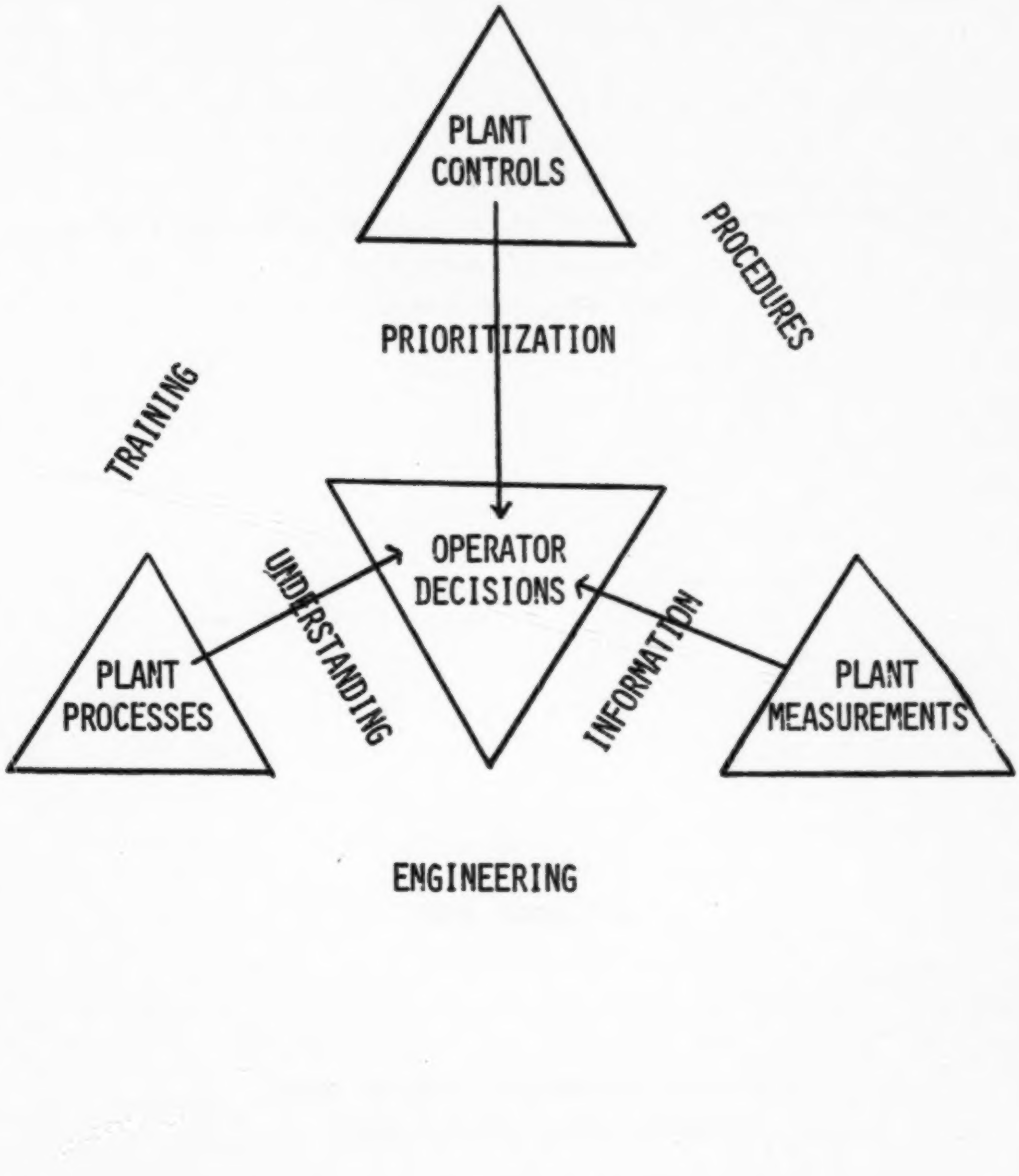
PLANT CONTROLS
PROCEDURES
PRIORITIZATION
TRAINING
OPERATOR DECISIONS
UNDERSTANDING
INFORMATION
PLANT PROCESSES
PLANT MEASUREMENTS
ENGINEERING

RK/AD 10/24/80

ADVANCED DISPLAY AND DIAGNOSTICS AT LOFT

Presented at
The Eighth Water Reactor Safety Research Information Meeting
October 27-31, 1980
Gaithersburg, Maryland

O. R. Meyer
EG&G Idaho, Inc.

Idaho National Engineering Laboratory
Idaho Falls, Idaho 83415

ADVANCED DISPLAY AND DIAGNOSTICS AT LOFT

O. R. Meyer
EG&G Idaho, Inc.

The behavior of light water reactors (LWR's) under steady state, transient, and accident conditions has been analyzed extensively. The behavior is comparatively well defined in engineering documentation, for example, the final Safety Analysis Reports (FSAR's) and their referenced reports. However, this large amount of documented information is of little use to the LWR operator in the main control room (MCR) because of the outdated state of the MCR man-machine interface.

The dominant feature of the man-machine interface in the LWR MCR is the direct display of a large number of readings (∿2000) of individual plant instruments and component position detectors. Relating these readings during a transient to the predicted behavior as documented in technical curves, charts, and equations is manifestly impractical. Instead, the basic principle of LWR operation is to recognize patterns of instrument and alarm readings and to respond by following preset rules for action. This is an acceptable, recognized principle in human engineering but it has serious limitations. First, there are a virtually unlimited number of sets of instrument and alarm readings. For each set, specific definitions need to be developed and rules for operator action determined, followed by training to imprint the definition and rule on the operator. The current activities in developing more extensive, plant specific simulations, and more intensive training programs are related to this limitation.

Secondly, and more importantly, the preset-rule principle of operation makes little use of the operator's education and training to recognize the functional state of the plant and determine the appropriate action.

The documented technical information on plant behavior, discussed above, is in the form of the functional state of the plant. Further, the number of sets of functional states of the plant is much less than the number of sets of individual instrument and alarm readings. A higher principle of operation could be applied to LWR MCR's if the actual functional state of the plant could be related to the existing analytical predictions of behavior and this relation displayed to the operators.

The current state-of-the-art computer technology permits this functional relationship to be displayed. A developmental model of an Operational Diagnostics and Display System (ODDS) was installed in the LOFT MCR to explore the potentials of an intelligent man-machine interface and to help define the research and development needed to transfer this concept to the MCR's of licensed LWR's. This ODDS system consists of a computer which receives instrument data from the LOFT data acquisition computers (which are analogous to LWR process computers). The ODDS computer can exercise computational programs and display results rapidly enough to be of direct use to the reactor operator, that is, "real time" or "on-line" computation. A set of color-graphic cathode ray tube terminals was chosen for displaying the computer output. A key board for reactor operator input is provided and more flexible input techniques are being studied; touch panel, voice input, and light pen.

The ODDS is capable of exploring what is termed "advanced diagnostic graphics." Advanced diagnostic graphics are being developed by

1. Selecting a graphic format that relates real time plant behavior to predicted, analyzed behavior, and defines safety-related limits of operation

2. Constructing a graphics display program which is consistent with the principles of human engineering and information science

3. Developing an interactive program between the computer and the reactor operator that allows the operator to make the final diagnosis and decision.

The following types of diagnostic graphics were defined to initiate this development and are operational for trial use and evaluation:

1. Process Schematics (minic diagrams). These are the predominate graphics in the LWR advanced control rooms. These consist of individual instrument readings arranged in a pattern based on fluid flow and heat transfer.

2. Operating Maps. This type of graphics exists in plant operating manuals as a means of defining allowable, multidimensional regions of operation. Considerable experience in naval and aerospace applications demonstrates their usefulness.

3. Event (Accident) Signatures. Related research programs, for example, Plant Status Monitoring, are defining the plant states that define a specific type of event or accident.

4. Trends. Strip chart recorders are well known, but these computer graphics versions are not restricted to X-Y coordinates and permit other features, for example, selectable sets of parameters, adjustable time window, and predicted future conditions.

5. Procedural Tools. This is merely a name for another family of computer graphics, that is open-ended, itself. Response trees and system coolant inventory are examples.

A study of the basic scientific methods of graphing the LWR safety state is reported separately.[1] Five of the types of graphics that may be applicable for a safety state vector display or a top-level safety parameter display are

1. Deviation Bar
2. Fourfold Circular Display
3. Linear Profile
4. Circular Profile
5. Chernov Face.

REFERENCE

1. Techniques for Displaying Multivariate Data on Cathode Ray Tubes with Applications to Nuclear Process Control, Dr. Michael M. Damchak, Hartford Graduate Institute, (to be published by EG&G Idaho, Inc.).

EIGHTH WATER REACTOR SAFETY RESEARCH INFORMATION MEETING
October 27-31, 1980
Gaithersburg, Maryland

CURRENT PERSPECTIVES IN SAFETY R&D

by

Walter B. Loewenstein

and

Achilles G. Adamantiades

ELECTRIC POWER RESEARCH INSTITUTE
Nuclear Safety & Analysis Department

ELECTRIC POWER RESEARCH INSTITUTE

Current Perspectives in Nuclear Safety R&D

General

In planning and executing a national, goal-oriented nuclear safety R&D program, a number of principles must be observed (Slide 1). First, proper balance must be maintained between short-term and long-term goals. Present and immediate needs must not detract from the pursuit of long-term objectives. At the same time the steadiness of purpose must be tempered with a necessary degree of flexibility and adaptability to the everchanging requirements and problems in nuclear power development. This necessary flexibility not only assures the capability of prompt responses to emerging needs but also allows for the recognition of past errors and for the redirection and reorganization of efforts in an environment of limited resources. A third important guideline is to recognize the need to keep the necessary coordination and perspective among the various parts of a multifaceted and highly interdisciplinary work in order to ensure maximum benefit from the overall effort and to concentrate the attack on the points of highest importance.

In the light of events of the past two years a significant reevaluation of emphasis and direction has taken place. Many of the ideas and concepts that are now attracting attention have been propounded for quite some time but the events of the last two years have raised our conscious level vis-a-vis their significance. Such ideas are, (Slide 2) among others, the importance of analyzing small break accidents, the potential of natural circulation as an adequate cooling mode, the prediction of plant transient behavior under a wide range of parameters, the analysis of certain degraded core and plant scenaria, the realistic assessment of radioactivity releases and transport under accident conditions, the need for analytic and experimental assessment of structural integrity, the conversion of probablistic risk assessment into a useful tool of reactor design and operation, etc.

Considerable efforts are also expended at EPRI in areas of materials and systems behavior, as well as in operational and engineering aspects of nuclear plants. Such efforts, with direct bearing on safety, are the integrity of the pressure boundary, human factors, radiation control, etc. A companion paper in this session presents the status of the intergranular stress corrosion cracking research program for BWRs.

The EPRI nuclear safety research program, while striving for continuity and consistency of effort, incorporates these concerns and affords an integral gleaning of current perspectives in nuclear safety. Examples from the EPRI safety program will be presented in the following to illustrate these basic themes that demonstrate the effort and to outline advances made in the past year in several important areas.

Emphasis on Operational and Plant Data

The gradual accumulation of operational experience(1) has given new insights into the problems of nuclear plants and has influenced the impetus of research and development work. Consequently the performance of tests and measurements at operating plants has been emphasized. These investigations provide:

(1) an improved understanding of the behavior of the system as a whole made up of interacting parts, (2) a means of testing and qualifying the computer codes, and (3) a narrower range of the parameters that need to be investigated analytically and experimentally.

Three examples will be mentioned here: first, the extensive gamma-scans and special TIP detector measurements, performed in both PWRs and BWRs for measuring power distributions, have provided two most complete and accurate set of benchmarks for qualification of core calculational methods(2). Slide 3 shows a cross section of the Hatch 1 core, the TIP locations and the 106 bundles on which gamma-scans were performed, including a complete core octant and six additional four-bundle cells chosen to reveal any power asymmetries. The insert in the figure shows a comparison between measurement and calculation performed with the code SIMULATE, which is now ancillary of the Advanced Recycle Methodology Program. The ARMP package, comprising a set of about 20 codes and being continuously expanded, has been extentively tested and qualified with the data from the gamma-scan measurements.

The SIMULATE code results are, generally, in good agreement with the gamma-scan measurements. In cases of deeply inserted control blades, however, the code tends to overpredict the power peak. Comparisons were also made between code predictions and axial power distributions derived from the process computer (either P-I or BUCLE) at selected intermediate points of the cycle. Since the process computer distributions have been shown to be quite accurate(3) these comparisons provide a good test of the predictive capabilities of the code SIMULATE. The qualification process has helped define with confidence the uncertainties in the calculations and has allowed possible reduction in the operating margins, thereby increasing the safety and the productivity of the plant.

A second example of plant test data is the transient and stability test performed at the Peach Bottom-2(4). Three turbine trip tests, from varying power levels and coolant flows, were performed with extensive measurement of plant parameters taken with both regular and special instrumentation. Analysis of the plant transient response with the RETRAN code gave new and valuable insights in plant behavior and in the sensitivity of various important variables (such as vessel dome pressure) on a number of plant parameters and component behavior. The interaction between neutronic calculations and thermohydraulic analysis were highlighted.

These BWR turbine trips and their analysis provide a particularly stringent test of any system dynamic code because of: strong coupling between pressure, core void and reactivity; dominance of acoustic phenomena during the early part of the transient; and the significance of the later transient stages when pressure begins to drop.

The Peach Bottom-2 plant investigations also included a series of stability test performed by means of pressure perturbation at low core flow rates as shown in Slides 4 and 5. It was demonstrated (a) that this technique can provide data superior to those obtained with the rod oscillator technique with minimal disturbance to plant operation; (b) that there is considerable stability margin designed into a large BWR, with decay ratios estimated between 0.12 and 0.35; (c) that safe opertion can be obtained at low flow conditions above the rated power/flow rod line. This latter demonstration can yield increased operational flexibility and allow a reduction in the number of precondition ramps on the ascent to full power. It is also possible to realize considerable fuel cycle economic gain by allowing operation at full power but less than full flow since this condition hardens the spectrum and causes higher plutonium production.

These stability tests along with data from overseas as reactors (Barsebäck 2, in Sweden and TVO-1, in Finland), will be used in the qualification of a BWR stability code which is currently being developed under EPRI sponsorship for utility use. This code with several others are intended for incorporation in the reload safety analysis methodology package being assembled by EPRI.

The extensive code verification and validation work by use of plant data will culminate with the assembly of this integrated and qualified package for use by the electric utility industry. A general view of the various codes or code groups and their interrelationships is shown in Slide 6. The activity aims at a calculational tool applicable to both conservative, licensing procedures and best estimate predictions with minimum variation in computer code models. As shown in Slide 7 the purpose of this package, scheduled for completion in mid-1983, is to provide the utility industry with an independent, verified and qualified calculational capability for both licensing and operational flexibility and optimization.

In the structural area, significant experience will be gained through the dynamic testing and analysis program on a piping system of the Indian Point-1 plant(5). The first phase of this program, already completed, consisted of dynamic testing of an as-built, lightly supported 8-in diameter pipeline. Both snapback and forced harmonic vibration were used to excite the piping system. Subsequent phases will include testing and analysis of the same pipeline without insulation, with modern seismic constraints (mechanical and hydraulic snubbers) and under high-level excitation (with strong nonlinear response). The test results will have two importnt functions: (a) to assess the accuracy of alternative analytical methods and possibly lead to improved and more realistic models of piping systems subjected to seismic, hydraulic, operating and other dynamic loads; (b) to demonstrate that damping values permitted by current regulations entail significant conservatisms. It is also possible that new guidelines can be established for development and use of simplified piping designs.

The Importance of Scaled Tests

Data from operating plants go hand-in-hand with results from properly scaled tests. These latter tests provide useful data where gaps exist in information from operating plants due to various reasons, e.g., inadequate data collection systems. Also, they can extend the range of parameters to accident limits which operating plants are not allowed to approach. The following examples can be cited (Slide 8): A number of natural circulation tests have been and will be performed at operating LWR plants. Since a number of limitations exist in the performance of these tests, scale model experiments are essential in supplementing the operational data. A 4-loop natural circulation model has been constructed, under EPRI sponsorship at the Stanford Research Institute to simulate the Trojan PWR 4-loop plant. The 2-loop reflux boiling facility simulates an actual 2-loop Combustion Engineering System 80 plant. The experimental results have been compared with analytical models. A model of the TMI-2 primary system has been used to show that natural circulation was effective for a range of core resistances, primary water inventories and secondary flow rates(6). Experiments with non-condensible gases (helium and nitrogen) injected in the primary system demonstrated the stability of reflux boiling even with non-condensible gases present.

Thermal-hydraulics models in conjunction with scaled and full-size test data can supplement the existing guidelines and provide an improved basis for operational decisions. Such an analysis of core uncovering and phase separation was performed and compared with single tube, rod bundle and TMI-2 accident available data(7). The agreement between theory and experiments is encouraging. Experiments on level indicators were carried out (jointly with NRC/GE) with TLTA for small-break transients. New work in level indicators for PWRs is underway with utility support and involvement.

Transients on the secondary side, including loss-of-feedwater and steamline break, have been studied with a full-scale model of a U-tube steam generator. Finally, the coolability of a degraded reactor core, resulting from a severe reactor accident, was investigated through a scale model with spaced rubble beds.

In the light of recent experience, primarily stemming from the events at TMI-2, the importance of a variety of properly designed and operated and accurately interpreted scaled-model experiments cannot be overemphasized.

Large Scale Demonstrations

In several cases, where small-scale tests are insufficient because of uncertainties in scaling laws and procedures, or where plant tests are impractical, large or full scale tests under controlled conditions are necessary.

Extentive missile testing has been conducted with the rocket sled facility at Sandia Laboratories over a number of years. After the tornado missile tests, on which reports were presented last year, a series of impact test with turbine missiles have been conducted. A companion paper in this session will elaborate on technical details of these tests. Suffice it to mention here the following two outcomes: (a) the turbine missile tests impinging, under various conditions, on turbine casings have demonstrated that a large amount of the missile energy (65-100%) is absorbed by the casing in the breakthrough process thus reducing considerably the threat of the missile to containment; and (b) a series of tests featuring actual-size turbine fragments impinging on full-thickness, reinforced-concrete wall segments have shown the capacity of the latter to withstand the impact without loss of containment function even under severe overspeed conditions. Empirical formulae presently used to predict scabbing and wall perforation were shown to be quite conservative.

Another example of large-scale testing is the intensive effort of the valve-testing program undertaken to resolve questions of primary system valve performance. Spring-loaded safety valves, pilot-actuated safety valves and power-operated relief valves will be tested to demonstrate their capability to operate satisfactorily under steam inlet conditions, as well as a range of subcooled water and transition (steam to water) flows. The program is responsive to regulatory document NUREG 0578 Section 2.1.2 and includes, in addition to testing, an analytical activity and a technical support program. This is a dedicated, intensive R&D program with heavy involvement of operating utilities and separate funding. Due to the stringent schedule imposed by NUREG 0578 the tests have been divided among three facilities namely, Combustion Engineering, Wyle and Marshall of Duke Power Company. Preliminary test results of relief valves from the Marshall facility under steam-flow are encouraging, showing the valves have performed (opened and closed), for the most part, as expected.

Realism in Accident Effects and Consequences

The main challenge posed to the R&D community by the potential of nuclear accidents is to narrow down to realistic bands the potential range of accident effects and consequences and to afford validated and reliable tools for risk assessment (Slide 9).

While the future course of degraded core studies is not totally clear, some combination of experimental and analytical effort will proceed. Given a set of assumed conditions, the magnitude of the effort can be easily circumscribed on a technical basis; however, non-technical considerations will certainly have an effect. If technical answers are required to specific issues it seems that the procurement of data from highy visible demonstration tests as benchmarks to the analytical efforts would be prudent if not necessary. The question might be: "What test size?" This decision will most certainly be affected by value/impact considerations and the availability of resources.

A number of degraded core studies are complete or underway or tentatively planned to address phenomena ranging from flow blockage and fuel failure to severely degraded core configurations, hydrogen generation, combustion and management and the potential for interaction with containment. Small-scale experiments for investigating basic phenomena, can be combined with large-scale tests for integral effects and with modeling and code evaluation efforts. The small-scale experiments emphasize common elements of a core melting accident such as the coolability of deep debris beds and the interaction of molten materials with water in typical LWR geometries. Large-scale tests are now scheduled to be performed primarily in the hydrogen combustion and management area to study the effects of turbulance, sprays, and controlled ignition methods. The analytical work will concentrate on phenomena that may lead to containment overpressurization, failure, and fission product release. The code MARCH/CORRAL will be evaluated and improved.

With the data and analyses from the degraded core studies a reevaluation of containment integrity and effectiveness can be made. These investigations are expected to provide renewed confidence that most present containment designs are conservative with respect to maximum conditions, expected in an accident. They could also lead to improved design methods that are based on physical observations more than on assumptions with large margins of conservatism.

The overall risks accruing from the potential of nuclear reactor accidents can now be quantified through risk assessment methodologies incorporating a large number of assumptions and numerical parameters. Both the methodologies and data used in probabilistic analysis and consequence evaluation can stand considerable improvement, if they are to be used increasingly in reactor safety evaluations. Considerablee effort has been and is being expended by EPRI to improve and to validate probabilistic risk assessment as discussed in a companion paper in this session. One of the means toward accomplishing this validation is to apply available in-plant and ex-plant consequence models to actual accident situations such as the SL-1 accident and its radioactive releases(8).

The Goal of Quantifying and Improving Safety

The overall thrust of the various safety R&D activities focuses on two main points: to provide an accurate quantification of existing margins of safety and to provide guidelines and means of improving the safety of the plant and of minimizing the overall risk. Two closely related efforts at EPRI aim directly at these two goals (Slide 10): the Power Shape Monitoring System (PSMS) on which considerable effort has been expended over he past few years and the Disturbance Analysis and Surveillance System (DASS) on which more will be said in a later presentation.

Monitoring the status of the reactor core can lead to a refinement in the knowledge of its thermal margins. An on-line core monitoring system (PSMS) installed at the Oyster Creek BWR plant has demonstrated the usefulness of the system particularly during feedwater transients. Plant monitor readings refined with core physics codes have resulted in point heat ratings and thermal limits to an accuracy of a few percent.

Considerable progress has been worked in the development of a DASS, as a useful tool not only in increasing plant factor and availability but also in ensuring the safety of the plant. Considerable attention has been given in the past year to safety status monitoring and the analysis of "small break" transients, a topic on which a companion paper is given in this session. Although this involves multiple faults in the plant, primary emphasis was given on the steam generator as a heat sink and the core as a heat source. The modeling of the LWR plants is proceeding by building individual simulation models for plant components and by attempting to describe the system to the operator by interconnected and interacting modules.

The result of this effort, mounted in collaboration with the Department of Energy, is intended to provide a rapid and user-adapted computational tool for plant operational transients. The initial PWR models are being developed and will be benchmarked against existing elaborate codes (e.g., RETRAN) and existing plant data. Improving and focusing the operator's understanding of plant status, particularly under transient conditions, will result in better visibility and controllability of plant operations which implies improved safety in nuclear plants.

Another example of safety quantification and improvement is the EPRI involvement in quantifying the probabilities of an anticipated transient without scram (ATWS) a subject of long-standing concern. The EPRI program has contibuted to a quantification of the relative probabilities involved in an ATWS event and in the understanding of the relative merits of various proposed fixes. Efforts continue to establish a widely accepted value/impact methodology (Slide 11) for application in this and other similar situations. By making informed judgements on the technical merits and risks involved the appropriate authorities can ensure that funds are expended with maximum efficacy and maximum benefit for the public.

The Collaborative Character of Safety

To achieve a desired level of safety in nuclear plants a synergistic approach is necessary. Solid design, proper operating and maintenance procedures, a rigorous but rational and enlightened regulatory oversight, and sound management practices are all indispensable. Although the technical research and development efforts can provide valuable inputs to all these aspects they do not always contribute directly to the fulfillment of the formal safety requirements and goals. Consequently other organizations have an important role to play in the process of transfer and application of the research results (Slide 12).

The Nuclear Safety Analysis Center (NSAC), also under EPRI but with a separate status and funding, was initiated in the aftermath of TMI-2 and is now continuing its function mainly as a technical evaluation, communication and liaison organization with a capability of fast response to current problems and emergency situations. Its main topical areas are the collection and analysis of significant event reports; the "what-if" studies to determine the additional margins existing at TMI for increasingly severe additional failures; and the communication and coordination function.

The Institute for Nuclear Power Operations (INPO), on the other hand, is an independent organization, also supported by the electric power industry. Its function is to set and to implement plant operational standards in the safety area and to encourage and promote high dedication to operational safety.

Also important to the overall success of the safety research effort is EPRI's cooperation with a number of foreign organizations primarily representing R&D arms of the utility industry abroad for the exchange of information and for the conduction of cooperative efforts. Examples of such exchanges are those with CEGB of the UK, EDF of France, BMFT of the Federal Republic of Germany, CRIEPI of Japan, CISE of Italy and others.

Summary and Conclusions

The EPRI safety R&D program has been guided by a set of guiding principles to be effective within given constrains of limited resources, and responsive to the needs of the electric power industry. Many concerns that surfaced in the post-TMI atmosphere have been topics of investigation of EPRI before that event. Such instances include research in human factors, disturbance analysis, small break events, and integrated system response methodology under transient conditions.

Although we perceive no need for dramatic shifts in our general R&D direction and emphasis the necessary flexibility must be a continuing part of the program. As one looks into the future the following trends may be discerned:

a. A definition of R&D needs and efforts to support conclusion of the current debate on Class 9 accidents by either mechanistic or probabilistic or a combination of approaches.

b. An increased use of data collected at operating plants.

c. The analysis and interpretation of selective large-scale demonstrations notably in the area of seismic data collection and design methods.

d. An emphasis on faster, more efficient and more reliable analytical methods and codes in the areas of thermohydraulics, fuels and materials behavior, structural integrity, fluid/structure interaction.

e. An improved knowledge and predictive capability in fission product behavior, transport and attenuation.

EPRI recognizes the requirements in all these areas and intends to structure its program to provide the technical data and analyses needed for problem resolution. The program will thus be responsive to both the formal and substantive requirements placed upon the electric power industry. The fruit of EPRI's research as well as that of other organizations in the field, will in the final analysis, be judged by the degree to which it responds to real and perceived safety problems and to which it enhances the safe and efficient operation of nucler power plants.

NOTES AND REFERENCES

1. As of June 30, 1980, over 1800 reactor-years of experience had been accumulated worldwide, 565 of which in the US. 74 reactors in the US and about 160 reactors operating abroad represent a total installed capacity of about 125 GW. Source: Atomic Industrial Forum Info, Sept. 1980.

2. N. S. Folk and W. R. Cobb, "Core Performance Benchmarking, Edwin I. Hatch Nuclear Plant Unit 1, Cycle 1," EPRI NP-1235, November 1979.

3. J. F. Carew,"Process Computer Performance Evaluation Accuracy," Licensing Topical Report, General Electric Co., NEDP-20340, 1974.

4. L. A. Carmichael and R. O. Niemi,"Transient and Stability Tests at Peach Bottom Atomic Power Station Unit 2 at End of Cycle 2," EPRI NP-564, June 1978.

5. "Seismic Piping Test and Analysis," Vols. 1, 2, and 3, EPRI NP-1505, Sept. 1980.

6. K.H. Sun, R.B. Duffey, and C.M. Peng, "The Prediction of TwoPhase Mixture Level and Hydrodynamically-Controlled Dryout Under Low Flow Conditions," EPRI NP-1359-SR, March 80.

7. S.D. Kalra, R.B. Duffey and G. Adams, "Loss-of-Feedwater Transients in PWR U-Tube Steam Generators: Simulation Experiments and Analysis," EPRI NP-1367-SR, March 1980.

8. "Consequence Analysis of the SL-1 Reactor Accident," EPRI Report in preparation.

NUCLEAR SAFETY R&D GENERAL GUIDELINES

- Long-term objectives must be pursued undetracted by immediate concerns
- Steadiness of purpose must be blended with a degree of flexibility
- Coordination and perspective among the various parts of the effort must be maintained
- Maximum effort must be directed toward items of maximum importance

MAJOR THEMES OF NUCLEAR SAFETY R&D

- Importance of analyzing small-break and other lesser accidents
- Natural circulation as a cooling mode
- Adequate prediction of plant transient behavior under a wide range of parameters
- Analysis of degraded core conditions
- Realistic assessment of radioactive releases
- Analytical and experimental assessment of structural integrity
- Convert probabilistic risk assessment into a useful tool for reactor design and operation

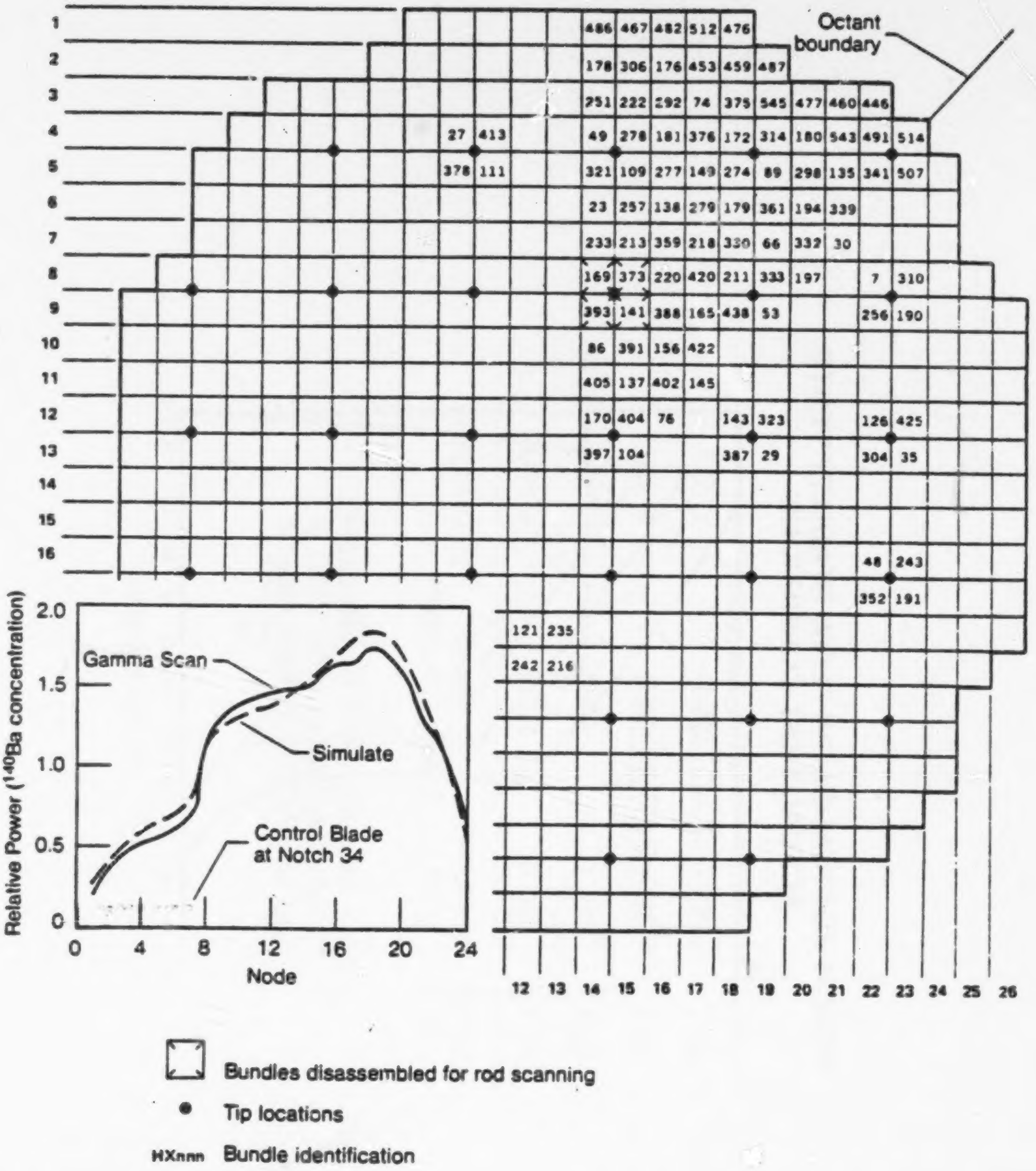
Octant boundary
1
2
3
4
5
6
7
8
9
10
11
12
13
14
15
16
486 467 482 512 476
178 306 176 453 459 487
251 222 292 74 375 545 477 460 446
27 413 49 278 181 376 172 314 180 543 491 514
378 111 321 109 277 149 274 89 298 135 341 507
23 257 138 279 179 361 194 339
233 213 359 218 330 66 332 30
169 373 220 420 211 333 197 7 310
393 141 388 165 438 53 256 190
86 391 156 422
405 137 402 145
170 404 76 143 323 126 425
397 104 387 29 304 35
48 243
352 191
121 235
242 216
12
13
14
15
16
17
18
19
20
21
22
23
24
25
26
Relative Power (140Ba concentration)
2.0
1.5
1.0
0.5
0
0
4
8
12
16
20
24
Node
Gamma Scan
Simulate
Control Blade at Notch 34
Bundles disassembled for rod scanning
Tip locations
HXnnn Bundle identification

Octant Normalized Axial Power Distribution - Bundle 393 (Edwin I. Hatch Unit 1 BWR)

PEACH BOTTOM-2 LOW-FLOW STABILTY TESTS: ACTUAL TEST CONDITIONS

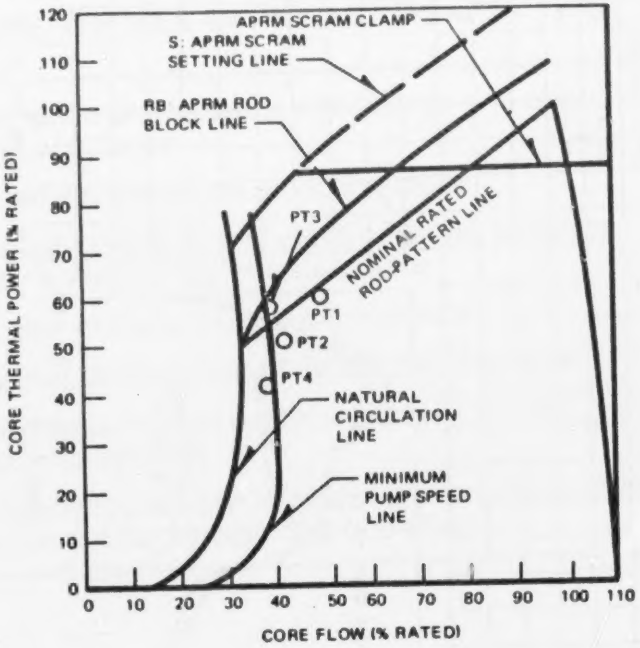

LOW FLOW STABILITY TESTS
AT PEACH BOTTOM-2, EOC 2
Core Stability Margin Estimates

Test Number	*Power (% rated)*	*Core Flow Rate (% rated)*	*Decay Ratio*
PT1	60.6	51.3	0.259
PT2	51.7	42.0	0.303
PT3	59.2	38.0	0.331
PT4	43.5	38.0	0.271

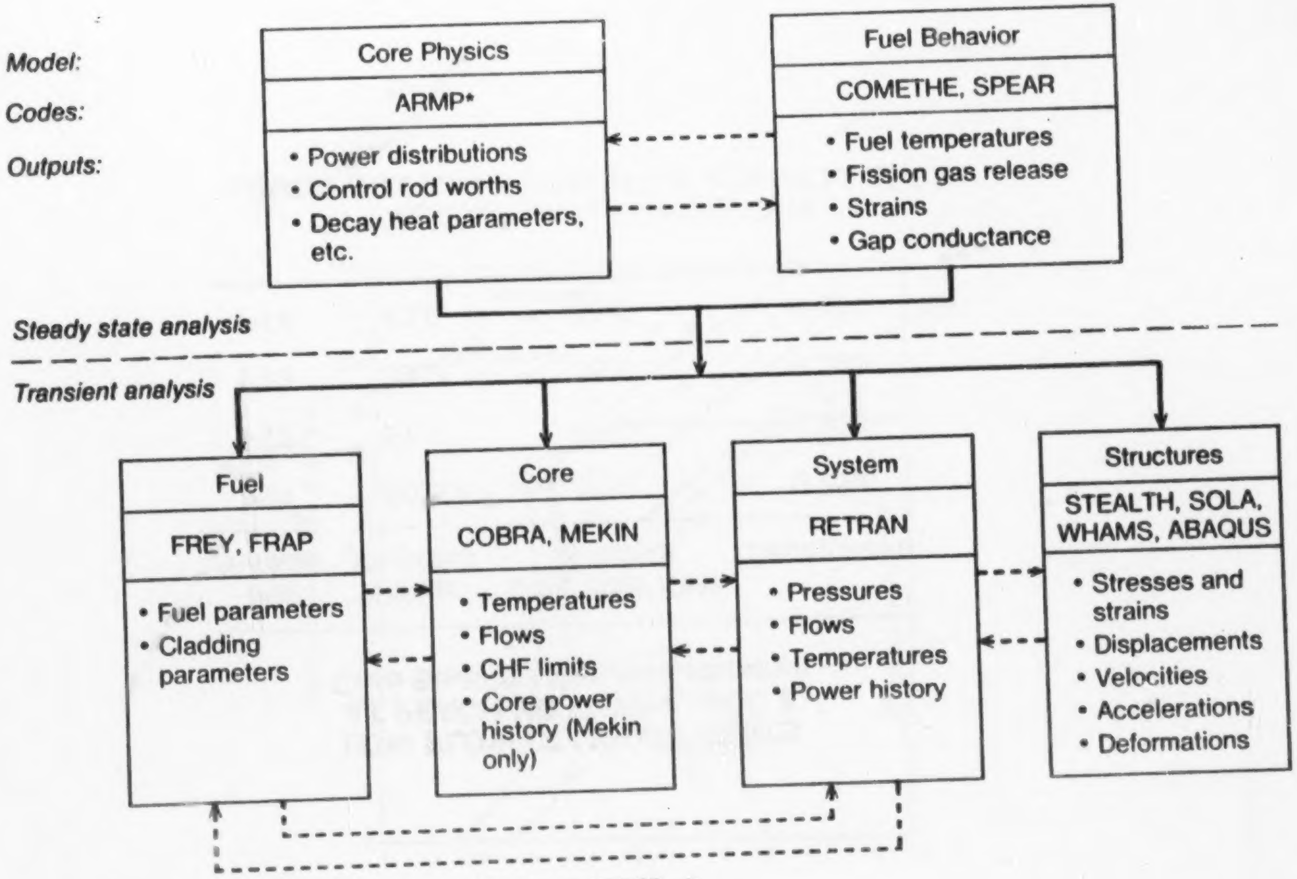
Model:
Codes:
Outputs:
Core Physics
ARMP*
• Power distributions
• Control rod worths
• Decay heat parameters, etc.
Fuel Behavior
COMETHE, SPEAR
• Fuel temperatures
• Fission gas release
• Strains
• Gap conductance
Steady state analysis
Transient analysis
Fuel
FREY, FRAP
• Fuel parameters
• Cladding parameters
Core
COBRA, MEKIN
• Temperatures
• Flows
• CHF limits
• Core power history (Mekin only)
System
RETRAN
• Pressures
• Flows
• Temperatures
• Power history
Structures
STEALTH, SOLA, WHAMS, ABAQUS
• Stresses and strains
• Displacements
• Velocities
• Accelerations
• Deformations

*Includes EPRI-CELL, CPM, PDQ-7, SIMULATE, NODE-P, -B, NORGE, etc.

Figure 7. Code Interfaces

RP1761

DEVELOPMENT OF RELOAD SAFETY ANALYSIS METHODOLOGY AND CODE PACKAGE

Applications

- Licensing activities
- Best estimate predictions of plant behavior in various steady state and transient situations

Purpose

- Increase utility independence from fuel suppliers;
- Offer more flexibility in tailoring plant performance to utility system operating needs
- Improve utility understanding of plant behavior and performance

---

SCALED TESTS

- 4-loop natural circulation model; simulates the Trojan PWR plant
- 2-loop reflux boiling facility, simulates an actual 2-loop PWR plant
- Model of TMI-2 primary system to investigate effectiveness of natural circulation
- Comparison of core uncovery and phase separation model with single tube, rod bundle and TMI-2 data
- Level indicator experiments
- U-tube steam generator scale model with freon
- Coolability of a bed of debris, simulating a severely degraded core

REALISM IN ACCIDENT EFFECTS AND CONSEQUENCES

Small-scale tests to emphasize common elements of a core melting accident

- Coolability of deep debris beds
- Interaction of molten materials with water

Large-scale tests

- Hydrogen combustion and management
- Effect of turbulance, sprays and ignition methods

Analytical work

- Containment over-pressurization
- Containment failure
- Fission product release
- MARCH/CORRAL code evaluation and improvement

QUANTIFYING AND IMPROVING SAFETY

Power shape monitoring system (PSMS)

- Monitors and predicts core power distributions
- Predicts fuel performance
- Provides greater operating margins
- Provides more efficient load maneuvers

Disturbance analysis and surveillance system (DASS)

- Verifies, analyses, integrates and assigns priorities to plant information
- Assists operator to improve plant safety and availability

QUANTIFYING AND IMPROVING SAFETY

Development of a widely accepted value/impact methodology to

- Assess the relative merits of various research and development strategies
- Assess the merits of alternative, proposed technical fixes to safety concerns (e.g. ATWS)
- Ensure funds are expended with maximum efficacy and benefit to the public

THE COLLABORATIVE CHARACTER OF SAFETY

Role of NSAC

Functions

- Technical evaluation
- Technical communication
- Liaison with industry groups
- Fast response to current problems and emergencies

Topical areas

- Significant event reports
- "What-if" studies
- Communication and coordination

Role of INPO

Functions

- Set standards of operational safety
- Conduct plant-by-plant evaluations and help implement standards
- Promote high dedication to operational safety

FUTURE TRENDS

- DEFINITION OF R&D TO SUPPORT CONCLUSION OF DEBATE ON CLASS 9 ACCIDENTS
- INCREASED USE OF OPERATING PLANT DATA
- ANALYSIS & INTERPRETATION OF SELECTED LARGE-SCALE DEMONSTRATIONS (PARTICULARLY IN SEISMIC AREA)
- EMPHASIS ON FASTER, MORE EFFICIENT & MORE RELIABLE ANALYTICAL TOOLS
- IMPROVED PREDICTIVE CAPABILITY IN FISSION PRODUCT RELEASE, TRANSPORT, & BEHAVIOR

STATUS OF EPRI TURBINE MISSILE RESEARCH PROGRAM

by
George E. Sliter
Project Manager
Nuclear Division
Electric Power Research Institute

Presented at
Eighth Water Reactor Safety Research Information Meeting
October 27-31, 1980

OVERALL PROGRAM

The objective of the turbine missile research program sponsored by the Electric Power Research Institute (EPRI) is to provide test data and supporting analyses that may be used to identify and quantify the conservatisms in current estimates of turbine missile risk in nuclear power plants. The program focuses on postulated failures of the shrunk-on disks in the low-pressure sections of 1800-rpm steam turbines, particularly in plants with a non-peninsula turbine arrangement. The three project areas in the program are impact of casing structures, impact of reinforced concrete structures, and probabilistic analysis of turbine missile risk.

The objectives and main efforts in each area are described briefly below, followed by preliminary results from recent turbine missile impact tests of concrete structures.

Casing Impact

The objective of projects involving casing impact is to provide data for determining whether fragments resulting from disk failure would be contained by the steel turbine casing or, if they are ejected, for estimating the initial conditions (velocity, rotation and direction) of their subsequent trajectories. Benchmark data in this area were provided by full-scale casing tests performed at the rocket sled facility of Sandia National Laboratories in 1978 [1]. Two tests were run with a non-spinning, 3365-lb. (1526 kg), Westinghouse disk segment without blades impacting a simple, first-order model of a turbine casing. In both tests the impact velocity was 490 fps (150 m/s), representing a 120 percent design overspeed condition. The target structures consisted of a 5-in.-thick (12.7-cm-thick) inner ring and a 1 1/4-in.-thick (3.2-cm-thick) outer shell. In one test, with a sharp pointed end of the missile striking first, the missile was slowed to 285 fps (187 m/s); 65 percent of its energy was dissipated by the impact. In the other test, with the curved blunt end of the missile striking first, the missile was brought almost to rest. Data from these tests are benchmarks for analyses and scale model studies.

Small-scale versions of the full-scale Sandia tests have been performed by SRI International to assess the validity of replica scaling laws for impact on steel structures. An explosively-driven piston launched one-fifth-scale missiles at one-fifth-scale casing structures. Target deformation, fracture modes and post-impact missile motion were remarkably similar to those observed in the full-scale tests. The results, scheduled to appear in a report in Spring of 1981, demonstrated the usefulness and cost-effectiveness of scale-modeling for studying casing impact effects.

In contrast with the conditions in the tests described above, actual turbine fragments have lightweight blades and are spinning as they impact casing structures. Small-scale tests are in progress at the Naval Air Propulsion Center spin pit facility to examine the effects of blade deformation on the containment or breakthrough of spinning turbine segments. The tests consist of 360° steel rings struck by three fragments from jet engine rotors modified to represent one-eleventh-scale versions of nuclear turbine disks with and without blades.

Concrete Impact

The objective of projects involving concrete impact is to provide data for evaluating the effectiveness of reinforced concrete walls and roofs in protecting safety-related plant areas against turbine missiles. Information from projects in the casing impact area helps to define the impact conditions used in concrete impact tests. The main purpose of this paper is to present preliminary results of full-scale and scale-model turbine-missile impact tests of concrete structures.

Risk Analysis

The objective of projects in this area is to provide an analytical basis for evaluating the safety characteristics of nuclear plant layouts and barrier design requirements related to turbine missile effects. The research in progress at Batelle Pacific Northwest Laboratories and Research Triangle Institute includes a review of existing methodologies for evaluating turbine missile risk, revised estimates of missile generation probability, examination of casing exit conditions from a probabilistic viewpoint, improved calculations of missile trajectories and impact damage, and application of an improved risk methodology in typical case studies. Results from the casing and concrete impact studies will be incorporated into the risk study as they become available. The risk study is scheduled for completion in 1981.

The results of full-scale and scale-model concrete impact tests presented below are preliminary and subject to verification.

FULL-SCALE CONCRETE IMPACT TESTS

To provide full-scale benchmark data on the resistance of reinforced concrete containment building walls to turbine missile impact, four tests were conducted at the rocket sled facility of Sandia National Laboratories.

Test Description

The target panels in the tests represented a section of the wall of a conventionally reinforced concrete PWR reactor containment building. The 4.5-foot-thick (1.37-m-thick) panels (cross-section shown in Figure 1) were fabricated from heavily reinforced concrete with a nominal compressive strength of 3800 psi (26.2 MPa). For the last two tests, the panels had a steel plate 3/8 in. (0.95 cm) thick anchored to its rear surface during construction. This represented the leakproof liner plate installed in all conventional PWR containment buildings. The panels in the first two tests did not have a steel liner to allow any backface cracking to be visible.

The panels were cast horizontally next to the test facility and rolled into place for testing at the end of the rocket-sled track. They were suspended from and supported against a massive concrete and soil backup structure. Tie rods held panels in place against the 2-foot-thick support-structure walls. Dynamic panel response was measured with acceleration, velocity and displacement gages on the panel backfaces and with strain gages bonded to the reinforcing bars.

The first three tests were performed with a 3250-pound (1477-kg), 120° sector of a Westinghouse last stage shrunk-on disk without blades (Figure 2). A heavier (4540 pound, 2064 kg) 137° sector of a General Electric disk was used in the fourth test (Figure 3).

The impact velocity in the first test was 295 fps (90 m/s). This is nominally the same as the exit velocity of the full-scale sharp-end casing test performed earlier by Sandia [1] and therefore accounts for the substantial energy reduction from casing breakthrough. It represents an upper bound on the exit velocity of a fragment from a postulated failure at 120 percent overspeed in the sense that (1) of all possible orientations, the sharp-end orientation leads to the greatest exit velocity; and (2) the impact velocity in the casing test (490 fps, 150 m/s) was arrived at by lumping both the translational and rotational energy of the failed fragment into translational velocity. It is also expected that a missile leaving a casing would have a portion of its energy in rotation and would impact the containment building (if at all) in an oblique and non-sharp manner. Hence, the non-spinning, perpendicular, and sharp-end impacts in the concrete tests represent a conservative condition.

The photographs in Figure 4 show the overall test arrangement with the panel hanging in place and the missile approaching and striking the panel. The carrier sled is deflected downward by the intervening structure prior to impact.

Test Results

The crater produced by the impact in the first test is shown in Figure 5 (the checkerboard on the surface has one foot squares). The missile penetrated 17 in. (47 cm), about one-third the panel thickness. Rear face damage was limited to cracking as shown in Figure 6 (cracks have been marked for visibility). No concrete pieces were scabbed from the rear face.

Since the impact orientation of a tumbling missile would be random, the effect of impact orientation was examined by turning the missile 90° to strike on its curved blunt edge in the second test. The same impact velocity as in the first test produced less penetration, 13 in. (33 cm). Rear face cracking was similar; again, no scabbing occurred.

In the third test, the missile was turned again to strike sharp-end first and impact velocity was increased to 428 fps (130 m/s), which corresponds to a disk failure at about 50% overspeed. The missile penetrated 24 in. (61 cm) into the panel and produced a slight bulge (1.6 in. [4.1 cm] high) in the backface liner plate.

The fourth and final test in the series was performed with a 4540-lb. (2064-kg) GE missile impacting sharp-end first. The test velocity was specified to be the same as in the third test (428 fps, 130 m/s), giving 40% greater missile kinetic energy. However, because 2 out of 16 rockets misfired, the actual impact velocity was only 377 fps (115 m/s), giving an 8% kinetic energy increase over the third test. The slightly greater impact energy produced slightly greater target response. The missile penetrated 26 in. (66 cm) into the wall and produced a 2-in. (5 cm) bulge in the liner plate. Therefore, although the desired increase in impact energy was not achieved, the test result was useful in its demonstration of consistency; even though the missile shapes in the third and fourth tests differed somewhat, a small increase in energy gave a consistently small increase in damage.

Cores drilled through the panel thickness in several places showed that all four impacts produced the conical plug usually observed in concrete walls under missile impact. The plug was held in place by the heavy reinforcing.

Results of the four full-scale tests are summarized in Table 1. An important general result is that in all cases the damage fell far short of that which would breach the containment in a reactor building. Furthermore, as discussed below, the observed backface damage is much less than would be predicted by formulas currently used in plant design.

Comparison With Design Calculations

Design calculations of impact effects are made traditionally using empirical formulas. The most widely-accepted is known as the NDRC formula [2,3]. This formula gives penetration depth into reinforced concrete in terms of impact velocity, concrete strength, and missile diameter and weight. Although derived from data on circular cylindrical missiles, the formula is commonly applied to irregularly shaped turbine missiles by using an "effective" diameter. Another NDRC formula gives the wall thickness for incipient scabbing or perforation in terms of penetration depth and missile diameter.

The NDRC formulas were applied to a 3250-lb. (1477-kg) missile with sharp-end orientation to calculate the velocities required for scabbing (with no liner) and perforation (with or without a liner). These velocities are plotted against target thickness in Figure 7 and compared with the conditions in the first and third tests. In the first test, no scabbing was produced at 295 fps (90 m/s), whereas the formula predicted incipient scabbing at 130 fps (40 m/s). In the third test, with a 428 fps (130 m/s) impact, a substantial margin against perforation remained (penetration was less than half the wall thickness), whereas the formula predicted incipient perforation at 340 fps (104 m/s). This additional resistance of the panels to scabbing and perforation over that predicted by the design formula may be due to the relatively large amount of reinforcing in the targets and to the inapplicability of the formula for predicting backface damage from missiles with highly irregular shape (as described below, predicted frontface penetration was close to measured values).

Because of the high cost of these tests, no further full-scale testing is planned at present.

SCALE-MODEL CONCRETE IMPACT TESTS

To assess the usefulness of scale-model testing for examining a wide range of missiles, targets, and impact conditions at a reasonable cost, a preliminary series of nine small-scale tests were conducted in the gas gun laboratory of SRI International.

Scaling Technique

The scaling technique employed, called "replica scaling", is commonly used to examine the dynamic response of structures [4]. In replica scaling, all prototype dimensions are reduced by the same scale factor to give geometric similarity, and the same materials as in the prototype are used in the model to give material or strength similarity. Because it is not possible to scale all sizes of the concrete aggregate, the sizes are scaled approximately and care is taken to maintain as closely as possible the same compressive strength in the model concrete as in the prototype concrete.

The scale factor in the tests, one eleventh (1/11), was selected on the basis of fitting the scale-model missile in the sharp orientation into the 4-in. (10-cm)-diameter barrel of the SRI gas gun (Figure 8). This scale factor led to a model target 21.8 in. (0.55 m) square and 4.9 in. (12.4 cm) thick. The 0.2-in. (0.5 cm)-diameter steel reinforcing was installed in a pattern geometrically similar to the full-scale reinforcing.

The scale models of the 3250-lb. (1477-kg) Sandia missile weighed 2.5 lb. (1.1 kg) and were fabricated from high-strength steel similar to turbine disk material. According to replica scaling laws, impact velocity in the scale model tests should be the same as in full scale. The laws further state that, if strain-rate effects (increased strength with increased strain rate) are negligibly small, structural response of the model such as penetration depth and backface cracking/scabbing would be the same in the model as in the prototype. However, strain-rate effects and the inability to reproduce all details of a prototype in small scale may lead to differences between model and prototype response. The main purpose of the SRI tests was to examine these differences.

Impact velocities in the nine tests ranged from 305 to 647 fps (93 to 197 m/s). Concrete strength was 3,600 ± 280 psi (24.8 ± 1.9 Mpa). In three of the tests the concrete target had a scale model version of a 3/8-in. (0.95-cm)-thick steel liner plate anchored into its back surface.

Test Results

Seven tests were performed with scale models of the 4.5-ft.-thick full-scale panels. Figure 9 is a photograph of the 1.2-in. (3-cm)-deep front-surface crater produced in the 4.9-in. (12.4 cm)-thick target by an impact at 305 fps (93 m/s). Another test at the same impact velocity produced a penetration of 1.6 in. (4.1 cm). Multiplying the average of these two measurements by the scale factor of eleven gives 15 in. (38 cm), compared with a measured penetration of 17 in. (43 cm) in the full-scale test at 295 fps (90 m/s). The back surface in the two scale model tests at 305 fps (93 m/s) had no visible cracks, whereas the full-scale test at 295 fps (190 m/s) produced slight cracking (see Figure 6).

Additional tests at greater impact velocities were performed on the remaining five models of 4.5-ft. (1.37-m)-thick panels. The severity of backface cracking increased as impact velocity was increased to 430 fps (131 m/s). At 550 fps (168 m/s) a small piece of concrete was scabbed from the back of the model. Scabbing was eliminated in tests at 550 and 630 fps (168 and 192 m/s) by a 0.034-in. (0.9 mm)-thick liner plate anchored to the back surface. The impact at 630 fps (192 m/s) produced a 2.8-in. (7.1-cm)-deep crater and a maximum deflection of 0.3 in. (0.8 cm) in the liner plate. These results are plotted in Figure 10 with circles and triangles. The solid curve is the NDRC prediction of penetration. The calculated curve agrees with the measured depths to within the scatter of ±10 percent commonly encountered in concrete impact testing.

The same NDRC formula applied to a full-scale target gave the dashed curve in Figure 10. Note that the formula predicts about 25 percent greater normalized penetration in a thicker target, whereas exact replica scaling would predict the same normalized penetration in both target sizes. The square and diamond points denoting the full-scale data from the first and third Sandia tests are in reasonable agreement with both the NDRC prediction and the model data.

For the scale model targets and missiles in these tests, the NDRC formula gives the impact velocity for incipient scabbing (with no liner) as 170 fps (52 m/s), and for incipient perforation as 425 fps (130 m/s). In contrast, the data showed that no scabbing occurred at 430 fps (131 m/s) and no perforation occurred at 630 fps (192 m/s).

Two additional tests were performed with scale-model versions of a 3.5-ft. (0.89-m)-thick full-scale panel, thinner than those tested at Sandia. In one of these tests, a scaled-down 3250-lb. (1477-kg) missile at 647 fps (197 m/s) penetrated 3.3 in. (8.4 cm) into the 3.8-in. (9.6-cm)-thick panel, but perforation was prevented by the rearmost layers of rebar and all fragmented concrete was contained by the liner plate (Figure 11 is a photo of a sawcut cross-section). The NDRC formula predicts that perforation would occur at less than half the velocity in this test.

SUMMARY AND CONCLUSIONS

Four full-scale turbine missile impact tests of reinforced concrete structures have demonstrated that containment building walls are substantially more resistant to impact than reflected by current design methods. Additional data are required to quantify this conservatism and provide a basis for developing improved design methods. This information can be used to make more realistic estimates of the overall risk from turbine missiles effects.

Nine scale-model tests have demonstrated the feasibility of using this low-cost approach for extending the data base over a broader range of missile weights, target types, and impact conditions (such as oblique impact) at reasonable cost. The damage produced in 4.9-in. (12.4-cm) targets by 2.5-lb. (1.1-kg) model missiles was remarkably similar to that produced in 4.5-ft. (1.37-m) targets by 3250-lb. (1477-kg) prototype missiles at the same velocities.

Measured penetration depths in both full-scale and scale-model tests were in close agreement with the predictions of the NDRC formula. On the other hand, agreement between calculated scabbing/perforation and that observed was poor. Test structures withstood substantially more impact energy without scabbing or perforation than predicted by the current design method.

Final reports on the impact tests to date are scheduled for publication in the Spring of 1981. Scale-model testing will continue into 1981. The entire EPRI turbine missile research program, including the risk analysis, is scheduled to be completed by the end of 1981.

REFERENCES

1. Yoshimura, H. R., J. T. Schamaun, "Preliminary Results of Turbine Missile Casing Tests," EPRI Preliminary Report, October 1978.

2. Sliter, G. E., "Assessment of Empirical Concrete Impact Formulas," Journal of the Structural Division, ASCE, May 1980.

3. USNRC Regulatory Guide 1.115, "Protection Against Low-Trajectory Turbine Missiles," Revision 1, July 1977.

4. Baker, W. E., P. S. Westine, and F. T. Dodge, Similarity Methods in Engineering Dynamics, Spartan Books, Rochelle Park, NJ, 1973.

EPRI TURBINE MISSILE RESEARCH PROGRAM (Sliter)

W30-1380 Coral 3/1 R2 10/23/80 (ml)

(For WPC information, please do not discard this sheet; it should be attached at the end of the document when it is returned for revision.)

Table 1 Summary of Full-scale Test Results

Test No.	Missile Weight (lb.)	Impact Orientation	Impact Velocity (fps)	Kinetic Energy (10^6 ft-lb)	Penetration Depth (in.)	Backface Response
1	3250 (W)	Sharp	295	4.4	17	Cracks
2	3250 (W)	Blunt	300	4.5	13	Cracks
3	3250 (W)	Sharp	428	9.3	24	1.6-in. Liner Deflection
4	4540 (GE)	Sharp	377	10.0	26	2-in. Liner Deflection

(NOTE: 1 lb. = 0.453 kg; 1 in. = 2.54 in; 1 fps = 0.305 m/s; 1 ft.-lb. = 1.356N-m)

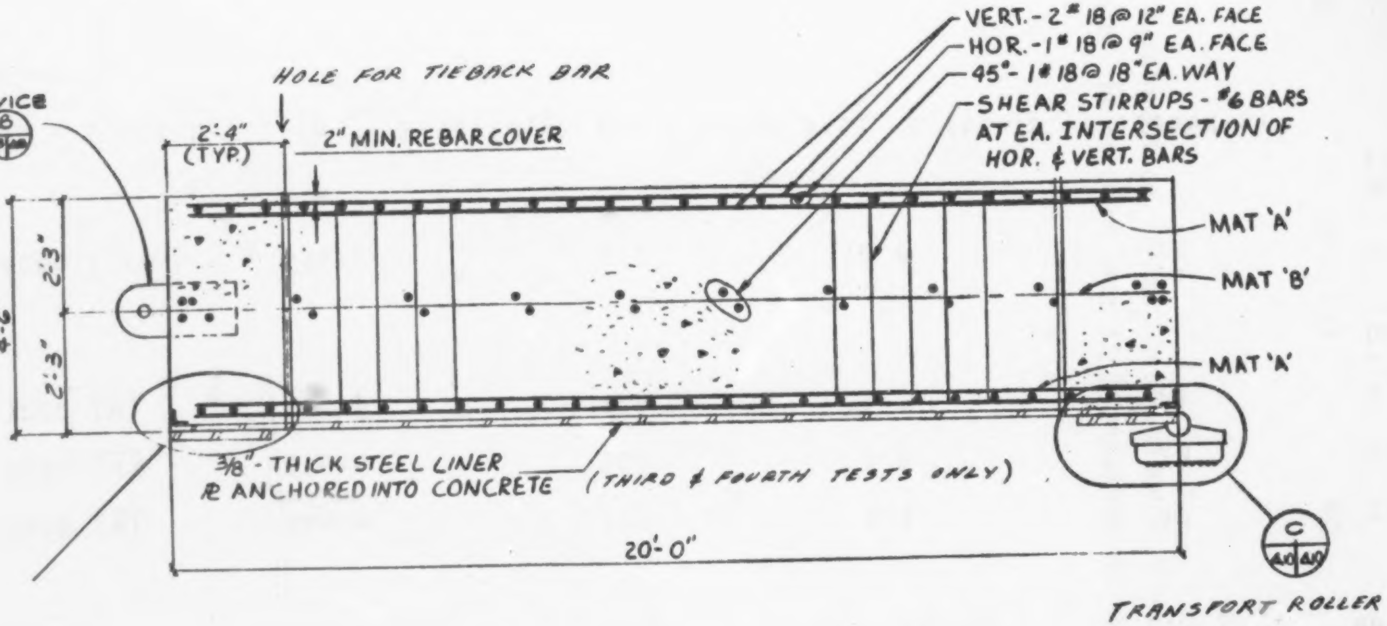
VERT. - 2# 18 @ 12" EA. FACE
HOR. - 1# 18 @ 9" EA. FACE
45° - 1# 18 @ 18" EA. WAY
SHEAR STIRRUPS - #6 BARS AT EA. INTERSECTION OF HOR. & VERT. BARS
HOLE FOR TIEBACK BAR
LIFTING DEVICE SEE DET. B A10 A10
2'-4" (TYP.)
2" MIN. REBAR COVER
MAT 'A'
MAT 'B'
MAT 'A'
4'-6"
2'-3"
2'-3"
3/8" - THICK STEEL LINER
℞ ANCHORED INTO CONCRETE
(THIRD & FOURTH TESTS ONLY)
20'-0"
C A10 A10
TRANSPORT ROLLER

Fig. 1 Cross-section of Full-scale Reinforced Concrete Targets

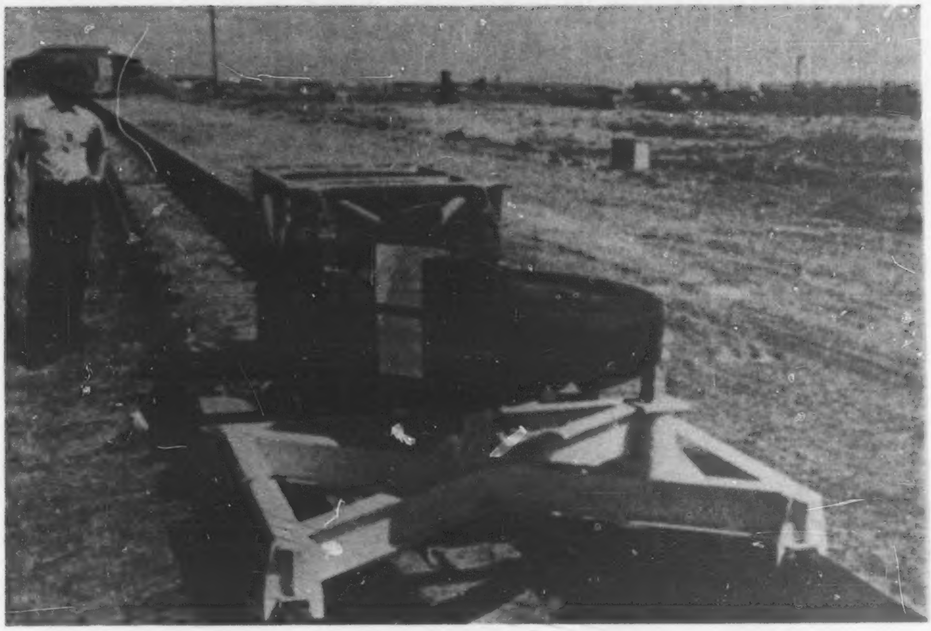

Fig. 2 Westinghouse Missile in Tests 1, 2, and 3 (3250 lb., 120°)

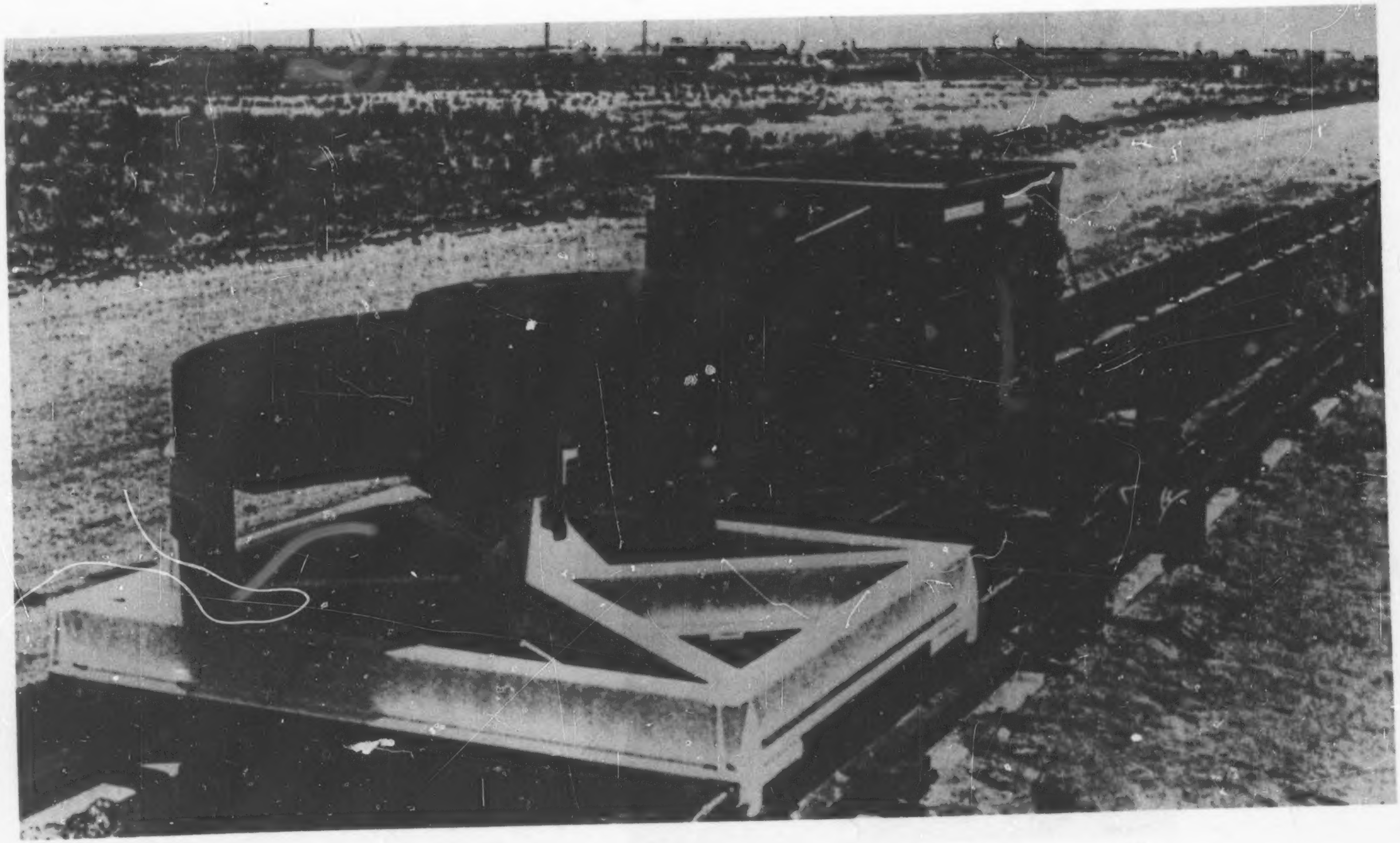

Fig. 3 General Electric Missile in Test 4 (4540 lb., 137°)

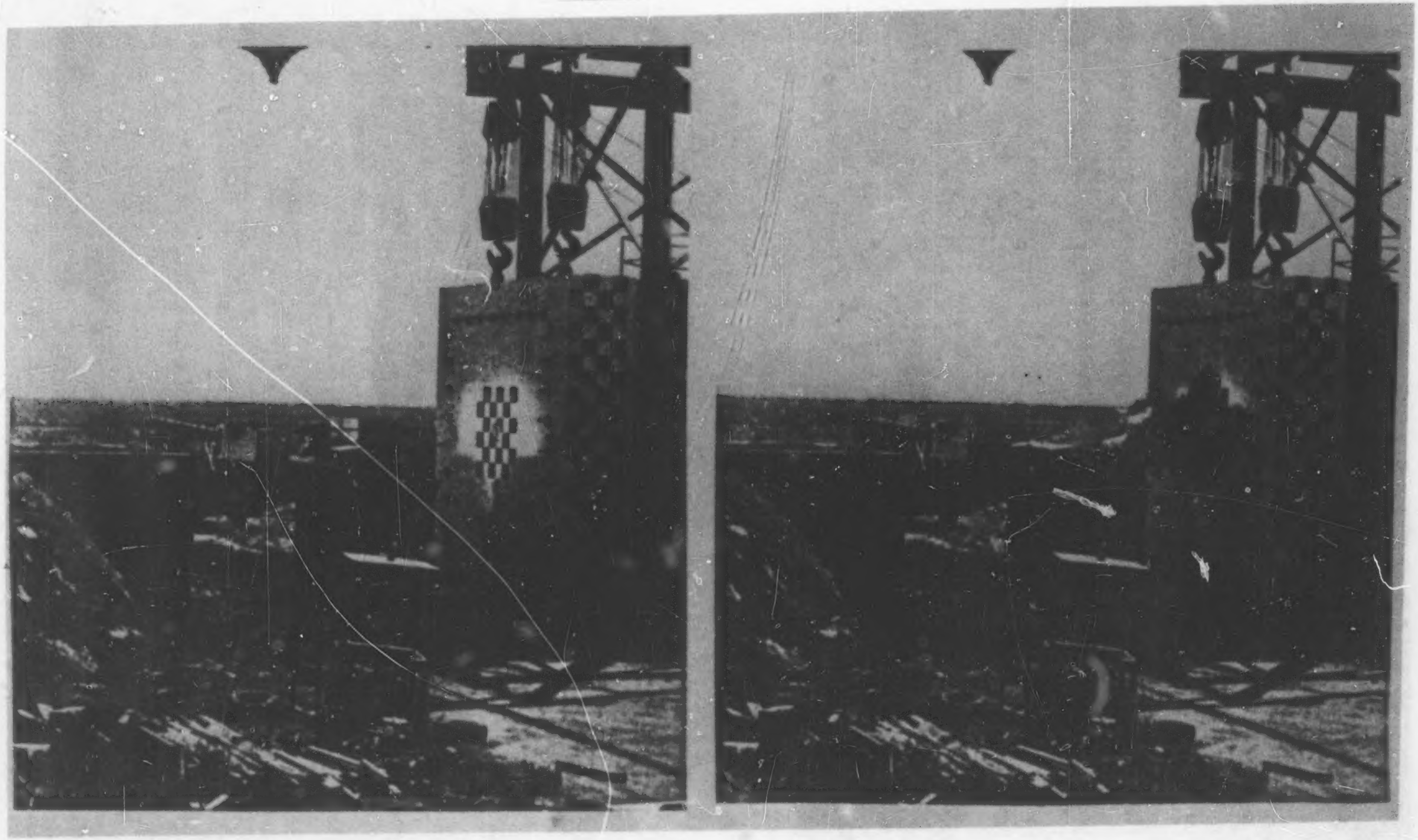

Fig. 4 Turbine Missile Approaching and Striking Target Panel

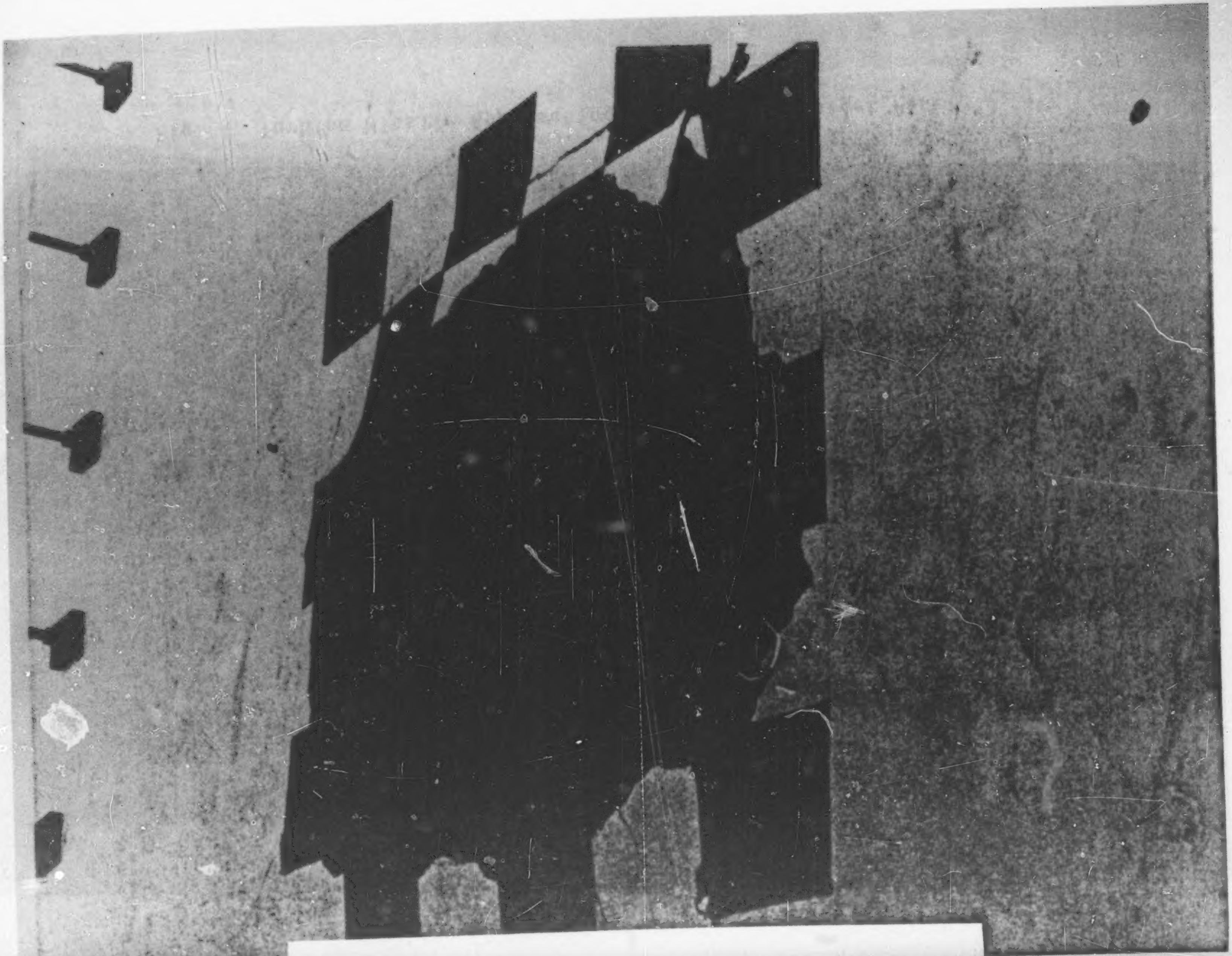

Fig. 5 Frontface Crater - Test 1 (295fps)

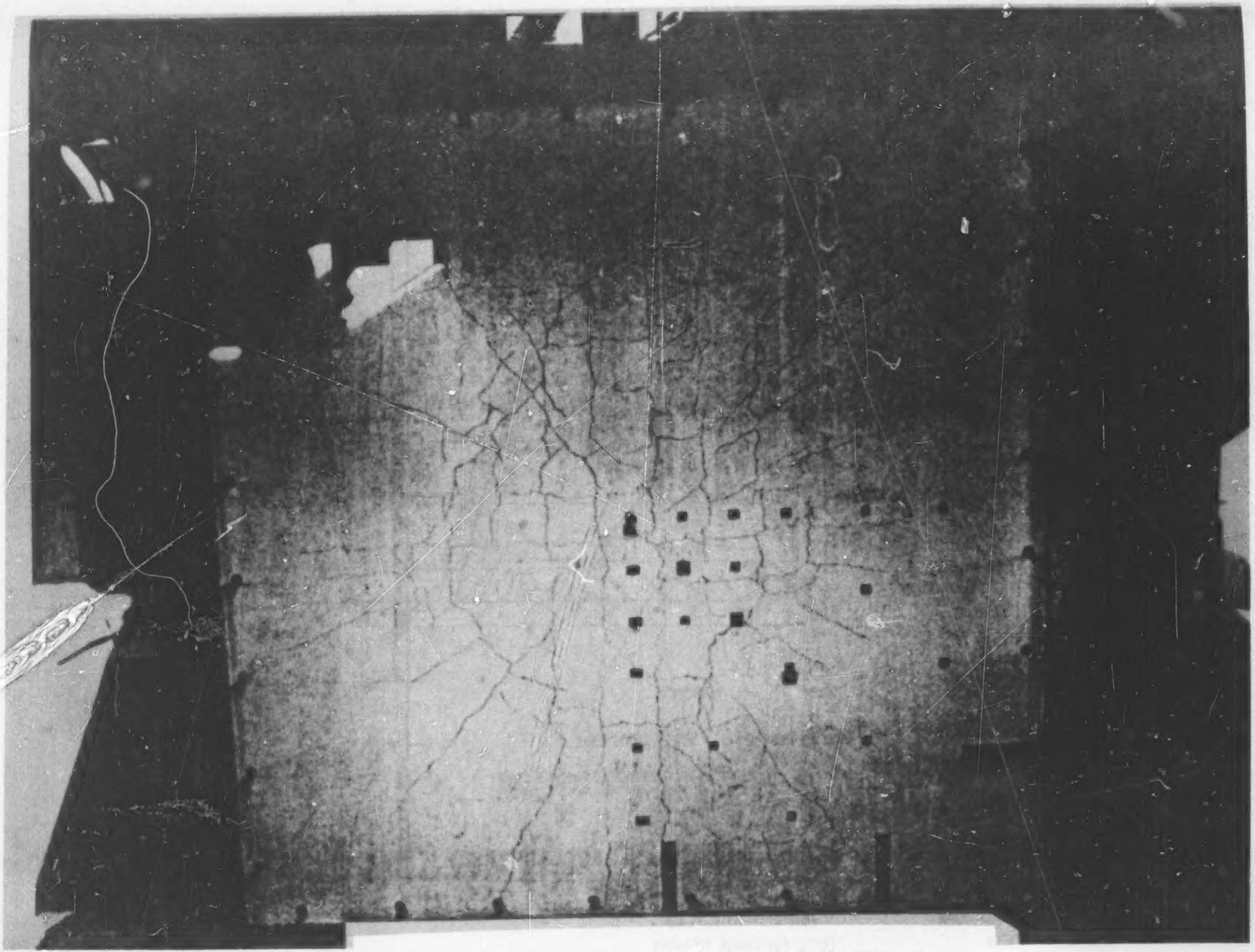

Fig. 6 Backface Cracks - Test 1 (295fps)

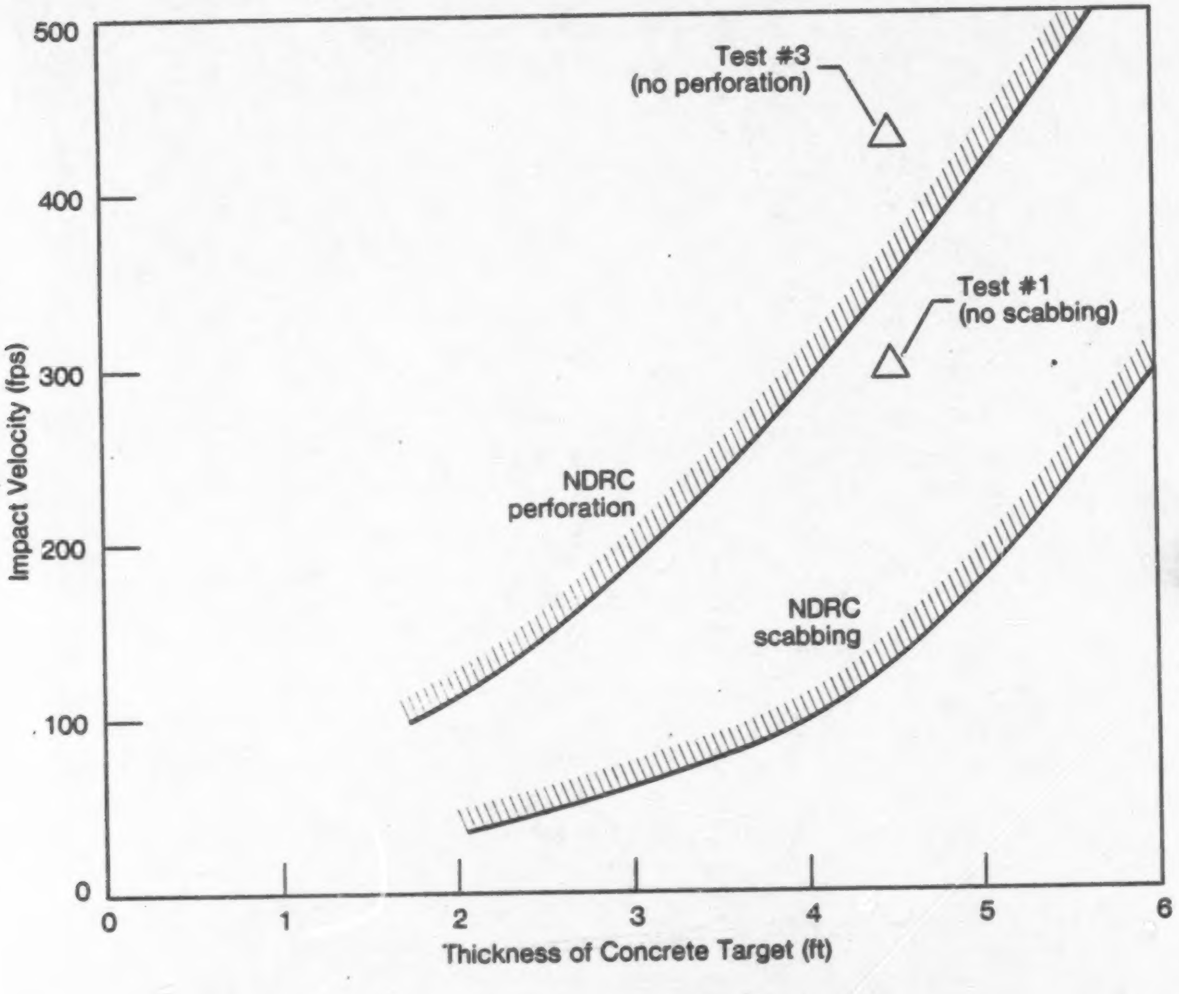

g. 7 Comparison of Full-scale Test Results with Predictions of NDRC Design Formula (3250-lb. Missile, Sharp-end Impact)

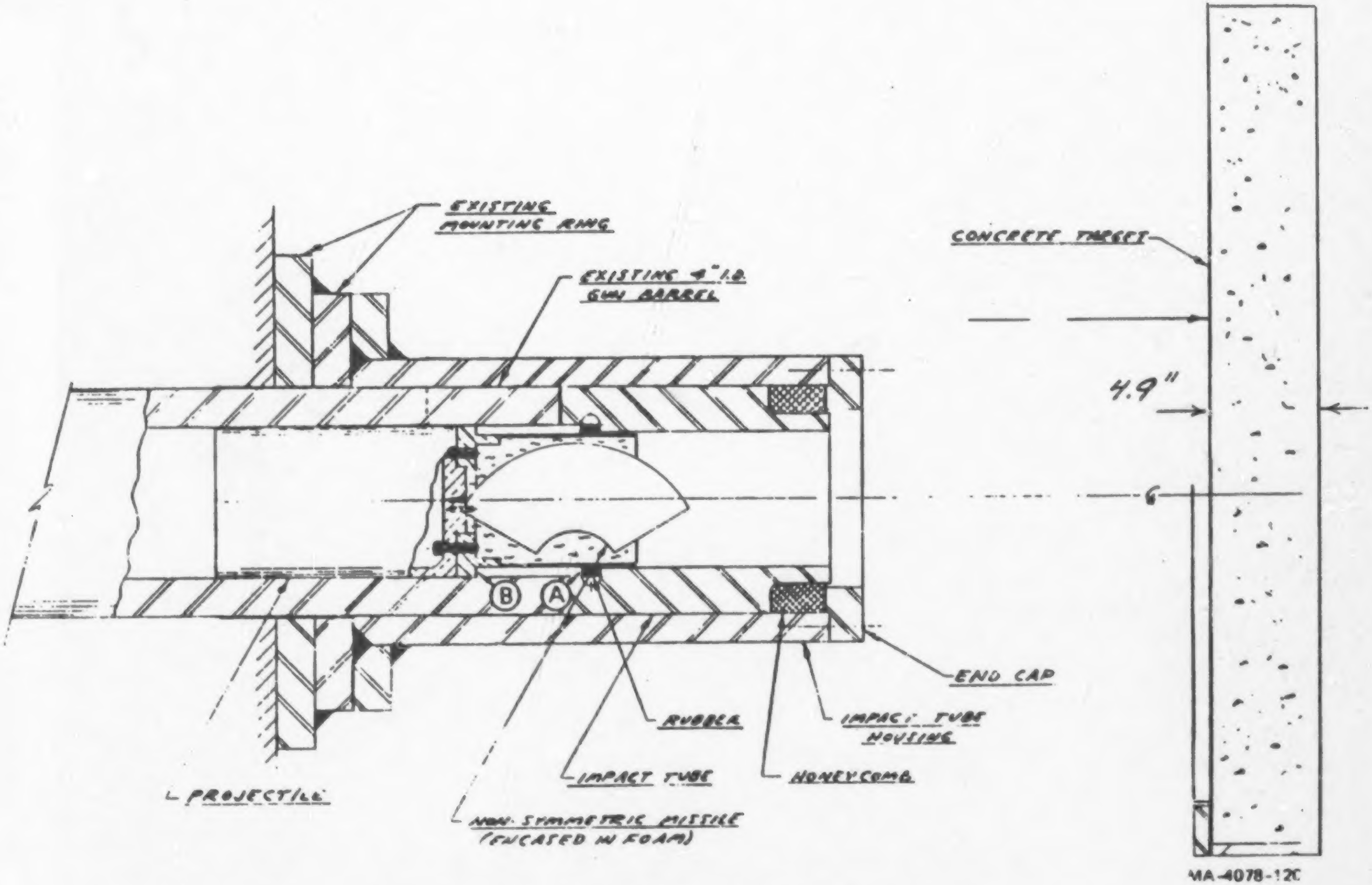
EXISTING MOUNTING RING
EXISTING 4" I.D. GUN BARREL
CONCRETE TARGET
4.9"
B
A
END CAP
RUBBER
IMPACT TUBE HOUSING
IMPACT TUBE
HONEYCOMB
PROJECTILE
NON-SYMMETRIC MISSILE (ENCASED IN FOAM)
MA-4078-12C

Fig. 8 Test Arrangement for 1/11-scale Gas Gun Tests

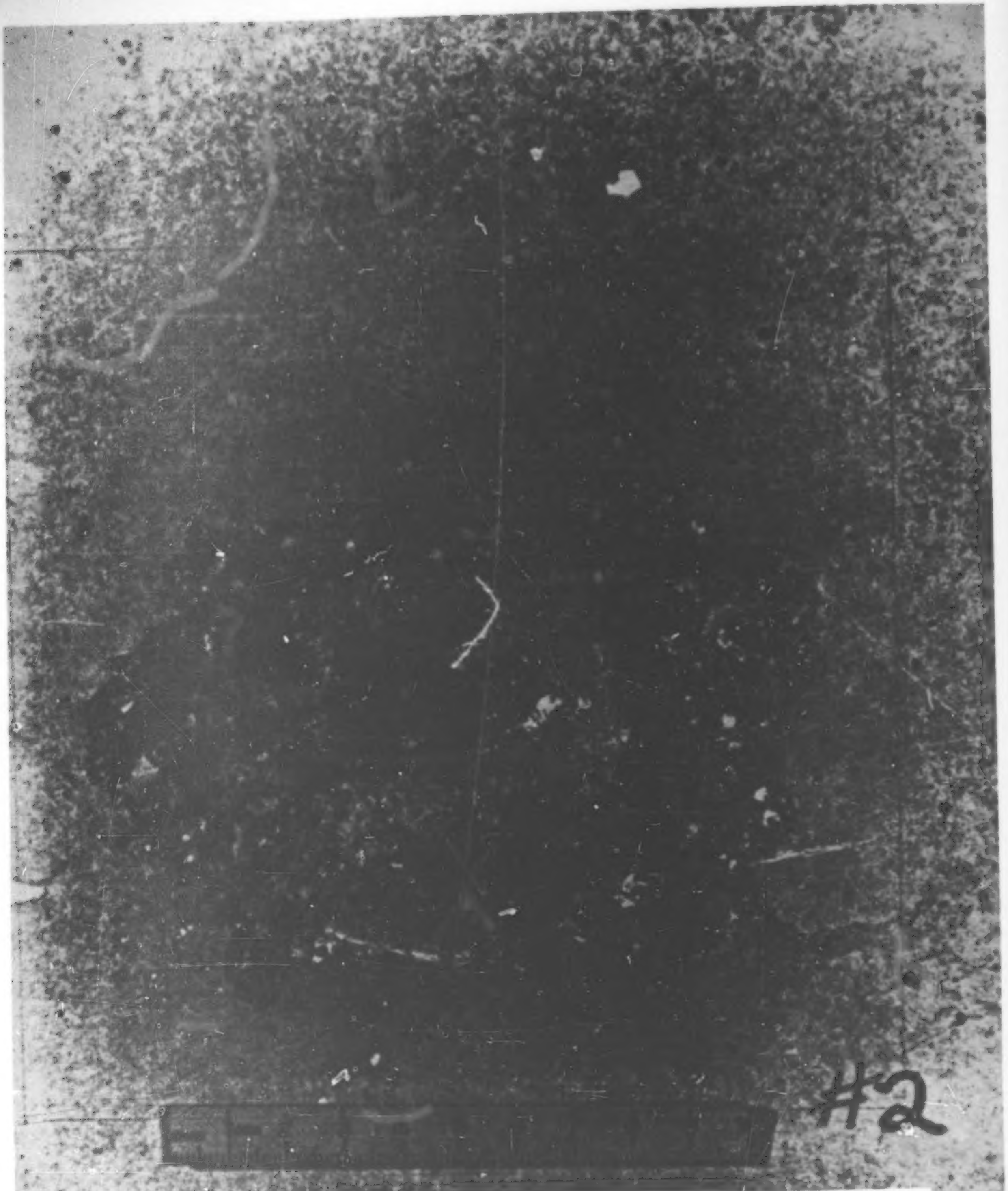

Fig. 9 Frontface Crater in Scale-Model Panel (305fps)

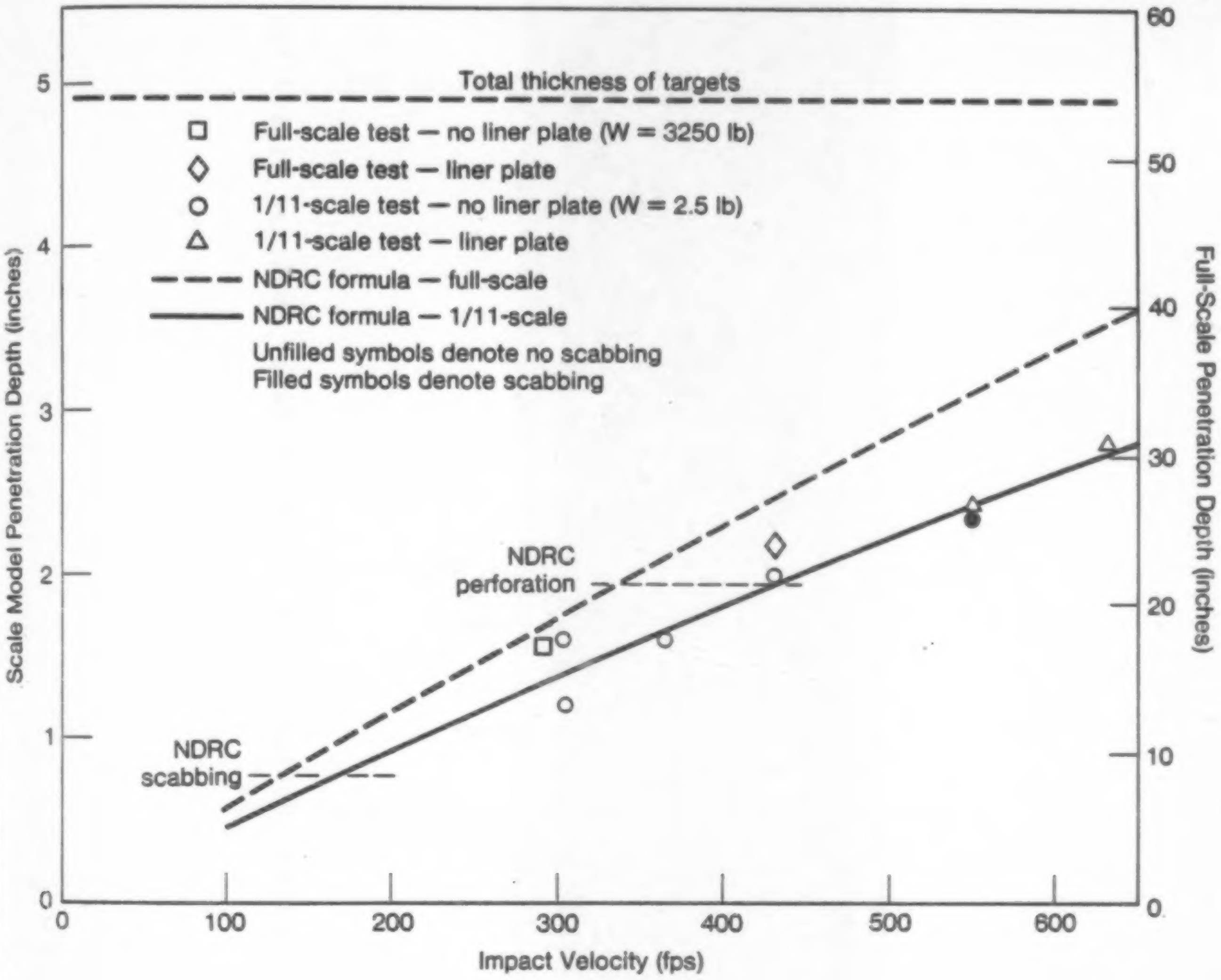

Fig. 10 Penetration versus Impact Velocity in Scale-model and Full-scale Tests

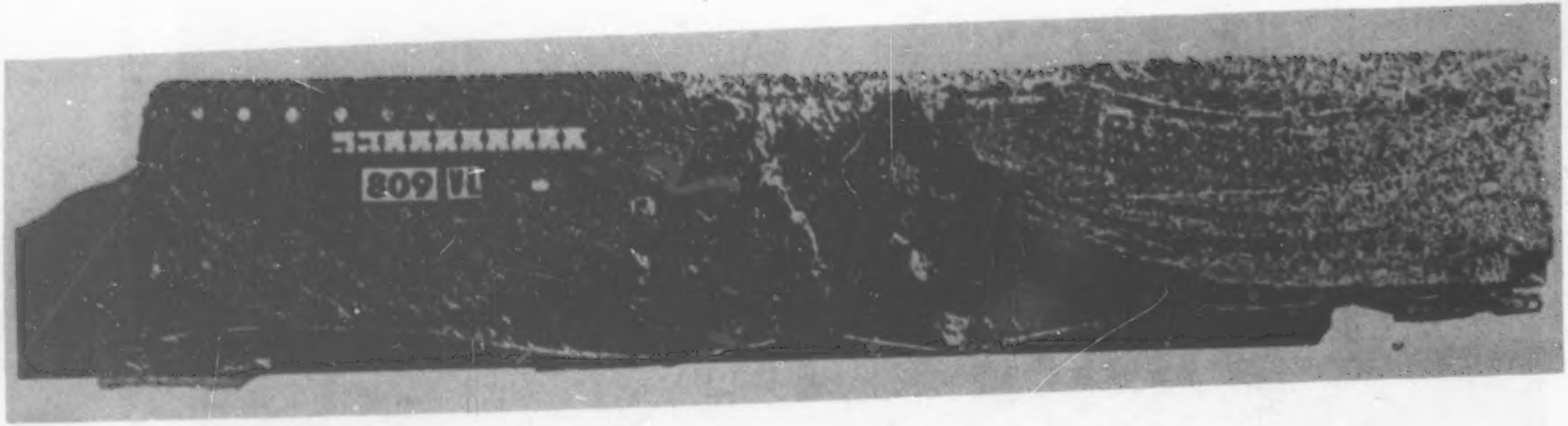

Fig. 11 Cross-section of 3.8 in. thick Panel Impacted at 647 fps

THE ANALYSIS OF SMALL BREAK TESTS

R. B. Duffey
K. H. Sun
S. P. Kalra
Y. Zvirin

Electric Power Research Institute
3412 Hillview Avenue
Palo Alto, CA 94303

Paper Presented at:

NRC Water Reactor Safety Information Meeting
Gaithersburg, Maryland
October 29, 1980

best copy available

THE ANALYSIS OF SMALL BREAK TESTS

Introduction

The need to analyze the consequences of small breaks on the operational behavior of LWRs has recently come to the forefront. There are four main areas of interest in PWRs as the liquid inventory initially decreases and then increases:

1) the transition from forced flow to single-phase natural circulation;

2) the breakdown of single-phase circulation and the onset of two-phase natural circulation;

3) the onset of core uncovery and the potential for core dryout and heat up;

4) the cooling of distorted cores and the recovery of the fuel to restore natural circulation.

Natural Circulation

Present procedures call for tripping of the reactor pumps (which also may occur for a station blackout), so that natural circulation must cool the reactor until safety injection or RHR is operative. The analysis of PWR natural circulation proceeds traditionally using the one-dimensional loop flow equations for mass, momentum, and energy. The irreversible friction and form losses are treated by correlations, so that the steady-state core ΔT is given by

$$\Delta T = (Q/\rho_\ell c_\ell)^{2/3} \, (r/2g\beta\Delta z)^{1/3} \qquad (1)$$

where Δz is the effective driving head for the loop.

Comparison to plant and experimental is shown in Fig. 1, and the agreement is generally within the uncertainties in the loop flow resistance, r, and reactor power, Q.

Now natural circulation represents an ultimate passive heat rejection capability and, provided adequate subcooling is maintained, is both stable (following loss of pumps) and predictable. This is supported by the available full-scale plant data for both tests and operational transients, and by model experiments with a four-loop representation.

Single-phase natural circulation can break down if the water inventory continues to fall due to a break or leaks thus interrupting the flow path. The remaining fluid would then temporarily stagnate in the loops, until boiling commences in the core and vessel. Two-phase natural circulation can then occur, with the steam generators condensing the vapor and cooling the primary water.

We can analyze the resulting pressure transient by treating the loop as a "lumped" system with the following result. The primary pressure variation, P, is related to the primary/ secondary heat transfer mismatch, ΔQ, through the relation

$$P \sim P_o \exp\left[\Delta Q / \left(\frac{RT^2 M_\ell C_\ell}{h_{fg}} + \rho_s V_s h_{fg}\right)\right] t$$

where V_s is the volume of steam in the primary loop.

The system is pressure-controlled by saturated vapor in the vessel head and "U" tubes, and not by the pressurizer. Thus any change in the primary to secondary heat transfer reflects as a pressure transient. Comparison to a model "U" tube experiment is shown in Fig. 2, where the two-phase circulation proceeds to a final stable state after some unstable flow and pressure transients.

Loss-of-Feedwater

One other process which affects the natural circulation behavior is the secondary side two-phase level, since this represents the effective heat sink elevation to supply the buoyancy force. We can therefore rewrite eq. (1) with

$$\Delta z = 1/2\ (z_{2s} - z_c) + \Delta L$$

where z_c and z_{2s} are the core and secondary-side mixture elevations, respectively, and ΔL the physical elevation difference between the core and steam generator.

Hence, modelling the secondary side level, z_{2s}, is extremely important. Loss-of-feedwater transients can cause the generator to eventually boil dry if auxiliary feedwater is not available. Tests at the Semiscale facility have shown that primary side natural circulation may continue for a while, presumably due to small heat loss and fluid inertia effects, ensuring the stability of the initial condition.

The variation of the secondary side level can be estimated utilizing two mass conservation equation, the mixture energy equation, and a void fraction correlation. The variation in level is linear until the tube bundle starts to uncover, from when it varies exponentially. The two-phase level variation is approximately given by

$$z_2 \sim Z_{20} \exp - [A]t \qquad (2)$$

where

$$A = 4\, C_o q^{11}/(C_o - 1)\, \rho_\ell\, h_{fg}\, D_e\, (1 + a_d/a_b)$$

The above is for the case of total loss-of-feedwater and hence gives the generator dryout time. We have shown that such an analysis agrees with model experiments and correlates with multidimensional computations.

Core Uncovery

Continued loss of inventory can eventually lead to core uncovery. The two-phase mixture level is the location of the hydrodynamically controlled dryout location for the core, and the definition of a "collapsed-liquid" level, z_1, enables the core flow to be estimated from a loop momentum balance. For PWRs this flow is from the downcomer; for BWRs with a core shroud, it is provided by leakage from the core bypass through the channel leakage orifice. Basically both cases are two-phase natural circulation. The calculation of the mixture height can again neglect momentum effects within the channel. It can be shown that the two-phase mixture level is simply related to the other thermal-hydraulic parameters [cf. eq. (2)].

Comparison to experimental data shows that the exact form of the void-fraction correlation is not important at high pressure. Results for both BWR and PWR data are shown in Fig. 3, and the analysis has been compared with single tube, bundle, and low and high pressure data.

Core heat up above the two-phase mixture level is part of a joint Westinghouse/EPRI effect. Here results from large (330 pin) bundle boil-off experiments are being made freely available by W for analysis of the heat transfer. The results will examine the extent to which modification to simple forced convective correlations are necessary. The flow regime is mixed forced and free-convection above the two-phase level when the mixture levels are low.

Cooling Distorted Cores

If sufficient clad heat up occurs coupled with reactor depressurization, local swelling of the clad can result. Since the core must be recovered by injected water, the flow blockage effect on heat transfer must be analyzed. Earlier theory for reflooding is applicable which estimates the flow diversion based on flow resistances. Recent comparison to data includes cases of: (a) 65% blockage in a 4-rod zircaloy bundle; (b) 90% blockage in the 25 rod KFK bundle; and (c) 65% blockage in the NRC/EPRI/W-FLECHT/SEASET 21 rod bundle. These three tests have significant bypass flow, and both long and short blockages, and all are in agreement with the theory. They all show an effect of the heat transfer enhancement in the low flow region downstream of the blockage. Thus the heat removal is not degraded as much as might have been expected on the basis of the local flow diversion alone.

Final Remarks

The above outline indicates the main areas of analysis and research necessary for small breaks. These are:

1. natural circulation, both single- and two-phase;

2. pressure transients due to nonequilibrium flows and phase-separation;

3. two-phase level modelling in the steam generator, reactor vessel, and reactor core;

4. analysis of low flow heat transfer;

5. estimation of the cooling of distorted clad geometry and partially blocked reactor cores.

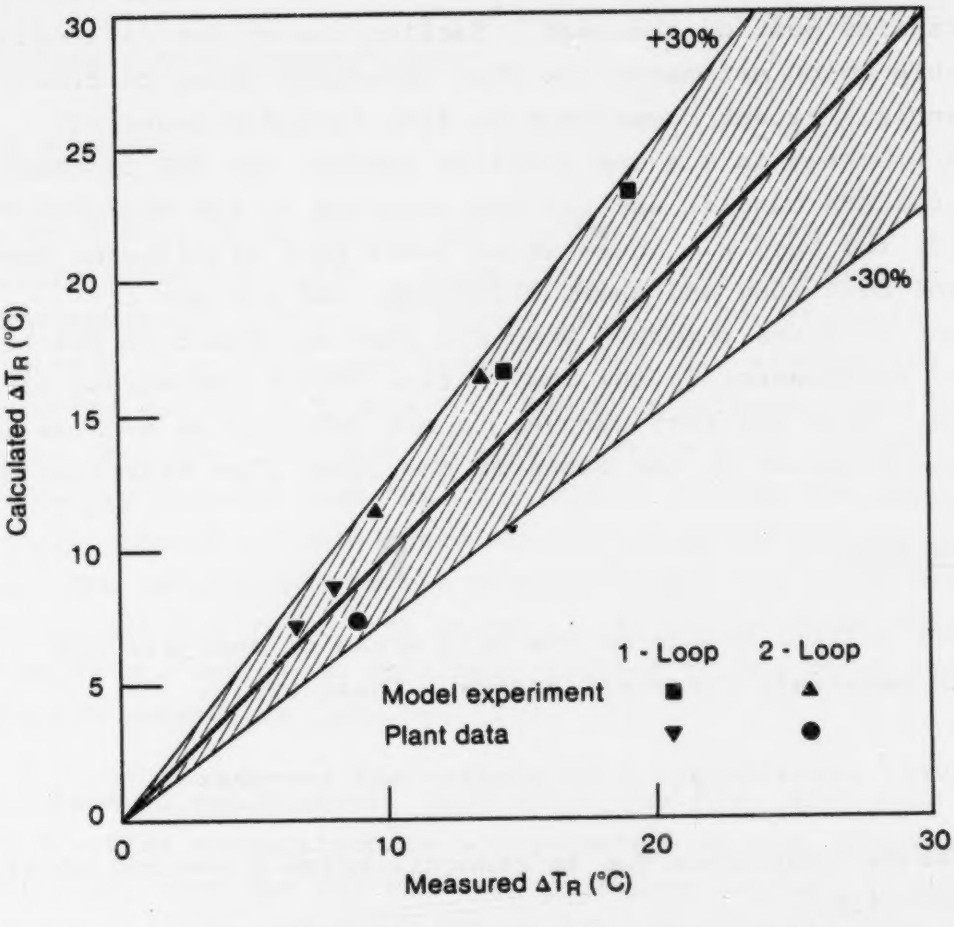

Figure 1 Comparison of experimental and plant data and theoretical calculations.

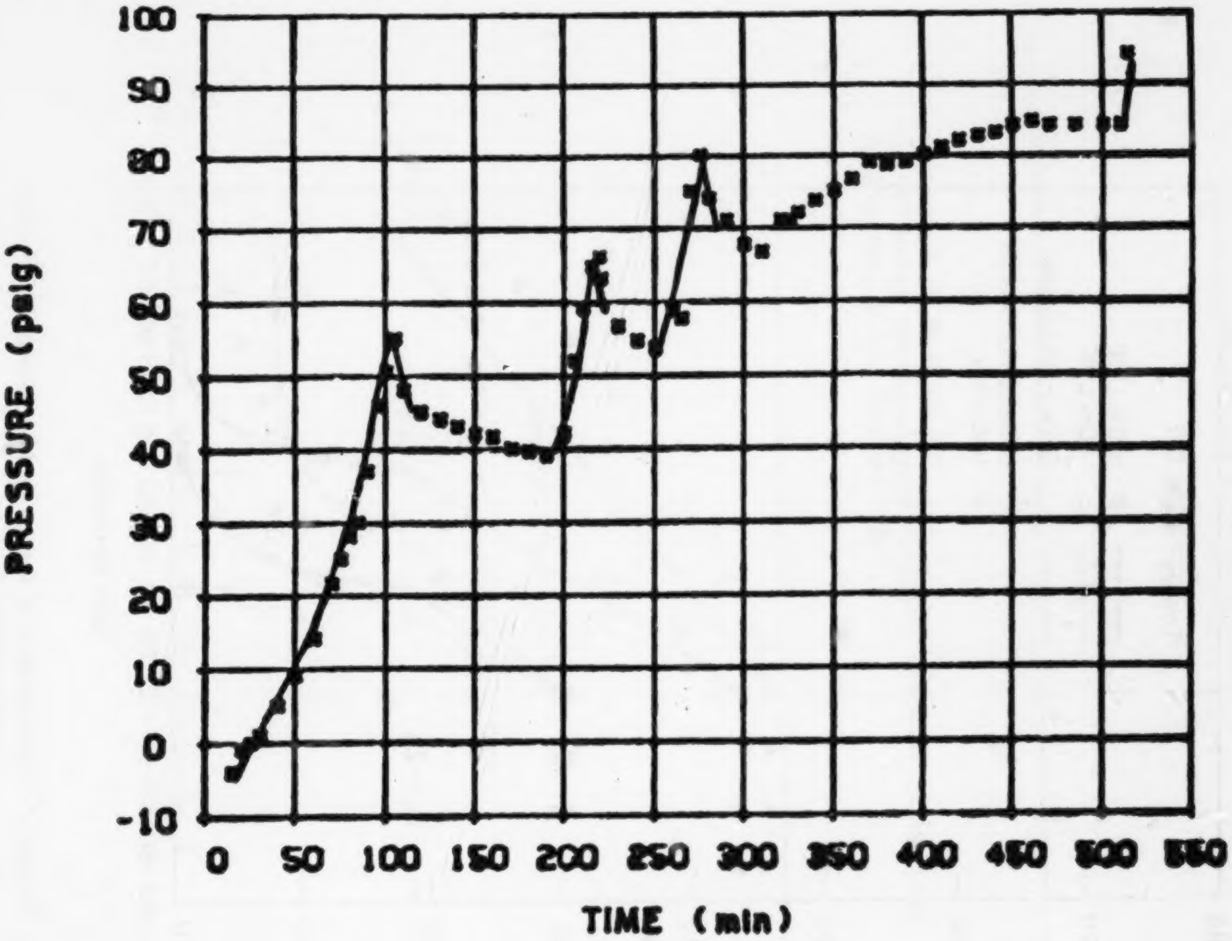

PRESSURE HISTORY

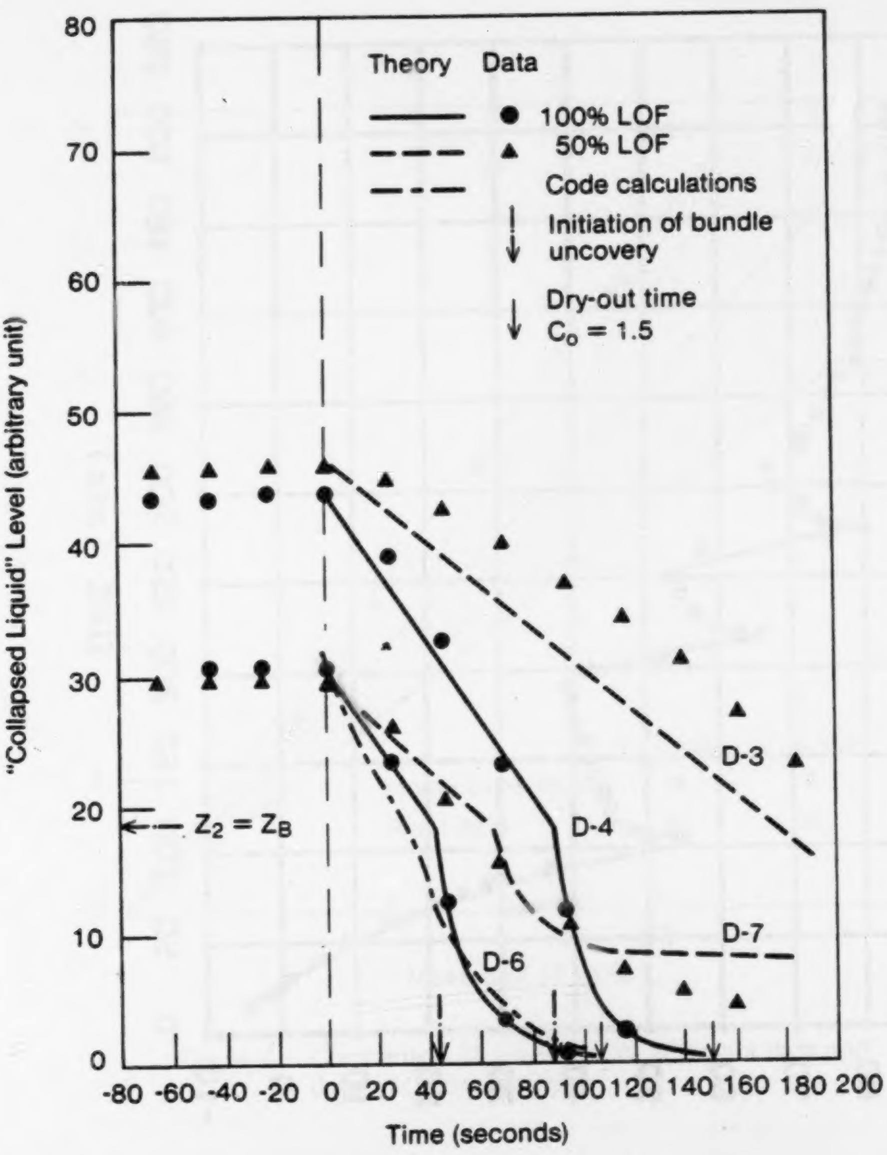

Figure 3 Comparison of theory and experiment: the tube bundle uncovers when $Z_2 \angle Z_B$.

EPRI

VALIDATING RISK ANALYSIS
TWO ASPECTS

Presented at the
Eighth Water Reactor Safety Research Information Meeting
Washington, D.C., October 1980

Gerald S. Lellouche
Nuclear Safety and Analysis Department

ELECTRIC POWER RESEARCH INSTITUTE

VALIDATING RISK ANALYSIS
TWO ASPECTS

Introduction

The work we wish to present today is not complete. It is, however, sufficiently suggestive to make it interesting and demonstrates that PRA has many facets that can be fruitfully polished. We shall touch on two continuing areas of EPRI research:

- Experimental verification of system behavior through time compression
- Competing risks

The value in studies of this sort are, we believe, clear and important to the industry. They deal with two topics of interest:

- Data base uncertainties
- The value of safety related fix.

I. EXPERIMENTAL VERIFICATION OF SYSTEM BEHAVIOR

ERMA
EPRI Reliability and Maintainability Analyzer

How good is a fault tree? How important are the uncertainties associated with a few hundred reactor-year data base? How important are common mode/cause phenomena? These were the questions that were in our minds several years ago when we started to search for a way to design an experiment which could be run to gather the system behavior which would answer them.

The first phase of the experiment is complete. We have a method of achieving a time compression of 10^{10} which allows a year of operation to run in about 3 milliseconds. We have built several subsystem mock ups and gathered lifetime data on them. We have not yet fully addressed the underlying questions which started the study but we have raised new ones and perhaps answered still other questions not originally asked.

ERMA is an electronic gadget. It is made up of items called Fast Failure Components (FFCs) and is connected to a batch of electronic intrumentation and recorders which monitor the behavior of the device. A modular schematic of an FFC appears in Fig. 1. where:

FRG = Failure Rate Generator
RRG = Repair Rate Generator
RPG = Random Pulse Generator
SRG = Scheduled Repair Generator

All rate information can be either constant or time dependent or distributed and time dependent (Bayesian), mixtures are allowed as well. These devices can be connected together to form a system configuration. Such a configuration can be in a tree form or in an actual series/parallel circuit diagram. One configuration for an 18 component low pressure coolant injection system (LPIC) is found in Fig 2. The operation of ERMA requires a fair amount of periferal equipment which drives and monitors the hardware. This is illustrated in Fig. 3.

For the case at hand, ERMA was run for three independent experiments of this fault tree using constant failure and repair rates. Each run consisted of recording system unavailability over 50,000 - 60,000 years, with a plant lifetime of 50 years. Figure 4 is a plot of system unavailability as a function of total elapsed time for each of the three runs. This figure illustrates (1) the convergent behavior of the system after long times to an unavailability about 9.5×10^{-4}, and (2) the unique and random approach to convergence (i.e., fluctuation) for independent runs.

It is this unique approach to equilibrium which opens up the question of an initial fluctuation which may produce a long term system behavior better or worse than the asymptatic value would indicate. Although we have not investigated it as yet, it may be that plant behavior and maintainence in the first year largely determines future behavior and this may be the origin of plant variability as exemplified by total number of scrams (for example). A second feature which was unexpected has to do with the impact of wearout phenomena (bathtub curves). In a twelve component configuration of an LPIS we examined the differences in system response induced by using failure rates that are constant as opposed to time dependent rates with an average equal to the constant rate value. In this case, we ran some 2300 lifetimes of 50 years each and plotted up the year by year failure rates. These are found in Fig. 5. Firstly, the constant failure rate model while having only small variation from year to year does show some structural regularities. The bathtub situation, however, shows detailed structure closely related to the wearin-wearout behavior, and does not have the same average value as the constant failure rate case. Again, the implications of these results are not yet clear but are very intriguing. A full report on ERMA will be available by the end of the year.

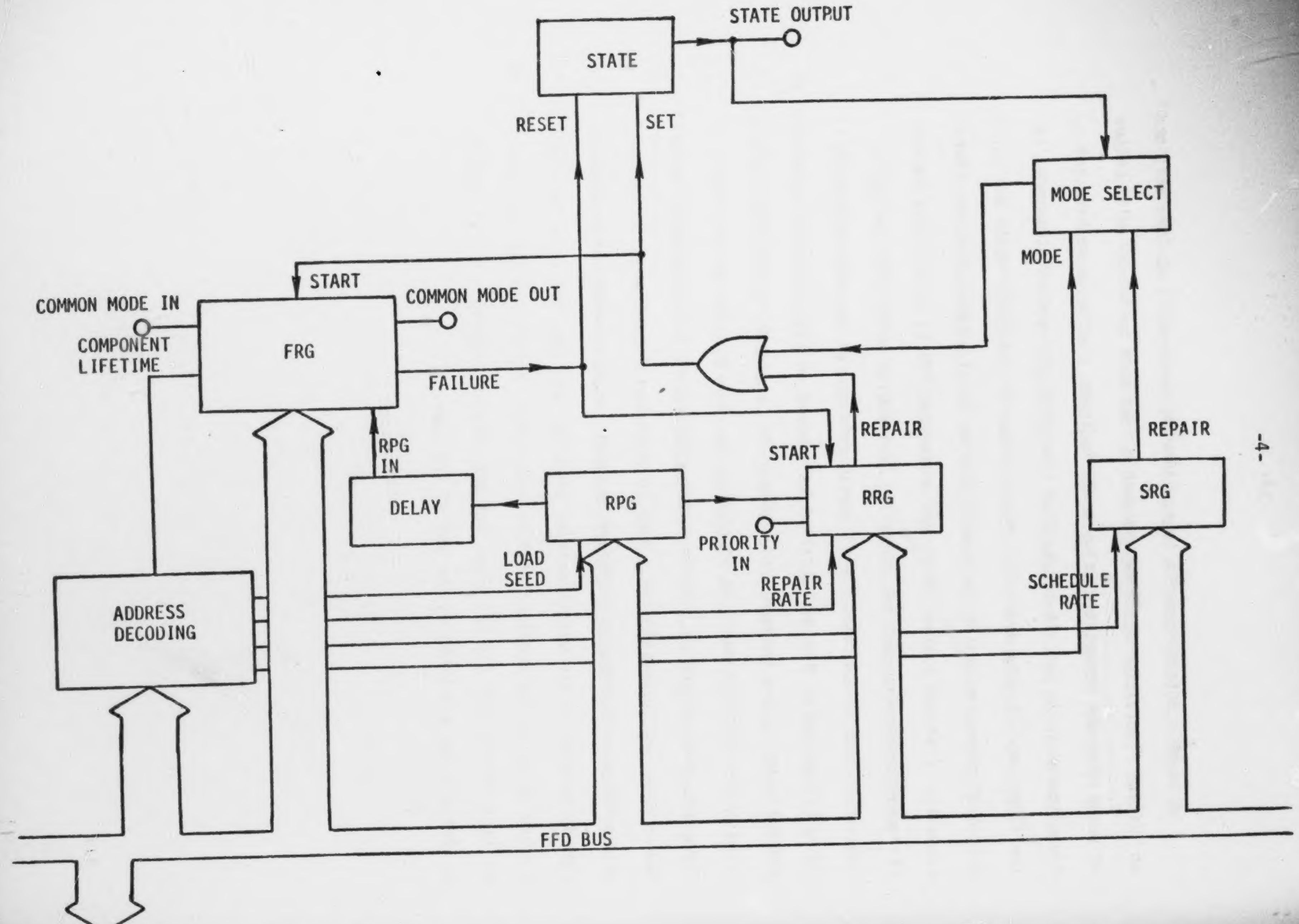
STATE
STATE OUTPUT
RESET
SET
MODE SELECT
MODE
START
COMMON MODE IN
COMMON MODE OUT
COMPONENT LIFETIME
FRG
FAILURE
RPG IN
DELAY
RPG
START
REPAIR
RRG
REPAIR
SRG
PRIORITY IN
LOAD SEED
REPAIR RATE
SCHEDULE RATE
ADDRESS DECODING
FFD BUS

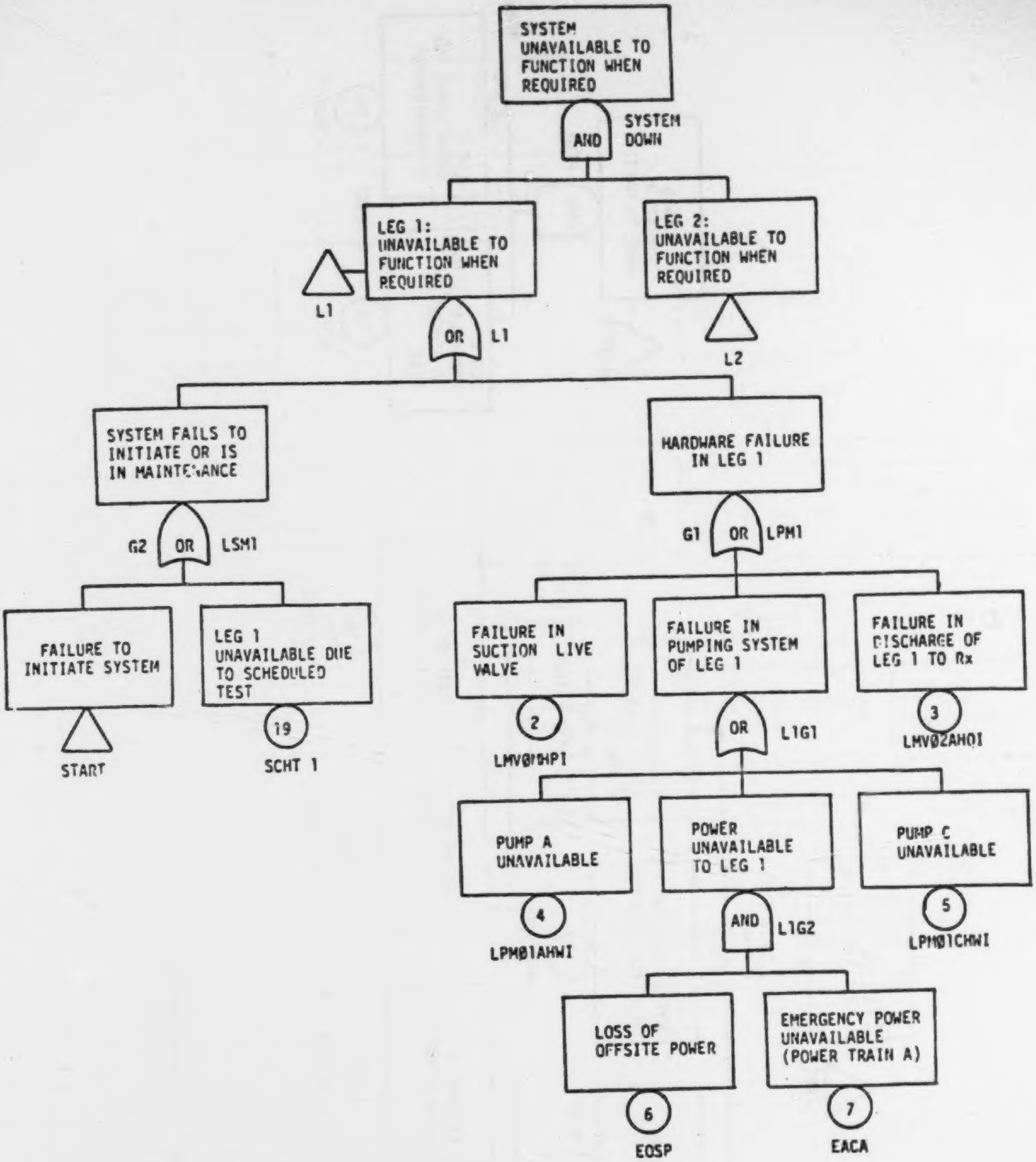
SYSTEM UNAVAILABLE TO FUNCTION WHEN REQUIRED
AND
SYSTEM DOWN
LEG 1: UNAVAILABLE TO FUNCTION WHEN REQUIRED
L1
LEG 2: UNAVAILABLE TO FUNCTION WHEN REQUIRED
L2
OR
L1
SYSTEM FAILS TO INITIATE OR IS IN MAINTENANCE
G2
OR
LSM1
HARDWARE FAILURE IN LEG 1
G1
OR
LPM1
FAILURE TO INITIATE SYSTEM
START
LEG 1 UNAVAILABLE DUE TO SCHEDULED TEST
19
SCHT 1
FAILURE IN SUCTION LIVE VALVE
2
LMV0MHPI
FAILURE IN PUMPING SYSTEM OF LEG 1
OR
L1G1
FAILURE IN DISCHARGE OF LEG 1 TO Rx
3
LMV02AHOI
PUMP A UNAVAILABLE
4
LPM01AHWI
POWER UNAVAILABLE TO LEG 1
AND
L1G2
PUMP C UNAVAILABLE
5
LPM01CHWI
LOSS OF OFFSITE POWER
6
EOSP
EMERGENCY POWER UNAVAILABLE (POWER TRAIN A)
7
EACA

Figure 2. Fault Tree Configuration for Eighteen-Component Low Pressure Coolant Injection System

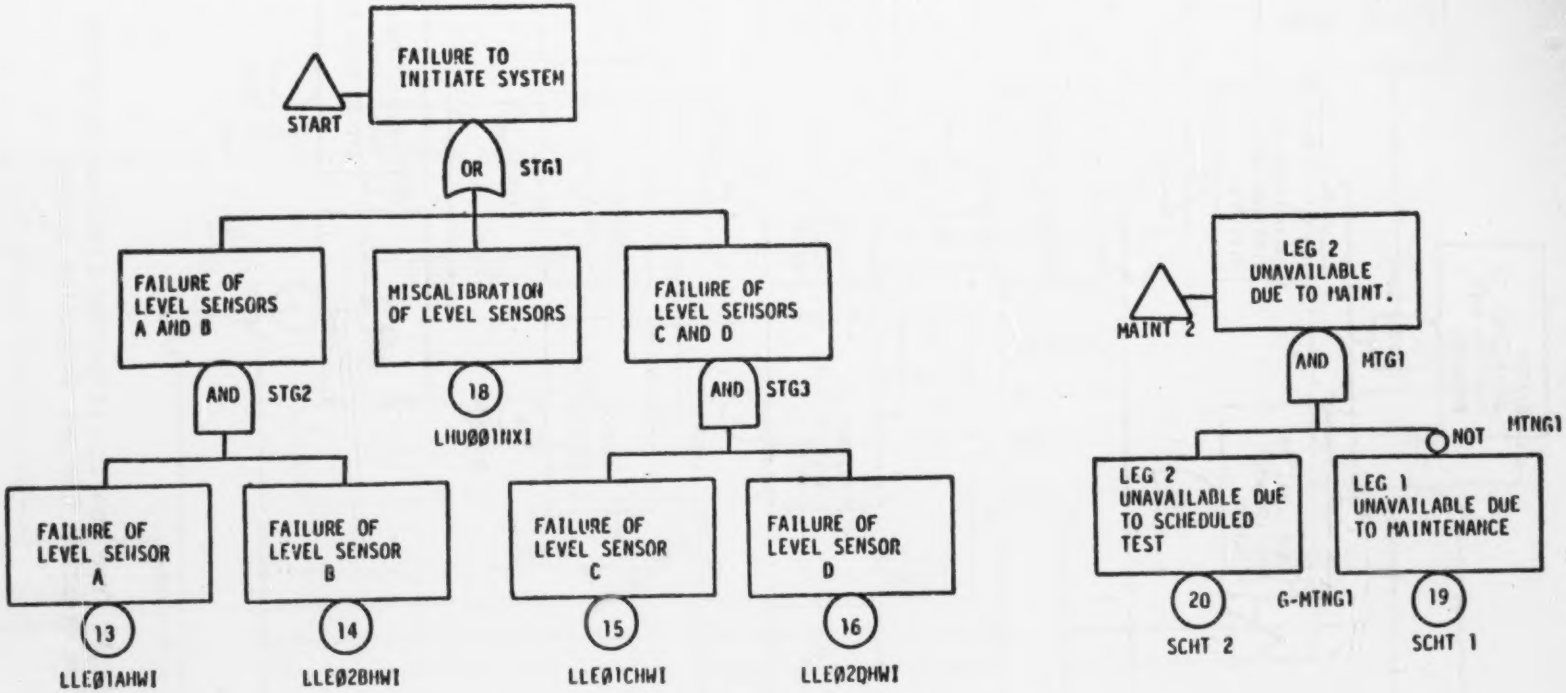
START
FAILURE TO INITIATE SYSTEM
OR
STG1
FAILURE OF LEVEL SENSORS A AND B
AND
STG2
MISCALIBRATION OF LEVEL SENSORS
18
LHU001HXI
FAILURE OF LEVEL SENSORS C AND D
AND
STG3
FAILURE OF LEVEL SENSOR A
13
LLE01AHWI
FAILURE OF LEVEL SENSOR B
14
LLE02BHWI
FAILURE OF LEVEL SENSOR C
15
LLE01CHWI
FAILURE OF LEVEL SENSOR D
16
LLE02DHWI
MAINT 2
LEG 2 UNAVAILABLE DUE TO MAINT.
AND
MTG1
NOT
MTNG1
LEG 2 UNAVAILABLE DUE TO SCHEDULED TEST
20
SCHT 2
G-MTNG1
LEG 1 UNAVAILABLE DUE TO MAINTENANCE
19
SCHT 1

Figure 2. (Continued)

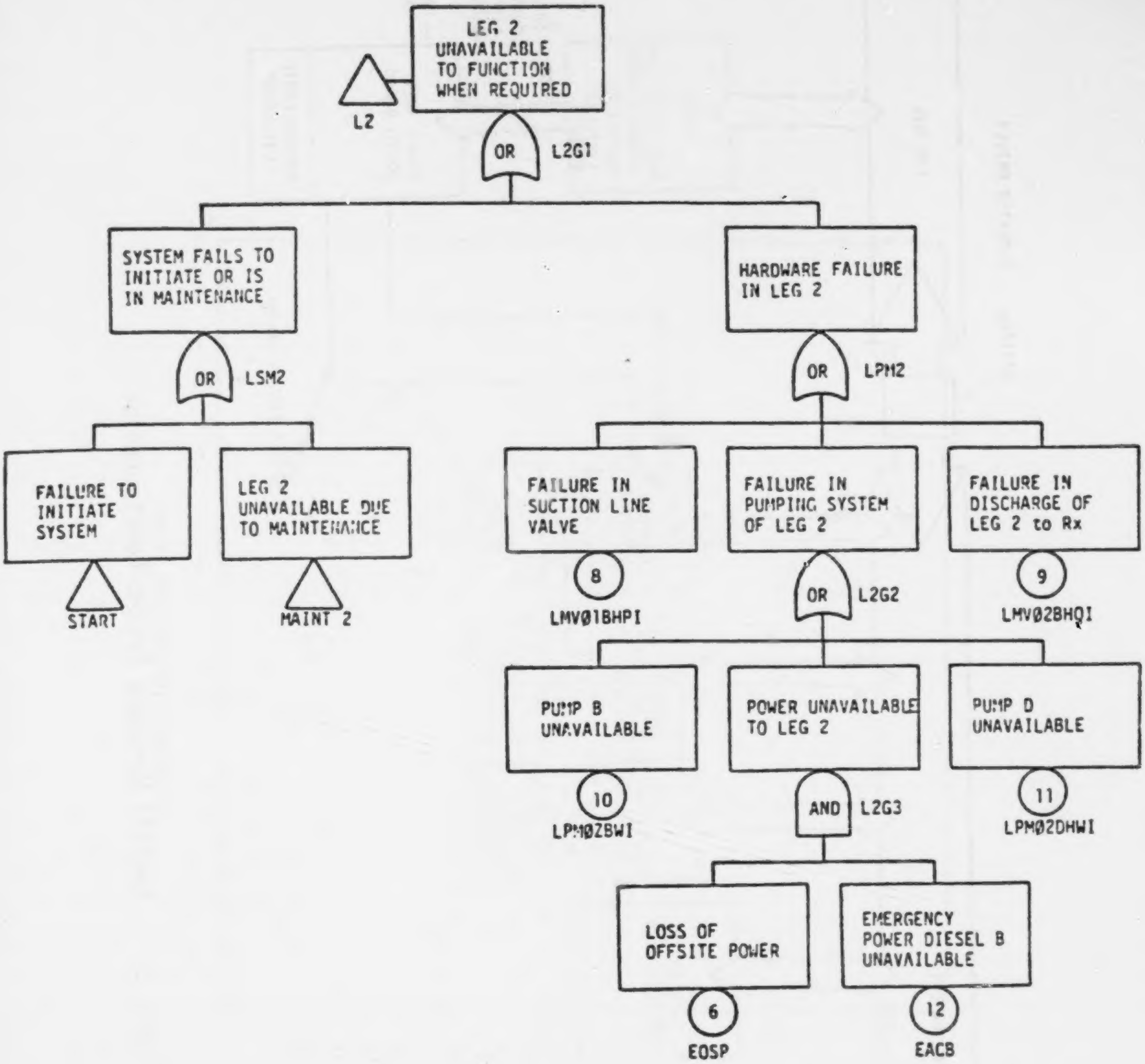
LEG 2 UNAVAILABLE TO FUNCTION WHEN REQUIRED
L2
OR
L2G1
SYSTEM FAILS TO INITIATE OR IS IN MAINTENANCE
OR
LSM2
HARDWARE FAILURE IN LEG 2
OR
LPM2
FAILURE TO INITIATE SYSTEM
START
LEG 2 UNAVAILABLE DUE TO MAINTENANCE
MAINT 2
FAILURE IN SUCTION LINE VALVE
8
LMV01BHPI
FAILURE IN PUMPING SYSTEM OF LEG 2
OR
L2G2
FAILURE IN DISCHARGE OF LEG 2 to Rx
9
LMV02BHQI
PUMP B UNAVAILABLE
10
LPM0ZBWI
POWER UNAVAILABLE TO LEG 2
AND
L2G3
PUMP D UNAVAILABLE
11
LPM02DHWI
LOSS OF OFFSITE POWER
6
EOSP
EMERGENCY POWER DIESEL B UNAVAILABLE
12
EACB

Figure 2. (Continued)

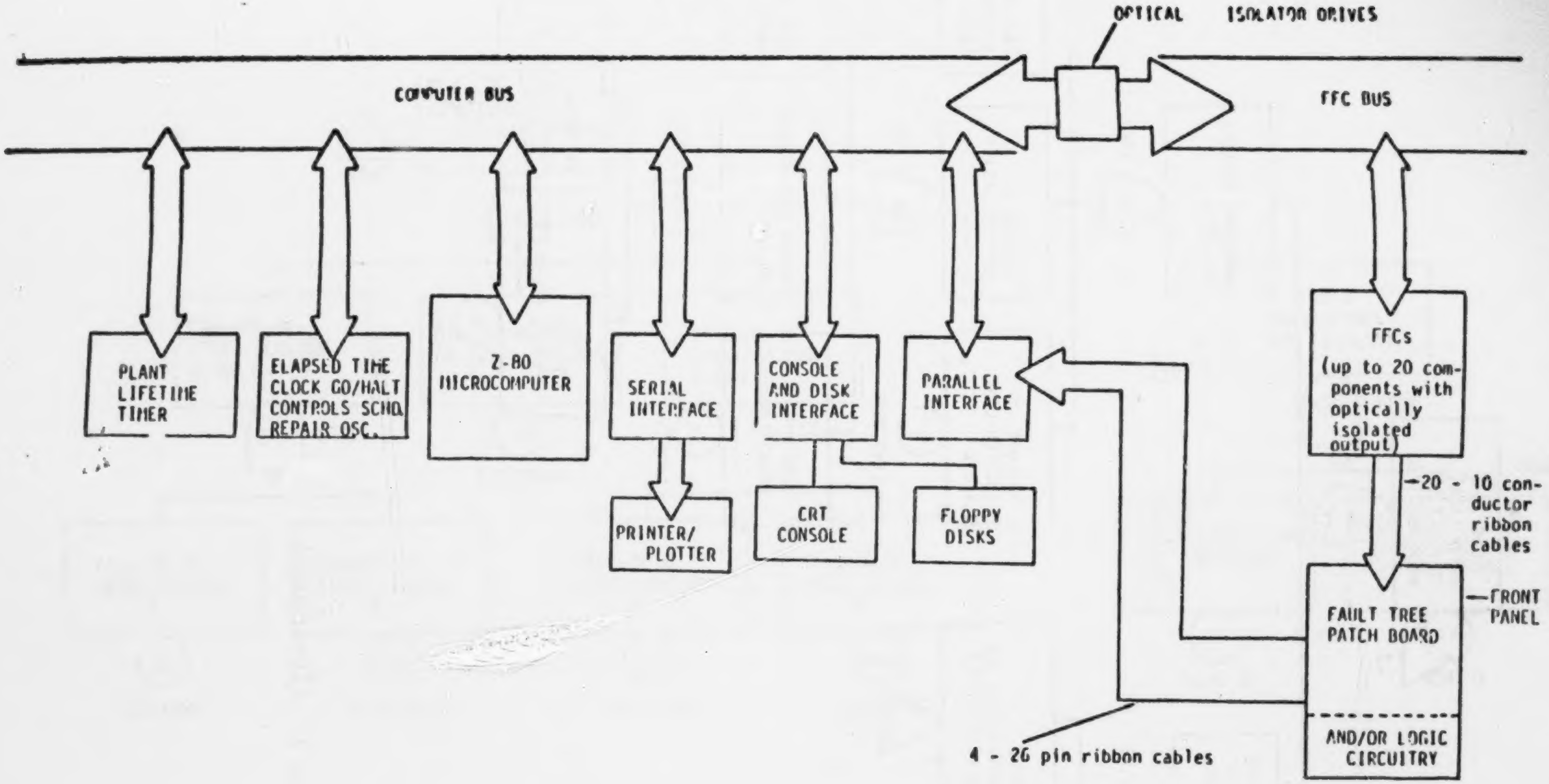
OPTICAL ISOLATOR DRIVES
COMPUTER BUS
FFC BUS
PLANT LIFETIME TIMER
ELAPSED TIME CLOCK GO/HALT CONTROLS SCHD. REPAIR OSC.
Z-80 MICROCOMPUTER
SERIAL INTERFACE
PRINTER/ PLOTTER
CONSOLE AND DISK INTERFACE
CRT CONSOLE
FLOPPY DISKS
PARALLEL INTERFACE
FFCs (up to 20 components with optically isolated output)
20 - 10 conductor ribbon cables
FRONT PANEL
FAULT TREE PATCH BOARD
AND/OR LOGIC CIRCUITRY
4 - 26 pin ribbon cables

Figure 3. Overall Hardware System Configuration

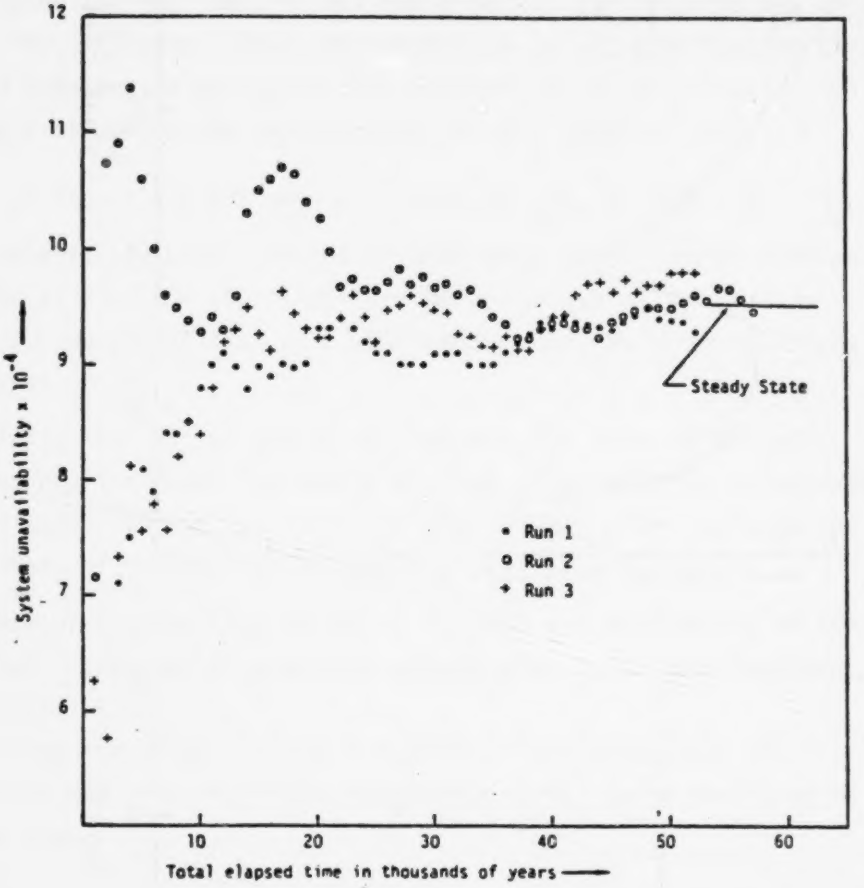

Figure 4. Low Pressure Coolant Injection System Results with ERMA

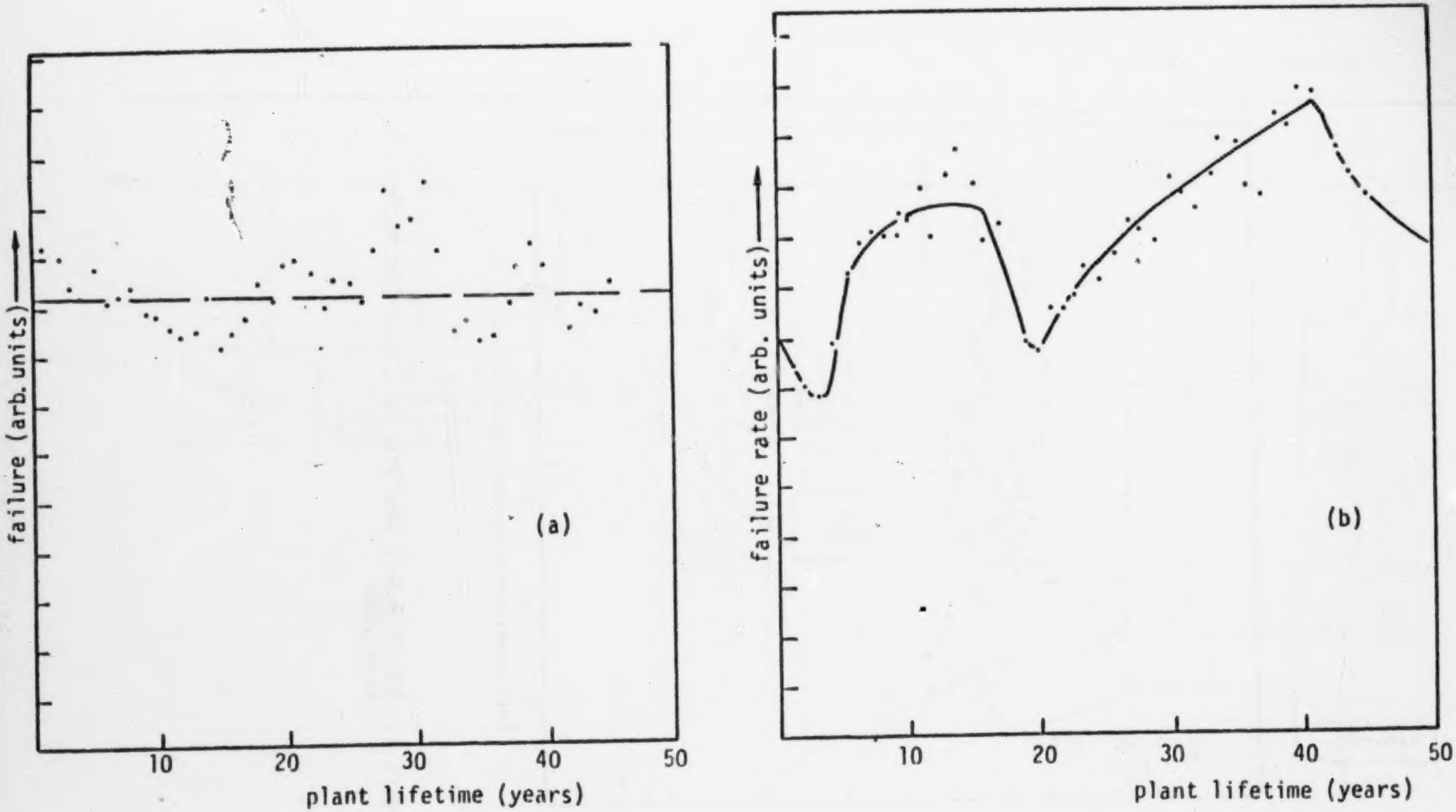

Figure 5. Measure Failte Rate vs. Plant LIfetime for a Six-Component System With (a) Constant Component Failure RAtes, and (b) Time Dependent Component Failure Rates

II. COMPLETING RISKS

ATWS

Any safety-oriented plant modification contains within it the probability of accomplishing the goal desired and the potential for creating new or altered pathways for accidents. Thus, the usefulness of any modification lies in a trade-off between the decreased risk inherent in the modification and the increased risk due to the new accident pathways created by it.

Examples of this trade-off are well known and some of them are:

1. The Interfacing LOCA (Event V of WASH 1400) where locking open an MOV to eliminate a single failure point for use of the LPIS increased the probability of a LOCA through the two check valves by a factor of 10.
2. Requiring the auxfeed system to actuate (post TMI) for certain events has increased the number of pressurizer emptying transients which appear to the operator as a LOCA and therefore increase the liklihood of operator misaction.
3. Closure of the blocking valves on the PORV and maintenance of the HPI has increased the number of safety valve actuations (and led to Crystal River).

Each of these are competing risk situations where unexpected results and increased risk are obtained from a supposedly safety based modification intended to reduce risk.

In the case of ATWS the staff has suggested that increasing the number of valves on C.E. and B&W plants will reduce ATWS risk. The following analysis shows that this modification induces a competing risk situation and the increased competing risk is greater than the ATWS risk reduction. The competing risk here is a failure of a valve to reseat after it has opened (e.g. TMI-2, Crystal River).

In the following analysis, we shall deal with WASH-1400 for a category characterization of the event sequence but it will be made reasonable that for B&W and C.E. there should be no real differences.

ATWS RISK

An ATWS event sequence leading to potential damage depends on the time into the fuel cycle. Early in the fuel cycle, insufficient fission products have built up so that a large amount of boron is in solution. Up to a time t_1 (Figure 6), even if all the valves open during an ATWS the moderator temperature coefficient will be insufficiently negative to terminate the transient before an excessive pressure level is reached. In this time period the ATWS transient of importance is:

$$(TK\ ,\ 0 - t_1)^*$$

where T stands for the frequency of ATWS transients of significance and K stands for the failure probability per demand of the scram system.

In the second part of the fuel cycle (see Figure 6) the moderator coefficient is sufficiently negative so that, if all the relief valves open, no excessive pressure will be reached, but, if one valve fails to open (symbolized by p^1), then an excessive pressure will be reached. Further into the fuel cycle, two valves would be required to fail to open to cause excessive pressure (p^2); still further 3 valves (p^3), etc. For our purposes, we do not at this time differentiate between one or more valves and denote this sequence and its time range by

$$(T\ K\ P,\ t_1 - t_2)^{**}$$

t_2 is the time in fuel cycle after which even if all valves fail to open no excessive pressure will be reached. This scheme is illustrated in the following figure:

---

* It is important to note that since ATWS is not a homogeneous set of events (some lead to higher pressures than others) the numbers T, t_1 actually comprise a set of pairs (T^1, t_1^1) (T^2, t_1^2)..... (T^i, t_1^i) ordered here so that $t_1^j < t_1^{j+1}$, and the peak pressure due to transient type T^j is less than that due to T^{j-1}. That is, it takes a more negative moderator coefficient to ameliorate transient type T_1^{j+1} than is necessary for type T^j.

** Here also the pair (T, t_2) is not single but depends on transient type as in the time range $(0 - t_1^2)$. Beyond t_2 ATWS is not of safety significance.

Figure 6

ATWS Event Sequences During
the Fuel Cycle

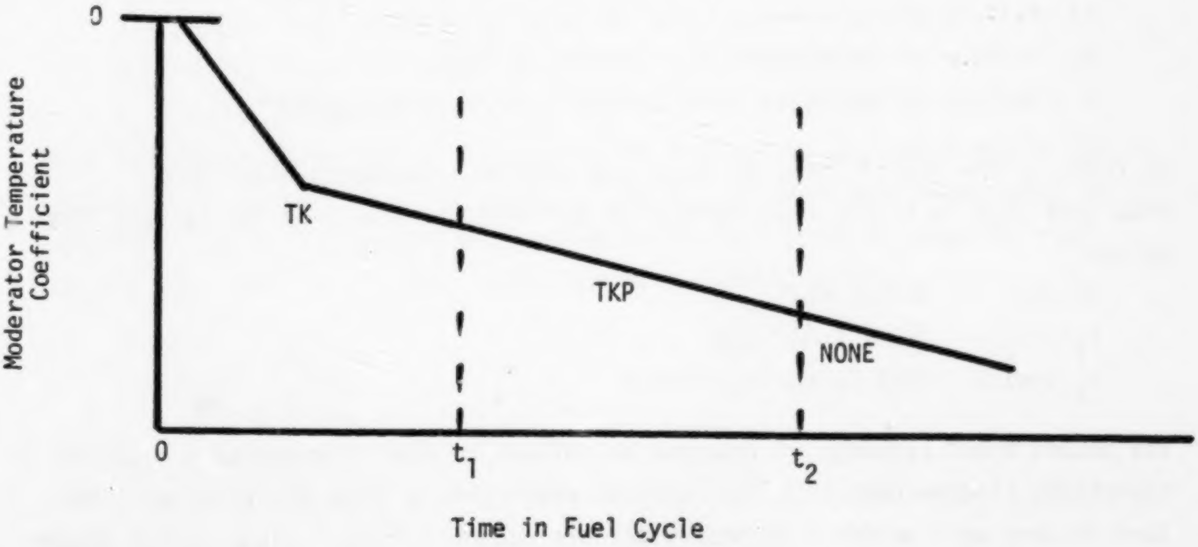

We estimate t_1 to be greater than about 30% of the cycle time and t_2 about 60%. For the very worst transients (total loss of feedwater), t_1 may be about 50% and t_2 may not apply. For our purposes we assume t_1 to be 40% and t_2 to be 80%.

COMPETING RISKS

The only competing risk we deal with here is failure of a valve to reseat. This event is denoted by Q. Clearly, for Q to occur the valve must have opened. The number of stuck open PWR valves is determined from LERs* to be 9. Using a 300 PWR reactor-year experience base, this leads to a transient frequency of 0.03/ reactor year.

There are two types of event sequences where failure to reseat is significant. The first is the ATWS event itself where the sequence - TKQ - leads to a small LOCA during the entire fuel cycle. Any additional serious failure (of HPI or other necessary system) leads to a core melt. In WASH 1400 terminology these additional failures are:

C - Failure of Containment Spray Injection System
D - Failure of Emergency Core Cooling Injection
F - Failure of Containment Spray Circulation System
G - Failure of Containment Heat Removal System
H - Failure of Emergency Core Cooling Recirculation System

We refer to the sum of these as X and the core melt sequences are: TKQX. Note that TKQX is a core melt during the entire fuel cycle. In the various time period

$0 - t_1$: TK >> TKQX
$t_1 - t_2$: TKP < to << TKQX
t_2 onward: TKQX is the total risk

The second event sequence of interest to failure to reseat is due to a class of transients (independent of scram failure) which lift a valve but which will not lead to core melt unless a secondary failure occurs. These include most T events and other events as well. All of these together include (but are not limited to):

---

* A search of the NTIS tape shows 9 stuck-open valves at various power levels. See App. 1.

Westinghouse	B&W	Combustion
Loss of external Load	Loss of External Load	Loss of External Load
Turbine Trip	Turbine Trip	Turbine Trip
Loss of Normal Feedwater	Loss of Normal Feedwater	Loss of A.C. Power
Loss of all A.C. Power	Cold Pressurization	Cold Pressurization
Cold Pressurization		

and, for all types of operator or maintenance misaction. The totality of these events are denoted by T*. These events have the same potential for failure to reseat as the ATWS events do. In fact, all failures to reseat have occurred for non-ATWS transients, hence the product of T*Q is: $T^*Q = 0.03$/reactor-year. Note that T*Q defines a type of small-small LOCA denoted in WASH 1400 by S_2. In WASH 1400 terms the following S_2 transients lead to core melt:

$S_2D = 9\times10^{-6}$/Reactor Year
$S_2F = 1\times10^{-7}$/Reactor Year
$S_2G = 6\times10^{-6}$/Reactor Year
$S_2H = 6\times10^{-6}$/Reactor Year
$S_2C = 2\times10^{-6}$/Reactor Year

Note that these events occur throughout the fuel cycle with about equal liklihood but can be expected to increase in the future since new operational requirements[†] have resulted in an increase in T* (a different competing risk situation). Returning to WASH 1400, the data indicated that:

$D = 9\times10^{-3}$/demand
$F = 1\times10^{-4}$/demand
$G = 6\times10^{-3}$/demand
$H = 6\times10^{-3}$/demand
$C = 2\times10^{-3}$/demand

hence that

$$(T^*Q)\ (D + F + G + H + C) \equiv T^*QX = 7\times10^{-4}$$

we may now establish a structure for the ATWS competing risk situation based on Figure 7. In this structure the competing risks are independent of the fuel cycle. In order to determine the effect of adding valves one must compare

$$TK\ (t_1) + TKP\ (t_2 - t_1)$$

versus

$$TKQX + T^*QX$$

[†] Arising out of TMI-2 considerations relative to closing blocking valves.

Figure 7

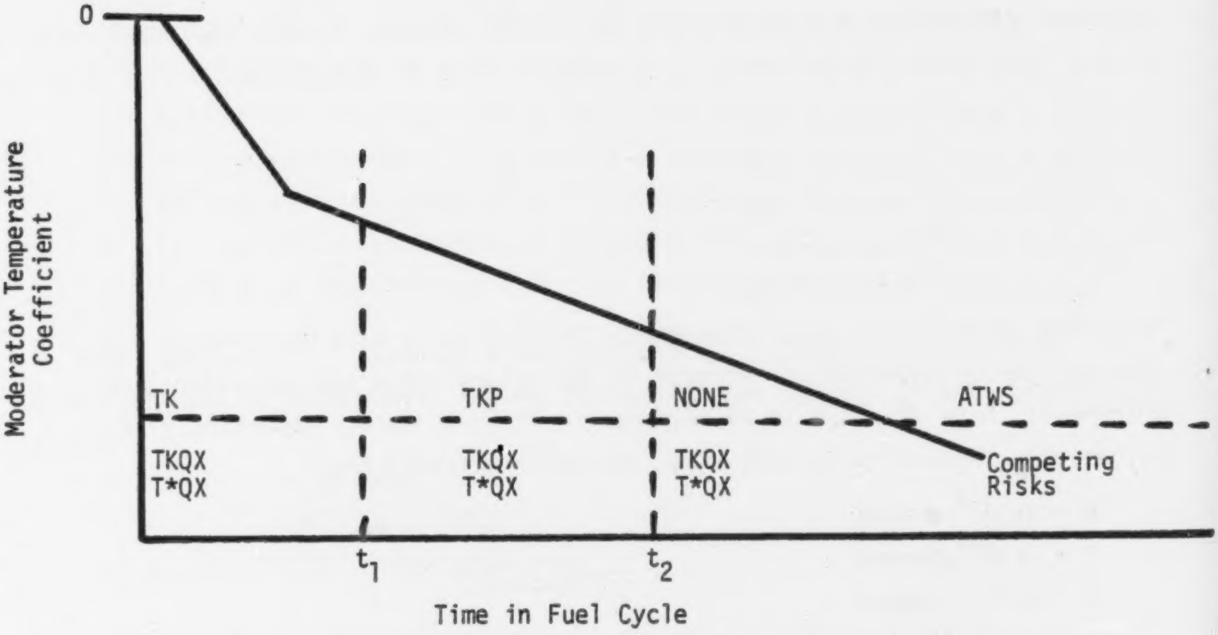
0
Moderator Temperature Coefficient
TK
TKP
NONE
ATWS
TKQX
T*QX
TKQX
T*QX
TKQX
T*QX
Competing Risks
t_1
t_2
Time in Fuel Cycle

We maximize the ATWS risk reduction by assuming $t_1 \sim 1$ in which case we can compare

TK vs. TKQX + T*QX

Since $K \ll 1$, we can neglect (for now) TKQX. NUREG 0460+estimates

$$TK = 1.6\times10^{-4}\text{/Reactor Year}$$

Since $T^*QX = 7\times10^{-4}$/Reactor Year, valve failures to reset already dominate ATWS risk hence any additional valves can only increase the risk.

Note that except for the use of WASH 1400, values for D, F, G, etc. have not been vendor specific. It is for this reason we believe our analysis applies to B&W and C-E as well as Surry. However, plant specific design does make a difference and we can expect that the following changes in C, D, F, G, H are valid:

C - Surry does not contain fan coolers; for plants with fans as well as sprays C is negligable.
D - Plant changes should not significantly affect this parameter.
F - Plant variations imply that F and H are coupled hence that F should not be called out separately; since H >> F this does not impact.
G,H - Plant variations do not indicate that these should change signifisignificantly.

With these considerations we recalculate T*QX for non-Surry type of plants to be

$$X = 2.1\times10^{-3}\text{/demand}$$

and

$$T^*QX = 6\times10^{-4}\text{/reactor year}$$

hence for non-Surry plants ATWS is still only ¼ of T*QX hence additional valves will increase risk. If we use $t_1 \approx 0.4$ the Q failure core melt probability dominates ATWS by a factor of 10.

COMPETING RISKS AND RELEASE CATEGORIES

We have so far only looked at melt probabilities. From a risk viewpoint this is insufficient. All Surry (WASH 1400) scram failure events are classified in release categories 3, 5, and 7. The release magnitude for PWR-3 is much greater

---

+Although we strongly disagree with the staff assessment which leads to $TK=1.6\times10^{-4}$ we use this value for this analysis. The EPRI assessment places TK at lease an order of magnetude lower which makes the competing risk still worse.

than for PWR-5 and PWR-7. If we use equivelent I-131[a] as an indicator we find

		Release as Equivelent Iodine-131
$\frac{\text{PWR-3}}{\text{PWR-5}}$	=	20
$\frac{\text{PWR-3}}{\text{PWR-7}}$	=	20,000

NUREG 0460 states (App. X-7, Vol. 2) that there is some possibility that an ATWS could fall into PWR-2 or PWR-3 but does not quanitify this statement. It concludes the most likely failure mode is PWR-7. For the purposes of this presentation we do quantify this effect.

From Appendix V of WASH 1400 PPV14-16, we take the event sequences by PWR category. We do not assume additional failures for the ATWS sequences and use the NRC staff number (which we believe is high by at least a factor of 20)

$$TK = 1.6\text{x}10^{-4}/\text{year}$$

for ATWS liklihood. The containment failure modes for ATWS by Category are then

Category 7 $TK\text{-}\varepsilon = 1.6\text{x}10^{-4}$
Category 5 $TK\text{-}\beta = 6.4\text{x}10^{-7}$
Category 3 $TK\text{-}\alpha \quad 1.6\text{x}10^{-6}$

Notice that we do not need to deal with TKF or and other lower sequence since TK subsumes TKF. The total ATWS risk is

$$(TK\text{-}\varepsilon)\ C_7 + (TK\text{-}\beta)\ C_5 + TK\text{-}\alpha)\ C_3$$

The competing risk we examine arises from $S_2 = T^*Q$ and only bother to account for the Category 3 releases. The competing risk is then

$$(T^*Q(D+H)\text{-}\alpha + T^*Q(F+C+G)\text{-}\delta+TKQ\text{-}\alpha)\ C_3$$

and the risk ratio is

$$\frac{\text{Competing Risk}}{\text{ATWS Risk}} = \frac{\{T^*Q[(D+H)\text{-}\alpha+(F+C+G)\text{-}\delta]+TKQ\text{-}\alpha\}C_3}{[TK(\varepsilon C_7+\beta C_5+\alpha C_3)]t_1}$$

R.E. Hall "A Risk Assessment of a PWR for Class 3 - 3 Accidents" NUREG/CR-0603, October 1979.

Quantifying this relation yields

$$\frac{\text{Competing Risk}}{\text{ATWS Risk}} = \frac{4.5\text{x}10^{-4}\ C_3}{6.9\text{x}10^{-5}\ [C_7 + .004\ C_5 + .01\ C_3]}$$

$$\approx 7/(.01 + .004/20 + 1/20000)$$

$$\approx 700$$

This analysis points out first that ATWS risk for PWRs is trivially small compared to other reactor risks and second the likelihood of increased risk due to addition of valves. Any additional valves installed are not likely to have set points at the lowest pressure levels but it is inconceivable that such valve additions would not increase T*Q by 1%. Since the T*Q risk outweighs ATWS by 700 the net change in risk due to eliminating ATWS by adding valves must be unfavorable. If a 3% increase in T*Q is reasonable, the public risk is increased by 20 times the original ATWS risk. We believe that analyses of this type are extremely important. The classical procedure of presuming that a fix solves a problem is insufficient and must be replaced by detailed analyses which allow a discrimination of any competing risks.

APPENDIX

List of (Stuck Open) Pressurizer Valves

1. Palisades, 1971, PORV
2. Oconee 1, 1973, Block Valve
3. Oconee 3, 1975, PORV
4. Davis Besse, 1977, PORV
5. TMI-2, 1978, PORV
6. Cook 3, 1978, PORV
7. Ft. Calhoun, 1979, 2 PORV
8. TMI-2, 1979, PORV
9. Crystal River, 1980, Safety Valve

Major Objectives of Metallurgy and Materials Research Branch Research for Application to Reactor Safety and Regulation

8th Information Meeting, October 31, 1980

1. ORNL - HSST

   - ° Validate analysis method and prove integrity and margin to failure of flawed vessels under thermal shock from large LOCA, and smaller breaks giving rise to pressurized thermal shock.
   - ° Develop method to measure and evaluate crack arrest and provide validation through a crack run/arrest test of a vessel having a low ductile shelf toughness, simulating older A302-B or more recent B&W-welded RPVS.
   - ° Support TAP A-11 effort to develop a practical methodology for application of elastic-plastic fracture mechanics in RPV safety evaluations.

2. NRL - Structural Integrity of LWR Pressure Boundary Components

   - ° Measure fracture toughness of irradiated low ductile shelf B&W weld metals for evaluation of RPV condition relative to 10CFR50 toughness limits.
   - ° Measure realistic but conservative rate of crack growth for steels, welds and piping to upgrade ASME Section XI curves used by NRR for safety evaluations for cracks found in operating reactors.
   - ° Establish data base and trends for licensing evaluation of annealing recovery of irradiation embrittlement.

3. NSRDC - J-R Curve Methodology Development

   - ° Develop and validate a method for testing compact tension specimens in the ductile range to establish upper shelf fracture toughness values, especially for irradiated weld metals.
   - ° Develop experimental verification of the Tearing Instability theory, using medium-diameter piping.

4. USNA - Rapid J-R Curve Evaluation

   ° Perfect a method for extraction of ductile shelf fracture toughness values from compact tension specimen load-deflection traces for licensing evaluation of condition of older reactors.

5. Sandia - Two-Phase Jet Loads

   ° Provide basis for revision of Reg. Guide 1.46 on Pipe Whip Inside Containment by developing improved model for two-phase jet impingement and moment loading of failed piping system.

6. LLL/U Cal Berkeley - Dynamic Analysis of Pipe Whip

   ° Support revision of rules in Reg. Guide 1.46 on Pipe Whip, through development of a special purpose code to describe pipe whip and moment loading from pipe breaks.

7. SAI - Piping Systems Reliability

   ° Support Load Combinations Program, and possible revision of Reg. Guide 1.46, through development of criteria for postulating pipe breaks based on a probabilistic model for reliability of typical piping systems.

8. HEDL - LWR Surveillance Dosimetry
   ORNL - PV Surveillance Experiment
   NBS - Dosimetry Measurement Data Base

   ° Establish methods to accurately predict fluence and embrittlement in RPV walls, especially for older reactors and for those whose surveillance program is inadequate or lost.

   ° Provide basis for Office of Standards for revision of Reg. Guide 1.99 on Effect of Residual Elements on Radiation Embrittlement of Steels, through accurate fluence values and information on chemical composition effects (especially Cu and P).

9. PNL - Steam Generator Tube Integrity

   - Establish integrity and margin to failure under burst and collapse loads of flawed and degraded steam generator tubing to support licensing decisions on tube plugging.
   - Using retired steam generator, evaluate existence and causes of tube deformation, cracking, denting, corrosion or wastage, and support plate deformation and cracking. Determine the source of and recommend ways to eliminate the crud and corrosion products.
   - Validate improved non-destructive examination methods for tube degradation, and recommend improved tube inspection and plugging schedules.

10. BNL - Steam Generator Tube Corrosion

    - Support the licensing request for a capability to assess and predict the stress corrosion cracking behavior of steam generator tubes under postulated service conditions.

11. ANL - Environmentally Assisted Cracking in LWR Piping Systems

    - Provide independent licensing background of information on environmental parameters affecting pipe cracking, including data on critical ranges of parameters, and an evaluation of proposed fixes and their long-term applicability.
    - Provide background information on operating stresses, temperature, loads and water chemistry on IGSCC in BWR stainless steels and on SCC in PWR carbon steels.

12. PNL - Integration of NDE Reliability and Fracture Mechanics

    - Resolve licensing question on best way to test with UT for optimum flaw detection and evaluation, and upgrade ASME code procedure endorsed by federal regulation for UT testing.

13. University of Michigan - Ultrasonic NDE Technology
    Southwest Research Institute - Field Implementation - SAFT-UT

    - Provide significantly enhanced UT flaw evaluation quality using SAFT-UT system, develop real-time SAFT-UT detection capability, and transfer technology to field for ISI coupled with enhanced display for positive ASME-XI licensing evaluation of detected flaws.

14. ORNL - Improved Eddy Current In-Service Inspection for Steam Generator Tubing

    - Use improved multi-frequency eddy current instrumentation to support licensing requests for independent ISI of steam generator tubing, including tube sheet crevice cracking, dented region, cracking, thinning, etc., not detected by single frequency testing.

15. PNL - Acoustic Emission Material Study

    - Provide technology to support final licensing branch position on use of AE for crack detection, and for warning of crack extension long before breach of integrity.
    - Provide technology to support on-line monitoring of areas of limited accessibility or areas of high potential for cracking.

16. Daedalean Associates - Incipient Flaw Prediction

    - Provide method for I&E to warn of incipient IGSCC in piping.

WIPS: Computer Code for Whip and Impact Analysis of Piping Systems

by

Graham H. Powell
Professor of Civil Engineering
University of California, Berkeley

Prepared for Eighth Water Reactor Safety Research
Information Meeting, Gaithersburg, Oct. 31, 1980

1. INTRODUCTION: PROGRAM OBJECTIVES

A computer code is being developed to assist in formulating design guidelines for the protection of piping following rupture. The problem of primary interest is the local behavior of straight pipe and piping elbows at regions of pipe-to-pipe and pipe-to-wall impact. Problems of secondary interest are the overall behavior of large piping systems following rupture and the design of pipe whip restraints.

The objectives of the program are to develop a special purpose computer code for pipe whip analysis; to verify the code by comparison with available experimental results; and to perform parameter studies to assist in the development of design guidelines. The computer code is to be implemented on a minicomputer (32-bit word "super" mini) in interactive mode. The code must be capable of performing pipe-to-pipe and pipe-to-wall impact analyses as well as analyses of the interaction of piping with pipe whip restraints. Large displacements of the piping system and large distortions of individual piping components are to be considered.

The project began in October 1978 and is scheduled to be completed in September 1981.

2. COMPUTER CODE DESIGN

The major challenge in the project is the design and implementation of the computer code. The most important considerations in the design of the code are (a) that it be possible to perform complex analyses with only a small number of man-hours devoted to data preparation and (b) that the code by easily modified so that its capabilities can be extended in the future.

Ease of use is being obtained (a) by using special purpose data input modules and (b) by using a highly automatic strategy for solution of the nonlinear structural analysis problem. A number of separate input modules accept, in interactive mode, data on the geometry of the complete piping system, the loading, and the properties of the piping components and restraints. A number of geometry generation options are available to reduce the data preparation effort. The data is stored permanently and may be modified or added to as desired. Any part of the complete system may then be specified to be an "analysis model" by defining the parts of the system to be included and the pipe and restraint properties to be used. Any number of different analysis models may be constructed from a single set of system data to study different break locations, different finite element idealizations, different contact geometries, etc.

During the modelling phase, input data is generated for the analysis module, which performs the nonlinear dynamic response analysis. This module is based on the linear structural analysis code FACTS (Finite Element Analysis of Complex Three-Dimensional Systems) developed by Structural Software Development, Inc., Berkeley, California. The code is highly modular, has a multi-level substructuring capability,

and makes use of a powerful Data Base Manager developed specifically for structural analysis. The FACTS code has been extended to perform nonlinear dynamic analysis, using a step-by-step strategy with automatic time step selection. The automatic time step selection greatly reduces the skill required of the analyst.

The analysis module produces results files which can be accessed by printing and plotting post-processors. At the time of writing, only preliminary consideration has been given to the features required in the post-processors.

The code is being implemented in FORTRAN77 on a DEC-VAX 11/780 computer. The few machine-dependent features in the code have been collected in well-defined subroutines to allow easy conversion for different computers.

3. IMPACT ANALYSIS

Impact of piping components with rigid boundaries can be analyzed relatively easily because the geometry of one contact surface (the rigid boundary) is known in advance. In WIPS, this type of analysis will be performed by specifying gap elements which become very stiff when the gap closes. The time step selection algorithm automatically reduces the time step to account for the rapid changes in velocity which occur at impact.

Impact of piping components with deformable boundaries (including other piping components) is much more difficult to analyze because the geometry at the contact interface is not known in advance but must be calculated in each time step by satisfying equilibrium and compatibility requirements at the interface. In WIPS, this type of impact problem is solved by a compatibility procedure in which the contacting surfaces are first allowed to overlap, and self-equilibrating contact forces are then applied to re-establish geometric compatibility.

4. STRUCTURAL ELEMENTS

Elements for straight pipe, elbows and restraints have been developed, plus an arbitrary shell element to allow detailed modelling of local effects in piping components. The nonlinear kinematic hardening theory of Mroz, extended to allow for strain rate dependence, has been used to model inelastic behavior.

The procedures for adding elements to the code have been standardized so that new elements can be added with relative ease.

5. OTHER STUDIES

Analyses to compare computed behavior with available test results are being carried out, and parameter studies will be carried out to assist in developing design guidelines. Simplified analysis procedures, suitable for hand computation, are also being studied and compared with computer analyses.

A detailed software management system has been developed to provide control over development and implementation of new features for the code.

PIPE WHIP AND IMPACT SAFETY ISSUES

(A) PIPE BREAK CRITERIA

(B) JET FORCES

(C) SUBSEQUENT STRUCTURAL INTEGRITY

  (1) IMPACT WITH ADJACENT PIPES

  (2) IMPACT WITH WALLS AND FLOORS

  (3) DESIGN OF PIPE WHIP RESTRAINTS

  (4) OVERALL DYNAMIC EXCITATION

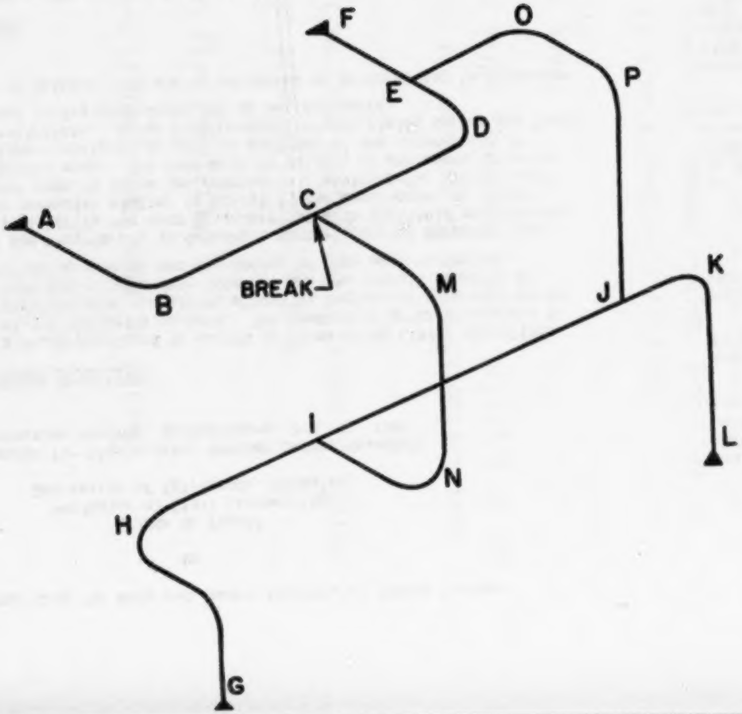
F
O
P
E
D
C
A
BREAK
B
M
J
K
I
L
N
H
G

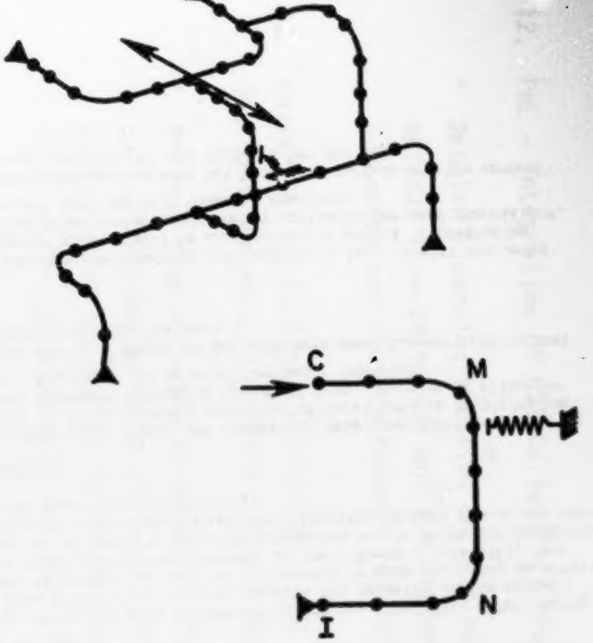

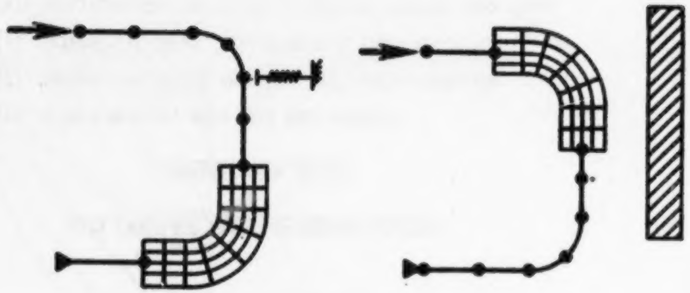

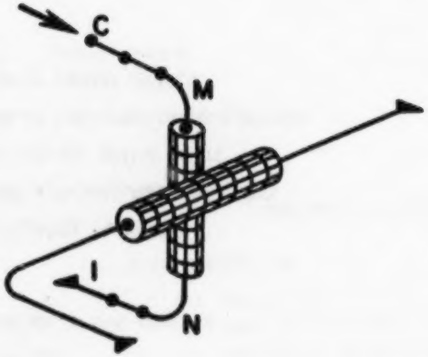

ISSUE OF PRIMARY INTEREST

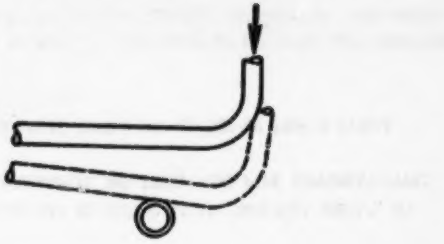

(1) LOCAL DAMAGE IN PIPES AT IMPACT POINT

(2) RESPONSE OF TARGET PIPE

CURRENT CRITERION (NUREG-75/087)

RUPTURE OF TARGET PIPE IF SMALLER DIAMETER. LEAK IN TARGET PIPE IF SMALLER THICKNESS UNLESS TEST OR ANALYSIS SHOW OTHERWISE.

ISSUES OF SECONDARY INTEREST

(1) PIPE-TO-WALL IMPACT
    IMPACT VELOCITY
    PIPE AND WALL DAMAGE

(2) PIPE WHIP RESTRAINTS
    CONFIRMING DESIGN CALCULATIONS

(3) OVERALL DYNAMIC EXCITATION
    VALVE ACCELERATIONS
    SUPPORT LOADS
    PIPE STRESSES

DELIVERABLES

(1) COMPUTER CODE
    (a) CONVENTIONAL PIPE WHIP ANALYSIS
    (b) IMPACT ANALYSIS WITH RIGID TARGETS
    (c) IMPACT ANALYSIS WITH DEFORMABLE TARGETS
    (d) BOTH LOCAL AND OVERALL RESPONSE CALCULATION
    (e) INTERACTIVE I/O
    (f) IMPLEMENTATION ON MINI-COMPUTER

(2) ANALYSIS RESULTS
    (a) QUALITY ASSURANCE EXAMPLES
    (b) COMPARISONS WITH AVAILABLE EXPERIMENTS
    (c) PARAMETER STUDIES, DESIGN CHARTS
    (d) ASSESSMENT OF SIMPLIFIED ANALYSIS METHODS
    (e) ASSESSMENT OF CURRENT CRITERIA

WIPS (WHIP AND IMPACT OF PIPING SYSTEMS)

COMPUTER CODE DESIGN

(1) HIGHLY MODULAR, WITH DATA BASE MANAGER
(2) SUBSTRUCTURING, TO ALLOW DETAILED LOCAL MODELLING
(3) INTERACTIVE INPUT, WITH EXTENSIVE ERROR CHECKING
(4) NONLINEAR SOLUTION STRATEGY REQUIRES MINIMUM USER SKILL
(5) INTERACTIVE EXAMINATION OF RESULTS
(6) NEW I/O MODULES EASILY ADDED
(7) NEW STRUCTURAL ELEMENTS EASILY ADDED

CURRENT STAGE OF CODE DEVELOPMENT

(OCTOBER 1980)

(1) END OF YEAR 2 OF 3 YEAR EFFORT.

(2) 3 MONTHS BEHIND SCHEDULE. EXPECT TO MAKE UP TIME IN YEAR 3.

(3) ANALYSIS MODULE COMPLETED AND TESTED AS STAND-ALONE CODE WITHOUT VARIABLE CONFIGURATION CONTACT.

(4) MODULES FOR VARIABLE CONFIGURATION CONTACT DEVELOPED AND BEING TESTED.

(5) INTERACTIVE INPUT MODULES DEVELOPED, TESTED, AND COUPLED WITH ANALYSIS MODULE.

(6) OUTPUT AND GRAPHICS MODULES BEING DESIGNED.

DATA INPUT

(1) IMPORTANT AIM IS MINIMIZATION OF MAN-HOURS.

(2) DATA ON PIPE SYSTEM GEOMETRY, PIPE COMPONENT PROPERTIES, AND DYNAMIC LOADS ARE INPUT USING SEPARATE MODULES AND SAVED.

(3) INPUT IS INTERACTIVE, WITH ERROR CHECKING.

(4) DATA MAY LATER BE MODIFIED AND/OR EXTENDED.

(5) ANY PART OF SYSTEM MAY BE SET UP AS AN "ANALYSIS MODEL", BY DEFINING MODEL BOUNDARIES AND SPECIFYING PIPE COMPONENT TYPES.

(6) ANY NUMBER OF ANALYSIS MODELS MAY BE SET UP FROM A SINGLE PIPE SYSTEM.

(7) ACTUAL ANALYSIS OF MODEL IS INITIATED BY DEFINING LOAD LOCATIONS AND A SMALL AMOUNT OF ANALYSIS CONTROL INFORMATION. ANY NUMBER OF ANALYSES MAY BE SPECIFIED FOR A SINGLE MODEL.

(8) RESULTS ARE SAVED, FOR SUBSEQUENT PRINTING, PLOTTING, OR INTERACTIVE EXAMINATION.

WIPS PROGRAM STRUCTURE

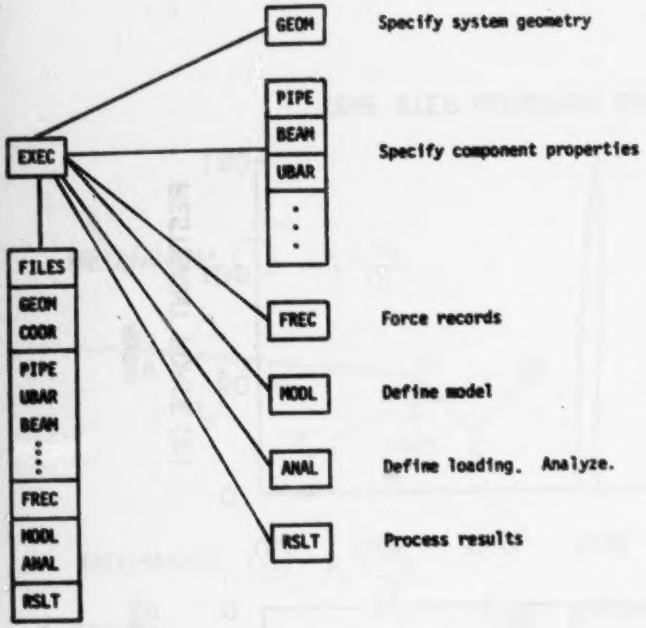
EXEC
GEOM
PIPE
BEAM
UBAR
FREC
MODL
ANAL
RSLT
FILES
GEOM
COOR
PIPE
UBAR
BEAM
FREC
MODL
ANAL
RSLT

Specify system geometry

Specify component properties

Force records

Define model

Define loading. Analyze.

Process results

SOLUTION STRATEGY

(1) EVENT-TO-EVENT. NO ITERATION.

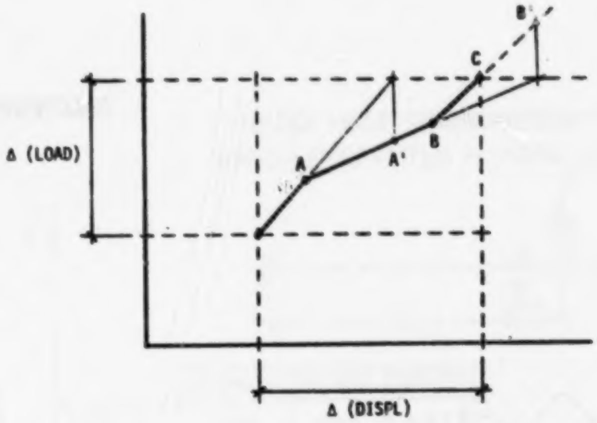
Δ (LOAD)
A
A'
B
C
B'
Δ (DISPL)

NONLINEAR SOLUTION STRATEGY

(1) MAJOR CONCERNS ARE:

- (a) RELIABILITY
- (b) TIME STEP SELECTION
- (c) ANALYSIS OF VARIABLE CONFIGURATION CONTACT

(2) RELIABILITY OBTAINED USING EVENT-TO-EVENT STRATEGY

AVOIDS LARGE EQUILIBRIUM ERRORS
AVOIDS RELIABILITY PROBLEMS OF ITERATION SCHEMES

(3) TIME STEP SELECTED AUTOMATICALLY

VARIES AS NEEDED DURING ANALYSIS
SELECTION BASED ON EQUILIBRIUM ERROR AT MID-STEP

(4) VARIABLE CONFIGURATION CONTACT BY COMPATIBILITY STRATEGY

OVERLAP ALLOWED; OVERLAP DISTANCES CALCULATED
EQUAL-AND-OPPOSITE FORCES APPLIED TO ELIMINATE OVERLAP

SOLUTION STRATEGY

(2) AUTOMATIC TIME STEP SELECTION

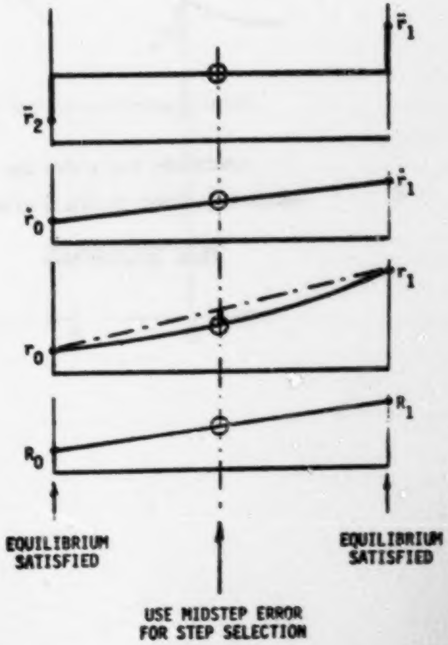
$\ddot{r}_1$
$\ddot{r}_2$
$\dot{r}_0$
$\dot{r}_1$
r_0
r_1
R_0
R_1
EQUILIBRIUM SATISFIED
EQUILIBRIUM SATISFIED
USE MIDSTEP ERROR FOR STEP SELECTION

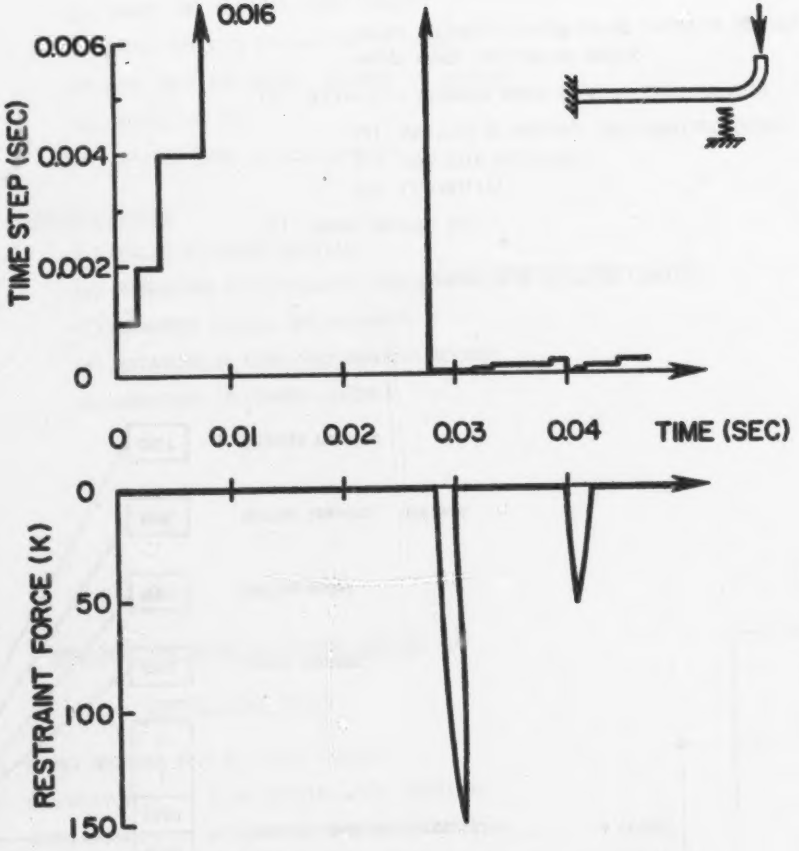

TIME STEP VARIATION DURING ANALYSIS

MROZ MATERIAL MODEL

NONLINEAR KINEMATIC HARDENING EXTENDED

FOR STRAIN RATE DEPENDENCE

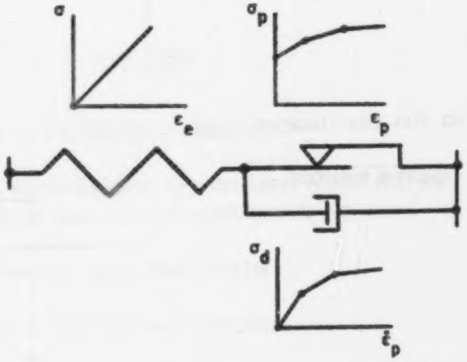
σ
ε_e
σ_p
ε_p
σ_d
$\dot{\varepsilon}_p$

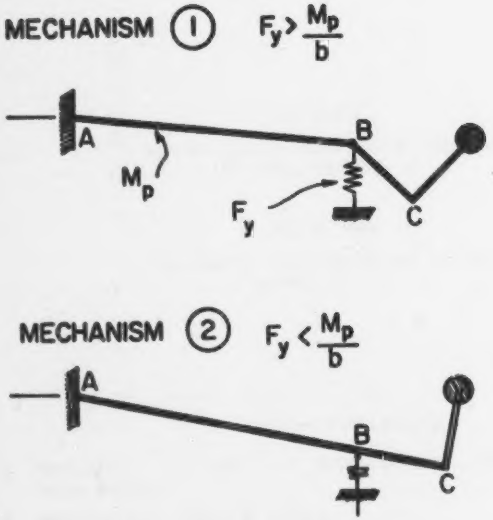
MECHANISM ①
$F_y > \frac{M_p}{b}$
A
B
C
M_p
F_y
MECHANISM ②
$F_y < \frac{M_p}{b}$
A
B
C

ALTERNATIVE MECHANISMS

DECO TEST CONFIGURATION
RIGID—PERFECTLY PLASTIC BEAM

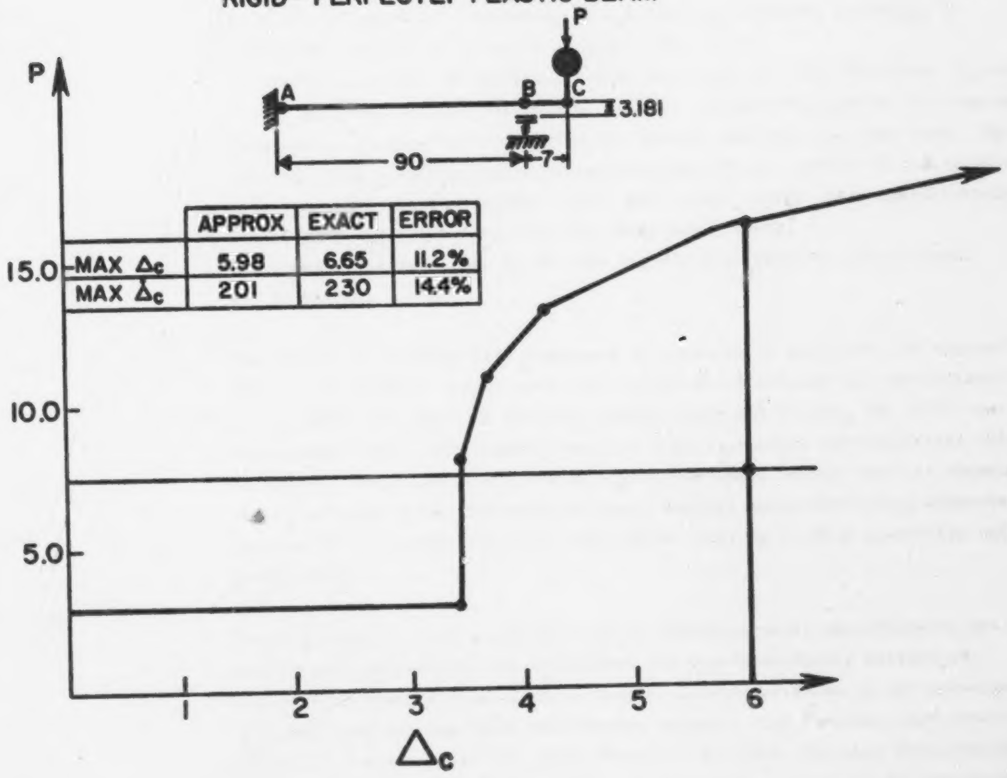

	APPROX	EXACT	ERROR
MAX Δ_c	5.98	6.65	11.2%
MAX $\dot{\Delta}_c$	201	230	14.4%

RESULTS AND IMPLICATIONS OF THE INITIAL NEUTRONIC CHARACTERIZATION OF TWO HEAVY SECTION STEEL TECHNOLOGY (HSST) IRRADIATION CAPSULES AND OF THE PSF SIMULATED LWR PRESSURE VESSEL IRRADIATION FACILITY

A. FABRY
assisted by F. COPS and S. VAESSEN
MOL, BELGIUM

F.B.K. KAM
assisted by C. BALDWIN and E. EASTHAM
ORNL, USA

with contributions by

F.W. STALLMANN, S.S. HURT, T.M. SIMS, the PCA, ORR and BSR operation teams (ORNL)
L.S. KELLOGG, W.N. McELROY (HEDL)
G. and S. DE LEEUW, G. MINSART, H. TOURWE, J. LACROIX, D. LANGELA (MOL)
E.D. McGARRY (NBS)
A.A. ALBERMAN, M. BENOIST, M. THIERRY (SACLAY)
W. ZIMMER (EGG/ORTEC)
D.J. KETEMA, H.J. NOLTHENIUS, W.L. ZIJP (PETTEN)

for presentation at

NCR Eighth Safety Research Information Meeting,
Metallurgy and Materials Research Branch Session
Gaithersburg, Maryland, October 27-31, 1980.

SUMMARY OF CONTENTS

Whenever the steel pressure vessel of a Light Water Reactor (LWR) power plant is approaching end-of-life (EOL) embrittlement conditions, it becomes more and more desirable, with the view to a sane safety-economy trade-off, to know its neutronic exposures, at all beltline weldment locations in particular, within an accuracy of ± 10 - 15 % (1 σ).
The USNRC-sponsored LWR Pressure Vessel Surveillance (PVS) Dosimetry Improvement program, coordinated by W.N. McELROY, Hanford Engineering Development Laboratory, is aimed at addressing the issues stemming from such need. This involves some pressing responsibilities relative to a number of oldier plants with comparatively low initial steel upper shelf energy, high embrittlement sensitivity and eventually marginal chemistry records.
The program has been open to and was rapidly gratified by international participation.

Two clean, low neutron flux benchmark arrangments of simulated LWR thermal shield and pressure vessel have been realized and extensively investigated at the ORNL Pool Critical Assembly (PCA); these PCA 8/7 and PCA 12/13 configurations [X/Y : water gaps from core edge to thermal shield/thermal shield to vessel] have been the focus of an international "blind test" of transport theory methods in LWR-PVS applications. Current uncertainties on absolute quarter thickness neutron flux predictions range up to 25 % (generally underprediction).

Comparatively as large uncertainties of in-vessel steel embrittlement predictions or projections may arise from the unsatisfactorily settled influences of neutron flux spectrum (safety non-conservative if not accounted for) and neutron flux level/self-anneal exposure time (economy non-conservative if not accounted for while actual). The high flux Pool Side Facility (PSF) metallurgy-dosimetry LWR-PVS test simulator is intended to cast more appropriate light on these questions.

The primary purpose of the work outlined in this paper was to define PSF beginning-of-life (BOL) neutronic exposure parameters - $\phi_{> 1\ \mathrm{MeV}}$, dpa , $\phi_{> 0.1\ \mathrm{MeV}}$, ... - to within ± 10 - 15 % (1 σ).

Emphasis is placed upon the consistent application of a robust, accurate and transportable neutron flux dosimetry technology (MOL) and of transport theory analysis (ORNL). Advantage is taken throughout of the EURATOM "equivalent fission flux" standard concept for threshold nuclear processes, and of the precise NBS - MOL experimental implementation of this concept via actual fission spectrum standard benchmark field referencing.

The analysis of the results and their implications encompasses :

1) low flux NBS - MOL fission chamber and MOL - HEDL radiometric measurements at the PCA/PSF mock-up (PCA 4/12 SSC, e.g. 4/12 with simulated surveillance capsule at back of the thermal shield)

2) low power MOL - HEDL - ORTEC flux radiometric measurements in PSF during its "start-up programme"

3) high power MOL - HEDL flux measurements at PSF beginning-of-cycle (BOC) and end-of-cycle (EOC) conditions

4) high power PSF/BOC SACLAY flux damage monitor measurements

5) preliminary PETTEN and MOL results of international PSF high power neutron fluence intercomparisons

6) some integral and MOL ^{6}Li(n,α) systematics observed in PCA 8/7 and PCA 12/13

7) an array of transport theory calculations.

Finally, a first radiometric and transport theory link with the FY 1980 Heavy Section Steel Technology (HSST) program irradiations is explored; it is likely to prove most benefitial in terms of assessing the significance of test reactor versus power reactor steel embrittlement observations.

The following is an outline of the generally most interesting conclusions and implications of this work.

- Combined HSST and PSF metallurgical irradiations appear to offer good potentials for the separation and assessment of neutron flux spectral effects and flux regime effects (if any) on steel embrittlement; such data would be quite transferable to LWR in-vessel 1/4 T conditions.

- Within engineering margins of 10 %, the attenuation of neutron flux spectra by steel displays essentially identical and simple integral features in all PCA/PSF/HSST configurations; this is suggested to be representative also of power reactor vessels irrespective of the spectral and angular distributions of incident neutrons

- Relatively to the above, current neutron transport theory does not reproduce accurately the integral and differential features of this attenuation; the biases are small for integral data, but are generally consistent with ^{6}Li(n,α) neutron spectrometry; further study is warranted.

- Development of a dedicated neutron dosimetry for ex-vessel cavities (or other ex-vessel access holes) of LWR power plants is recommended as a cheap and accurate approach to certify EOL in-vessel exposures and accuracies, including effects of azimuthal flux variations; these azimuthal effects are important and deserve on another hand independent reference benchmark field investigation.

- Accuracies of ± 10 % can readily be attained for all steel LWR-PVS neutronic exposure parameters by application of current transport theory calculations combined to a few well selected and benchmark field referenced integral flux/fluence/damage neutron monitors. A high flux/fluenc LWR-PVS secondary reference neutron field, consistently characterized in a way traceable to primary fission spectrum standards, can provide ideal calibration, sensor QA, and overall certification of commercial surveillance dosimetry while by-passing unrewarding and unnecessary paperwork.

- For metallurgical test reactor irradiations, initial flux characterization and/or eventual low flux mock-up measurements, if cautiously organized and applied, can provide adequate control of design details and irradiation times needed to reach the exposure goals; the resulting flux spectrum information may also most valuably be combined to in-situ neutron fluence results obtained a-posteriori.

- Damage monitors will be most essential if it is found that adequate steel embrittlement correlations require a damage function with lower energy response than dpa, such as $\phi_{> 0.1\ \mathrm{MeV}}$, suggested by some experiments in France (CEA, Grenoble).

LWR LICENSING AND SAFETY ISSUE

IMPROVEMENT AND APPLICATION OF THE EMBRITTLEMENT TREND CURVES FOR LWR PRESSURE VESSEL STEELS REQUIRE

- DEFINITION OF NEUTRONIC EXPOSURE PARAMETERS TO ±10% (1σ) IN TEST REACTOR AND POWER REACTOR SURVEILLANCE IRRADIATIONS
- EVALUATION OF IN-VESSEL END-OF-LIFE NEUTRONIC EXPOSURE PARAMETERS TO ±10-15% (1σ)

PRINCIPAL NEUTRONIC EXPOSURE PARAMETERS ARE

$$\phi_{>1\,\mathrm{MeV}},\ \mathrm{dpa},\ \phi_{>0.1\,\mathrm{MeV}}$$

SCOPE

- CONSISTENT MEASUREMENTS AND ANALYSIS OF INITIAL (BOL) NEUTRON SPACE AND ENERGY DISTRIBUTIONS FOR
  1) PSF SIMULATED LWR PRESSURE VESSEL IRRADIATION FACILITY
  2) HSST IT-CS CAPSULE A AND B FY1980 METALLURGICAL IRRADIATIONS
- IMPLICATIONS OF DATA TRENDS FOR POWER REACTOR SURVEILLANCE APPLICATIONS

SUMMARY OF RESULTS (HIGHLIGHTS)

- ACCURACY GOAL OF ±10% (1σ) ON PSF/HSST INITIAL NEUTRONIC EXPOSURE PARAMETERS ATTAINED
- RELEVANCE OF POWER REACTOR EX-VESSEL DOSIMETRY FOR IN-VESSEL EOL NEUTRONIC CHARACTERIZATION CONFIRMED

SUMMARY OF RESULTS (HIGHLIGHTS)

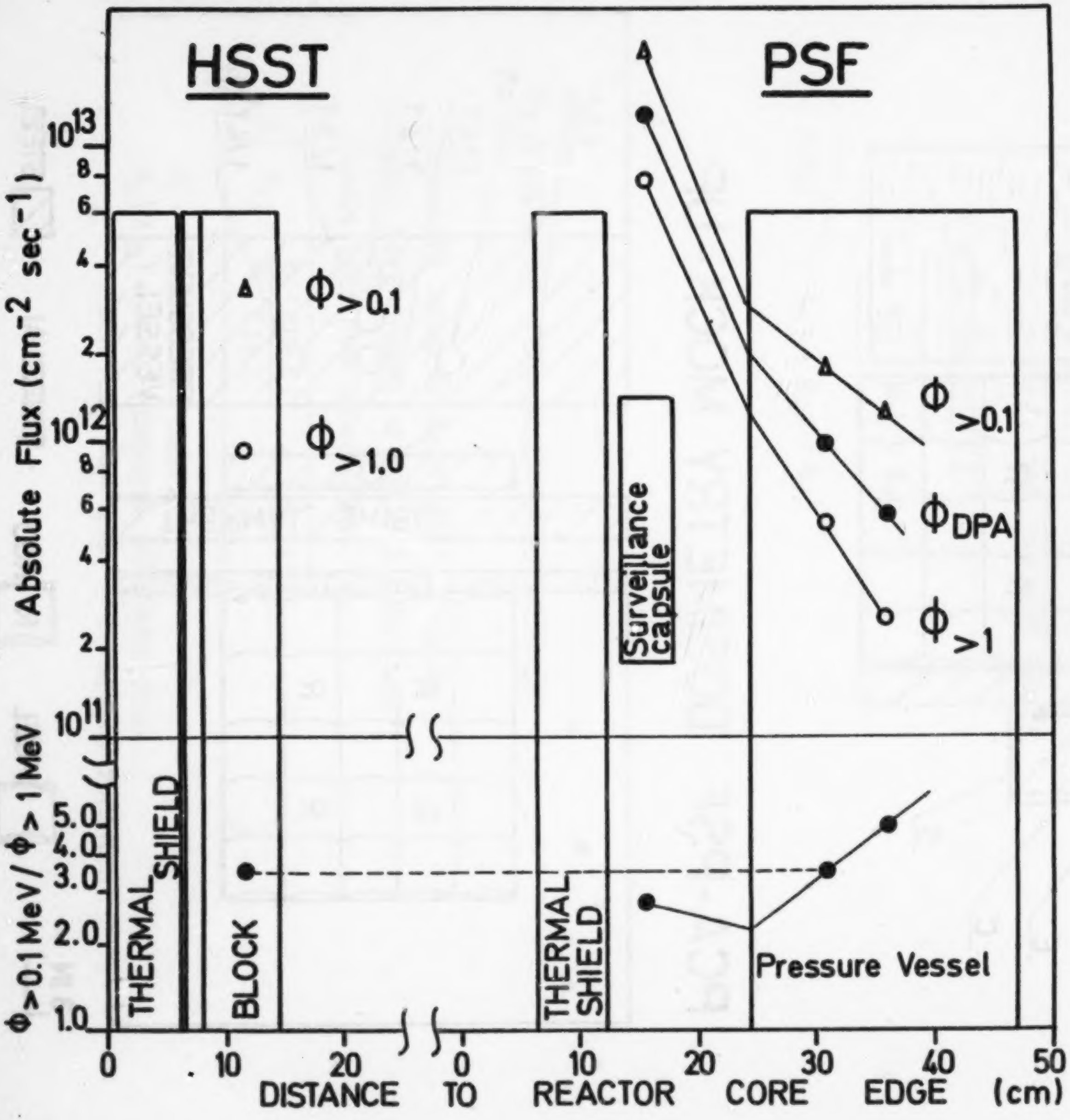

POTENTIALS OF PSF
AND HSST IRRADIATIONS
TO SEPARATE METALLURGICAL
EFFECTS OF :

- DIFFERENT NEUTRON EXPOSURE UNITS
- DIFFERENT NEUTRON FLUX LEVEL REGIMES

BSR-HSST DOSIMETRY MOCK-UP

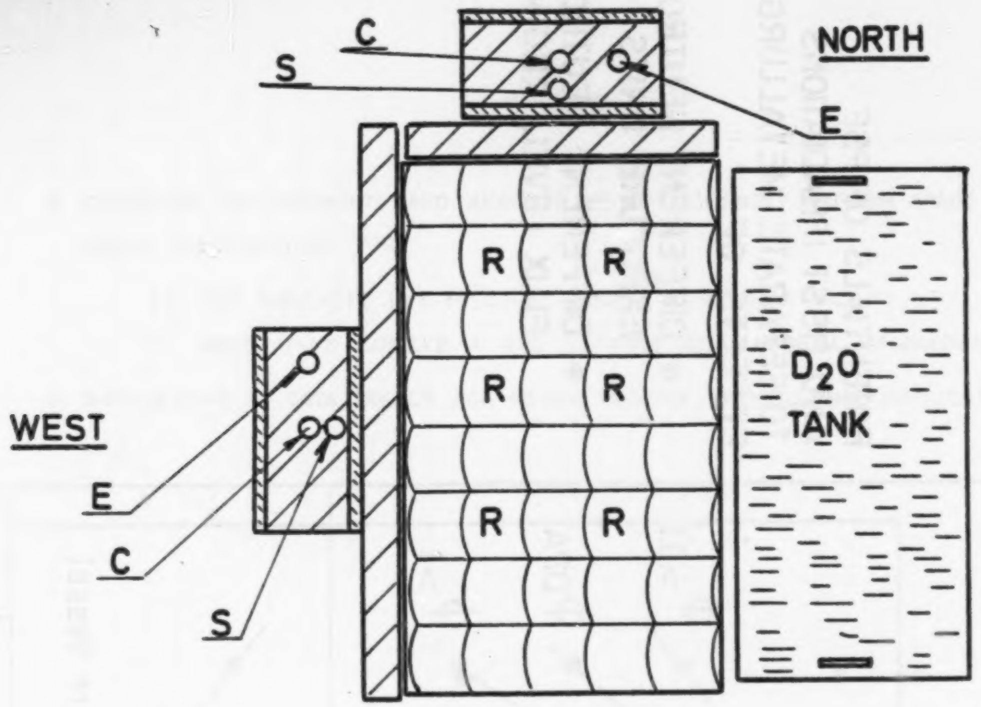
C
S
NORTH
E
R
R
R
R
R
R
D₂O TANK
WEST
E
C
S

PCA-PSF DOSIMETRY MOCK-UP

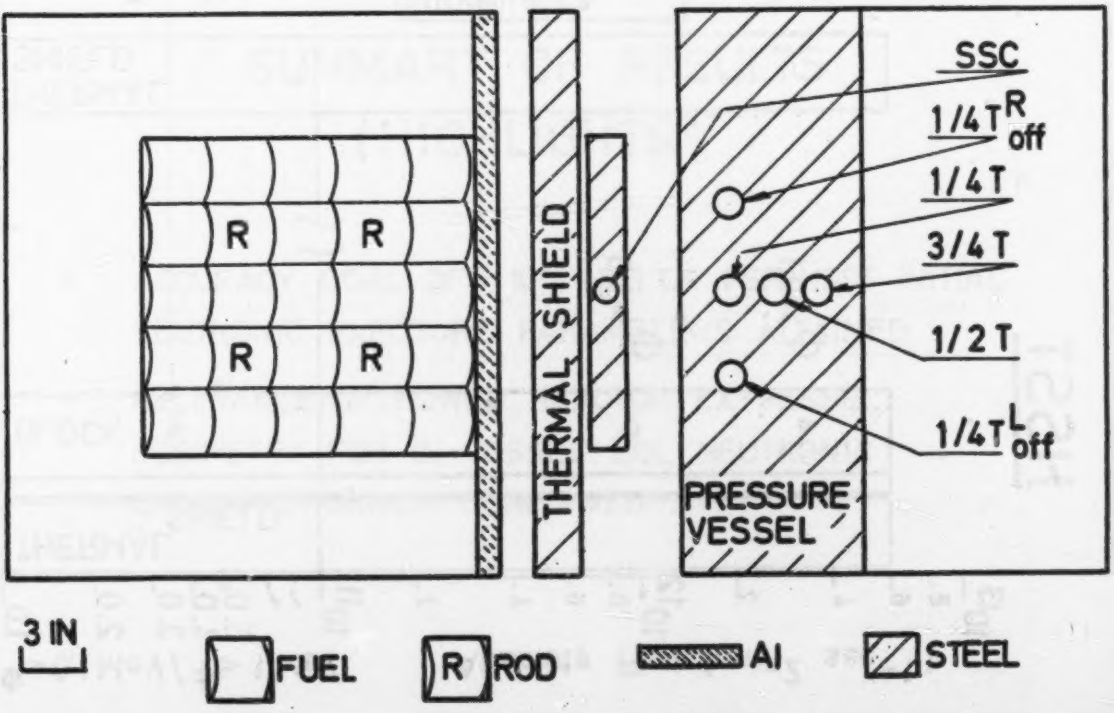
SSC
1/4T R off
1/4T
3/4T
1/2T
1/4T L off
R
R
R
R
THERMAL SHIELD
PRESSURE VESSEL
3 IN
FUEL
R ROD
Al
STEEL

DOSIMETRY FORMALISM AND METHOD

DOSIMETRY AND DAMAGE CORRELATION PARAMETERS :

- (EQUIVALENT) FISSION FLUX FOR REACTION

  $r_i(E)$ IN FIELD $\Phi(E)$:

$$\boxed{\Phi_{f,i} = \int_0^\infty r_i(E)\,\Phi(E)\,dE \Big/ \int_0^\infty r_i(E)\,X_{25}(E)\,dE}$$

WITH $X_{25}(E)$ = URANIUM - 235 FISSION SPECTRUM

$r_i(E) = \sigma_i(E)$ FOR DOSIMETERS

$= \varepsilon(E)$ FOR EXPOSURE UNIT ε

- SPECTRAL INDICES

$$\boxed{S_{i,j} = \Phi_{f,i} \,/\, \Phi_{f,j}}$$

also $S_{\varepsilon,i} = \Phi_{f,\varepsilon} / \Phi_{f,i}$

DOSIMETRY FORMALISM AND METHOD (contd.)

DOSIMETRY MEASUREMENTS BY BENCHMARK FIELD REFERENCING AT MOL AND NBS CAVITY FISSION SPECTRUM STANDARDS :

$$\boxed{\Phi_{f,i} = \frac{R_i\,(\text{FIELD})}{R_i\,(X_{25})} \cdot \Phi_f\,(X_{25})}$$

R_i = INTEGRAL RESPONSE.

$\Phi_f(X_{25})$ = TOTAL ABSOLUTE STANDARD FLUX DERIVED FROM NBS ^{252}Cf SOURCE STRENGTH

DOSIMETRY FORMALISM AND METHOD (contd.)

DOSIMETRY DATA ANALYSIS BY COMBINATION WITH TRANSPORT THEORY CALCULATIONS :

(EQUIVALENT) " EXPOSURE FISSION FLUX " IS

$$\Phi_{f,\varepsilon} = \Sigma_i \; w_i \; \Phi^{(i)}_{f,\varepsilon}$$

WHERE $\boxed{\Phi^{(i)}_{f,\varepsilon} = (S_{\varepsilon,i})_{CALC.} \; \Phi^{EXPT.}_{f,i}}$

WITH WEIGHT FACTORS

$$W_i = \left| 1 - (S_{\varepsilon,i})_{CALC.} \right|^{-1} \; \sigma^{-2}_{\Phi^{EXPT}_{f,i}}$$

AND CORRELATION COEFFICIENTS

$$\rho_{i,j} = \left| 1 - (S_{i,j})_{CALC.} / (S_{i,j})_{EXPT.} \right|$$

NOTE THAT $\boxed{\Phi^{(j)}_{f,\varepsilon} / \Phi^{(i)}_{f,\varepsilon} = (S_{i,j})_{CALC.} / (S_{i,j})_{EXPT.}}$

CORRELATION OF FISSION FLUX AND EXPOSURE PARAMETERS FOR SELECTED PSF NEUTRON DOSIMETERS

REACTION COUPLE		$(S_{\varepsilon i}-1) / S_{\varepsilon,i}$ CALC.			
ε (EXPOSURE)	i (DOSIMETER)	SSC	1/4T	1/2T	3/4T
DPA STEEL	^{237}Np (n,f)	-9.4%	-7.5%	-6.2%	-3.7%
DPA STEEL	^{103}Rh (n,n')	+5.2%	+9.0%	+12.9%	+16.6%
> 1 MeV	COMPOSITE Rh, In	+4.7%	+1.2%	-3.5%	-9.4%
> 0.1 MeV	DPA GRAPHITE	-1.0%	-0.3%	+0.4%	+0.6%

- DPA STEEL FISSION FLUX AND ^{237}Np FISSION FLUX EQUAL WITHIN < 10%
- $\Phi > 0{,}1$ MeV AND GRAPHITE FISSION FLUX EQUAL WITHIN ± 1%

ELEMENTS OF PSF NEUTRONIC CHARACTERIZATION

- TRANSPORT THEORY
- AN ENGINEERING MOCK-UP (PCA 4/12 SSC) USED FOR :
  - DESIGN OPTIMIZATION
  - RADIOMETRIC, SSTR AND FISSION CHAMBER INTEGRAL DOSIMETRY
  - NEUTRON SPECTROMETRY (PROTON RECOIL)
- A START-UP INTEGRAL DOSIMETRY PROGRAMME AT LOW AND HIGH ORR CORE POWER NEEDED FOR :
  - VALIDATION OF MOCK-UP DATA APPLICABILITY
  - CONTROL OF REQUIRED METALLURGICAL EXPOSURE TIMES
  - BOL RADIOMETRIC AND DAMAGE MONITOR CHARACTERIZATION
  - INTERNATIONAL VALIDATION/CALIBRATION OF FLUENCE DOSIMETERS
- EXTENSIVE IN-SITU INTERNATIONAL FLUENCE DOSIMETRY .

ELEMENTS OF HSST NEUTRONIC CHARACTERIZATION

- TRANSPORT THEORY
- A DOSIMETRY MOCK-UP USED FOR
  - CONTROL OF REQUIRED METALLURGICAL EXPOSURE TIMES
  - RADIOMETRIC FLUX DOSIMETRY LINK WITH EXTENSIVE PCA/PSF STANDARDIZATION EFFORT
- INTERLABORATORY IN-SITU FLUENCE DOSIMETRY .

SPECTRAL INDICES AND ABSOLUTE FISSION FLUXES IN PSF SIMULATED SURVEILLANCE CAPSULE

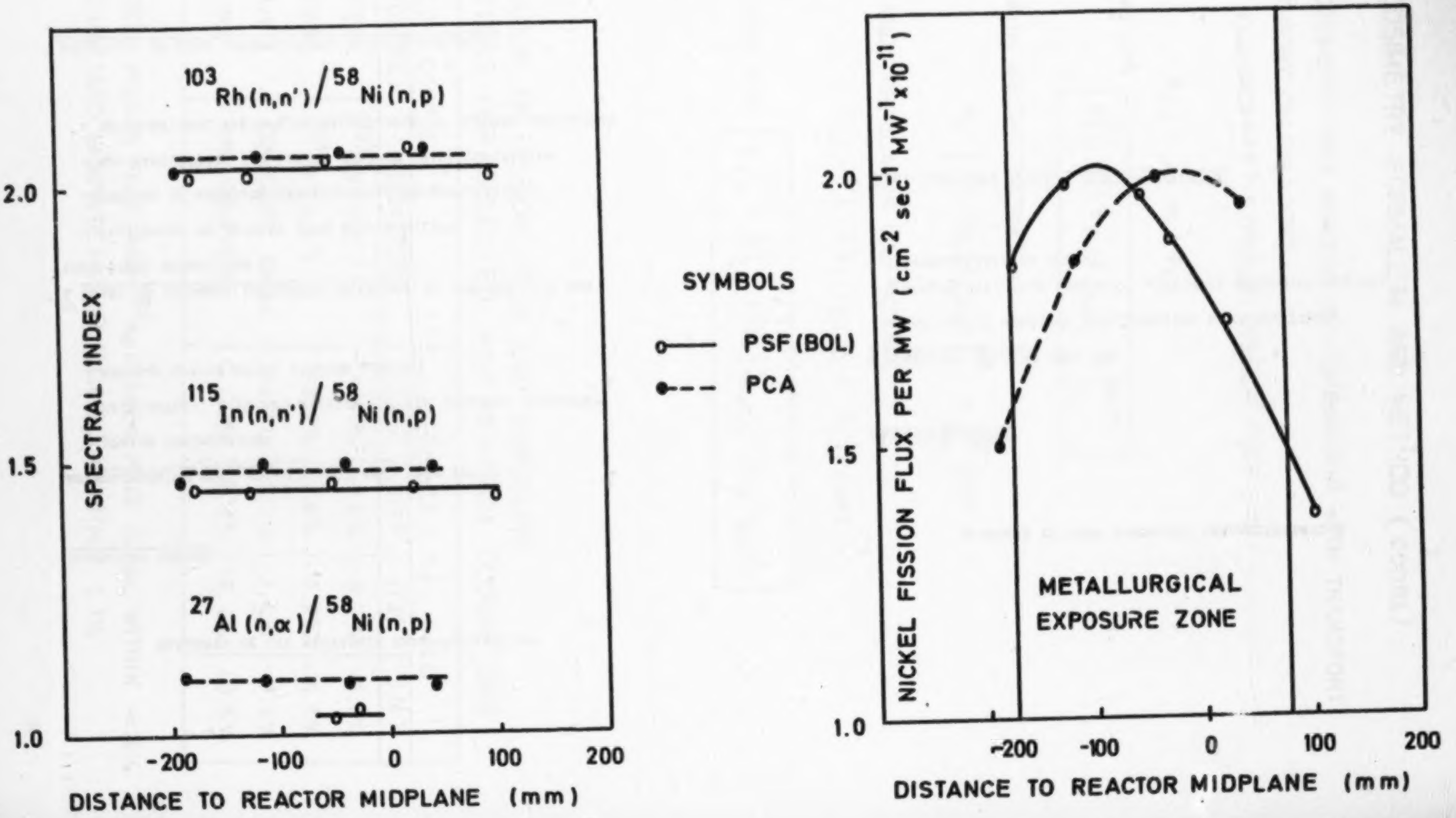

INFLUENCE OF ORR CORE ASSYMETRY ON PSF FISSION FLUX TRAVERSES (VESSEL SIMULATOR)

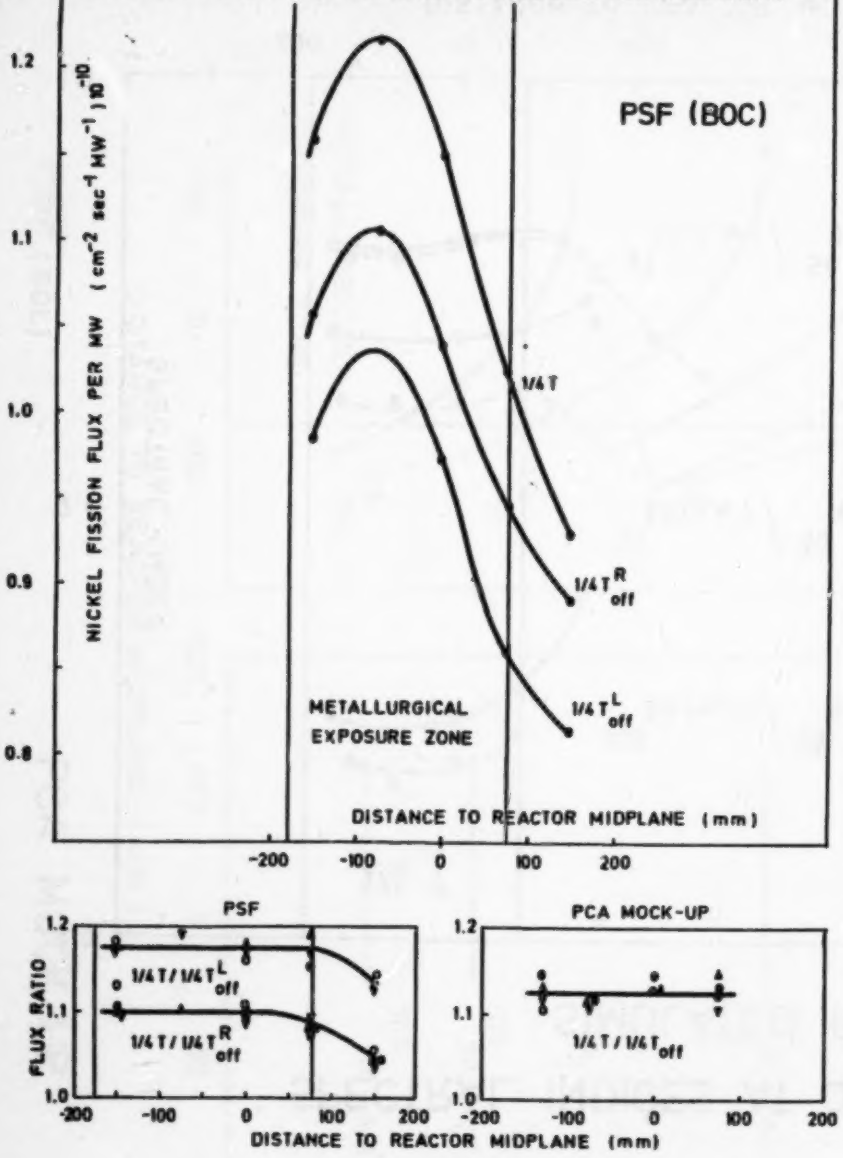

ABSOLUTE VERTICAL FISSION FLUX DISTRIBUTIONS AT QUARTER THICKNESS OF PSF SIMULATED LWR PRESSURE VESSEL WALL

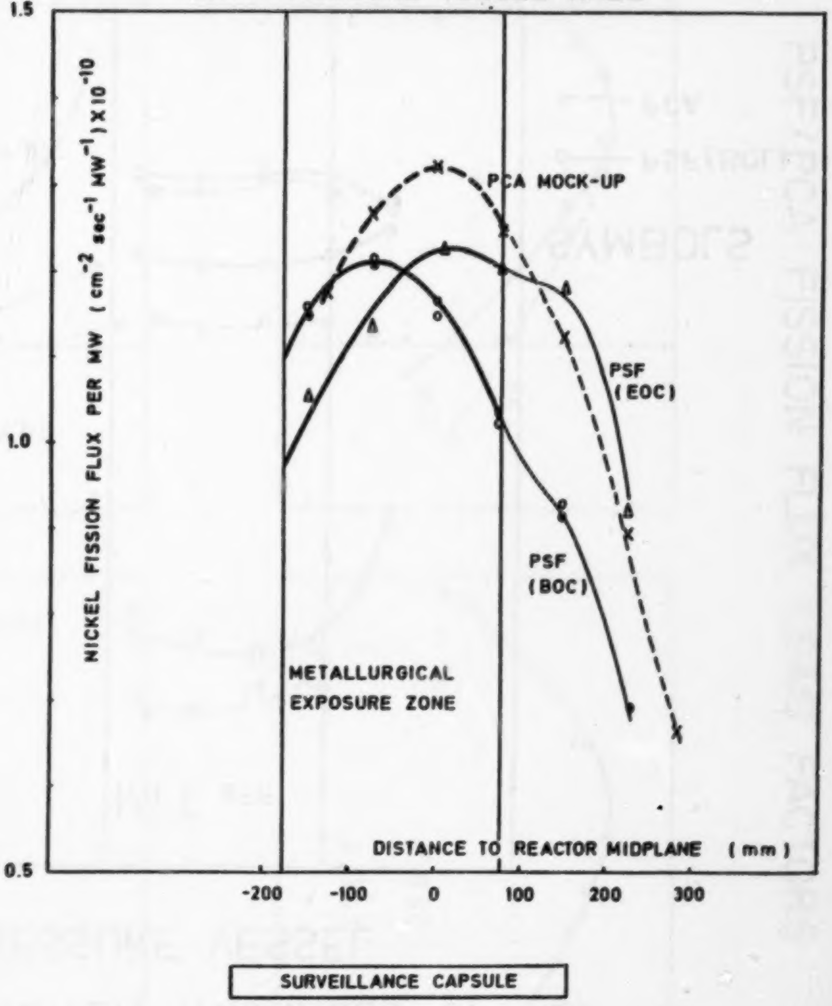

SPECTRAL INDICES AT QUARTER THICKNESS OF PSF SIMULATED PRESSURE VESSEL

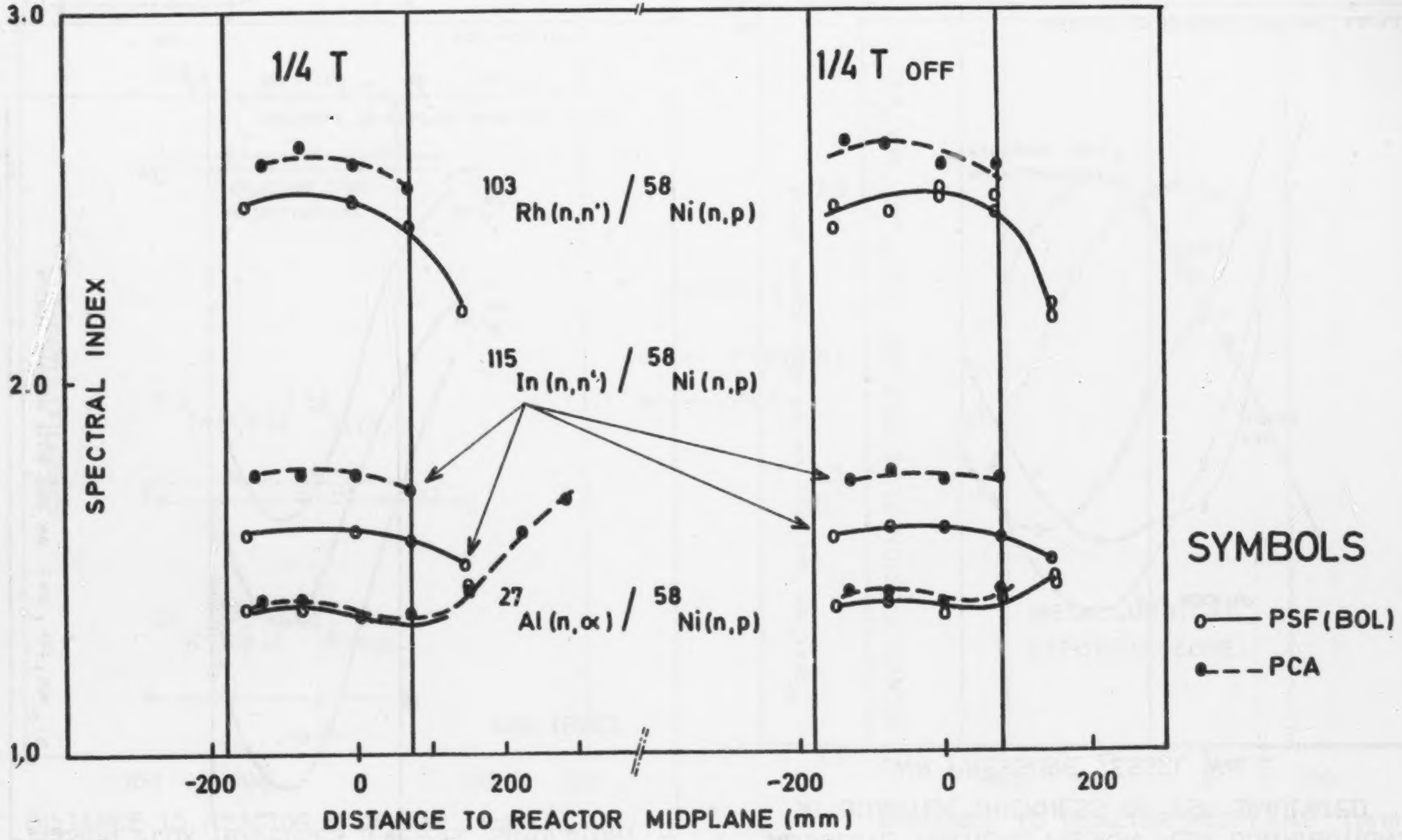

PSF/PCA FISSION FLUX LEAD FACTORS

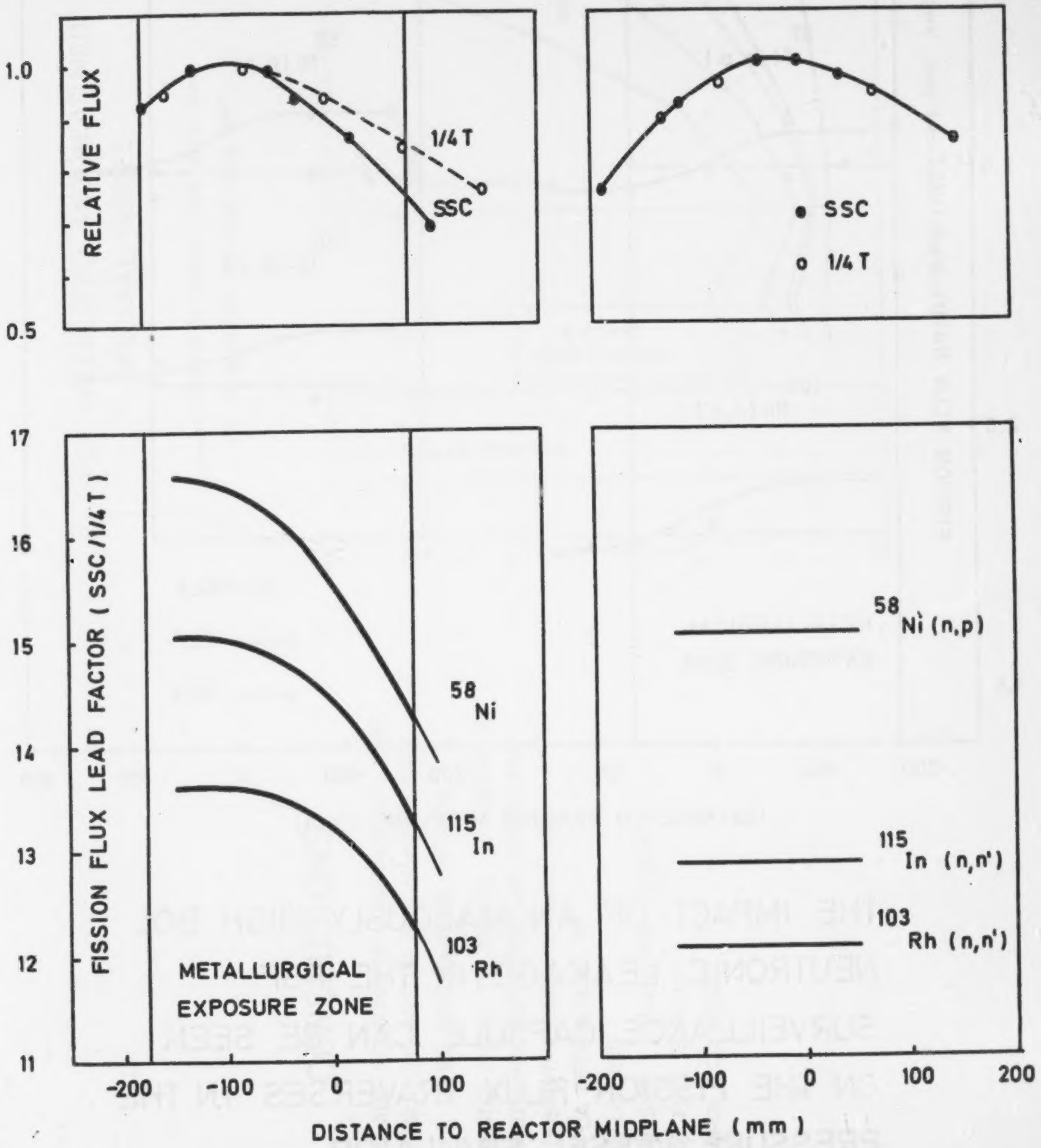

PSF (BOL)

PCA MOCK-UP

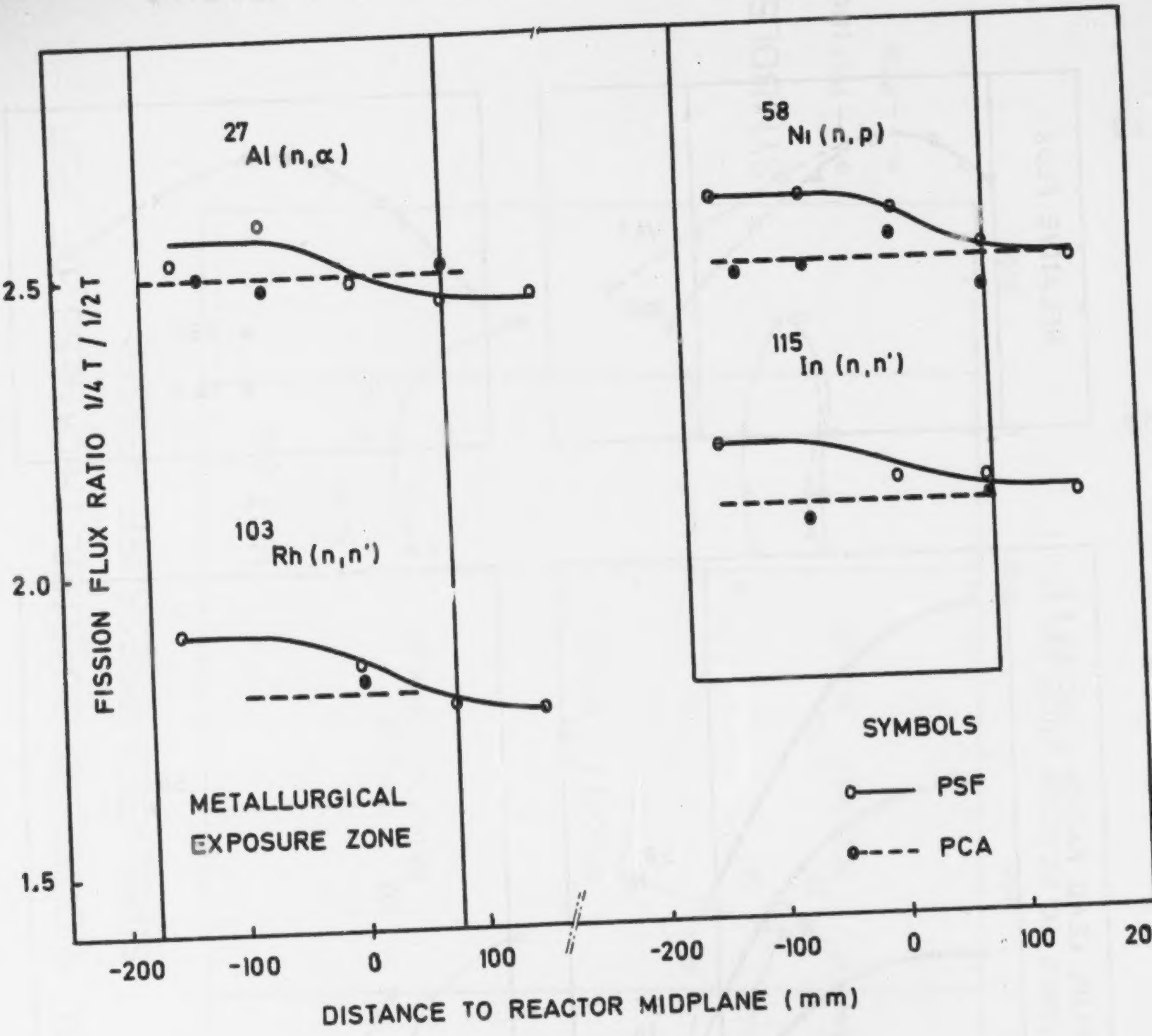

THE IMPACT OF ANOMALOUSLY HIGH BOL NEUTRONIC LEAKAGE IN THE PSF SURVEILLANCE CAPSULE CAN BE SEEN ON THE FISSION FLUX TRAVERSES IN THE PRESSURE VESSEL SIMULATOR

CONCLUSIONS

- IMPACT AND REASONS OF ANOMALOUSLY HIGH NEUTRONIC LEAKAGE OF PSF SURVEILLANCE CAPSULE TO BE INVESTIGATED FURTHER
- APPARENTLY SMALL OR TRIVIAL INFLUENCE IN PSF NEUTRONIC EXPOSURES AS ASSESSABLE FROM DOSIMETRY MEASUREMENTS OF PSF / PCA DIFFERENCES IN
  - CORE LOADING
  - CORE SIZE (TRANSVERSE LEAKAGE)
  - CORE FUEL BURN-UP
  - CONTROL ROD MOVES

PSF CALCULATED AND MEASURED SPECTRAL INDICES

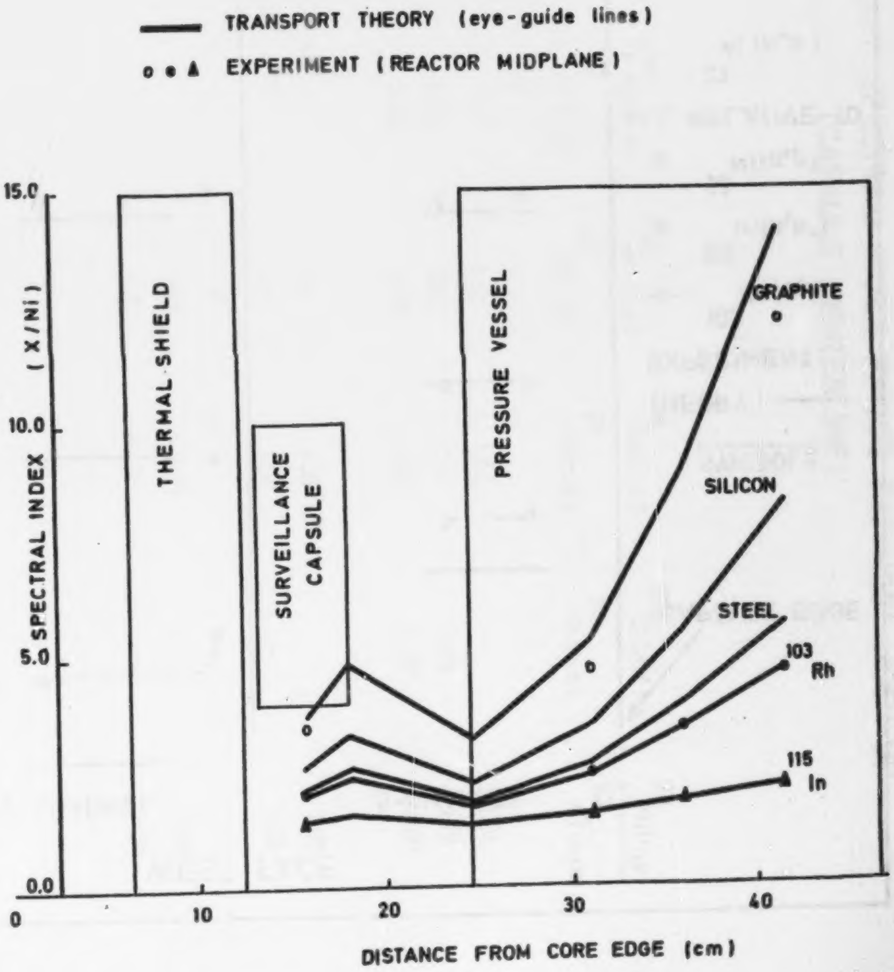

SPECTRAL INDICES IN BSR-HSST DOSIMETRY MOCK-UP (IT-CS CAPSULES)

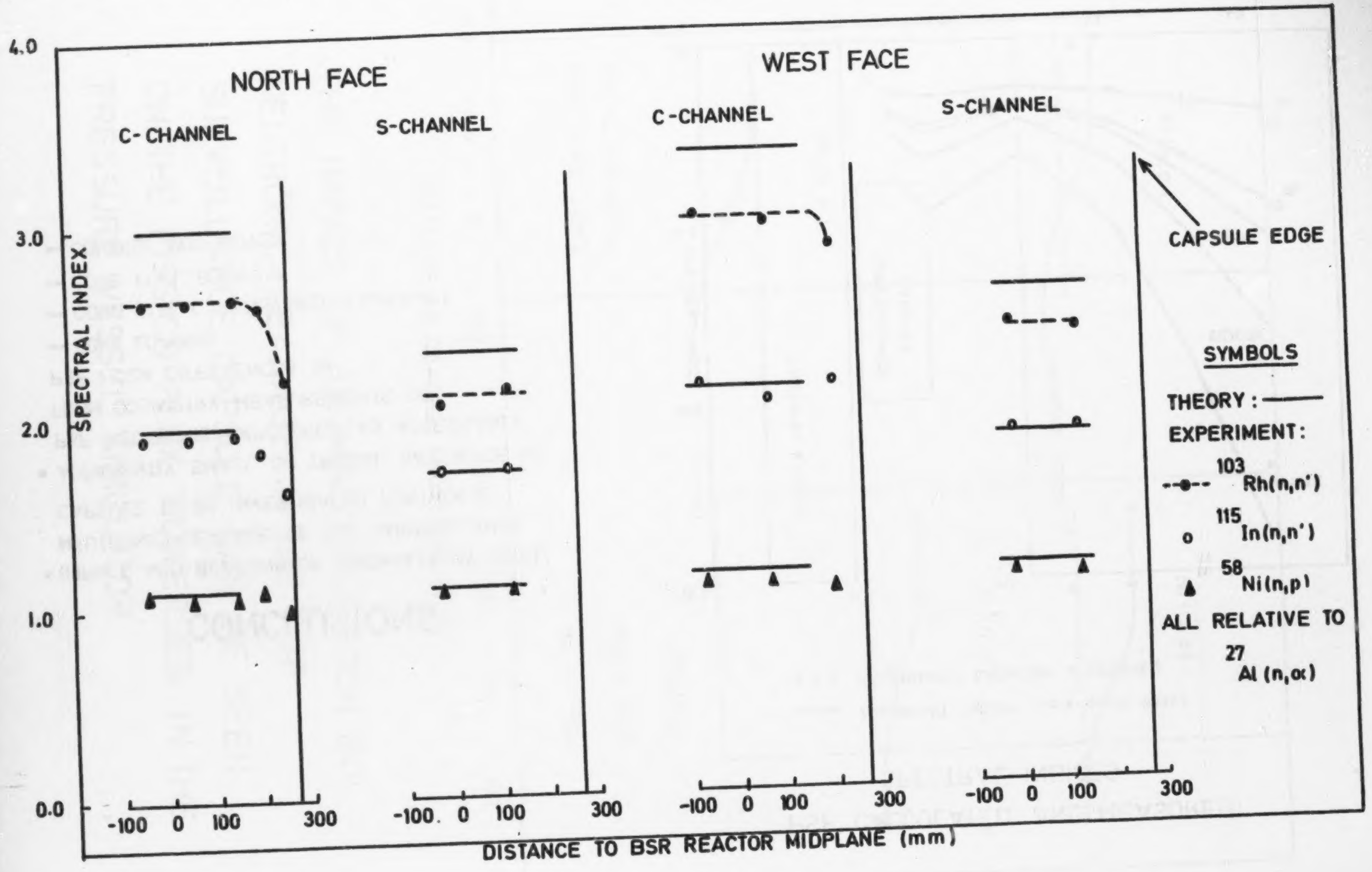

CALC/EXPT SPECTRAL INDEX RATIOS PSF/HSST MOCK-UP (CAPSULE CENTERLINE)

	$^{237}Np(n,f)$ / $^{27}Al(n,\alpha)$	$^{103}Rh(n,n')$ / $^{27}Al(n,\alpha)$	$^{115}In(n,n')$ / $^{27}Al(n,\alpha)$	$^{238}U(n,f)$ / $^{27}Al(n,\alpha)$	$^{58}Ni(n,p)$ / $^{27}Al(n,\alpha)$
PSF MOCK-UP					
SSC	-	1.01	1.04	-	1.04
1/4 T	0.89	0.93	0.91	0.89	1.01
1/2 T	0.95	0.89	0.87	0.89	0.97
HSST NORTH					
S-CHANNEL	-	1.11	1.00	-	1.00
C-CHANNEL	-	1.14	1.02	-	1.01
HSST WEST					
S-CHANNEL	-	1.09	0.99	-	1.05
C-CHANNEL	-	1.12	1.01	-	1.02

PSF/HSST EXPOSURE PARAMETERS (±10%, 1σ)

	$\phi_{>1MeV}$ [(a)] ($cm^{-2}\ sec^{-1}$)	$\phi_{>0.1MeV} / \phi_{>1MeV}$	DPA FISSION FLUX / $\phi_{>1MeV}$
ORR-PSF (30 MW)			
SSC	7.70,12	2.77	1.67
1/4 T	5.15,11	3.50	1.90
1/2 T	2.50,11	5.01	2.21
BSR-HSST (2 MW)			
NORTH CAPSULE	9.73,11	3.57	–
WEST CAPSULE	9.21,11	3.59	–

(a) AT MAXIMUM VERTICAL FLUX, NOMINAL CORE POWER AND ON CENTERLINE OF METALLURGICAL EXPOSURE ZONE

RADIAL FISSION FLUX ATTENUATION BY STEEL IN TYPICAL LWR PRESSURE VESSEL ENVIRONMENTS

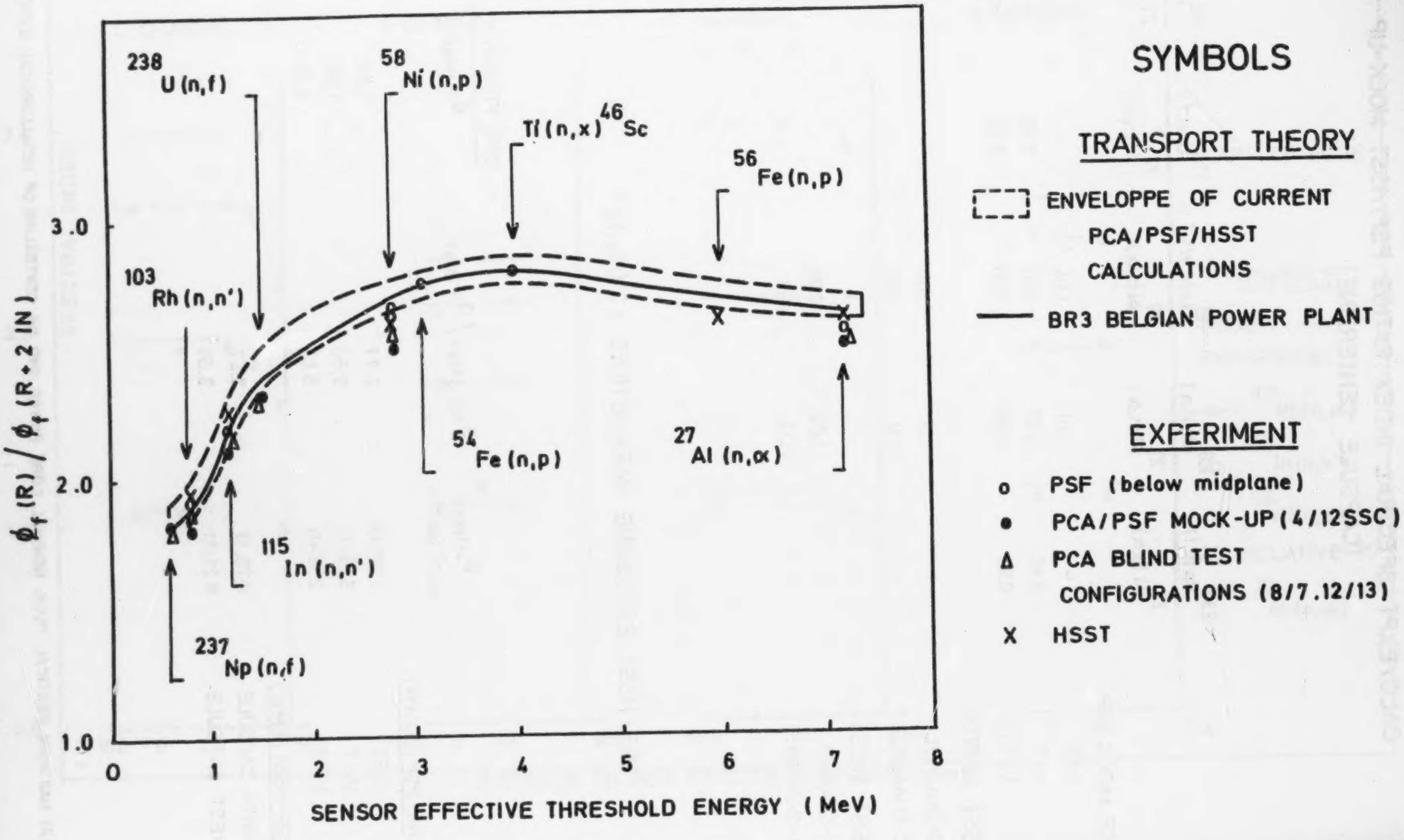

RADIAL NEUTRON FLUX SPECTRUM ATTENUATION BY STEEL IN SIMULATED LWR PRESSURE VESSEL ENVIRONMENTS

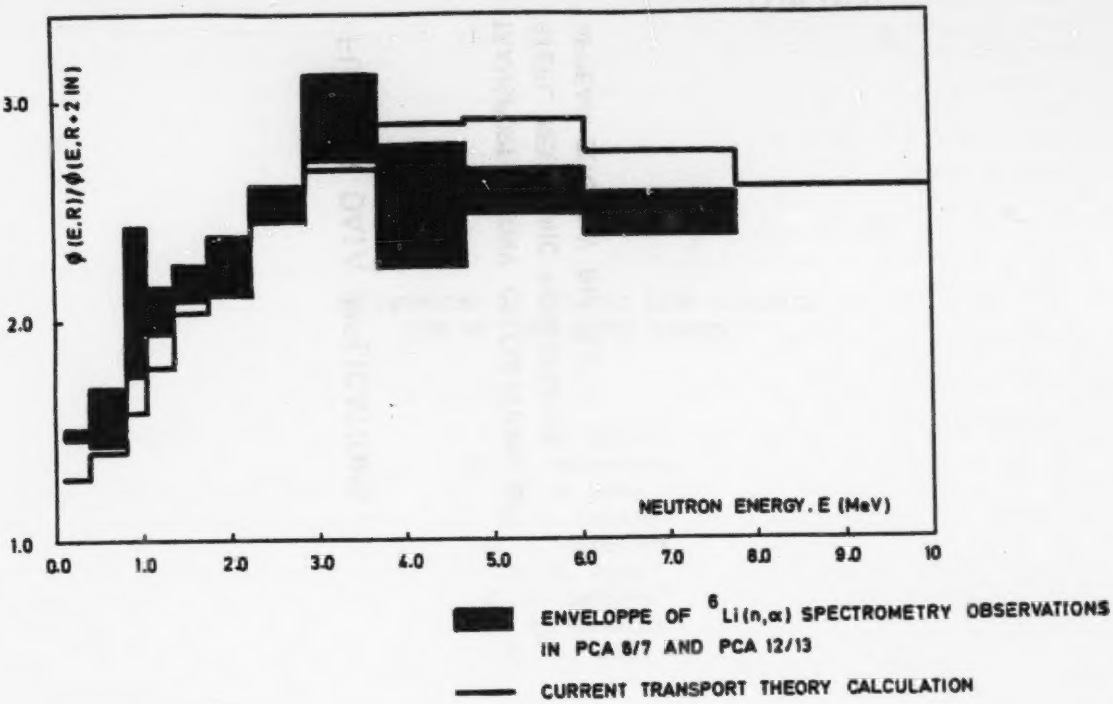

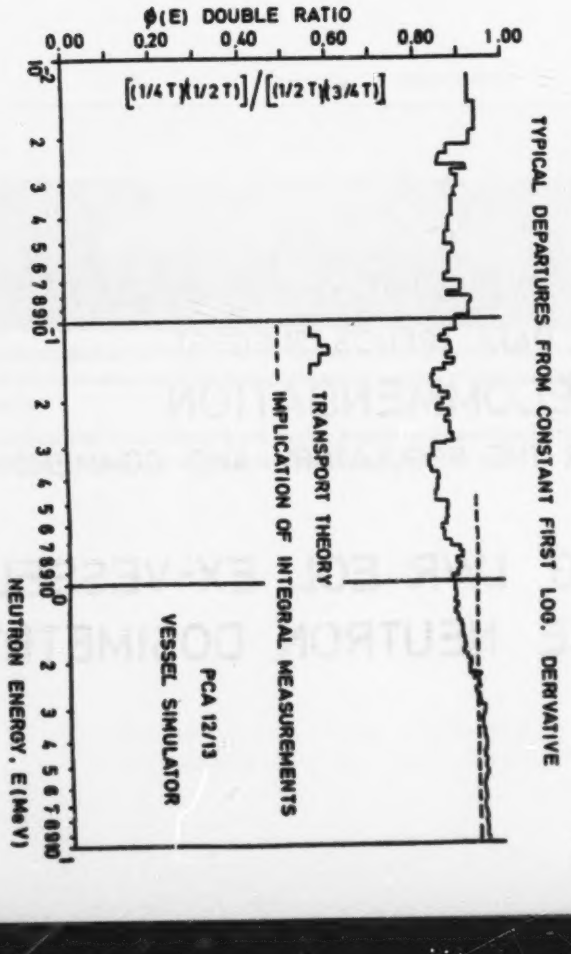

TYPICAL DEPARTURES FROM CONSTANT FIRST LOG. DERIVATIVE

PRIMARY DATA IMPLICATIONS

WITHIN ENGINEERING MARGINS OF 10% THE FIRST LOG. SPACE DERIVATIVE OF THE ABSOLUTE NEUTRON FLUX SPECTRUM IN LWR STEEL PRESSURE VESSELS APPEARS TO BE :

- UNIQUE
- CONSTANT

THEREFORE DEFINABLE BY PCA BENCHMARKING

FURTHER DATA IMPLICATIONS

- TRANSPORT THEORY CALCULATIONS OF STEEL NEUTRONIC PENETRATION APPEAR SLIGHTLY BIASED

ECONOMIC / SAFETY CONSIDERATIONS AND PCA / PSF / HSST NEUTRON DOSIMETRY DATA TRENDS SUGGEST :

RECOMMENDATION

TO ANALYZE FURTHER THE REGULATORY AND COMMERCIAL MERITS OF :

IMPLEMENTING LWR EOL EX-VESSEL SURVEILLANCE NEUTRON DOSIMETRY

UCID-18680

AN OVERVIEW OF SEISMIC RISK ANALYSIS FOR NUCLEAR POWER PLANTS

P. D. Smith
D. L. Bernreuter
M. P. Bohn
T. Y. Chuang
G. E. Cummings
R. G. Dong
J. J. Johnson*
R. W. Mensing
J. E. Wells

*Structure Mechanics Associates, San Ramon, CA

September 11, 1980

Lawrence
Livermore
Laboratory

This is an informal report intended primarily for internal or limited external distribution. The opinions and conclusions stated are those of the author and may or may not be those of the Laboratory.

This work was supported by the United States Nuclear Regulatory Commission under a Memorandum of Understanding with the United States Department of Energy.

DISCLAIMER

This book was prepared as an account of work sponsored by an agency of the United States Government. Neither the United States Government nor any agency thereof, nor any of their employees, makes any warranty, expressed or implied, or assumes any legal liability or responsibility for the accuracy, completeness, or usefulness of any information, apparatus, product, or process disclosed, or represents that its use would not infringe privately owned rights. Reference herein to any specific commercial product, process, or service by trade name, trademark, manufacturer, or otherwise, does not necessarily constitute or imply its endoresment, recommendation, or favoring by the United States Government or any agency thereof. The views and opinions of authors expressed herein do not necessarily state or reflect those of the United States Government or any agency thereof.

Available from : National Technical Information Service - U.S. Department of Commerce
5285 Port Royal Road - Springfield, VA 22161 - $8.00 per copy - (Microfiche $3.50)

ABSTRACT

Earthquakes, which present a unique design condition for nuclear power plants, are an example of a common-cause event which affects all single and redundant safety systems simultaneously. The potential size of an earthquake is uncertain; hence, nuclear power plant structures are designed for an estimated low probability event. Seismic risk analysis is an efficient method of assessing the effect of seismic hazards relative to other design conditions and of providing a framework within which to assess the relative importance of various seismic issues. The three elements of a seismic risk analysis are described: earthquake hazard or probability of occurrence of an earthquake, response of the nuclear power plant to the hypothesized event, and an evaluation of the failure of the plant. The last element includes component, structure, and system failure and any failure combination which produces an accident condition of consequence to the public. A methodology for this is described including a brief review of previous studies.

[illegible]
[illegible]

[illegible]

[illegible]

CONTENTS

Introduction 1

Aspects of Seismic Hazards to Nuclear Power Plants 4

General Perspective of Risk Analysis 10

Risk Analysis 12

Earthquake Hazard 13

Plant Response 20

Evaluation of Failure 32

Component-Related Probabilistic Considerations 32

System-Related Probabilistic Considerations 34

Examples of Event Trees 38

Event Tree for Transients with the Power Conversion System (PCS) 39

Event Tree for Transients without Power Conversion System (PCS) 46

Example of a System Fault Tree 49

Calculation of Failure of a Single Component 52

Calculation of Failure of Redundant Components in Fault Trees 55

Seismic Redundancy and Component and System Failure Targets 58

Seismic Redundancy and Plant Risk Targets 63

Event Tree Failure Calculations 64

Summary of Risk Calculations 70

Conclusions 72

Appendix: Risk Studies 75

Reactor Safety Study 75

Canadian Nuclear Power Plant Study 75

A Study by Hsieh and Okrent 76

A Study by Cornell and Newmark 76

Diablo Canyon Study 76

A Study by Ang and Newmark on Diablo Canyon 77

Clinch River Study 77

Oyster Creek Study 77

Seismic Risk Study in Great Britain 77

Seismic Safety Margins Research Programs 78

References 79

LIST OF ILLUSTRATIONS

1. Location of past destructive earthquakes in the United States 7
2. Isoseismal contours for 1906 San Francisco and 1811 New Madrid earthquakes 8
3. Components of seismic safety analysis 11
4. Earthquake hazard curves 14
5. Schematic of construction of probabilistic hazard function 15
6. (a) Seismic hazard density function (b) Seismic hazard complementary cumulative distribution function 18
7. Accelerogram of the 1940 Imperial Valley, California earthquake recorded at El Centro, California 19
8. Schematic of response calculations 21
9. Support-component model (a) and corresponding transfer function (b) used to calculate response spectra 24
10. Acceleration response history, $\ddot{y}(t)$, obtained by using the 1940 El Centro North-South component acceleration record as the foundation motion, $\ddot{x}(t)$, of the simple mechanical system shown in Fig. 9 . . 25
11. Peak acceleration response of the component in a subsystem with a natural frequency of 1.0 Hz 25
12. Peak acceleration response of the component in subsystems with various natural frequencies, where each subsystem was excited by the same motion $\ddot{x}(t)$ in Fig. 9 26
13. Acceleration response spectrum obtained by using the North-South component of the 1940 El Centro acceleration record 27
14. Acceleration response spectra obtained using time histories from 46 real earthquakes, each of which was scaled to 1.0 g peak horizontal acceleration 29
15. (a) Cumulative distribution function for component response conditional on free-field peak acceleration, a. (b) Density function for component response conditional on free-field peak acceleration, a 30
16. Graphical interpretation of the integrand of Eq. (4) 35

17. (a) Cumulative distribution function for the resistance (failure level) of a component/subsystem. (b) Probability density function for the response at a component/subsystem . . . 36
18. (a) Complementary cumulative distribution function for the response of a component/subsystem. (b) Density function for the resistance (failure level) of a component/subsystem 37
19. Class 1 transient event tree 44
20. Class 2 transient event tree 48
21. Simplified auxiliary feedwater system models. (a) system block diagram, (b) system fault tree 50
22. Graphical description of assumptions for calculation of component failure probability, $P_F(C)$, for simple example in text 53
23. Same as Fig. 22, except the r_i are shown 57
24. Graphical description of assumptions for calculation of system failure probability, $P_F(S)$, for simple example in text 61
25. Event tree for simple system 65
26. Fault tree for system 2 66
27. Computational procedure used in the Seismic Safety Margins Research Program (SSMRP) 71

LIST OF TABLES

1. Definition of events used on transient event trees 40
2. Calculation of the conditional probability of failure of the component, $P_F(C)$, where the load on the component and the resistance of the component are given in Figs. 21 and 22 . . . 56
3. Calculation of the conditional probability of failure of a system, $P_F(S)$, which is composed of three redundant identical components 58
4. Calculation of the conditional probability of failure of a system, $P_F(S)$, which is composed of three redundant identical components 63
5. Calculation of failure probabilities in an event sequence 69

INTRODUCTION

Almost three years ago, an important perspective on probabilistic seismic analysis of nuclear power plants was given by Cornell, Newmark, and Vanmarcke.[1] It is repeated here verbatim, because it addresses major concerns that arise repeatedly:

> "It is apparent in retrospect that the seminar did not provide a simple consensus of the speakers much less of the other participants. It can be said that it failed to provide a set of recommendations for next steps, either in development of regulatory procedures consistent with probabilistic analysis or in planning research. It could have better provided a perspective across the various parts of the total problem of the relative degrees of uncertainty in the procedures and parameters and the relative contributions to total seismic risk.
>
> "But it must be remembered that this may have been the first opportunity for many of the representatives of one discipline (e.g., seismology or nuclear systems analysis) to see in such depth the nature of the questions and procedures in another (e.g., structural dynamics or material behavior). Also, despite the fact that virtually all of the methods discussed have been utilized in one degree or another in one way or another in NPP practice, there are no examples of an application in which they have been brought together coherently. In short the seminar may have simply set the stage for these more unified, comprehensive and comparative studies of the problem.
>
> "Finally, a large number of the participants were cautious if not openly critical of the application of probability to NPP seismic analysis. One visitor observed that the tone of the seminar 'started at real optimism' and 'ended at skepticism' about applicability of highly sophisticated methods given such small data bases.
>
> "At least one of the editors would like to finish with a touch of optimism. It should be remembered that any incompleteness of information or understanding faced by probabilistic approaches is fundamentally just as significant for deterministic safety procedures. Failure of probabilistic analyses to include modes later identified as significant has its direct parallel in the history of current safety practice. In short, most of the objections to probabilistic safety analysis apply generally to safety analysis. Probabilistic methods seek in fact only to apply to the problem more of the information which does exist. They should never use less data or theoretical knowledge than the parallel deterministic models. Concerns about the 'sophistication' and 'complexity' of probabilistic methods probably reflect more the current lack of familiarity with probability by many engineers than fundamental difficulties (there are no new mathematical tools needed, for example).
>
> "The unavoidable fact is that probability has been used for some time in isolated parts of the NPP seismic safety problem.

> Unfortunately, those applications have been localized and largely uncoordinated. (For example, mean plus one sigma response spectra are used, but acceleration versus intensity relationships, based on statistical regressions, ignore in practice the resulting standard deviation.) The aim of a coordinated probabilistic seismic safety assessment should be simply to be consistent and logical as it passes through the entire problem. It should discourage regulatory practices which are demonstrably inconsistent with even the simplest rules for dealing rationally with uncertainty. At best, probabilistic seismic safety analysis should provide positive bases for the development of design, analysis, and regulation schemes which are logical, realistic, and consistent with the existing knowledge and lack of knowledge in the field. The seminar did, we believe, both present (with frankness) the weaknesses in knowledge and outline the procedures by which a probabilistic approach can improve (if never perfect) engineering practice in the NPP seismic safety field."

The optimism of one of the editors appears to have been well founded. The state-of-the-art of probabilistic seismic analysis and risk analysis has steadily advanced since that time.

Earthquakes, which represent a potential hazard for all nuclear plants, are almost a unique hazard because of their potential to compromise redundancy.

A number of limited studies on risk of earthquakes to nuclear power plants have been performed. Although the Reactor Safety Study[2] reached the conclusion that earthquakes were not a major contributor of risk of radioactive release from nuclear power plants, a later Canadian study of seismic risk and nuclear power plants[3] showed that the risk may have been underestimated. A further study by Hsieh and Okrent[4] indicated that design errors could be an important, but previously overlooked, contributor to seismic risk.

In 1978 the U.S. Nuclear Regulatory Commission (NRC) established the Seismic Safety Margins Research Program (SSMRP) to examine the question of seismic risk[*] to the public. This multi-year program is directed towards estimating the degree of conservatism or unconservatism in the NRC seismic safety requirements with the ultimate goal of developing improved requirements and evaluation methods. The SSMRP approach uses risk analyses (event trees and fault trees) combined with detailed analytical modeling and an extensive component failure (fragility) data base. As a later part of this program, detailed calculations of the seismic risk of a typical commercial nuclear reactor are to be made.

---

[*] In the SSMRP, a nonstandard definition of risk is used, that is, probability of release of radioactive material.

This paper outlines the basic aspects of risk analysis in general and its application to nuclear reactor risk in particular. Risk analysis is divided into three topics:

- Earthquake hazard
- Plant response
- Failure analysis

These three topics are considered in detail in the following sections. A summary of important nuclear risk studies is presented in the appendix.

ASPECTS OF SEISMIC HAZARDS TO NUCLEAR POWER PLANTS

Earthquakes constitute a unique hazard to nuclear power plants. Several observations lead to this conclusion:

- Earthquakes threaten redundancy. For example, redundant systems are often installed in plants to provide additional safety. However, an earthquake induces mechanical effects such as stress or displacement in the entire plant simultaneously, and this tends to compromise redundancy. For example, if an earthquake causes a diesel generator to fail, it is quite likely that a second, redundant, diesel generator will also fail. This scenario essentially means a loss of some of the benefits of redundancy.
- Steady advances continue to be made in the state-of-the-art of earthquake engineering which leads to frequent changes in the licensing process. For example, the effects of the discovery of the Hosgri fault on the Diablo Canyon plant license application are well-known, and the Ramapo fault earthquake at the Indian Point plant site in New York raises the specter of the potential for an East Coast "Diablo Canyon."
- We do not design or evaluate the plant for the maximum possible earthquake. For example, the Imperial Valley earthquake of October 15, 1979 produced one record with a peak vertical ground acceleration of 1.74 g, which is more than twice the design value for any plant. This single record also provides two examples of possible licensing instability:
  - The peak acceleration was about 0.5 g larger than any previously measured in the United States.
  - The ratio of the vertical to horizontal acceleration was 2.35 whereas a typical licensing value is 0.67.
- We do not design for the maximum possible earthquake with a given peak acceleration. For example, typical design basis response spectra are roughly equivalent to the mean plus one standard deviation (MSD) of spectra from a certain set of recorded earthquakes. This MSD value is less than the maximum of this set, and this maximum is less than the maximum for all recorded earthquakes.

- Measures taken to increase seismic safety may lead to decreased overall safety. For example, the present seismic design methods tend to result in stiffer systems when additional strength is provided for the earthquake loading. A stiff system is subjected to greater cyclic thermal stress than a flexible one under normal thermal operating loads, with a resulting reduction in reliability under normal conditions. Trade-off studies may thus be required to find the most appropriate seismic design level.
- Measures taken to increase seismic safety through the addition of strength may lead to reduced reliability of the element strengthened. For example, when more and more reinforcing is added to concrete for the earthquake loading, we increase its strength but reduce its ductility.
- Measures taken to increase seismic safety in one element of the seismic design methodology chain may lead to decreased safety in another element of the chain. For example, if a containment or auxiliary structure is overdesigned for seismic loads, the actual structural damping we can expect to be mobilized during an earthquake may be less than the damping assumed in the structural response analysis, because of the low earthquake stresses resulting from the overdesign. The lower damping values arise as a result of low stress in the structure, and thus it is unlikely that the structural design adequacy will be questioned. However, the earthquake loads to systems mounted on the structure may be increased as a result of the overdesign, that is, because of the low damping.
- There may not be a clear choice of a single value for a parameter that is agreed to be "conservative." For example, concrete cracks occur before and during earthquake loading and this affects stiffness and hence structure frequencies. These frequencies have a profound effect on the design of piping systems. While a stiffness might possibly be selected so as to provide a "conservative" design for one piping system, it would be quite unexpected that we would be able to determine a single structural stiffness that would result in "conservative" designs for all piping systems. An analogous issue arises in choosing values for foundation dynamic parameters for use in soil-structure interaction analyses, except the effects of such

parameter choices then affect not only subsystem but also structural design.

- Seismic safety analyses rely on the "design envelope" concept, but this does not always guarantee "conservative" results are used in design. For example, seismic safety analyses most often use analyses based on the safe shutdown earthquake peak acceleration. In some cases, separate (not necessarily safety) analyses are also performed based on the operating basis earthquake peak acceleration. Except in a few cases, the latter acceleration is typically one-half the former. Yet, instances have been noted where the calculated response for the operating basis earthquake exceeded that due to the safe shutdown earthquake; for example, in-structure response spectra over some frequency range.
- Seismic safety assessments and design are based largely on analyses that have little experimental verification. For example, soil-structure interaction analyses have yet to be convincingly corroborated with test or field results.
- The data base on earthquakes is a poor relative to the needs of the nuclear industry. For example, most of the reactors in the United States are located east of the Rocky Mountains, but most of the high-quality data is for earthquakes which occurred in the west.

Many engineers believe earthquakes to be primarily a California issue for conventional structures in the United States; however, earthquakes have occurred in every state, and as shown in Fig. 1, damaging earthquakes have also had a wide distribution. The 1811-12 series of earthquakes near New Madrid, Missouri is believed by some to have been the most severe earthquakes that have occurred in the United States, which is certainly true on the basis of the areas over which equivalent damage might have been expected, (see Fig. 2). This characteristic of Eastern United States earthquakes (large felt areas) was recently reconfirmed, even for small events, by the July 28, 1980 earthquake near Lexington, Kentucky. Earthquakes are thus a hazard that should be considered for conventional design in every state.

Earthquakes are of even greater significance in nuclear than in conventional design. This can be seen by considering four factors:

- The reliability of nuclear plants under normal operating and accident conditions has increased to the point where some studies now estimate

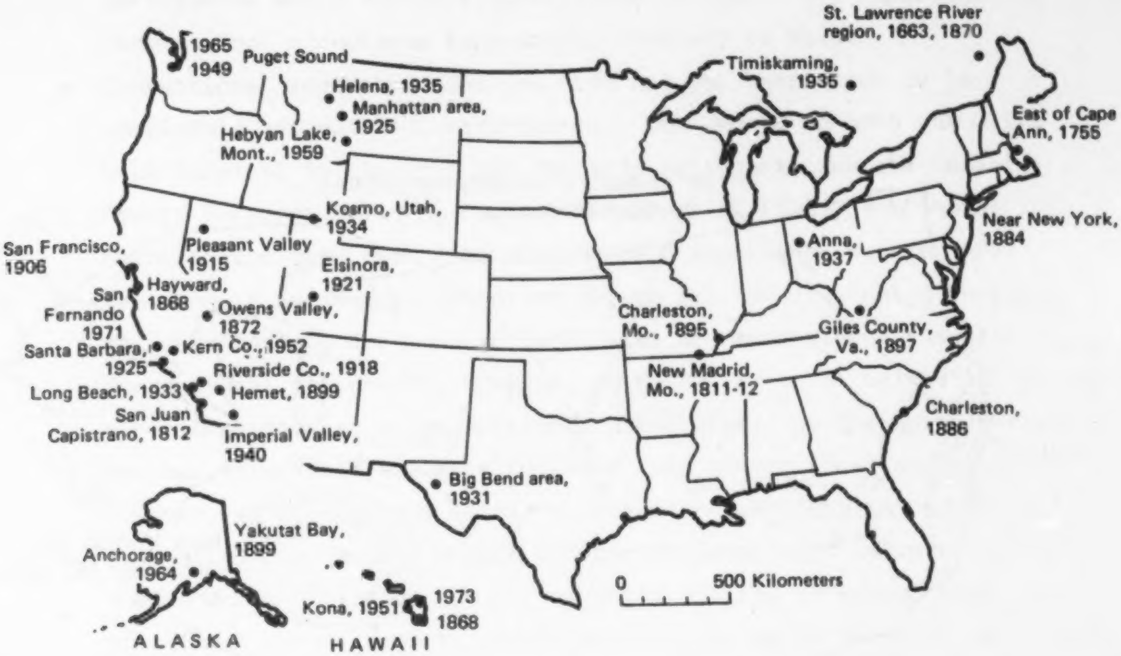
1965
1949
Puget Sound
Helena, 1935
Manhattan area, 1925
Hebyan Lake, Mont., 1959
St. Lawrence River region, 1663, 1870
Timiskaming, 1935
East of Cape Ann, 1755
Near New York, 1884
Kosmo, Utah, 1934
Pleasant Valley 1915
San Francisco, 1906
Elsinora, 1921
Hayward, 1868
San Fernando 1971
Owens Valley, 1872
Santa Barbara, 1925
Kern Co., 1952
Riverside Co., 1918
Long Beach, 1933
Hemet, 1899
San Juan Capistrano, 1812
Imperial Valley, 1940
Anna, 1937
Charleston, Mo., 1895
Giles County, Va., 1897
New Madrid, Mo., 1811-12
Charleston, 1886
Big Bend area, 1931
Yakutat Bay, 1899
Anchorage, 1964
ALASKA
Kona, 1951
1973
1868
HAWAII
0
500 Kilometers

FIG. 1. Location of past destructive earthquakes in the United States (Hays).[5]

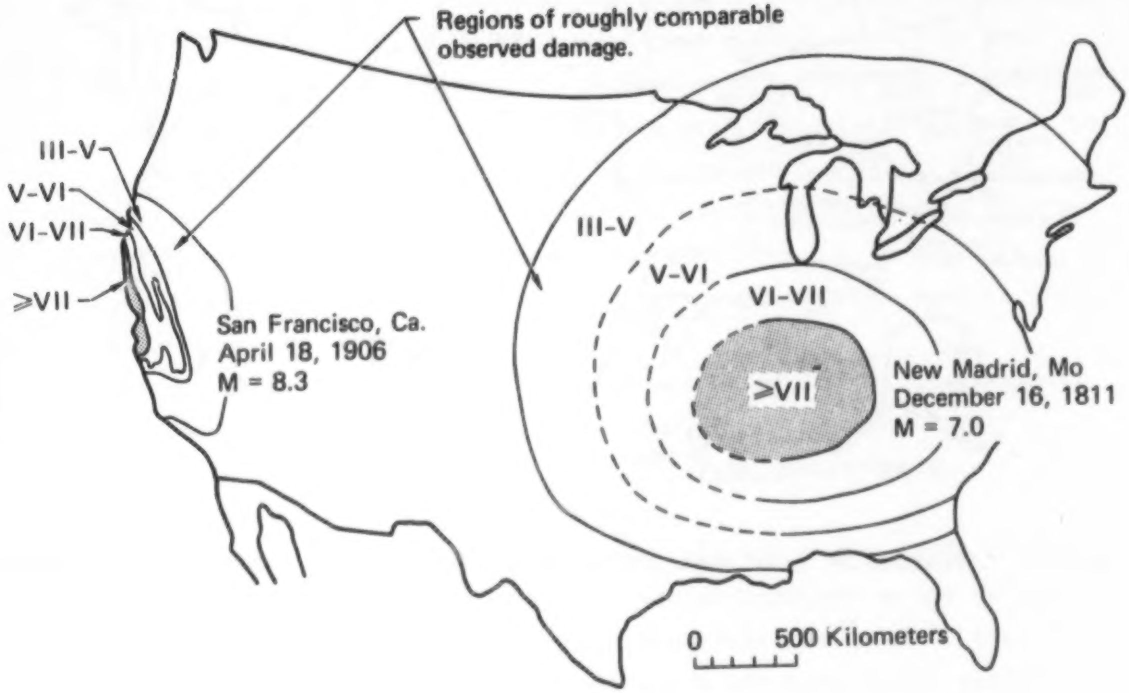
Regions of roughly comparable observed damage.
III-V
V-VI
VI-VII
≥VII
San Francisco, Ca.
April 18, 1906
M = 8.3
III-V
V-VI
VI-VII
≥VII
New Madrid, Mo
December 16, 1811
M = 7.0
0
500 Kilometers

FIG. 2. Isoseismal contours for 1906 San Francisco and 1811 New Madrid earthquakes (modified from Nuttli).[6]

earthquakes are a dominant contributor to risk. Our experience in conventional structures is probably contrary to this.

- Conventional engineered designs have not yet been shown to be completely adequate for earthquakes. The damage to both the Olive View Hospital in the 1971 San Fernando earthquake and the Imperial County Services Building in the 1979 Imperial Valley earthquake demonstrates that even with considerable experience we are still learning in earthquake resistant design for conventional structures. The requirements for nuclear facilities are more severe than for conventional structures, however, we do not have the extensive experience base as in conventional structures. We are quite certain nuclear structures are more reliable than conventional structures; however, we do not know if the increased reliability is "adequate."
- Nuclear design imposes unique non-conventional requirements. For conventional structures we may be quite willing to accept some structural damage from an earthquake as long as it does not cause loss of life. For nuclear design, an earthquake could cause virtually no damage to the structures, but could damage the mechanical or electrical operating or safety systems mounted on the structures and thereby cause a release of radioactivity. The failure of an integrated system of this type is a relatively rare concern in conventional design. In addition, we do not have a broad base of engineering experience on the survivability of complex systems of this type during severe earthquakes. Certainly our experience is not as extensive as in the case of conventional (more simple) structural systems where unexpected failures still occur. Alternately, since we do not test the entire nuclear plant for earthquake-like loadings, nuclear designs for earthquakes must still be considered as unproven, in spite of the perception--and perhaps the reality--that nuclear designs are quite reliable.
- Seismic risk analysis for plants in the Eastern United States may have to consider the possible effects from more than one site, in certain cases, because of the large felt areas characteristic of Eastern earthquakes.

Risk analyses provide one method to integrate and evaluate these various issues. For example, risk analysis is one way to study the trade-offs between measures taken to increase seismic safety and the postulated consequent decrease in operating safety. Another type of risk analysis is to study the consequences of not designing for the maximum possible earthquake or maximum possible earthquake for a given peak acceleration.

GENERAL PERSPECTIVE OF RISK ANALYSIS

This section presents a general perspective on earthquake risk analysis, drawing heavily on the work of Cornell and Newmark.[7]

The analysis of risk caused by earthquakes requires the integration of a variety of elements summarized in Fig. 3. We begin with a probabilistic description of the seismic hazard, and end with the risk to the public.

The seismic hazard at a site depends predominantly on seismological issues which are virtually independent of the plant. Ideally, the description of the seismic hazard should include all possible scenarios, including the timing and intensities of aftershocks, surface faulting, vibratory motion, and so forth. The ground motions are transmitted (possibly with some interaction between the soil and structures) through the soil in the neighborhood of the plant to the structures. The structures play three major roles:

- The structures may directly initiate accidents by collapsing upon critical equipment.
- The structures act as transmitters (possibly with feedback or interaction) of motion to piping, mechanical, foundation, and electrical components.
- The performance of the containment structure as a secondary pressure vessel affects accident mitigation and consequences.

Accident sequences are derived from the behavior of the entire "plant system" with its various "subsystems" (for example, nuclear steam supply system, "emergency core cooling system", residual heat removal system) with their various components (for example, vessels, pipes, valves, electrical equipment) under the seismic environment (for example, support motion histories, possible pipe breaks with consequent pressure-temperature conditions). The induced pressure-temperature conditions, acting during and after the earthquake, mechanically influence the containment structure as a pressure vessel. Off-site power may also be influenced by the earthquake, and this too affects risk. The net result may be one of a family of patterns of release of radioactivity from the plant as a function of time.

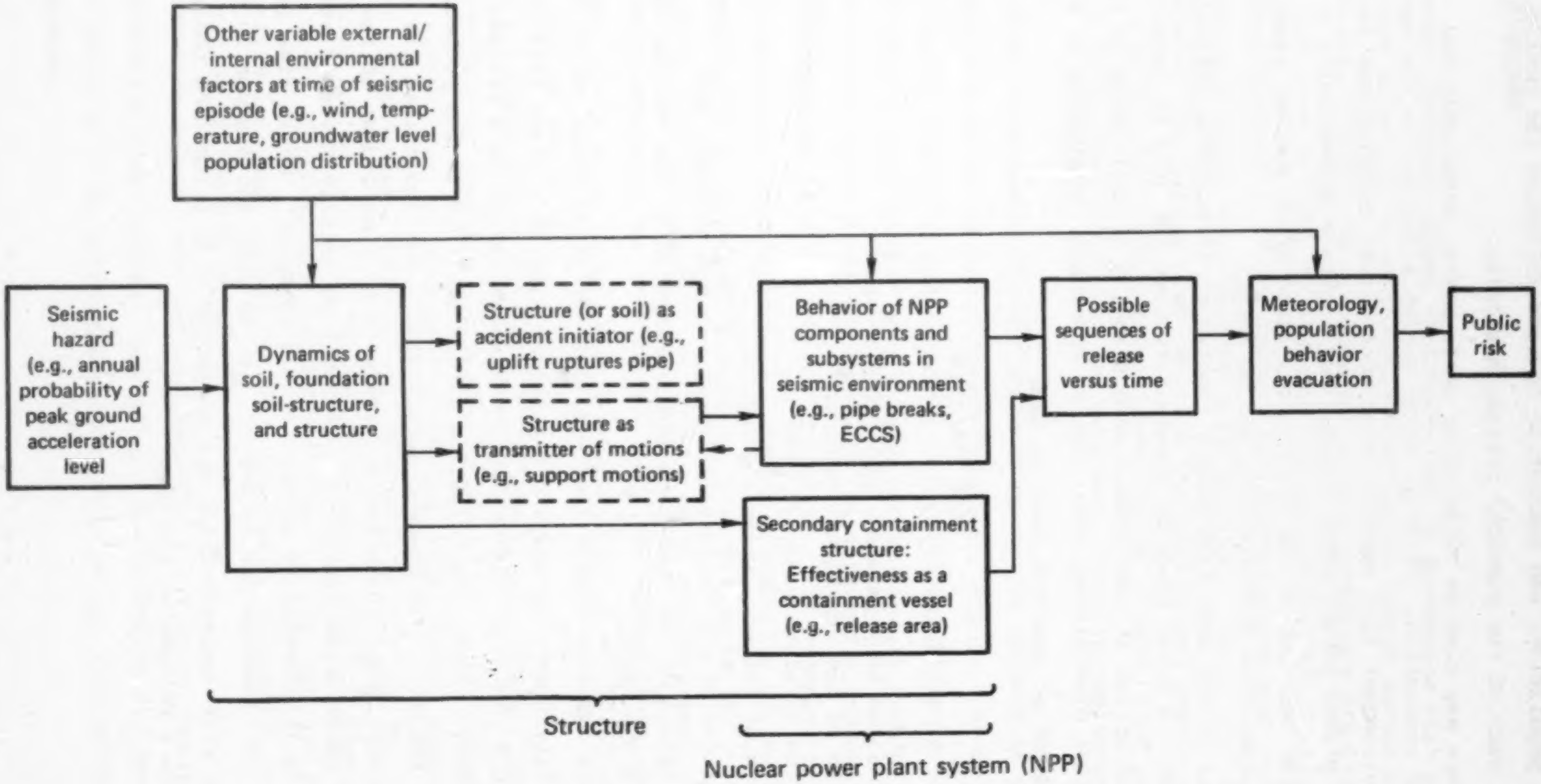
Other variable external/ internal environmental factors at time of seismic episode (e.g., wind, temperature, groundwater level population distribution)
Seismic hazard (e.g., annual probability of peak ground acceleration level
Dynamics of soil, foundation soil-structure, and structure
Structure (or soil) as accident initiator (e.g., uplift ruptures pipe)
Structure as transmitter of motions (e.g., support motions)
Behavior of NPP components and subsystems in seismic environment (e.g., pipe breaks, ECCS)
Secondary containment structure: Effectiveness as a containment vessel (e.g., release area)
Possible sequences of release versus time
Meteorology, population behavior evacuation
Public risk
Structure
Nuclear power plant system (NPP)

FIG. 3. Components of seismic safety analysis (Cornell and Newmark).[7]

Meteorological, population, and evacuation factors determine the public consequences of each of the possible release histories.

These factors may also be affected by earthquakes, especially the effectiveness of evacuation. Finally, other variable factors in the natural and man-made environment (for example, wind conditions, temperatures inside and outside the plant, ground water levels) may interact mechanically or otherwise with the behavior of the foundation, structures, nuclear steam supply system, population distribution, and so forth.

The analysis of the risk from such a complex of interacting phenomena is a formidable task. A broad range of specialists must not only be involved but must interact and arrive at some common understanding of the issues in the different technical disciplines, and, just as important, compromise on some balance in the depth of approach used in each.

RISK ANALYSIS

Risk analysis can be separated into three areas:

- Definition of the earthquake hazard,
- Calculation of plant response, and
- Evaluation of failure, which depends on
  - Definition of the failure of components and systems, and
  - Description of the operation and interaction of the various systems within the plant.

Risk analysis combines inputs from all three of these areas using the rules of probability theory to compute the probability of a plant failure. Failure events of primary importance are those which result in a release of radioactive material. Thus, one output of a risk analysis is the probability of a radioactive release. The Reactor Safety Study[2] has shown that the most likely way to release significant radioactivity is by a melt-down of the core.

Each of the three areas mentioned above will be briefly reviewed and the method of analysis illustrated by several simple examples. While risk implies an assessment of the consequences to the public, we will not discuss further those elements of risk analysis which are concerned with estimating the public consequences given a release at the plant.

EARTHQUAKE HAZARD

The most important aspect to account for in earthquake risk analysis is the pervasive effect of an earthquake: earthquakes induce mechanical effects such as stress, strain, and displacement in all components simultaneously. If there is more than one unit at the site, we must expect all facilities to be excited simultaneously. In the Eastern United States, we must even expect widely separated sites to be excited simultaneously. Next, the "intensity" of the earthquake, for example, the level of the peak ground acceleration, may vary over a wide range. These two characteristics suggest that probabilistic methods should be used to perform the analysis. This is explained in the following.

The first requirement for the application of the methods of probability to risk analysis is to develop a hazard function. Figure 4 shows typical graphs of hazard functions that describe a derived relationship between peak free-field ground acceleration at the site and the annual probability of an earthquake occurring in some region around the site which induces a site peak acceleration greater than the value of interest. For example, graph 1, used in studies on Diablo Canyon, shows the annual probability of the occurrence of an earthquake with an acceleration greater than 0.75 g as 10^{-4}. The 0.75 g corresponds to the safe shutdown earthquake (SSE) acceleration. (This is an example where accelerations used in risk analyses exceed those used in design, as the upper limit shown in graph 1 for Diablo Canyon is 1.2 g, which is 0.45 g greater than the SSE value.)

Figure 5 shows one process used to develop these hazard functions. The basic seismicity description (frequency information) is the $\log_{10}N$ (N is the number of earthquakes larger than a given magnitude) versus magnitude (or intensity) relationships shown in the upper portion of Fig. 5b. These relationships are derived from historical seismic records. There may be several sources of earthquakes (three are shown in Fig. 5a) and a relationship can be derived for each. These relationships give information on earthquakes at the location of the earthquake.

Attenuation rules (lower part of Fig. 5b) are used to specify how the peak acceleration (for example) decreases with increasing distance from the source to the site. The attenuation relationships are also derived from data on earthquakes.

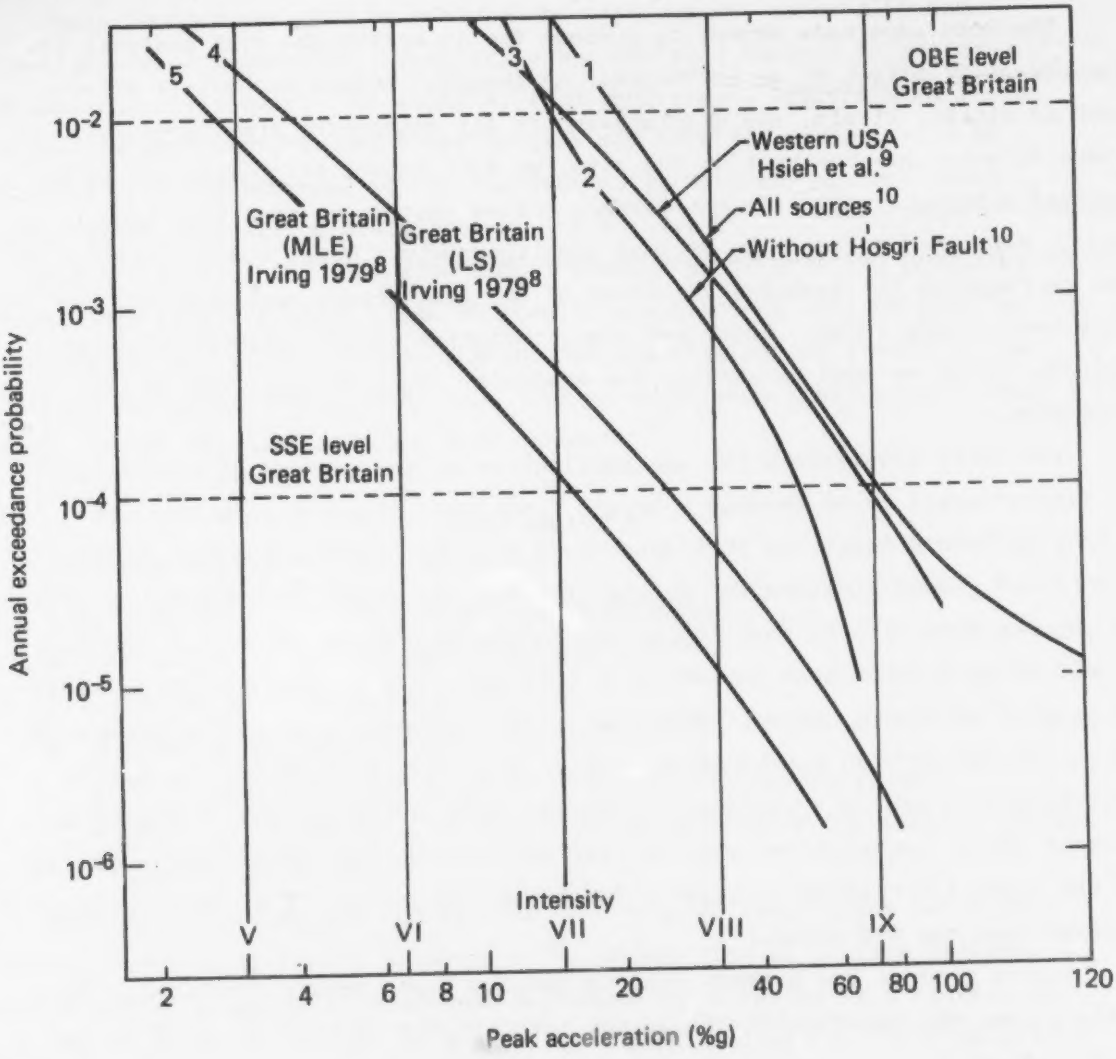

FIG. 4. Earthquake hazard curves (modified from Irving).[8] Each curve is a complementary cumulative distribution function.

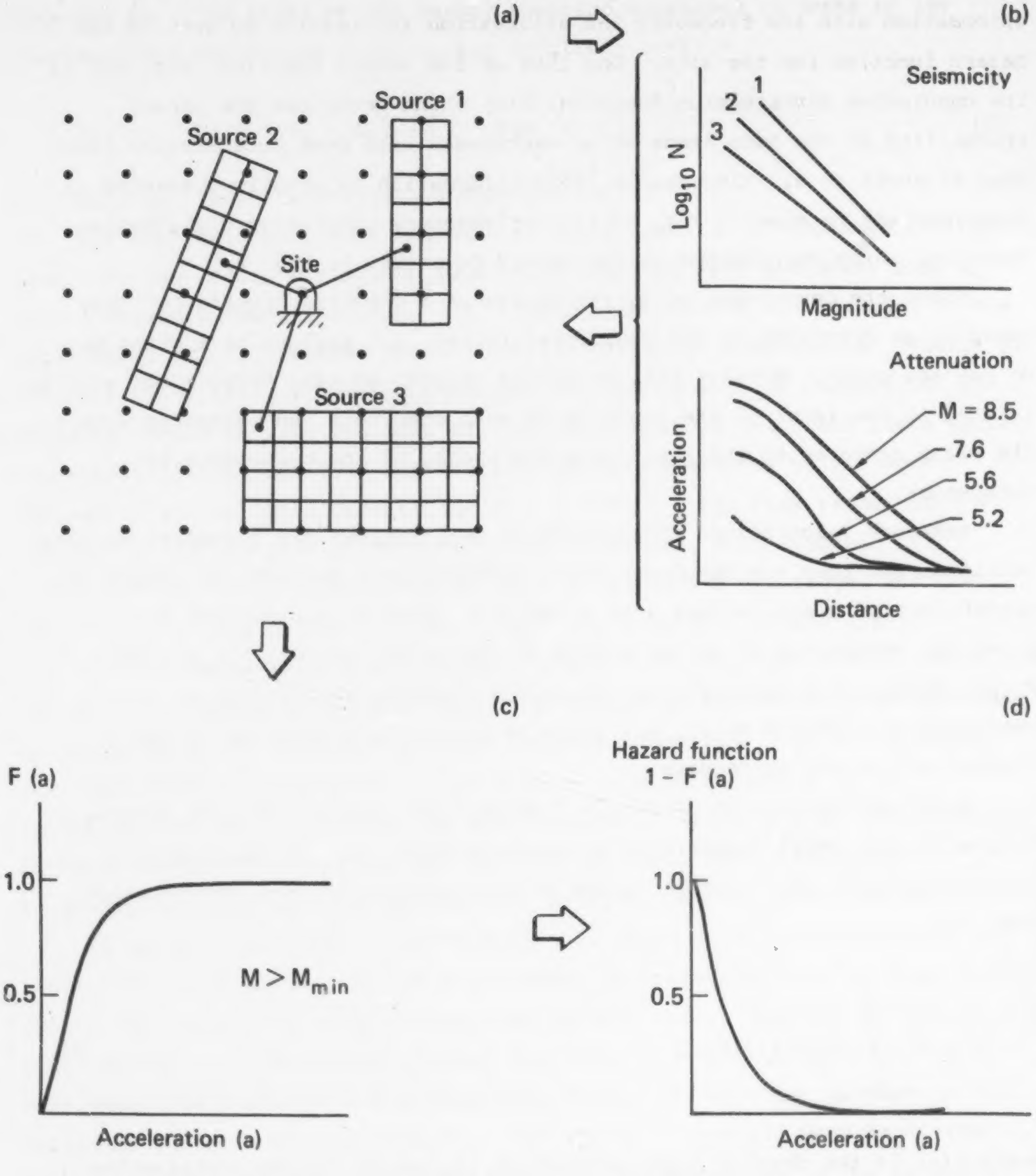
(a)
Source 1
Source 2
Site
Source 3
(b)
Seismicity
1
2
3
Log$_{10}$ N
Magnitude
Attenuation
M = 8.5
7.6
5.6
5.2
Acceleration
Distance
(c)
F (a)
1.0
0.5
M > M$_{min}$
Acceleration (a)
(d)
Hazard function
1 − F (a)
1.0
0.5
Acceleration (a)

FIG. 5. Schematic of construction of probabilistic hazard function: (a) Three typical seismic source zones and the site; (b) seismicity for the three source zones and acceleration attenuation curves for the region; (c) depicts a typical cumulative probability distribution F(a) of ground acceleration at site; (d) is the complementary cumulative distribution form of C. Modified from Hays.[33]

Probabilistic methods are used to combine the earthquake source information with the frequency and attenuation information to develop the hazard function for the site. One form of the hazard function (Fig. 5c) is the cumulative distribution function, F(a) which describes the annual probability of the occurrence of an earthquake with peak acceleration less than or equal to a. Alternately, this information is usually presented in complimentary form as in Fig. 5d (a complementary cumulative distribution function) which corresponds to the hazard functions in Fig. 4.

Given the occurrence of an earthquake of a specific "intensity" (for example, as described by its peak acceleration, a_i) failure of a plant may or may not occur. Whether failure occurs depends on many factors but will be related to the level of the response of each component and subsystem within the plant compared to the resistance (strength) of the components and subsystems.

Response calculations and resistance descriptions are discussed in later sections, and they are combined, using probabilistic methods, to obtain the probability of plant failure (for example, release of radioactive material) given the occurrence of an earthquake of the given "intensity", a_i. Let $P_F(a_i)$ denote this probability. Since the response and failure of each component will depend on a_i, the value of $P_F(a_i)$ is a function of the "intensity" of the earthquake.

Since earthquakes of different "intensities" will occur with varying frequency, the total probability of plant failure, P_{FT}, is calculated by integrating over all possible values of site free-field peak acceleration. That is:

$$P_{FT} = \int_0^\infty P_F(a) f(a) da \tag{1}$$

where f(a) is the density function form of the hazard (which contains the basic information on frequency). This expression is approximated by:

$$P_{FT} = \sum_{i=1}^{n} P_F(a_i) \Delta F(a_i) \tag{2}$$

where $\Delta F(a_i)$ is the probability the peak acceleration will be in the interval Δa_i. In terms of the hazard function expressed in terms of the complementary cumulative distribution function, 1-F(•):

$$\Delta F(a_i) = \left[1 - F(a_i - \Delta)\right] - \left[1 - F(a_i + \Delta)\right] \tag{3}$$

for small Δ. These relations are depicted in Fig. 6.

One implication of this approach is quite important: The acceleration level for the design earthquake (operating basis or safe shutdown) does not play a direct fundamental role. All acceleration levels are included in the integral of Eq. 1. Because of this consideration, we describe our results as probability of failure from earthquakes, not probability of failure for an operating basis or safe shutdown earthquake. We could calculate these latter two probabilities, but they are of little interest because we are more interested in the total probability of failure or total risk rather than a somewhat arbitrary smaller portion of it. (However, some studies[7] have shown that the risk is dominated by the 1 x SSE to 2 x SSE range, and the upper limit of the integral of Eq. 1 has some practical finite limit.)

So far, we have described seismic hazard functions (see Fig. 4) which are typically developed in terms of only peak ground acceleration. The best data on earthquakes are acceleration time histories (see Fig. 7). We recognize that peak acceleration alone is too simple a characterization of an earthquake, which, because of its complex nature, could also be characterized in terms of additional parameters such as duration, number of cycles, frequency content, peak ground velocity or displacement, and so forth.

We could develop the hazard function in terms of both acceleration and these additional parameters, in which case the horizontal axis in Fig. 6 and the integral in Eq. 1 would become multi-dimensional. However, in the current state of the art, the seismic hazard function is developed with respect to site peak free-field ground acceleration alone and the other parameters are accounted for in some other manner. The reader can obtain a sense of the variety of possible approaches by reviewing the references in the Appendix.

In the remainder of this report, we will adopt the conventional assumption which is to characterize the hazard function in terms of only the site peak free-field ground acceleration and make the assumption that these other parameters will be used in the response or failure calculations.

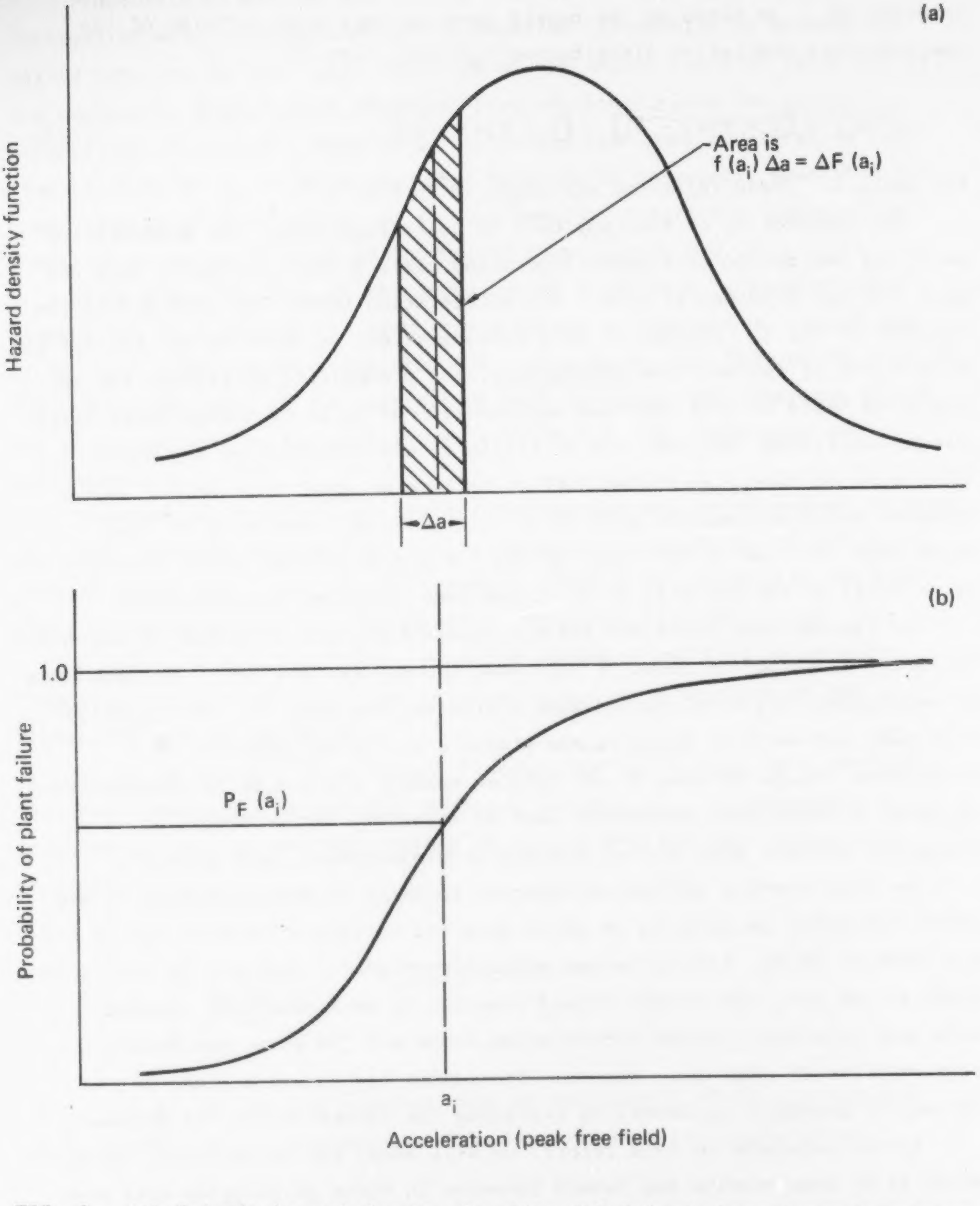

FIG. 6. (a) Seismic hazard density function (b) Seismic hazard complementary cumulative distribution function.

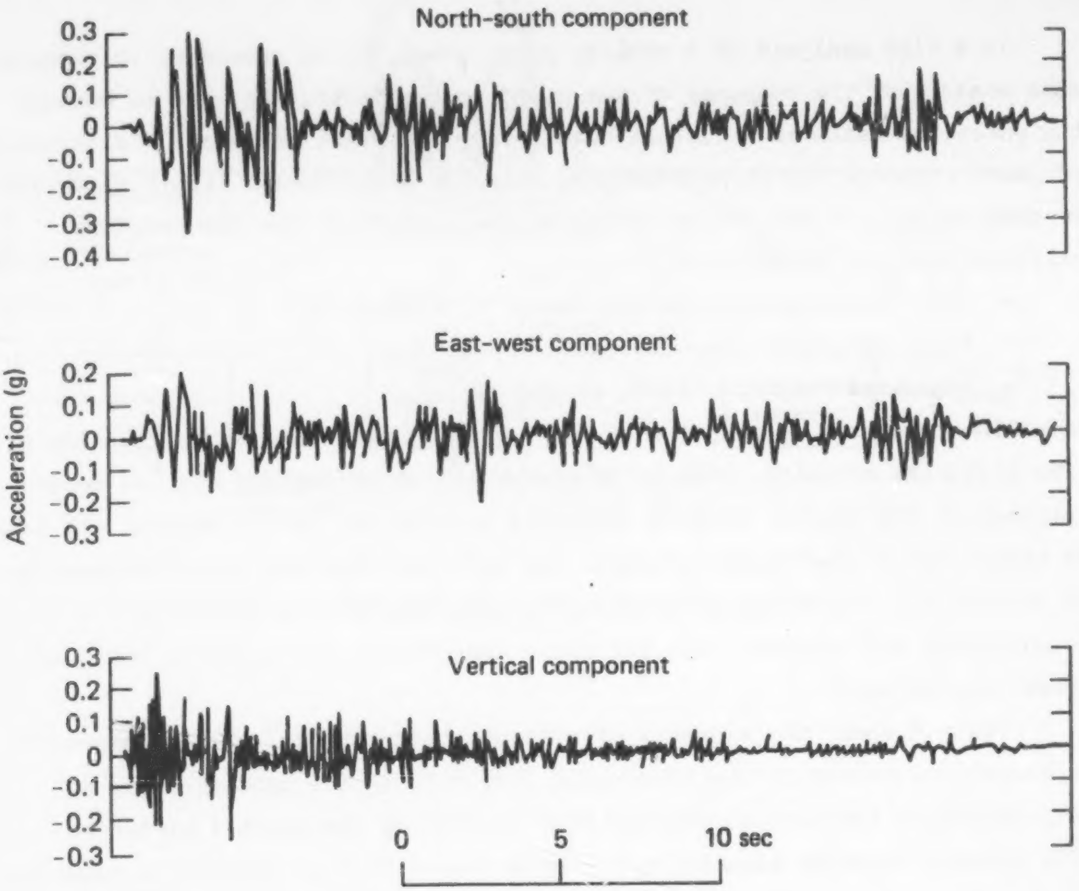

FIG. 7. Accelerogram of the 1940 Imperial Valley, California earthquake recorded at El Centro, California.

PLANT RESPONSE

In a risk analysis of a nuclear power plant, it is necessary to compute some measure of the response of the plant to the earthquake, and to compute the potential failures which can result from the plant response. Calculations of plant response can be performed at a number of different levels of detail or complexity. In the current state of the art, we divide the response calculations into three areas:

- Soil Structure Interaction (Refs. 11 through 16)
- Major structure response (Refs. 17 and 18)
- Subsystem response (Refs. 19 and 20)

and assume that the description of the nuclear plant response is in terms of time histories of force, moment, displacement, acceleration, etc. at points of interest in the plant. Such calculations are related to but are not the same as those used in the design process. We will not describe these differences in any detail, but, a key point in a risk analysis is that response calculations are required only for those components identified on the fault trees (see below).

Figure 8 shows the elements of response calculations. Three components of earthquake motion in the free-field (see Fig. 7) are used as input to soil-structure interaction calculations to develop the basemat histories. (The basemat is often assumed to be rigid, and then its response is described by three translational and three rotational time histories.) There may be dynamic coupling, interaction, or feedback, between the structure and foundation (particularly in the case of a soil foundation) or soil-structure interaction, which is highly dependent on the dynamic properties of the structure and foundation, and the incoming wave motion. (This area is the subject of a great deal of controversy.) Soil-structure interaction results may also be used to evaluate the stability of the foundation, for example, in liquefaction studies.

The basemat time histories are then used to calculate the response of the structure for two purposes:

- To evaluate the integrity of the structure, and
- To obtain motions at the supports of subsystems (for example, piping systems).

There may also be coupling between the subsystems and structure (particularly for subsystems like a reactor vessel-coolant loops) which is a

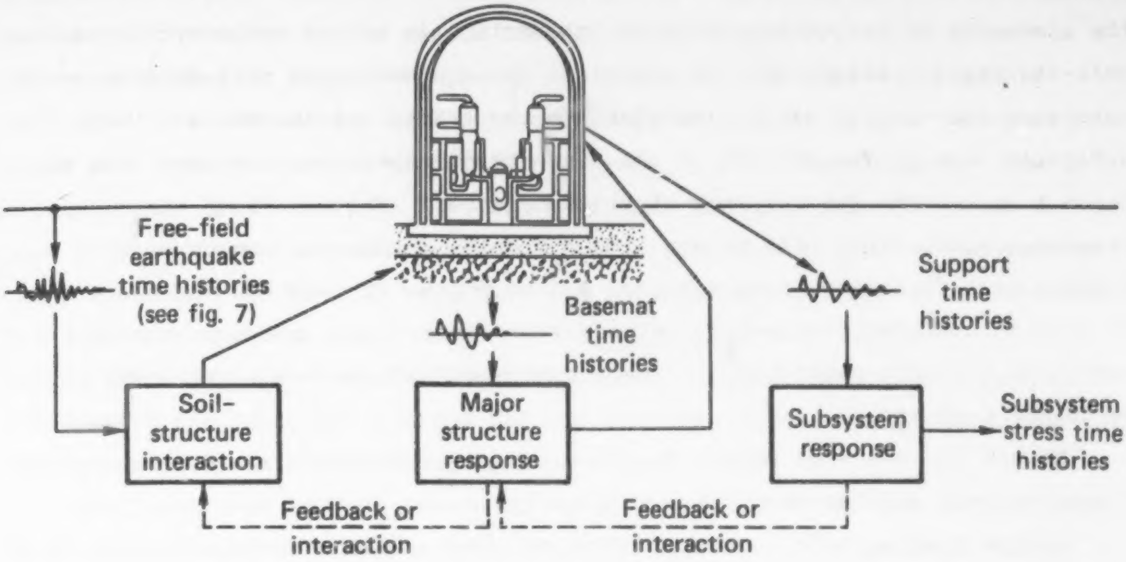
Free-field
earthquake
time histories
(see fig. 7)
Basemat
time
histories
Support
time
histories
Soil-
structure
interaction
Major
structure
response
Subsystem
response
Subsystem
stress time
histories
Feedback or
interaction
Feedback or
interaction

FIG. 8. Schematic of response calculations.

phenomena analogous to soil-structure interaction. (Surprisingly, however, the phenomena of structure-subsystem interaction is not as controversial as soil-structure interaction. In addition, the phenomenon of soil-structure-subsystem interaction may be important in the reactor vessel-coolant loops subsystem case.) The motions at the supports of subsystems are then used as input to calculate the response of the subsystems. The result of the subsystem response calculations will be the time histories of stress, moment, displacement, velocity, acceleration, and so forth, at selected points in the various subsystems (for example, stress time history at a point in a piping system or electric cable tray). These subsystem responses are then used to calculate failures.

We now go into some detail to establish probabilistic concepts related to responses that are important in a risk analysis.

Assume that we have a single component whose support is attached to point A of a structure. Assume further that there is a single natural response frequency, f_r, associated with the motion of this support-component subsystem, and that the damping of this subsystem is denoted by c. The frequency (f_r) depends on the mass (m), spring stiffness (k), and damping coefficient (c) of the support-component (subsystem) model. Finally, assume that failure of this component is determined by the peak acceleration it experiences (the component response). Thus peak acceleration is the primary quantity of interest in a failure or risk analysis.

An example of such a subsystem would be a piece of electrical equipment in a cabinet mounted on a floor. The failure of electrical equipment can be sensitive to its acceleration response and the cabinet has dynamic response characteristics which we may represent by a single frequency, f_r, and damping, c. These assumptions are depicted in Fig. 9, which shows a simple block diagram of mass, m, stiffness, k, and damping, c, for the support-component subsystem in our example. A given free-field earthquake will produce a history of motion $\ddot{x}(t)$ in Fig. 9 at the support point A of our subsystem which then results in a history of response motion $\ddot{y}(t)$ in Fig. 9 at the component by solving the governing equation of motion,

$$m\ddot{y}(t) + c\left[\dot{y}(t) - \dot{x}(t)\right] + k\left[y(t) - x(t)\right] = 0.$$

A result typical of a component response history is shown in Fig. 10 which also identifies the peak acceleration which the component experiences during a particular earthquake. (As a point of interest Fig. 10 was actually derived from a free-field earthquake history in Fig. 7.) If we locate this component peak acceleration on a plot versus frequency, we obtain Fig. 11. If we had a number of different support-component subsystems, where each subsystem is excited by the same motion (all subsystems are located at or near point A) but where each subsystem had a different frequency (but the same damping) and if we repeat the above analysis for each subsystem we can obtain the locus of peak accelerations indicated by the circled points in Fig. 12. If we connect the points shown in Fig. 12 we obtain the curve called a "response spectrum." This response spectrum curve displays the spectrum of component peak acceleration responses obtained from subsystems with different frequencies. For example the response spectrum for the 1940 El Centro earthquake (North-South component) is shown in Fig. 13.

While response spectra have many uses, the key concept here is that each point on the response spectrum (see Fig. 12) is obtained by exciting single degree of freedom systems (Fig. 9) which each have different frequencies by the same motion. Response spectra then have two main applications:

- They can be used to process and evaluate information. For example, they can be used to reduce the amount of information contained in a given (free-field, support point, stress, strain, moment, average daily temperature, and so forth) time history (the one used to excite the single degree of freedom systems) to some more manageable lower level, for the purpose of evaluating the time history, while still retaining some portion of the information contained in the history. For example, a response spectrum is one general way to infer the relative "strengths" of the various frequencies present in the history. This is difficult to do by direct inspection of the history (see Fig. 7) and impossible to do if we reduce the information in the history to something as simple as its peak value.
  Response spectra are also related to Fourier and power spectra. (See Brillinger[21] and Vanmarcke.[22])
- They can be used to make inferences about the possible response of subsystems, even subsystems more complex than our example, for instance, a three-dimensional piping system.

This latter application is the one in which we are most interested here, that is, we will use response spectra as a convenient tool to describe various aspects of the possible response of subsystems.

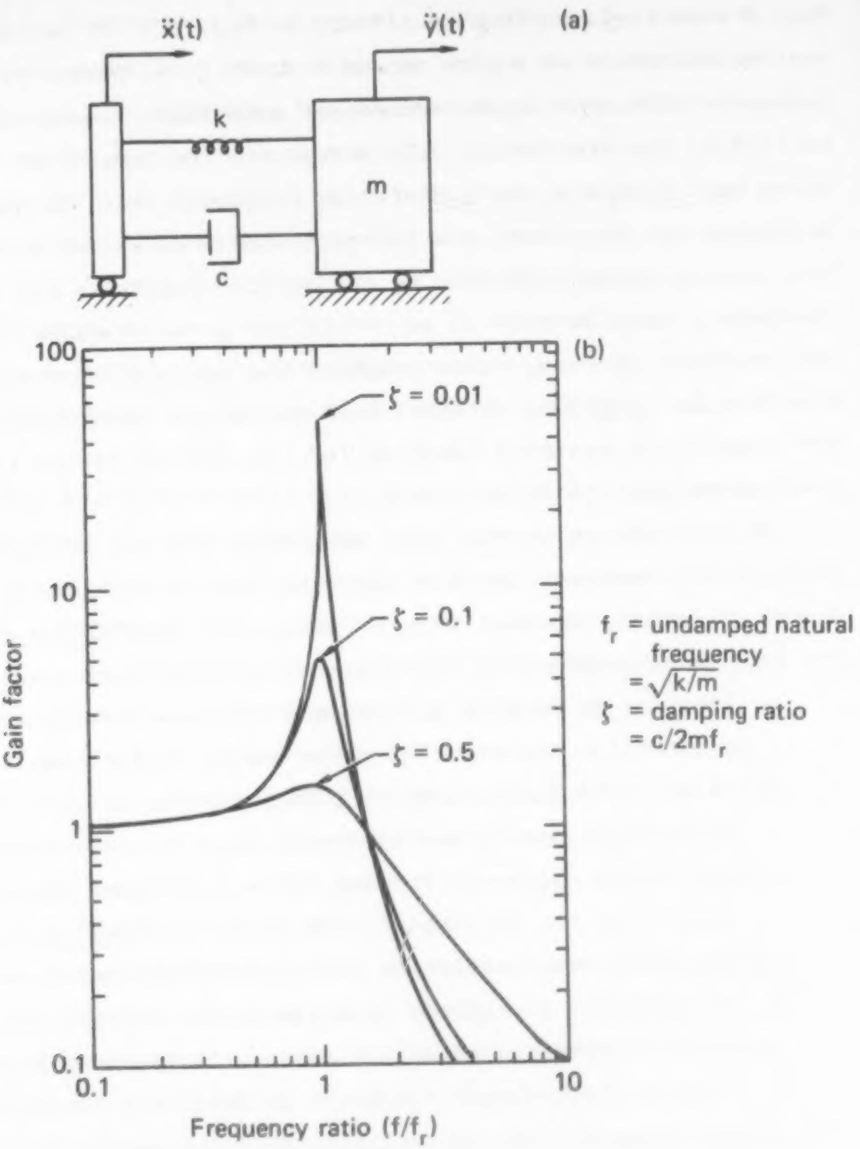

FIG. 9. Support-component model (a) and corresponding transfer function (b) used to calculate response spectra. The transfer function, which depends on the fraction (ζ) of critical damping at any model frequency, f_r, determines how the complex frequency content (f) or the input time history, $\ddot{x}(t)$, is translated to the response history, $\ddot{y}(t)$, of the mass, m, of a component. The frequency f_r depends on the mass (m), spring stiffness (k), and damping coefficient (c) of the support-component (subsystem) model.

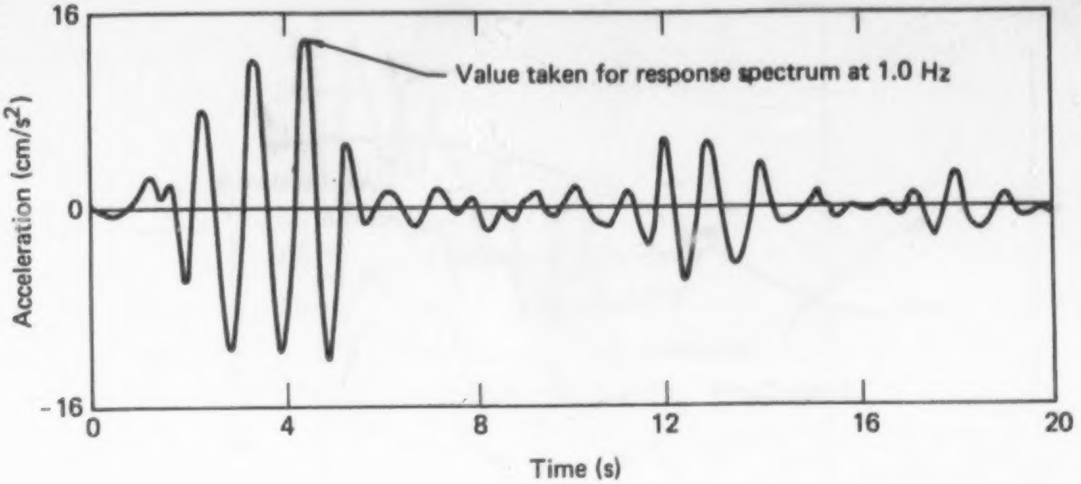

FIG. 10. Acceleration response history, $\ddot{y}(t)$, obtained by using the 1940 El Centro North-South component acceleration record as the foundation motion, $\ddot{x}(t)$, of the simple mechanical system shown in Fig. 9. The damping was 5% of critical ($\zeta = 0.05$) and the fundamental frequency, f_r, was 1.0 Hz. The peak absolute acceleration of this response history determines the value of the response spectrum at 1.0 Hz.

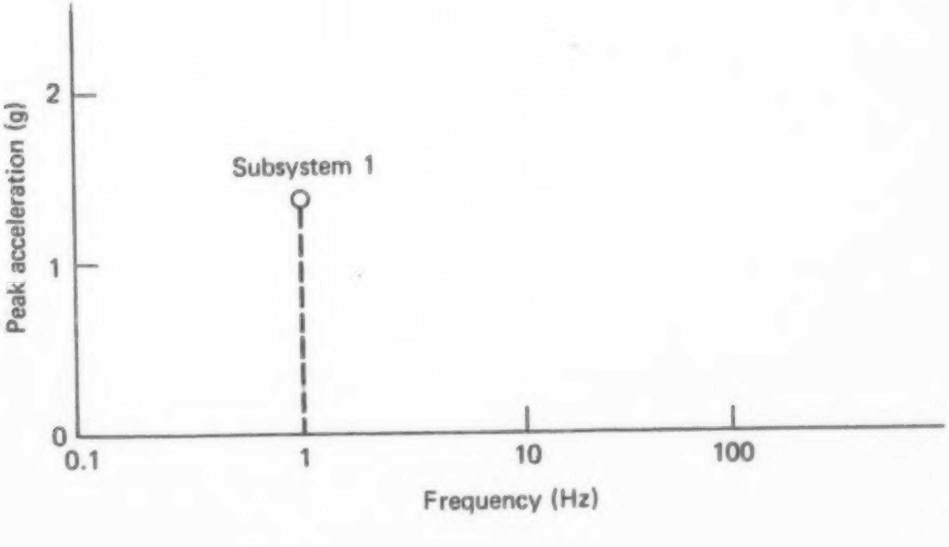

FIG. 11. Peak acceleration response of the component in a subsystem with a natural frequency of 1.0 Hz. (See Figs. 9 and 10.)

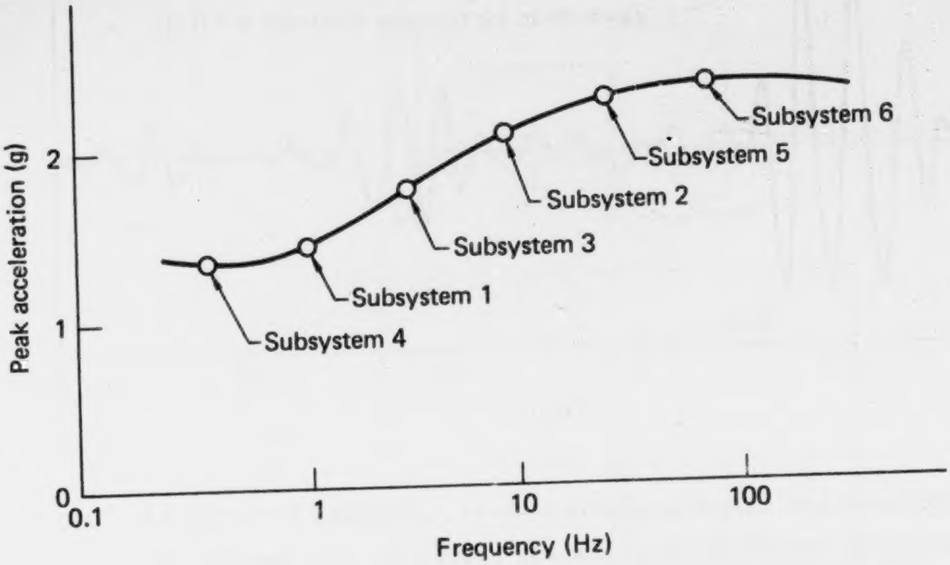

FIG. 12. Peak acceleration response of the component in subsystems with various natural frequencies, where each subsystem was excited by the same motion $\ddot{x}(t)$ in Fig. 9.

best copy available

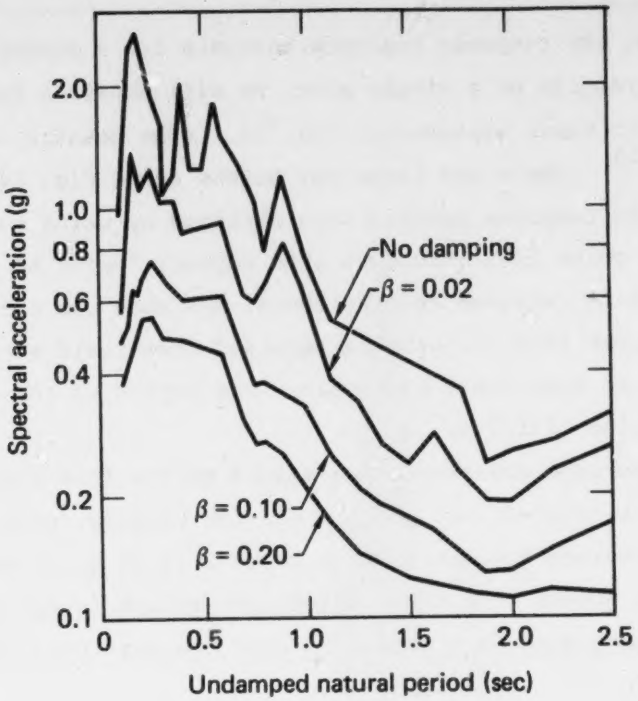

FIG. 13. Acceleration response spectrum obtained by using the North-South component of the 1940 El Centro acceleration record.

If we repeat the response spectrum analysis for a number of earthquakes and display the results on a single plot, we will obtain a family of response spectra similar to those depicted in Fig. 14. (The details behind Fig. 14 are in Bumpus et al.[23]) There are three key points about Fig. 14:

- All of the response spectra were obtained by using response histories at a single point in a structure (the support "point A" described above).
- There are 46 response spectra shown, and each was obtained by response calculations (Fig. 8) using a recorded free-field earthquake.
- Each of the free-field earthquakes was scaled to the same peak acceleration of 1.0 g.

The most important observation we should derive from Fig. 14 is the variability of the results. At about 4 Hz, for example, we see that the component peak acceleration varies from about 2 to 27 g, or more than an order of magnitude. We stress that this variability exists in spite of the fact that each free-field earthquake was scaled to have the same peak acceleration. There are two sources of this variability:

- Variations in the "relative strengths" of the various "frequency contents" from one recorded free-field earthquake to another.
- Variations in the dynamic parameters (for example, structural frequency and damping) of the models (for example, structural model) used in each of the 46 response calculations. (See Bumpus et al.,[23] for details.) This variation exists because we do not have precise knowledge of the values we should use for the dynamic parameters.

We do not yet know which of these two kinds of variability is most important, although many believe the former is dominant. We will soon have research results on this question.

The existence of such variations suggests that for a given free-field peak acceleration, component response can be considered a random variable rather than a fixed (deterministic) value. Thus, it is appropriate to describe the distribution of values of component response by a cumulative distribution function, $F_R(r|a)$, (see Fig. 15a) or by a probability density function, $f_R(r|a)$, (see Fig. 15b) where r denotes the response variable (for example, acceleration). The fact that the response distribution will depend on the value of the free-field peak acceleration is recognized by writing the distribution and density functions as conditional functions, conditional on the value of peak acceleration, a.

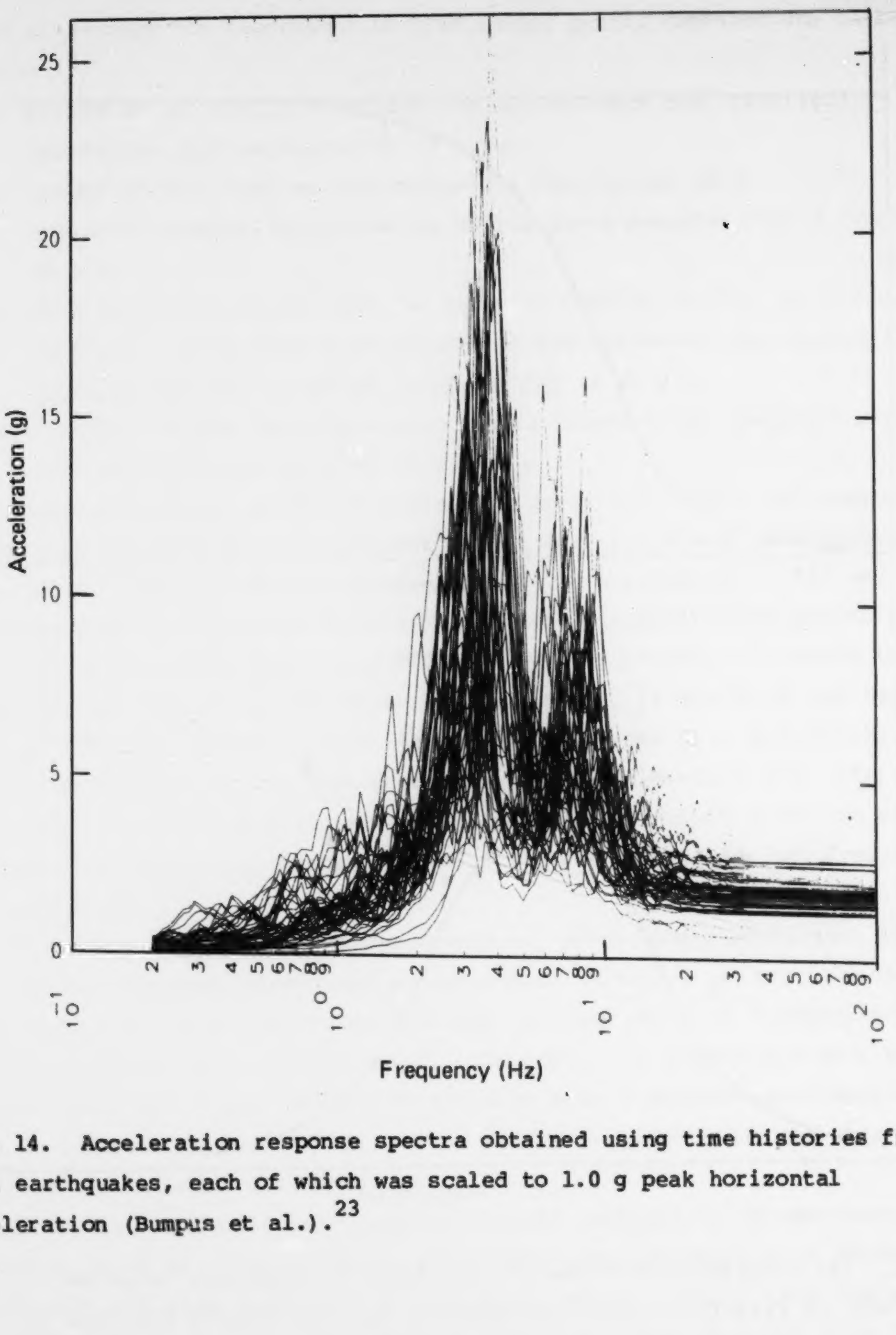

FIG. 14. Acceleration response spectra obtained using time histories from 46 real earthquakes, each of which was scaled to 1.0 g peak horizontal acceleration (Bumpus et al.).[23]

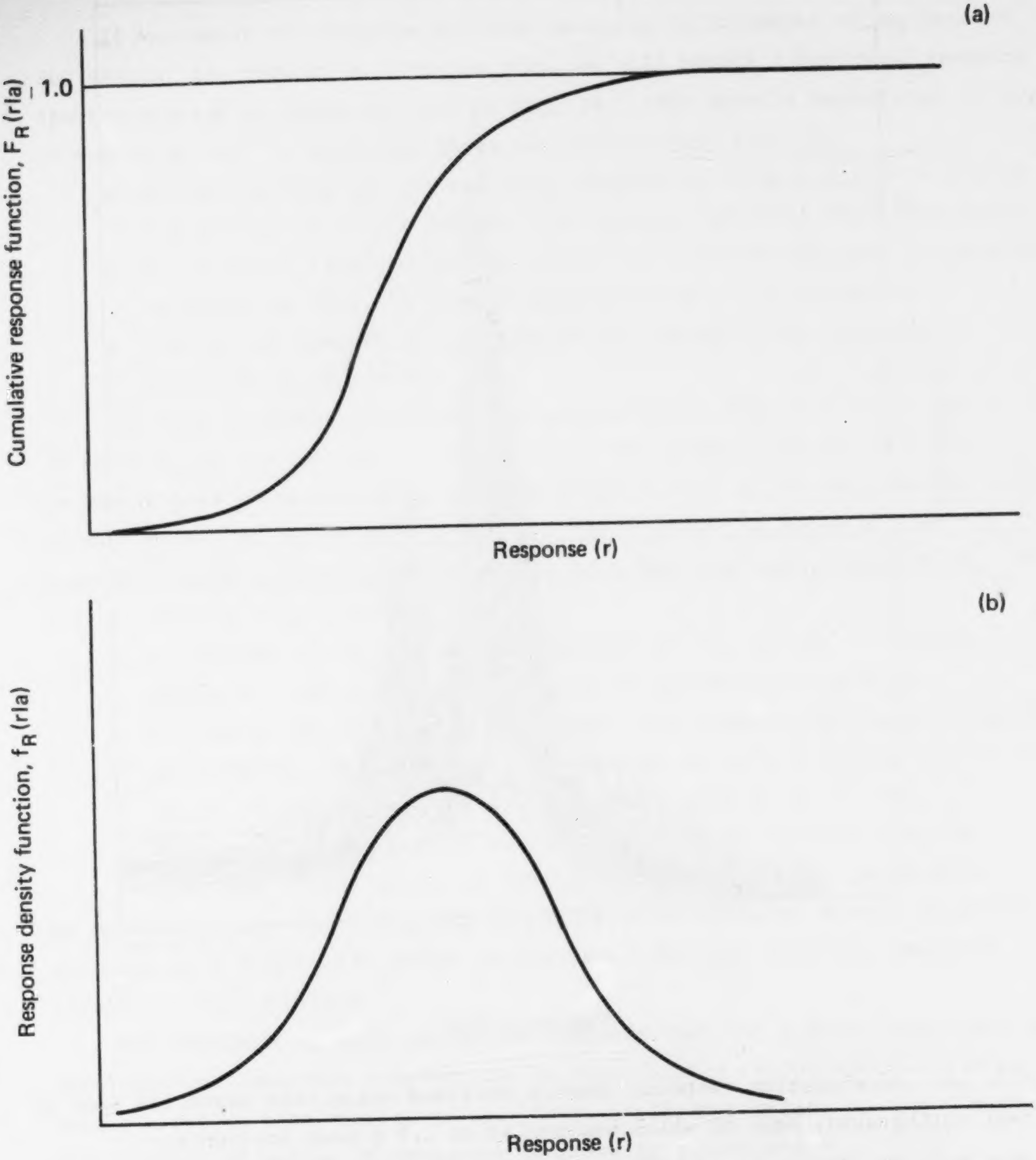

FIG. 15. (a) Cumulative distribution function for component response conditional on free-field peak acceleration, a. (b) Density function for component response conditional on free-field peak acceleration, a.

To illustrate the importance of this latter point, consider the following scenario:

- Assume we are making a failure evaluation where the free-field earthquake peak acceleration is 1.0 g.
- Assume further that we are evaluating the failure of a support-component subsystem (as in the above example) with a frequency of 4 Hz.
- With these two assumptions the analysis results in Fig. 14, are of interest. (Note that this means that the component response may be at least as low as 2 g and at least as high as 27 g.)
- Finally, assume the acceleration level at which the component will fail is known precisely to be 15 g.

With these assumptions, we cannot state with certainty whether the component will or will not fail if an earthquake with a free-field peak acceleration of 1.0 g occurs. The best statement we can make is something like, "If an earthquake with an acceleration of 1.0 g occurs, the conditional probability of failure of the component is about 0.5." This is roughly equivalent to the assumption that 50% of the responses at 4 Hz in Fig. 14 are above and below the 15 g. Thus by characterizing the response in terms of a distribution function conditional on the site free-field peak acceleration (Fig. 15a) and knowing the criteria for failure (for example, failure at 15 g) we are able to calculate the conditional probability of component failure for any free-field peak acceleration.

Obviously, the response values depend on, among other quantities, the value of the site peak free-field acceleration. However, even in the case of linear analysis, we may choose to increase the mean value of damping, for example, with the level of excitation. The resulting responses from linear analyses would not simply scale with the site free-field peak acceleration. Thus, in general, it is possible to have different conditional response distributions for each excitation level.

If desired, we could calculate the (total) probability of component failure by using Eq. 1 to integrate the conditional probability of component failure over all peak free-field acceleration values. Rather than taking this last step, common practice is to combine the conditional probabilities for several components and subsystems to obtain the conditional probability of failure of the systems and plant and then use Eq. 1 to get the (total) probability of failure of the plant. This is explained below.

EVALUATION OF FAILURE

Component-Related Probabilistic Considerations

We can calculate the conditional and, if desired, the (total) probability of failure for the various components (the supported equipment in the example) once we obtain the three types of information below:

- Seismic hazard function (Fig. 4).
- Response values for the various components at each free-field acceleration level (for example, the spectral accelerations in Fig. 14).
- Criteria for failure of the various components (the 15 g in the example).

Since we are not restricted to consideration of responses like peak acceleration as in our above example (recall we used response spectra only as a convenient tool), we can use any appropriate response quantity like peak strain, displacement, stress, or time histories of these quantities (and possibly include consideration of cumulative damage or fatigue) and determine the conditional and then the total failure probabilities for the various components (electrical equipment, piping systems, structures, pumps, valves, vessels, foundation, etc.) which are considered in the particular risk analysis.

Two considerations led to the conclusion that failure should be represented as a random event:

- The decision to measure the "intensity" of an earthquake by the free-field peak acceleration, which is a random variable over all earthquakes (Fig. 4) and,
- The decision to perform detailed response calculations (Fig. 8) which leads to there being variation in component response from one earthquake to another, even when each earthquake has the same free-field peak acceleration (Fig. 14).

Alternately, we could use simpler response methods (such as using only the average response value) and apparently eliminate the need to evaluate conditional failure using probabilistic techniques.

However, there are additional reasons for representing component failure as a random event:

- Typically, we do not test components to establish the level at which they fail. This leads to some uncertainty on the failure level, thus it is convenient to model the failure level of a component as a random variable.
- There are natural variations in materials, manufacturing processes, installation, operating environment, and so forth, all of which lead to variations in the failure level of a component.
- The earthquake is not the only loading experienced by a component that can contribute to its failure. Other normal operating and accident conditions lead to temperatures, pressures, stresses, and so forth, which we may have to combine with the effects due to an earthquake. These other loads have natural variations which lead to variations in the failure level of a component.

Thus, just as the response (as measured, for example, by acceleration) is viewed as a random variable, the level (for example, acceleration) at which a component will fail should also be treated as a random variable. Let $F_S(r)$ denote the cumulative distribution function for the failure of a component. That is,

$$F_S(r) = P(S \leq r)$$

denotes the probability that the strength, S, of a component is less than or equal to the response r. Similarly let $f_S(r)$ denote the corresponding probability density function for the failure level.

In the previous example the (conditional) probability of failure was dependent on only the relative frequency of response being greater than a fixed level (15 g). Now, since both component response (for example, Fig. 14) and failure level (see the reasons given immediately above) are to be treated as random variables, the probability of component failure for a given free-field acceleration level must be obtained by integration. In particular, the conditional probability of component failure, $P_{CF}(a_0)$, given free-field peak acceleration, a_0, can be calculated by:

$$P_{CF}(a_0) = \int_0^\infty F_S(r) f_R(r|a_0) dr \quad , \tag{4}$$

where $F_S(\cdot)$ is the cumulative distribution function for the failure level defined above and $f_R(\cdot|a_0)$ is the conditional (on the acceleration a_0) density function for the response. The computations involved in Eq. 4 are illustrated in Fig. 16. This expression can be approximated by

$$P_{CF}(a_0) \doteq \sum_{i=1}^{n} F_S(r_i)\Delta F_R(r_i|a_0) \tag{5}$$

where $\Delta F_R(r_i|a_0)$ is the conditional probability that the response is in the interval Δr_i (see Figs. 17a and 17b).

The conditional probability of component failure can also be written as:

$$P_{CF}(a_0) = \int_0^{\infty} \left[1 - F_R(s|a_0)\right] f_S(s)ds \quad , \tag{6}$$

where $1 - F_R(\cdot|a_0)$ is the complementary cumulative distribution function for the response and $f_S(\cdot)$ is the density function for the failure level; see Figs. 18a and 18b. This expression is approximated by

$$P_{CF}(a_0) = \sum_{i=1}^{n} \left[1 - F_R(s_i|a_0)\right] \Delta F_S(s_i) \quad , \tag{7}$$

where $\Delta F_S(S_i)$ is the probability the component failure level is in the interval Δs_i (the shaded area in Fig. 18b).

System-Related Probabilistic Considerations

In principle, we could use expressions like Eq. 4 or 6 to arrive at the conditional failure probabilities for all the components in a plant, but, we still would not have enough information to calculate the risk to the public from radioactive release. Some method must be devised to combine the individual component failures into accident scenerios which can lead to a release. For example, we might calculate the probability of a loss of coolant

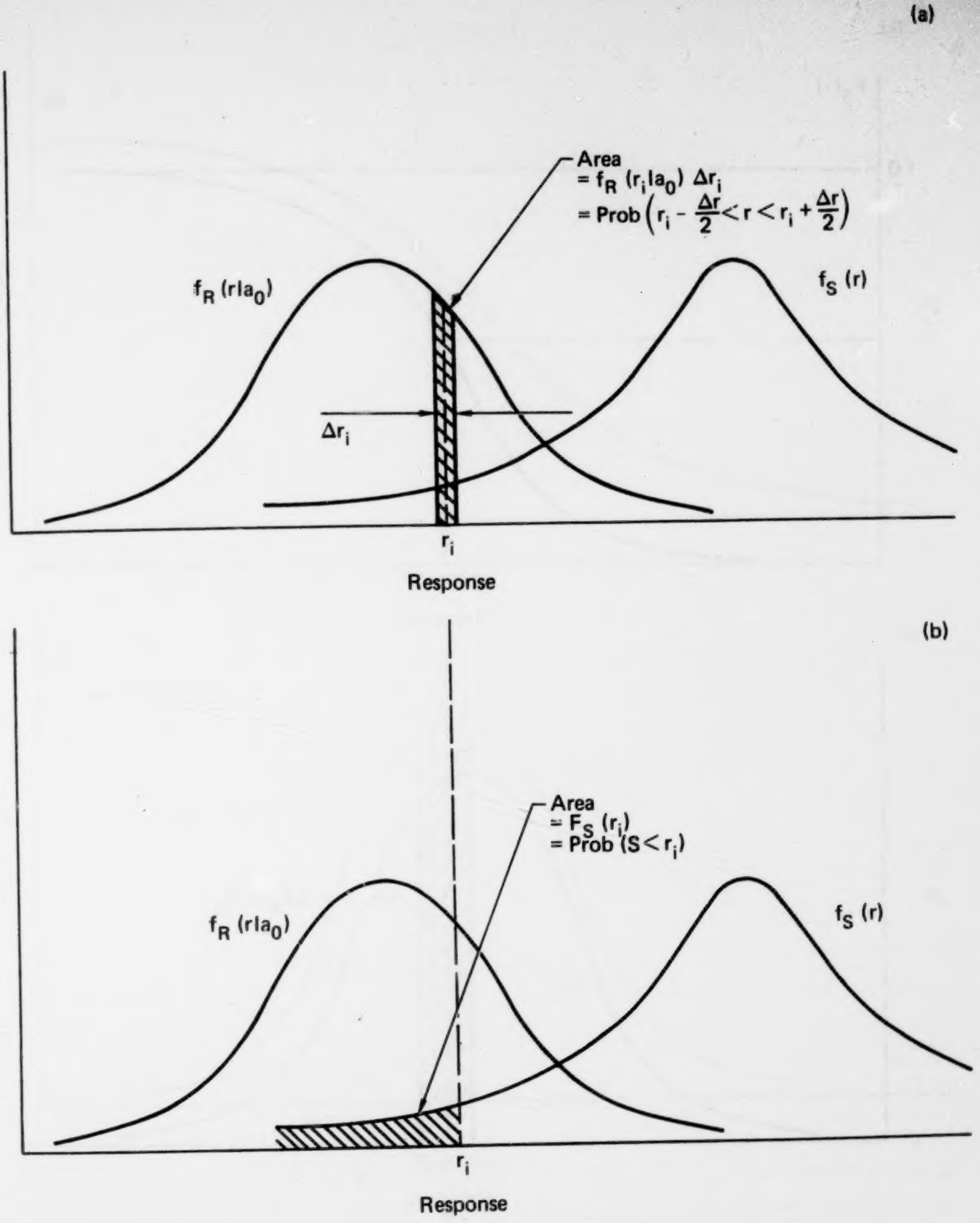
(a)
Area
$= f_R (r_i|a_0)\ \Delta r_i$
$= \text{Prob}\left(r_i - \frac{\Delta r}{2} < r < r_i + \frac{\Delta r}{2}\right)$
$f_R (r|a_0)$
$f_S (r)$
Δr_i
r_i
Response
(b)
Area
$= F_S (r_i)$
$= \text{Prob} (S < r_i)$
$f_R (r|a_0)$
$f_S (r)$
r_i
Response

FIG. 16. Graphical interpretation of the integrand of Eq. (4).

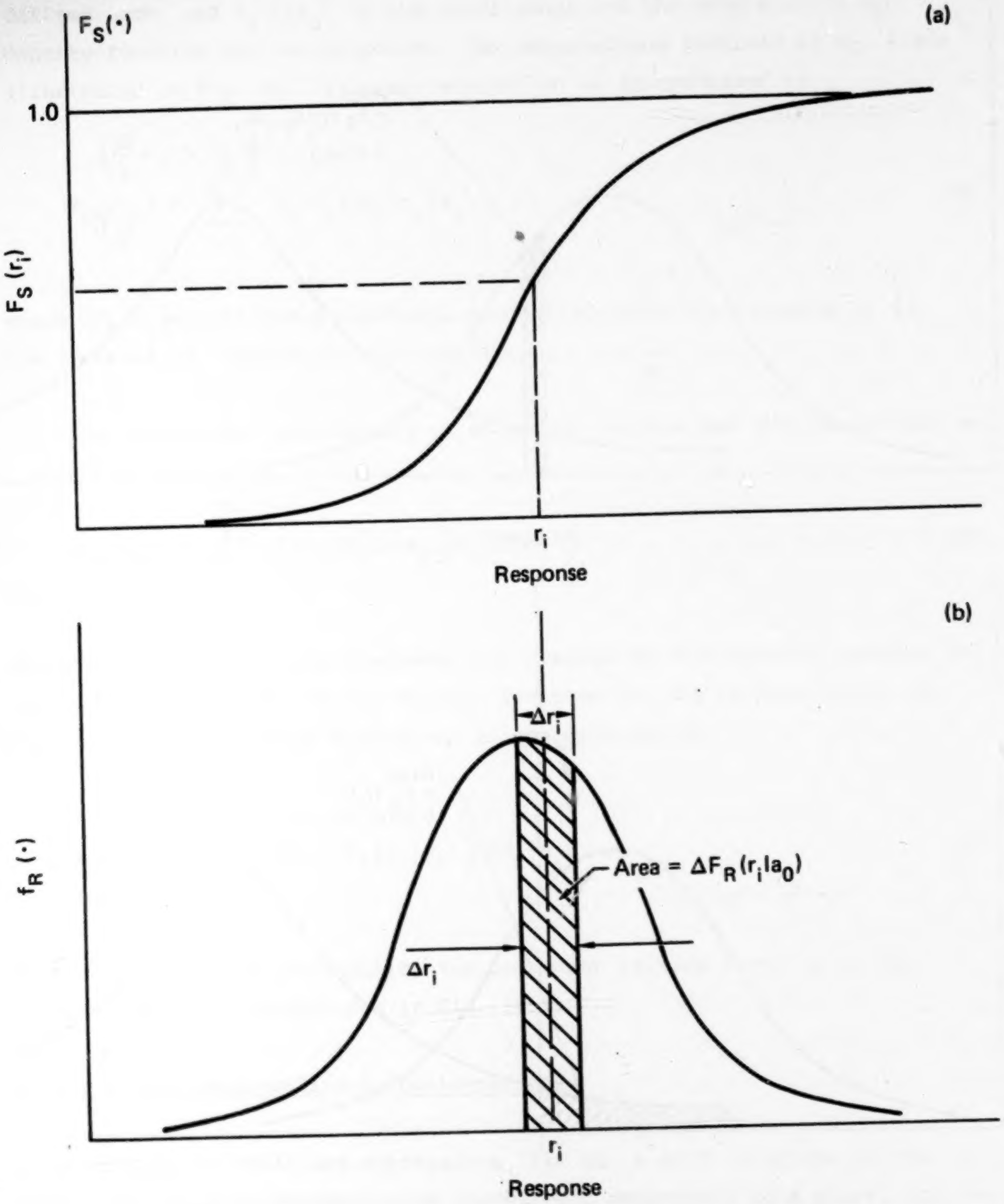

FIG. 17. (a) Cumulative distribution function for the resistance (failure level) of a component/subsystem. (b) Probability density function for the response at a component/subsystem.

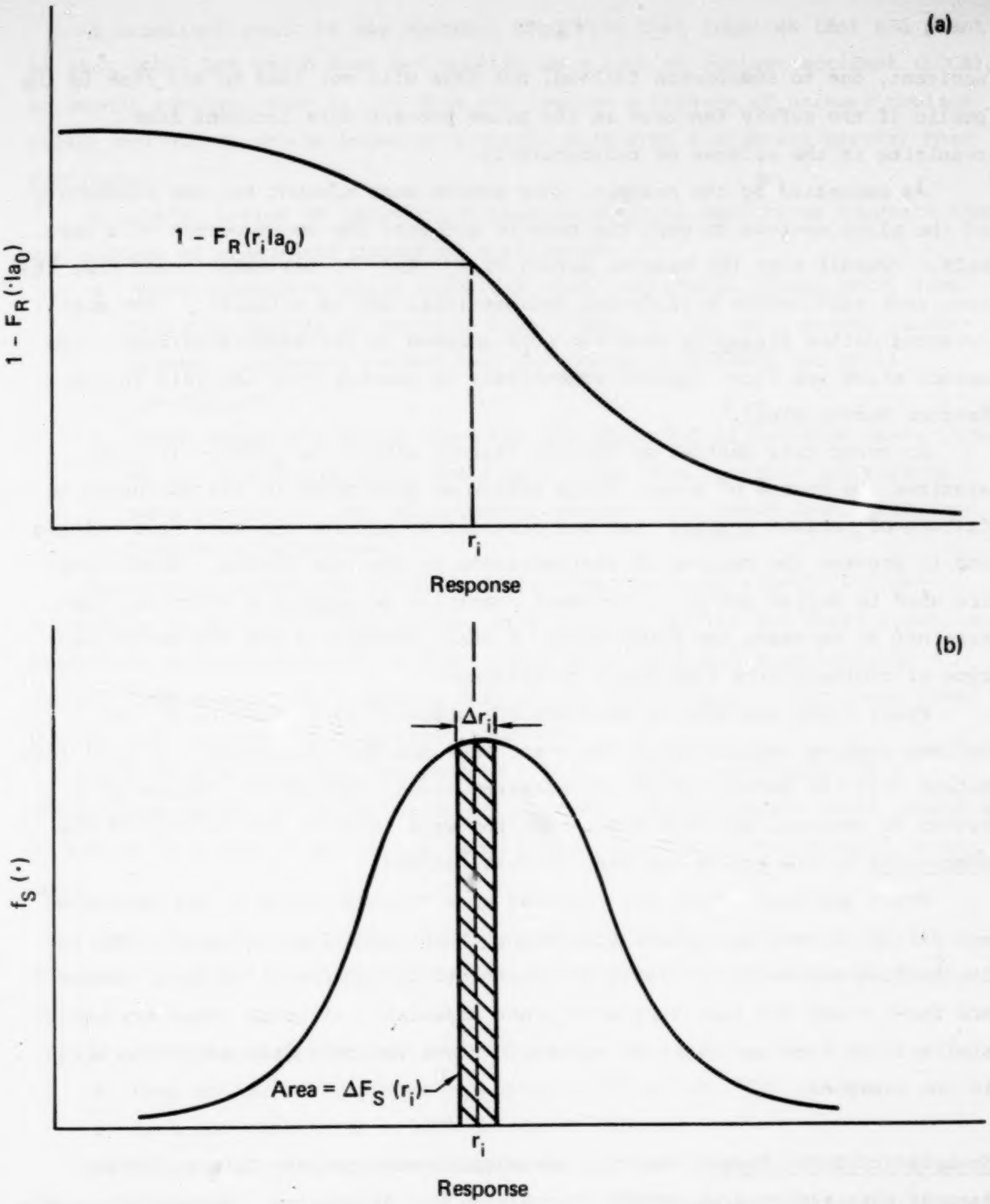

FIG. 18. (a) Complementary cumulative distribution function for the response of a component/subsystem. (b) Density function for the resistance (failure level) of a component/subsystem.

accident, due to components failing, but this will not lead to any risk to the public if the safety features in the plant prevent this accident from resulting in the release of radioactivity.

As suggested by the example, this method must account for the capability of the plant systems to cool the core or mitigate the consequences of a core melt. (Recall that the Reactor Safety Study, Ref. 2, has established that the core must melt before significant radioactivity can be released.) The most advanced method presently used for this purpose is the event-tree/fault tree method which was first applied extensively to reactor risk analysis in the Reactor Safety Study.[2]

An event tree defines an initial failure within the plant. It then examines the course of events which follow as determined by the operation or failure of various systems that are provided to prevent the core from melting and to prevent the release of radioactivity to the environment. Event trees are used to define potential accident scenarios or sequences which are then examined to estimate the probability of their occurrence and the amount and type of radioactivity that might be released.

Fault trees are used to estimate the probability of failure of the various systems identified in the event tree accident sequences. A fault tree starts with the definition of an undesired event, such as the failure of a system to operate, and then determines the ways in which the failure of the components in the system can lead to this failure.

Event and fault trees are obtained by a thorough study of the operating and safety systems in a particular plant, their functional capabilities, and the logical sequences of events that can lead to success or failure. Event and fault trees are thus very much plant dependent, although there may be similarities from one plant to another. These two definitions are clarified in the examples.

Examples of Event Trees. We will use event trees from the Seismic Safety Margins Research Program (SSMRP) to clarify the discussion. Both of the trees we describe are concerned with a transient event. The remainder of this section follows Garcia and Kelly.[24]

A transient event is any abnormal condition that requires that the plant be shut down, but which does not qualify as a loss of coolant accident (LOCA) or vessel rupture, that is, it does not involve a rupture of primary coolant piping equivalent to the break of a single pipe with a diameter greater than 0.5 inches.

A careful review of various information on plant operations suggests that two classes of transients should be considered:

- Those transients which leave the power conversion system (PCS) (see Table 1) capable of removing heat. That is, the main steam, turbine bypass, condenser, condensate, and feedwater systems are still operating.*
- Those transients which leave the PCS incapable of removing heat. Some of the transients which would fall under this category are loss of main feedwater, loss of condenser vacuum, main steam line break, and loss of offsite power.

As a rule, transients which initiate a reactor trip signal (followed eventually by a turbine trip signal) will usually fall in the first class, and transients which initiate a turbine trip signal (followed eventually by a reactor trip signal) will usually fall in the second class. The event trees for the two classes are discussed in detail.

Note that a transient can lead to a LOCA. This could happen if a pressurizer relief or safety valve sticks open. This accident could change a transient to a small, medium, or large LOCA, depending on which valve sticks open.

Event Tree for Transients with the Power Conversion System (PCS). A transient with PCS event is defined as any abnormal condition in the plant which

- requires that the plant be shut down,
- does not directly affect the operability of the PCS, and
- does not qualify as a LOCA or vessel rupture.

That is, all of the systems which make up the PCS (main steam, turbine bypass, condenser, condensate, and feedwater) are still operating and there is no rupture of the reactor coolant system (RCS) piping equivalent to the break of a single pipe whose diameter is greater than 0.5 inches. This type of transient will be referred to as a class 1 transient (T_1).

---

*Note that the circulating water system is also required for heat removal.

TABLE 1. Definition of events used on transient event trees.

EVENT	NAME	DESCRIPTION
T_1, T_2	TRANSIENTS	Transients - Any abnormal condition in the plant which requires that the plant be shut down, but which does not qualify as a LOCA (that is, it does not involve a rupture of primary coolant piping equivalent to the break of a single pipe whose diameter is greater than 0.5 inches). ● Class 1 Transients (T_1) - A transient which does not directly affect the operability of the PCS ● Class 2 Transient (T_2) - A transient which directly affects the operability of the PCS, causing it to become inoperative.
K	RPS	Reactor Protection System - The RPS is designed to shut down the nuclear reaction in the core if an abnormal condition exists, in order to reduce the amount of heat which is produced and make it possible to put the plant in a safe condition. Success is defined to be bringing the reactor to a subcritical (shutdown) condition.
M	PCS	Power Conversion System - Designed as the normal method of removing heat from the reactor coolant system (RCS). Steam created in the steam generators is sent through the main steam lines to the main turbine or turbine bypass and on to the condenser. The condensate is then pumped through the condensate and feedwater systems and returned to the steam generator to be turned to steam again. For a transient, success is defined as the steam from the steam generators being sent to the condenser by way of the turbine bypass, condensed, and the condensate returned to the steam generator by the condensate and feedwater pumps.
L	AFWS & SSR	Auxiliary Feedwater System & Secondary Steam Relief - The AFWS & SSR is designed to remove heat from the RCS to help prevent core melt. Water is added to the steam generators by three AFW pumps (two motor driven, one steam turbine driven) which take suction from the condensate storage tank or the service water system. The water is allowed to boil in the steam generator, removing heat from the RCS. This steam is then released through the SSR valves. Success is defined as at least 1 out of 3 AFW pumps delivering water to the steam generators from either the condensate storage tank or the service water system, and release of the created steam through the SSR valves.

TABLE 1. (Continued).

EVENT	NAME	DESCRIPTION
P	S/RV-O	Safety/Relief Valves - Open - The pressurizer S/RVs are designed to relieve excess pressure in the RCS in order to prevent possible subsequent damage to the RCS piping and vessels. Small amounts of excess pressure are relieved by one or both of the two power operated relief valves (PORVs). If the pressure spike is excessive, or the PORVs fail to open, pressure will be relieved by one, two, or three of the three safety valves (SVs). Success is defined as the opening of the necessary number of S/RVs to prevent RCS overpressurization.
Q	S/RV-R	Safety/Relief Valves - Reclose - The pressurizer S/RVs are also designed to reclose once the excess RCS pressure has been relieved. This reclosing keeps most of the water inventory within the RCS, preventing a LOCA type accident. Success is defined as the reclosing of all the S/RVs which opened, once the excess RCS pressure is relieved. (If any PORVs are stuck open, the operator can manually close a motor operated block valve if he realizes what is happening, which will stop flow through the PORVs. This valve closure will satisfy the success criteria.)
U	CVCS	Chemical and Volume Control System - The CVCS is designed to maintain water inventory in the RCS for most normal operations and transients. Excess water is drained from the RCS and eventually brought to the volume control tank. If water is needed it is added from the volume control tank by three charging pumps. During a transient, success is defined as maintaining water inventory in the RCS above the core.
W	RHRS	Residual Heat Removal System - The RHRS is designed to bring the reactor to cold shutdown once the RCS temperature and pressure have been brought down to about 350°F and 400 PSI respectively. The RCS is cooled by passing the RCS water through heat exchangers which cool the water by passing the heat to the component cooling water system, and from there to the service water system. The RHRS consists of two RHR pumps taking suction from the Loop A hot leg, two RHR heat exchangers which take discharge from the pumps (and which themselves discharge back to the RCS), the component cooling water system which circulates water in a closed loop, taking heat from the RHR heat exchangers and passing it out from component cooling water heat exchangers, and the service water system, which takes heat from the component cooling water system and discharges it to the environment.

TABLE 1. (Continued).

EVENT	NAME	DESCRIPTION
W (continued)	RHRS	Success is defined as at least 1 out of 2 RHR pumps delivering water from the Loop A hot leg through its respective RHR heat exchanger and on back to the RCS, the component cooling water system passing water through the same heat exchanger and removing heat, and the service water system taking the heat from the component cooling water system.

The event tree developed is shown in Fig. 19. It includes all the functions required to bring the plant to a cold shutdown condition. Shutting down of the nuclear reaction is accomplished by the RPS (Table 1). Removing the heat from the RCS is accomplished by either (a) the PCS or (b) the AFWS & SSR (Table 1). Prevention of RCS overpressure is accomplished by S/RV-O (Table 1). S/RV-R prevents the transient from becoming a LOCA. The CVCS maintains the water level in the reactor vessel and the RHRS allows the plant to be brought to a cold shutdown. Descriptions of the events and their success criteria are compiled in Table 1.

The class 1 transient event tree (see Fig. 19) identifies 24 accident sequences involving the operation (and operability) of seven mitigating systems--the RPS, PCS, AFWS & SSR, S/RV-O, S/RV-R, CVCS, and RHRS. Successful operation of these systems will prevent a class 1 transient from resulting in core melt.

Across the top of Fig. 19 we have identified seven different systems (columns 2 through 8) which may or may not function given that a class 1 transient has occurred (column 1). The systems in columns 2 through 8 are described in Table 1. In the tree network underneath columns 2 through 8 (the event tree) an upward branch means the system did not fail (success) and a downward branch means the system did fail (failure). For example, under column 2 there is only one success-failure branch for RPS, while under column 8 there are seven locations in the event tree where a success-failure branch of CVCS occurs. Column 9 lists the 24 possible logical paths or sequences. (The event notation is that of Table 1.) The Y (YES) or N (NO) under column 10 indicates whether or not the event sequence leads to a core melt. Note that event sequences 7, 8, 9, 10, 14, 15, 16, 20, 21 22, 23, and 24 can lead to failure.

The event tree was constructed by considering the timing sequence of the accident as well as the functional and operational interrelationships between systems. These interrelationships are:

- If RPS and PCS succeed (events $\overline{K}$ and $\overline{M}$), then S/RV-O and S/RV-R are of no consequence. The justification for this is that the pressure in the RCS would not exceed normal operating pressure, thus the pressure control functions are not required. This also applies to those cases where RPS succeeds, PCS fails, and AFWS & SSR succeeds (events $\overline{K}$, $\overline{M}$, and $\overline{L}$) because AFWS & SSR provides the same function as PCS (see below).

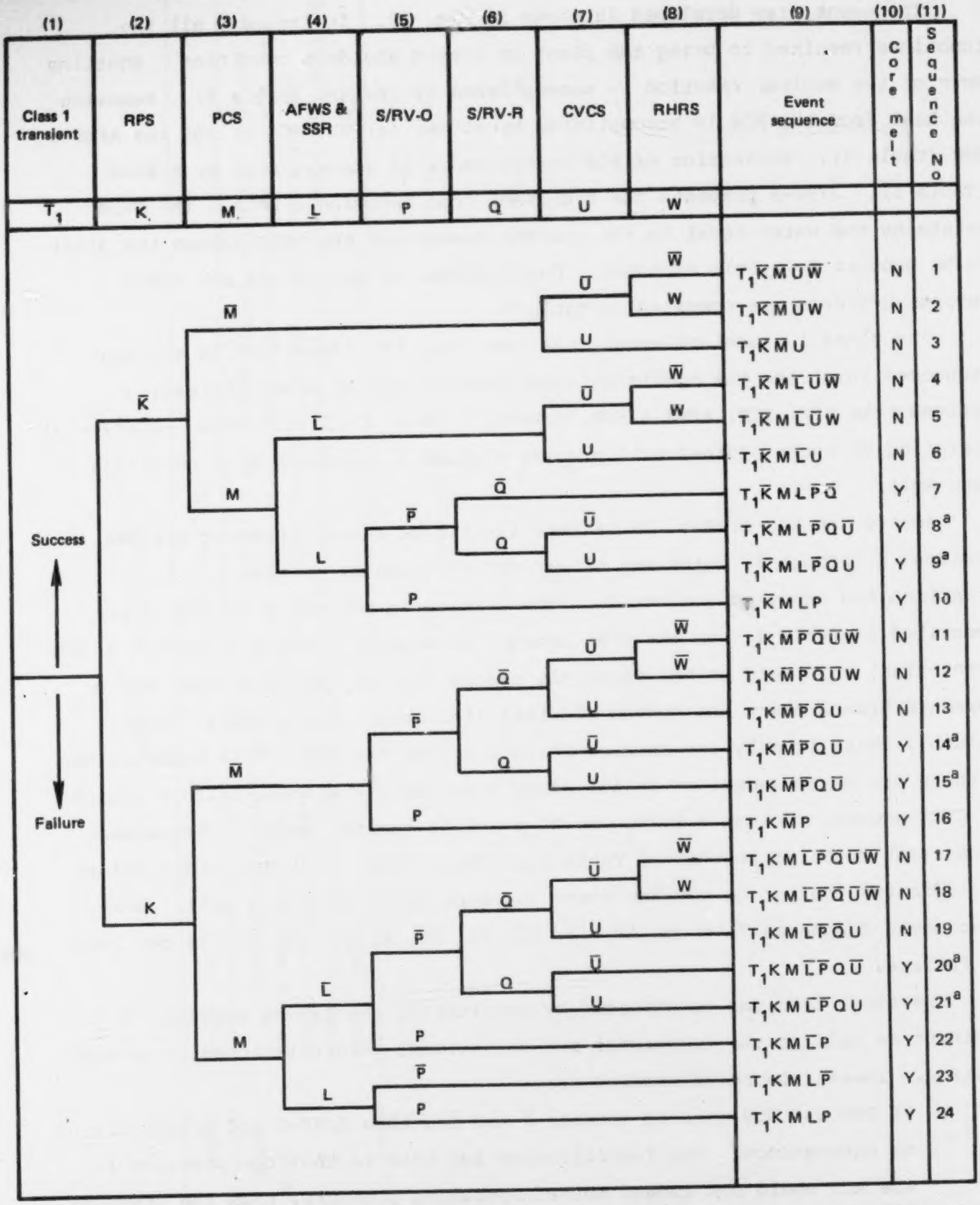

(1) Class 1 transient T_1
(2) RPS K
(3) PCS M
(4) AFWS & SSR L
(5) S/RV-O P
(6) S/RV-R Q
(7) CVCS U
(8) RHRS W
(9) Event sequence
(10) Core melt
(11) Sequence No
Success
Failure
$T_1\bar{K}\bar{M}\bar{U}\bar{W}$ N 1
$T_1\bar{K}\bar{M}\bar{U}W$ N 2
$T_1\bar{K}\bar{M}U$ N 3
$T_1\bar{K}M\bar{L}\bar{U}\bar{W}$ N 4
$T_1\bar{K}M\bar{L}\bar{U}W$ N 5
$T_1\bar{K}M\bar{L}U$ N 6
$T_1\bar{K}ML\bar{P}\bar{Q}$ Y 7
$T_1\bar{K}ML\bar{P}Q\bar{U}$ Y 8[a]
$T_1\bar{K}ML\bar{P}QU$ Y 9[a]
$T_1\bar{K}MLP$ Y 10
$T_1K\bar{M}\bar{P}\bar{Q}\bar{U}\bar{W}$ N 11
$T_1K\bar{M}\bar{P}\bar{Q}\bar{U}W$ N 12
$T_1K\bar{M}\bar{P}\bar{Q}U$ N 13
$T_1K\bar{M}\bar{P}Q\bar{U}$ Y 14[a]
$T_1K\bar{M}\bar{P}Q\bar{U}$ Y 15[a]
$T_1K\bar{M}P$ Y 16
$T_1KM\bar{L}\bar{P}\bar{Q}\bar{U}\bar{W}$ N 17
$T_1KM\bar{L}\bar{P}\bar{Q}\bar{U}\bar{W}$ N 18
$T_1KM\bar{L}\bar{P}\bar{Q}U$ N 19
$T_1KM\bar{L}\bar{P}Q\bar{U}$ Y 20[a]
$T_1KM\bar{L}\bar{P}QU$ Y 21[a]
$T_1KM\bar{L}P$ Y 22
$T_1KML\bar{P}$ Y 23
T_1KMLP Y 24

[a] These sequences, although marked as core melt, realistically feed into the appropriate LOCA event tree.

FIG. 19. Class 1 transient event tree.

- If PCS succeeds (event $\overline{M}$), then AFWS & SSR are of no consequence. The justification for this is that both PCS and AFWS & SSR perform the same function, that is providing water to the secondary side of the steam generators in order to remove heat from the RCS. Thus, only one of these systems is needed for any given sequence.
- If RPS succeeds and both PCS and AFWS & SSR fail (events $\overline{K}$, M, and L), then RHRS is not important since core melt is assumed. The justification for this is that with failure of both PCS and AFWS & SSR, the core decay heat is not removed and core melt will occur. In addition, the RCS pressure will never drop low enough for the RHRS to be used. (Exception: see the last interrelationship.)
- If S/RV-O fails (event P) or is not important, then S/RV-R is not important. The justification for this is that the S/RVs do not open, they cannot reclose.
- If RPS and AFWS & SSR all fail (events K, M, and L), then S/RV-R, CVCS, and RHRS are not important since core melt is assumed. The justification for this is that RPS failure will cause large amounts of heat to be added to the RCS, and failure of PCS and AFWS & SSR will leave no way for the heat to be removed, thus resulting in core melt. The RCS pressure will remain very high, therefore even if the S/RVs open the pressure will be too high for them to close, and the pressure will also be too high to use the RHRS. The CVCS will be ineffectual because it cannot provide enough flow to make up for the coolant loss.
- If S/RV-R fails (event Q), the result is a LOCA event of some type. The justification for this is that a stuck open valve is physically the same as a broken pipe, in that coolant will flow uninterrupted from the RCS. The resultant LOCA size will depend on the number and type of valves sticking open. A small LOCA will result from (a) one stuck open RV or (b) two stuck open RVs. A medium LOCA will result from (a) one stuck open SV, or (b) two stuck open SVs, or (c) one stuck open RV and one stuck open SV, or (d) two stuck open RVs and one stuck open SV. Any other combination of open valves will result in a large LOCA. Sequences involving this interrelationship would have to be continued on the appropriate LOCA event tree.

These interrelationships reduce the numbers of possible sequences from 128 to 24.

There are 12 non-melt sequences on the event tree. For the sequences numbered 1 through 6, core melt is avoided by RPS success (shutting down the nuclear reactor) and removal of the decay heat by either the PCS or the AFWS & SSR. For the sequences numbered 11 through 13 and 17 through 19, core melt is avoided by removal of core heat by either the PCS or the AFWS & SSR and by the S/RVs opening (to relieve the pressure spike caused by failure of the RPS) and then reclosing to avoid a LOCA).

There are six sequences on the event tree which lead to LOCAs. These are indicated in Fig. 19 by the superscript a to the right of the last column on the tree. The explanation of the treatment of these sequences is detailed in the above last interrelationship. It is important to note that even though core melt is conservatively indicated for these sequences, core melt is avoidable if the LOCA mitigating systems are capable of functioning.

Event Tree for Transients without Power Conversion System (PCS). A transient without PCS event is defined as any abnormal condition in the plant which:

- requires that the plant be shut down,
- causes the PCS to become inoperative, and
- does not qualify as a LOCA or vessel rupture.

That is, one or more of the system which make up the PCS (main steam, turbine bypass, condenser, condensate, or feedwater) is no longer operating and there is no rupture of RCS piping equivalent to the break of a single pipe whose diameter is greater than 0.5 inches. This type of transient will be referred to as a class 2 transient (T_2).

It is commonly believed, and it seems quite plausible, that for the range of earthquake "intensities" thought to dominate the seismic risk (for example, the 1 x SSE to 2 x SSE range) offsite power will be lost, which means that the PCS will become inoperative. With these assumptions, the class 2 transient is much more important than a class 2 transient in a seismic risk analysis.

The class 2 transient event tree identifies 15 accident sequences involving the operation (and operability) of six mitigating systems: the RPS, AFWS & SSR, S/RV-O, S/RV-R, CVCS, and RHRS. Successful operation of these systems will prevent a class 2 transient from resulting in a core melt.

The event tree developed is shown in Fig. 20. It includes the same functions as the class 1 transient tree discussed above. The difference between the two trees is that the PCS will not be available to remove heat from the RCS, so that only the AFWS & SSR will be able to perform this function. Descriptions of the events and their success criteria are compiled in Table 1.

The event tree was constructed by considering the timing sequence of the accident as well as the functionability and operability interrelationships between systems. These interrelationships are the same as those described for the class 1 transients, except that those interrelationships which include PCS success do not apply, since class 2 transients assume PCS failure. Elimination of the PCS event from the tree results in 64 potential sequences (as compared to 128 for the class 1 transients). Consideration of the system interrelationships reduces that number to 15.

There are six non-melt sequences on the event tree. These are indicated in Fig. 20 by the "N" in the core melt column. The reasoning for declaring these to be non-melt sequences is the same as that described for the class 1 transient tree. The sequences numbered 1 through 3 on the class 2 transient tree correspond to the sequences numbered 4 through 6 on the class 1 transient tree. The sequences numbered 8 through 10 on the class 2 transient tree correspond to the sequences numbered 17 through 19 on the class 1 transient tree.

There are four sequences on the event tree which lead to LOCAs. These are indicated in Fig. 20 by the sequence number with a superscript a. The explanation of these sequences is detailed in the last interrelationship in the section on the class 1 transient tree and is the same as that for the similarly indicated sequences on the class 1 transient tree.

In general, for an analysis involving the entire plant, the various failure sequences can lead to different consequences even though each is a failure of some kind. These consequences are defined by means of a containment failure event tree attached to the end of each accident sequence (not shown). For example, we might have a wide range of release possibilities, ranging from a catastrophic immediate large release due to the rupture of the reactor pressure vessel to a delayed longer term small release as at Three Mile Island, and the magnitude of release in such a range has a significant effect on the consequences to the public or risk.

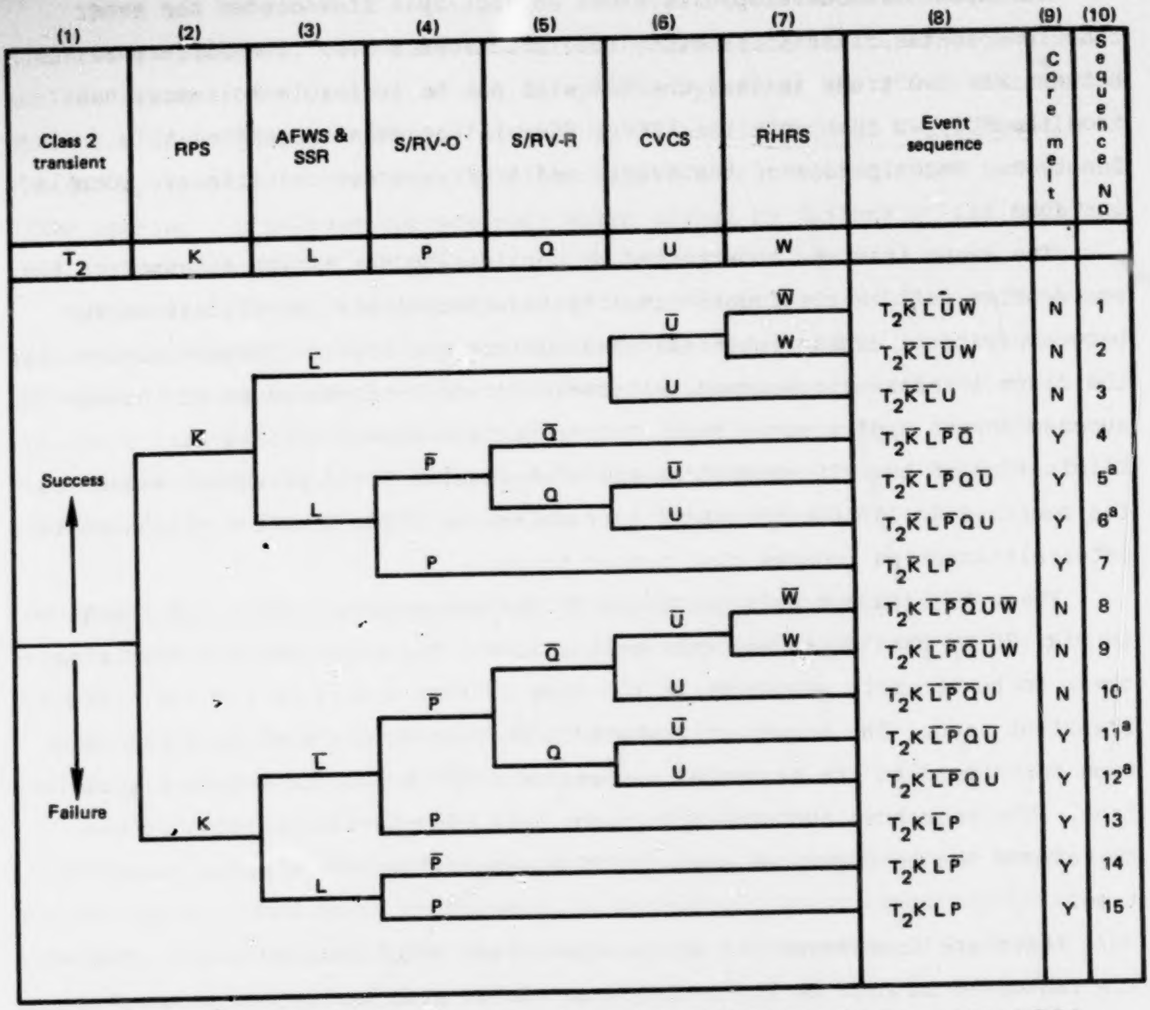
(1) Class 2 transient T_2
(2) RPS K
(3) AFWS & SSR L
(4) S/RV-O P
(5) S/RV-R Q
(6) CVCS U
(7) RHRS W
(8) Event sequence
(9) Core melt
(10) Sequence No
Success
Failure
$\bar{K}$
K
$\bar{L}$
L
$\bar{P}$
P
$\bar{Q}$
Q
$\bar{U}$
U
$\bar{W}$
W
$T_2\bar{K}\bar{L}\bar{U}\bar{W}$ N 1
$T_2\bar{K}\bar{L}\bar{U}W$ N 2
$T_2\bar{K}\bar{L}U$ N 3
$T_2\bar{K}L\bar{P}\bar{Q}$ Y 4
$T_2\bar{K}L\bar{P}Q\bar{U}$ Y 5ᵃ
$T_2\bar{K}L\bar{P}QU$ Y 6ᵃ
$T_2\bar{K}LP$ Y 7
$T_2K\bar{L}\bar{P}\bar{Q}\bar{U}\bar{W}$ N 8
$T_2K\bar{L}\bar{P}\bar{Q}\bar{U}W$ N 9
$T_2K\bar{L}\bar{P}\bar{Q}U$ N 10
$T_2K\bar{L}\bar{P}Q\bar{U}$ Y 11ᵃ
$T_2K\bar{L}\bar{P}QU$ Y 12ᵃ
$T_2K\bar{L}P$ Y 13
$T_2KL\bar{P}$ Y 14
T_2KLP Y 15

(a)These sequences, although marked as core melt, realistically feed into the appropriate LOCA event tree.

FIG. 20. Class 2 transient event tree.

Example of a System Fault Tree. To illustrate how a fault tree can be used to compute the probability of a system failure, consider the system in Fig. 21 which is a simplified version of the auxiliary feedwater system both in fault tree and block diagram form. This example is taken from a paper by Cornell and Newmark.[7] This tree is a simplified version of a more detailed one in the Reactor Safety study.

The reasoning and assumptions leading to this model are as follows: The earthquake will likely lead to the loss of off-site power and this in turn will probably lead to a transient. The main feedwater system is not seismically designed and is likely to be lost at high seismic levels. Loss of containment by overpressure can then occur if the auxiliary feedwater system fails.

The fault tree in Fig. 21b assumes the auxiliary feedwater system fails if:

- All three of the three stored water facilities fail or
- All three pumps fail.

One pump is driven by turbine and the other two by electricity. The accident sequence has already assumed the loss of off-site power and thus the electrically driven pumps depend on one of the two diesel generators operating.

We stress that this model is a simplified one presented for the purposes of illustration only. It is simplified in a number of ways including:

- It is a part of only one sequence leading to a release, and
- Much detail (piping, valves, control systems, etc.) has been omitted.

We now illustrate how system failure probabilities are calculated using a fault tree such as given in Figure 20b. For a system with only components in parallel, that is redundant components, failure of all components is required to cause system failure. Thus, if a system S1 is composed of only two components, C1 and C2, in parallel, the event (S1 FAILS) is equivalent to C1 failing and C2 failing. That is,

$$\text{(S1 FAILS)} = \text{(C1 FAILS) and (C2 FAILS)}$$

Thus, the probability that S1 fails, $P_F(S1)$, is

$$P_F(S1) = P(\text{C1 FAILS and C2 FAILS}) \quad . \qquad (8)$$

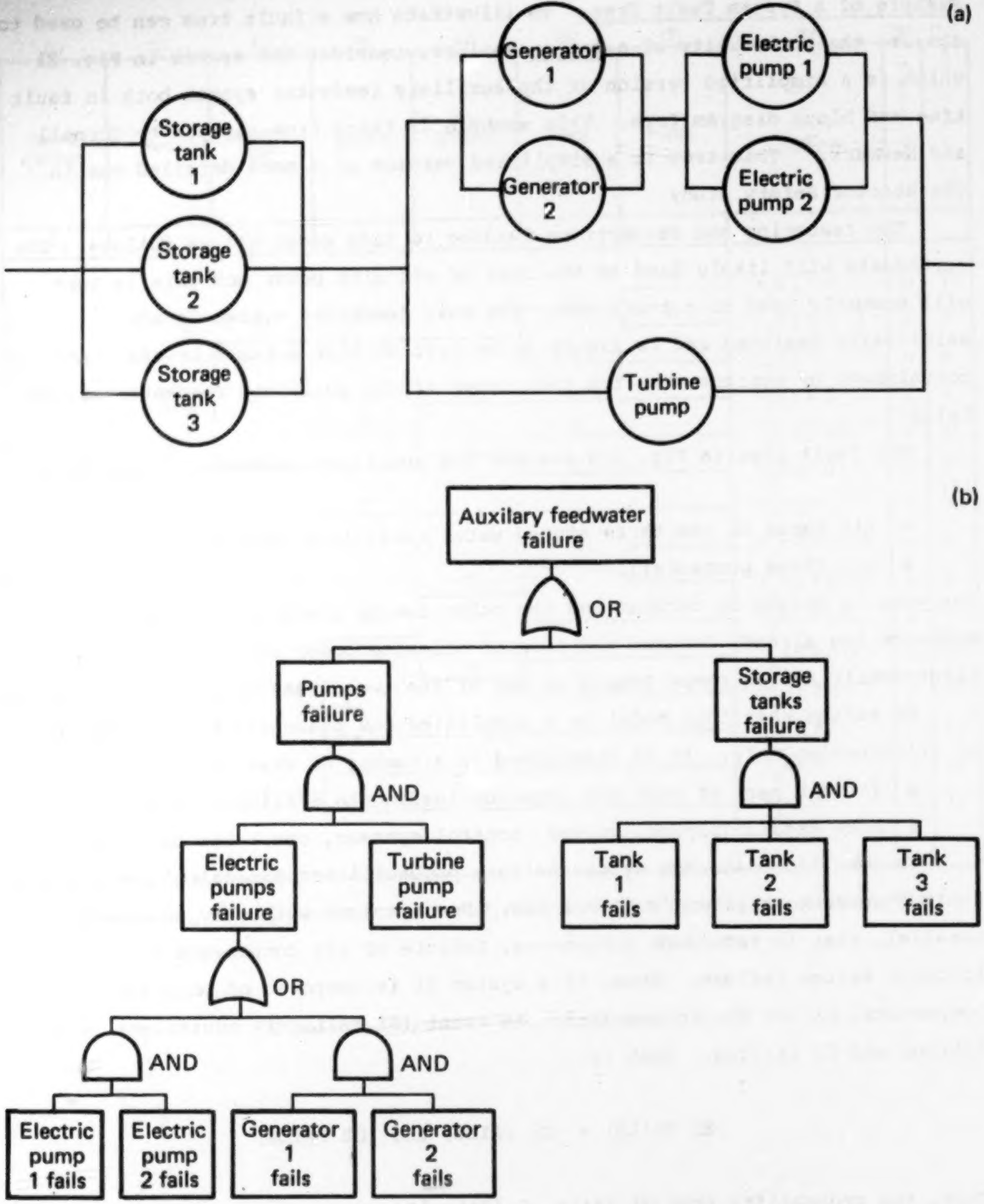
(a)
Storage tank 1
Storage tank 2
Storage tank 3
Generator 1
Generator 2
Electric pump 1
Electric pump 2
Turbine pump
(b)
Auxilary feedwater failure
OR
Pumps failure
Storage tanks failure
AND
AND
Electric pumps failure
Turbine pump failure
Tank 1 fails
Tank 2 fails
Tank 3 fails
OR
AND
AND
Electric pump 1 fails
Electric pump 2 fails
Generator 1 fails
Generator 2 fails

FIG. 21. Simplified auxiliary feedwater system models. (a) system block diagram, (b) system fault tree (Cornell and Newmark).[7]

If the events (C1 FAILS) and (C2 FAILS) are probabilistically independent, $P_F(S1)$ can be expressed in terms of the probabilities of the individual components failing. In particular,

$$P_F(S1) = P_F(C1)\,P_F(C2) \quad , \tag{9}$$

where $P_F(C1)$ and $P_F(C2)$ are the probability that C1 fails and C2 fails, respectively.

For a system with only components in series, a failure of any component will cause system failure. Specifically, if a system S2 consists of two components, C3 and C4, in series, S2 fails if C3 fails or C4 fails. Thus,

$$P_F(S2) = P(\text{C3 FAILS or C4 FAILS}) \quad . \tag{10}$$

Since the complement of the event (C3 FAILS or C4 FAILS) is the event (C3 NOT FAIL and C4 NOT FAIL), $P_F(S2)$ in Eq. 10 can be rewritten as

$$P_F(S2) = 1 - P(\text{C3 NOT FAIL and C4 NOT FAIL}) \quad . \tag{11}$$

If the failures of components C3 and C4 are independent events, and noting that for a component, C,

$$\begin{aligned} P(\text{C NOT FAIL}) &= 1 - P(\text{C FAILS}) \\ &= 1 - P_F(C) \end{aligned}$$

the probability of system failure in Eq. 11 can be rewritten as

$$P_F(S2) = 1 - \left[1 - P_F(C3)\right]\left[1 - P_F(C4)\right] \quad , \tag{12}$$

using the same reasoning used in going from Eq. 8 to 9.

Using the basic relations given in Eqs. 9 and 12, and assuming the failure of all components are independent events, the probability of failure of the system in Fig. 21 is:

$$\begin{aligned} P_F(AFW) = 1 - &\left\{1 - P_F(TP)\left[1 - \left\langle 1 - P_F(G1)\,P_F(G2)\right\rangle\left\langle 1 - P_F(EP1)\,P_F(EP2)\right\rangle\right]\right\} \\ &\left\{1 - P_F(ST1)\;P_F(ST2)\;P_F(ST3)\right\} \quad , \end{aligned} \tag{13}$$

where $P_F(AFW)$ is the probability of failure of the system in Fig. 20, $P_F(G1)$ and $P_F(G2)$ are the failure probabilities of the two generators, $P_F(EP1)$ and $P_F(EP2)$ are the failure probabilities of the electrically operated pumps, $P_F(TP)$ is the failure probability of the turbine pump, and $P_F(ST1)$, $P_F(ST2)$ and $P_F(ST3)$ are the failure probabilities of the three stored water facilities.

Note that the components appearing on the fault trees are those for which the probability of failure can be calculated as described in the beginning of this section.

The calculation of the probability of system failure as given in Eqs. 9 and 12 for components in series and parallel, respectively, and in Eq. 13 for the system in Fig. 21 depended on the failure of the components being independent events. Unfortunately, an earthquake simultaneously excites the entire plant, including redundant components and safety systems. Thus, the failures of individual components (or systems) are no longer independent and this fact must be taken into consideration when computing the probability of system (or plant) failure. We next illustrate how the probability calculations given in Eqs. 4 to 7 can be used when an earthquake simultaneously affects the response of all components within a system.

Calculation of Failure of a Single Component. We make two slight generalizations about the support equipment subsystem example of the previous section:

- Fig. 22a characterizes the response at 4 Hz from Fig. 14 as a uniform probability density function with a probability of 0.0 that responses will occur below 2 g or above 27 g. (Note that this is a conditional probability, conditional on the free-field peak acceleration being equal to 1.0 g.)
- Fig. 22b characterizes the component failure level as a random variable (whereas in the previous example the component was assumed to have a deterministic failure level of 15 g) for the reasons given in the beginning of this section. The uncertainty in the failure level is assumed to be described by a cumulative distribution function with a probability of failure of 0.0 if the component response is below 8 g, a probability of failure of 1.0 if the response is above 22 g, and a linear relationship between these two points.

These forms correspond to Figs. 17a and 17b and Eqs. 4 and 5.

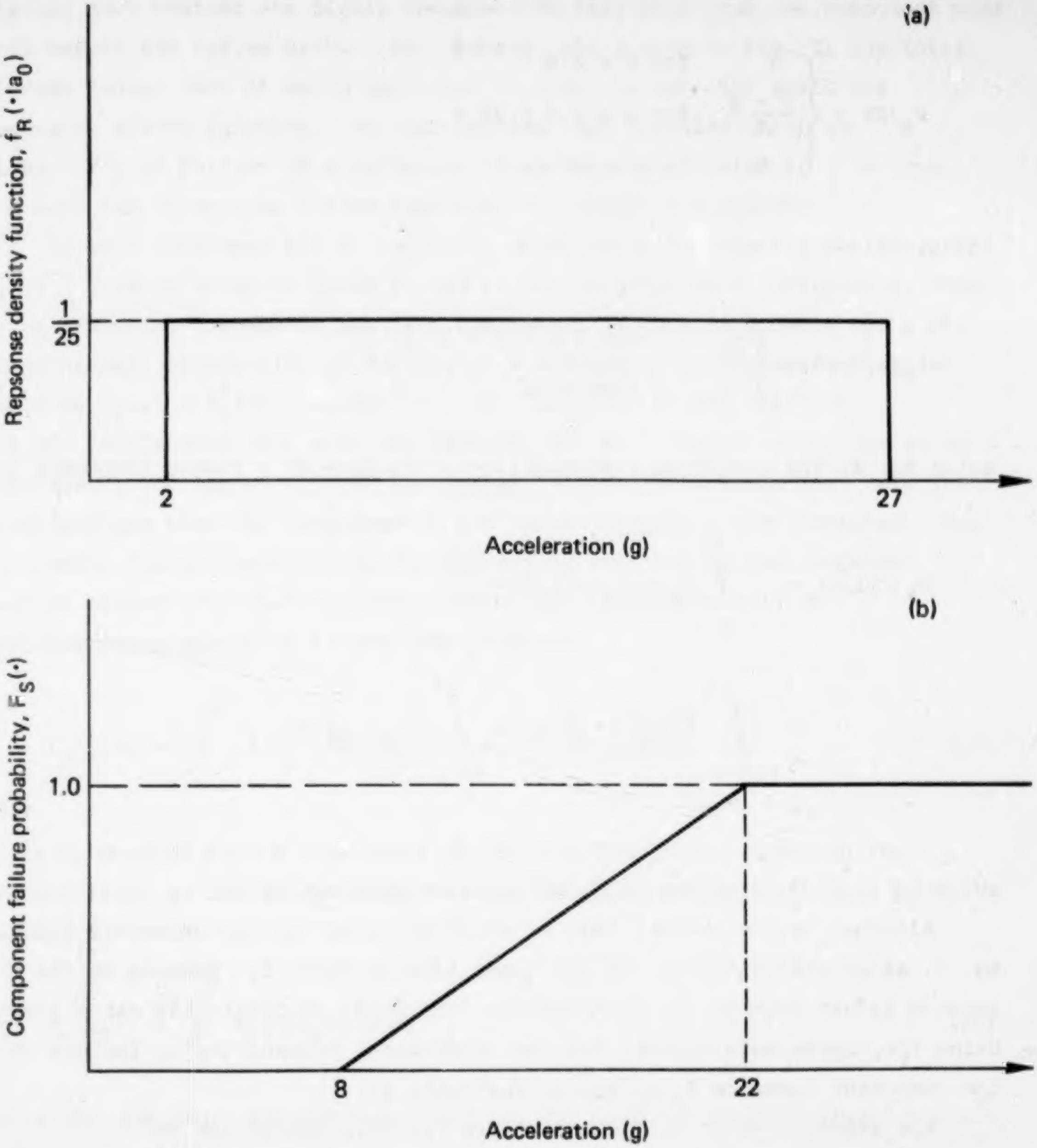

FIG. 22. Graphical description of assumptions for calculation of component failure probability, $P_F(C)$, for simple example in text. (a) Assumed density function for the response of a component. This function corresponds to Fig. 17b. (b) Assumed distribution function for resistance of the component. This function corresponds to Fig. 17a.

Because of the assumed probabilities, it is easy to express the density function and distribution functions mathematically. In particular,

$$F_S(S) = \begin{cases} 0 & \text{for } S < 8\text{ g} \\ \dfrac{S-8}{14} & \text{for } 8\text{ g} \le S \le 22\text{ g} \\ 1.0 & \text{for } S > 22\text{ g} \end{cases} \tag{14}$$

and given a = 1.0 g,

$$f_R(r|1.0) = \begin{cases} \dfrac{1}{25} & \text{for } 2\text{ g} < r < 27\text{ g} \\ 0 & \text{otherwise} \quad . \end{cases} \tag{15}$$

Using Eq. 4, the conditional probability of failure of a single component is

$$\begin{aligned} P_F(C|1.0) &= \int_0^\infty F_S(r) f_R(r|1.0)\,dr \\ &= \int_8^{22} \frac{r-8}{14} \cdot \frac{1}{25}\,dr + \int_{22}^{27} 1 \cdot \frac{1}{25}\,dr \quad , \\ &= 0.48 \end{aligned} \tag{16}$$

which is in good agreement with our previous estimate of 0.5.

Alternately, we perform this calculation using the approximate formula, Eq. 5, as described in Fig. 22 and summarized in Table 2. Because of the assumed linear form of the distribution functions, we obtain the exact answer using the approximate formula for the conditional probability of failure of the component (compare P_F in Eq. 16 and Table 2).

The assumptions in this example (see Fig. 22) should not be misinterpreted. Recall that the response density function, Fig. 22a, is a conditional one, conditional on the site peak free-field acceleration. Since the integration in Eq. 1 has a practical (but theoretically, no finite) limit, we should not be surprised to find some value of the site peak free-field acceleration for which response values will exceed resistance capability (27 g is greater than 22 g in Fig. 22, for example).

Calculation of Failure of Redundant Components in Fault Trees. In nuclear plants, many systems are highly redundant so that more than one component must fail before the system fails. For example, the system in Fig. 21 has three storage tanks, each of which must fail in order to lose the auxiliary feedwater system function. We next consider the calculation of the probability of failure of a redundant three-component system of this type. The next few paragraphs follow Anderson, Charlwood, and Chapman.[3]

If each component had an identical conditional failure probability, say $P_F(C) = 0.48$ as given in Table 2, and if the failures were independent, then since redundant components are like components in parallel, using Eq. 9 the (conditional) probability of failure of a redundant three-component system would be $P_F(S) = P_F^3(C) = (0.48)^3 = 0.11$. However, if the failures are not independent, but are, for example, due to a common cause such as an earthquake, the computation of the system failure probability must take into consideration that the responses at the three components are identical, thus the system failure probability is computed by convoluting the component failure probability distributions. Since all components will be simultaneously subjected to the same response,

$$P_F(S|a) = \int_0^{\infty} P(S_1 \leq r,\ S_2 \leq r,\ S_3 \leq r) f_R(r|a)\,dr \quad , \tag{17}$$

where S_i denotes the failure level of the ith component. Assuming the failure level of the three components are independent and identical, Eq. 17 reduces to

$$P_F(S|a) = \int_0^{\infty} F_S^3(r) f_R(r|a)\,dr \quad . \tag{18}$$

Using the component distribution function and response density function given in Eqs. 14 and 15 respectively,

$$P_F(S|1.0) = \int_8^{22} \left(\frac{r-8}{14}\right)^3 \cdot \frac{1}{25}\,dr + \int_{22}^{27} 1^3 \cdot \frac{1}{25}\,dr$$

$$= 0.14 + 0.20 = 0.34 \quad . \tag{19}$$

TABLE 2. Calculation of the conditional probability of failure of the component, $P_F(C)$, where the load on the component and the resistance of the component are given in Figs. 21 and 22. The calculation is performed using Eq. (5).

(1) r_i	(2) $F_R(r_i)$	(3) $F_S(r_i)$	$F_S(r_i)\ F_R(r_i) = (2) \times (3)$
2-9	-	0	0
9	0.08[a]	1/14[a]	0.006
11	0.08	3/14	0.017
13	0.08	5/14	0.029
15	0.08	7/14	0.04
17	0.08	9/14	0.051
19	0.08	11/14	0.063
21	0.08	13/14	0.074
24.5	0.2	1	0.2
			$\sum = 0.48 = P_F(C\|1.0)$

[a] See Fig. 23.

Table 3 gives the computations based on the approximation given in Eq. 5, and is similar to Table 2 except that it now applies to three redundant components rather than a single component. The result is a conditional system failure probability of 0.34, or over half the component failure of 0.48, and about three times the system failure probability of 0.11 which is obtained if independence of failures is assumed.

The large difference in the failure probabilities between common and independent causes, and the surprisingly small decrease in the system failure from the component failure probability occurs because, at the higher response (in this case, acceleration) levels, the component failure probability approaches 1.0, and so the system probability approaches 1.0 also, despite being the cube of the component probability (see the second integral in Eq. 19).

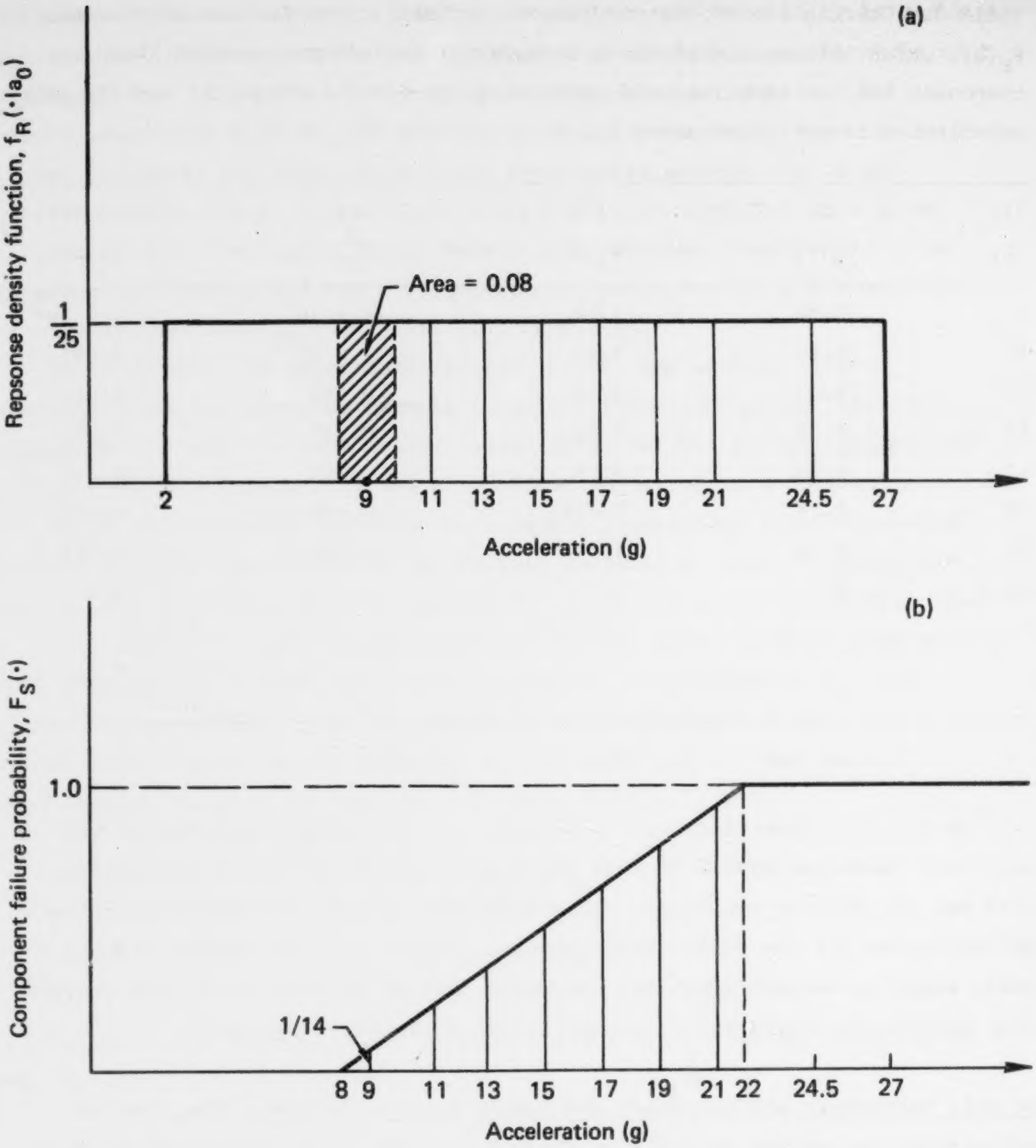

FIG. 23. Same as Fig. 22, except the r_i are shown. (See Table 1.)

TABLE 3. Calculation of the conditional probability of failure of a system, $P_F(S)$, which is composed of three redundant identical components. Each component has the same load and resistance described in Figs. 22 and 23. The calculation is performed using Eq. 5.

(1) r_i	(2) $F_R(r_i)$	(3) $F_S(r_i)$	(4) $F_S^3(r_i)$	(5) = (2)(4) $P_F(S)$
9	0.08	1/14	4×10^4	3×10^5
11	0.08	3/14	1×10^{-2}	0.001
13	0.08	5/14	0.046	0.004
15	0.08	7/14	0.125	0.01
17	0.08	9/14	0.266	0.021
19	0.08	11/14	0.485	0.039
21	0.08	13/14	0.801	0.064
24.5	0.2	1	1	0.2

$$\sum = 0.34 = P_F(S)$$

In the more general case, for example, in the failure analysis of the auxiliary feedwater system in Fig. 20, a generalized functional expression, like Eq. 13, must be evaluated. Allowance must be made for different failure probabilities for the different components, rather than the simple example we used, where we assumed identical component failure probabilities, and we must also account for different responses at the different components.

Seismic Redundancy and Component and System Failure Targets. The previous calculation for system probability assumed that the three subsystems all had the same natural frequency and, therefore, for a given earthquake each component would experience the same response. However, if the three subsystems have different natural frequencies, then they will have different component response. This occurs because the probability is small that one particular earthquake will produce high response over the whole range of frequencies. This can be seen by close inspection of Fig. 14. For example, above about 12 Hz, one particular earthquake clearly contributes the highest response, but below 12 Hz other earthquakes produce the higher response values. Thus, if the three subsystems were subjected to a given earthquake, then component 1 might have a high response, component 2 a low response, and component 3 some intermediate response in the case where the three subsystems had different natural frequencies.

To illustrate the importance of this effect, the system failure probability for the previous example is calculated assuming that the three components all have the same failure level (Fig. 24) but the subsystems have different natural frequencies and so would be subjected to different responses.

Since all responses are based on a common source they will be related. That is, although the values of the dynamic parameters, like frequency and damping, are uncertain, when an earthquake occurs the entire plant will have or is interpreted to have certain physical characteristics, which although not known with precision, are functionally related. In particular, R_2, the response at component 2 and, R_3, the response at component 3, are functionally related to the response, R_1, at component 1. The assumed relationships as given in Fig. 24, are respectively,

$$R_2 = 2 + 5(R_1 - 2)^{1/2}$$

$$R_3 = 27 - 5(27 - R_1)^{1/2}.$$

In this case, the system failure probability for three redundant components is (see Eq. 17).

$$P_F(S|a) = \int_0^\infty P(S_1 \le r_1, S_2 \le r_2, S_3 \le r_3) f_{R_1}(r_1|a)dr_1 \quad . \tag{20}$$

The relationships between the three responses for this example are shown in Fig. 24. Since all three components are assumed to have the same failure distribution function, $F_S(\cdot)$, Eq. 20 reduces to

$$P_F(S|a) = \int_0^\infty F_S(r_1)F_S(r_2)F_S(r_3)f_{R_1}(r_1|a)dr_1 \quad , \tag{21}$$

which can be approximated by (for a = 1.0)

$$P_F(S|1.0) = \sum_{i=1}^{n} F_S(r_{1i})F_S(r_{2i})F_S(r_{3i})\Delta F_R(r_{1i}|1.0) \quad . \tag{22}$$

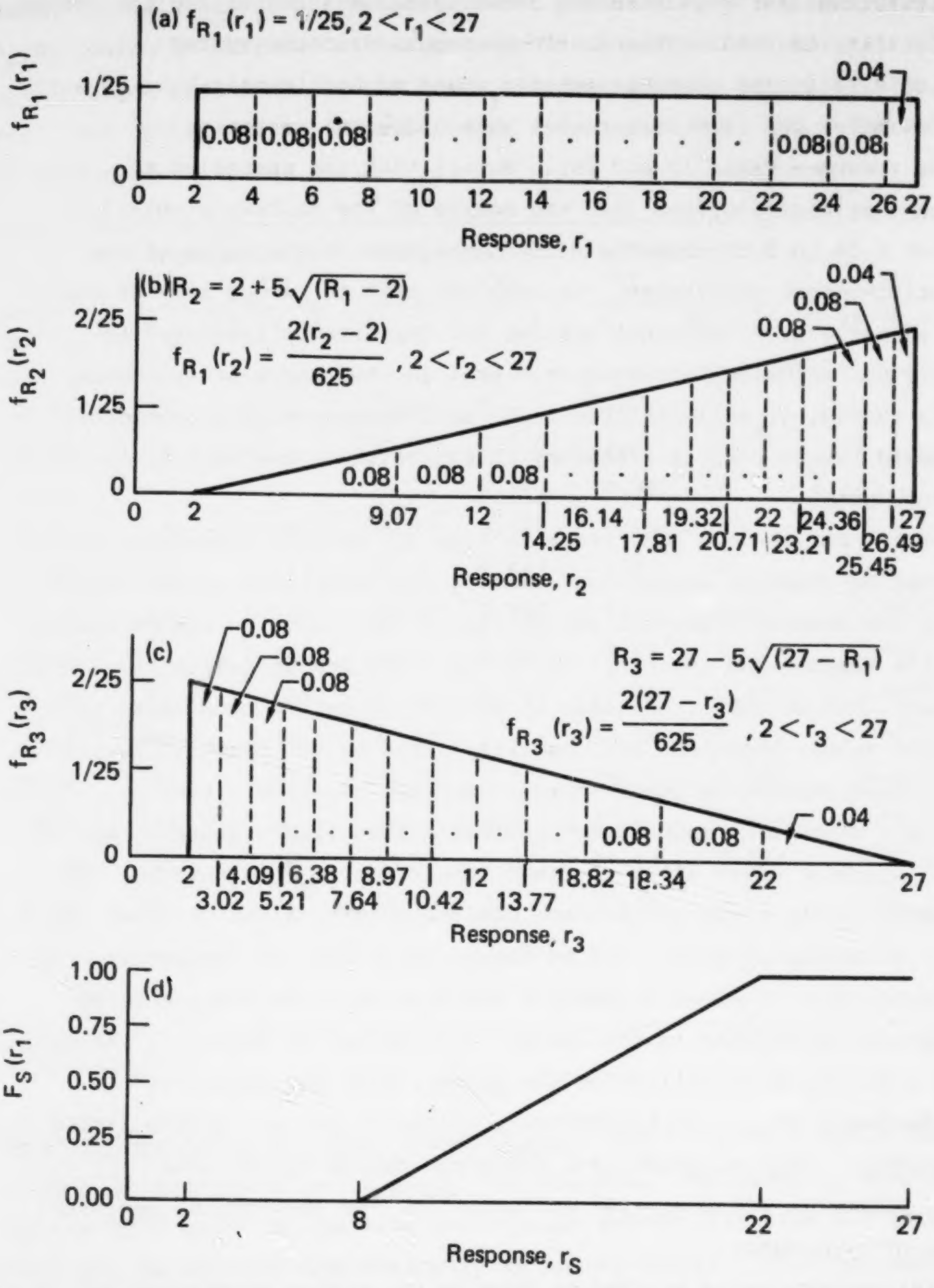

FIG. 24. Graphical description of assumptions for calculation of system failure probability, $P_F(S)$, for simple example in text. (a), (b), and (c) are the assumed density functions for the response of the three components in the system. These functions correspond to Fig. 17b. (d) is the assumed distribution function of the resistance of each of the three components. This function corresponds to Fig. 17a and is the same as the function in Fig. 21b.

The calculations for this case are shown in Table 4 and we see the system failure probability is 0.23. This should be compared to the system probability of 0.34 in the previous example where we had identical components (as in this example) and identical rather than different response distributions (compare Figs. 17 and 18). Recall that the source of the different response distributions (and the source of the failure probability reduction from 0.34 to 0.23) was the different natural frequencies of the three support-component subsystems. We conclude that to recoup some of the reliability advantages of redundant systems for the seismic loading, the systems should be "seismically redundant," that is, the transfer functions (like the one in Fig. 9) relating free-field earthquake motion to component responses should have different frequency characteristics for each of the redundant components.

For example, for the two generators in Fig. 21, seismic redundancy might be accomplished by physical separation (placing the generators at different elevations in the same or different structures) or by attaching one generator directly on the basemat and the other to an isolation system (which is mounted on the basemat), and so forth. Seismic redundancy is seldom considered in present reactor safety practice, and, as illustrated by our example, the absence of seismic redundancy leads to some increase in seismic risk.

The concept of seismic redundancy provides a good illustration of one of the ways risk analyses could affect seismic safety design requirements. For example, present safety requirements have evolved to give a set of rules (load combinations, allowable stresses, and so forth) to design all components. No explicit consideration is given to whether there is only one component, or multiple component redundancy in the system. If instead we defined a target or allocated a failure probability for the system, then the degree of component redundancy would lead to different allowable failure probabilities for the components. Thus we might have different design rules (load combinations, allowable stresses, and so forth) for the components, dependent on the degree of redundancy.

Plant risk targets could be used to develop the system target failure probabilities, perhaps by inverse calculations using event and fault tree analysis. With these probabilities we can then determine component design rules as outlined above. This approach is described in more detail in Chou, et al.[25]

TABLE 4. Calculation of the conditional probability of failure of a system, $P_F(S)$, which is composed of three redundant identical components. The distribution functions for the loads are described in Figs. 24a, 24b, and 24c. The resistance of the components is shown in Fig. 24d. The calculation is performed using Eq. (5).

	Component 1		Component 2		Component 3			
(1)	(2)	(3)	(4)	(5)	(6)	(7)	(8)	(9)
$F_{R_1}(r_{1i})$	r_{1i}	$F_s(r_{1i})$	r_{2i}	$F_s(r_{2i})$	r_{3i}	$F_s(r_{3i})$	= (3)(5)(7)	= (1)(8)
0.08	3	0	7.0	0	2.51	0	0	0
0.08	5	0	10.66	0.190	3.55	0	0	0
0.08	7	0	13.18	0.370	4.64	0	0	0
0.08	9	0.071	15.23	0.516	5.79	0	0	0
0.08	11	0.214	17.0	0.643	7.0	0	0	0
0.08	13	0.357	18.58	0.756	8.29	0.021	0.0057	0.0005
0.08	15	0.500	20.03	0.859	9.68	0.120	0.0515	0.0041
0.08	17	0.643	21.36	0.954	11.19	0.228	0.1399	0.0112
0.08	19	0.786	22.62	1.0	12.86	0.347	0.2727	0.0218
0.08	21	0.929	23.79	1.0	14.75	0.482	0.4478	0.0358
0.08	23	1.0	24.91	1.0	17.0	0.643	0.6430	0.0514
0.08	25	1.0	25.98	1.0	19.93	0.852	0.8520	0.0682
0.04	26.5	1.0	26.75	1.0	23.46	1.0	1.0	0.0400
								$\sum$ = 0.23

Seismic Redundancy and Plant Risk Targets. The issue of seismic redundancy extends to consideration of plant risk targets. For example, whether there is one, or more units at the site affects the public risk from earthquakes since each unit is excited simultaneously by an earthquake. This may mean that plant (unit) risk targets might have to be lower for multi-unit compared to single unit sites in order to achieve some target public risk.

The issue of seismic redundancy also extends to consideration of site risk targets in the Eastern United States. Because of the large felt areas characteristic of earthquakes in the east and the large number of reactors in the east, we must expect an eastern earthquake to simultaneously excite a number of sites (see Fig. 2). Thus we may arrive at the surprising result that the allowable site risk in the Eastern United States could be lower than in the Western United States. This probably does not mean SSE accelerations in the east must exceed those in the west.

Event Tree Failure Calculations. So far, our failure probability calculations have been applicable to systems with redundant components, that is, it is applicable to a system in which all components must fail for the system to fail. Such calculations are necessary to compute the probability associated with a fault tree. We now consider how these probabilities can be used in the context of an event tree.

Recall, (see Fig. 19) given an initial event (for example, a transient) within a plant, an event tree is used to define the potential accident scenarios (depending on the successful operation or failure of engineered safety systems) which might lead to release of radioactive material. To illustrate how the probability of a release can be calculated based on an event tree, consider the very simple event tree given in Fig. 25. In this example, there is no release if both systems function properly; if one of the two systems function, there is a category 2 release; and if both systems fail, there is a category 1 release. For illustration, we will only calculate the probability of a category 1 release, that is, when both systems fail. (The Reactor Safety Study[2] defined seven release categories.)

Suppose, for illustration, that system 1 is the auxiliary feedwater system diagramed in Fig. 21. The fault tree for system 2 is given in Fig. 26. Since we are concerned with a category 1 release, we need to determine what sequence of component failures result in a failure of both systems. Starting with system 1, failure occurs if

- all pumps fail, or
- all storage tanks fail.

In the former case, this requires both the turbine pump and the electric pumps to fail. The electric pumps fail if

- both electric pump 1 and electric pump 2 fail or
- both generator 1 and generator 2 fail.

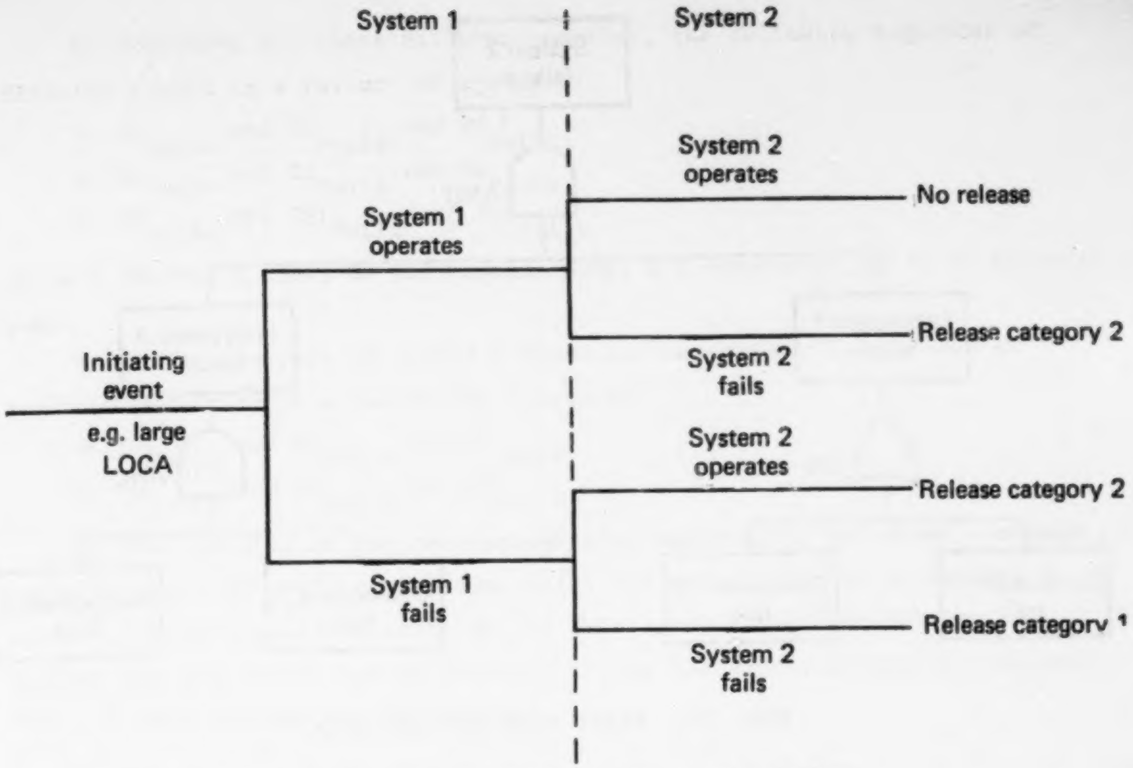
System 1
System 2
System 2 operates
No release
System 1 operates
Release category 2
System 2 fails
Initiating event
e.g. large LOCA
System 2 operates
Release category 2
System 1 fails
Release category 1
System 2 fails

FIG. 25. Event tree for simple system.

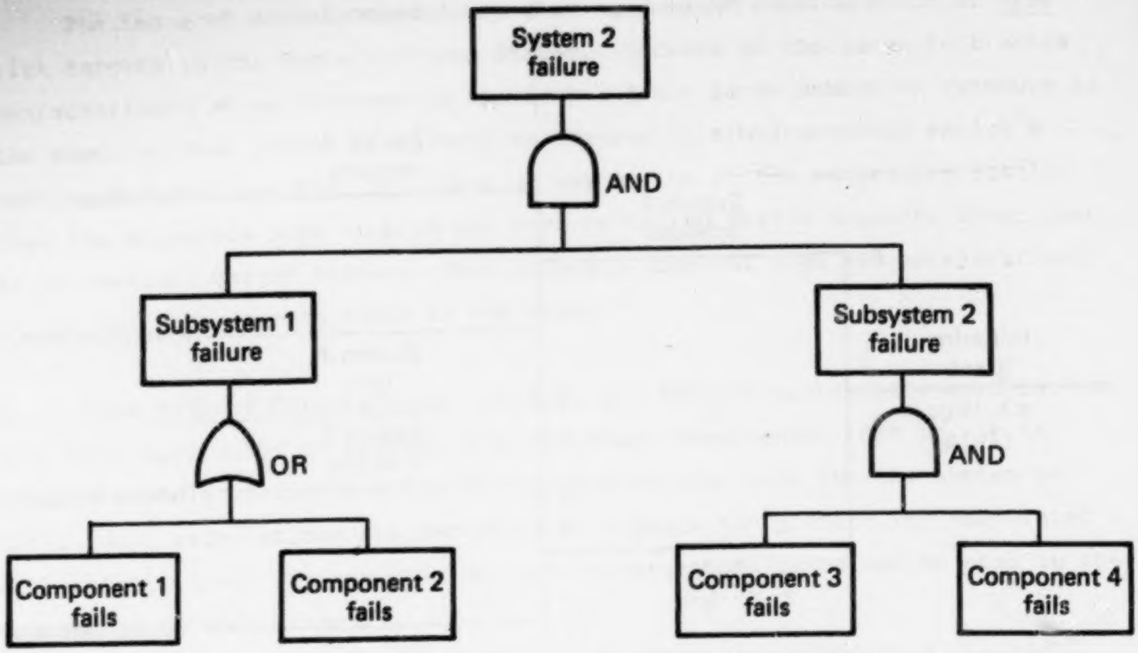
System 2 failure
AND
Subsystem 1 failure
OR
Subsystem 2 failure
AND
Component 1 fails
Component 2 fails
Component 3 fails
Component 4 fails

FIG. 26. Fault tree for system 2.

By combining all these failures together, the following sequences of failures result in a failure of system 1:

- $T1_{Fails}$ and $T2_{Fails}$ and $T3_{Fails}$
- TP_{Fails} and $G1_{Fails}$ and $G2_{Fails}$
- TP_{Fails} and $EP1_{Fails}$ and $EP2_{Fails}$

where T denotes a tank, TP the turbine pump, G a generator and EP an electric pump.

A similar analysis of system 2 leads to the following sequences of failures resulting in a failure of system 2:

- $C1_{Fails}$ and $C3_{Fails}$ and $C4_{Fails}$
- $C2_{Fails}$ and $C3_{Fails}$ and $C4_{Fails}$

If the failures of the two systems are independent, and since a category 1 release occurs only if both systems fail, the probability of a category 1 release can be calculated using Eq. 12 (where now the components are the systems and the event, system failure, is now the event, category 1 release). Thus, if both systems are independent,

$$P(\text{Category 1 Release}) = P_F(S1) \quad P_F(S2). \tag{23}$$

The probability of system failure, $P_F(S1)$ or $P_F(S2)$, could be obtained by methods similar to our previous examples.

However, in the case of common cause failures, such as when an earthquake is the source of failure, both systems are subject to responses from the same source and hence the failure of the systems are not independent. Thus, the identity in Eq. 23 is not applicable and we must make a series of calculations similar to that performed for the single system with redundant components. In particular, failure of both systems occurs if one of the sequences listed for system 1 occurs and one of the sequences listed for system 2 occurs. Thus, there are six sequences which define the failure of both systems:

- $T1_{Fails}$ and $T2_{Fails}$ and $T3_{Fails}$ and $C1_{Fails}$ and $C3_{Fails}$ and $C4_{Fails}$
- $T1_{Fails}$ and $T2_{Fails}$ and $T3_{Fails}$ and $C2_{Fails}$ and $C3_{Fails}$ and $C4_{Fails}$
- TP_{Fails} and $G1_{Fails}$ and $G2_{Fails}$ and $C1_{Fails}$ and $C3_{Fails}$ and $C4_{Fails}$
- TP_{Fails} and $G1_{Fails}$ and $G2_{Fails}$ and $C2_{Fails}$ and $C3_{Fails}$ and $C4_{Fails}$

- TP_{Fails} and $EP1_{Fails}$ and $EP2_{Fails}$ and $C1_{Fails}$ and $C3_{Fails}$ and $C4_{Fails}$.
- TP_{Fails} and $EP1_{Fails}$ and $EP2_{Fails}$ and $C2_{Fails}$ and $C3_{Fails}$ and $C4_{Fails}$.

The probability of each of these sequences can be calculated using the methods described in our previous example. The computations for the first sequence, $T1_{Fails}$ and $T2_{Fails}$ and $T3_{Fails}$ and $C1_{Fails}$ and $C3_{Fails}$ and $C4_{Fails}$, are summarized in Table 5. For simplicity, we have assumed that the responses for the three tanks are identical to those given in Table 4 and that the responses for C3 and C4 are identical. We also have assumed that the failure level (resistance) distribution of the three tanks are identical. Similarly, we assume the failure distribution for C3 and C4 are identical. From Table 5, the probability that the first sequence occurs, given a large LOCA (and an earthquake of intensity 1.0 g) is 0.196. A similar calculation can be performed for the other sequences as well. For illustration purposes, suppose such calculations led to the probabilities, respectively, 0.12, 0.007, 0.006, 0.01 and 0.009 (Note: this has no resemblence to reality; they are given only for illustration). Summing these, we see that the probability of a category 1 release, given a large LOCA (and conditional on a 1 g earthquake) is 0.352. Note that summing, as we have done, assumes that the sequences cannot occur simultaneously. This is not strictly true, so our method only provides an approximation. Fortunately, by summing we have an upper bound for the actual probability, thus our approximation is conservative.

Once analogous probabilities are calculated for all initiating events (e.g. large LOCA, small LOCA, etc.), the conditional probability of failure (in this case, a category 1 release), given an earthquake of an intensity of 1.0 g, is calculated by summing, i.e.

$$P_F(1.0) = \sum_{\substack{\text{all} \\ \text{initiating} \\ \text{events}}} P(\text{initiating event} \mid 1.0) P_F(1.0, \text{ initiating event}) \quad , \qquad (24)$$

where, for example, the term $P_F(1.0, \text{initiating event}) = 0.352$ in the case of a large LOCA, as illustrated.

To evaluate the "total" probability of failure (category 1 release), the value of $P_F(a)$, such as that given above for $a = 1.0$ g, would be calculated

TABLE 5. Calculation of failure probabilities in an event sequence.

	Component T1		Component T2		Component T3		Component C1		Component C3 & Component C4				
(1)	(2)	(3)	(4)	(5)	(6)	(7)	(8)	(9)	(10)	(11)	(12)	(13)	(14)
$\Delta F_R(r_i \vert 1.0)$	r_{1i}	$F_{S1}(r_{1i})$	r_{2i}	$F_{S1}(r_{2i})$	r_{3i}	$F_{S1}(r_{3i})$	r_{4i}	$F_{SC1}(r_{4i})$	r_{5i}	$F_{C3}(r_{5i})$	$F^2_{C3}(r_{5i})$	(3)×(5)×(7) ×(9)×(12)	(13)×(1)
0.08	3	0	7.0	0	2.51	0	1.06	0	5.6	0	0	0	0
0.08	5	0	10.66	0.190	3.55	0	1.11	0	9.8	0.01	1×10^{-4}	0	0
0.08	7	0	13.18	0.370	4.64	0	1.15	0	14.0	0.03	9×10^{-4}	0	0
0.08	9	0.071	15.23	0.516	5.79	0	1.20	3×10^{-4}	18.2	0.08	6.4×10^{-3}	0	0
0.08	11	0.214	17.0	0.643	7.0	0	1.25	4.6×10^{-3}	22.4	0.17	0.03	0	0
0.08	13	0.357	18.58	0.756	8.29	0.021	1.30	0.036	26.6	0.31	0.10	2.0×10^{-5}	1.6×10^{-6}
0.08	15	0.500	20.03	0.859	9.68	0.120	1.35	0.159	30.8	0.49	0.24	2.0×10^{-3}	1.6×10^{-4}
0.08	17	0.643	21.36	0.954	11.19	0.228	1.40	0.421	35.0	0.67	0.45	2.7×10^{-2}	2.1×10^{-3}
0.08	19	0.786	22.62	1.0	12.86	0.347	1.46	0.726	39.2	0.82	0.67	1.3×10^{-1}	1.1×10^{-2}
0.08	21	0.929	23.79	1.0	14.75	0.482	1.52	0.919	43.4	0.92	0.85	3.5×10^{-1}	2.8×10^{-2}
0.08	23	1.0	24.91	1.0	17.00	0.643	1.58	0.986	47.6	0.97	0.94	6.0×10^{-1}	4.8×10^{-2}
0.08	25	1.0	25.98	1.0	19.93	0.852	1.65	0.999	51.8	0.99	0.98	8.4×10^{-1}	6.7×10^{-2}
0.04	26.5	1.0	26.75	1.0	23.46	1.0	1.70	1.0	55.0	1.0	1.0	1.0 ×	4.0×10^{-2}
													$\sum = 0.196$

as we have illustrated and then integrated over all values of acceleration using Eq. 1. However, such calculations are quite extensive and thus are beyond the scope of this report.

Summary of Risk Calculations

In summary, a risk analysis involves a sequence of calculations leading to the probability of a failure (where, for example, failure is defined to be a category 1 release). Once a description of the seismic hazard is defined, the sequence of calculations involves

- Response calculations (Figs. 8 and 14)
- Component failure calculations (Eqs. 4 through 7 and Table 2)
- System failure calculations (Tables 2, 3, 4, and 5)

This sequence of risk calculations, as used in the Seismic Safety Margins Research Program (SSMRP), is diagrammed in Fig. 27, where the sequence of calculations proceeds from the bottom to the top of the figure. In the SSMRP, the calculations are performed by two separate software packages:

- SMACS (Seismic Methodology Analysis Chain with Statistics) which performs the seismic dynamic response calculations in a manner that couples soil-structure interaction, and major structure and subsystem response; and
- SEISIM (Seismic Evaluation of Important Safety Improvement Measures) which performs failure calculations for
  - components,
  - systems, and
  - core melt (release)

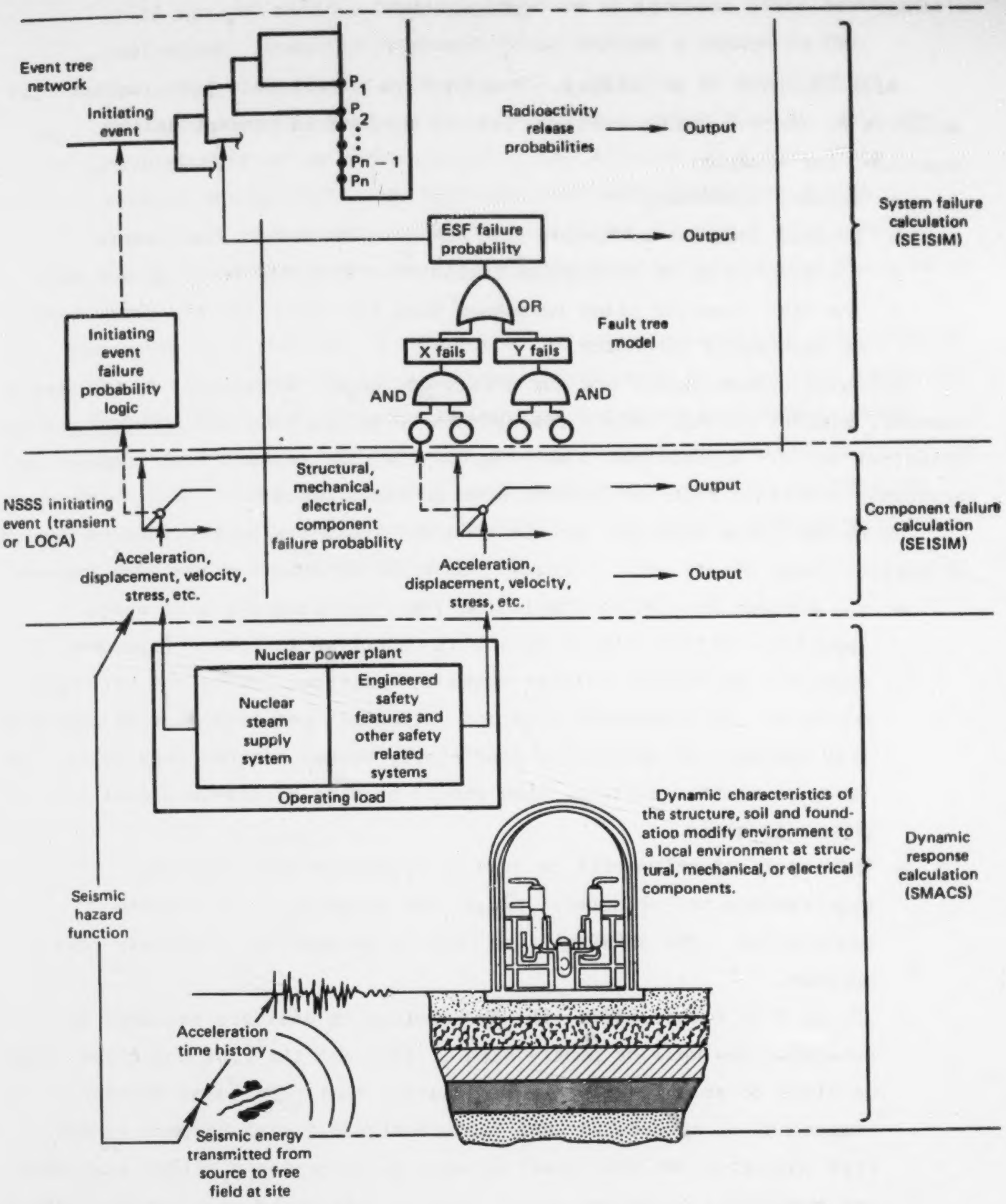
Event tree network
Initiating event
P1
P2
Pn – 1
Pn
Radioactivity release probabilities
Output
ESF failure probability
Output
System failure calculation (SEISIM)
OR
Fault tree model
X fails
Y fails
AND
AND
Initiating event failure probability logic
Structural, mechanical, electrical, component failure probability
Output
NSSS initiating event (transient or LOCA)
Component failure calculation (SEISIM)
Acceleration, displacement, velocity, stress, etc.
Acceleration, displacement, velocity, stress, etc.
Output
Nuclear power plant
Nuclear steam supply system
Engineered safety features and other safety related systems
Operating load
Dynamic characteristics of the structure, soil and foundation modify environment to a local environment at structural, mechanical, or electrical components.
Dynamic response calculation (SMACS)
Seismic hazard function
Acceleration time history
Seismic energy transmitted from source to free field at site

FIG. 27. Computational procedure used in the Seismic Safety Margins Research Program (SSMRP).

CONCLUSIONS

Risk analysis is no panacea. However, the unavoidable fact is that risk analyses do address issues that are largely ignored in present safety practice, for example:

- seismic redundancy
- logical accident scenarios that can lead to harm to the public
- the wide range of earthquake intensities that may occur at any site
- the wide range of plant responses that may occur for any given level of earthquake intensity.

Moreover, these issues are not merely addressed (after all, in one way or another, present seismic safety assessments do this), they are integrated into a logical whole. Probabilistic methods are the only mathematical tool presently available that can address some of these issues.

As seismic risk analysis becomes more developed its application to design of nuclear power plants will increase. Examples of such applications include:

- The Nuclear Regulatory Commission (NRC) and Congress will agree (possibly, within a year) on a risk objective for power reactors. This is a political decision based on technical inputs and national policy on the acceptable risk and ultimately required cost of one mode (say nuclear) of generating electricity versus another (say coal). It is by no means a decision that should be made by the technical community alone.
- This risk objective will be used to establish design safety requirements in the several areas, for example, in earthquake engineering. The SSMRP will be able to be used for precisely this purpose.
- If, at this future stage, the NRC decides to evaluate reactors to determine how well or poorly each of them met the risk objective, then we might be able to make a determination that particular systems, components or structures were "underdesigned," with respect to the risk objective (we will never be able to determine a priori that they are absolutely "underdesigned," this is determined only through future performance, if then).
- If a determination is made that particular structures, systems, or components are "underdesigned" with respect to earthquakes, it is

still not yet obvious that the "fix" is to increase their earthquake resistance! Possible alternate fixes include a change in the operating or maintenance procedures, a lowering of power output, modifications of other structures, systems, and components (not the ones thought to be underdesigned), the addition of a new safety system, and so forth, as there are many ways to achieve a risk objective. A systems analysis approach can provide a more rational basis for deciding the best fix on the basis of minimizing the risk or cost.

The point is clear that the future of seismic risk analysis will include closer interactions with design practices, development of practical designing tools, and the identification of implications for other engineering areas. One example is testing. Failure modes of significance to seismic risk will be more thoroughly identified for components and structures. The tendency to test to failure will increase as opposed to testing only to qualification levels. Many other examples can be cited.

APPENDIX:
RISK STUDIES

Nine risk studies relating to seismic risk and nuclear power plants are described in terms of general features. All were carried out within the past six years. Most of the more recent studies dealt with specific plants, whereas earlier ones dealt with generic systems. The latest, and on going, study, the Seismic Safety Margins Research Program (SSMRP),[26] embodies a significant research effort in every element of the seismic design methodology chain.

REACTOR SAFETY STUDY

The Reactor Safety Study, reported in 1975,[2] established a probabilistic computational procedure which was followed later by several later studies. A generic system was addressed in the seismic risk section. A single fragility curve was used and was based on the work of Newmark.[27] The seismic hazard description was that developed by Hsieh, Okrent, and Apostolakis.[28] The measure of risk was the probability of core melt. A major conclusion was that the seismic contribution to risk is low compared to other contributions, but there have been questions regarding the basis for the conclusion.

CANADIAN NUCLEAR POWER PLANT STUDY

A study of seismic risk and Canadian nuclear power plants by ACRES Consulting Services, Ltd.,[3] was reported in 1975. A three-component generic system was addressed. Four fragility curves were developed to reflect the uncertainty in fragility levels, and were based on information on design practices and assumptions. The seismic hazard was established specifically for Canadian sites. The measure of risk was the probability of system failure. A major finding was that the seismic contribution to risk is important.

A STUDY BY HSIEH AND OKRENT

The study by Hsieh and Okrent[4] reported in 1976 included design errors and system degradation. A generic system consisting of ten components in series was addressed, that is, the failure of any one component means failure of the system. Three fragility curves of lognormal shape, based on the work of Newmark,[27] were generated corresponding to normal, minimal, and maximal design errors. The seismic hazard was based on the results of Hsieh, Okrent, and Apostolakis.[28] The measure of risk was the probability of system failure. A significant finding was that design errors can be important.

A STUDY BY CORNELL AND NEWMARK

A generic system consisting of eight components, modeled after an auxiliary feedwater system, was studied by Cornell and Newmark[7] and reported in 1978. Fragility descriptions of lognormal form were developed from a set of multiplicative factors related to design safety factors. The seismic hazard was a modification of the results of Hsieh, Okrent, and Apostolakis.[28] Risk was measured by the probability of failure of the system. A conclusion was that the seismic contributions to risk could be important.

DIABLO CANYON STUDY

A risk study on the Diablo Canyon nuclear power plant[29] was carried out by the Pacific Gas and Electric Company (PG&E) in 1977, following the realization that the Hosgri fault is a potential major seismic hazard source. Seven safety systems were modeled by fault trees, and event trees were generated for five initiating events. Several forms of fragility curves were developed based on PG&E's information. Random failure was accounted for through the tails of the fragility curves. The fragility parameter for all curves was the peak ground acceleration. The seismic hazard was developed based on PG&E's information. Risk was measured by the cumulative probability distribution of radioactive exposure at various locations, taking into consideration the weather and dose constants. A major finding was that the seismic contribution to risk is low, and that the non-category 1 Turbine Building was the source of most of the risk due to earthquakes.

A STUDY BY ANG AND NEWMARK ON DIABLO CANYON

As a result of the PG&E study on the Diablo Canyon nuclear power plant, Ang and Newmark[10] in 1977 carried out a study to help answer questions such as: (1) how much decrease in the operational life of the plant resulted from the increased seismic hazard, and (2) if a recovery of operational life is desired what retrofitting or upgrading may be necessary. The results of this study confirmed the seismic contribution to risk for the plant is low.

CLINCH RIVER STUDY

A risk study on the Clinch River breeder reactor nuclear power plant[30] was reported in 1977. The seismic hazard was based on the work of Hsieh, Okrent, and Apostolakis.[28] The measure of risk was the probability of core melt. The results indicated earthquakes are significant contributors to risk, and that the risk was sensitive to the degree of seismic hazard.

OYSTER CREEK STUDY

A study on the Oyster Creek nuclear power plant was carried out, but the final results are not yet published. The procedures used to establish the fragility curves and the seismic hazard were described by Kennedy, Campbell, Cornell, Perla, and Kaplan[31] in 1979. Fragility curves were developed following the procedure of Cornell and Newmark.[7] The results of the study indicate that non-category 1 systems can be important contributors to seismic risk.

SEISMIC RISK STUDY IN GREAT BRITAIN

The Central Electricity Generating Board carried out a seismic risk study for Great Britain[32] which was reported in 1979. The seismic hazard was developed from information for Great Britain. Generic equipment, pipe work, and structures were studied to establish the ground motion levels to cause failure in terms of limit states. Limit states, for example, can be defined in general terms as the elastic limit state, the yield limit state, and malfunction or collapse. The results were used to specify required OBE and SSE design ground motion levels for nuclear power plants, based on achieving a risk objective.

SEISMIC SAFETY MARGINS RESEARCH PROGRAMS

The Seismic Safety Margins Research Program (SSMRP)[25] is the first risk study to include an extensive research effort in every element of the seismic design methodology chain. The construction and demonstration of a probabilistic computational procedure is being carried out in Phase I which will be completed by January 1981. The Zion Nuclear Power Plant near Chicago, Illinois, USA, owned by Commonwealth Edison Company (CECo), was selected as the demonstration plant. Zion specific analyses and/or characterizations are being made for the seismic input, soil-structure interaction, major structural response, subsystem response, and fragility curves. The event trees and fault trees being used are similar to those of the Diablo Canyon study[29] and the Reactor Safety Study[2] except they are developed specifically with earthquakes in mind. Five safety systems are modeled in Phase I; modeling of additional systems will be carried out in Phase II. Sensitivity studies to assess the effects of uncertainties in modeling parameters will be started in Phase I and completed in Phase II. Several probabilistic norms are provided, that is, probability of release (risk), probability of failure of the various systems, probability of failure of the various components, and responses at various locations in the plant. Phase II will also include a ranking of the various contributions to risk. Included in the effort planned for Phase III will be recommendations for improving the design requirements for nuclear power plants. In the SSMRP, every aspect of the above overview is covered in at least the detail described, and in some cases in more detail.

The key to the success of the program was the extraordinary cooperation extended to the SSMRP by CECo.

REFERENCES

1. C. A. Cornell, N. M. Newmark, and E. H. Vanmarcke, Eds., "Concluding Report of the Seminar on Probabilistic Seismic Analysis of Nuclear Power Plants," Bundesanstalt fur materialprufing, Berlin-Dahlem (January 16-19, 1978).
2. Reactor Safety Study--An Assessment of Accidents in New U.S. Commercial Nuclear Power Plants, U.S. Nuclear Regulatory Commission, WASH-1400 (NUREG-75/014) (1975).
3. D. L. Anderson, R. G. Charlwood, and C. B. Chapman, Seismic Risk Analysis Procedures for Canadian Nuclear Power Plants," Acres Consulting Services Limited (1975).
4. T.-M. Hsieh and D. Okrent, Some Probabilistic Aspects of the Seismic Risk of Nuclear Reactors, School of Engineering and Applied Science, University of California, Los Angeles, CA, UCLA-ENG-76113 (1976).
5. W. W. Hays, "Procedures for Estimating Earthquake Ground Motions," in Professional Paper 1114, U.S. Geological Survey (U.S. Government Printing Office, Washington, D.C., 1980).
6. O. W. Nuttli, "The Mississippi Valley Earthquakes of 1811 and 1812, Intensities, Ground Motion, and Magnitudes," in Seismological Society American Bulletin, Vol. 63, pp. 227-248 (1973).
7. C. A. Cornell and N. M. Newmark, "On the Seismic Reliability of Nuclear Power Plants," Topical meeting on Probabilistic Reactor Safety, American Nuclear Society, Newport Beach, CA (May 8-10, 1978).
8. J. Irving, "National Summary of U.K. Trends in Extreme Load Design Criteria," invited lecture, Post-SMiRT Seminar on Extreme Load Design of Nuclear Power Plant Facilities, Berlin, Germany (August 20-21, 1979).
9. T. Hsieh, D. Okrent, and G. E. Apostolakis, "On the Average Probability Distribution of Peak Ground Acceleration in the U. S. Continent Due to Strong Earthquakes," Annals of Nuclear Energy, 2, pp. 615-624 (1975).
10. A. H-S. Ang and N. M. Newmark, A Probabilistic Seismic Safety Assessment of the Diablo Canyon Nuclear Power Plant, report to the United States Nuclear Regulatory Commission (November 1977).
11. J. J. Johnson, A Summary of Soil-Structure Interaction Review Reports, Lawrence Livermore National Laboratory draft Report, July 28, 1960.
12. J. E. Luco, Linear Soil-Structure Interaction, Lawrence Livermore National Laboratory, draft Report, July 1980.

13. J. M. Roesset, A Review of Soil-Structure Interaction, Lawrence Livermore National Laboratory, UCRL-15262 (1980).

14. H. B. Seed and J. Lysmer, The Seismic Soil-Structure Interaction Problem for Nuclear Facilities, Lawrence Livermore National Laboratory, UCRL-15254 (1980).

15. J. T. Christian, J. R. Bull, and E. Kausel, Soil-Structure Interaction, Lawrence Livermore National Laboratory, UCRL-15230 (1980).

16. J. Isenberg, D. K. Vaughan, G. L. Wojcik, F. S. Wong, and J. P. Wright, A Review of Structure-Medium Interaction Analysis Methods with Application to SSMRP, Lawrence Livermore National Laboratory, UCRL-15255 (1980). Prepared by Weidlinger Associates, Menlo Park, CA.

17. Structural Building Response Review, Lawrence Livermore National Laboratory, UCRL-15183, USNRC Report NUREG/CR-1423, Vol. II, January 1980. Prepared by Sargent and Lundy.

18. J. J. Healey, S. T. Wu, and M. Murga, Structural Building Response Review, Lawrence Livermore National Laboratory, UCRL-15185, NUREG/CR-1423, Vol. I, February 1980. Prepared by Ebasco Services.

19. J. Fogelquist, M. K. Kaul, R. Koppe, S. W. Tagart, Jr., H. Thailer, and R. Uffer, Subsystem Response Review, Lawrence Livermore National Laboratory, UCRL-15214 (1980). Prepared by Nuclear Services Corporation/Quadrex Corporation.

20. R. P. Kennedy, R. D. Campbell, D. A. Wesley, H. Kamil, A. Gantayat, and R. Vasudevan, Subsystem Reponse Review, Lawrence Livermore National Laboratory, UCRL-15216 (1980). Prepared by Engineering Decision Analysis Co.

21. D. R. Brillinger, "Fourier Analysis of Stationary Processes", Proceedings of the IEEE, Vol. 62 No. 12, pp. 1628-1643 (1974).

22. E. H. Vanmarcke, Seismic Risk and Engineering Decision, Eds. C. Lomnitz and E. Rosenblueth, Elsevier, N.Y. (1976).

23. S. E. Bumpus, J. J. Johnson, and P. D. Smith, Best Estimate Method vs Evaluation Method: A Comparison of Two Techniques in Evaluating Seismic Analysis and Design, UCRL-52746, USNRC Report NUREG/CR-1489 (1980).

24. A. A. Garcia and J. E. Kelly, Event Tree Development and Construction for the Seismic Safety Margins Research Program, Science Applications, Inc., Bethesda, MD and Palo Alto, CA, August 1979.

25. C. K. Chou, R. W. Mensing, P. D. Smith, K. Vepa, J. D. Collins, C. A. Cornell, R. P. Kennedy, M. K. Ravindra, *Seismic Safety Margins Research Program, Load Combination Project--Task 3, Load Combination Methodology Development, Interim Report I*, Lawrence Livermore National Laboratory, UCID-18149 (1980).

26. P. D. Smith, F. J. Tokarz, D. L. Bernreuter, G. E. Cummings, C. K. Chou, V. N. Vagliente, J. J. Johnson, and R. G. Dong, *Seismic Safety Margins Research Program--Program Plan, Revision II*, UCID-17824 (1978).

27. N. M. Newmark, "Inelastic Design of Nuclear Reactor Structures and its Implications on Design of Critical Equipment," *Transactions of the 4th SMiRT Conference* (1977), paper K4/1.

28. T. -M. Hsieh, D. Okrent, and G. E. Apostolakis, *Probability Distribution of Peak Ground Acceleration in the U. S. Continent Due to Strong Earthquakes*, School of Engineering and Applied Science, University of California, Los Angeles, CA., UCLA-ENG-7516 (1975).

29. Pacific Gas and Electric Company, *Seismic Evaluation for Postulated 7.5M Hosgri Earthquake, Units 1 and 2, Diablo Canyon Site, Vol. V: Analysis of the Risk to the Public from Possible Damage to the Diablo Canyon Nuclear Power Station from Seismic Events*, U.S. Nuclear Regulatory Commission, docket no. 50-275 and 50-323 (1977).

30. Clinch River Breeder Reactor Plant, *CRBRP Safety Study, an Assessment of Accident Risk from CRBRP*, CRBRP-1, March 1977.

31. R. P. Kennedy, R. D. Campbell, C. A. Cornell, H. F. Perla, and S. Kaplan, "Probabilistic Seismic Safety Study of an Existing Nuclear Power Plant," *5th International Conference on Structural Mechanics in Reactor Technology*, Berlin, Germany, August, 1979.

32. J. Irving, *Seismic Risk and the Design of Nuclear Power Stations in Great Britain*, C.E.G.B., G.D. & C.D., report no. C/JI/SD/142.0/R016 (1979).

33. W. W. Hays, "Program and Plans of the U.S. Geological Survey for Producing Information Needed in National Seismic Hazards and Risk Assessment, Fiscal Years 1980-84," *Geological Survey Circular 816* (1979).

Technical Information Department · Lawrence Livermore Laboratory
University of California · Livermore, California 94550

SEISMIC SAFETY MARGINS
RESEARCH PROGRAM (Phase I)

REPORTS GENERATED BY THE SEISMIC SAFETY MARGINS RESEARCH PROGRAM

September 1980

P. D. Smith
R. G. Dong
D. L. Bernreuter
M. P. Bohn
T. Y. Chuang
G. E. Cummings
J. J. Johnson

Manuscript submitted: xx/xx/xx
Date published: xx/xx/xx

Prepared for the
Office of Nuclear Regulatory Research
U. S. Nuclear Regulatory Commission
Washington, DC 20555
NRC FIN Nos. A0126, A0130, A0138, A0139, and A0142
by
Lawrence Livermore National Laboratory
Livermore, CA 94550
Operated by the University of California
for the U. S. Department of Energy

REPORTS GENERATED BY THE SSMRP

INTRODUCTION

This document compiles the reports generated by the Seismic Safety Margins Research Program (SSMRP). This compilation is kept up to date at the Lawrence Livermore National Laboratory, and is included near the end of each quarterly progress report for the SSMRP. Because of the high interest in the reports this compilation is periodically issued separate from the quarterly progress reports when significant progress takes place before the end of a quarter.

The compilation of reports is arranged according to the technical areas corresponding to the projects of the program. Under the technical areas are identified deliverables, each of which is designated by a two or three letter code accompanied with a brief description. Following each deliverable are the generated reports.

Projected due dates and completion status are indicated. The reports produced for each deliverable are identified, and the status of release as a NUREG is shown. Changes or additions to the preceding month's tabulation is indicated by a vertical bar on the right hand margin. Changes, if any, are explained by a footnote. The completed reports are available on request from: Oak Ridge Technical Information Center, P.O. Box 62, Oak Ridge, Tennessee 37830.

REPORTS GENERATED IN EACH TECHNICAL AREA

SEISMIC INPUT

Deliverables and Corresponding Reports	Original Due Date	Revised Due Date	Status of Completion	Status of NUREG
SI-1 Feasibility of using ARMA models to simulate earthquake time histories	9/79		Completed 7/79	
M. K. CHANG, J. W. KWIATKOWSKI, R. F. NAU R. M. OLIVER, and K. S. PISTER, ARMA Models for Earthquake Ground Motions," University of California, Report No. UCB/EERC-79/19, July 1979.				Camera ready copy being procured
SI-2 Simulation of time histories parameterized by magnitude, epicentral distance, and site conditions using ARMA models.	12/80		Completed 6/80	
R. F. NAU, R. M. OLIVER, and K. S. PISTER "Simulating and Analysing Artificial Non-Stationary Earthquake Ground Motions," University of California, ORC 80-16, June 1980				Camera ready copy being procured
SI-3 Differences between body wave magnitude in the Eastern and Western U.S. and the interrelation between local body and surface wave magnitudes.	4/80		Completed 4/80	

SEISMIC INPUT (Continued)

Deliverables and Corresponding Reports	Original Due Date	Revised Due Date	Status of Completion	Status of NUREG
D. H. CHUNG and D. L. BERNREUTER "Regional Relationships Among Earthquake Magnitude Scales," Lawrence Livermore National Laboratory, April 1980, NUREG/CR-1457.				NUREG
SI-4 Assessment and expansion of the strong ground motion data base.	4/80		Completed 4/80	
C. B. CROUSE, J. A. HILEMAN, B. E. TURNER, and G. R. MARTIN "Compilation, Assessment and Expansion of the Strong Earthquake Ground Motion Data Base," Lawrence Livermore National Laboratory, UCRL-15227, NUREG/CR-1660. Prepared by Fugro, Inc., April 1980.				NUREG [a]
SI-5 Relative effect of Q on the strong ground motion from earthquakes between the Eastern and Western U.S.	7/80		Completed 7/80	
D. H. CHUNG and D. L. BERNREUTER "The Effect of Regional Variation of Seismic Wave Attenuation on the Strong Ground Motion from Earthquakes," Lawrence Livermore National Laboratory, July 1980.				Submitted for NUREG
SI-6 Improved Bayesian methodology for development of site dependent spectra.	12/80			

---

a. NUREG Completed.

SOIL-STRUCTURE INTERACTION

Deliverables and Corresponding Reports	Original Due Date	Revised Due Date	Status of Completion	Status of NUREG
SSI-1 Soil-Structure Interaction (SSI) Review Reports assessing the state-of-the-art of SSI analysis methodology, accuracy, uncertainties, and itemizing benchmarck problems.	6/80		Completed 8/80	
J. J. JOHNSON A Summary of Soil-Structure Interaction Review Reports," Draft, Lawrence Livermore National Laboratory Report, July 28, 1960.				
J. E. LUCO "Linear Soil-Structure Interaction," Lawrence Livermore National Laboratory, Draft Report, July 1980.			Consolidated with J. J. Johnson's report.	
J. M. ROESSET A Review of Soil-Structure Interaction," Lawrence Livermore National Laboratory UCRL-15262, June 1980.			"	
H. B. SEED and J. LYSMER "The Seismic Soil-Structure Interaction Problem for Nuclear Facilities," Lawrence Livermore National Laboratory, UCRL-15254, April 1980.			"	
J. T. CHRISTIAN, ET. AL. "Soil-Structure Interaction, "Lawrence Livermore National Laboratory, UCRL-15230, February 1980.			"	

b. Deliverable completed

SOIL-STRUCTURE INTERACTION (Continued)

Deliverables and Corresponding Reports	Original Due Date	Revised Due Date	Status of Completion	Status of NUREG
J. ISEMBERG, ET. AL. "A Review of Structure-Medium Interaction Analysis Methods with Application to SSMRP," Lawrence Livermore National Laboratory, UCRL-15255, May 1980.			"	
SSI-2 Sensitivity Study of Soil-Structure Interaction phenomenon for structure-structure interaction, soil properties and soil configuration, wave passage, and azinmuth effects for Zion nuclear power station using continuum analysis approach.	6/80		Partially completed 6/80	
H. L. WONG "Identification of Sensitive Parameters for Statistical Simulation of Soil-Structure Interaction," June 1980.				
SSI-3 Sensitivity study comparing linear finite analysis with continuum analysis approach for Zion nuclear power station.	9/80			
SSI-4 Summary of nonlinear analysis task with evaluation of future work to be done for the development, verification, and comparison of nonlinear SSI methods with linear techniques.	11/80			

MAJOR STRUCTURAL RESPONSE

Deliverables and Corresponding Reports	Original Due Date	Revised Due Date	Status of Completion	Status of NUREG
STR-1 General structural building response analysis review with special emphasis on damping and nonlinearity.	2/80		Completed 2/80	
"Structural Building Response Review," Lawrence Livermore National Laboratory, UCRL-15183. Prepared by Sargent and Lundy, January 1980, NUREG/CR-1423,SL-3759, Vol. II.				NUREG
J. J. HEALEY, S. T. WU, and M. MURGA "Structural Building Response Review," Lawrence Livermore National Laboratory, UCRL-15185. Prepared by Ebasco Services, February 1980, NUREG/CR-1423, Vol. I.				NUREG
STR-2 Response of nuclear power plant structures to three input components.	6/80		Completed 4/80	
S. E. BUMPUS, J. J. JOHNSON, and P. D. SMITH "Best Estimate Method vs. Evaluation Method: A Comparison of Two Techniques in Evaluating Seismic Analysis and Design," Lawrence Livermore National Laboratory, UCRL-52746, NUREG/CR-1489, May 1980.				NUREG
STR-3 Effect of structural damping on nuclear power plant structures. This is another study by expanding LLL/DOR Seismic Conservatism Program (Parts III & IV) to typical nuclear power plant structures (Zion station).	6/80		Completed 6/80	

MAJOR STRUCTURAL RESPONSE (Continued)

Deliverables and Corresponding Reports	Original Due Date	Revised Due Date	Status of Completion	Status of NUREG
D. A. WESLEY, P. S. HASHIMOTO, R. B. NARVER Seismic Safety Margins Research Program 'Phase I) Task (sic) IV, Structures Response, "Variability of Dynamic Characteristics of Nuclear Power Plant Structures," UCRL-15267, NUREG/CR-1661. Lawrence Livermore National Laboratory prepared by Structural Mechanics Associates, SMA 12205.02, June 1980.				NUREG
STR-4 Identify modeling variables, systematic or random, in the major structure response analysis. Rank in terms of their effect on the uncertainty of structural response.	3/80		Completed 3/80	
T. K. HASSELMAN and S. S. SIMONIAN "Structural Uncertainty in Seismic Risk Analysis," Lawrence Livermore National Laboratory, UCRL-15218 Prepared by J. H. Wiggins Company, March 1980, NUREG/CR-1560.				NUREG
STR-5 Accuracy of finite element method and lumped mass method in seismic analysis.	9/80			

a. NUREG completed

SUBSYSTEM RESPONSE

Deliverables and Corresponding Reports	Original Due Date	Revised Due Date	Status of Completion	Status of NUREG
SUB-1 Subsystem Response Review Reports assessing the state-of-the-art of subsystem response determination, accuracy, and uncertainties.	2/80		Completed 3/80	
J. FOGELQUIST, M. K. KAUL, R. KOPPE, S. W. TAGART, JR., H. THAILER, and R. UFFER, "Subsystem Response Review," Lawrence Livermore National Laboratory, UCRL-15215. Prepared by Nuclear Services Corporation/Quadrex Corporation, March 1980.				Submitted for NUREG
R. P. KENNEDY, R. D. CAMPBELL, D. A. WESLEY, H. KAMIL, A. GANTAYAT, and R. VASUDEVAN, "Subsystem Response Review," Lawrence Livermore National Laboratory, UCRL-15216. Prepared by Engineering Decision Analysis Co., March 1980.				Submitted for NUREG
SUB-2 Sensitivity study investigating the effects of uncertainties on subsystem response.	10/80	Merged with SUB-4		
SUB-3 Sensitivity study on nonlinear analysis of a key safety system.	10/80	FY 82		
SUB-4 Sensitivity study to rank contributions to uncertainty in subsystem response. (Added 7/10/80.)	None	11/80		

FRAGILITIES

Deliverables and Corresponding Reports	Original Due Date	Revised Due Date	Status of Completion	Status of NUREG
FRA-1 NPRDS listing of Zion component in-service operational history.	6/79		Completed 6/79	Not Appropriate for NUREG
FRA-2 Report on gathered fragilities related information.	9/80			
FRA-3 Report on Expert opinion received on component fragility.	9/80			
FRA-4 Reports on failure modes for components and structures for a representative PWR plant.			Completed	
Components	2/80		6/79	
Buildings	2/80		10/79	
R. D. CAMPBELL and D. A. WESLEY "Preliminary Failure Mode Predictions for the SSMRP Reference Plant (Zion 1 and 2)," Lawrence Livermore National Laboratory, UCRL-15042. NUREG/CR-1703. Prepared by Engineering Decision Analysis Co., June 1979.				NUREG[a]
"Potential Seismic Structural Failure Modes Associated with the Zion Nuclear Plant," Lawrence LivermoreNational Laboratory, UCRL-15140, NUREG/CR-1704. Prepared by Engineering Decision Analysis Co. Inc., October 1979.				NUREG[a]

---

a. NUREG completed.

FRAGILITIES (Continued)

Deliverables and Corresponding Reports	Original Due Date	Revised Due Date	Status of Completion	Status of NUREG
FRA-5 Fragility curves for components and structures for a representative PWR plant.	1/81			
FRA-6 Documentation of an overall fragility description development methodology.	4/81			

SYSTEMS ANALYSIS

Deliverables and Corresponding Reports	Original Due Date	Revised Due Date	Status of Completion	Status of NUREG
SYS-1 Description of computational methodologies for prediction of core melt probabilities in a nuclear power plant due to seismic events.	4/79		Completed 2/79	
I. B. WALL, M. K. KAUL, R. I. POST, S. W. TAGART, JR., and T. J. VINSON "Specification of Computational Approach," Lawrence Livermore National Laboratory, UCRL-13985, NUREG/CR-1702. Prepared by Nuclear Services Corp., February 1979.				NUREG
J. D. COLLINS, J. M. HUDSON, and J. D. CHROSTOWSKI, "Specifications of Computational Approach," Lawrence Livermore National Laboratory, UCRL-13986, NUREG/CR-1701. Prepared by J. H. Wiggins Company, February 1979.				NUREG
SYS-2 Description of a design concept for calculating probability of radioactive release, core melt, safety system, structural and component failure probabilities from a set of nuclear plant seismic responses.	8/79		Completed 6/79	
"SEISIM Code Design Concept," Technical Report 78-1645-2. J. H. Wiggins Company, June 1979.				Not ready for NUREG

a. NUREG completed.

SYSTEMS ANALYSIS (Continued)

Deliverables and Corresponding Reports	Original Due Date	Revised Due Date	Status of Completion	Status of NUREG
SYS-3 Operating Seismic Safety Analysis Code-SEISIM (Option 1 only).	1/81		Partially completed 4/80	
J. H. HUDSON, J. D. GASCA, and J. D. COLLINS "SEISIM Option I Design Specification (Revision 1)," J. H. Wiggins Company Draft Report 80-1366-1, April 1980.				Not ready for NUREG
SYS-4 Accident sequences as the result of earthquakes at Zion 1 nuclear power plant.	10/79		Completed 8/79	
A. A. GARCIA and J. E. KELLY "Event Tree Development and Construction," Science Applications, Inc., SAI-003-79-BE, August 1979.				Not ready for NUREG
SYS-5 Fault trees of some safety systems of Zion 1 nuclear plant. (auxiliary feedwater system, service water system, emergency core cooling system, residual heat removal system, parts of the electric power and instrumentation and control system pertaining to the above).	1/81		Partially completed 5/80	
Draft Version of the Zion Unit 1 Auxiliary Feedwater System Fault Tree on the Seismic Safety Margins Research Program (SSMRP), May 14, 1980. (1 tree)				Not appropriate for NUREG
Draft Version of the Zion Unit 1 Electrical Power System Fault Tree on the Seismic Safety Margins Research Program (SSMRP), May 30, 1980. (1 tree)				Not appropriate for NUREG

SYSTEMS ANALYSIS (Continued)

Deliverables and Corresponding Reports	Original Due Date	Revised Due Date	Status of Completion	Status of NUREG
Draft Version of the Zion Unit 1 Service Water System Fault Tree on the Seismic Safety Margins Research Program (SSMRP), June 27, 1980. (3 trees.)				Not appropriate for NUREG
Draft Version of the Zion Unit 1 Emergency Core Cooling System Fault Tree on the Seismic Safety Margins Research Program (SSMRP), July 1980. (4 trees.)				Not appropriate for NUREG

OTHER REPORTS

	Status of NUREG
C. K. CHOU, K. VEPA, L. GEORGE, and P. D. SMITH "Seismic Safety Margins Research Program Project VIII Load Combination Project-Work Plan," Lawrence Livermore National Laboratory, UCID-18126, July 10, 1979.	
C. K. CHOU, R. W. MENSING, P. D. SMITH, K. VEPA, J. D. COLLINS, C. A. CORNELL, R. P. KENNEDY, and M. K. RAVINDRA "Seismic Safety Margins Research Program Load Combination Project--Task 3, Load Combination Methodology Development Interim Report I," Lawrence Livermore National Laboratory, UCID-18149, January 31, 1980.	
C. K. CHOU, S. C. LU, M. W. SCHWARTZ "Load Combination Program, Phase II Work Plan," Lawrence Livermore Laboratory Draft Report, April 15, 1980.	
R. G. DONG and P. D. SMITH "Seismic Safety Margins Research Program (Phase I)Long Range Plan, Report I," Lawrence Livermore National Laboratory, April 2, 1980.	Submitted for NUREG 7/30/80
P. D. SMITH, F. J. TOKARZ, D. L. BERNREUTER, G. E. CUMMINGS, C. K. CHOU, V. N. VAGLIENTE, J. J. JOHNSON and R. G. DONG, "Seismic Safety Margins Research Program, Program Plan, Revision II," UCID-17824, Rev. II, August 11, 1978.	
R. L. SHARPE, J. W. REED, and C. B. WAUGH "Seismic Safety Margins Research Program (Phase I), Project I - Plant/Site Selection Assessment Report," Lawrence Livermore National Laboratory, UCRL-15110, NUREG/CR-1705. Prepared by Engineering Decision Analysis Company, Inc., July 20, 1979.	Submitted for NUREG 9/15/80
DENNIS C. BLEY, CARROLL L. CATE, DOUGLAS C. IDEN, B. JOHN GARRICK, JAMES M. HUDSON, "Seismic Safety Margins Research Program (Phase I), Project VII - Systems Analysis Event Tree Methodology Development," Report PLG-0110, Pickard, Lowe,and Garrick, Inc., and J. H. Wiggins Company, September 1979.	Submitted for NUREG
ABEL A. GARCIA, JOHN E. KELLY, PAUL J. AMICO, WILLIAM J. PARKINSON, FREDERICK L. LEVERENZ "Seismic Safety Margins Research Program (Phase I),Interim Report, Project VII Systems Analysis, Event Tree Development and Construction," Report No. SAI-003-79-BE, Science Applications, Inc., Bethesda, Maryland, August 1979.	Submitted for NUREG

OTHER REPORTS (Continued)

	Status of NUREG
P. D. SMITH, and R. G. DONG "Seismic Safety Margins Research Program (Phase 1), Definition of Terms." Lawrence Livermore National Laboratory, September 1980.	Submitted for NUREG 7/30/80
P. MOIENI, G. APOSTOLAKIS, and G. E. CUMMINGS "Interim Report on Systematic Errors in Nuclear Power Plants," Lawrence Livermore National Laboratory, UCRL-15274, NUREG/CR-1722, September 22, 1980.	NUREG
A. MOSLEH AND G. APOSTOLAKIS "Some Properties of Distributions Useful in the Study of Rare Events," August, 1980. Prepared by the University of California, Los Angeles, CA.	Submitted for NUREG 10/80

B. Report completed.

Application of Systems Analysis Techniques to the Study of Reactor Seismic Safety*

G. E. Cummings and J. E. Wells

University of California, Lawrence Livermore National Laboratory
P.O. Box 808 - L-90
Livermore, California 94550

SUMMARY

We will (1) describe the probabilistic-based systems model used in the Seismic Safety Margins Research Program (SSMRP), (2) discuss how the model interfaces with SSMRP, and (3) discuss the systems modeling as it pertains to the safety systems at Zion 1 nuclear power plant. This model was developed as part of the SSMRP to give the U.S. Nuclear Regulatory Commission (NRC) additional information about the conservatism in seismic analysis methodology as applied to U.S. nuclear power plants. SEISIM (Seismic Evaluation of Important Safety Improvement Measures) is the computer program used to implement the probabilistic based systems model and event-tree/fault tree methodology is used to construct the model. Input to SEISIM are responses of plant structures and components to seismic events, failure descriptions of structures and components (fragilities), and event-tree/fault-tree system descriptions. SEISIM outputs include probability of radioactive release for a given release category, system failure probabilities, and dominance rankings.

The responses of the components and structures at the plant are generated by a separate computer code which uses earthquake time histories as the

---

*This work was supported by the United States Nuclear Regulatory Commission under a Memorandum of Understanding with the United States Department of Energy.

Related Papers

1. G. E. Cummings and J. E. Wells, "Systems Analysis Methods Used in the Seismic Safety Margins Research Program," Transactions of the 5th International Conference on Structural Mechanics in Reactor Technology, Berlin, Germany, August 1979, Paper K3/2.

2. G. E. Cummings, "An Application of Systems Analysis Techniques to the Study of Reactor Seismic Safety," Nuclear Eng. & Design 59 (1980).

3. G. E. Cummings, J. E. Wells, L. C. Lewis, "Nuclear Reactor Seismic Safety Analysis Techniques," Proceedings of the 4th International System Safety Conference, San Francisco, California, July 1979.

4. J. E. Wells, L. L. George, "SEISIM: Simulation of Seismic Events on Nuclear Power Plants," Proceedings of the 4th Biennual CUBE Symposium, Livermore, California, October 1980.

5. I. B. Wall, M. K. Kaul, R. I. Post, S. W. Tagart, Jr., and T. J. Vinson, "Specification of Computational Approach," Lawrence Livermore National Laboratory, UCRL-13985, NUREG/CR-1702, Prepared by Nuclear Services Corp., February 1979.

6. J. D. Collins, J. M. Hudson, and J. D. Chrostowski, "Specifications of Computational Approach," Lawrence Livermore National Laboratory, UCRL-13986, NUREG/CR-1701, Prepared by J. H. Wiggins Company, February 1979.

7. "SEISIM Code Design Concept," Technical Report 78-1645-2, J. H. Wiggins Company, June 1979.

8. J. H. Hudson, J. D. Gasca, and J. D. Collins, "SEISIM Option I Design Specification (Revision 1)," J. H. Wiggins Company Draft Report 80-1366-1, April 1980.

9. A. A. Garcia and J. E. Kelly, "Event Tree Development and Construction," Science Applications, Inc., SAI-003-79-BE, August 1979.

10. D. C. Bley, C. L. Cate, D. C. Iden, B. J. Garrick, J. M. Hudson, "Event Tree Methodology Development," Pickard, Lowe and Garrick, Inc., PLG-0110, September 1979.

11. P. Moieni, G. Apostolakis, and G. E. Cummings, "Interim Report on Systematic Errors in Nuclear Power Plants," Lawrence Livermore National Laboratory, UCRL-15274, NUREG/CR-1722, September 22, 1980.

12. A. Mosleh and G. Apostolakis, "Some Properties of Distributions Useful in the Study of Rare Events," August 1980, Prepared by the University of California, Los Angeles, California.

forcing function. Soil-structure interaction effects, structure and subsystem responses, and non-seismic loads are accounted for in this calculation. These responses are coupled to fragility functions (cummulative distribution functions of component and structural strengths) to calculate component and structural failure probabilities. These fragility based failure probabilities along with random failure probabilities (human error, test and maintenance outage, etc.) are used to quantify the accident sequence fault trees. These accident sequence probabilities are then used to calcuate the probability of radioactive release for PWR release categories. Uncertainties related to the responses and fragilities are propagated through the computation using analytical methods.

The quantification of the event-trees and fault trees are done conditional on a given seismic event and the conditional probabilities thus calculated unconditioned by integrating the results over the seismic hazard curve. In this way, most of the dependency between event failures resulting from the seismic event itself is removed making fault tree analysis quantification techniques applicable. The outputs from the computation will be used in sensitivity studies to determine the key elements involved in seismic analysis of nuclear power plants. Dominance ranking of accident sequences, component groups, and individual components is also used to aid in determining seismic design adequacy and to identify areas for further study.

Results of this analysis are the most comprehensive in terms of detail in the event-tree/fault tree model and effort put into developing the fragility functions.

SOIL-STRUCTURE INTERACTION
SEISMIC SAFETY MARGINS RESEARCH PROGRAM

Presented By:
Dr. James J. Johnson

Structural Mechanics Associates

For:
Lawrence Livermore National Laboratory

Presented At:
8th Water Reactor Safety Research
Information Meeting
Sponsored By:
U. S. Nuclear Regulatory Commission
Office of Nuclear Regulatory Research
Division of Reactor Safety Research
Gaithersburg, Maryland
October 30, 1980

SUMMARY

The U.S. NRC Seismic Safety Margins Research Program (SSMRP) is developing methods to examine the current seismic analysis and design process of nuclear power plants in a system context. This system analysis approach encompasses the entire Seismic Methodology Chain (SMC), (seismic input, soil-structure interaction, major structure response, and subsystem response), the systematic representation of nuclear power station's reactor system using event/fault tree methodology, a description of the fragility of structures, components, and systems due to seismic loading conditions, and a computational approach which computes the probability of radioactive releases. The systems analysis computational approach was implemented in the computer program SEISIM. One of the input requirements for SEISIM is the local seismic responses corresponding to the fault tree and fragility descriptions. The computer program SMACS was developed to compute these responses. The computer programs SEISIM and SMACS are described separately.

The analysis of each aspect of the SMC is characterized by two items: the analysis should be realistic; and uncertainties should be modeled using probabilistic methods. This discussion presents side studies performed in the soil-structure interaction (SSI) area which support the SMACS and SEISIM analyses.

Side studies serve a number of purposes in support of our systems analysis. The results provide guidance to the calculations by identifying sources of uncertainty which must be considered. In addition, they provide guidance on phenomena not included directly in our SMACS calculations but approximated in SEISIM, e.g., nonlinear behavior. Finally, they provide preliminary information to the U.S. NRC of a licensing nature. Comparative calculations using alternate methodologies (SSI analysis by the direct method as substructure approach, etc.) is an example.

In the SSI area, the following tasks were performed: SSI state-of-the-art review; an investigation of the effects of embedment, non-vertically incident waves, and structure-to-structure interaction for the Zion nuclear power station; comparative SSI analysis of Zion by the substructure approach (CLASSI) and the direct method (FLUSH); and some limited nonlinear SSI analysis.

Our SSI state-of-the-art review task had a number of objectives: to identify and assess the relative importance of the various facets of SSI; to review existing methods and methods under development for performing SSI analyses and to estimate their accuracy; to identify sources of uncertainty in the SSI process; to recommend benchmark analysis and test problems to be used in the verification of SSI analysis procedures; and to recommend procedures for Phase I of the SSMRP. Five individual reports were generated and a summary written. The purpose of the summary was to highlight the salient features of the five reports and act as a pointer to pertinent sections of the five.

Our systems analysis is being demonstrated on the Zion nuclear power station which, hence, becomes the subject of many of our side studies. An assessment of the importance of embedment and the assumption on non-vertically incident seismic waves was completed. The embedment study considered the Zion reactor building as embedded vs. a surface-founded structure. The results showed embedment to be an important consideration in predicting response.

The effect on structural response of the wave propagation mechanism of the earthquake was also investigated. Apparent wave velocities were obtained for the Zion site through source modeling studies performed by the SSMRP Seismic Input Project. Two cases were analyzed: one case corresponding to best estimate apparent wave velocities; the second to a bounding case. The results showed non-vertically incident waves to have a minimum effect on structural response. It is important to note these conclusions are site, structure, and earthquake dependent.

In our systems analysis, it is important to identify and quantify sources of uncertainty in seismic response predictions. SSI analysis techniques are a potential source of significant uncertainty. Two categories of analysis procedures are available to treat SSI: the direct method, which analyzes the soil-structure system in a single step; and the substructure approach, which treats the problem in a series of steps. The Zion nuclear power station was analyzed by the direct method (FLUSH) and the substructure approach (CLASSI). A comparison of the results provides insight into this source of variability.

A limited investigation of nonlinear SSI was performed. Both one-dimensional wave propagation analyses and fully three-dimensional nonlinear SSI were treated. In the former case, a shallow soil layer of thickness similar to Zion but differing in material behavior was considered. The three-dimensional case studied a relatively simple structure similar in characteristics to the Zion reactor building. In both cases, linear and nonlinear response was computed and compared.

REFERENCES

Christian, J. T., J. R. Hall, and E. Kausel, 1980, Soil-Structure Interaction, Lawrence Livermore National Laboratory, Livermore, Calif., UCRL-15230.

Isenberg, J., D. K. Vaughan, G. L. Wojcik, F. S. Wong, and J. P. Wright, 1980, A Review of Structure-Medium Interaction Analysis Methods with Applications to SSMRP, Lawrence Livermore National Laboratory, Livermore, Calif., UCRL-15255.

Johnson, J. J., Soil-Structure Interaction: The Status of Current Analysis Methods and Research, Lawrence Livermore National Laboratory, Livermore, Calif., NUREG/CR-1780, (UCRL-53011).

Luco, J. E., 1980, Linear Soil-Structure Interaction, Lawrence Livermore National Laboratory, Livermore, Calif., UCRL-15272.

Roesset, J. M., 1980, A Review of Soil-Structure Interaction, Lawrence Livermore National Laboratory, Livermore, Calif., UCRL-15262.

Seed, H. B., and J. Lysmer, 1980, The Seismic Soil-Structure Interaction Problem for Nuclear Facilities, Lawrence Livermore National Laboratory, Livermore, Calif., UCRL-15254.

Wong, H. L. and J. E. Luco, Identification of Sensitive Parameters for Soil-Structure Interaction, in review.

[illegible]

[illegible]

[illegible]

[illegible]

[illegible]

[illegible]

[illegible]

MAJOR STRUCTURAL RESPONSE
SEISMIC SAFETY MARGINS RESEARCH PROGRAM

Presented By:
Dr. James J. Johnson

Structural Mechanics Associates

For:
Lawrence Livermore National Laboratory

Presented At:
8th Water Reactor Safety Research
Information Meeting
Sponsored By:
U. S. Nuclear Regulatory Commission
Office of Nuclear Regulatory Research
Division of Reactor Safety Research
Gaithersburg, Maryland
October 30, 1980

SUMMARY

The U.S. NRC Seismic Safety Margins Research Program (SSMRP) is developing methods to examine the current seismic analysis and design process of nuclear power plants in a system context. This system analysis approach encompasses the entire Seismic Methodology Chain (SMC), (seismic input, soil-structure interaction, major structure response, and subsystem response), the systematic representation of nuclear power station's reactor system using event/fault tree methodology, a description of the fragility of structures, components, and systems due to seismic loading conditions, and a computational approach which computes the probability of radioactive releases. The systems analysis computational approach was implemented in the computer program SEISIM. One of the input requirements for SEISIM is the local seismic responses corresponding to the fault tree and fragility descriptions. The computer program SMACS was developed to compute these responses. The computer programs SEISIM and SMACS are described separately.

The analysis of each aspect of the SMC is characterized by two items: the analysis should be realistic; and uncertainties should be modeled using probabilistic methods. This discussion presents side studies performed in the major structure response area which support the SMACS and SEISIM analyses.

Side studies serve a number of purposes in support of our systems analysis. The results provide guidance to the calculations by identifying sources of uncertainty which must be considered. In addition, they provide guidance on phenomena not included directly in our SMACS calculations but

approximated in SEISIM, e.g., nonlinear behavior. Finally, they provide preliminary information to the U.S. NRC of a licensing nature. The comparison of alternative modeling idealizations for typical nuclear power plant structures is an example.

In the major structure response area, several side studies were performed: structural building response review; sensitivity studies to investigate eigensystem and damping effects on structural response; and a comparative study of several model idealizations for complex nuclear power plant structures.

Our review of the state-of-the-art had several objectives: to review techniques for modeling of structures and dynamic response determination; to identify sources of uncertainty; and to recommend appropriate techniques of modeling structures for Phase I of the SSMRP. Sargent and Lundy and Ebasco Services, Inc., performed this task producing two reports addressing these issues. Their results identified a number of sources of uncertainty, e.g., material behavior characterization, modeling techniques, and nonlinear behavior of structures. In addition, our review task indicated an appropriate mechanism to incorporate uncertainties into our SMACS calculations was shifts in frequencies and damping.

An investigation of the dynamic characteristics of structures and their representation by their eigensystem (mode shapes and frequencies) was completed. The result being a methodology which may be applied to the evaluation of structural models and the parameters to fit these models from tests. The effort concentrated on an eigensystem representation. The proposed methodology had several levels of sophistication to meet the requirements and available data. We anticipate its application in a later stage of the SSMRP.

A study of the sensitivity of structural response to variations in structural damping was made. Time history analyses of the Zion auxiliary-turbine-building were performed for the structure fixed at its base and excited by a series of recorded earthquake motions. Statistics of in-structure response, such as forces and response spectra, were computed and evaluated. Representative results are presented.

Our state-of-the-art review identified major uncertainty associated with structural modeling. Describing structural behavior at the point level, structural element level (beam, wall, slab, etc.), and as an overall structure is subject to uncertainty. In addition, the translation of engineering drawings into a mathematical model is subject to the judgment of the analyst. In terms of a linear model, the mass, stiffness, and damping characteristics are affected. This variability leads to a non-unique description of the structure's dynamic behavior. We sought to quantify the variability due to model idealizations by performing a modeling sensitivity study. Results of this study are presented.

A typical nuclear power plant building was the subject of the investigation. The heavy, shear-wall structure was constructed of reinforced concrete. In plan view, it was T-shaped with one assumed plane of symmetry which leads to uncoupled horizontal response along the plane of symmetry and coupled horizontal and torsional response in the perpendicular plane. We applied four modeling idealizations to the subject structure--a detailed finite element model, a detailed finite element model with mass lumping to reduce the number of dynamic degrees of freedom, a detailed finite element model with the constraint of rigid floors, and an equivalent beam model.

The models were evaluated according to two criteria: the dynamic characteristics of the models were compared directly, i.e., modal characteristics, and the dynamic response of the models were compared. In the first case, frequencies of comparable modes were compared. In the second case, multiple time history analyses were performed using recorded earthquakes as excitation. In-structure response, in the form of peak values and response spectra, and their statistics were computed and compared. Soil-structure interaction was not included in the calculations.

REFERENCES

Bumpus, S. E., J. J. Johnson, and P. D. Smith, Best Estimate Method vs. Evaluation Method: A Comparison of Two Techniques in Evaluating Seismic Analysis and Design, Lawrence Livermore National Laboratory, NUREG/CR-1489, UCRL-52746, May 1980.

Hasselman, T. K. and S. S. Simonian, Structural Uncertainty in Seismic Risk Analysis, Lawrence Livermore National Laboratory, NUREG/CR-1560, UCRL-15218, March 1980.

Healey, J. J., S. T. Wu, and M. Murga, Structural Building Response Review, Lawrence Livermore National Laboratory, NUREG/CR-1423, Vol. I, UCRL-15185, February 1980.

Singh, A. K., T. I. Hsu, and T. P. Khatua, Structural Building Response Review, Lawrence Livermore National Laboratory, NUREG/CR-1423, Vol. II, UCRL-15183, January 1980.

Wesley, D. A., P. S. Hashimoto, and R. B. Narver, Variability of Dynamic Characteristics of Nuclear Power Plant Structures, Lawrence Livermore National Laboratory, NUREG/CR-1661, UCRL-15267, June 1980.

Wesley, D. A., P. S. Hashimoto, Preliminary Evaluation of Nonlinear Seismic Response Effects for Nuclear Power Plant Shear Wall Structures, Lawrence Livermore National Laboratory, in review.

SUBSYSTEM RESPONSE
SEISMIC SAFETY MARGINS RESEARCH PROGRAM

Presented By:
Dr. Tien-Yuh Chuang

Lawrence Livermore National Laboratory

Presented At:
8th Water Reactor Safety Research
Information Meeting
Sponsored By:
U. S. Nuclear Regulatory Commission
Office of Nuclear Regulatory Research
Division of Reactor Safety Research
Gaithersburg, Maryland
October 30, 1980

SUMMARY

In order to evaluate the conservatisms in the seismic design of nuclear power plants, a probabilistic approach is employed by the Seismic Safety Margins Research Program (SSMRP). The system model of SSMRP consists of a series of functions representing the various stages in seismic analysis process, i.e., seismic input, soil structure interaction, major structural response, subsystem response, fragility of structures and components, and the event/fault tree chain leading to core melt. The subsystem denotes those components and systems whose behavior during a seismic event may be determined decoupled from the major structural response.

A review of the state-of-the-art of seismic qualification methods of subsystem has been performed by two subcontractors - EDAC and NSC/Quadrex. This task assesses the accuracy of seismic analysis techniques to predict dynamic response, and also identifies and quantifies sources of random and modeling uncertainty in subsystem response determination. Reports from both subcontractors are listed in the reference.

Eight safety related systems are identified for the subsystem response analysis. The function of these systems are briefly described. For SSMRP Phase I, the dynamic models of the following systems are created: the auxiliary feedwater system (AFW), portion of service water system provided backup water supply for AFW system, residual heat removal (RHR) system, portion of safety injection system connected to RHR system and reactor coolant system.

Multiple input time history method is used to determine the seismic response of piping systems. Pseudostatic mode method will be used for SSMRP, since it is a better method than either absolute displacement method or datum acceleration and relative displacement method.

A SMACS sensitivity study has been initiated. Its objective is to determine which areas of the seismic methodology chain (SMC), i.e., seismic input, soil structure interaction, major structural response and subsystem response, contribute most to the uncertainty in the subsystem response. Key parameters are identified in each area of SMC. Statistical experiments will be performed. Statistical results, i.e., mean, variance and coefficient of variation, will be used to rank the contribution to the subsystem response due to SMC.

Finally, three major tasks are identified for the SSMRP Phase II, i.e., construct dynamic models for the safety systems not included in Phase I, perform sensitivity study of subsystem utilizing SEISIM and study the effect of piping systems due to support failure.

References:

1. Subsystem Response Review, NUREG/CR-1700, UCRL-15215, March 1979, J. Fogelquist et al., Nuclear Service Corporation/Quadrex.

2. Subsystem Response Review, NUREG/CR-1706, UCRL-15215, March 1979, K. P. Kennedy, et al., Engineering Decision Analysis Company, Inc.

FRAGILITIES DEVELOPMENT
SEISMIC SAFETY MARGINS RESEARCH PROGRAM

Presented By:
Dr. M. P. Bohn

Lawrence Livermore National Laboratory

Presented At:
8th Water Reactor Safety Research
Information Meeting
Sponsored By:
U. S. Nuclear Regulatory Commission
Office of Nuclear Regulatory Research
Division of Reactor Safety Research
Gaithersburg, Maryland
October 30, 1980

Summary

The Seismic Safety Margins Research program (SSMRP) is an NRC-funded multi-year program directed towards estimating the conservatism in the Standard Review Plan seismic safety requirements with the ultimate goal of developing improved seismic requirements. As part of this program, calculations of the seismic risk from a typical commercial nuclear reactor are being made. These calculations require a knowledge of the conditional probability of failure (fragility) of safety related components in the reactor system which actively participate in the hypothesized accident scenarios.

Component failure is defined as either loss of pressure boundary integrity or loss of operability. Failure (fragility) is characterized by a cumulative distribution function which describes the probability that the failure has occurred given a value of loading. In the context of the SSMRP, loading may be spectral acceleration, zero period acceleration or internal force resultant such as moment or shear, depending on the component and failure mode under consideration, but contrary to other similar studies, fragility is not related directly to the seismic hazard characterization, for example, free-field peak acceleration.

The first phase of the determination of the necessary fragility functions has been completed. As a first step, all the components identified in the reactor fault tree analyses have been grouped into 48 generic categories, and fragility functions have been determined for each category. For example, all motor operated valves located on piping with diameters

between 2-1/2 and 8 inches are placed into a single generic category, and similarly, all motor control centers have been placed into another generic category. All piping, tees, elbows, butt welds, and reducer sections have been placed into one generic category, and scaling factors (dependent on size, material and temperature) are utilized to relate the individual piping components to a single master fragility curve.

Fragility functions for the 48 generic categories have been developed, based on a combination of design analysis reports, experimental data and an extensive expert opinion survey. In this survey, questionnaires were sent to over 250 recognized specialists in the nuclear industry (representing nuclear power system vendors, utilities, testing laboratories, nuclear component manufacturers, architect-engineers, and consultants) which resulted in 147 detailed responses covering (to varying degrees) virtually all the 48 generic catergories. The responses to the questionnaires identified various failure modes as well as the percentile failure rates as a function of loading. The statistical methods used to combine multiple respondent data and to combine failure data for multiple failure modes are outlined.

The experimental data utilized in developing fragility curves were obtained from the results of component manufacturers qualification tests, independent testing lab failure data and data obtained from the U.S. Corps of Engineers SAFEGUARDS Subsystem Hardness Assurance Program.

Finally, ongoing work (namely Phase II of the SSMRP) aimed at improving and further benchmarking the preliminary fragility functions obtained to date is described.

FRAGILITIES DEVELOPMENT
SEISMIC SAFETY MARGINS RESEARCH PROGRAM

Presented by:

Dr. M.P. Bohn

Lawrence Livermore National Laboratory

Presented at:

8th Water Reactor Safety Research
Information Meeting

Sponsored by:

U.S. Nuclear Regulatory Commission
Office of Nuclear Regulatory Research
Division of Reactor Safety Research

Gaithersburg, Maryland

October 30, 1980

FRAGILITIES WITHIN THE SSMRP

- SSMRP will compute probability of plant failure and probability of radioactive release due to earthquakes
- Methodology uses Event Trees and Fault Trees to relate failure of basic components (pipes, electrical equipment, buildings, etc.) to plant failure
- To date, over 7000 basic events are being considered in Fault Trees
- Probabilistic failure criteria (fragilities) required for each basic event

TYPICAL FRAGILITY CURVE

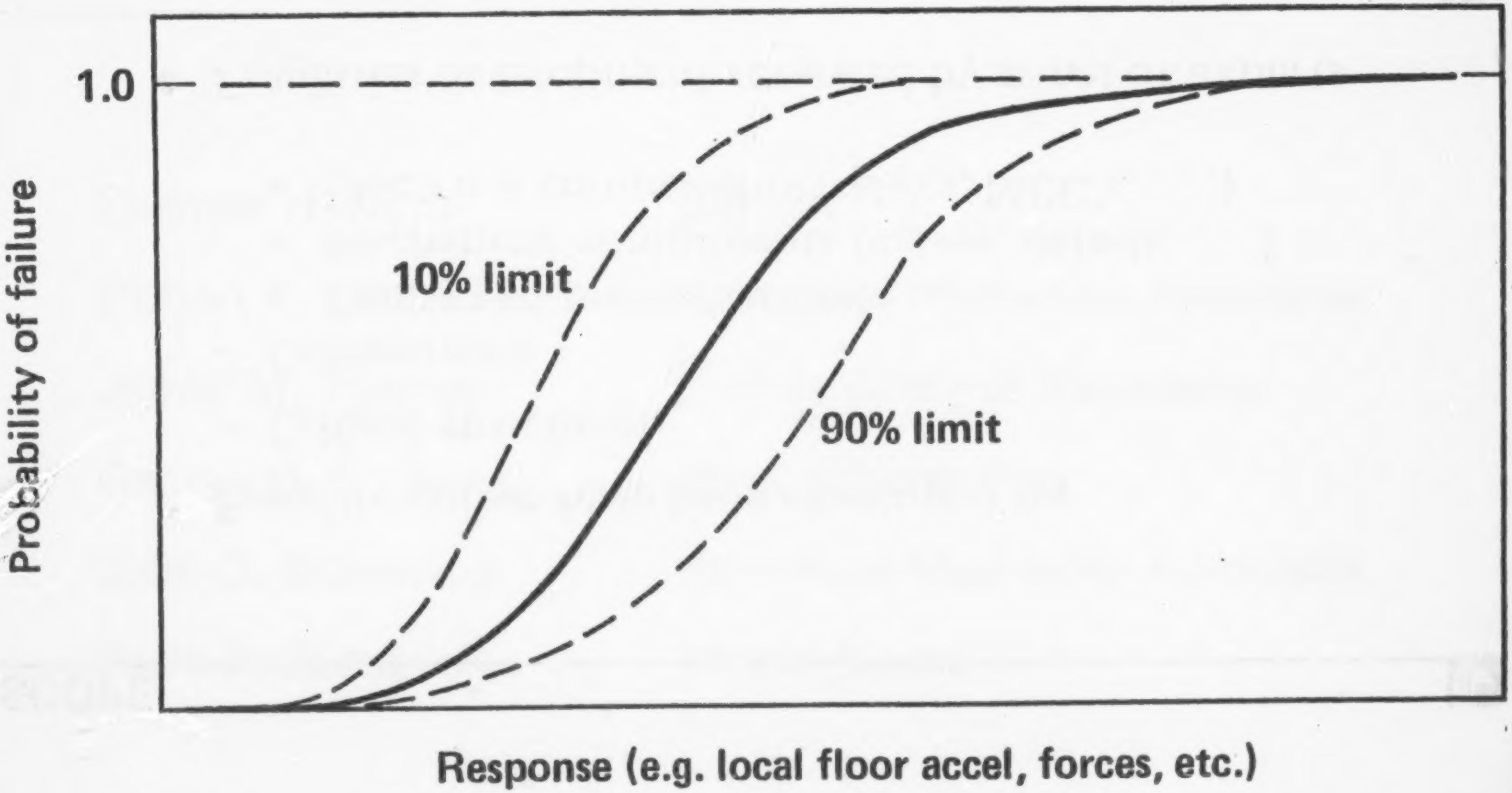

SCOPE

- Fragility curves have been developed for
  - – Critical structures
  - – Components
    - Piping and pressure vessels
    - Mechanical components (valves, deisels, . . .)
    - Electrical components (relays, MCC's, . . .)
- Fragilities development reviewed by panel of experts

THE SSMRP FRAGILITIES PANEL CONSISTED OF HIGHLY EXPERIENCED MEMBERS

Spencer H. Bush	Battelle
Robert P. Kennedy	Structural Mechanics Associates
Jerrell M. Thomas	Failure Analysis Associates
George D. Shipway	Wyle Laboratories
John D. Stevenson	Structural Mechanics Associates
Peter P. Zemanick	Westinghouse

BUILDING FRAGILITIES DEVELOPED FOR:

- Reactor building
- Turbine/auxiliary building
- Crib house
- Storage tanks
- Buried piping

BUILDING FRAGILITIES DEVELOPMENT PROCEDURE

- Used Newmark's procedure which assumes log-normal capacity (fragility) relation

- Acceleration at failure taken as

  $$A_F = FS \cdot A_D$$

  where A_D ~ acceleration used in original design

  FS ~ estimate of factor of safety in original design (assumed log-normal)

- Acceleration at failure thus has the form

  $$A_F = \check{A}_F \, \epsilon_R \, \epsilon_U$$

FACTORS OF SAFETY

$$FS = F_{strength} * F_{\mu} * F_{response}$$

where

$F_{strength}$ = ratio of actual strength to design forces

F_{μ} = factor relating actual capacity with energy absorption to equivalent elastic ultimate strength used in design

$F_{response}$ = factors accounting for conservatisms in original design analysis

RESPONSE FACTOR ACCOUNTS FOR

- Spectral shape
- Damping
- Modelling accuracy
- Combination of modes
- Combination of earthquake components
- Input reduction with depth
- Soil structure interaction

Only required if no new structural analysis is performed

BUILDING FAILURE DEFINITION

- Failure is taken to be when inelastic deformation of structure are estimated to interfere with operation of safety related equipment

- This does not imply collapse. For most cases examined, considerably greater margins of safety for collapse are believed to exist.

best copy available

FRAGILITY DESCRIPTION

Auxiliary Building Roof Diaphragm

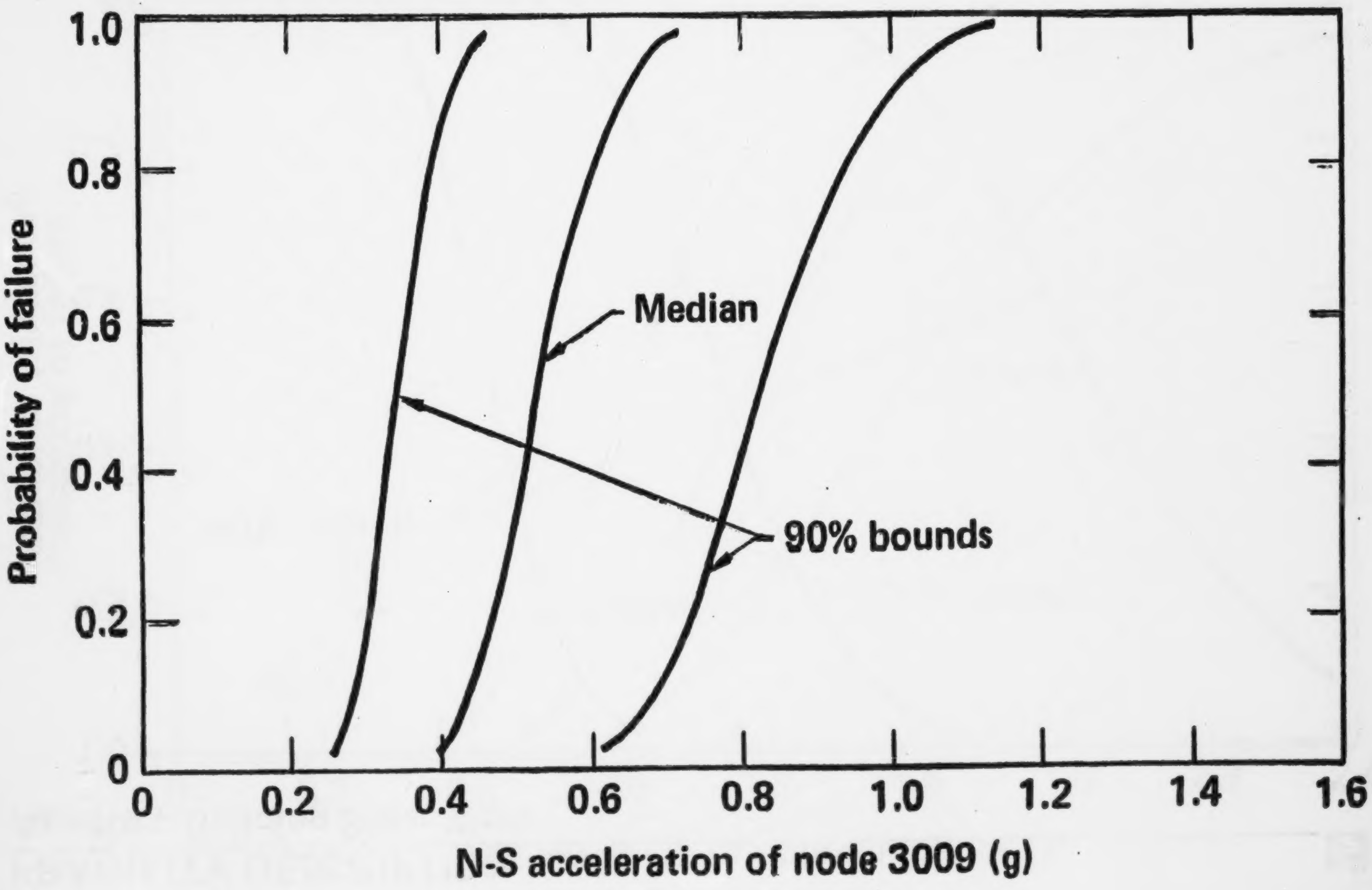

FRAGILITY DESCRIPTION

Auxiliary Building Shear Walls

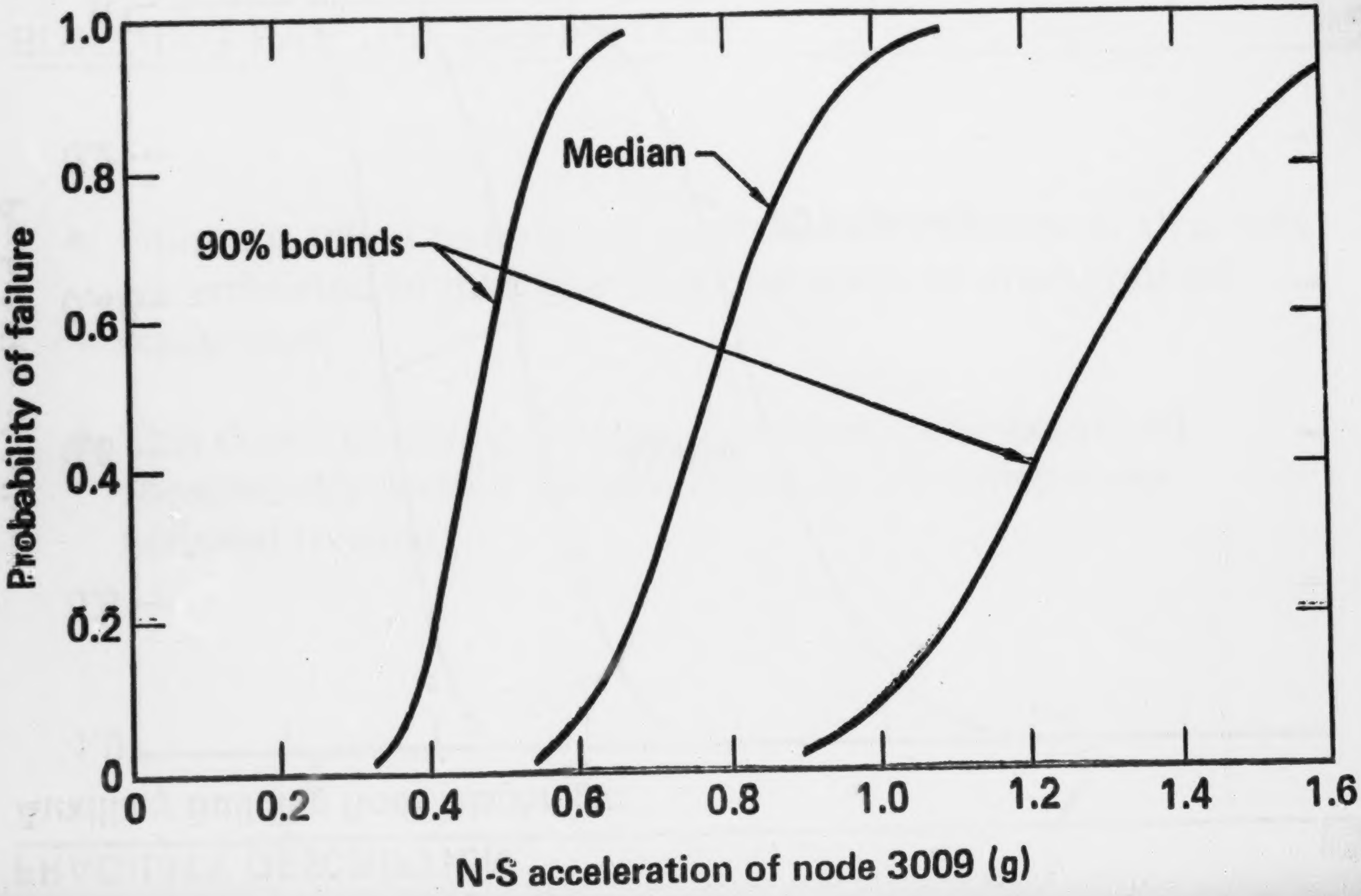

FRAGILITY DESCRIPTION

Reactor Building Pressurizer Enclosure

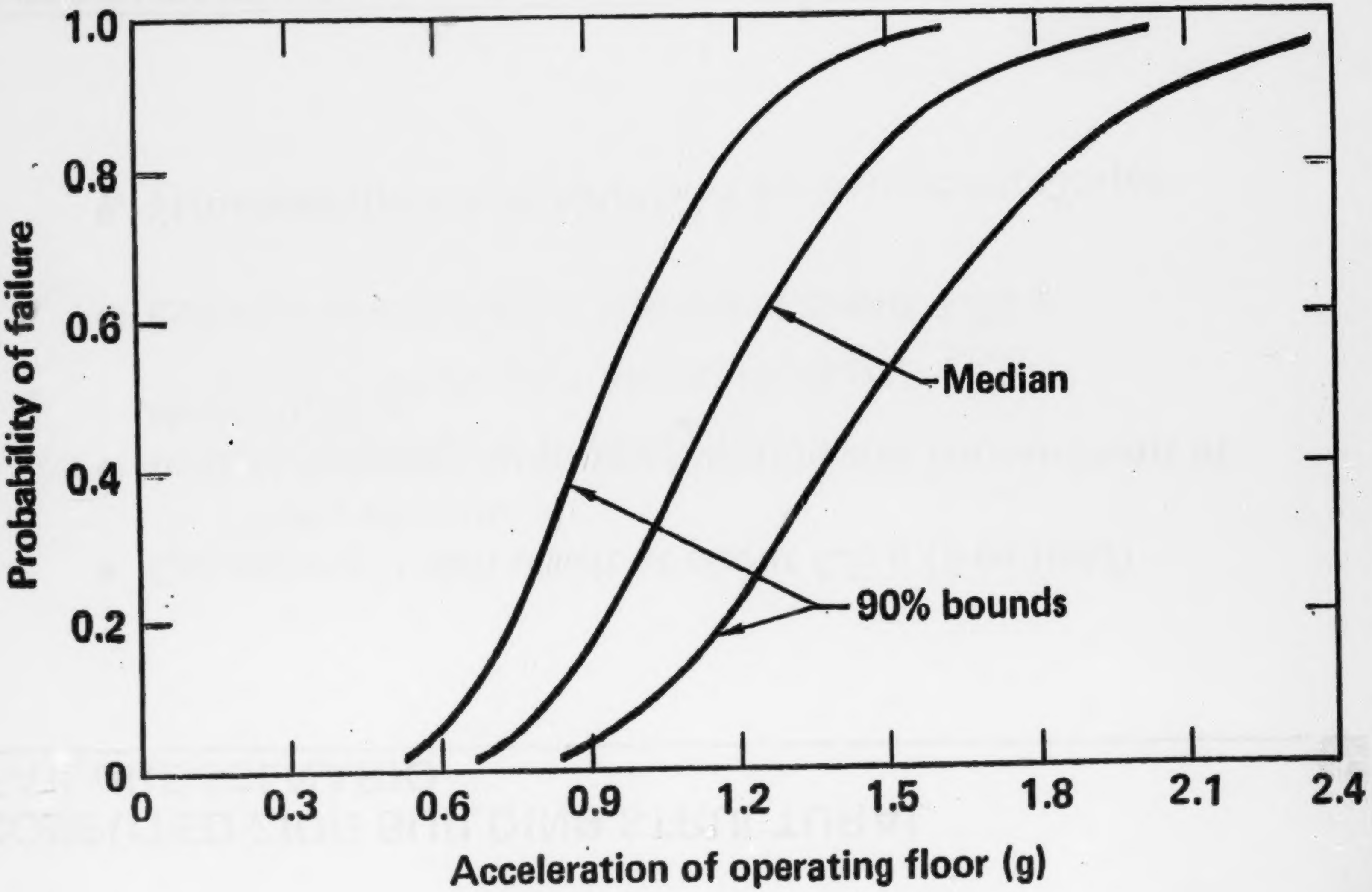

COMPUTED ZION BUILDING STRUCTURAL FAILURE SCENARIO

- Containment slab uplift at about 0.5 g (free field)
- Impact between auxiliary building and containment at about 0.75 g
- Damage to pressurizer closure at about 1.25 g
- Structural failure at about 2.5 g

MECHANICAL/ELECTRICAL COMPONENT FRAGILITIES

- Grouped all components into 48 generic categories
- Data obtained from 3 sources
  - ZION specific data/design reports
  - SAFEGUARDS program data
  - Expert opinion

GENERIC CATEGORIES FOR COMPONENTS

- Reactor core assembly
- Reactor coolant system vessels
  - RPV
  - Pressurizer
  - Steam generator
- Primary coolant piping
- Large diameter piping
- Intermediate piping
- Small pipes
- Large vertical storage vessels with formed heads

Mechanical

- Large vertical storage tank — flat bottom
- Large horizontal vessel — diesel fuel oil tank
- Small-medium vessels and heat exchangers
- Buried pipe
- Reactor coolant pump
- Large vertical centrifugal pumps with motor drive
- Large vertical pumps
- Motor driven compressors
- LMOV's (Large motor operated valves)
- Large relief and check valves
- Small valves

GENERIC CATEGORIES FOR COMPONENTS (Cont)

Electrical

- Horizontal motors
- Generators
- Battery racks
- Switchgear
- Dry transformers
- Control panels and racks
- Auxiliary relay cabinets
- Breaker panels
- Local instruments
- Motor control centers
- Computers
- Light fixtures
- Communications equipment
- Invertors
- Cable trays
- Circuit breakers
- Relays
- Ceramic insulators

GENERIC CATEGORIES FOR COMPONENTS (Cont)

Miscellaneous

- Air handling units
- Chemical and biological filters
- Instrument racks
- Duct work
- Hydraulic snubbers
- Generator accessories
- Gas turbine generators
- Water purification units
- Water chillers
- Dampers, diffusers, extractors
- Recombiners (hydrogen)
- Storage racks (fuel storage)

ZION SPECIFIC DATA/DESIGN REPORTS

- Design reports/qualification data provided by Comm Edison and Westinghouse Corporation for 18 specific components
- Used same capacity evaluation approach (Newmark) as used for building fragilities
- Obtained both "best-estimate" fragility curves and "confidence bounds" based on modeling uncertainty
- Results to be combined with expert opinion survey results

FRAGILITY DESCRIPTION

Cable Trays

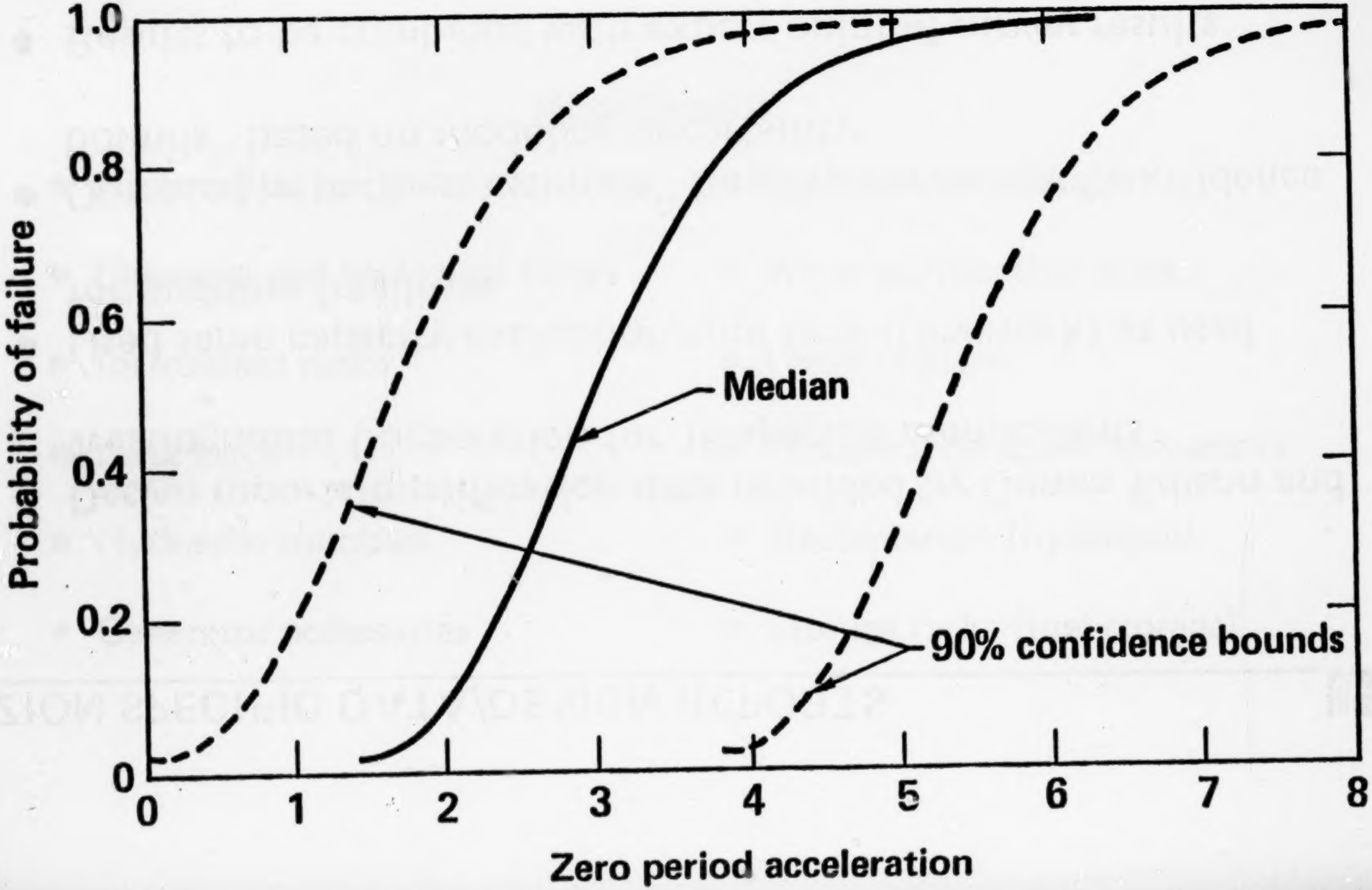

FRAGILITY DESCRIPTION

Steam generator supports

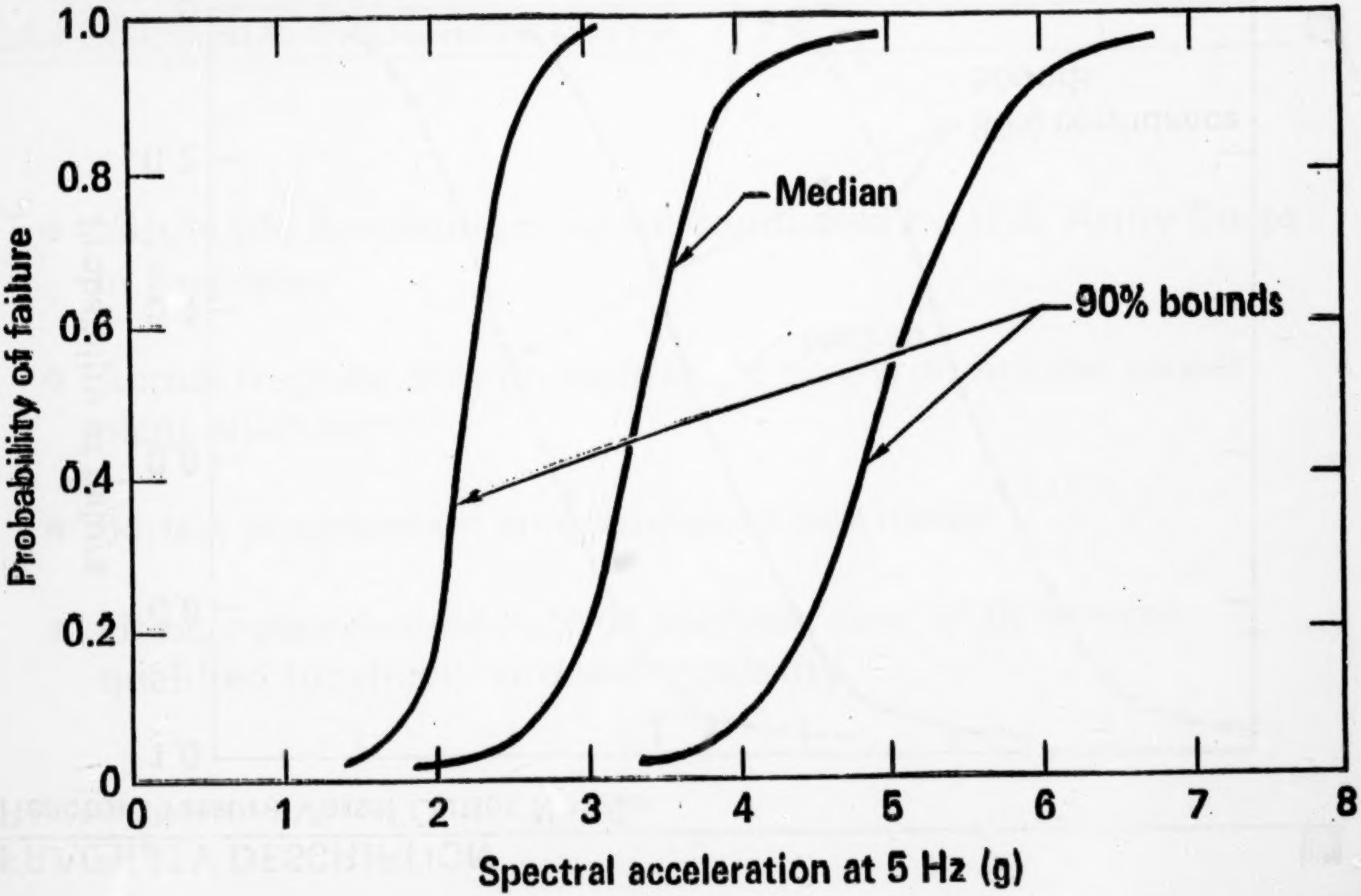

FRAGILITY DESCRIPTION

Reactor Pressure Vessel Outlet Nozzle

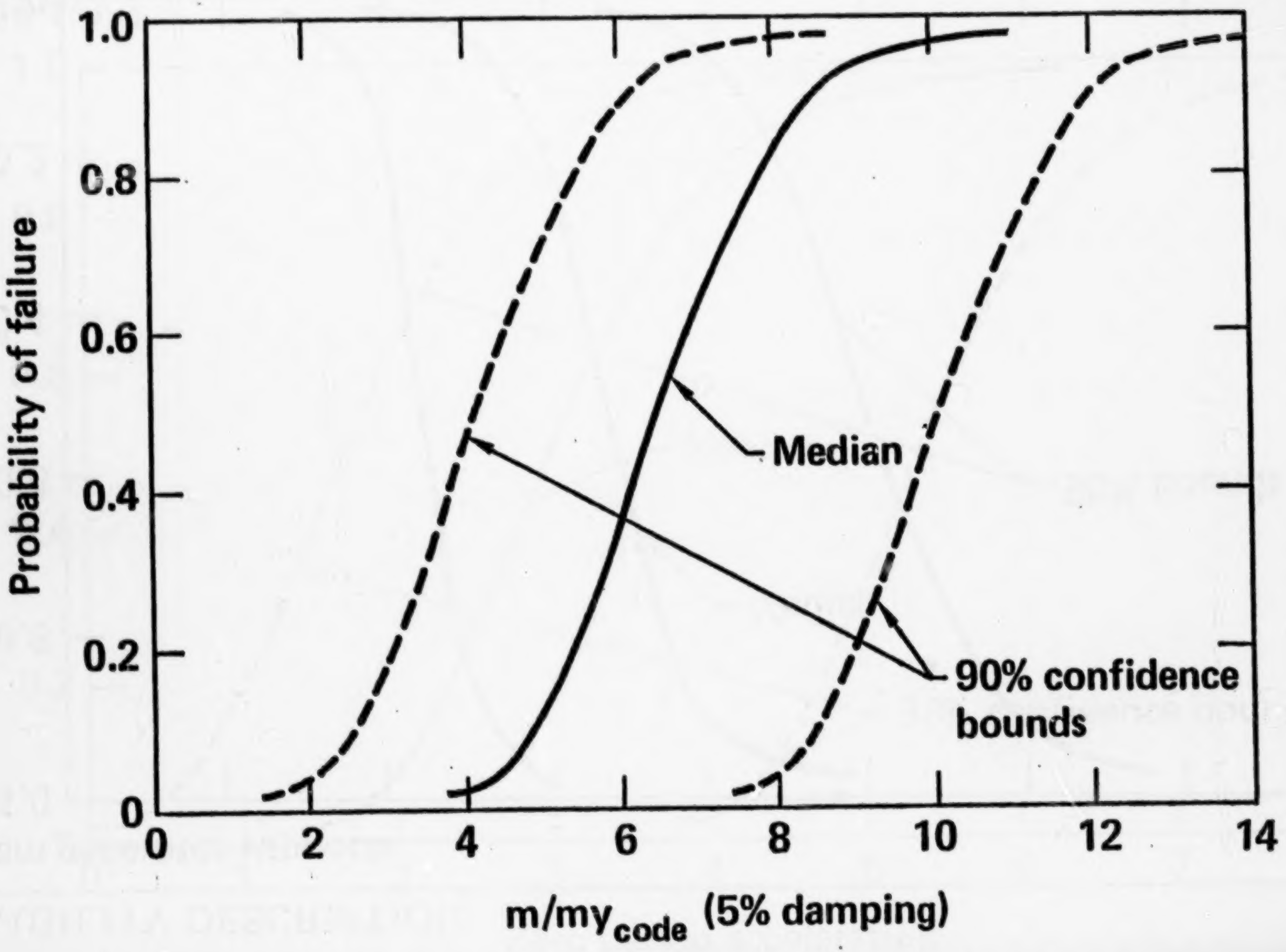

SAFEGUARDS PROGRAM DATA

- Missile site hardening program conducted by U.S. Army Corps of Engineers
- Actual fragility data on equipment similar to nuclear power plant equipment
- 64 test programs on approximately 300 items
- Using a pseudo-probabilistic method, over 18,000 items qualified for shock hardness capability

SAFEGUARDS TESTING

- All equipment monitored for function during testing
- An undamped shock spectra was specified
- Complex waveform shock tests of 2–5 seconds duration
- Very little upgrading required for qualification

PHASE 1 EXPERT OPINION SURVEY

- 400 experts identified
- 250 agreed to participate
- 150 completed questionnaires returned
- All but 4 generic categories received at least one response

QUESTIONNAIRE FOR EXPERT OPINION SURVEY

- Considered one generic equipment category
- Asked for
  - Most important failure modes
  - Appropriate response quantity for each mode
  - 10%, 50%, 90% failure probability values in each mode
  - Source of information (data, analysis, opinion)

TYPICAL RESPONSE – ONE GENERIC CATEGORY – ONE MODE

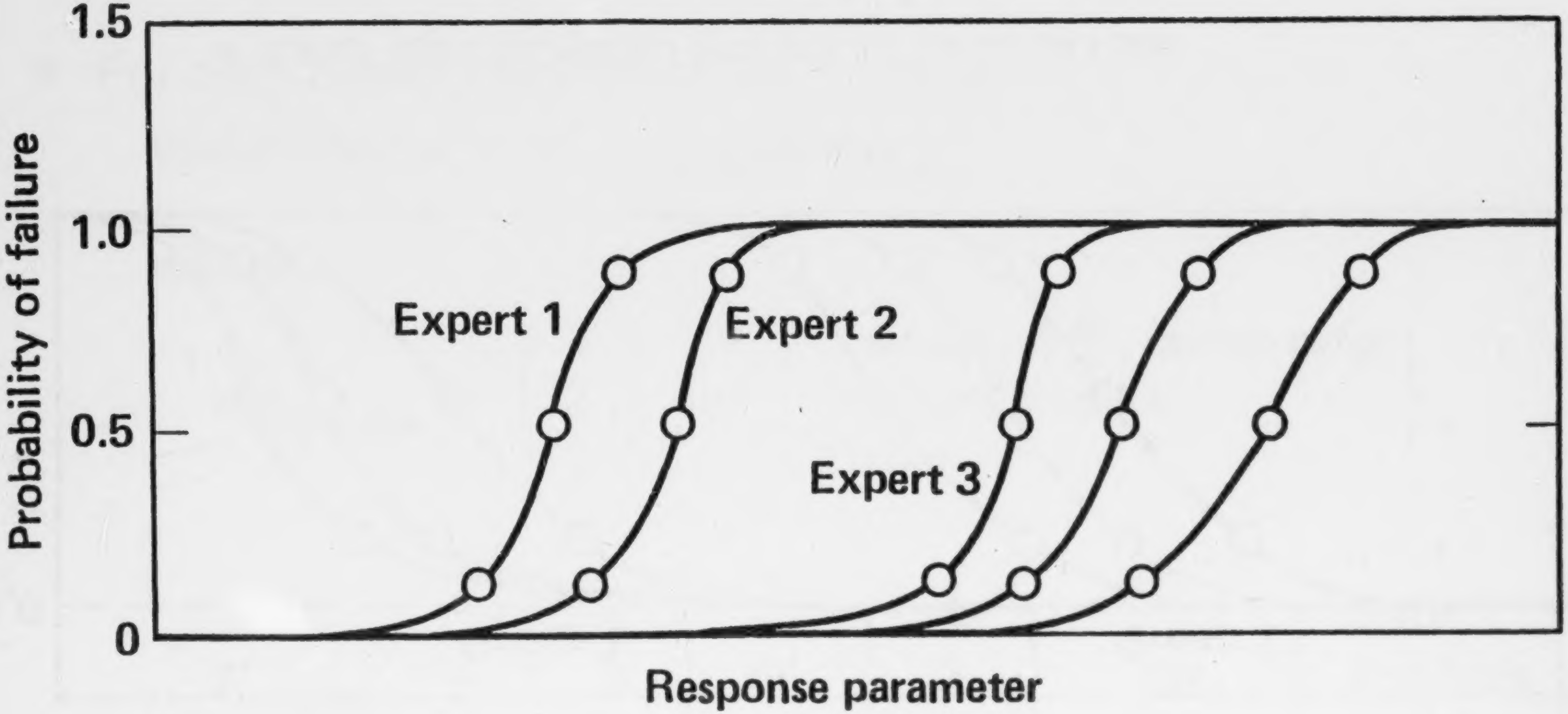

COMBINATION OF EXPERT OPINION DATA INTO A SINGLE FRAGILITY CURVE (FOR EACH MODE)

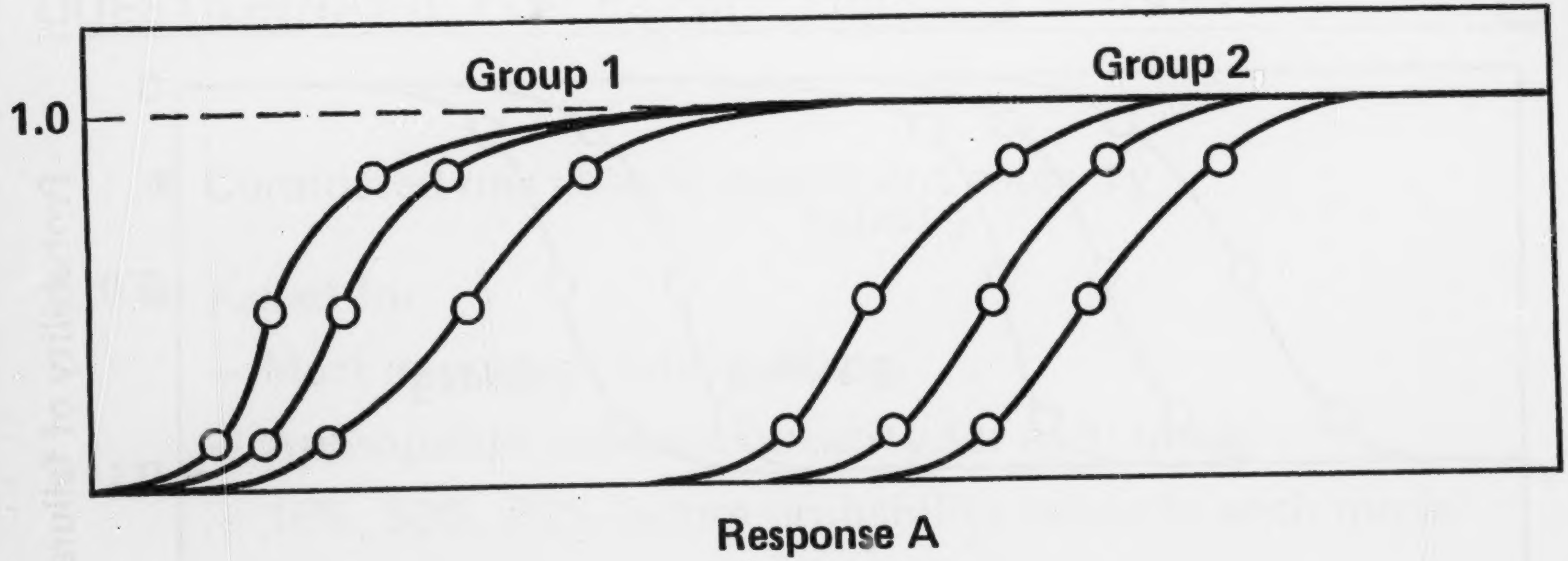

- Least squares/nested analysis of variance used
- Model

$$A_{ijq} = A_q + T_j + \epsilon_{ijq}, \quad \begin{cases} i = \text{expert} \\ j = \text{group} \\ q = \text{fractile level} \end{cases}$$

- Variance = $\hat{\sigma}^2 + \hat{\sigma}_T^2 + \hat{\sigma}_\epsilon^2$

WEIGHTING OF EXPERT OPINION

- A weighted least squares procedure used
- For each expert, multiplicative factor is

  $$\text{Weight factor} = W_{\text{expertise}} \cdot W_{\text{source}}$$

  where

  $$W_{\text{expertise}} = \left\{ \begin{matrix} 3 \\ 2 \\ 1 \end{matrix} \right\} \text{ for } \left\{ \begin{matrix} \text{Vendor, A/E, comp mfgr} \\ \text{Military expert} \\ \text{Other} \end{matrix} \right\}$$

  $$W_{\text{source}} = \underset{\text{Pressure}}{\left\{ \begin{matrix} 4 \\ 3 \\ 1 \end{matrix} \right\}} \text{ or } \underset{\text{Functional}}{\left\{ \begin{matrix} 4 \\ 2 \\ 1 \end{matrix} \right\}} \text{ for } \left\{ \begin{matrix} \text{Data} \\ \text{Analysis} \\ \text{Opinion} \end{matrix} \right\}$$

COMBINING MODES INTO SINGLE FRAGILITY CURVE FOR EACH COMPONENT

- Given fragility curve for each of several failure modes, a single fragility curve is derived such that probability of failure is the union of probabilities of failure of individual modes

- For single mode, $P_F = \int_0^\infty F_S(r)\ f_R(r)\ dr$

- For multiple modes,

$$P_F = \int_0^\infty \underbrace{\left\{1 - \left[1 - F_S^{(1)}\right] \left[1 - F_S^{(2)}\right] \left[\cdots\right]\right\}}_{\text{Effective fragility curve}} f_R(r)\ dr$$

LMOV MODE 3 ELECTRICAL FAILURE

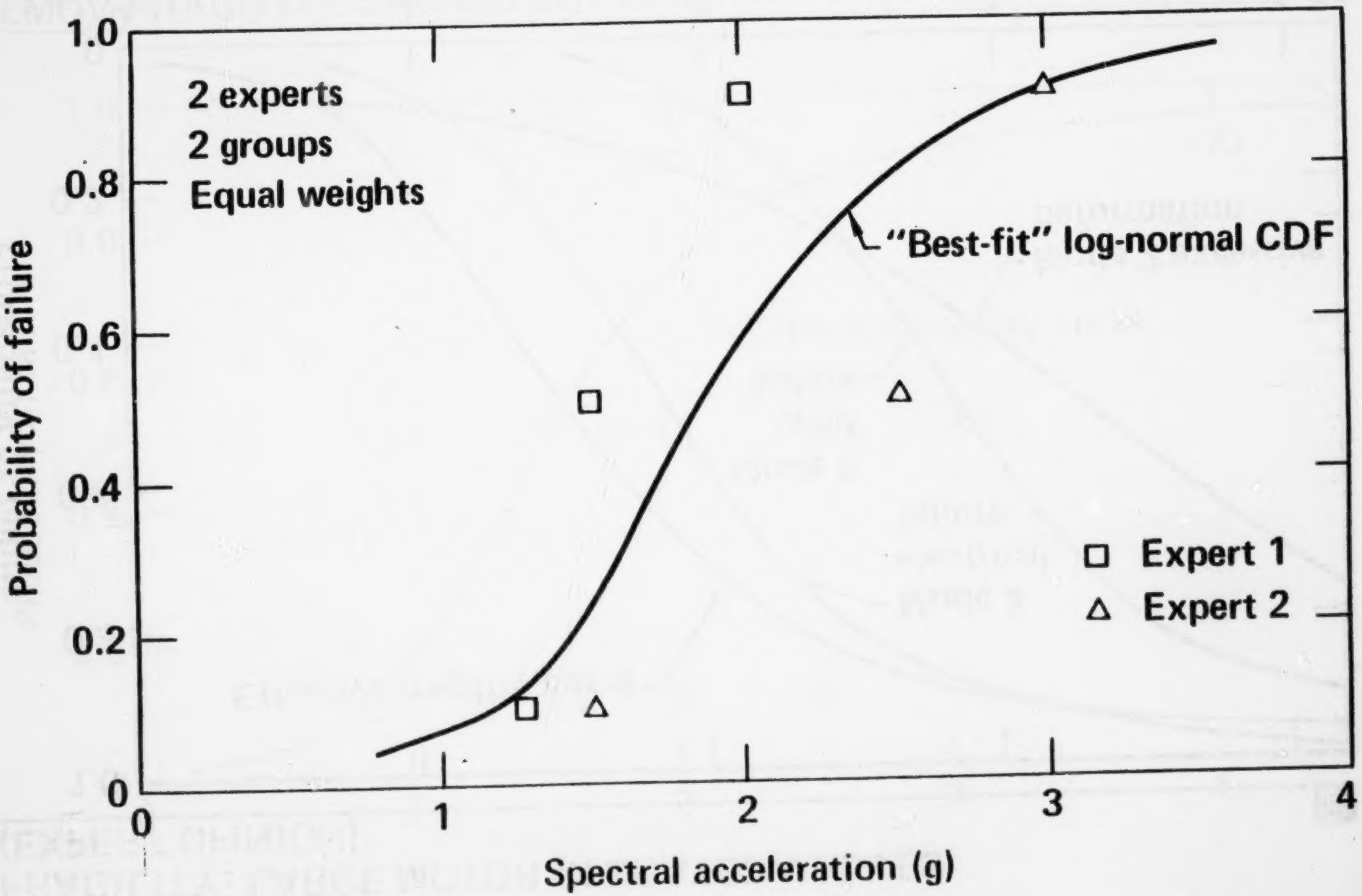

FRAGILITY: LARGE MOTOR OPERATED VALVES (EXPERT OPINION)

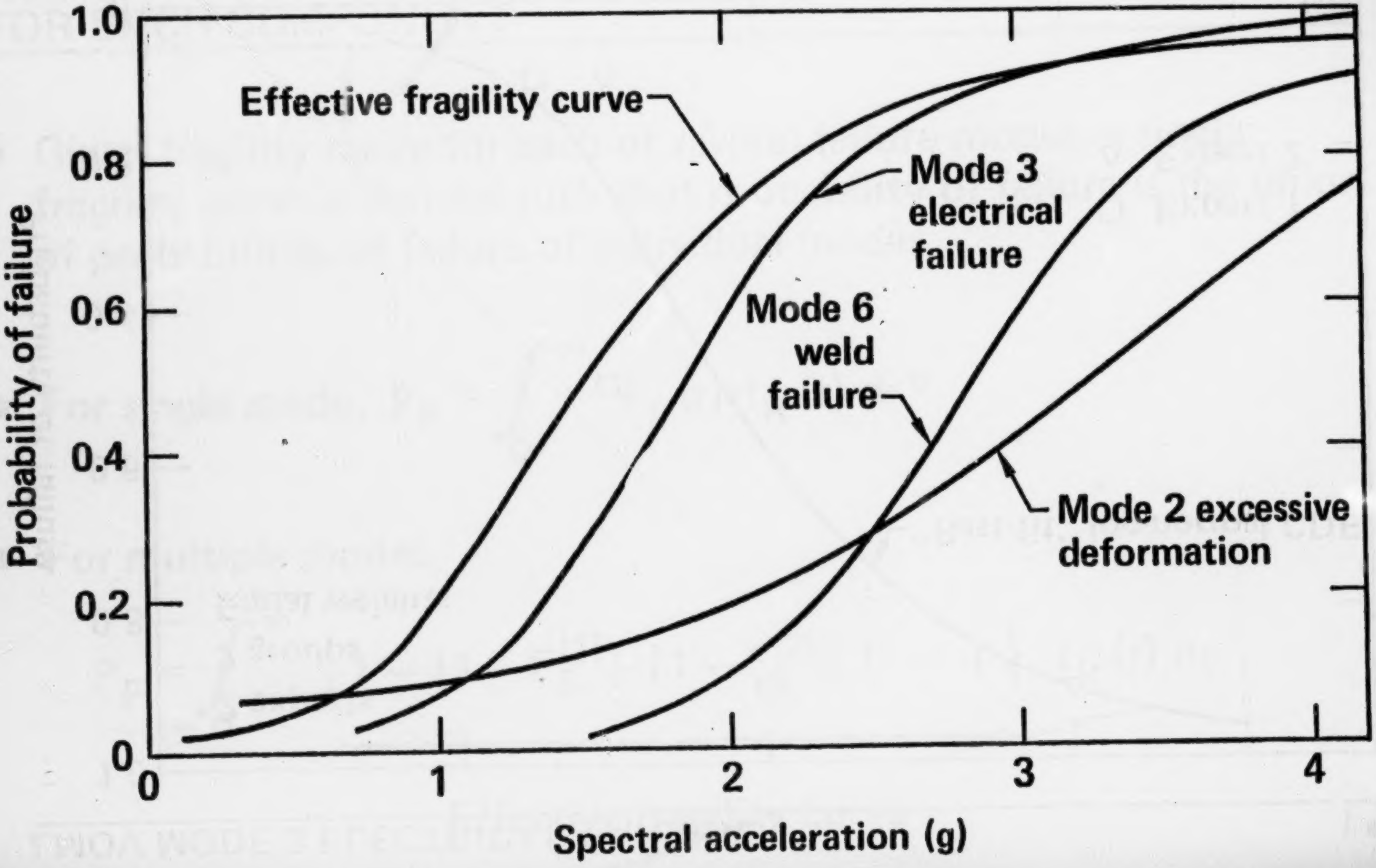

LMOV FRAGILITY AND EXPERT OPINION DATA BASE

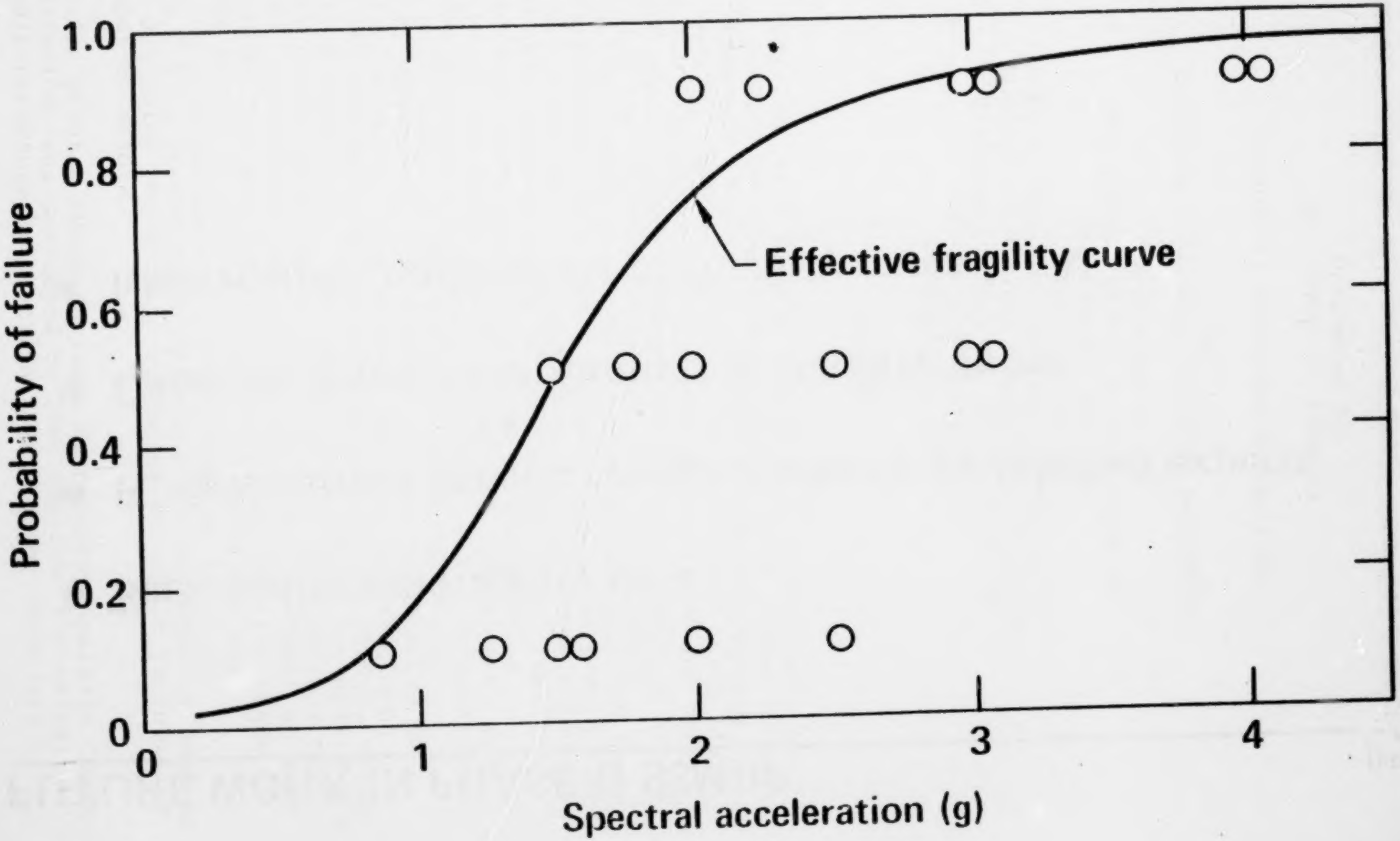

FUTURE WORK IN PHASE II SSMRP

- Seek additional fragility data
- Review current generic category scheme by selected experts
- Generate upper/lower bounds to fragility curves
- Issue revised, updated set of fragility curves

SMACS
SEISMIC METHODOLOGY ANALYSIS CHAIN WITH STATISTICS

Presented By:
Dr. James J. Johnson

Structural Mechanics Associates

For:
Lawrence Livermore National Laboratory

Presented At:
8th Water Reactor Safety Research
Information Meeting
Sponsored By:
U. S. Nuclear Regulatory Commission
Office of Nuclear Regulatory Research
Division of Reactor Safety Research
Gaithersburg, Maryland
October 30, 1980

SUMMARY

A methodology that will examine the current seismic analysis and design process of nuclear power plants in a system context is being developed in the U.S. NRC Seismic Safety Margins Research Program (SSMRP). Clearly, examining the total plant including the functional requirements of operating and safety systems and their interdependence, is the most complete manner of addressing the various issues and this is the SSMRP approach. The systems analysis approach encompasses the entire Seismic Methodology Chain (SMC) (seismic input, soil-structure interaction, major structure response, and subsystem response), the systematic representation of the nuclear power station's reactor systems using event/fault tree methodology, a description of the fragility of structures, components, and systems due to seismic loading conditions, and a computational approach which computes the probability of failure of structures, components, and systems and the probability of radioactive releases. The systems analysis computational approach was implemented in the computer program SEISIM, which is described separately. The input requirements for SEISIM are the system event/fault trees, the fragility descriptions of structures, components, and systems related to a local seismic response quantity, and the seismic responses for the range of earthquake levels of consideration. In addition, the probability of occurrence of each earthquake level is necessary. This presentation describes the methodology used in SSMRP to determine the seismic responses and their variability to be input to SEISIM.

The computer program SMACS (Seismic Methodology Analysis Chain with Statistics) was developed to link together the seismic input, soil-structure interaction (SSI), major structure

response, and subsystem response calculations. The seismic input is defined by ensembles of acceleration time histories in three orthogonal directions (two horizontal and vertical) on the surface of the soil. SSI and detailed structural response are determined simultaneously by the substructure approach to SSI which analyzes the coupled soil-structure system in a series of steps (determination of the foundation input motion, determination of the foundation impedances, and analysis of the coupled system). The substructure approach as implemented by Professors Luco and Wong in the computer program CLASSI was used extensively. In fact, CLASSI forms the basis for the SSI and structural response calculations in SMACS. Solution of the final step of the substructure approach, analysis of the coupled soil-structure system, by the CLASSI methodology permits very detailed models of the structures to be considered; in our case more than a hundred modes were included. Hence, detailed structural response in the form of time histories of accelerations, displacements, and forces are computed. The time history response of subsystems is likewise calculated in SMACS. Piping systems are analyzed assuming independent piping support motions obtained from the detailed structural response.

The response determined with SMACS is the input to the systems analysis program SEISIM. Hence, a compatibility between the responses and the fragility descriptions of structures, components, and systems must be maintained. The fragility of many components (pumps, valves, etc.) is tied to the spectral acceleration at the component's support location. The fragility of piping is tied to the vector sum of the moments in the pipe. Structural fragilities are related to forces in structural elements or to peak accelerations at particular locations in the structure. In all cases, these fragility parameters correspond to the response quantity calculated.

Several items require emphasis. The SSMRP response calculations should be as realistic as possible and uncertainties should be modeled using probabilistic methods. Best estimate models of the entire SMC were used. Uncertainty in each phase was incorporated as follows: In the seismic input, the largest source of variability was incorporated through ensembles of time histories; in the SSI phase, the mechanism to include variability was the shear modulus and damping in the soil; in the structures and subsystems stages, variations in the eigensystem and modal damping properties were the mechanism. These variations were treated in SMACS. Next, the response calculations must be performed for a range of excitation levels reflecting the fact that the systems analysis yields the probability of failure and radioactive release for the earthquake hazard which includes earthquakes of small amplitude up to very large events.

Examples of response including variability are presented.

The
University of Oklahoma at Norman

School of Aerospace, Mechanical
and Nuclear Engineering

September 29, 1980

L. C. Shao
Assistant Director for General Reactor Safety Research
Division of Reactor Safety Research
United States Nuclear Regulatory Commission
Washington, D.C. 20555

Dear Mr. Shao:

Enclosed are copies of my visual aids for the Eighth Water Reactor Safety Research Information Meeting to be held on October 27-31, 1981 in Washington D.C. Also enclosed is a two-page summary of my presentation.

Very truly yours,

Martin C. Jischke
Professor and Director

MCJ/jc
Encl.

cc: Dr. Robert Abbey, NRC

865 Asp Avenue, Room 212, Norman, Oklahoma 73019 (405) 325-5011

MEASURED PRESSURE LOADS ON MODEL STRUCTURES IN SIMULATED TORNADO-LIKE FLOW

Martin C. Jischke
University of Oklahoma

Ward's tornado simulator has been modified to study the interaction of tornadic flowfields with structures. Measurements with and without swirl have been made of the pressure on the surface of a cylindrical model and a rectangular model placed in the simulator. The cylindrical model, intended to represent the containment building of a nuclear reactor, is a circular cylinder 17.1 cm high and 11.4 cm in diameter with a hemispherical roof. The rectangular model, intended to represent the turbine building of a nuclear power plant, is a rectangular prism 12.7 cm high with a planform 14.6 cm by 25.4 cm.

Results are presented for the surface pressure coefficient and the total force and moment coefficients for imposed swirl angles of 0° and 45°, with the models placed at three locations within the simulator: 1) the convergent zone, 2) the boundary of the convergent zone and convection zone, 3) the convection zone.

The measurements on the cylindrical model show that in the swirling flow case, the nonuniform flow due to the tornado-like vortex induces a side-force, reckoned with respect to the local wind direction, that increases as the distance between the model and vortex decreases. The magnitude of the force coefficient on the structure increases with swirl, especially as the vortex and model come closer together. The horizontal force coefficient has a value of 1.01 or less under all conditions. The overturning moment coefficient on the model increases with swirl, the maximum value being 0.45 when the model is in the convergent zone. These measurements show that in the convergent zone and outer part of the convection zone, the pressure distribution on the model would tend to cause a structure of this shape to failure by overturning. When the model's inner edge is tangent to the undisturbed position of the vortex, the vortex attaches itself to the model and the pressure coefficient on the model has a more symmetric distribution around the model and has a relatively large negative value. Typical values of the pressure coefficient on the cylindrical portion of the model are as low as -2.78. Because of this high suction pressure force, another mode of failure, referred to as the bursting mode, becomes possible when the vortex attaches itself to the structure.

The data for the rectangular model shows that the effects of the imposed swirl can be dramatic and important. Increases in the horizontal force coefficient and overturning moment coefficient by a factor of four over the zero swirl values can occur when the model is at the boundary of the convergent and convection zones. The maximum measured horizontal force coefficient is 6.04. The vertical force on the roof can more than double, achieving a maximum value with swirl of 3.65. In addition, extremely high suction pressure forces can occur locally on the structure. The minimum measured pressure coefficient is -6.00. Thus, in addition to the possibility of failure by overturning, the structure can fail by a sequence which involves a local bursting due to the high suction force that then allows the high tornadic winds to tear away major parts of the structure.

These results show that the tornadic wind loads on structures cannot always be accurately estimated from the loads caused by boundary-layer-type winds.

References:

1. Jischke, M. C. and Light, B. D., "Laboratory Simulation of Tornadic Wind Loads on a Cylindrical Structure", Fifth International Conference on Wind Engineering, Fort Collins, Colorado, July, 1979.

2. Jischke, M. C. and Light, B. D., "Laboratory Simulation of Steady Tornadic Wind Loads on Structures", NUREG/CR-1183, December, 1979.

MEASURED PRESSURE LOADS ON MODEL STRUCTURES IN SIMULATED TORNADO-LIKE FLOWS

MARTIN C. JISCHKE
UNIVERSITY OF OKLAHOMA

LICENSING AND SAFETY ISSUES

- WHAT ARE THE FORCES EXERTED ON TYPICAL NUCLEAR REACTOR POWER PLANT STRUCTURES BY A TORNADIC WIND FIELD ?
- CAN THESE RESULTS BE ESTIMATED FROM RESULTS FOR THE MORE COMMON BOUNDARY-LAYER-TYPE WINDS ?
- ARE PRESENT DESIGN PRACTICES FOR TORNADO-PROOF STRUCTURES ADEQUATE ?

APPROACH

- SIMULATE TORNADIC WINDFIELD IN LABORATORY USING WARD-TYPE SIMULATOR
- PLACE SCALED MODELS OF TYPICAL STRUCTURES IN SIMULATOR AND MEASURE SURFACE PRESSURES
- USE MEASURED PRESSURE COEFFICIENTS AND SCALING LAWS TO DEDUCE FULL-SCALE FORCES

TORNADIC WINDFIELD FEATURES SIMULATED

- "REALISTIC" SURFACE PRESSURE PROFILE
- "REALISTIC" CORE RADIUS
- VORTEX BREAKDOWN
- MULTIPLE VORTEX FORMATION
- VERTICALLY SHEARED VELOCITY PROFILE
- SURFACE ROUGHNESS

FORCE AND MOMENT COEFFICIENTS

CYLINDRICAL MODEL

LOCATION	SWIRL ANGLE	C_{F_x}	C_{F_y}	C_{F_z}	C_{M_x}	C_{M_y}	C_{M_z}
CONVERGENT ZONE	0°	1.00	0.00	0.35	0.00	0.42	0
	45°	1.00	-0.11	0.32	0.04	0.45	0
CONVECTION-CONVERGENT ZONE BOUNDARY	0°	0.60	-0.05	0.35	0.01	0.28	0
	45°	0.82	-0.46	0.35	0.18	0.34	0
CONVECTION ZONE	0°	0.01	0.00	0.03	0.00	0.00	0
	45°	0.90	0.20	0.82	-0.15	0.33	0

POSSIBLE DAMAGE MECHANISMS
(CYLINDRICAL STRUCTURE)

- AWAY FROM VORTEX, HIGH EXTERNAL PRESSURE ON WINDWARD PORTION CAN CAUSE FAILURE BY OVERTURNING MOMENT MODE
- NEAR VORTEX, THE LOW ROUGHLY SYMMETRIC PRESSURE DISTRIBUTION CAN CAUSE FAILURE BY A BURSTING MODE

FORCE AND MOMENT COEFFICIENTS

RECTANGULAR MODEL

LOCATION	SWIRL ANGLE	ORIENTATION	C_{F_x}	C_{F_y}	C_{F_z}	C_{M_x}	C_{M_y}	C_{M_z}
CONVERGENT ZONE	0°	0°	1.54	0.02	0.95	0.00	0.80	0.02
		45°	3.19	-1.08	2.00	0.61	1.65	0.35
		90°	2.53	0.00	1.93	-0.01	1.40	0.03
	45°	0°	3.55	-1.30	2.37	1.14	1.79	0.42
		45°	4.08	-0.93	2.40	0.53	2.40	0.32
		90°	3.44	0.48	1.40	-0.20	1.73	0.10
		135°	1.91	-0.26	0.95	0.16	1.11	0.27

FORCE AND MOMENT COEFFICIENTS

RECTANGULAR MODEL

LOCATION	SWIRL ANGLE	ORIENTATION	C_{F_x}	C_{F_y}	C_{F_z}	C_{M_x}	C_{M_y}	C_{M_z}
CONVERGENT-CONVECTION ZONE BOUNDARY	0°	0°	0.59	0.01	0.93	-0.01	0.42	0.01
		45°	1.32	-0.45	1.48	0.23	0.74	0.22
		90°	1.46	-0.01	1.51	0.00	0.77	0.00
	45°	0°	3.85	-1.26	3.31	1.39	1.88	0.29
		45°	5.90	-1.33	3.65	0.93	3.45	0.60
		90°	3.04	0.36	1.81	0.05	1.07	0.01
		135°	1.96	-0.53	1.36	0.41	0.99	0.47

FORCE AND MOMENT COEFFICIENT

RECTANGULAR MODEL

LOCATION	SWIRL ANGLE	ORIENTATION	C_{F_x}	C_{F_y}	C_{F_z}	C_{M_x}	C_{M_y}	C_{M_z}
CONVECTION ZONE	0°	0°	0.01	0.00	0.08	0.00	0.01	0.00
		45°	0.03	-0.02	0.10	0.01	0.02	0.01
		90°	0.03	0.00	0.09	0.00	0.02	0.00
	45°	0°	0.75	0.18	1.03	0.42	0.06	0.30
		45°	1.02	1.35	1.15	0.55	0.52	0.37
		90°	0.85	0.25	1.10	0.10	0.45	0.55
		135°	0.87	0.14	1.02	0.15	0.01	0.50

HIGH LOCAL SUCTION PRESSURES

- MINIMUM C_p ON RECTANGULAR MODEL WITHOUT SWIRL IS -1.45 ON THE ROOF (MODEL ORIENTATION: 45° IN CONVERGENT ZONE)

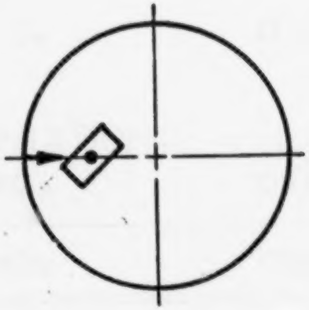

- MINIMUM C_p ON RECTANGULAR MODEL WITH 45° SWIRL IS -6.00 ON THE LEEWARD VERTICAL WALL (MODEL ORIENTATION: 45° AT BOUNDARY OF CONVERGENT AND CONVECTION ZONE)

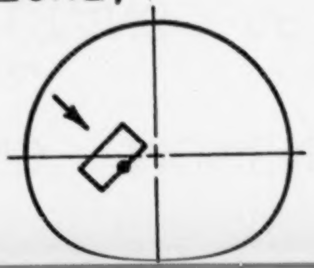

POSSIBLE DAMAGE MECHANISMS

(RECTANGULAR STRUCTURE)

- WHOLE STRUCTURE FAILURE BY DRAG FORCES AND OVERTURNING MOMENT
- LOCAL FAILURE BY HIGH SUCTION PRESSURES MAY INITIATE FAILURE SEQUENCE

CONCLUSIONS

- FORCES ON TYPICAL STRUCTURES DUE TO TORNADIC WINDS CAN BE ESTIMATED FROM RESULTS OBTAINED IN THIS RESEARCH
- THESE FORCES CANNOT BE ACCURATELY ESTIMATED FROM RESULTS FOR BOUNDARY-LAYER-TYPE WINDS
- PRESENT DESIGN PRACTICES ARE INADEQUATE FOR ESTIMATING TORNADIC WIND LOADS ON LARGE STRUCTURES

FUTURE WORK

- ADDITIONAL STATIC MEASUREMENTS
- EFFECT OF RELATIVE MOTION OF MODEL AND VORTEX
- ANALYSIS OF EFFECTS ON SCALE -- ESPECIALLY BUILDING SIZE

ATMOSPHERIC DISPERSION RESEARCH PROGRAM

Robert F. Abbey, Jr.
Office of Nuclear Regulatory Research
U.S. Nuclear Regulatory Commission

Isaac Van der Hoven
Air Resources Laboratories
National Oceanic & Atmospheric Administration

The main objective of the atmospheric dispersion research program is to provide improved bases for licensing decisions and for development and confirmation of regulations, standards, and guides. The emphasis in the atmospheric dispersion research program currently being supported is threefold: (1) to obtain high-quality, realistic data in order to verify current and proposed methods used to predict the transport and diffusion of airborne radioactive effluents, (2) to assess the adequacy of the NRC position outlined in various Regulatory Guides, e.g., 1.3, 1.4, 1.23, 1.111, 1.145, and (3) to evaluate meteorological dispersion models used to describe the spread of radioactive plumes.

Estimates of the dispersive capability of the atmosphere are needed for two purposes: (1) emergency response planning; and (2) site characterization. Research in atmospheric dispersion involves the development, execution, and analysis of empirical field and wind tunnel tracer tests. Such tests are necessary to acquire high-quality tracer and turbulence data needed to verify or evaluate diffusion and transport codes. Federal regulations, 10 CFR Part 100 and 10 CFR Part 50 Appendix E require an assessment be made of the meteorological characteristics surrounding each site for site acceptability and emergency response determinations, respectively.

The general outline of the atmospheric dispersion research program is shown in Tables 1 and 2; the functional relationships and responsibilities inherent in the program are detailed in Table 3. This program began in 1972 with the conduct of tracer experiments performed during low wind speed and inversion conditions over flat terrain. The effects on dispersion of topography, thermal stability and turbulence are being examined empirically and analytically. Tracer experiments are being conducted over a range of topographical features with concentrations being measured out to 50 miles. Dispersion models are being evaluated using existing high-quality tracer concentration data sets. This evaluation will demonstrate the range of models applicable to different meteorological and topographical regimes. Such an assessment will provide a basis for selecting a given model for use in emergency planning and environmental effects resulting from posutlated accidental releases of radioactive effluents for site evaluation purposes (Table 4). Field program plans have been initiated to obtain high quality concentrations and meteorological measurements under controlled conditions in river valley (Table 5) and shoreline environments. The three major projects that comprise the atmospheric transport and diffusion research program are described in Table 6; the contractor organizations and principal investigators are also listed therein.

TABLE 1

ATMOSPHERIC DISPERSION RESEARCH PROGRAM

-- DISTANCES (0 - 80 KM)

-- WIND SPEEDS (CALM - 10 MPS)

-- ALL STABILITY CONDITIONS

A. TERRAIN EFFECTS
   1. FLAT, EVEN
   2. ROUGH, HILLY
   3. COASTAL SHORELINE ENVIRONMENT
   4. CHANNELED FLOW
   5. IMPINGEMENT

B. MODEL EVALUATION
   1. TRANSPORT (TRAJECTORY)
   2. DIFFUSION (TURBULENCE)
   3. DEPOSITION
   4. COMPUTER CAPABILITY FOR EMERGENCY RESPONSE

C. VERTICAL DISPERSION

D. BUILDING WAKE EFFECTS

OBJECTIVE: VERIFICATION OF CURRENT AND PROPOSED METHODS USED TO PREDICT THE TRANSPORT AND DIFFUSION OF AIRBORNE RADIOACTIVE EFFLUENTS FOR EMERGENCY RESPONSE AND SITE EVALUATION PURPOSES

TABLE 2

ATMOSPHERIC DISPERSION PROGRAM
Site Safety Research Branch, RES

OBJECTIVE:
Verification of current and proposed methods used to predict transport and diffusion of airborne radioactive effluents.

CURRENT EFFORTS:

I. Microscale (0-1 km; minutes)
  A. Field experiments conducted under all atmospheric stability conditions and windspeeds < 2 $msec^{-1}$ and between 2 and 10 $msec^{-1}$
    1. Terrain effects (ground and elevated sources)
      a. Flat, even
      b. Rough, hilly
      c. Channeled (canyon, river valley)
      d. Coastal (land-sea breeze)
      e. Impingement
    2. Building wake effects (ground, vent and stack sources)--includes wind tunnel tests
      a. Small size, flat terrain
      b. Large size, flat terrain
      c. Small size, rough terrain
      d. Large size, rough terrain
    3. Vertical dispersion (ground and elevated sources)
      a. Flat, even terrain
      b. Rough, hilly terrain
  B. Theoretical analyses based on field and wind tunnel data

II. Mesoscale (1-100 km; hours)
  A. Field experiments -- all atmospheric stability conditions; windspeeds ≥ 2 $msec^{-1}$
    1. Terrain effects
      a. Flat, even
      b. Rough, hilly
      c. Coastal
      d. Impingement
      e. Channeled flow
    2. Vertical dispersion
      a. Flat, even terrain
      b. Rough, hilly terrain
  B. Theoretical analyses

III. Special Studies
  A. Diffusion of heavier and lighter than air gases--all stabilities, range of windspeeds
    1. Ground-level source
      a. No obstacles
      b. With buildings present
    2. Elevated source
      a. With buildings (vent, small stack)
      b. Isolated stacks
  B. Fumigation - field, wind tunnel, and theoretical studies
    1. Continental
    2. Coastal (buoyancy and forced convection)
  C. Atmospheric effects of heat and moisture dissipation

TABLE 3

ATMOSPHERIC TRANSPORT AND DIFFUSION RESEARCH PROGRAM

OUTLINE OF RESPONSIBILITIES

Steering Group

R. F. Abbey, Jr. NRC/RES, Chairman
R. N. Meroney, Colorado State University
I. Van der Hoven, NOAA
S. R. Hanna, NOAA/ATDL

Working Groups

Model Evaluation	Empirical Assessment
W. S. Lewellen, Aeronautical Research Associates of Princeton	C. R. Dickson, NOAA/ARL-ID
G. E. Start, NOAA/ARL-ID	W. B. Johnson, SRI International
F. C. Kornegay, ORNL	R. K. Hadlock, Battelle-PNL

TABLE 4

APPROACH TO EVALUATION OF REAL-TIME ATMOSPHERIC DISPERSION MODELS

1. Identify atmospheric transport, diffusion, and deposition models appropriate to estimate concentration patterns of effluents to 80 km.
   Model characteristics:
   a. Gaussian (statistical)
   b. K-theory
   c. 2nd-order closure

2. Identify tracer concentration data sets from point sources with simultaneous meteorological measurements taken out to 80 km.
   a. terrain and surface conditions
   b. atmospheric stability
   c. transition conditions
   d. wind fields

3. Determine evaluation criteria by which to assess models identified in 1 using data in 2.
   a. downwind 1 hr. surface concentration patterns to 80 km
   b. cost/benefit
   c. real time capability
   d. sensitivity of meteorological data input

4. Evaluate models using 3 and data in 2.
   a. models (not more than 6)
   b. experiments (not more than 50)

5. In consultation with NRC determine performance criteria for meteorological data needed, model output, and compatibility at plants.

6. Perform 1, 2, 3, and 4 with precipitation scavenging models.

7. Evaluate minicomputer capabilities that currently exist which may be applicable or easily adaptable to on-site emergency planning and response functions. This assessment shall, as a minimum, include the following:
   a. meteorological input
   b. sampling input
   c. storage and memory capacity
   d. processing speed and efficiency
   e. display techniques
   f. communications links
   g. atmospheric transport, diffusion, deposition, and precipitation scavenging models used

TABLE 5

PROPOSED ATMOSPHERIC DISPERSION FIELD EXPERIMENT AT INDIAN POINT

PROJECT DIRECTOR: Robert F. Abbey, Jr., NRC/RES

FIELD DIRECTOR: C. Ray Dickson
Air Resources Laboratory, NOAA-ID

PARTICIPANTS: NOAA/ARL
SRI International
Battelle-Pacific Northwest Laboratories
Consolidated Edison
State of New York

OBJECTIVE: To obtain high quality tracer concentration and coincident meteorological data in order to verify and evaluate ARAC and other dispersion models.

TEST PERIOD: Two weeks commencing May 1, 1981.

TEST CHARACTERISTICS:

1. Gaseous tracers released either concurrently from two different locations or consecutively to distinguish between day and night releases (SF_6, 12B2).
2. 50 km X 50 km square grid or 25 km X 70 km grid centered at Indian Point.
3. 200 portable samplers with four samples at each of 50 locations.
4. Continuous releases for two weeks with samplers changed every six hours.
5. Radiosondes released every six hours.
6. Tetroons tracked by radar, released every three hours for trajectory determination.
7. 6-8 150 ft instrumented towers.
8. Pibal stations and radar for wind field definition.
9. Mark IX mobile lidar system for concentration measurements in the vertical.
10. Acoustic sounder for stability and mixing height determinations.
11. Oil fog and plume photography.
12. ALPHA-1 airborne lidar.

TABLE 6

SITE SAFETY RESEARCH BRANCH/DIVISION OF REACTOR SAFETY RESEARCH

Evaluation of Real-Time Dispersion Models NOAA/Air Resources Lab. NOAA/Atmospheric Turbulence and Diffusion Laboratory Colorado State University Aeronautical Research Associates of Princeton SRI International Battelle-Pacific Northwest Lab. Oak Ridge National Lab.	Utilizing known atmospheric transport, diffusion, and deposition models appropriate to estimate concentration patterns of effluents to 80 km and previously developed high quality tracer concentration data sets, an objective evaluation of selected models will be performed. This evaluation will demonstrate the range of models applicable to different meteorlogical/topographical regimes, identify needed input data, and quantify model uncertainties. Such an assessment will provide a basis for selecting a given model for use in emergency planning and environmental effects resulting from postulated accidental releases of radioactive effluents for site evaluation minicomputer capabilities for on-site dispersion modeling as well as the Atmospheric Release Advisory Capability (ARAC) centered at LLL is being made.
Intermediate Range Atmospheric Transport Experiments NOAA/Air Resources Lab. SRI International Aeronautical Research Associates of Princeton Oak Ridge National Lab.	A continuous two week field program has been proposed to be conducted at Indian Point, NY, to obtain high quality concentration measurements with 400 fixed point samples located in a 20 km X 50 km grid. Concurrent meteorological measurements will be made and used as data input to selected atmospheric transport and diffusion models. The model evaluation effort will be conducted independently in order to assess objectively the performance of each model in predicting the maximum concentration and spread of the tracer.
Dispersion in Shoreline Environments SRI International NOAA/Air Resources Lab Battelle-Pacific Northwest Lab. The Research Corporation of New England	To quantify the spread of effluents from ground-level, point sources in shoreline environments during postulated accident conditions, a field program has been initiated to obtain high quality concentration measurements under controlled conditions. Tests are planned for the Texas Gulf Coast, Florida Atlantic Coast, and the shores of Lake Michigan. The measurements program will utilize state-of-the-art tracer technology and remote sensing techniques to determine the spread of the effluent in the horizontal and vertical, over water as well as over land. The data thus collected will be used to evaluate existing and proposed models of dispersion during accident conditions in coastal zones, both for emergency planning and site evaluation purposes.

NEAR-GROUND TORNADO WIND FIELDS

by

James R. McDonald, P.E.

Texas Tech University
Lubbock, Texas

NRC Contract NRC-04-76-345

NEAR-GROUND TORNADO WIND FIELDS

by

James R. McDonald, P.E.
Professor of Civil Engineering
Texas Tech University

The incentive for studying near-ground tornado wind fields comes from the need to design certain types of structures to resist the damaging effects of tornadoes. The basic flow chart for tornado-resistant design of structures is shown in Figure 1. A clear understanding of the near-ground tornado wind field is a necessary part of the entire design process.

Tornado wind fields have been studied theoretically for many years by meteorologists and those trained in fluid dynamics. The complexity of the tornado mechanism and the varying conditions under which a tornado can occur make it difficult, if not impossible, to understand from a theoretical point of view. The characteristics of the tornado wind field are difficult to measure because of the intensity of the winds, the rapid spatial variations, and the short life span of the storm. For this reason, scientists and engineers have resorted to indirect methods of determining characteristics of the near-ground wind field. The purpose of this research project is to learn as much as possible about near-ground wind fields by examining the damage and debris left by a tornado. Specific objectives of the project are listed in Figure 2.

The objectives of the project are accomplished by documentation of damage caused by severe wind storms. Although near-ground tornado wind fields are the primary interest, valuable information can be gained from studying other types of storms. Teams of engineers and scientists are sent to the field as soon as the significance of a windstorm is established. It is critical that the investigation team arrive at the scene as soon as possible because valuable storm damage evidence is quickly destroyed or distorted in the rescue, cleanup and recovery operations. The type of information gained from damage documentation is listed in Figure 3.

During the documentation effort, the damage and debris patterns are mapped and photographed for later analysis. The performance of various types of structures is documented in detail, with particular attention paid to "engineered" structures. Tornado-generated missiles are identified, their origin is determined, and their impact point is located. Characteristics of the missile (size, shape, weight, type of material and anchorage) are identified. The penetration or perforation of structures is noted. Attempts are made to authenticate stories of unusual events. Such stories as water removal from ponds, the transport of large or unusual objects, or the miraculous survival of a person or object often get widespread publicity in the news media. More often than not, stories which suggest extremely high wind speeds can be explained in a rational manner when examined by a scientific approach.

Analysis of the data obtained from the damage documentation provides information relating to near-ground wind fields. A summary of the type of information obtained from analysis of damage data is contained in Figure 4. The damage and debris patterns reveal evidence of rotational winds. Normally it will be known whether the winds are produced by a tornado or other type of windstorm. However, if the event occurs at night and intensity is relatively weak, the wind could be the result of a downburst or other type of straight line wind.

Much can be learned from an "autopsy" of a damaged building. Various types of failure modes can be identified and the performance of the structural system can be evaluated. As data is gathered on various types of structural systems (e.g., reinforced concrete, masonry or timber), conclusions can be drawn regarding the relative resistance of different structural systems to wind loads.

Estimates of wind speeds to cause a certain type of failure mechanism can be obtained by applying fundamental principles of structural analysis. Wind speeds associated with damage to a structural component give a lower bound wind speed estimate.

The correlation of wind speeds calculated from damage analysis with appearance of damage provides an indirect means of estimating tornadic wind speeds where a detailed damage documentation is not possible or practical. When used with an intensity classification such as the F-scale, estimates of maximum wind speed in a tornado based on certain types of observed damage is both practical and reliable.

Using the approach described above, numerous storms have been documented and the data analyzed in the past ten years. Figure 5 lists the most recent storms studied as a part of this research project. Some of the more significant results that can be stated at this point in time are summarized in Figure 6. They are not all a direct result of this particular study, but the study does substantiate these statements.

At one time (not more than 10-12 years ago), the technical literature and the press quoted tornadic wind speeds in the 500 to 800 mph range. Today, based on both damage documentation and theoretical studies, maximum wind speeds in tornadoes are thought to be in the 275-300 mph range. These speeds are produced in very rare tornadoes that make up less than one-tenth of one percent of all recorded tornadoes.

Except in buildings that are purposely sealed and designed to be tornado resistant, the principal damage mechanism is the aerodynamic flow of air over a building rather than the rapid change in atmospheric pressure (APC). Openings or vents in an ordinary building, such as a house, are sufficiently large to allow equalization of the pressure. The aerodynamic forces are outward on all parts of an ordinary building except on the windward wall. Thus, failure in a sense is "explosive," since all parts tend to fly outward, but it is caused by the wind, not the APC.

In virtually every tornado resistant design application, it is the tornado generated missile that controls the design of walls and roofs. This is true in power plant design as well as in the design of shelters for occupant protection. The problem is to identify what types of missiles are expected to fly in a tornado and to evaluate the hazard probability. Through tornado damage documentation, various types of missiles have been identified. Others have been included in design criteria based on speculation, but have not been observed in the field to date. Examples of missiles that have been observed to fly (or roll and tumble) and some that did not are listed in Figure 7. The missiles observed in the Bossier City, LA torando of December 3, 1978 are the most recent evidence of a formidable missile type. Six steel wide flange beams were picked up from the roof of an elementary school. The largest one weighed more than 700 lbs and traveled a distance of 1000 ft.

Studies were made to duplicate the missile trajectories using a theoretical trajectory model. The initial pickup points, the impact points, and the theoretical trajectories are shown in Figure 8. The impact points were matched with the theoretical trajectories by varying two parameters within a reasonable range of values. The two parameters are: (1) aerodynamic flight parameter, and (2) the wind speed at which the beam would be released from its anchorage. Preliminary conclusions from this study suggest that the steel wide flange beam may be a more likely missile threat than the 12 in. diameter steel pipe that is presently included in the criteria for nuclear power plant design.

The final result of damage documentation discussed in this brief summary report is a catalog of structural performance. By observing and analyzing the damage to many different buildings and structural types, patterns of damage emerge, which can be systematically cataloged and used for predicting potential damage to existing buildings.

There are numerous other applications that are being studied and which will be discussed in subsequent reports. It is only through continued studies of this type that we can improve our knowledge of the tornado phenomena and increase our confidence in the criteria for tornado resistant design.

TORNADO RESISTANT DESIGN

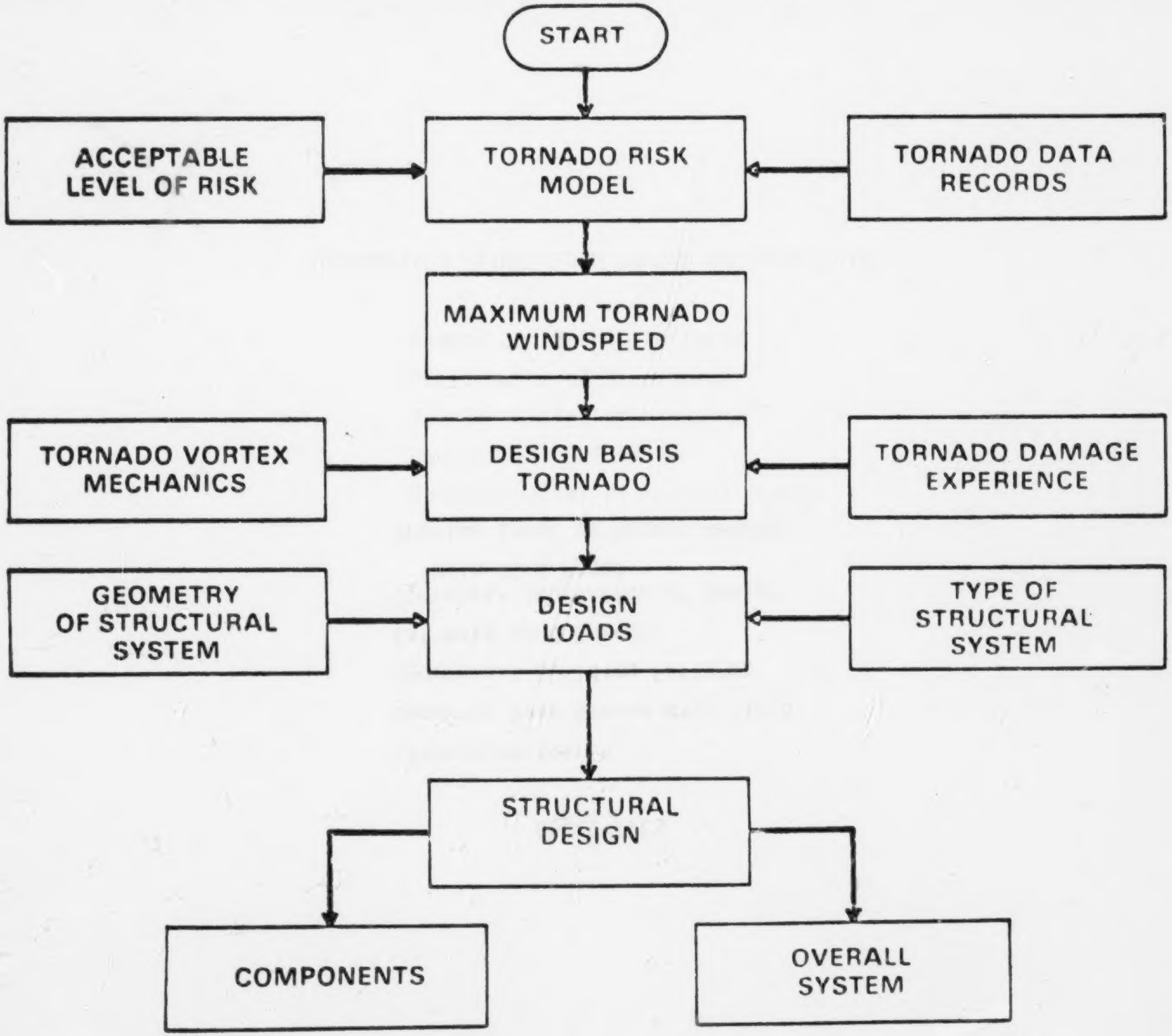
START
ACCEPTABLE LEVEL OF RISK
TORNADO RISK MODEL
TORNADO DATA RECORDS
MAXIMUM TORNADO WINDSPEED
TORNADO VORTEX MECHANICS
DESIGN BASIS TORNADO
TORNADO DAMAGE EXPERIENCE
GEOMETRY OF STRUCTURAL SYSTEM
DESIGN LOADS
TYPE OF STRUCTURAL SYSTEM
STRUCTURAL DESIGN
COMPONENTS
OVERALL SYSTEM

Figure 1

OBJECTIVES

Literature Search

Describe Near-Ground Wind Field

Understand Building Failures

Estimate Wind Speeds

Correlate Appearance of Damage
With Wind Speed

Provide Input to Record Keeping

Figure 2

INFORMATION GAINED FROM DAMAGE DOCUMENTATION

Damage and Debris Patterns
Performance of Structures
Identification of Missiles
Damage Path Definition
Authentication of Unusual Events

Figure 3

ANALYSIS OF DAMAGE DATA

- Type of Storm
- Failure Modes
- Estimated Wind Speeds
- Appearance of Damage versus Wind Speed

Figure 4

SPECIFIC STORMS

- Tornadoes
  - Bossier City, Louisiana
  - Wichita Falls, Texas
  - Kalamazoo, Michigan
  - Grand Island, Nebraska
- Hurricanes
  - Frederic
  - Allen

Figure 5

RESULTS

Tornadic Wind Speeds Are Not Astronomical
Wind is the Principal Damage Mechanism
Missiles Control Design Criteria
Cladding is More Likely to Fail Than Structure

Figure 6

SOME MISSILES THAT FLEW

Lubbock Fertilizer Tank
Bossier City Wide Flange Beams
Lillis Railroad Car
McComb School Busses
Grand Island Roof Planks
Plainview Roof Timbers

AND SOME THAT DID NOT

Brandenburg Utility Poles and Storage Yard
Washita Pipes
Grand Gulf Storage Yard

Figure 7

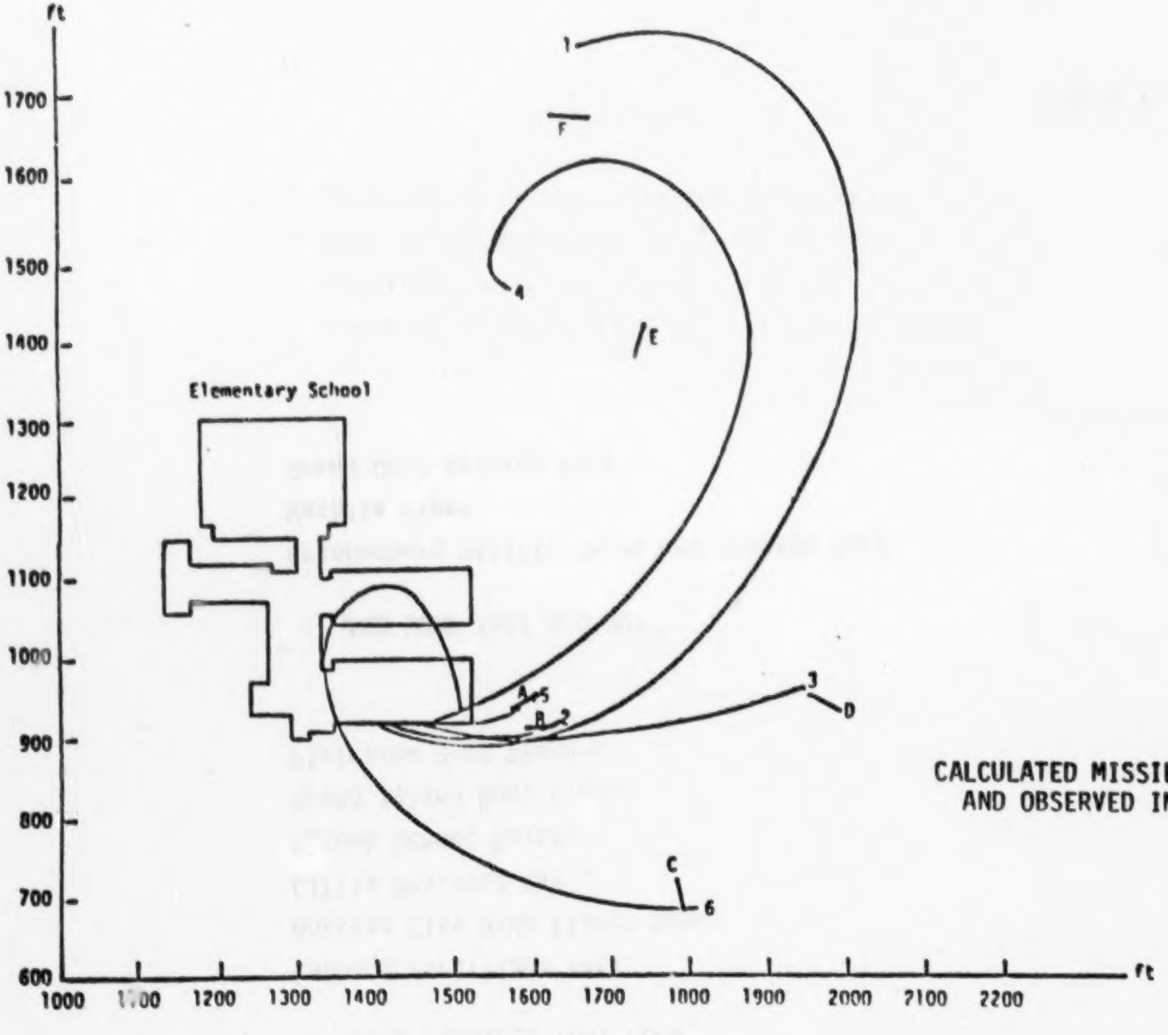

CALCULATED MISSILE TRAJECTORIES
AND OBSERVED IMPACT POINTS

Figure 8

AUTOMOBILE IMPACT FORCES ON CONCRETE WALLS

by

R. L. Chiapetta* and J. F. Costello**

SUMMARY

The objective of the study described in this paper was to develop force-time impact signature data for use in the design or evaluation of nuclear power plant structures subject to tornado-borne automotive vehicle impact. The approach was based on the use of analytical vehicle models to calculate impact forces.

Current design procedures were reviewed and a few candidate analytical models for impact force predictions were evaluated. The one-dimensional vehicle model finally selected for subsequent calculations consists of a distributed mass representation of a car with variable strength and mass properties along its length. The engine, however, was considered to be rigid.

The vehicle data base for this investigation consisted of detailed strength and mass distribution information, as well as test data from low-speed, head-on impact with flat concrete barriers, for nine cars ranging from full-size to minicars. The test data were utilized to validate the analytical vehicle model.

The one-dimensional model was used to calculate impact force-histories on rigid walls due to head-on impact of each of the nine vehicles considered over an impact speed of 20 to 60 meters/sec. The sensitivity of computed forces to variations in mass and strength distributions was determined.

---

* Principal, Chiapetta, Welch & Associates; Palos Hills, IL, USA

**Structural Engineer, Division of Reactor Safety Research, U.S. Nuclear Regulatory Commission, Washington, DC, USA

A three-dimensional lumped-mass vehicle model was used to predict the effect of various impact orientations on the force-histories for variation of impact angle in one plane. A lumped-mass structural model was then employed for a typical panel to determine the effect on structural response of impact orientation using the rigid wall, force-time histories generated by the three-dimensional vehicle model.

To assess the significance of vehicle/structure interaction on the head-on impact force-histories, the simple lumped-mass model of a reinforced concrete wall panel was coupled to the one-dimensional vehicle model for numerous panel design configurations within the range of practical interest. Vehicle-structure interaction was found to have relatively little effect on the force-histories.

The sensitivity of structural response to variations in force signature characteristics was established and idealized impact force-time relations were developed for five distinct impact speeds ranging from 20 to 60 meters/sec. The use of these relations produce less conservative estimates of structural deflection, for all impact speeds considered, than the currently accepted design procedure.

AUTOMOBILE IMPACT FORCES ON CONCRETE WALLS

ISSUE ADDRESSED

- DESIGN OF CATEGORY I STRUCTURES AGAINST TORNADO-GENERATED DEBRIS — SOFT MISSILE IMPACT PROBLEM — AUTOMOBILES
- DESIGN LOADS — CURRENTLY ACCEPTABLE PROCEDURE — INSTANTANEOUS TRANSFER OF VEHICLE MOMENTUM TO STRUCTURE
- RECENT HIGHER ESTIMATES OF ATTAINABLE VEHICLE IMPACT VELOCITIES — SOFT MISSILE IMPACT LOAD FREQUENTLY GOVERNS CERTAIN DESIGN ASPECTS OF R/C WALL PANELS
- A BETTER DEFINITION OF AUTOMOBILE IMPACT LOADS IS DESIRED

OBJECTIVE

- DEVELOP VEHICLE IMPACT FORCE FUNCTIONS APPLICABLE TO R/C WALL PANEL DESIGN

SCOPE

- CONSIDER AUTOMOBILE IMPACT INTO TYPICAL R/C WALLS AT VELOCITIES UP TO 60 METERS/SEC
- USE OF ANALYTICAL MODELS
- CONSIDER STRUCTURAL AS WELL AS VEHICLE DEFORMATION EFFECT ON FORCE
- ESTIMATE CONSEQUENCES OF DIFFERENT VEHICLE IMPACT ORIENTATIONS

METHOD OF APPROACH

- USE ONE-DIMENSIONAL ANALYTICAL MODELS TO CALCULATE FORCES DUE TO HEAD-ON ORIENTATION VEHICLE IMPACT WITH RIGID WALLS — BASELINE CONFIGURATION
- VALIDATE MODELS BY CORRELATION WITH EXISTING VEHICLE CRASH TEST DATA FOR HEAD-ON, LOW SPEED IMPACT
- EXTRAPOLATE MODELS TO HIGH SPEED IMPACT
- DETERMINE EFFECT OF STRUCTURAL DEFORMATION ON FORCES BY COUPLING OF A STRUCTURAL DEFORMATION MODEL WITH VEHICLE MODEL
- CONSIDER EFFECT OF IMPACT ORIENTATION WITH USE OF THREE-DIMENSIONAL VEHICLE MODEL
- APPLY DEFORMATION AND ORIENTATION FACTORS TO BASELINE CONFIGURATION FORCE FUNCTIONS TO DERIVE EQUIVALENT FUNCTIONS FOR OTHER CONFIGURATIONS

PROGRAM OUTLINE

TASK 1 - PRELIMINARY INVESTIGATION

- REVIEW CURRENT DESIGN PROCEDURES
- COMPILE AVAILABLE TEST DATA ON AUTOMOTIVE VEHICLE IMPACT
- COLLECT VEHICLE DATA NECESSARY FOR ANALYTICAL MODELS

TASK 2 - VEHICLE IMPACT FORCES ON RIGID WALLS

- SELECT CANDIDATE ANALYTICAL MODELS FOR IMPACT FORCE PREDICTIONS
- COMPARE MODEL PREDICTIONS WITH TEST DATA AT LOW SPEED
- USE MOST PROMISING MODELS TO CALCULATE HIGH SPEED IMPACT FORCES
- DETERMINE SENSITIVITY OF FORCES TO VARIATIONS IN MASS AND STRENGTH DISTRIBUTIONS OF A GIVEN VEHICLE
- ESTIMATE THE EFFECT OF IMPACT ORIENTATION ON FORCE MAGNITUDE
- DEVELOP PRELIMINARY IMPACT FORCE-TIME DEFINITIONS

TASK 3 - STRUCTURAL RESPONSE

- COUPLE A SIMPLE STRUCTURAL MODEL WITH VEHICLE MODEL
- DEFINE RANGES OF PARAMETERS FOR STRUCTURAL COMPONENTS OF INTEREST
- ASSESS SIGNIFICANCE OF VEHICLE/STRUCTURAL INTERACTION
- DETERMINE SENSITIVITY OF STRUCTURAL RESPONSE TO VARIATIONS IN CHARACTERISTICS OF FORCE SIGNATURE
- CONSTRUCT ENVELOPE OF FORCE SIGNATURES

SUMMARY OF RESULTS

- RELATIVELY SMALL EFFECT OF STRUCTURAL DEFORMATION ON IMPACT FORCE FUNCTION FOR PRACTICAL RANGE OF STRUCTURAL PARAMETERS

- SIDE-ON IMPACT ORIENTATION MAY RESULT IN SIGNIFICANTLY GREATER IMPACT FORCES AND STRUCTURAL DEFLECTION THAN THE BASELINE HEAD-ON ORIENTATION

- APPLICATION OF THE DEVELOPED IMPACT FORCE FUNCTION TO R/C WALL PANELS PRODUCES SUBSTANTIALLY LESS STRUCTURAL DEFLECTION THAN DOES THE CURRENTLY ACCEPTED METHOD OF INSTANTANEOUS MOMENTUM TRANSFER — FOR THE IMPACT VELOCITY RANGE OF 20 TO 60 METERS/SEC

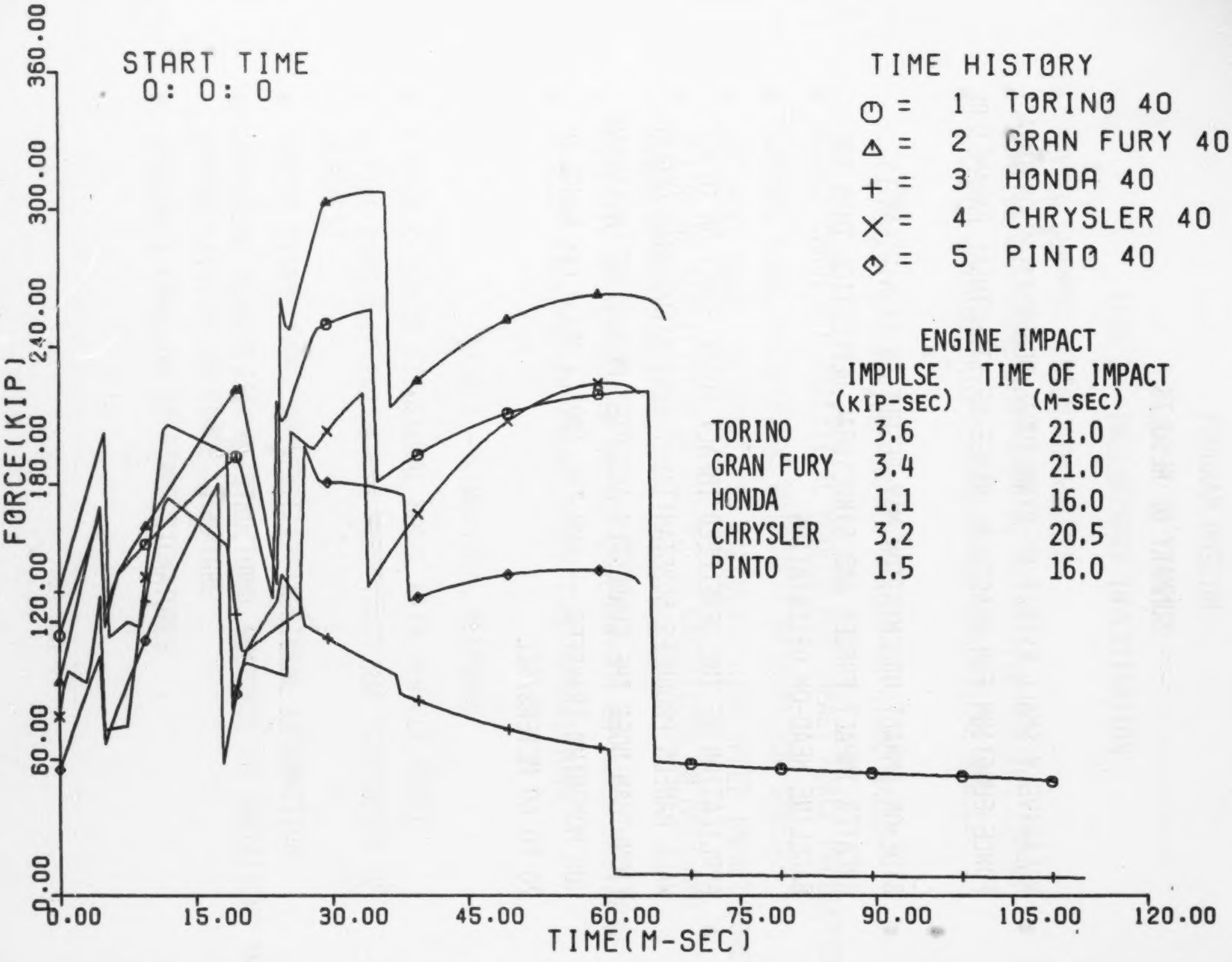

ENGINE IMPACT

	IMPULSE (KIP-SEC)	TIME OF IMPACT (M-SEC)
TORINO	3.6	21.0
GRAN FURY	3.4	21.0
HONDA	1.1	16.0
CHRYSLER	3.2	20.5
PINTO	1.5	16.0

IMPACT FORCE FOR VARIOUS CARS — BASELINE CONFIGURATION, 40 METERS/SEC·IMPACT

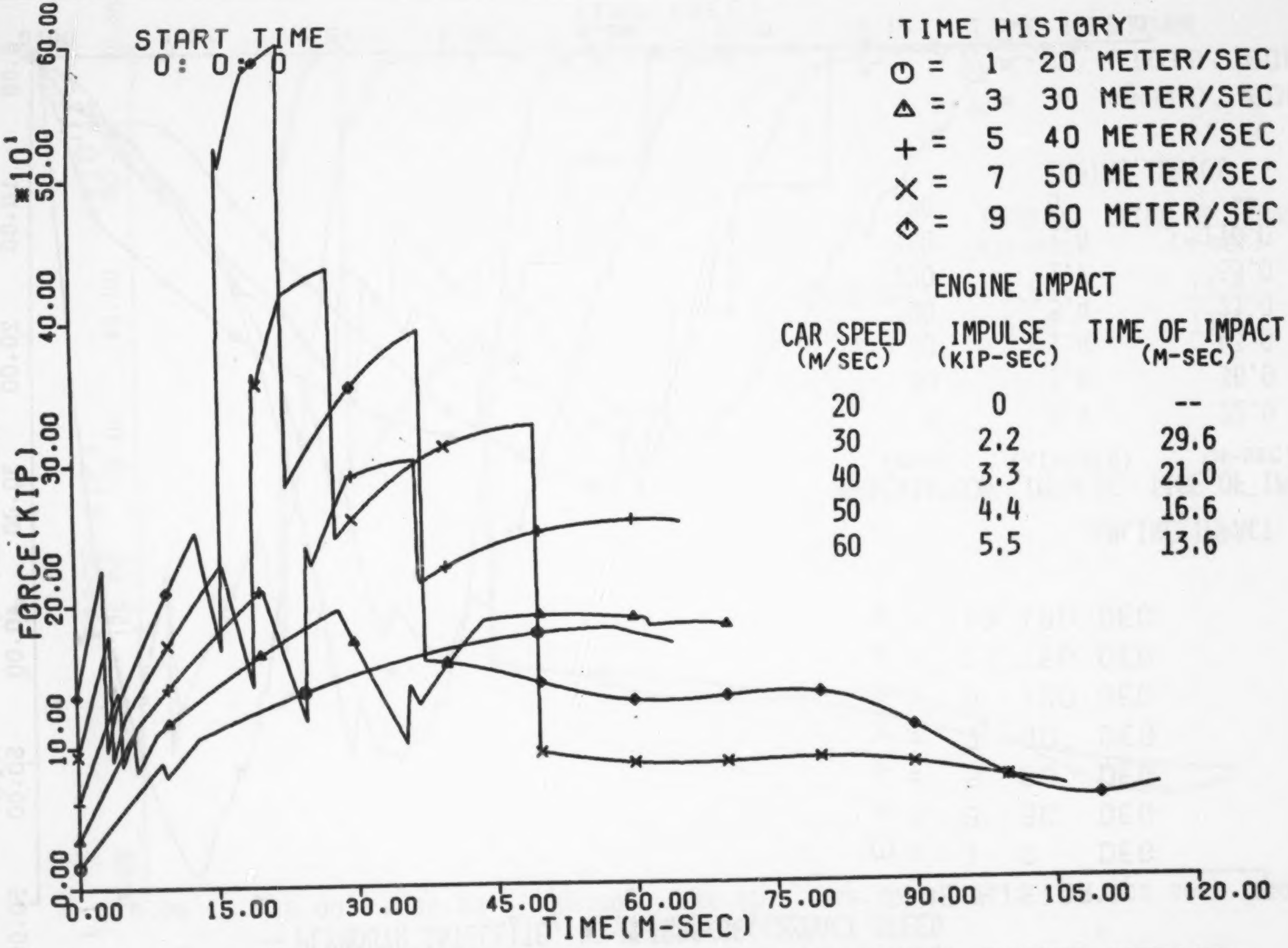

ENGINE IMPACT

CAR SPEED (M/SEC)	IMPULSE (KIP-SEC)	TIME OF IMPACT (M-SEC)
20	0	--
30	2.2	29.6
40	3.3	21.0
50	4.4	16.6
60	5.5	13.6

IMPACT FORCE FOR VARIOUS IMPACT SPEEDS — BASELINE CONFIGURATION, PLYMOUTH SATELLITE

EFFECT OF VEHICLE YAW ORIENTATION ON IMPACT FORCE
— PLYMOUTH SATELLITE, 40 METERS/SEC IMPACT SPEED

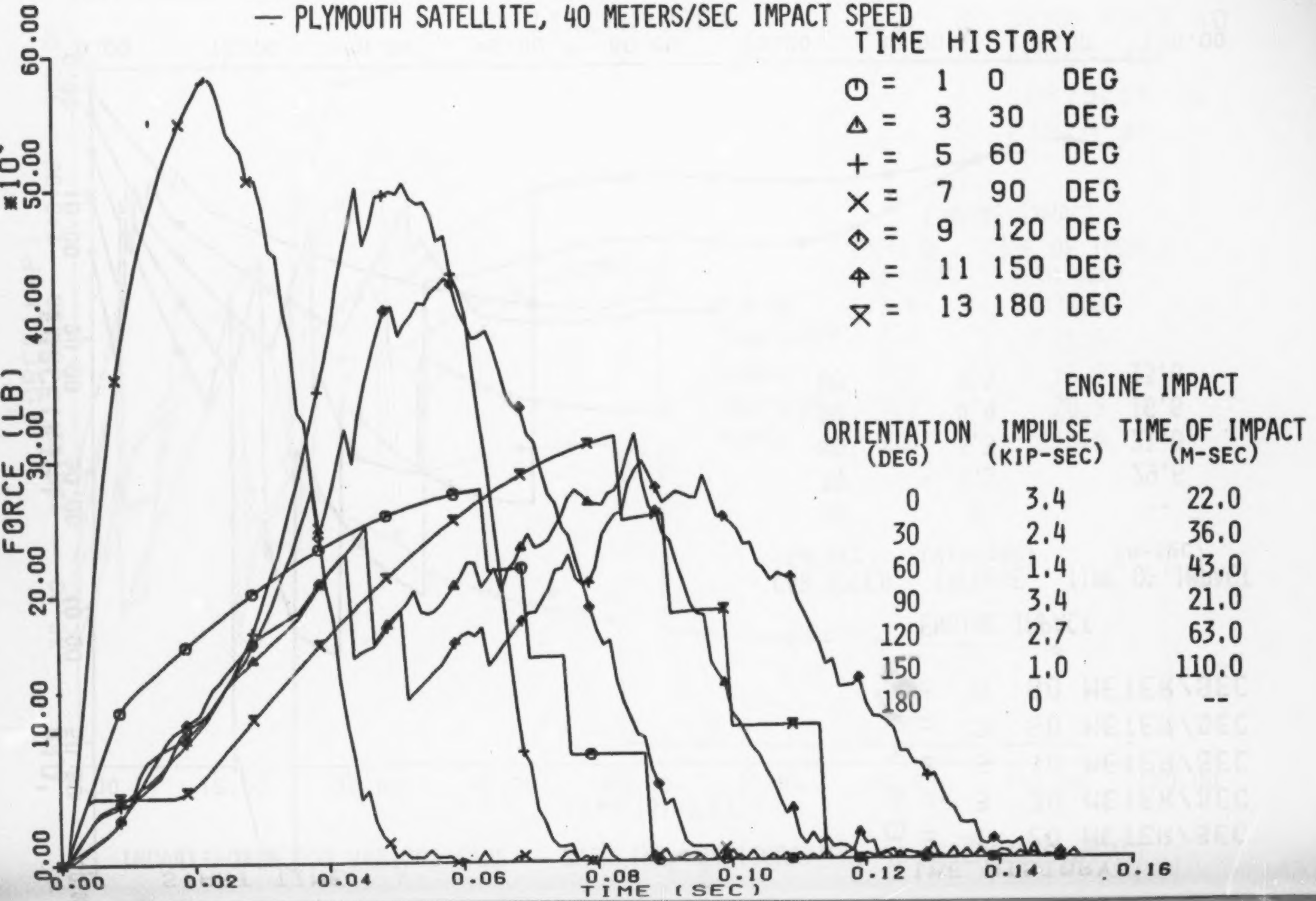

ENGINE IMPACT

ORIENTATION (DEG)	IMPULSE (KIP-SEC)	TIME OF IMPACT (M-SEC)
0	3.4	22.0
30	2.4	36.0
60	1.4	43.0
90	3.4	21.0
120	2.7	63.0
150	1.0	110.0
180	0	--

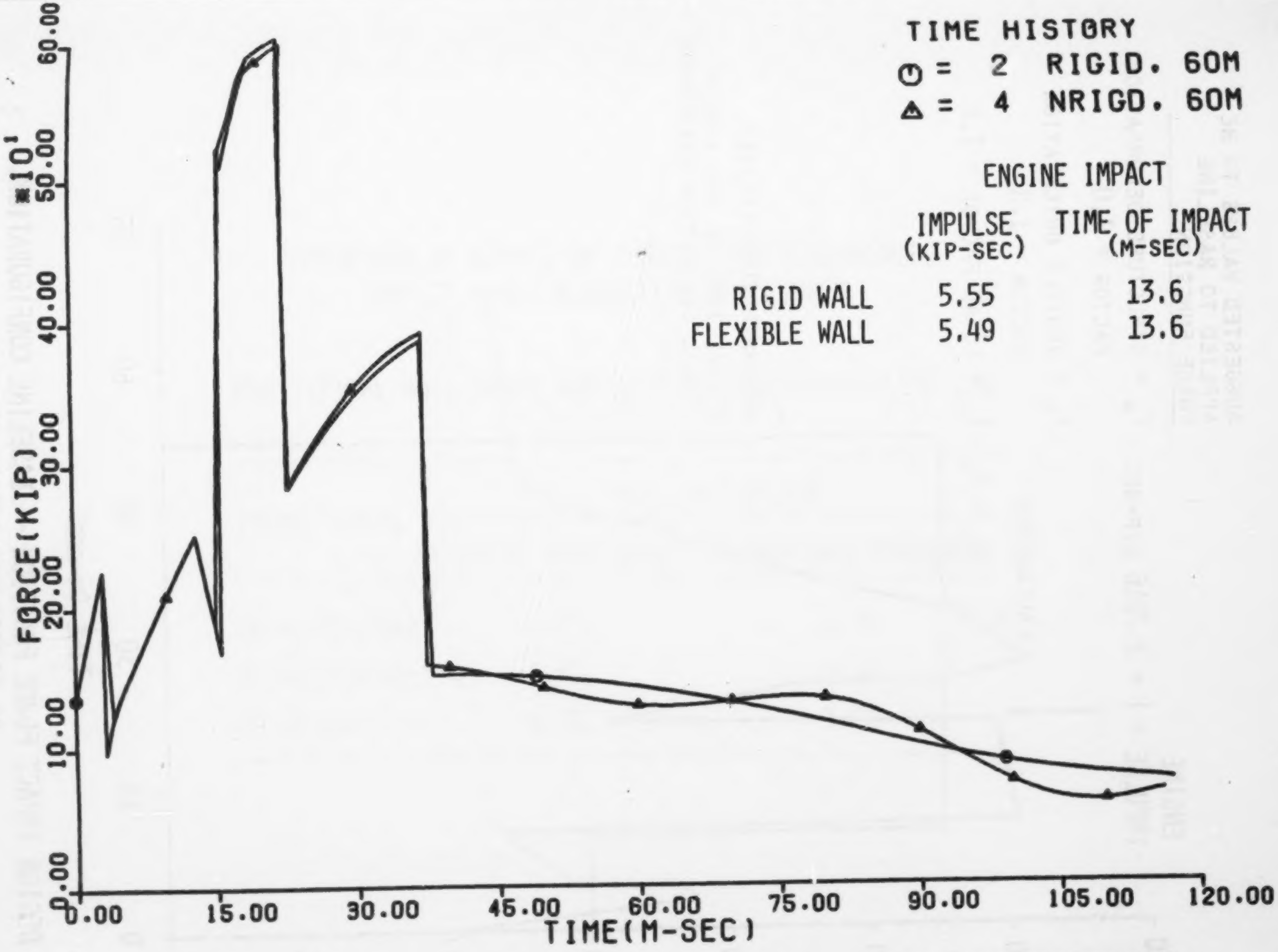

EFFECT OF STRUCTURAL DEFORMATION ON IMPACT FORCE — BASELINE CONFIGURATION,
PLYMOUTH SATELLITE, 60 METERS/SEC

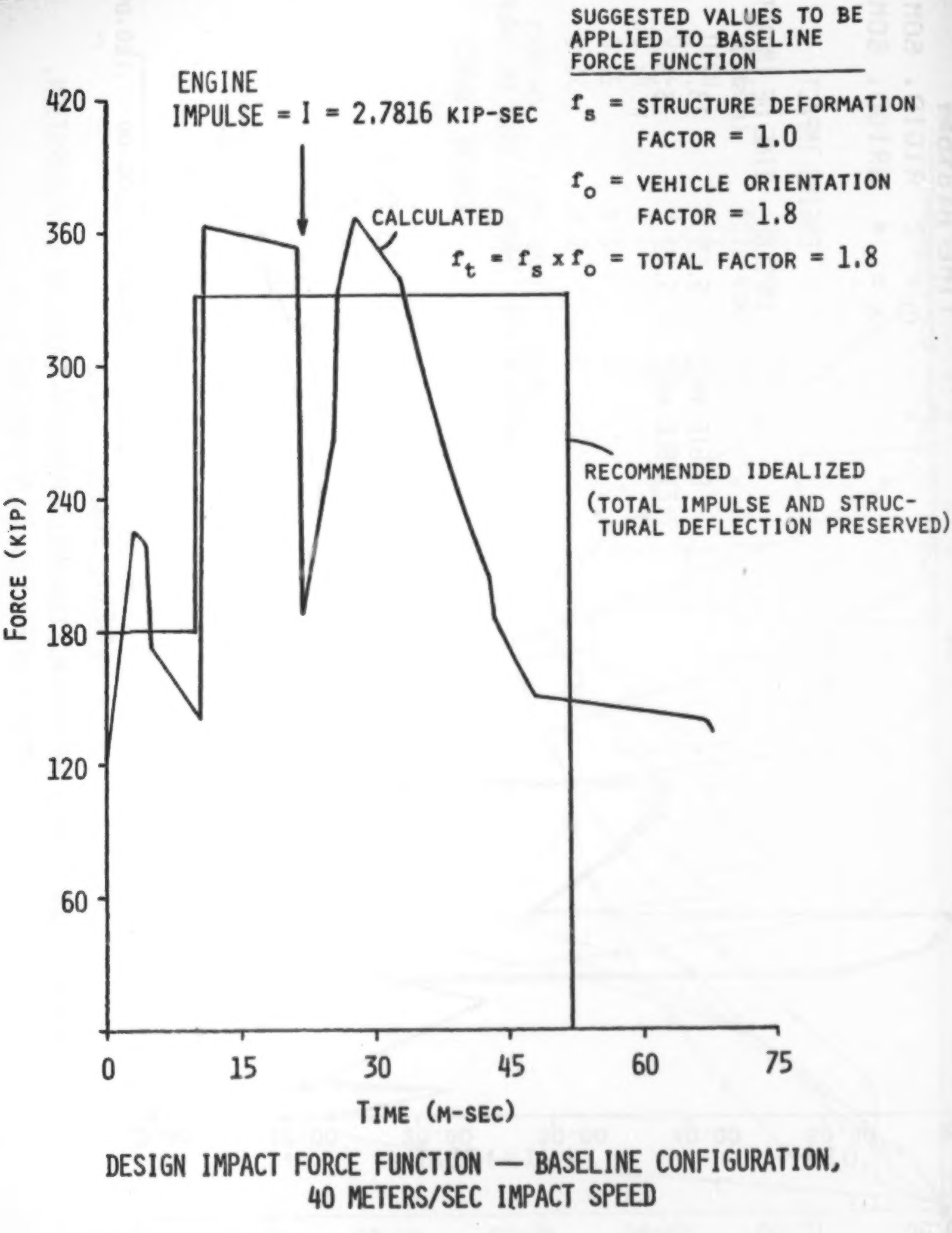

DESIGN IMPACT FORCE FUNCTION — BASELINE CONFIGURATION,
40 METERS/SEC IMPACT SPEED

COMPARISON OF EFFECT OF CURRENT AND RECOMMENDED IMPACT LOAD CALCULATION PROCEDURES

FOR TYPICAL WALL PANEL AND 1973 PLYMOUTH SATELLITE CAR

IMPACT SPEED	WALL DEFLECTION	
	CURRENT PROCEDURE	RECOMMENDED PROCEDURE
20 METERS/SEC	0.29	0.20
40 METERS/SEC	0.82	0.51
60 METERS/SEC	1.70	1.40

OVERVIEW OF NRC PROGRAMS
IN
SEISMOLOGY AND GEOLOGY

Jerry Harbour

1. Objectives

Integrated regional and topical programs in geology and seismology are conducted to improve the bases for reliably predicting the size and recurrence intervals of earthquakes used as design bases in different siting regions. This requires a better understanding of the causes of earthquakes, particularly in the Eastern U.S., and the variables influencing their locations and resultant ground motions. Both field and laboratory studies are included in research on the response of soil foundations to earthquakes. Research on volcanic and other geologic hazards is also included. Because of the continuing reevaluation of existing plants, results from these programs are applicable to operating plant sites as well as to future sites.

2. Organization of Subelements of the Site Safety Research Program

SEISMOLOGY AND GEOLOGY

Regional Studies

- Charleston, South Carolina and the Southeastern U.S.
- Northeastern U.S. and St. Lawrence Valley
- New Madrid, Missouri Region
- Mid-Continent Region (Ouachita Front, Nemaha Ridge)
- Western Ohio (Anna, Ohio)
- Pacific Northwest

Topical Studies

- Geological and Seismological Hazards
  - Stress Measurement and Evaluation
  - Hazards Evaluation
- Geotechnical Engineering and Soils Response

2.1 Regional Studies

Emphasis is placed on regional programs to collect, compile, and synthesize geological, geophysical, and seismological data in the more active regions of the eastern and northwestern U.S. Approximately 200 seismograph stations are deployed in 6 regional networks in the Eastern and Northwestern U.S. These collect records of small shocks (mainly magnitude 2 to 4.5) used (a) to identify areas of seismic energy release, (b) to use in statistical recurrence studies, and (c) to deduce orientation and direction of subsurface faulting and stress fields.

In addition to earthquake monitoring, field studies are conducted to help understand the reasons for localization of earthquakes in these mainly intraplate tectonic environments and to identify geologic features and methods for quantitatively defining earthquake hazards on a regional basis. Activities include examination and mapping of surface geological features, as well as subsurface exploration using geophysical techniques such as aeromagnetism, gravimetry, and active seismic surveying. Borings to depths of a kilometer or more have been made in selected areas and more will be required in the future. Also, offshore seismic reflection profiling has been conducted in some areas off the Atlantic Coast and in the Great Lakes to search for evidence of recent faulting. (This methodology was used to identify and date recency of movement on the Hosgri Fault offshore from Diablo Canyon a few years ago.)

2.2 Topical Studies

While knowledge of earthquake hazards and the methods for their quantitative assessment have improved markedly in the past five years, the general trend has been toward assigning larger, or statistically more frequent, earthquakes in site analyses. Continuation of recent emphasis on probabilistic risk analyses will require not only methodological research to assure proper application to seismic hazard assessment, but also extensive additions to the data base and deterministic studies to verify assumptions and reduce uncertainties in probabilistic models.

Explanatory models of earth crustal processes are being proffered by the earth science community to explain earthquake occurrece in the intraplate regions of the Eastern U.S. These models, or their elements, characteristically are simplified and not universally applicable to all areas. Examples include uniform east-west or northeast-southwest compressive stress, stress accumulation at discontinuities (e.g., hole-in-plate or peg-in-plate analogies), strain reversal on thrust faults and release of residual stress accumulated over long periods of geologic times. While some, or all, of these models may be applicable in some areas, the impact of their direct application to seismic hazard analysis can only continue the trend in upward revision of perceived danger from earthquakes in the relatively quiet Eastern U.S. Development of the unifying geomechanical hypotheses that are needed for adequate assessment of seismic hazards requires extensive surface and subsurface geological and geophysical information like that being gathered in these programs.

The topical studies on seismic hazards are intended to improve methodology for understanding earthquake occurrence and for extrapolating the "maximum" earthquake that can be expected to occur within a region during periods of time longer than the historic record. Current and planned projects will investigate methods of earth stress measurement and definition of stress fields, the possible role of vertical tectonic motions in seismic energy release, the methods for determining earthquake recurrence intervals in different source zones and definition of ground motion intensity at specific sites. The role and importance of reservoir filling in inducing earthquakes and the impact on local seismic hazard will also be investigated.

Topical programs in geology and seismology include the following:

Geological and Seismological Hazards Program
(Earthquake Recurrence Intervals, Earth Stress Measurements, Vertical Crustal Movements, Volcanic Hazards)

Geotechnical Program
(Soil Subsidence and Liquefaction, Influence of Soil and Structures on Strong Motion Accelerograph Records).

3. Relation to Other Programs

Increasing national and international attention to potential seismic hazards has resulted in major increases in programs of other agencies. Under provisions of the Earthquake Hazards Reduction Act of 1977, large programs of fundamental and applied research in earthquake prediction and hazards mitigation have been started in the U.S. Geological Survey and the National Science Foundation.

The Site Safety research program is coordinated with and, to some extent, integrated into these national efforts. Staff members have participated in interagency planning and review sessions to ensure that (a) adequate attention is given to NRC seismic research requirements, (b) research in other agencies and the NRC is complimentary rather than duplicatory, and (c) schedules of other agency research include consideration, when possible, of NRC priorities for accomplishment of specific needs.

To a large extent, these agency goals are accomplished through cooperative funding of different parts of regional programs, such as in the Northeast and in the New Madrid, Missouri earthquake zones, and by direct NRC support of other agency efforts, such as those of the U.S. Geological Survey in the Charleston, South Carolina, region, and of the Corps of Engineers and National Bureau of Standards studies of the liquefaction potential and settlement of soils during earthquake shaking.

SITE SAFETY RESEARCH BRANCH
FUNDING HISTORY FY 1977-84

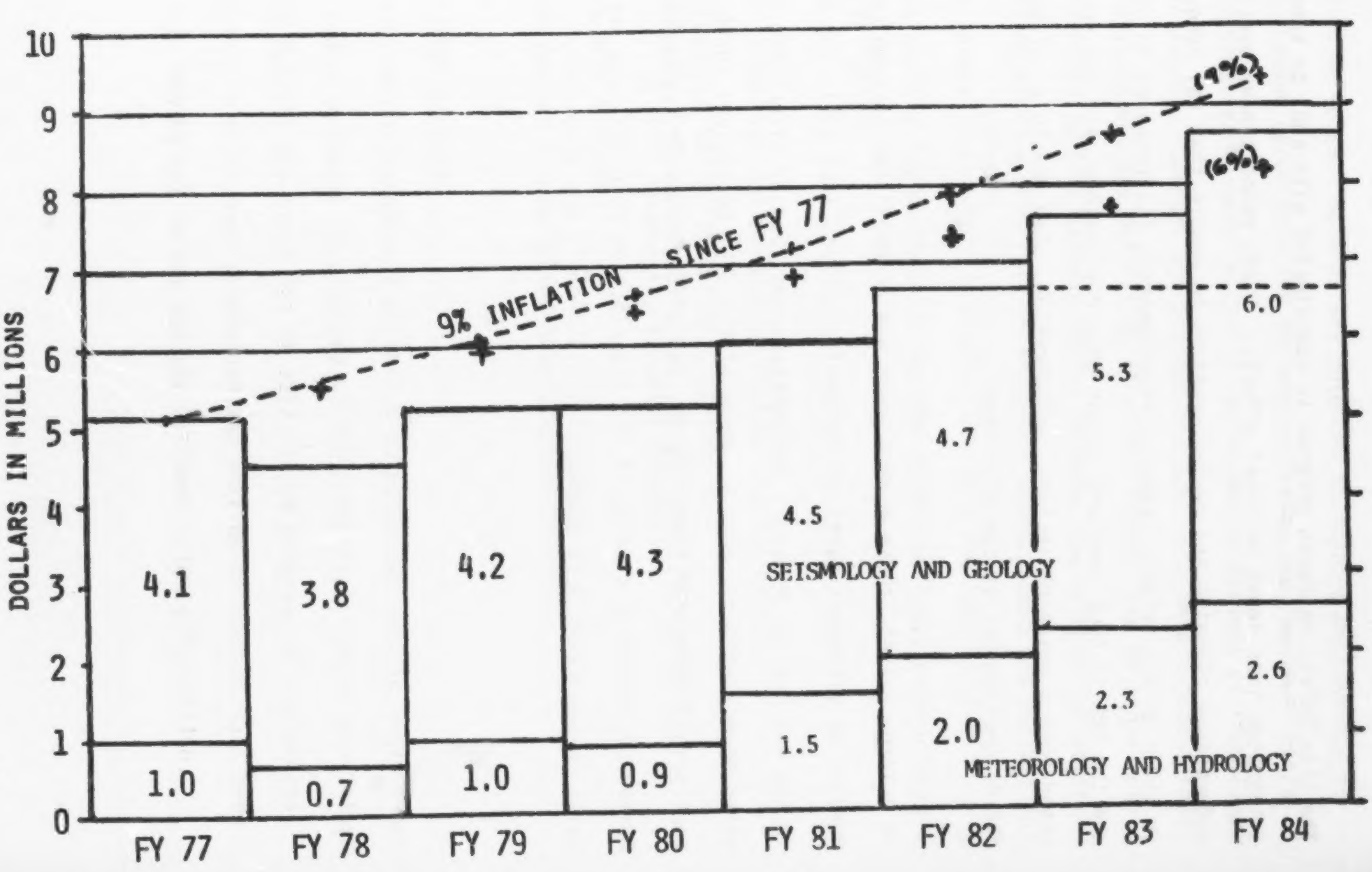

SITE SAFETY RESEARCH BRANCH

DISTRIBUTION OF FUNDS BY CONTRACTOR TYPE (FY-81)

	NUMBER OF CONTRACTS		DOLLARS IN 1,000'S
	24	UNIVERSITIES	$2,495
	13	OTHER FEDERAL AGENCIES	$2,045
	11	STATE AGENCIES	$ 775
	7	COMMERCIAL FIRMS	$ 685
TOTALS:	55		$6,000

Reservoir Induced Seismicity

A Review

presented by

Andrew J. Murphy
U.S. N.R.C., Washington, D.C.

This presentation is a review of the state of knowledge about Reservoir Induced Seismicity (RIS). A considerable number of papers have been reviewed in preparing this presentation, but I have drawn heavily from five papers, three by David Simpson, one by M. Lee Bell and Amos Nur, and the last by a group of Woodward Clyde Consultants, headed by Duane Packer. Full bibliographic data are provided.

Table 1 is an outline of the presentation.

ABSTRACT

The Nuclear Regulatory Commission (NRC) has an active interest in the phenomenon of Reservoir Induced Seismicity. This interest is the direct result of the often intimate relationship between nuclear power plants and the use of man-made reservoirs or rivers with man-made reservoirs on them, as a source of cooling water. (There are two plants in the eastern United States where the problem of a reservoir built as a source of cooling water is being studied: one is the V. C. Summer plant in South Carolina where numerous microearthquakes have been recorded over a 3.5 year recording period, and the other is Shearon Harris plant in North Carolina where no local microearthquakes were recorded from Sept. 1977 to the end of 1979. The Oconee power plants are downstream from Lake Jocassee which is inducing earthquakes in the vicinity of the lake.)

The topic of RIS is introduced by defining RIS as a change in the natural, background seismicity that is induced by a reservoir. Figure 1 is a map compiled by Packer, et al., (1979) showing the locations of known cases of RIS and their relationship with world-wide seismicity. RIS, particularly on the microearthquake scale, may begin any time after impoundment starts. Simpson (1976), observed that with the exception of one case, the major earthquakes ($M \geq 5$) that were induced by reservoirs had delay times (impounding-to-earthquakes) at least as long as the precursory time predicted by the diffusion model of Scholz, et al., 1973 (Figure 2).

The number of documented cases of RIS currently exceeds 45, Table 2, (Packer, et al., 1980). The list of cases includes a) changes in seismicity with the largest earthquake to date greater than magnitude 5, such as Kariba and Koyna, b) changes in seismicity with the largest earthquake to date between magnitudes 3 and 5, such as Kurobe, Clark Hill and Jocassee, and c) changes in the level of microseismicity (largest event less than about magnitude 3), such as Monticello, Shasta and Kamafusa. To this list we must add the cases of transient changes in seismicity such as Qued Fodda and the cases of decreases in the level of seismicity such as Tarbela.

A static load/pore pressure model of stresses associated with reservoirs was formulated by Snow, 1972, and developed further by Simpson (1976) and by Bell and Nur (1978). The model describes the stress patterns associated with the three basic fault types; normal, strike-slip, and thrust faults, and considers the theoretical stability of the three fault types in the presence of the static load and pore pressure conditions produced by a reservoir (Figures 4 and 5).

1. Bell, M.L., A. Nur: Strength Changes Due to Reservoir-Induced Pore Pressure and Stresses and Applications to Lake Oroville, Journal of Geophysical Research, Vol. 83, No. B9, p. 4469-4483, 1978.

2. Packer, D., L.S. Cluff, P.L. Knuepfer, R.J. Withers: Study of Reservoir Induced Seismicity, Final Technical Report of USGS Contract No. 14-08-0001-16809, 1979.

3. Scholz, C.H., L.R. Sykes, and Y.P. Aggarwal: Earthquake Prediction: A Physical Basis Science, 181, p. 803-810, 1973.

4. Simpson, D.W.: Seismicity Changes Associated with Reservoir Loading, Engineering Geology, 10, p. 123-150, 1976.

5. Simpson, D.W.: Load, Pore Pressure and Reservoir Stability, in preparation, 1980.

6. Simpson, D.W., and S. Kh. Negmatullaer: Induced Seismicity at Nurek Reservoir, Tadjikistan, USSR, in preparation, 1980.

7. Snow, D.T.: Geodynamics of Seismic Reservoirs. Proceedings, Symposium on Percolation through Fissured Rocks. Dtsch. Ges. Evd-Grundbau, Stattgart, T2-J: 1-19, 1972.

Figure 1 and Table 2 after Packer, et al., 1979.

Figures 2-5 after Simpson, et al., 1976.

RESERVOIR INDUCED SEISMICITY

RIS

A. INTRODUCTION

THE WHAT, WHERE, AND WHEN OF RIS.

B. DOCUMENTED CASES OF RESERVOIR INDUCED CHANGES IN SEISMICITY

- A. MAJOR SEISMICITY
- B. MINOR SEISMICITY
- C. MICROSEISMICITY
- D. TRANSIENT CHANGES
- E. DECREASES
- F. QUESTIONABLE CASES

C. CHARACTERISTICS OF RIS

D. MECHANISM

- A. SNOW
- B. SIMPSON
- C. BELL & NUR

E. PREDICTION -

- A. DETERMINATION OF POTENTIAL
- B. ESTIMATING SIZE AFTER IMPOUNDMENT

F. AVENUES FOR RESEARCH

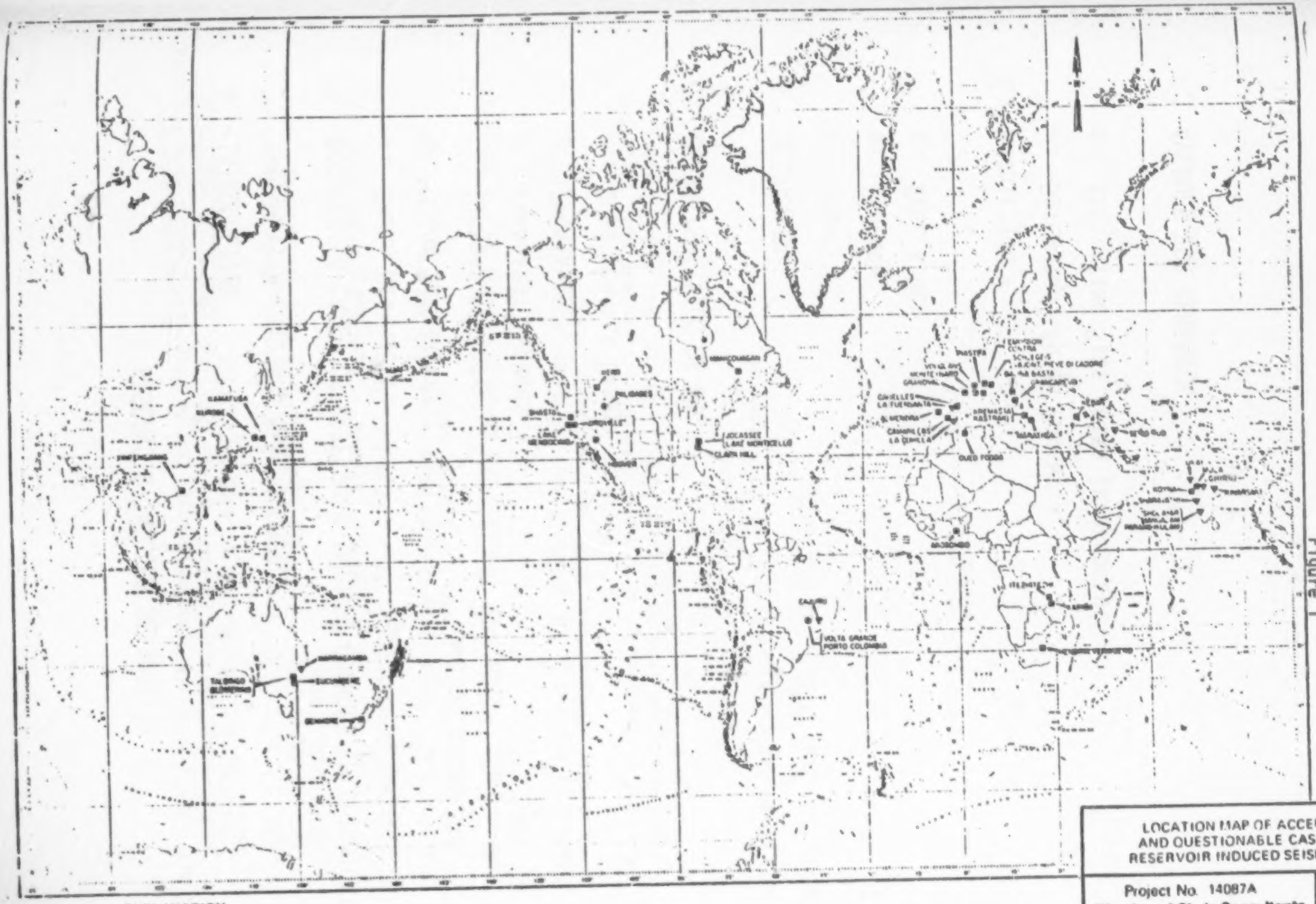
KAMAFUSA
KUROBE
SHASTA
ORVILLE
LAKE MENDOCINO
PALISADES
MANICOUAGAN
JOCASSEE
LAKE MONTICELLO
CLARK HILL
MONTEYNARD
GRANDVAL
CANELLES
LA FUENSANTA
EL GRADO
CAMARILLAS
LA CUHILLA
KREMASTA
KASTRAKI
MARATHON
VAJONT
PIEVE DI CADORE
OUED FODDA
KOYNA
KARIBA
VOLTA GRANDE
PORTO COLOMBIA
CAJURU
TALBINGO
EUCUMBENE
BENMORE

Figure 1

EXPLANATION

■ Accepted case of RIS ▼ Questionable case of RIS

Source: Base map from USGS World Seismicity Map, 1974

LOCATION MAP OF ACCEPTED
AND QUESTIONABLE CASES O
RESERVOIR INDUCED SEISMICIT

Project No. 14087A
Woodward-Clyde Consultants

Fig
P

Table 2

TABLE 1-1

REPORTED CASES OF RESERVOIR INDUCED SEISMICITY

No.*	Dam Name, Reservoir Name	Country	Classification of RIS	Magnitude Largest RIS Event
1.	Akosombo Main, Lake Volta	Ghana	Accepted, macro	Intensity V
2.	Almendra, Tormes Reservoir	Spain	Accepted, micro	less than 2
3.	Bajina Basta	Yugoslavia	Accepted, micro	less than 3
4.	Benmore	New Zealand	Accepted, macro and micro	5 (?)
5.	Blowering	Australia	Accepted, macro and micro	3.5
6.	Cabin Creek	USA	Not RIS	—
7.	Cajuru	Brazil	Questionable	approx. 4
8.	Camarillas	Spain	Accepted, macro	4.1
9.	Canelles	Spain	Accepted, macro	4.7
10.	Clark Hill	USA	Accepted, micro (macro?)	4.3 (?)
11.	Contra, Lake Vogorno	Switzerland	Accepted, micro	less than 3
12.	Coyote Valley, Lake Mendocino	USA	Accepted, macro	5.2
13.	El Grado	Spain	Not RIS	—
14.	Emosson	Switzerland	Accepted, micro	less than 3
15.	Eucumbene	Australia	Accepted, macro	~5 (?)
16.	Fairfield, Lake Monticello	USA	Accepted, micro	2.8
17.	Ghirni	India	Questionable	—
18.	Grancarevo	Yugoslavia	Accepted, micro	less than 3
19.	Grandval	France	Accepted, macro and micro	Intensity V
20.	Hendrik Verwoerd	South Africa	Accepted, micro	less than 2
21.	Hoover, Lake Mead	USA	Accepted, macro and micro	5.0
22.	Itezhitezhi	Zambia	Accepted, macro	4 or less (?)
23.	Jocassee	USA	Accepted, macro and micro	3.2
24.	Kamafusa	Japan	Accepted, micro	less than 3
25.	Kariba	Zambia/Rhodesia	Accepted, macro and micro	6.25
26.	Kastraki	Greece	Accepted, macro	4.6
27.	Keban	Turkey	Accepted, micro	less than 3
28.	Kerr, Flathead Lake	USA	Accepted, macro	4.9
	Kinnersani	India	Questionable	—
29.	Koyna, Shivaji Sagar Lake	India	Accepted, macro and micro	6.5
30.	Kremasta	Greece	Accepted, macro and micro	6.3
31.	Kurobe	Japan	Accepted, macro and micro	4.9
32.	La Cohilla	Spain	Questionable	—
33.	La Fuensanta	Spain	Questionable	—
34.	Mangalam	India	Questionable	—
35.	Mangla	Pakistan	Not RIS	—
36.	Manicouagan 3	Canada	Accepted, macro and micro	4.1
37.	Marathon	Greece	Accepted, macro	5.75
38.	Mica	Canada	Not RIS	—
39.	Monteynard	France	Accepted, macro	Intensity VII
40.	Mula	India	Accepted, micro	less than 1
41.	Nurek	USSR	Accepted, macro and micro	~4.5
42.	Oroville	USA	Accepted, macro	5.7
43.	Oued Fodda	Algeria	Accepted, micro	less than 3
44.	Palisades	USA	Accepted, micro	~3.7 (?)
45.	Parambikulam	India	Questionable	—
46.	Piastra	Italy	Accepted, macro and micro	~4.4
47.	Pieve di Cadore	Italy	Accepted, macro and micro	~Intensity V
48.	Porto Colombia	Brazil	Accepted, macro	—
49.	Rocky Reach	USA	Not RIS	—
50.	San Luis	USA	Not RIS	—
51.	Sanford	USA	Not RIS	—
52.	Schlegeis	Austria	Accepted, micro	less than 2
53.	Sefid Rud	Iran	Questionable	4.7
	Sharavathi	India	Questionable	—
54.	Shasta	USA	Accepted, micro	less than 3
55.	Sholayar	India	Questionable	—
56.	Talbingo	Australia	Accepted, macro and micro	~3.5
57.	Ukai	India	Questionable	—
58.	Vajont	Italy	Accepted, micro	less than 3
59.	Volta Grande	Brazil	Accepted, macro	~less than 4
60.	Vouglans	France	Accepted, macro	~4.4
61.	Warragamba, Lake Burragorang	Australia	Questionable	5.4
62.	Xinfengjiang	China	Accepted, macro and micro	6

*Numbers correspond to numbers on Figure 1-2; Kinersani and Sharavathi are unplotted because of insufficient data.

Figure 2

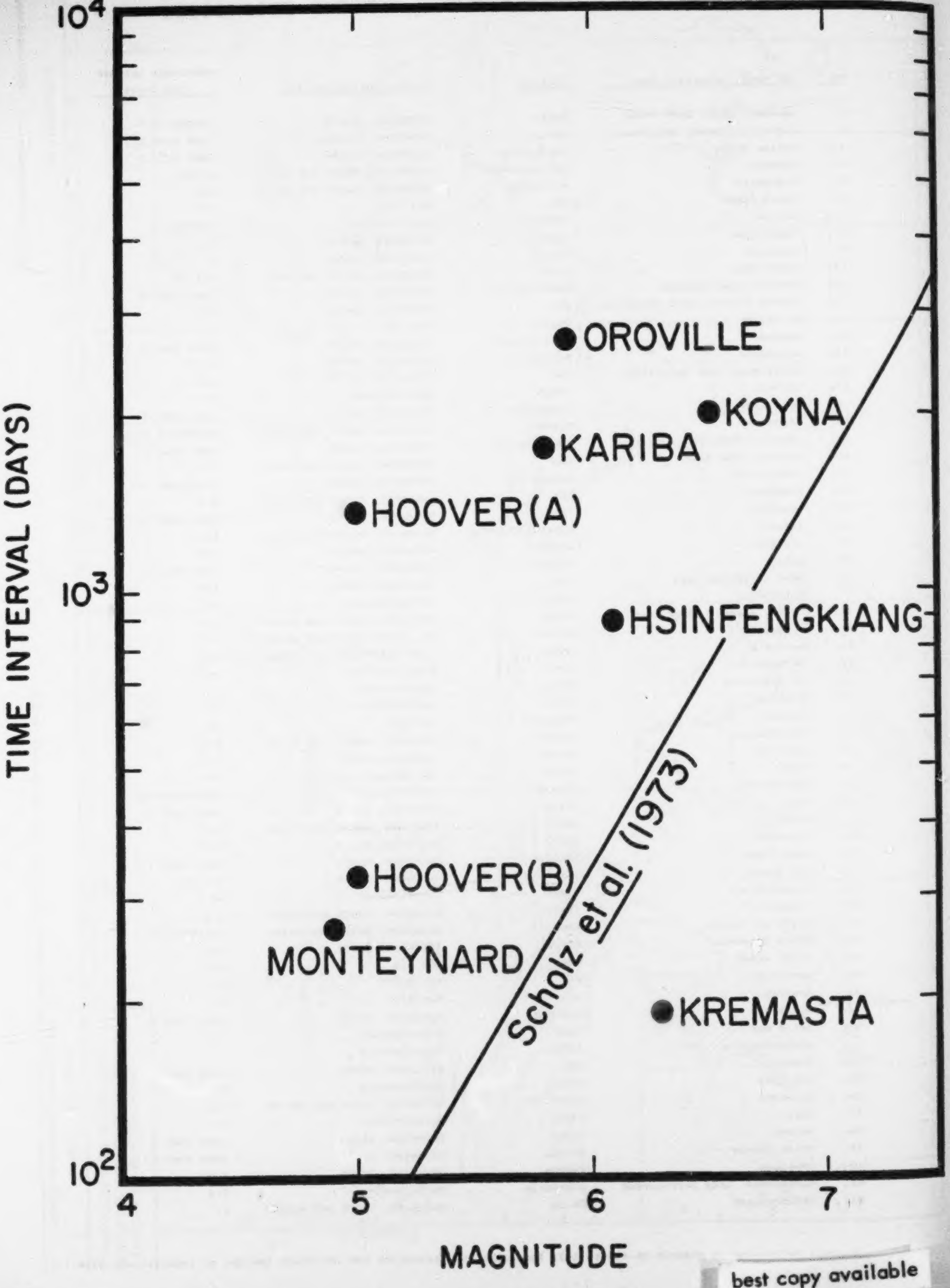

best copy available

Figure 4

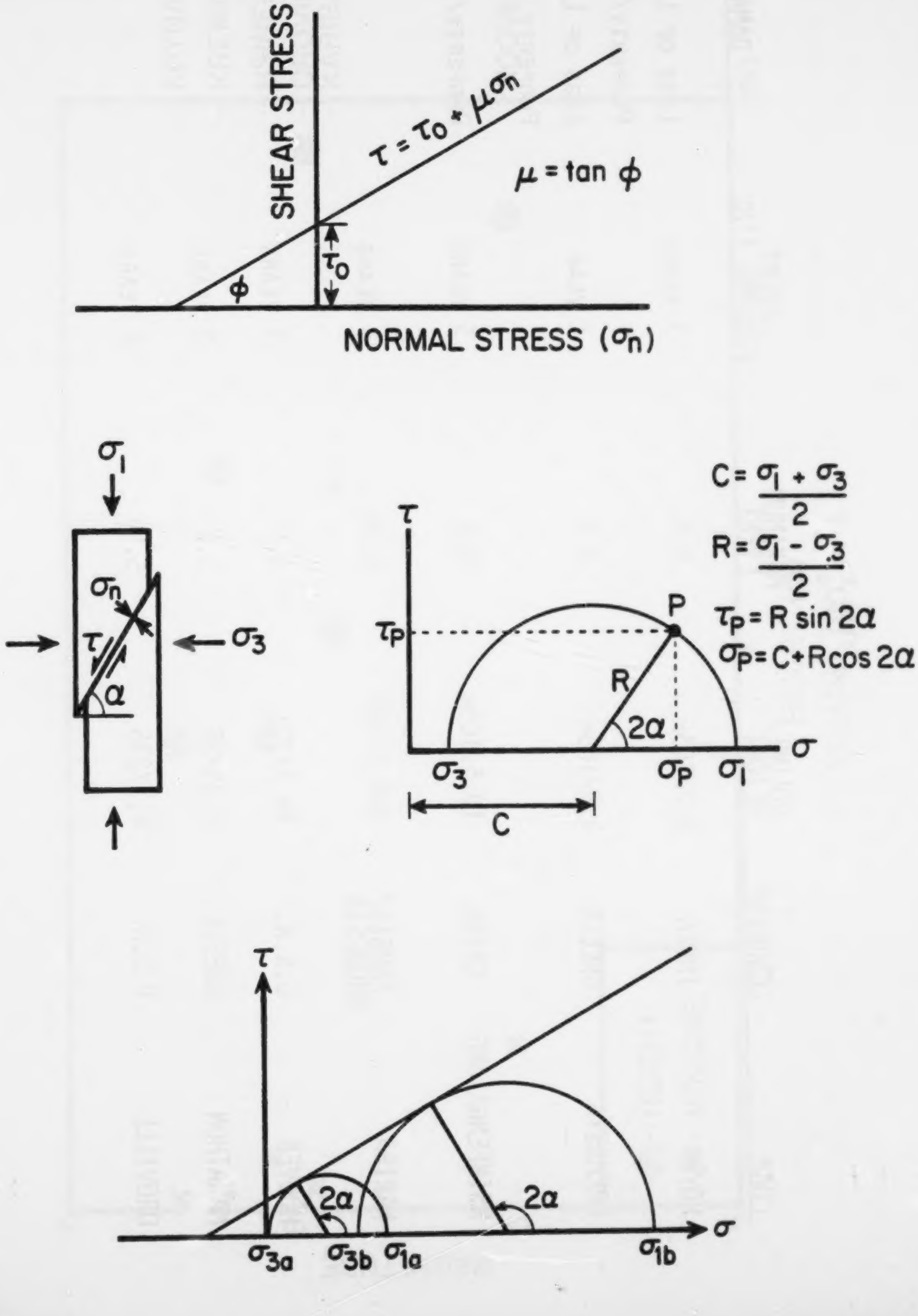
SHEAR STRESS (τ)
τ = τ0 + μσn
μ = tan φ
φ
τ0
NORMAL STRESS (σn)
σ1
σn
τ
α
σ3
C = (σ1 + σ3)/2
R = (σ1 - σ3)/2
τP = R sin 2α
σP = C+Rcos 2α
τ
P
τP
R
2α
σ
σ3
σP
σ1
C
τ
2α
2α
σ
σ3a
σ3b
σ1a
σ1b

Table 3

DAM	COUNTRY	VOLUME/ HEIGHT	MAXIMUM EVENT	EVENT FILLING TIME	DAMAGE
KOYNA	INDIA	2.7/103m	6.5	3 years	Loss of Life Property/Dam
KREMASTA	GREECE	4.8/165m	6.3	1 year	Loss of Life Property
HSINFENGKIANG	CHINA	10.5/105m	6.0	3 years	Property/Dam
KARIBA	ZAMBIA/ RHODESIA	160.3/128	6.25	4 years	
HOOVER	U.S.A.	36.7/221	5.0	3 years	
MARATHON	GREECE	0.04/63	5.75	8 years	
OROVILLE	U.S.A.	4.3/236	5.9	8 years	

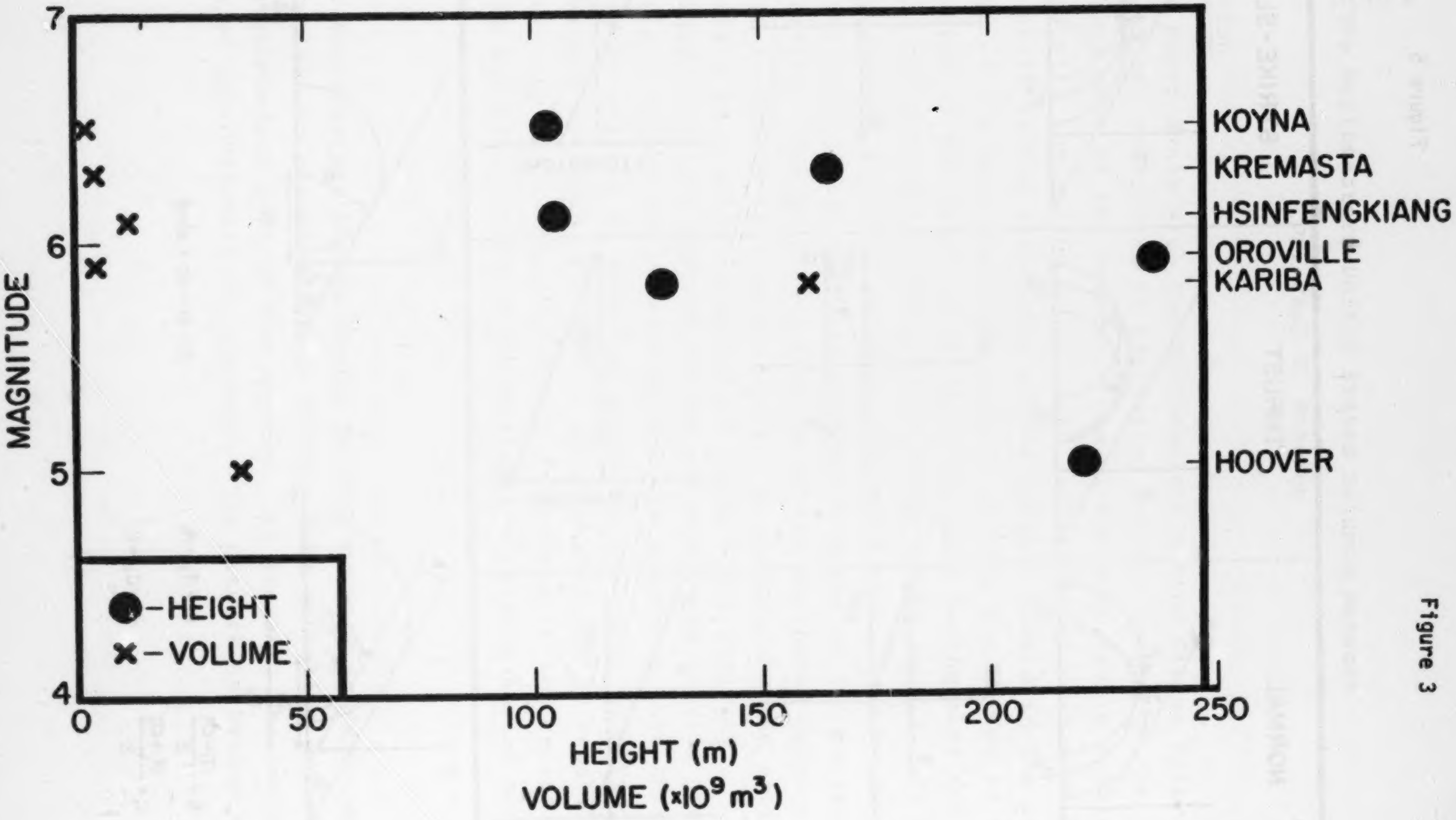
7
6
5
4
MAGNITUDE
0
50
100
150
200
250
HEIGHT (m)
VOLUME (×10^9 m^3)
KOYNA
KREMASTA
HSINFENGKIANG
OROVILLE
KARIBA
HOOVER
● - HEIGHT
× - VOLUME

Figure 3

Figure 5

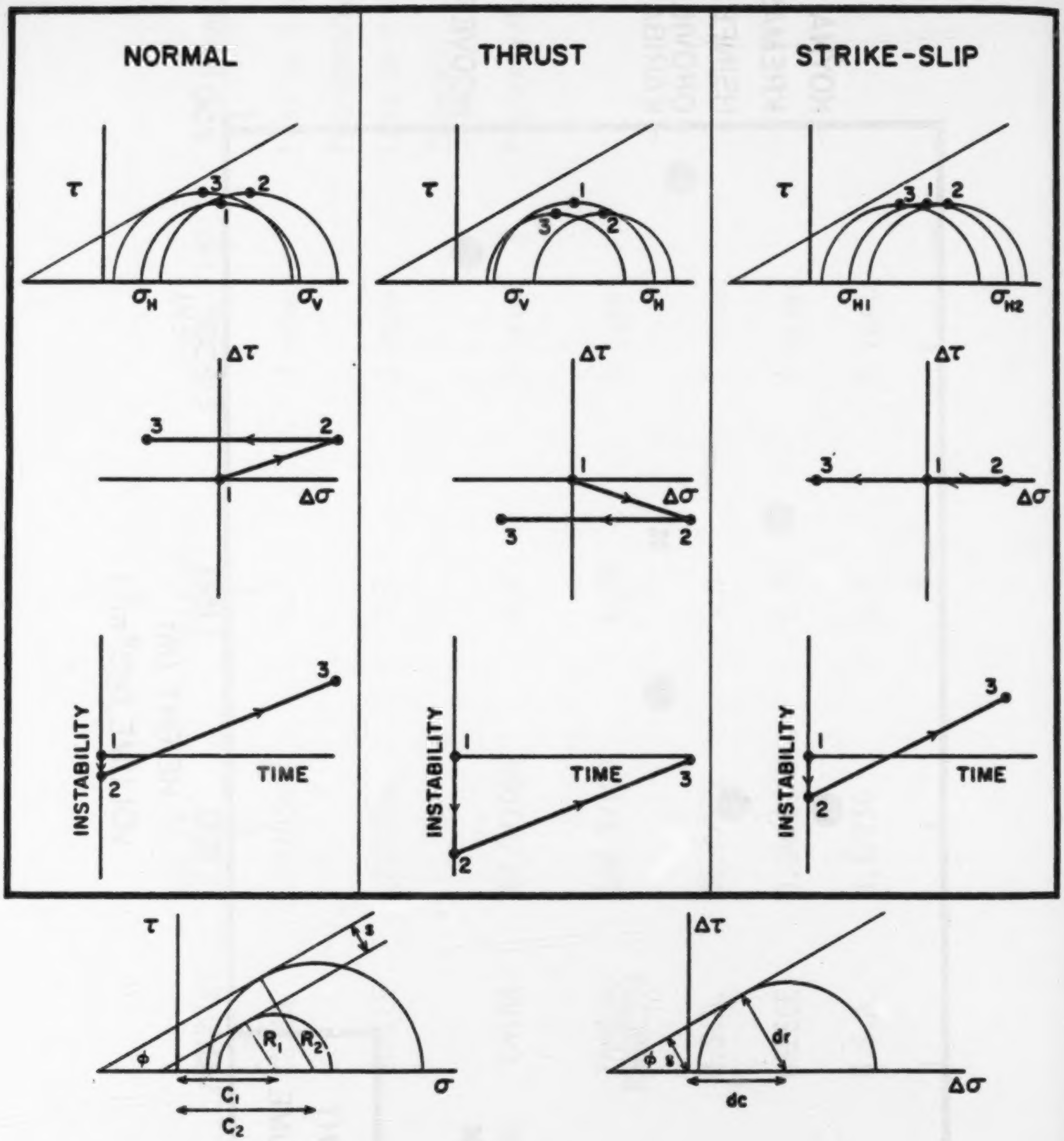
NORMAL
THRUST
STRIKE-SLIP
τ
σ_H
σ_V
σ_{H1}
σ_{H2}
1
2
3
Δτ
Δσ
INSTABILITY
TIME
s
φ
R_1
R_2
C_1
C_2
σ
dr
dc

$R = \dfrac{\sigma_1 - \sigma_3}{2}$

$C = \dfrac{\sigma_1 + \sigma_3}{2}$

$dr = R_2 - R_1$

$dc = C_2 - C_1$

$S = dr - dc = \sin\phi$

The Northeastern United States Seismic Network

Dr. Paul W. Pomeroy

Introduction

This paper deals with the Northeastern United States Seismic Network and its usefulness in evaluating seismic hazard in the northeastern part of the country. One of the most severe problems associated with the siting of critical facilities in this area has been and still is the evaluation of the seismic hazard in the region. One of the most important aspects of this evaluation is the determination of the location of large historic earthquakes and, of course, the potential locations of large future events. It has been demonstrated in other parts of the world that, in some cases, present day small scale activity delineates areas of future large scale activity. The principal purpose of the Northeast Seismic Network is to precisely locate present day microearthquake activity, and to relate that activity to future large scale activity.

Another important purpose of the network is to provide precise locations and mechanisms of microearthquake events so that these events may be related to specific causative geologic, geophysical or topographic features. If such a relationship can be established, future activity can be geographically restricted to the causative structures and more realistic evaluations of seismic hazard can be achieved.

Network

The Northeastern United States Seismic Network (NEUSSN) was formed in 1975 to promote uniform seismic data gathering activities in the northeastern part of the country. At present, the network consists of approximately 95 stations. The network is broken up into sub-networks operated by Weston Observatory of Boston College, the Massachusetts Institute of Technology, the Lamont-Doherty Geological Observatory of Columbia University, Pennsylvania State University and the Delaware Geological Survey. Southern New Hampshire stations are recorded at MIT while most of the remainder of the New England stations record at Weston. New York, New Jersey and some Vermont stations are recorded at Lamont. Pennsylvania stations are recorded at Penn State and Delaware stations at the Delaware Geological Survey. An overall map of the network is presented in Figure 1.

An important international cooperative program partially funded by the NRC is carried out by the Department of Energy, Mines and Resources in Canada. Under this program, a total of sixteen digital stations located throughout eastern Canada are being installed. Data is exchanged routinely between the Canadian network and the NEUSSN operators. All earthquakes occuring within 100 km of the international border are located and published by both groups. Data from utility operated networks, particularly the Consolidated Edison Ramapo Fault network are an important component of the Northeast Network.

Records are read daily at each sub-network center daily and information of interest is exchanged routinely with other network operators, as well as the National Earthquake Information Service. In the event of a significant event, over twenty portable microearthquake monitoring units are available for deployment in aftershock studies. For temporary but longer term studies, two 12 element digital recording monitoring systems are available to the network operators.

Data

Data from all the sub-networks are sent to the Weston Observatory which publishes quarterly bulletins of the NEUSSN group. A map showing typical seismicity during the three month period October through December 1979 is presented in Figure 2.

Results

A. Seismicity

Data from the northeast network for the period October 1975 to December 1979 are presented in Figure 3. These microearthquake results for a 4^+ year period can be compared and contrasted with those for larger events presented in Figure 4 for the period 1928 to 1959--a thirty year period and those in Figure 5 for the period 1534 to 1959--a four hundred twenty-five year period. Three important points should be made:

1. In a gross sense, the patterns of seismicity observed in the last four years are approximately the same as those of the thirty year period and the four hundred^+ year period. Thus, the microearthquakes are providing a picture of earthquake occurrence similar to that of the larger historic events. There are however, important exceptions to this general statement.
2. In the Attica, New York region, there is no evidence of earthquake activity prior to 1929 (contrast Figure 4 with Figure 6--the same map for the period 1534 to 1928). Yet, on August 14, 1929, an intensity VIII earthquake caused considerable damage in this region and sporadic activity is continuing at the present time. Although there is no way to determine if microearthquake activity was occuring in this region prior to 1929, any estimate of seismic hazard for this region would have changed remarkably between 1928 and 1930.
3. In the Boston, Massachusetts area, considerable seismic activity is apparent on the maps of historical seismicity (Figures 5 and 6) yet very little activity is present in the region during the period 1928 to 1959 (Figure 5) or in recent years (Figure 3). Thus, formerly active areas can be relatively aseismic over periods of thirty years or more.

B. Geological

Major geological and geophysical studies, funded by the NRC, are being carried out under a concomitant program entitled New England Seismotectonic Study. This program, involving a number of investigations at different institutions throughout New England and New York, has made many important contributions to the understanding of the occurrence of the intraplate earthquakes in this region.

Another study, also funded by the NRC, has analyzed the statistical association of earthquakes with any geologic or geophysical phenomena in this region that have been suggested as possible causative or at least geographically associated with the earthquakes. No single variable or combination of variables appear to explain the seismicity patterns as presently observed but further regional investigations are required to resolve the possible associations.

Examples of the use of seismic data in these studies are presented in Figures 7, 8 and 9. Figure 7 is a cumulative plot of the seismicity since 1534 to the present. Figure 8 is a plot of the frequency of occurrence of earthquakes and Figure 9 is a plot of cumulative strain release--all for the Northeastern United States.

Conclusions

The operation of the Northeastern United States Seismic Network has provided a valuable data source for investigations of causative relationships between earthquakes and known or postulated geologic and geophysical phenomena. As in the New Madrid case, to be discussed by the following speaker, more detailed work and continued network operations are required to delineate causative geologic structures.

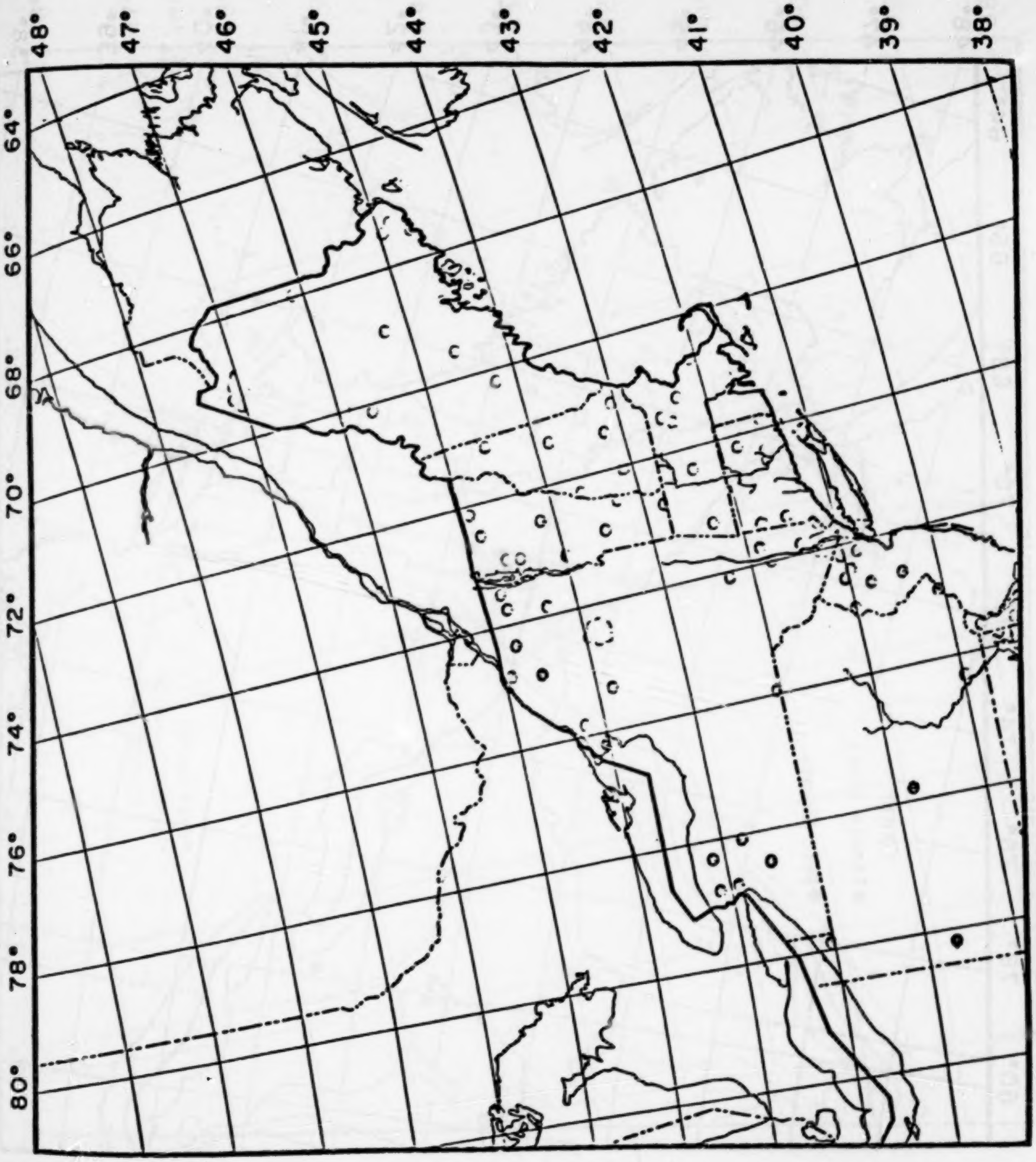
48°
47°
46°
45°
44°
43°
42°
41°
40°
39°
38°
64°
66°
68°
70°
72°
74°
76°
78°
80°

Figure 1. Seismic Stations operating during the period October-December, 1979.

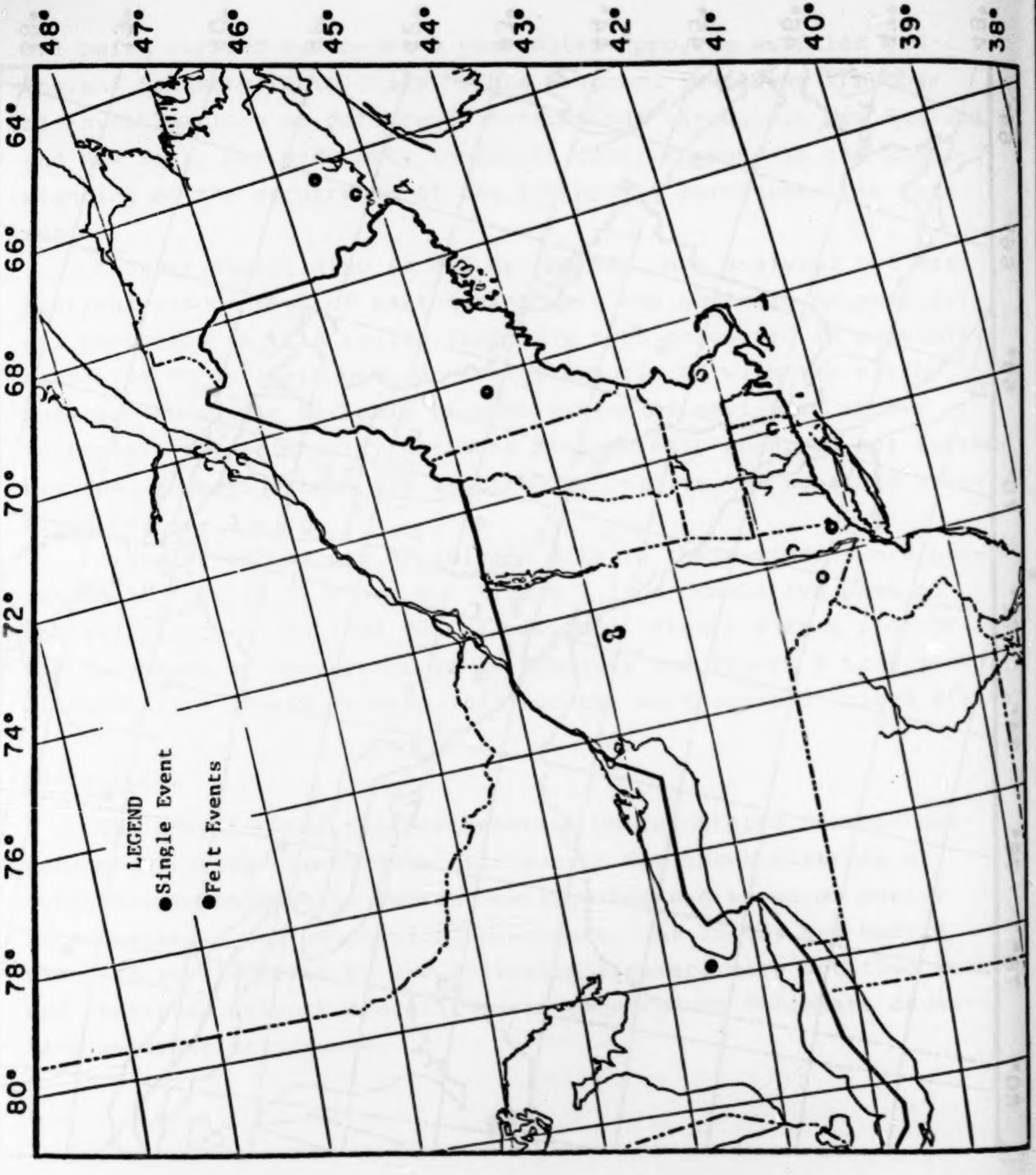
48°
47°
46°
45°
44°
43°
42°
41°
40°
39°
38°
64°
66°
68°
70°
72°
74°
76°
78°
80°
LEGEND
● Single Event
● Felt Events
3

Figure 2. Earthquake epicenters during period October - December, 1979.

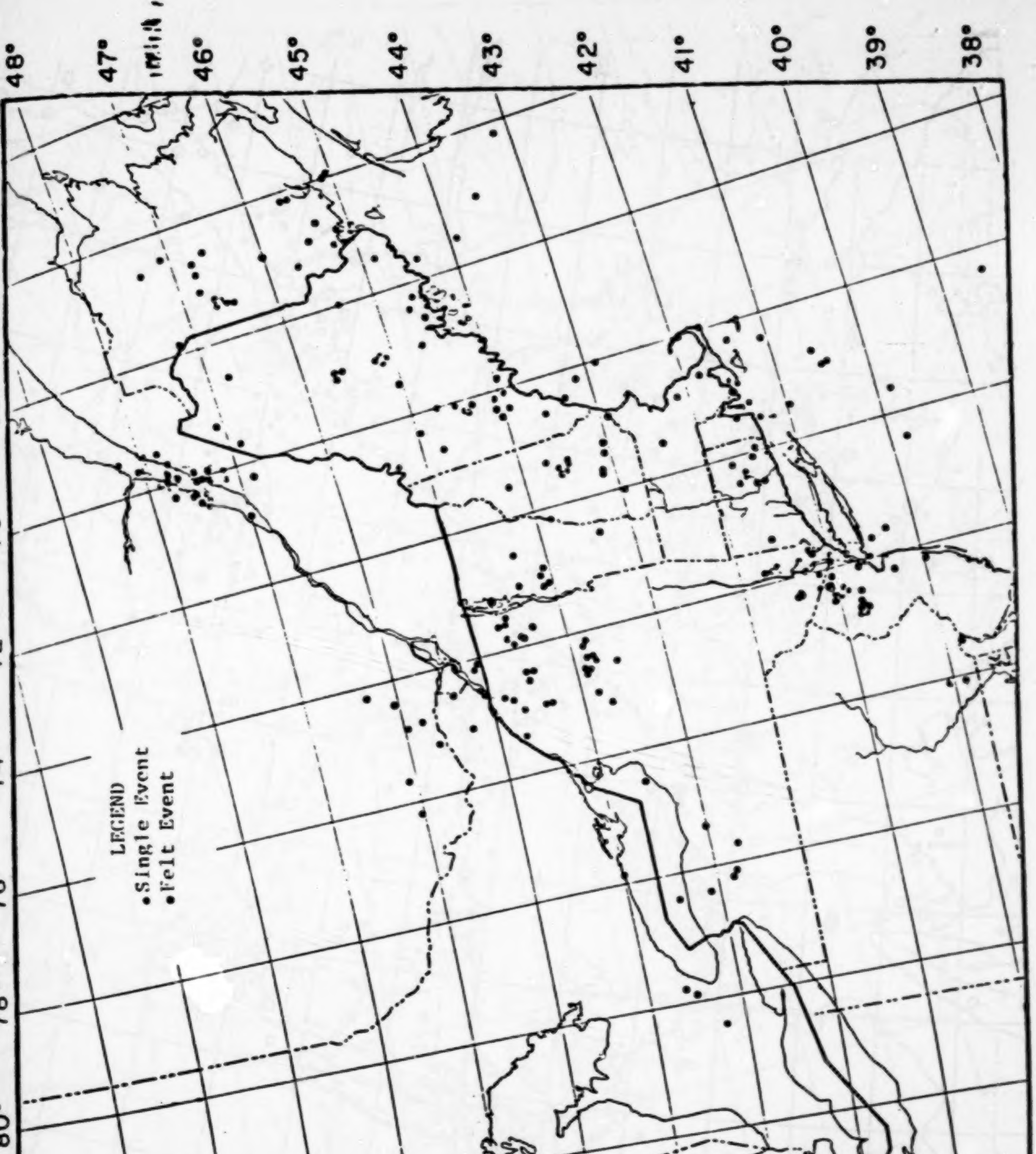
48°
47°
46°
45°
44°
43°
42°
41°
40°
39°
38°
64°
66°
68°
70°
72°
74°
76°
78°
80°
LEGEND
•Single Event
•Felt Event

Figure 3. Earthquake epicenters during the period October 1975 - December, 1979.

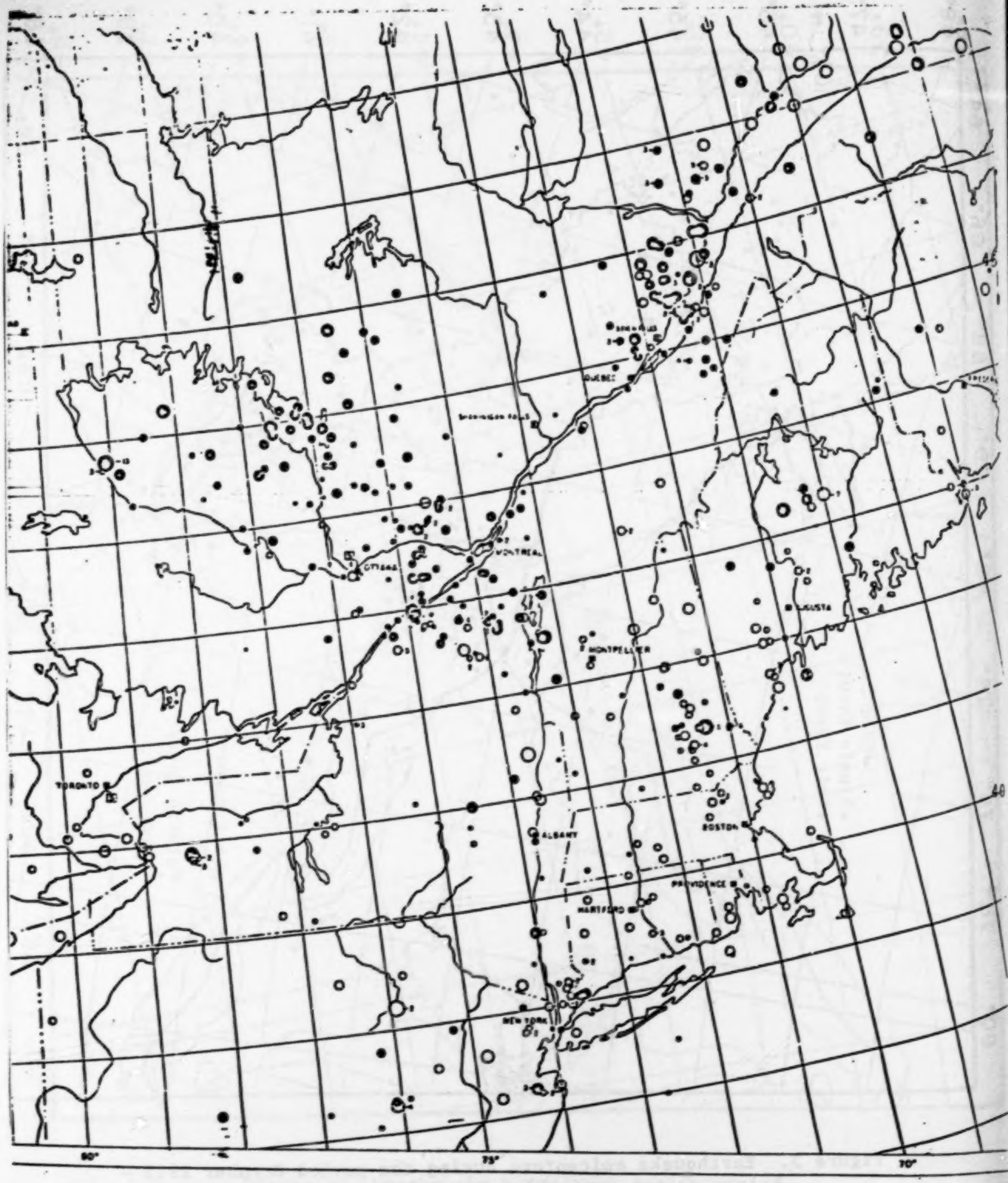

45
40
80°
75°
70°
TORONTO
OTTAWA
MONTREAL
QUEBEC
SHAWINIGAN FALLS
MONTPELIER
AUGUSTA
BOSTON
ALBANY
PROVIDENCE
HARTFORD
NEW YORK

Figure 4. Earthquakes of Northeastern North America, 1928 - 1959

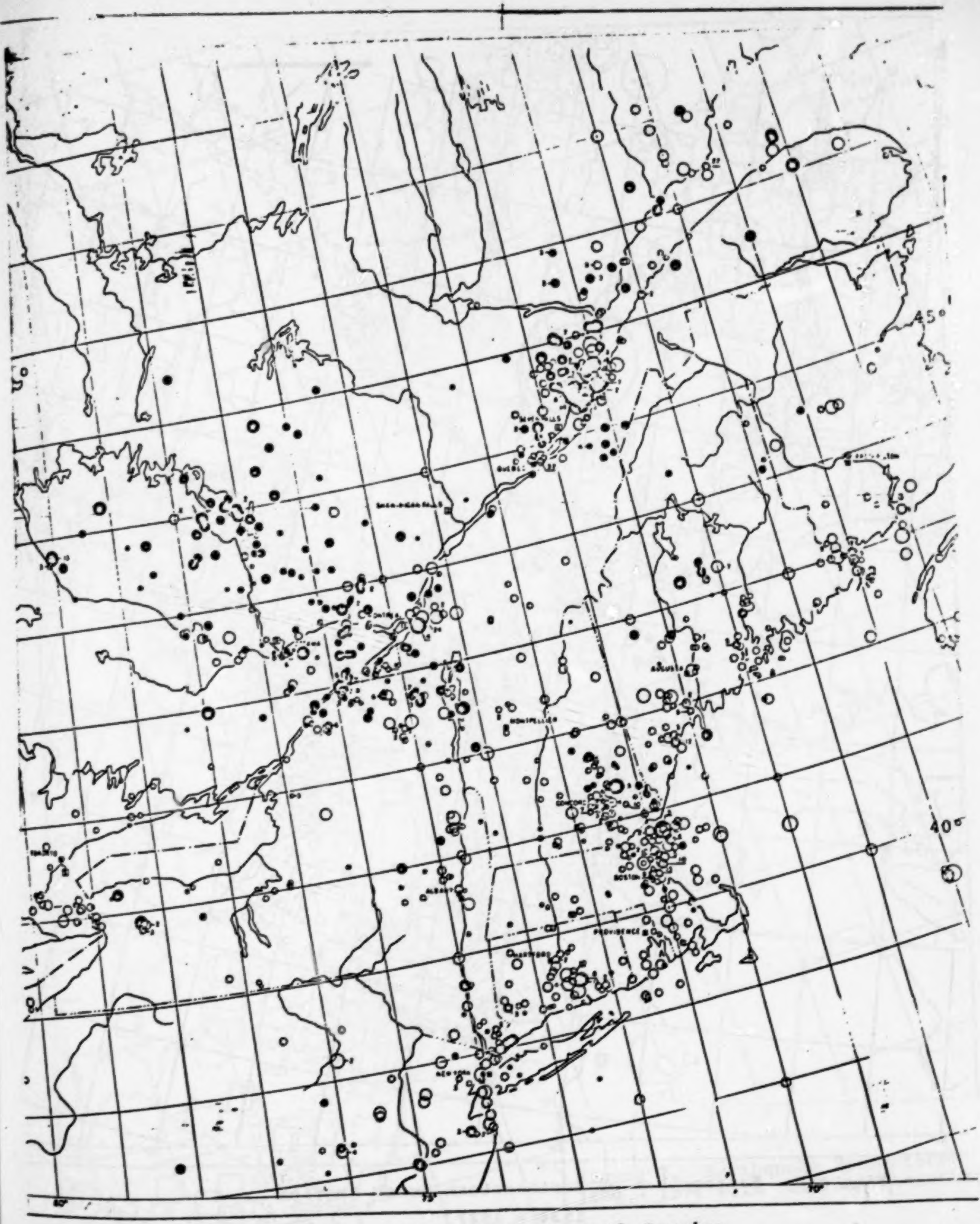
45°
40°
PROVIDENCE
BOSTON
NEW YORK
ALBANY
MONTPELIER
AUGUSTA
80°
75°
70°

Figure 5. Earthquakes of Northeastern North America 1534 - 1959

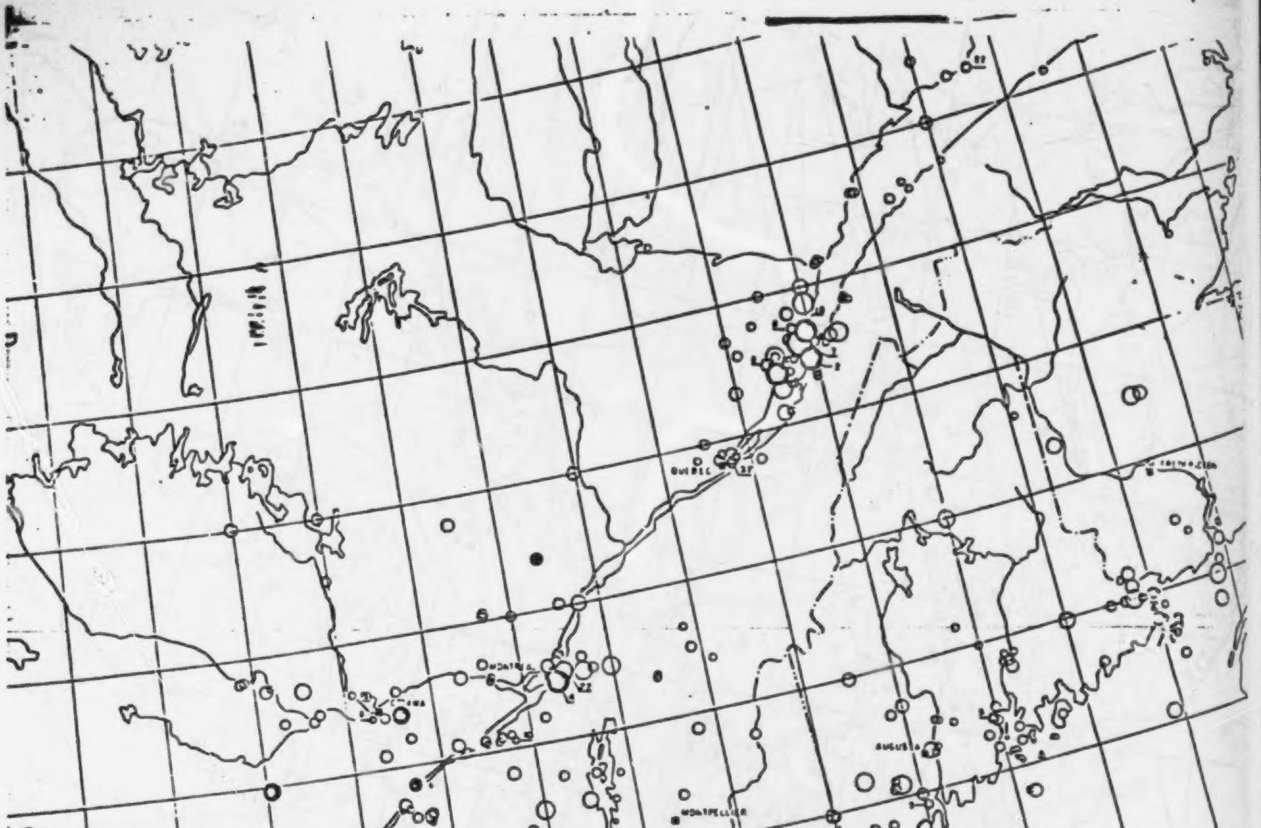
QUEBEC
MONTREAL
TORONTO
MONTPELIER
AUGUSTA
CONCORD
ALBANY
BOSTON
PROVIDENCE
HARTFORD
NEW YORK
40
80°
75°
70°

Figure 6. Earthquakes of Northeastern North America ,
1534 - 1927

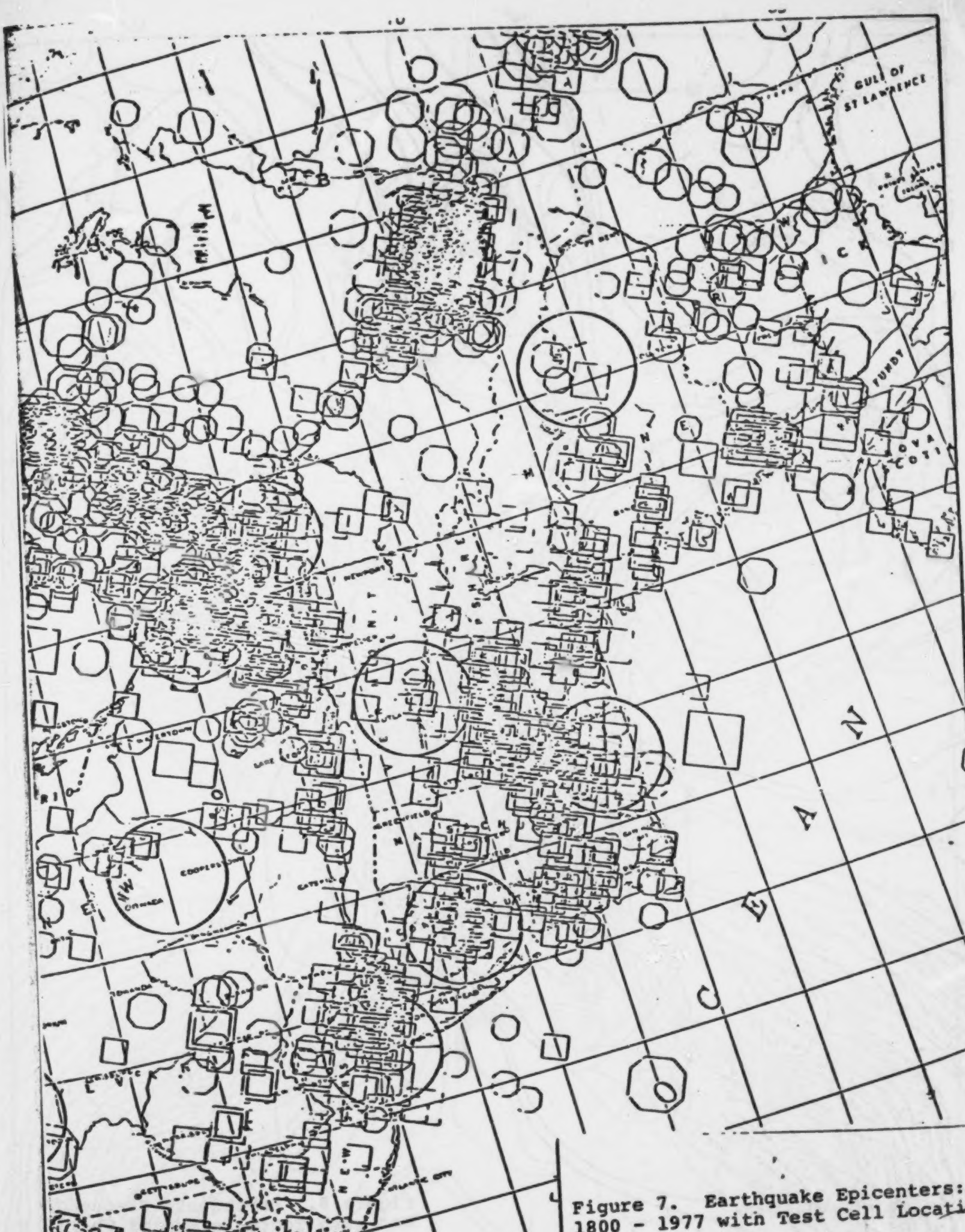
GULF OF ST LAWRENCE
FUNDY
NOVA SCOTIA
NEWPORT
GREENFIELD
COOPERSTOWN
ONEIDA
O C E A N

Figure 7. Earthquake Epicenters: 1800 - 1977 with Test Cell Locations

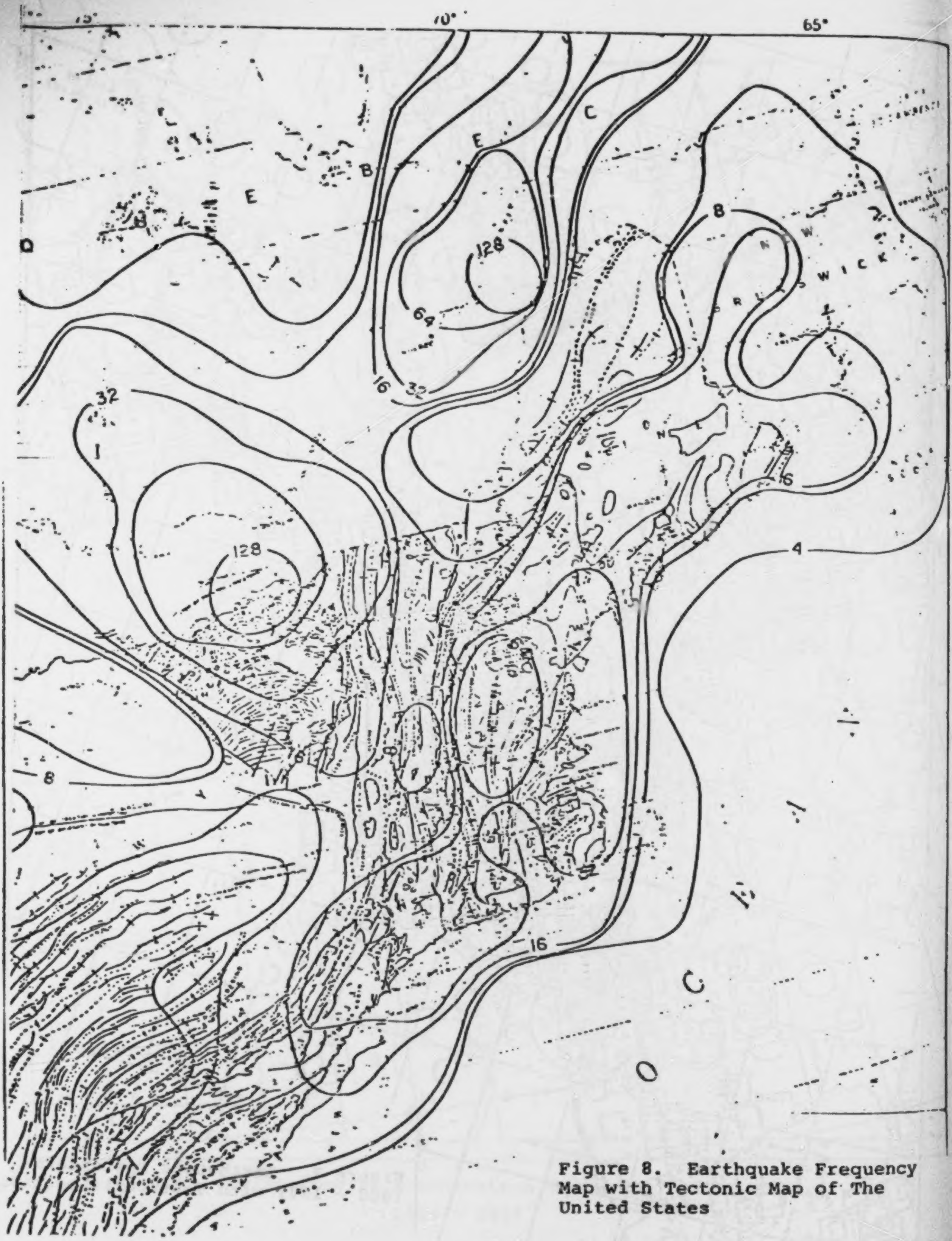
75°
70°
65°
D
B
E
B
E
C
128
64
32
16
8
NEW BRUNSWICK
32
128
8
16
4
16
OCEAN

Figure 8. Earthquake Frequency Map with Tectonic Map of The United States

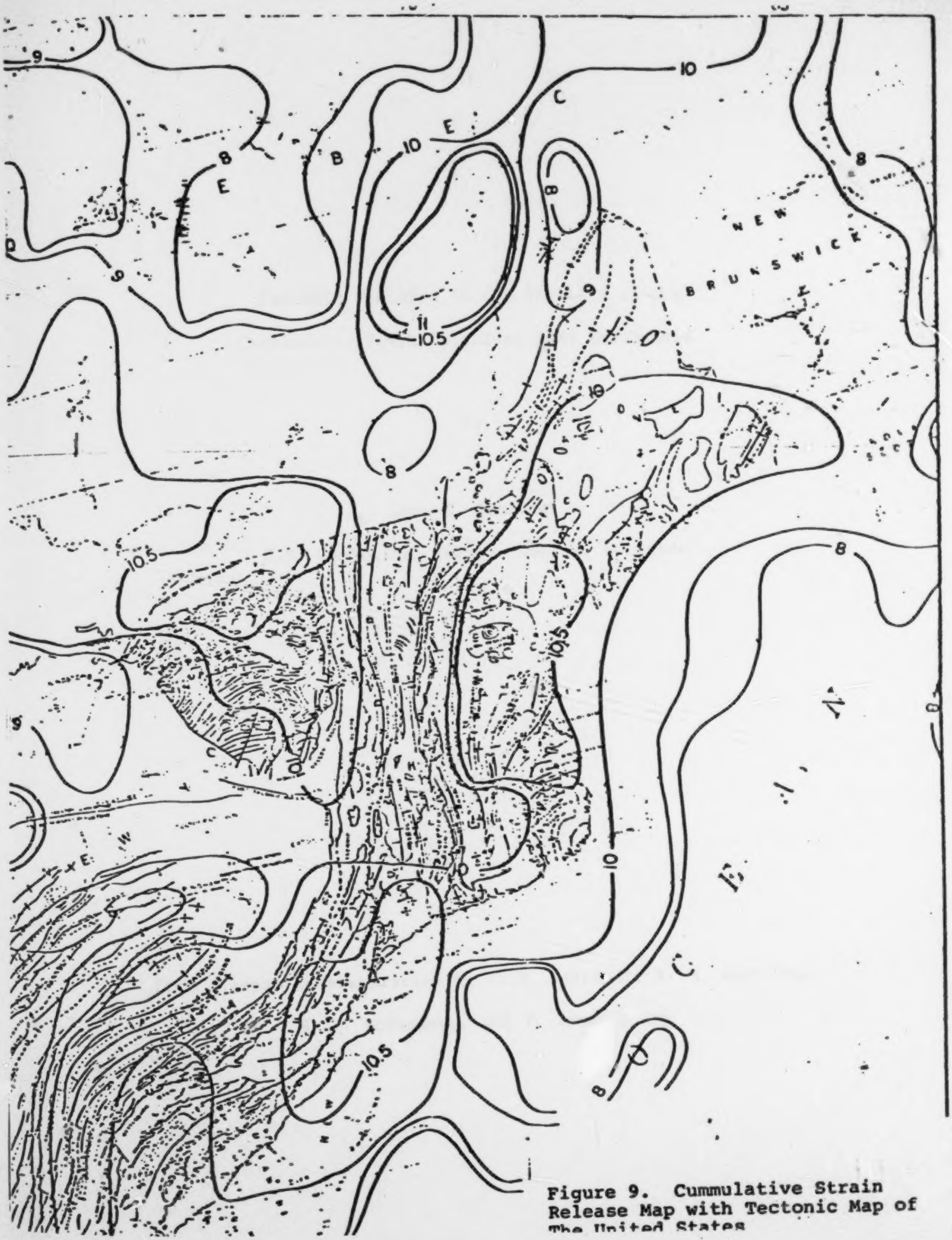
9
10
10
8
11
10.5
8
9
10
8
10.5
10.5
10
10.5
8
8
NEW BRUNSWICK
MAINE
OCEAN

Figure 9. Cummulative Strain Release Map with Tectonic Map of The United States

Tectonic Features in the Vicinity of the Charleston, South Carolina, 1886 Earthquake

by

John C. Behrendt
U.S. Geological Survey, Denver, Colorado

from a paper in preparation by J. C. Behrendt. R. M. Hamilton.
H. D. Ackermann, and V. James Henry

Multichannel seismic reflection profiles in the meizoseismal area of the 1886 Charleston earthquake and nearby offshore area show evidence of Cenozoic faulting. Deformation observed on two land profiles defines a northeast-striking reverse(?) fault zone named the Cooke fault. A Jurassic-age basalt layer at 750 m depth has 50 m vertical displacement, southeast side down. Overlying Upper Cretaceous and Cenozoic beds have decreasing displacement with decreasing depth. These displacements coupled with larger (~190 m) displacements of reflectors below the basalt indicate continuing Cenozoic movement of a post-basalt-flow, pre-late Cretaceous fault into Eocene time or later. The fault extends into a cluster of 1973-1978 epicenters, suggesting a possible causal relationship with seismicity. Marine multichannel seismic reflection data combined with single-channel, high-resolution reflection profiles reveal Cenozoic faulting beneath the continental shelf near Charleston. A reverse fault 12 km offshore, named the Helena Banks fault, extends for at least 30 km, and is observed as shallow as 10 m below the sea bottom, with the most recent movement in post-Miocene or Pliocene time. There is no known seismicity in the area of this fault. The reverse movement on the Helena Banks and Cooke faults is consistent with a northwest-southeast compressional stress regime. Elucidation of the relation, if any. between reactivated Triassic or older structures and/or a decollement (defined by diffractions at 11.4 ± 1.5 km depth) on the one hand and seismicity on the other will be important in assessing earthquake risk in many areas of similar tectonic setting outside of the Charleston region in the Atlantic coastal and continental margin area.

Multichannel seismic reflection profiles in the epicentral area of the 1886 Charleston earthquake [illegible]

FIGURE CAPTIONS

Figure 1. Map of Charleston, South Carolina region showing locations of: meizoseismal area of 1886 earthquake - dashed line (from Bollinger, 1977), seismic-reflection profiles epicenters of 1973-1978 seismicity (from Tarr and Rhea, in press), coreholes used for stratigraphic control, and zones of Cenozoic and Mesozoic faulting. The seismic lines are labeled SC for this study, C for the COCORP study by Schilt and others (in press). Evidence is presented here only for the Cenozoic Cooke fault; the other faults shown are discussed in Hamilton and others (in press).

Figure 2. Map showing information from Figure 1 and the locations of the marine seismic reflection profiles CH1-CH6. The single-channel data (collected by Skidaway Institute) also overlap lines CH1-CH6. The SE, BT and FC lines are reported by Dillon and others (1979). Evidence is presented here only for the Helena Banks fault; the other faults shown offshore are discussed in Behrendt and others (in press).

Figure 3. Parts of seismic reflection profiles SC5 (left) and SC10 (right) showing features that define the Cooke fault, the location of which is shown in Figure 1. The K reflection is from a layer about 0.5 km deep and correlates with a lithologic change within the Black Creek formation of Upper Cretaceous (Campanian) age. The J reflection is from the top of a Jurassic-age basalt layer at about 0.7 km depth. The B reflection is either crystalline basement or another basalt layer at about 1.4-1.5 km depth. The location of the inferred Cooke fault is indicated by the arrows, which indicate the zone of deformation. Note that all reflections drop across this zone, with the amount of drop increasing with depth (see Fig. 4). The interval between the J and B reflections increases by about 70ms (140 m) across the zone. The strike of the fault is about ~N 65°E.

Lines SC5 and SC10 cross the fault at angles of 22° and 49°, respectively which is the reason the fault zone is broader and less abrupt on line SC5 than on SC10. Gaps in data are the result of vibration points missed because of buildings and wells. The draping of reflections toward the gap on SC10 is an artificial effect.

Figure 4. Graph showing displacement on Cooke fault measured from the record section for line SC10 (Fig. 3) assuming velocities of 2.0 km/sec above J and 4.0 for the B-J interval. J_1 and J_2 refer to separate "legs" of the J and B reflections. The equation describes the least squares fit to the data from J to the shallowest measurement. R is the correlation coefficient.

Figure 5. Parts of seismic reflection profiles (Fig. 1) showing evidence for the Helena Banks fault indicated by arrows. (A) Multichannel profile CH4, (B) Vertically-compressed version of (A), (C) Single-channel profile along CH4, (D) Multichannel profile CH5, (E) Single-channel profile along CH5, and (F) Multichannel profile CH2. The strong reflection at about 1.1 sec on the multichannel records is J, which is probably from a basalt layer.

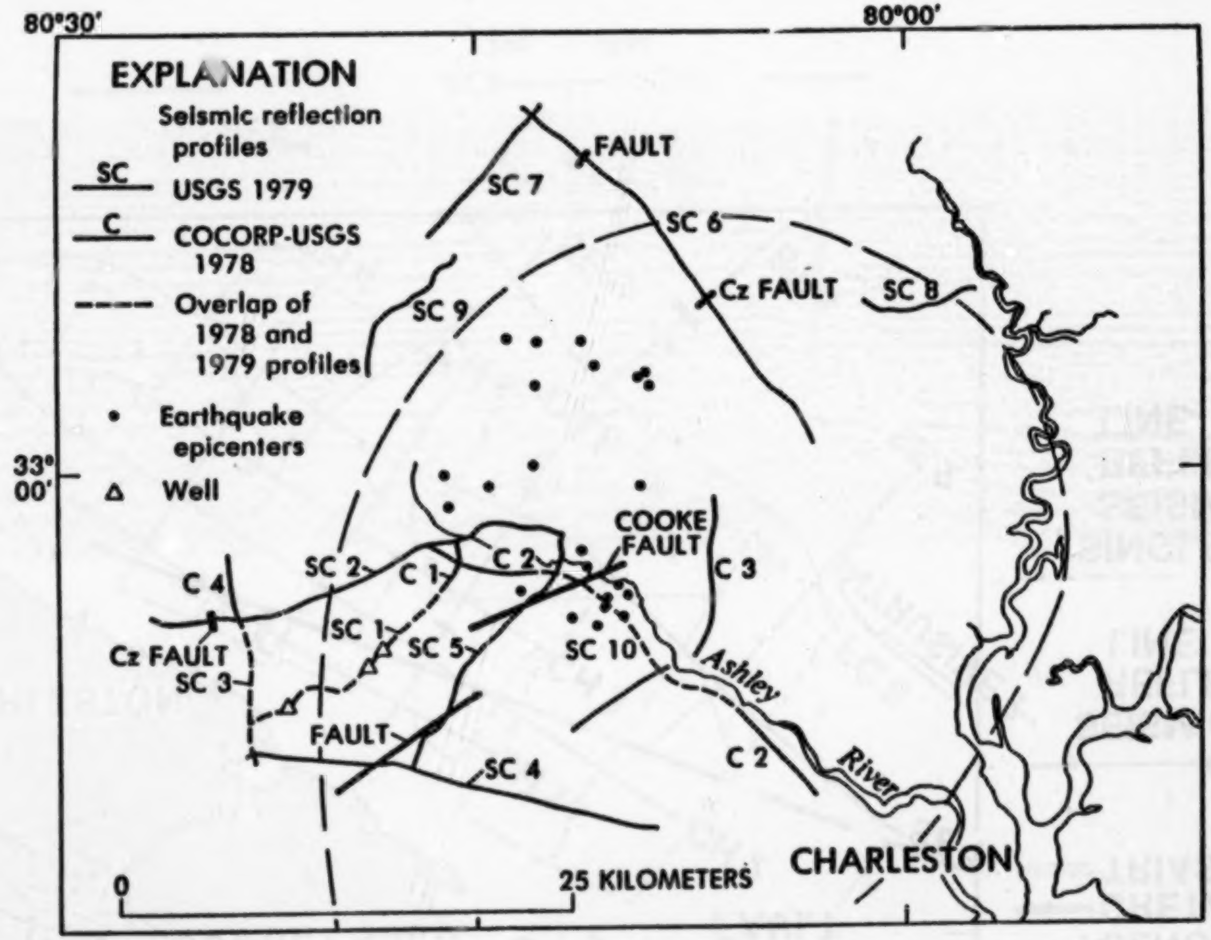
80°30'
80°00'
33° 00'
EXPLANATION
Seismic reflection profiles
SC USGS 1979
C COCORP-USGS 1978
Overlap of 1978 and 1979 profiles
Earthquake epicenters
Well
FAULT
SC 7
SC 6
Cz FAULT
SC 8
SC 9
COOKE FAULT
SC 2
C 1
C 2
C 3
C 4
Cz FAULT
SC 3
SC 1
SC 5
SC 10
Ashley
River
FAULT
SC 4
C 2
CHARLESTON
0
25 KILOMETERS

Figure 1

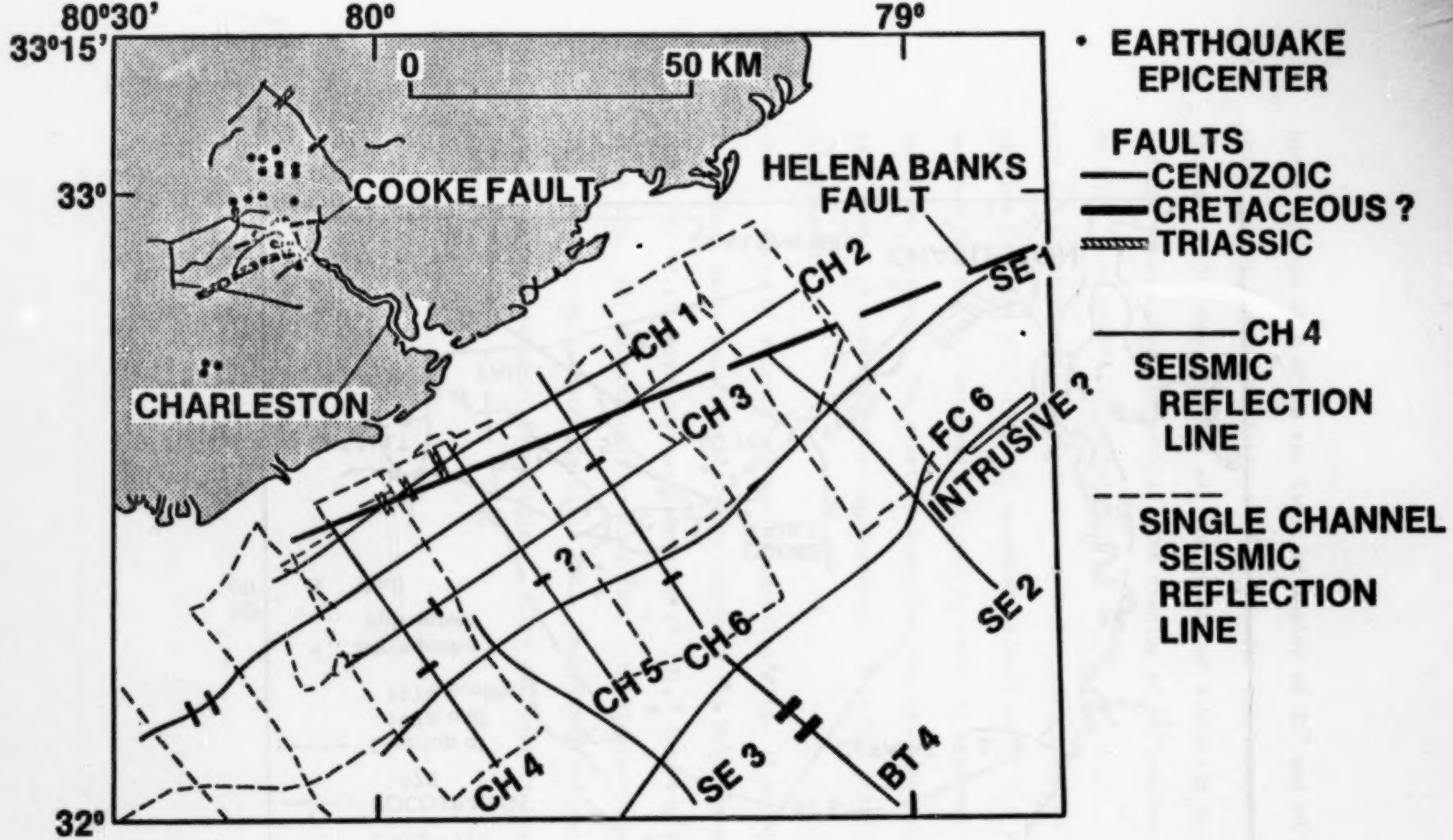
80°30'
80°
79°
33°15'
33°
32°
0
50 KM
COOKE FAULT
CHARLESTON
HELENA BANKS FAULT
CH 1
CH 2
CH 3
CH 4
CH 5
CH 6
SE 1
SE 2
SE 3
BT 4
FC 6
INTRUSIVE ?
?
• EARTHQUAKE EPICENTER
FAULTS
CENOZOIC
CRETACEOUS ?
TRIASSIC
CH 4
SEISMIC REFLECTION LINE
SINGLE CHANNEL SEISMIC REFLECTION LINE

Figure 3

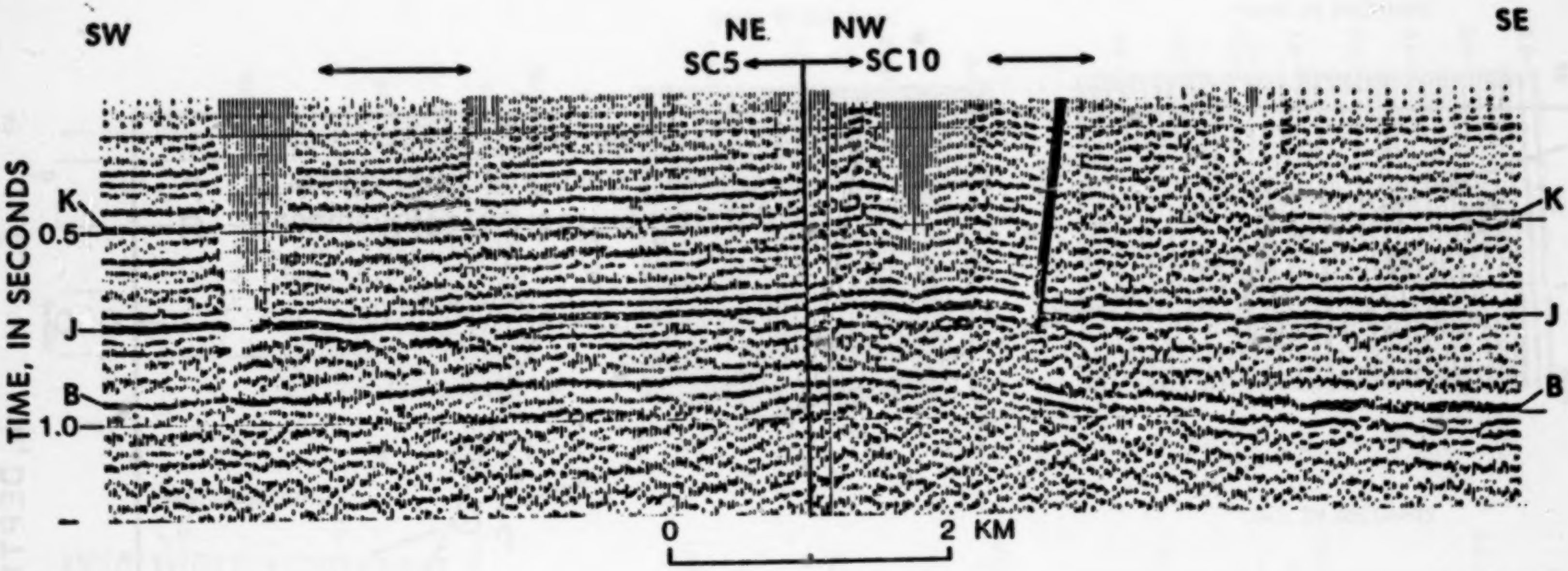

Figure 3

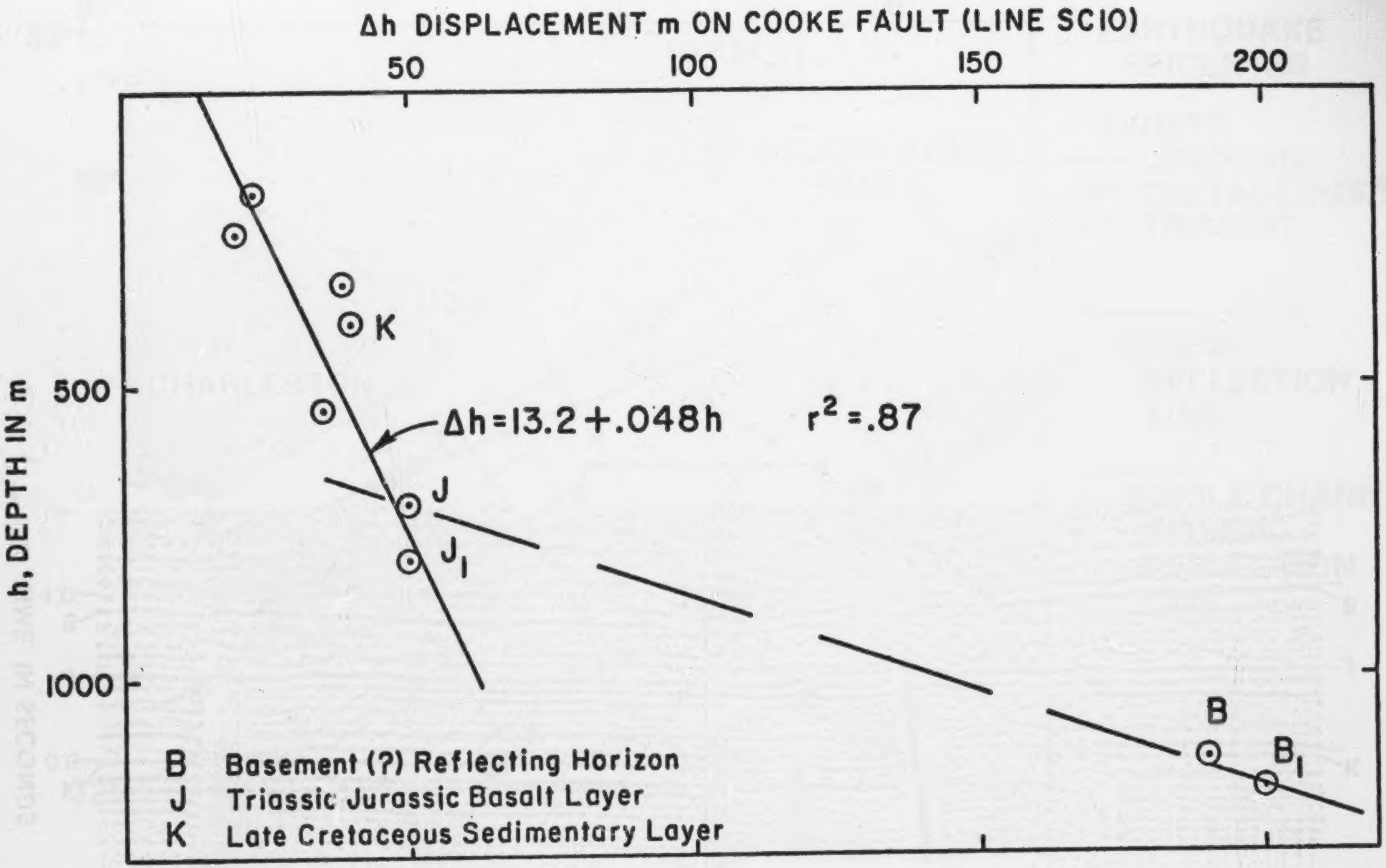
Δh DISPLACEMENT m ON COOKE FAULT (LINE SCIO)
50
100
150
200
h, DEPTH IN m
500
1000
K
J
J1
B
B1
Δh=13.2+.048h
r2 =.87
B Basement (?) Reflecting Horizon
J Triassic Jurassic Basalt Layer
K Late Cretaceous Sedimentary Layer

Figure 4

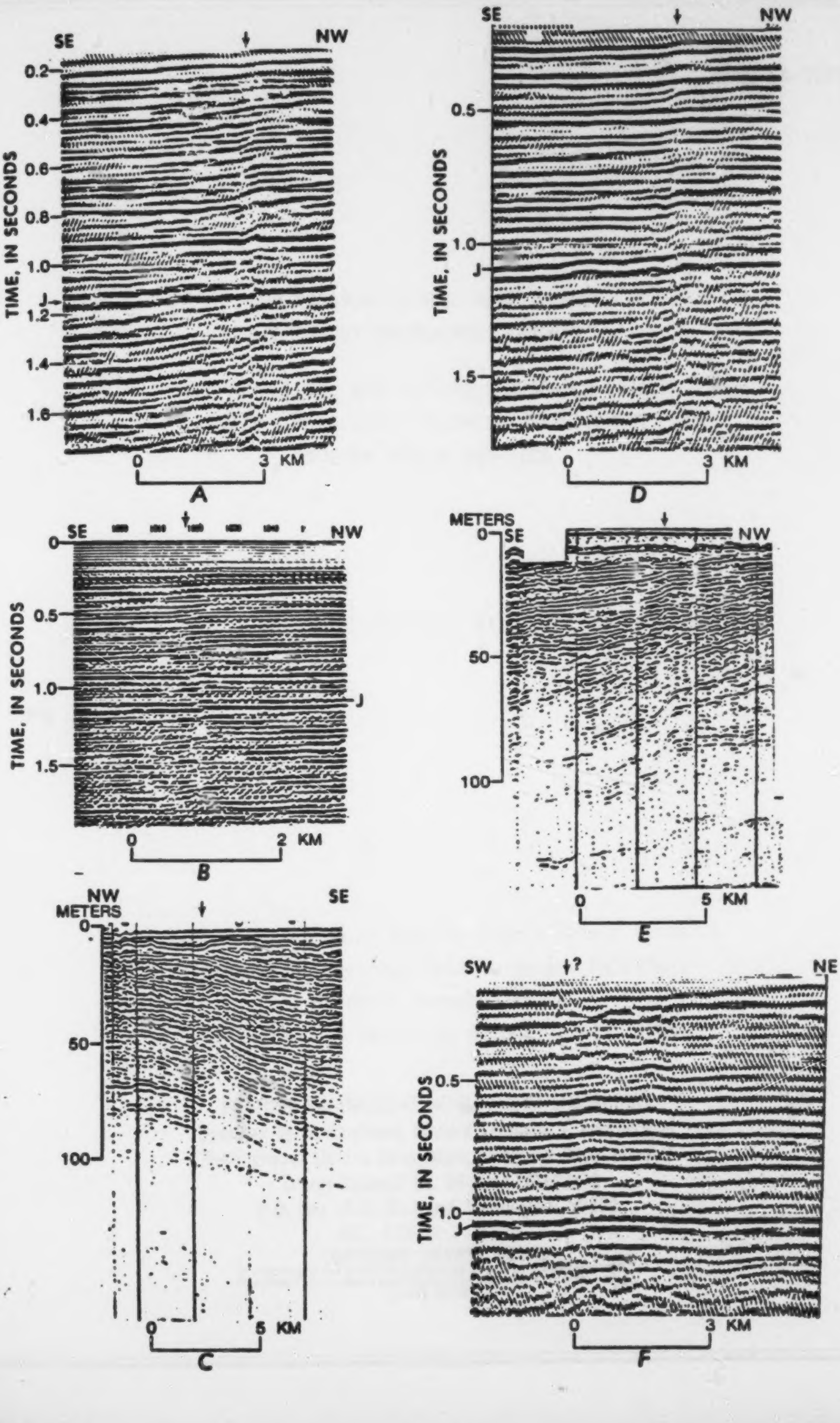
SE
NW
0.2
0.4
0.6
0.8
1.0
J
1.2
1.4
1.6
TIME, IN SECONDS
0
3 KM
A
SE
NW
0.5
1.0
J
1.5
TIME, IN SECONDS
0
3 KM
D
SE
NW
0
0.5
1.0
J
1.5
TIME, IN SECONDS
0
2 KM
B
METERS
0
SE
NW
50
100
0
5 KM
E
NW
SE
METERS
0
50
100
0
5 KM
C
SW
?
NE
0.5
1.0
J
TIME, IN SECONDS
0
3 KM
F

Figure 5

DEPTH IN m

HEDL SA-2225

LWR PRESSURE VESSEL SURVEILLANCE DOSIMETRY IMPROVEMENT PROGRAM

NRC METALLURGY AND MATERIALS RESEARCH BRANCH LWR-PV SURVEILLANCE DOSIMETRY IMPROVEMENT PROGRAM REVIEW GRAPHICS

W. N. McElroy, et al.

For presentation at the NRC Eighth Safety Research
Information Meeting, Metallurgy and Materials
Research Branch Session
Gaithersburg, Maryland, October 27-31, 1980

HANFORD ENGINEERING DEVELOPMENT LABORATORY
Operated by Westinghouse Hanford Company, a subsidiary of
Westinghouse Electric Corporation, under the Department of
Energy Contract No. DE-AC14-76FF02170
P.O. Box 1970, Richland, Washington 99352
NRC FIN No. B5988-7

COPYRIGHT LICENSE NOTICE
By acceptance of this article, the Publisher and/or recipient acknowledges the U.S. Government's right to retain a nonexclusive, royalty-free license in and to any copyright covering this paper.

[illegible]

[illegible]

[illegible]

[illegible]

[illegible]

[illegible]

[illegible]

[illegible]

[illegible]

[illegible]

[illegible]

HANFORD ENGINEERING DEVELOPMENT LABORATORY
Operated by Westinghouse Hanford Company, a subsidiary of
Westinghouse Electric Corporation, under the Department of
Energy Contract No. DE-AC14-76FF02170
P.O. Box 1970, Richland, Washington 99352
[illegible]

COPYRIGHT LICENSE NOTICE
[illegible]

LWR PRESSURE VESSEL SURVEILLANCE DOSIMETRY IMPROVEMENT PROGRAM

Principal participants and laboratories:

W. N. McElroy, K. W. Carlson, A. I. Davis, R. Gold,
G. L. Guthrie, L. S. Kellogg, E. P. Lippincott,
W. Y. Matsumoto, C. C. Preston, J. H. Roberts*,
F. H. Ruddy, R. L. Simons, L. E. Thomas, and C. A. Wilson
Hanford Engineering Development Laboratory (HEDL), USA

J. A. Grundl, C. M. Eisenhauer, E. D. McGarry, V. J. Spiegel
National Bureau of Standards (NBS), USA

F. B. K. Kam, R. E. Maerker, L. F. Miller, and F. W. Stallmann
Oak Ridge National Laboratory (ORNL), USA

A. Fabry, J. Debrue, G. DeLeeuw, S. DeLeeuw, G. Minsart, and
H. Tourwe
CEN/SCK, Mol, Belgium

D. Pachur, W. Schneider, and L. Weise, KFA, Jülich;
G. Prillinger and G. Hehn, IKE-Stüttgart; and U. Gröschel and
J. Koban, Kraftwerk Union, Germany

M. Austin, A. F. Thomas, and T. J. Williams, Rolls-Royce &
Associates Limited (RRAL); and A. J. Fudge, AERE, Harwell, UK

M. Galliani and F. Remondino
Italian Atomic Power Authority (ENEL), Italy

A. Sekiguchi and M. Nakazawa, University of Tokyo;
K. Sakurai, JAERI; and K. Takeuchi, SRI, Japan

A. A. Alberman and J. P. Genthon, CEA, Saclay; and P. Mas,
CEN, Grenoble, France

G. R. Odette and G. Lucas
University of California, Santa Barbara (UCSB), USA

R. A. Wullaert
Fracture Control Corporation (FCC), USA

---

*HEDL Consultant

B. A. Magurno and J. Carew
Brookhaven National Laboratory (BNL), USA

W. Zimmer
EG&G ORTEC, USA

H. Farrar IV and B. L. Oliver
Rockwell International (RI), USA

C. Cogburn
University of Arkansas (UA), USA

J. R. Hawthorne
Naval Research Laboratory (NRL), USA

E. B. Norris
Southwest Research Institute (SWRI), USA

J. S. Perrin and D. R. Farmelo
Battelle Memorial Institute (BMI), Columbus Laboratory, USA

S. L. Anderson
Westinghouse Electric Company (W), USA

R. H. Lewis, A. A. Lowe, Jr., J. K. Schmotzer, and C. L. Whitmarsh
Babcock & Wilcox Company (B&W), USA

G. C. Martin, Jr., and J. F. Copeland
General Electric Company (GE), USA

J. D. Varsik, G. P. Cavanaugh, J. J. Koziol, and D. W. Stephen
Combustion Engineering, Inc. (CE), USA

C. Z. Serpan
Metallurgy and Materials Research Branch,
U. S. Nuclear Regulatory Commission (NRL), USA

T. U. Marston, H. A. Till, and O. Ozer
Electric Power Research Institute and Contractors (EPRI), USA

Date: October 1980

TABLE OF CONTENTS

Page

Principal Participants and Laboratories iii

Figures vii

Tables ix

I. INTRODUCTION 1

II. FY 1980 RESEARCH RESULTS - SUMMARY 5

III. ASTM STANDARDS FOR SURVEILLANCE OF NUCLEAR REACTOR PRESSURE VESSELS 9

IV. LWR PHYSICS-DOSIMETRY TESTING IN THE ORNL POOL CRITICAL ASSEMBLY PRESSURE VESSEL BENCHMARK FACILITY (ORNL-PCA) 11

A. PCA CALCULATIONAL BLIND TEST 11

B. REVISED CALCULATIONS OF THE EFFECTS OF PHOTOFISSION IN THE PCA EXPERIMENTS 16

V. LWR STEEL METALLURGICAL TESTING IN THE PRESSURE VESSEL BENCHMARK FACILITY (ORR-PSF) 25

A. POWER AND TEST REACTOR METALLURGICAL DATA DEVELOPMENT AND TESTING 26

B. ORR-PSF TEST FACILITY IRRADIATION PROGRAM 29

C. ORR-PSF METALLURGICAL SPECIMEN TEST PROGRAM 42

VI. ANALYSIS AND INTERPRETATION OF RESEARCH AND POWER REACTOR TEST AND SURVEILLANCE RESULTS 53

A. SURVEILLANCE CAPSULE METALLURGICAL DATA DEVELOPMENT AND TESTING 53

B. SURVEILLANCE CAPSULE DOSIMETRY DATA DEVELOPMENT AND TESTING 56

1. Program Status 56
2. ORR-PSF Dosimetry/Perturbation Experiment 57
3. Benchmark Field Referencing 62
4. Surveillance Capsule Exposure Units and Values 68
5. Helium Accumulation Fluence Dosimetry for Reactor Vessel Surveillance 71

TABLE OF CONTENTS (Cont'd)

Page

C. OTHER REACTOR DATA DEVELOPMENT AND TESTING STUDIES 73

1. Spectral Effects Associated with the Extrapolation of TMI-2 PWR Surveillance Capsule Measurements 73
2. Status of Ex-Vessel Dosimetry Measurements in the Arkansas Power and Light Company's Unit #1 PWR 73
3. Status of Metallurgical and Dosimetry Measurements in the Garigliano BWR, Rome, Italy 74
4. Status of Dosimetry Measurements for the NRC-HSST Program 75

REFERENCES 87

FIGURES

Figure		Page
1	Interrelationships for ASTM Standards for Surveillance of Nuclear Reactor Pressure Vessels	3
2	Preparation, Validation, and Calibration Schedule for LWR Pressure Vessel Surveillance Standards	4
3	Pressure Vessel Wall Mock-up Schematic of Two Equivalent Facilities Constructed at ORNL	12
4	Experimental Configuration: Locations A1, A2, A3, A4, A5, A6, A7, A8 and B1 in the PCA 12/13 Configuration	14
5	Ratios of Calculated to Experimental Reaction Rates for the ^{58}Ni(n,p) Reaction at Various Points in the PCA 12/13 Configuration	15
6	Comparison of Calculated to Measured Spectral Indices Along the Horizontal Traverse in the 12/13 Configuration	17
7	Point Beach Unit No. 1 and Connecticut Yankee Trend Curve Results	27
8	Point Beach Unit No. 2 Trend Curve Results	28
9	The LWR Metallurgical Pressure Vessel Benchmark Facility	30
10	The Metallurgical Assembly Located in the Surveillance Capsule	31
11	The Metallurgical Assembly at the Inside Surface (Zero-Thickness Position, OT) of the Simulated Pressure Vessel Capsule	32
12	The Metallurgical Assembly Located at the Quarter-Thickness (1/4T) Position in the Simulated Pressure Vessel Capsule	33
13	The Metallurgical Assembly Located at the Half-Thickness (1/2T) Position in the Simulated Pressure Vessel Capsule	34
14	Exploded View of the Simulated Pressure Vessel Capsule	35
15	The Metallurgical Assembly Contained in the Void Box Capsule (VBC)	36

FIGURES (Cont'd)

Figure Page

16 As-Built Photograph of a Typical Metallurgical Assembly 37

17 Rear View of the Void Box Metallurgical Assembly, Showing Iron Gradient Wires and Holder Tubes Positioned in Charpy Notches 38

18 An Assembled Pressure Vessel Capsule, Showing Thermocouple Leads 39

19 The Process Control Panel for the Pressure Vessel Benchmark Facility 41

20 "MTS" Hydraulic Compression Testing Machine 43

21 Metallurgical Specimen Configuration 44

22 Space Compatible Compression Specimens 49

23 Space Compatible Hardness and TEM Specimens 51

24 Preliminary Design of the BSR-Simulated Dosimetry Measurement Facility (SDMF) 67

25 Relative Flux Distribution as a Function of the Distance from the Capsule Top, in the Dummy HSST Capsule at the BSR 82

26 Relative Equivalent Fission Flux Along the Center Channel of the Dummy HSST Capsule, as a Function of the Distance from the Capsule Top 83

TABLES

Table		Page
1	List of Neutron Fields for LWR-PV Dosimetry Validation and Calibration Studies	8
2	Summary of Photofission Effects in the PCA/LWR-PV Pressure Vessel Mockup at ORNL	18
3	Fast Neutron Reaction Rates[1] in the PCA/LWR-PV Pressure Vessel Mockup at ORNL	19
4	Photofission Reaction Rates[1] in the PCA/LWR-PV Pressure Vessel Mockup at ORNL	20
5	Calculated and Experimental Reaction Rate and Cd Ratios for ^{235}U(n,f) in the PCA/LWR-PV Mockup	22
6	Comparison of Minsart's (MOL) Revised Cadmium Ratios with those Calculated by Siman Tov (ORNL) for the 12/13 Configuration	23
7	Description of Compression Cylinder Specimens	45
8	Compression Cylinder Chemistry (wt%)	46
9	Charpy, Tensile, and CT Specimens for Each of Five Capsules for PSF*	47
10	Space Compatible Specimen Materials for PSF (Engineering Materials)	48
11	Proposal for TEM Annealing Heat Treatment Temperatures for Isochromal Anneals	52
12	Reported Surveillance Capsules Single Foil Flux/Fluence Values ($_i$ 1 MeV) - Relative to ^{54}Fe(n,p)	58
13	Range Evaluation (MAXIMA/MINIMA) Radiometric Results	61
14	Logistics of the Certified Fluence Irradiations of Nickel Foils in the NBS Cavity Fission (U-235) Spectrum	64
15	Comparison of Results of Interlaboratory Consistency in Measuring the Nickel Certified Fluence Standards	65
16	Re-Evaluated Exposure Values for Surveillance Capsules	69
17	Dosimetry/Physics Results*	70

TABLES

Table Page

18 Neutron Fluxes (E 1 MeV) in BSR-HSST Capsule Mock-up "A", at a BSR Core Power of 2.0 MW. 76

19 Neutron Fluxes (E 1 MeV) in BSR-HSST Capsule Mock-up "B", at a BSR Core Power of 2.0 MW. 77

20 Experimental Equivalent Fission Fluxes in BSR-HSST Capsule Mock-up "A" at a BSR Core Power of 2.0 MW. 78

21 Experimental Equivalent Fission Fluxes in BSR-HSST Capsule Mock-up "A" at a BSR Core Power of 2.0 MW. 79

22 Integral Spectral Indices in BSR-HSST Capsule Mock-up "A" 80

23 Integral Spectral Indices in BSR-HSST Capsule Mock-up "A" 81

24 Estimated Neutron Fluxes (E 1.0 MeV) in BSR-HSST Capsule "A", at a Core Power of 2 MW 85

25 Estimated Neutron Fluxes (E 1.0 MeV) in BSR-HSST Capsule "A", at a Core Power of 2 MW 86

LWR PRESSURE VESSEL SURVEILLANCE DOSIMETRY IMPROVEMENT PROGRAM

I. INTRODUCTION

Aging light water reactor pressure vessels (LWR-PV) are accumulating significant neutron fluence exposures, with consequent changes in their steel fracture toughness and embrittlement characteristics. Recognizing that accurate and validated measurement and data analysis procedures are needed to periodically evaluate the metallurgical condition of these reactor vessels, the U. S. Nuclear Regulatory Commission (NRC) has established the LWR-PV Surveillance Dosimetry Improvement Program. The primary concern of this program is to improve, standardize, and maintain dosimetry, damage correlation, and the associated reactor analysis procedures used for predicting the integrated effect of neutron exposure to LWR pressure vessels and support structures.

A vigorous research effort attacking the same measurement and analysis problems exists worldwide, and strong cooperative links between the USNRC supported activities at HEDL, ORNL, NBS and NRL and those supported by CEN/SCK (Mol, Belgium), EPRI (Palo Alto, USA), KFA (Jülich, Germany) and several UK laboratories have been extended to a number of other countries and laboratories.(1-7) These cooperative links have been strengthened by the active membership of the scientific staff of many of the participating countries and laboratories in the ASTM E10 Committee on Nuclear Technology and Applications. Several subcommittees of ASTM E10 are responsible for the preparation of LWR-PV surveillance standards.

The major benefit of this program will be a significant improvement in the accuracy of the assessment of the remaining safe operating lifetime of light water reactor pressure vessels and support structures. A primary objective of the multilaboratory program is to prepare an updated and improved set of dosimetry, damage correlation, and the associated reactor analysis ASTM standards for LWR-PV irradiation surveillance programs, as described in

Figures 1 and 2. Supporting this objective are a series of analytical and experimental validation and calibration studies in "Benchmark Neutron Fields," reactor "Test Regions," and operating power reactor "Surveillance Positions." These studies will establish and certify the precision and accuracy of the measurement and predictive methods which are recommended for use in these standards. Consistent and accurate measurement and data analysis techniques and methods, therefore, will have been developed and validated along with guidelines for required neutron field calculations. These calculations, in turn, are used 1) to correlate changes in material properties with the characteristics of the neutron radiation field and 2) to predict end-of-life (EOL) pressure vessel and support structure steel toughness and embrittlement from power and test reactor data.

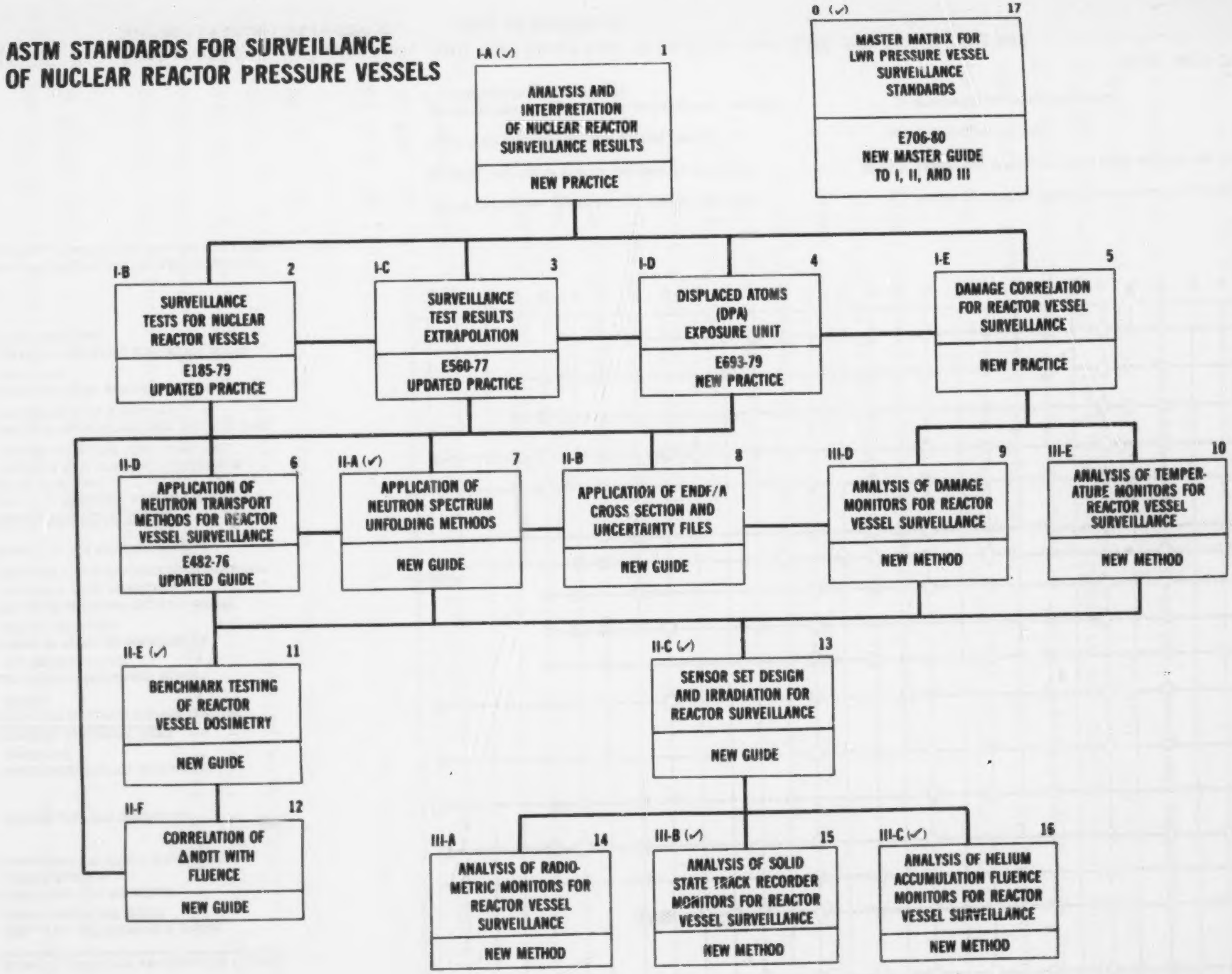
ASTM STANDARDS FOR SURVEILLANCE OF NUCLEAR REACTOR PRESSURE VESSELS
I-A (✓) 1
ANALYSIS AND INTERPRETATION OF NUCLEAR REACTOR SURVEILLANCE RESULTS
NEW PRACTICE
0 (✓) 17
MASTER MATRIX FOR LWR PRESSURE VESSEL SURVEILLANCE STANDARDS
E706-80
NEW MASTER GUIDE TO I, II, AND III
I-B 2
SURVEILLANCE TESTS FOR NUCLEAR REACTOR VESSELS
E185-79
UPDATED PRACTICE
I-C 3
SURVEILLANCE TEST RESULTS EXTRAPOLATION
E560-77
UPDATED PRACTICE
I-D 4
DISPLACED ATOMS (DPA) EXPOSURE UNIT
E693-79
NEW PRACTICE
I-E 5
DAMAGE CORRELATION FOR REACTOR VESSEL SURVEILLANCE
NEW PRACTICE
II-D 6
APPLICATION OF NEUTRON TRANSPORT METHODS FOR REACTOR VESSEL SURVEILLANCE
E482-76
UPDATED GUIDE
II-A (✓) 7
APPLICATION OF NEUTRON SPECTRUM UNFOLDING METHODS
NEW GUIDE
II-B 8
APPLICATION OF ENDF/A CROSS SECTION AND UNCERTAINTY FILES
NEW GUIDE
III-D 9
ANALYSIS OF DAMAGE MONITORS FOR REACTOR VESSEL SURVEILLANCE
NEW METHOD
III-E 10
ANALYSIS OF TEMPERATURE MONITORS FOR REACTOR VESSEL SURVEILLANCE
NEW METHOD
II-E (✓) 11
BENCHMARK TESTING OF REACTOR VESSEL DOSIMETRY
NEW GUIDE
II-C (✓) 13
SENSOR SET DESIGN AND IRRADIATION FOR REACTOR SURVEILLANCE
NEW GUIDE
II-F 12
CORRELATION OF ΔNDTT WITH FLUENCE
NEW GUIDE
III-A 14
ANALYSIS OF RADIOMETRIC MONITORS FOR REACTOR VESSEL SURVEILLANCE
NEW METHOD
III-B (✓) 15
ANALYSIS OF SOLID STATE TRACK RECORDER MONITORS FOR REACTOR VESSEL SURVEILLANCE
NEW METHOD
III-C (✓) 16
ANALYSIS OF HELIUM ACCUMULATION FLUENCE MONITORS FOR REACTOR VESSEL SURVEILLANCE
NEW METHOD

FIGURE 1. Interrelationships for ASTM Standards for Surveillance of Nuclear Reactor Pressure Vessels.
Neg 8010295-1

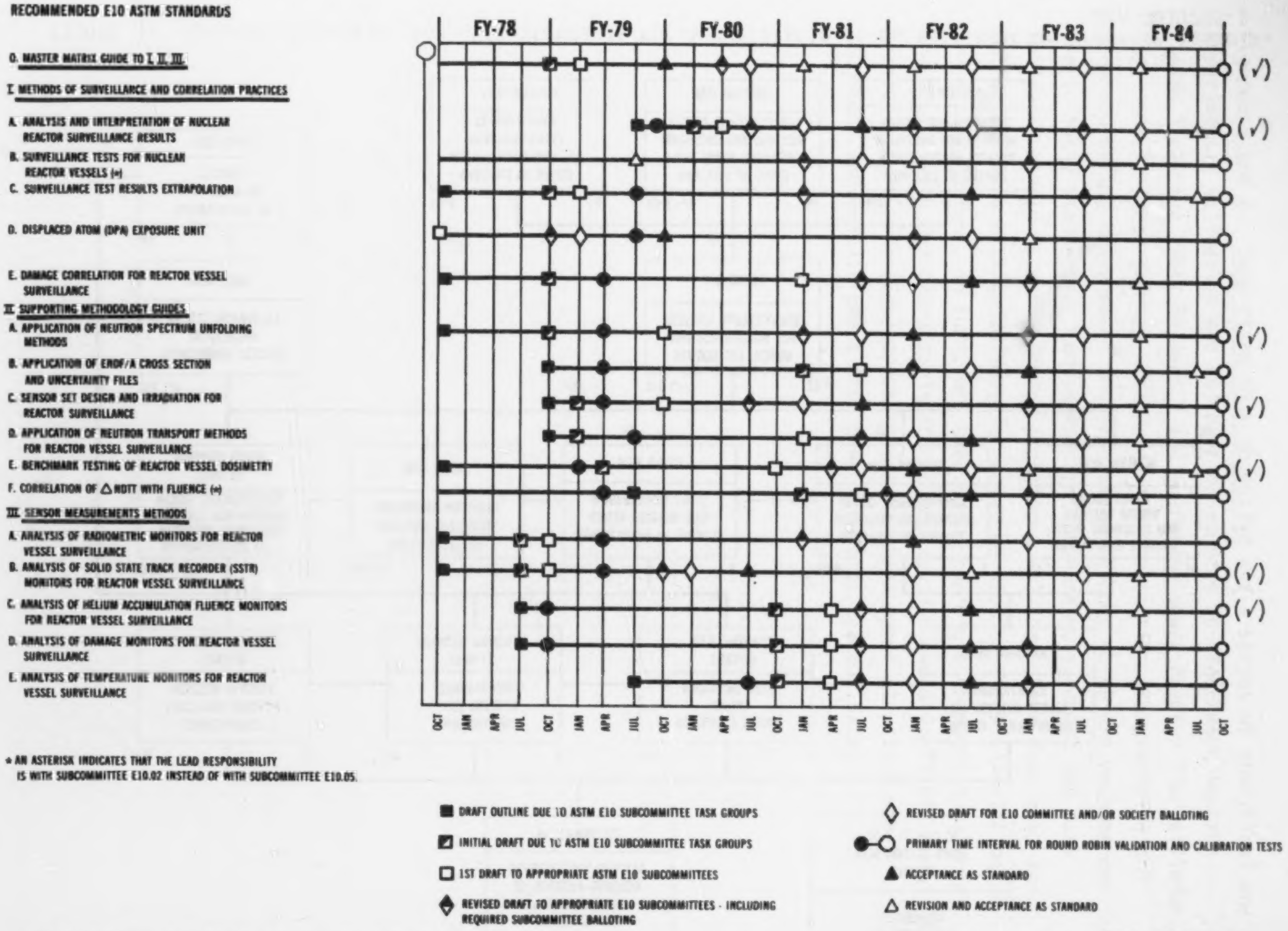

HEDL 8002-267.2

FIGURE 2. Preparation, Validation, and Calibration Schedule for LWR Pressure Vessel Surveillance Standards. Neg 8009009-1

II. FY 1980 RESEARCH RESULTS - SUMMARY

To account for neutron radiation damage in setting pressure-temperature limits and making fracture analysis(1-3, 6-23), neutron induced changes in reactor pressure vessel steel fracture toughness and embrittlement must be predicted, then checked by extrapolation of surveillance program data during the vessel's service life. Uncertainties in the predicting methodology can be significant. The main variables of concern are associated with:

- Steel chemical composition and microstructure
- Steel irradiation temperature
- Power plant configurations and dimensions - core edge to surveillance to vessel wall to support structure positions
- Core power distribution
- Reactor operating history
- Reactor physics computations
- Selection of neutron exposure units
- Dosimetry measurements
- Neutron spectral effects
- Neutron dose rate effects.

Variables associated with the physcial measurements of PV steel property changes are not considered here and are addressed separately in Appendices G and H of 10 CFR Part 50(19,20) in ASTM Standards(22), and elsewhere(6-17).

The U.S. Nuclear Regulatory Commission estimates that there are approximately 21 operating early generation U.S. pressurized water reactors (PWR) that will have beltline materials with marginal toughness, relative to the existing requirements of Appendices G and H and Regulatory Guide 1.99(21) sometime within their service life.(24)

As older vessels become more highly irradiated, the predictive capability for changes in fracture toughness and embrittlement must improve. Since during the vessel's service life an increasing amount of information will be available from test reactor and surveillance programs, better procedures to evaluate and use this information can and must be developed. The most appropriate way to make these procedures available is through voluntary consensus standards, such as those now being developed by ASTM Committee E10 on Nuclear Technology and Applications and discussed here.

Important summary highlights of FY 80 research activities of this multilaboratory program are:

A. The preparation of first, revised, or final drafts, Figures 1 and 2, of seven (✓) of seventeen ASTM standards which focus on the critical neutron exposure (dosimetry), damage analysis (data correlation), and the associated reactor analysis and interpretation aspects of the problem of guaranteeing the safety and integrity of the pressure vessel boundary of LWR power reactors.(23)

B. Initiation and completion of important supporting validation and calibration studies, reviews, and neutron field experimentation, Table 1, which demonstrate and certify the direct applicability of the sixteen ASTM standards (five "practices", six "guides", and five "methods").(2,4,5,25-27)

C. The completion of key experimental dosimetry/physics studies associated with the PCA low flux version of a PWR pressure vessel mockup, Figures 3-6 and Tables 2-6.(2,4,25-27)

D. The completion of a "Blind Testing" program using the PCA results to assist in the verification of the reliability of neutron physics calculations that are used for predicting PV steel toughness and embrittlement from power reactor surveillance data. The status of this effort is reviewed in a separate paper presented at the NRC 8th Safety Research Information meeting.(4) [Compared with measurements, most "Blind Test" calculations showed a trend towards underestimating the fluxes 5-25% and more so (50% and greater) for the cylindrical geometry. Only the one-dimensional calculations tended to overestimate the fluxes. If the same trend were found in the calculation of commercial power reactors, then the extrapolation from surveillance measurements to the interior of the pressure vessel could lead to significant nonconservative errors in flux, fluence, and damage estimates.]

E. The completion of the testing and the start in early 1980 of the Oak Ridge Research Reactor irradiaton of the metallurgy/dosimetry test assembly for the PSF experiment, which is a high flux version of a PWR pressure vessel mockup, Figures 9-23 and Tables 7 to 11.

F. The completion of initial work associated with the evaluation and reevaluation of exposure units and values for existing and new metallurgical data bases (Reg. Guide 1.99, MPC, EPRI, and others), Figures 7,8, and 24 and Tables 12-17. [This initial work involved the reanalysis of data from 19 PWR surveillance capsule reports for Westinghouse power plants. Using a consistent set of auxiliary data and dosimetry adjusted reactor physics results, the revised fluence values for E > 1 MeV averaged 42% higher than the originally reported values. The range of fluence values (new/old) was from a low of 1.08 to a high of 2.11. This indicates a definite need to re-evaluate other power reactor surveillance and test reactor exposure data.]

TABLE 1

LIST OF NEUTRON FIELDS FOR LWR-PV DOSIMETRY VALIDATION AND CALIBRATION STUDIES

Neutron Field	Type of Dosimetry*	Status
Benchmarks for Calibration		
• ^{252}Cf and ^{235}U Fission Neutron Irradiation Facilities at NBS (Standard)	Sensor calibrations	Preparation of fluence counting standards in progress for participating laboratories. ^{252}Cf is absolute fast neutron fluence standard.
• ^{235}U Fission Field at CEN/SCK (Standard)	Sensor calibrations	Applied routinely to RM, DM and other sensor calibrations for PCA and other neutron field measurements.
• ISNF Irradiation Facilities at NBS (Standard)	Sensor calibrations (particularly detectors with response range below 0.5 MeV)	Fission rate ratios established with fission chambers. Application to RM and other sensors planned.
• CRMF Irradiation Facility at EG&G (Reference)	Sensor calibrations	Planning stage.
• PCA/PSF Irradiation Facilities at ORNL (Reference)	Sensor validations and surveillance perturbation investigations	BSR-SDMF being established at ORNL.
Benchmarks for Transport Calculation Validation		
• Iron Shells Field at CEN/SCK (Reference)	Active and passive RM, SSTR, NE	CEN/SCK spectrometry in progress. NBS fission chamber measurements completed. Planning stage for passive sensors.
• PCA at ORNL (Reference)	Active and passive RM, SSTR, NE	Radiometric, fission chamber, track recorder, and neutron and gamma spectrometry measurements in progress. Results used for "Blind Test" program.
Test Regions for Dosimetry Method** Validation		
• BSR-HSST Dosimetry-Test (Test Reactor at ORNL)	Radiometric monitors (RM)	Irradiation and dosimetry counting completed. Analysis of Interlaboratory dosimetry in progress.
• FRJ-1 and FRJ-2 (Test Reactor at KFA, Germany)	RM, HAFM, TM (Melt Wires), DM (Quartz)	"Test Region" irradiations in metallurgical rigs in progress. Interlaboratory dosimetry analysis in progress.
• DIDO, PLUTO, and HERALD (Test Reactors in UK)	RM, HAFM, TM, DM	Planning stage, UK results are available.
• Buffalo NRL-NRC (Test Reactor at University of Buffalo)	Radiometric monitors	Planning stage, NRL results are available.
• University of Virginia (Test Reactor)	Radiometric monitors	Planning stage, Westinghouse results are available.
• BR-3 (PWR Power Reactor at CEN/SCK, Mol, Belgium)	RM, HAFM, DM (Quartz), TM (Melt Wires)	In- and Ex-Vessel "Test Region" irradiations in progress.
• Arkansas Power and Light Company PWR Unit #1 (Russelville, Arkansas)	Radiometric monitors	Ex-vessel "Test Region" irradiations and sensor counting and analysis in progress.
• Garigliano Reactor (BWR Power Reactor at Rome, Italy)	Radiometric monitors	In-vessel "Test Region" irradiation completed and analysis in progress.
• Brown's Ferry 3 (BWR)	RM, SSTR, Ionization Chambers	In- and ex-vessel "Test Region" irradiations completed and analysis in progress.
• McGuire I (PWR)	RM, SSTR, Proton Recoil	Ex-vessel "Test Region" irradiations planned and scheduled.

*RM: Radiometric Monitors
SSTR: Solid State Track Recorders
HAFM: Helium Accumulation Fluence Monitors
NE: Nuclear Emulsions
DM: Damage Monitors
TM: Temperature Monitors
BSR-SDMF: ORNL Bulk Shielding Reactor - Surveillance Dosimetry Measurement Facility.

**These neutron fields are also being used for physics and metallurgical damage correlation procedures and data validation and calibration studies.

III. ASTM STANDARDS FOR SURVEILLANCE OF NUCLEAR REACTOR PRESSURE VESSELS

The status of the preparation of the seventeen ASTM standards was very briefly summarized in Section II. The current schedule for the preparation, acceptance, and revision of all of the new and updated standards is shown in Figure 2. A summary listing of the type and the status of neutron field studies associated with the validation and calibration of the 16 ASTM Standards is provided in Table 1. The ASTM Master Matrix Standard provides more detailed information on the current 1) scope, 2) areas of application, and 3) interrelationships for the set of sixteen standards.(23)

With reference to Table 1, application, testing and the study of neutron dosimetry systems and individual detectors were accomplished for a number of "Benchmark Neutron Fields," research reactor "Test Regions," and PWR and BWR power reactor "In- and Ex-Vessel Surveillance Positions." The results of these dosimetry studies are being combined with available metallurgical data for use in the validation and calibration of 1) the established ASTM Standards and, 2) the currently applied reactor physics computational tools used for predicting PV steel toughness and embrittlement from test reactor and power reactor surveillance data.

With reference to Figures 1 and 2, a revised version of the Master Matrix Guide (0) was prepared by W. McElroy and successfully passed joint ASTM E10.05 and E10.02* ballot.(23) It is now being balloted at E10 and Society level. The Master Matrix Guide is now shown as one of a set of seventeen standards. In previous reports, fifteen standards were identified. A new ASTM Guide (IIF), "Correlation of ΔNDTT with Fluence," is shown in Figures 1 and 2. ASTM Subcommittee E10.02 will have the lead responsibility for its preparation, but the E10.05.06 Task Group on "Exposure Units" will assist E10.02 in its preparation. E10.02 has also taken the lead responsibility for the preparation of the ASTM Method (IIIE) "Temperature Monitors" of Figures 1 and 2.

---

*ASTM E10 Subcommittee E10.02 on Behavior and Use of Nuclear Metallurgical Materials in Nuclear Systems and Subcommittee E10.05 on Nuclear Radiation Metrology (formerly, on Dosimetry).

A first draft was prepared by S. Anderson of the new ASTM Master Practice (IA), "Analysis and Interpretation of Nuclear Reactor Surveillance Results," which defines a consistent set of procedures for reactor pressure vessel fracture toughness and embrittlement predictions. It can be 1) referenced as an instrument of regulation and 2) used for the establishment of improved metallurgical data bases.

Revised drafts of the ASTM Guide (IIA) for "Application of Neutron Spectrum Unfolding Methods" and the Guide (IIE) for "Benchmark Testing of Reactor Vessel Dosimetry" were prepared by F. Stallmann and E. McGarry/J. Grundl, respectively, and are in the process of review by program participants.

A revised draft of the ASTM Guide (IIC) for "Sensor Set Design," was prepared by G. Martin and a revised draft of the ASTM Method (IIIB) for "Solid State Track Recorder Monitors" was prepared by R. Gold, F. Ruddy, and J. Roberts for ASTM E10.05 Subcommittee ballot. The IIIB standard passed E10.05 ballot and is now being balloted at E10 and Society level.

A first draft of the ASTM Method (IIIC) for "Analysis of Helium Accumulation Fluence Monitors" was prepared by H. Farrar and B. Oliver and is in the process of review by program participants.

IV. LWR PHYSICS - DOSIMETRY TESTING IN THE ORNL POOL CRITICAL ASSEMBLY PRESSURE VESSEL BENCHMARK FACILITY (ORNL-PCA)

[Variables Studied: 1) Plant dimensions - Core Edge to Surveillance to Vessel Wall to Support Structures Positions; 2) Core Power Distribution; 3) Reactor Physics Computations; 4) Selection of Neutron Exposure Units; 5) Neutron Spectral Effects; and 6) Dosimetry Measurements.]

The PCA Pressure Vessel Benchmark Facility, Figure 3, is being used primarily in support of the improvement and validation of the following ASTM Standards, see Figure 1:

- Analysis and Interpretation of Nuclear Reactor Surveillance Results (IA)
- Surveillance Tests for Nuclear Reactor Vessels (IB)
- Surveillance Dosimetry Extrapolation (IC)
- Application of Neutron Spectrum Unfolding Methods, (IIA)
- Application of Neutron Transport Methods (IID)
- Benchmark Testing of Reactor Vessel Dosimetry (IIE)
- Correlation of ΔNDTT with Fluence (IIF)

Results of studies completed to date indicate that routine LWR power plant calculations of flux, fluence and spectrum, using current S_n transport methods can be as accurate as $\pm$ 15% (1σ) for a criterion of E >1.0 MeV if properly modeled and subjected to benchmark neutron field validation. Otherwise, errors can be a factor of two or more.

A. PCA Calculational Blind Test

The purpose of the PCA Calculational Blind Test is to determine how accurately transport theory calculations can predict neutron dosimetry measurements in a benchmark field which simulates a steel-water configuration of commercial light water reactors. A large number of dosimetry experiments were performed in the PCA-PV configuration which are used for comparison

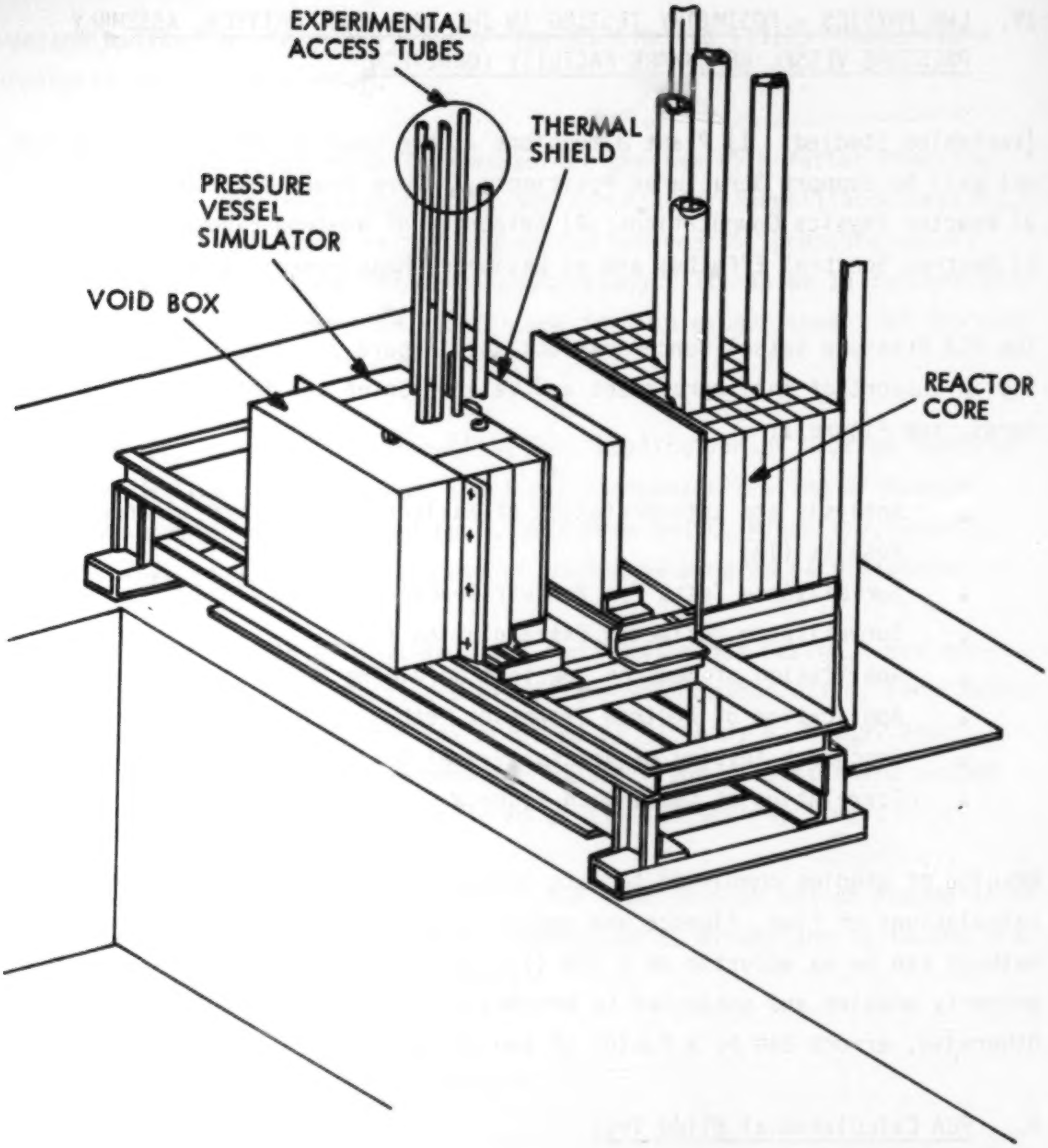
EXPERIMENTAL ACCESS TUBES
THERMAL SHIELD
PRESSURE VESSEL SIMULATOR
VOID BOX
REACTOR CORE

HEDL 7804-028

FIGURE 3. Pressure Vessel Wall Mockup Schematic of Two Equivalent Facilities Constructed at ORNL. The high-flux version at ORR (PSF) will include damage exposure of metallurgical test specimens; the low-flux version near a low-power critical assembly (PCA) will focus on active and passive dosimetry measurements.

Neg 8000085-4

with the calculations. To date, measurements of $^{237}Np(n,f)$, $^{103}Rh(n,n')$, $^{115}In(n,n')$, $^{238}U(n,f)$, $^{58}Ni(n,p)$, and $^{27}Al(n,\alpha)$ reaction rates are available at experimental locations A1, A3, A4, A5 and A6 in the PCA 12/13 configuration, and A4, A5, and A6 in the PCA 8/7 configuration, Figures 3 and 4.

To obtain the highest possible accuracy, all measurements (fission chambers and foils) were referenced to standard fission fields at NBS and CEN/SCK, Mol, Belgium. Active neutron and gamma spectroscopy and SSTR measurements have also been performed. Results of the neutron transport calculations of the PCA have been received from ten laboratories and vendors. The majority of them used a two-dimensional x-y geometry with some form of leakage correction. Two participants also submitted results from one-dimensional calculations and one participant used cylindrical geometry for the calculation. One Monte Carlo calculation was also submitted.

Compared with the measurements, most calculations showed a trend towards underestimating the fluxes by 5-25% and more so (50% and greater) for the cylindrical geometry. Only the one-dimensional calculations tended to overestimate the fluxes. Figure 5 shows an example of such a comparison in terms of the calculational to experimental (C/E) ratios for the $^{58}Ni(n,p)$ reaction at different locations in the PCA 12/13 configuration. This graph shows that not only are the calculations generally lower than the experimental values, but that the C/E ratios decrease also with increasing distance from the core.

If the same trend were found in the calculation of commercial power reactors, the extrapolation from surveillance measurements to the interior of the pressure vessel could lead to other large, nonconservative errors in flux and damage estimates. There is the possibility that leakage corrections may be responsible for the discrepancies. This and other possible explanations for the differences between calculated and measured results are being investigated.

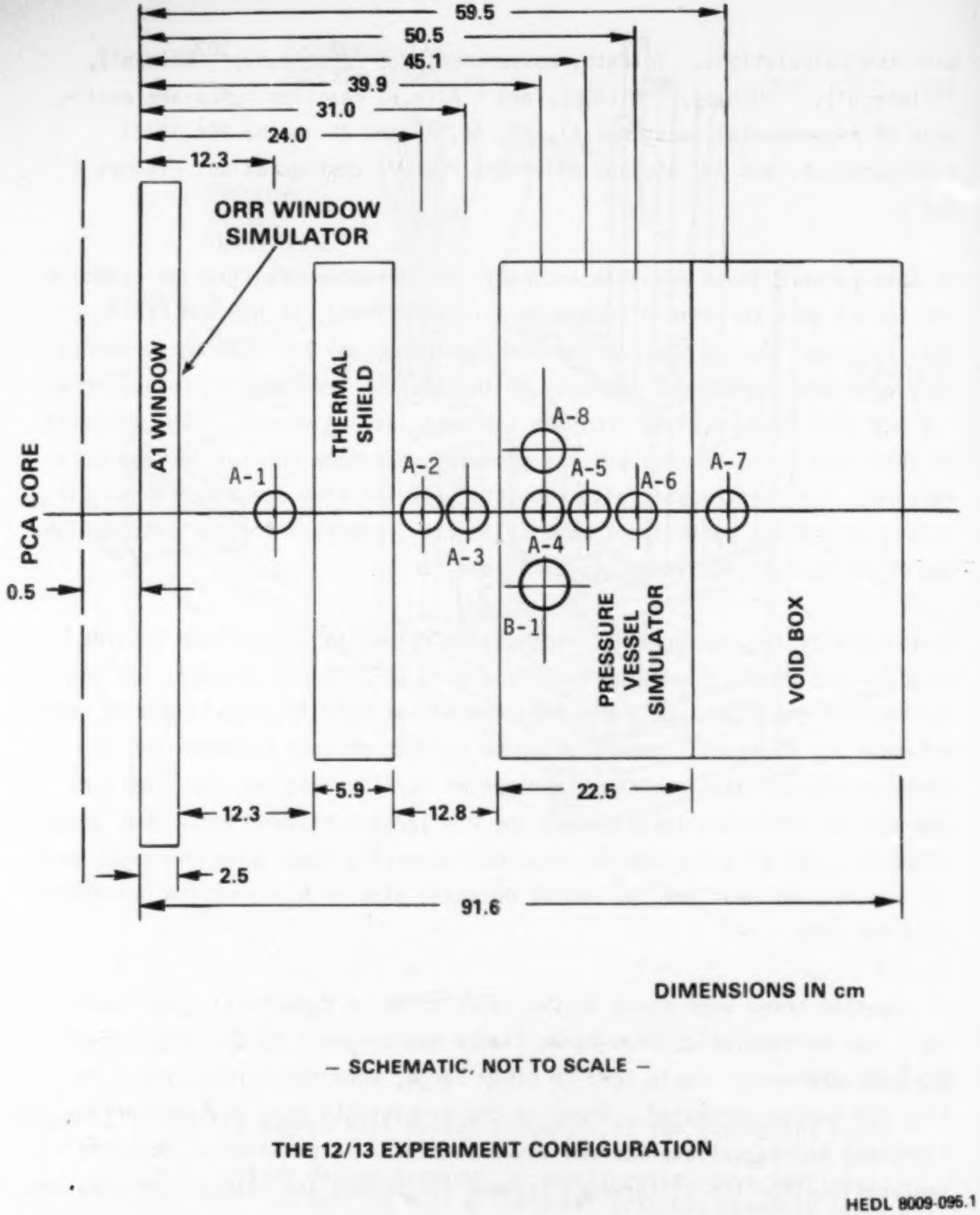
59.5
50.5
45.1
39.9
31.0
24.0
12.3
ORR WINDOW SIMULATOR
PCA CORE
A1 WINDOW
THERMAL SHIELD
A-1
A-2
A-3
A-4
A-5
A-6
A-7
A-8
B-1
PRESSURE VESSEL SIMULATOR
VOID BOX
0.5
12.3
5.9
12.8
22.5
2.5
91.6
DIMENSIONS IN cm
– SCHEMATIC, NOT TO SCALE –
THE 12/13 EXPERIMENT CONFIGURATION
HEDL 8009-095.1

FIGURE 4. Experimental Configuration: Locations A1, A2, A3, A4, A5, A6, A7, A8 and B1 in the PCA 12/13 Configuration.

ORNL-DWG 80-16516

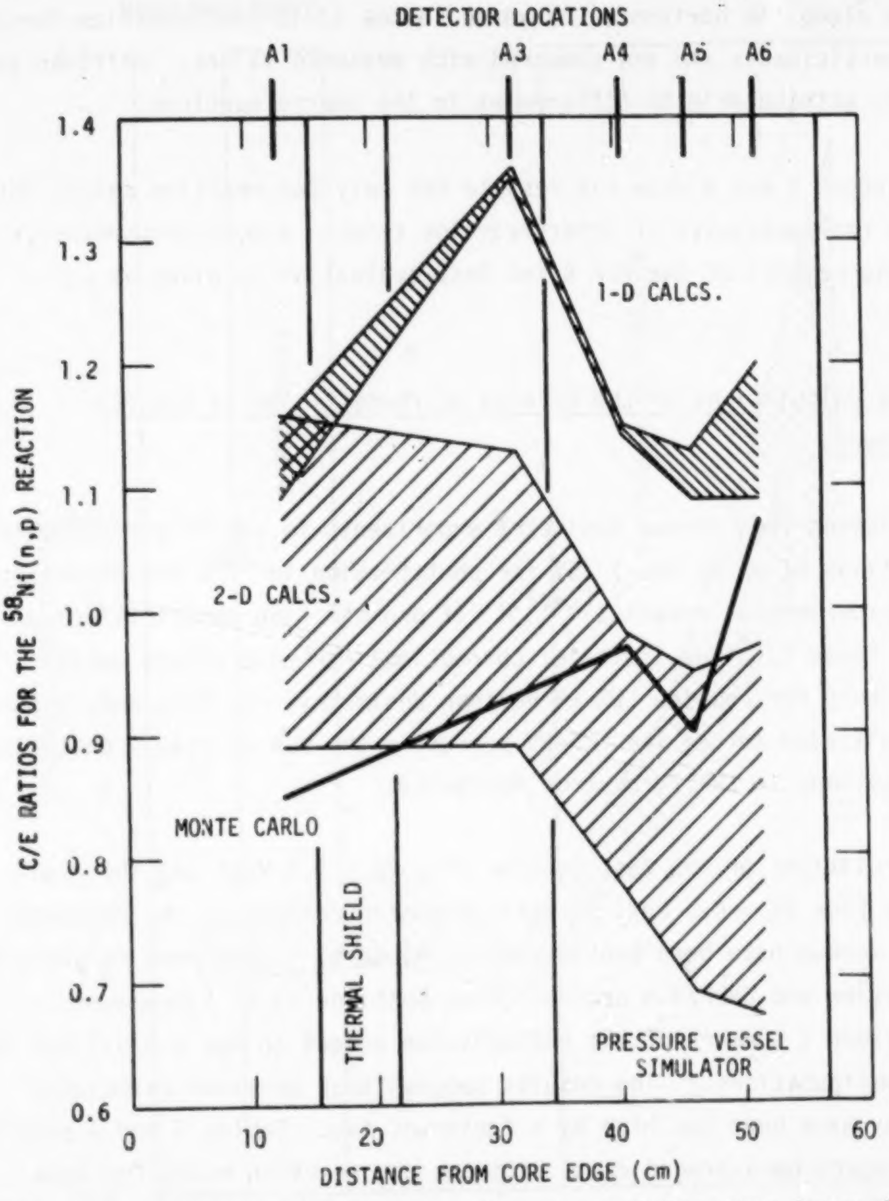

FIGURE 5. Ratios of Calculated to Experimental Reaction Rates for the ^{58}Ni(n,p) Reaction at Various Points in the PCA 12/13 Configuration. Cylindrical data not shown.

Neg 8010270-6

The spectral shape represented by spectral indices, the ratio between two reaction rates, seems to be fairly accurately calculated. This can be seen in Figure 6, where the calculated spectral indices of ^{237}Np(n,f)/^{58}Ni(n,p) are plotted along the horizontal traverse in the 12/13 configuration for the different participants and are compared with measured values. Differences are probably attributable to differences in the source spectrum.

Although Figures 5 and 6 show the results for only two reaction rates, these results are representative of other reaction rates. A more comprehensive report of the results of the PCA Blind Test evaluation is given in Reference 4.

B. Revised Calculations of the Effects of Photofission in the PCA Experiments

There is evidence from recent dosimetry experiments in LWR-PV environments that corrections of up to about 35% for photofission in ^{238}U are necessary to explain experimental results.(28,29) If photofission contributions are as large as these findings indicate, corrections for this effect would become mandatory for routine LWR-PV neutron dosimetry. To this end, efforts have been initiated to use the LWR-PV mockup in the PCA to assess photofission contributions in LWR-PV neutron dosimetry.

Revised calculations of the fast neutron flux ($E > 0.8$ MeV) and the high-energy gamma flux ($E > 6.5$ MeV) in various configurations of the PCA pressure vessel mockup have been provided by G. Minsart. These were folded with NBS photofission and ENDF/B-V neutron cross sections by C. Eisenhauer. Table 2 provides a summary of the photofission effect in the 8.4/6.7 and the 12.3/12.8 configurations.* The results suggest that previous calculated estimates may have been too high by a factor of two. Tables 3 and 4 provide the fluxes, spectrum-averaged cross sections and reaction rates for both

---

*The 8.4/6.7 and 12/3/12/8 are the actual dimensions (cm) of the 8/7 and 12/13 configurations, respectively.

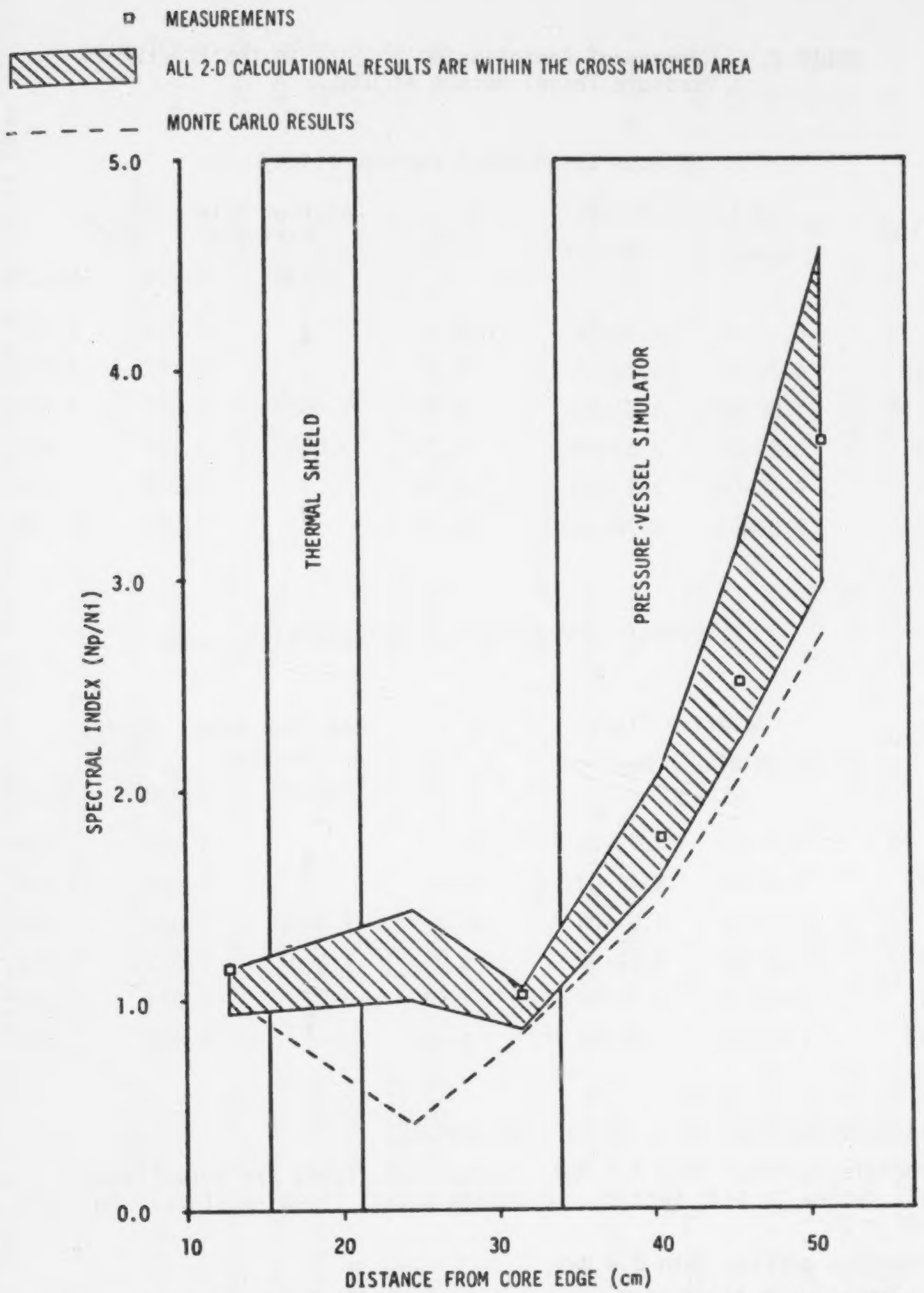

FIGURE 6. Comparison of Calculated to Measured Spectral Indices Along the Horizontal Traverse in the 12/13 Configuration.

ORNL-DWG 80-16372

HEDL 8009-095

TABLE 2. Summary of Photofission Effects in the PCA/LWR-PV Pressure Vessel Mockup at ORNL

Effects for 8.4/6.7 Configuration

Position	Relative Fluxes[1]		ϕ_γ/ϕ_n	Reaction Rate Ratios:[4] $\frac{R(\gamma+n)}{R(n)}$		
	Gamma[2]	Neutron[3]		U-235	U-238	Np-237
Before TS	8.92-01	4.38-02	20.4	↑	1.016	1.005
After TS	4.26-02	5.70-03	7.47		1.047	1.018
Before PV	4.02-02	4.81-03	8.36	1.0003	1.051	1.020
1/4 T	3.89-03	2.29-03	1.70	±.0003	1.024	1.006
1/2 T	9.95-04	1.47-03	0.68		1.015	1.003
3/4 T	7.03-04	8.70-04	0.81	↓	1.054	1.008

Effects for 12.3/12.8 Configuration

Position	Relative Fluxes[1]		ϕ_γ/ϕ_n	Reaction Rate Ratios: $\frac{R(\gamma+n)}{R(n)}$		
	Gamma[2]	Neutron[3]		U-235	U-238	Np-237
Before TS	6.70-01	1.79-02	37.4	↑	1.020	1.006
After TS	3.09-02	2.42-03	12.8		1.040	1.016
Before PV	2.21-02	7.01-04	31.5	1.0006	1.067	1.028
1/4 T	1.65-03	3.11-04	5.31	±.0004	1.037	1.010
1/2 T	3.63-04	1.97-04	1.84		1.019	1.004
3/4 T	1.45-04	1.26-04	1.15	↓	1.040	1.007

[1] Revised calculations by G. Minsart on 6/24/80.

[2] For energies greater than 6.5 MeV. Calculated fluxes are normalized. For all tables in this section, to obtain actual $(n/cm^2\text{-}s)/(n/s)$, multiply by 8.86×10^{-4}.

[3] For energies greater than 0.8 MeV.

[4] Folded with gamma and ENDF/B-V neutron cross sections by C. Eisenhauer. Reaction rates are per nucleus per 1 core neutron per second.

TABLE 3. Fast Neutron Reaction Rates[1] in the PCA/LWR-PV Pressure Vessel Mockup at ORNL

For the 8.4/6.7 Configuration

Position	Neutron Flux[2]	Spectrum-Averaged Cross Sections			Reaction Rates		
		U-235	U-238	Np-237	U-235	U-238	Np-237
Before TS	0.0438	14.90	0.1003	0.4772	6.5-01	1.39-03	2.09-02
After TS	0.00570	14.82	0.0801	0.4202	8.45-02	4.57-04	2.40-03
Before PV	0.00481	15.01	0.0804	0.4173	7.22-02	3.87-04	2.01-03
1/4 T	0.00229	8.207	0.0535	0.4163	1.88-02	1.23-04	9.53-04
1/2 T	0.00147	6.450	0.0373	0.3670	9.48-03	5.48-05	5.40-04
3/4 T	0.000870	6.334	0.0254	0.3120	5.51-03	2.21-05	2.71-04

For the 12.3/12.8 Configuration

Position	Neutron Flux[2]	Spectrum-Averaged Cross Sections			Reaction Rates		
		U-235	U-238	Np-237	U-235	U-238	Np-237
Before TS	0.0179	14.21	0.1130	0.5156	0.254	2.02-03	9.23-03
After TS	0.00242	14.11	0.0939	0.4650	0.0341	2.27-04	1.13-03
Before PV	0.000701	14.18	0.1141	0.5109	9.94-03	8.00-05	3.58-04
1/4 T	0.000311	7.350	0.0727	0.4929	2.28-03	2.26-05	1.53-04
1/2 T	0.000197	4.997	0.0520	0.4422	9.84-04	1.02-05	8.71-05
3/4 T	0.00126	5.743	0.0350	0.3637	7.24-04	4.41-06	4.58-05

[1] Revised flux calculations by G. Minsart (CEN/SCK, Mol, Belgium); folded with cross sections by C. Eisenhauer (NBS).

[2] Flux >0.8 MeV.

TABLE 4. Photofission Reaction Rates[1] in the PCA/LWR-PV Pressure Vessel Mockup at ORNL

For the 8.4/6.7 Configuration

Position	Gamma Flux[2]	Spectrum-Averaged Cross Sections			Reaction Rates		
		U-235	U-238	Np-237	U-235	U-238	Np-237
Before TS	0.8923	1.06-04	7.88-05	1.27-04	9.46-05	7.03-05	1.13-04
After TS	0.0426	8.27-04	5.00-04	9.98-04	3.52-05	2.13-05	4.25-05
Before PV	0.0402	8.13-04	4.93-04	9.76-04	3.27-05	1.98-05	3.92-05
1/4 T	0.00389	1.26-03	7.76-04	1.46-03	4.90-06	2.98-02	5.68-06
1/2 T	0.000995	1.37-03	8.39-04	1.58-03	1.36-06	8.35-07	1.57-06
3/4 T	0.000703	2.82-03	1.70-03	3.17-03	1.98-06	1.195-06	2.23-06

For the 12.3/12.8 Configuration

Position	Gamma Flux[2]	Spectrum-Averaged Cross Sections			Reaction Rates		
		U-235	U-238	NP-237	U-235	U-238	Np-237
Before TS	0.6698	7.28-05	5.88-05	8.64-05	4.88-05	3.94-05	5.79-05
After TS	0.0309	4.71-04	2.94-04	5.73-04	1.46-05	9.09-06	1.77-05
Before PV	0.0221	3.78-04	2.42-04	4.52-04	8.36-06	5.35-06	9.99-06
1/4 T	0.00165	8.00-04	5.00-04	9.25-04	1.32-06	8.25-07	1.53-06
1/2 T	0.000363	8.68-04	5.43-04	1.00-03	3.15-07	1.97-07	3.63-07
3/4 T	0.000145	1.97-03	1.20-03	2.23-03	2.86-07	1.74-07	3.23-07

[1] Revised flux calculations by G. Minsart (CEN/SCK, Mol, Belgium); folded with cross sections by C. Eisenhauer (NBS).

[2] Flux >6.5 MeV.

neutrons and gammas for the U-235, U-238 and Np-237 fissionable isotopes. Table 2 also shows truncated gamma and neutron fluxes and their ratios. The latter is generally a good indicator of the relative photofission effect. In these tables, the letters TS designate the thermal shield; PV, the pressure vessel; and 1/4-, 1/2-, and 3/4-T the quarter, half and three-quarter thicknesses within the pressure vessel simulator.

The largest photofission corrections are required for U-238 fission and they now appear to be less than 7% (rather than the 15% of previous estimates) for all Table 2 locations. Corrections for fission in Np-237 are only about one third as large, and those for U-235 are completely negligible. However, these results are still very preliminary, since the accuracy of the calculated corrections is very much in question.

Most of the photofission gammas are believed to arise from thermal-neutron capture in iron. In the PCA mockups, calculations indicate that the photofission gammas are generated locally in surrounding or nearby iron. For example, when gamma rays from the core are increased by a factor of 3, the gamma ray flux in the pressure vessel simulator increases by only about 20%. This is in contrast to PWR and BWR configurations where the gammas causing photofission in front of the pressure vessel are believed to be generated in the thermal shield. Therefore, calculated gamma fluxes are sensitive to the calculated neutron flux. The accuracy of calculated thermal fluxes can be assessed by comparison with some measured ^{235}U(n,f) reaction rates. Reaction rates calculated by G. Minsart are shown in Table 5 and are compared to some experimental data measured by F. Ruddy, R. Gold, and J. Roberts with bare and cadmium-covered solid state track recorders. Two experimental fission chamber data points by A. Fabry and E. McGarry are also shown. Since large discrepancies are observed between theory and measurement for the thermal neutron component, these calculated photofission contributions cannot be regarded as reliable.

Additional calculations have been performed, but these do not shed any light on the thermal neutron discrepancies. In this regard, Table 6 compares

TABLE 5

CALCULATED AND EXPERIMENTAL REACTION RATE AND Cd RATIOS FOR $^{235}U(n,f)$ IN THE PCA/LWR-PV MOCKUP

Position	Reaction Rate Ratio[1] (Cd-Covered)	Reaction Rate Ratio[1] (Bare)	Cd Ratio Calculated	Cd Ratio Experimental
		8.4/6.7 Configuration		
1/4T	1.00	1.37	2.54	1.86
1/2T	1.05	1.24	1.33	1.12
3/4T	1.30	6.52	6.00	1.20
		12.3/12.8 Configuration		
Before TS			127.	130[2]
Before PV			428.	125[2]
1/4T	1.10		6.10	
1/2T	0.93	1.20	1.61	1.25
3/4T	1.20	6.02	5.50	1.10

---

[1] G. Minsart's revised calculations are divided by experimental results obtained by HEDL with bare and cadmium-covered solid state track recorders. The ratio is normalized at the 8.4/6.7 1/4T position.

[2] Experimental data obtained with Mol fission chambers.

TABLE 6. Comparison of Minsart's (MOL) Revised Cadmium Ratios with those Calculated by Siman Tov (ORNL) for the 12/13 Configuration

Position	Siman Tov (12.3/12.8) Cadmium Ratios	G. Minsart (12.3/12.8) Cadmium Ratios
Before TS	77.0	127.
After TS	200.	160.
Before PV	480.	428.
1/4 T	4.25	6.10
1/2 T	1.65	1.61
3/4 T	25.0	5.50

G. Minsart's calculated cadmium ratios with the results of one-dimensional calculations by Siman Tov (ORNL). Except at the 3/4 T position where Siman Tov's results are significantly higher, agreement between the two calculations is good. Finally, the presence of Cd around the fission chambers may also produce a significant number of photofission gammas. Rough calculations by C. Eisenhauer indicate a 4% effect on ^{238}U(n,f) compared to estimates of up to 7% for gammas generated in iron.

Additional efforts are clearly required to adequately resolve photofission effects in LWR-PV neutron dosimetry. The forthcoming experimental schedule for the PCA reflects this need and, in particular, includes absolute gamma-ray spectrometry so that calculations can be directly tested.

V. LWR Steel Metallurgical Testing in the Pressure Vessel Benchmark Facility (ORR-PSF)

[Variables Studied: 1) Steel Chemical Composition and Microstructure; 2) Steel Irradiation Temperature; 3) Selection of Neutron Exposure Units; 4) Dosimetry Measurements; and 5) Neutron Spectra and Dose Rate Effects.]

The LWR Metallurgical Pressure Vessel Benchmark Facility (ORR-PSF) is being used primarily in support of the improvement and validation of the following ASTM Standards, see Figure 1:

- Analysis and Interpretation of Nuclear Reactor Surveillance Results (IA)
- Surveillance Tests for Nuclear Reactor Vessels (IB)
- Surveillance Dosimetry Extrapolation (IC)
- Displaced Atom (DPA) Exposure Unit (ID)
- Damage Correlation (IE)
- Application of Neutron Spectrum Unfolding Methods (IIA)
- Sensor Set Design (IIC)
- Correlation of ΔNDTT with Fluence (IIF)
- Five Methods, IIIA, IIIB, IIIC, IIID, and IIIE

There are a number of metallurgical programs and studies that have been established to determine the fracture toughness and Charpy properties of irradiated materials as a function of chemistry, microstructure, and irradiation conditions.(3,7-9,11,13-16,30-33,35-47) The ORR-PSF multilaboratory metallurgical-dosimetry improvement program(1,2,11,25-27), is expected to provide key irradiation effects data, under well controlled conditions, to help in 1) the validation and calibration of exposure units and values and 2) the analysis and correlation of property change data obtained from this and other programs. Summary information on recent results of power and test reactor data development and testing and the status of the ORR-PSF program work is presented in Sections V-A, B, and C.

A. Power and Test Reactor Metallurgical Data Development and Testing

Recent analyses of PWR surveillance capsule and test reactor data indicate that long-term LWR power plant surveillance capsule and short-term test reactor (~288°C irradiation temperature) neutron-induced property change data for steel (base metal, heat affected zone and weld metal) can show significantly different fluence dependencies.(2,3,14-16,30,31,33,36,46) For instance, for low-flux surveillance capsule irradiated materials, the neutron induced damage may increase at a rate per unit fluence similar to that of high flux test reactor irradiated materials, up to some level of exposure which appears to be a function of chemistry and microstructure. At exposures above this level, the rate of embrittlement is much reduced and it appears that the embrittlement saturates. As an example, Figure 7, the Point Beach Unit No. 1 and Connecticut Yankee vessel plate, weld material, and the A302B correlation materials do indicate apparent saturation at exposures up to about 2×10^{19} n/cm^2 (E > 1 MeV).[14,36] On the other hand, Figure 8, the Point Beach Unit No. 2 surveillance capsules V, T, and R vessel plate, weld material, and A533B correlation material results do not show such saturation.(31) Also, in Figure 8, the Point Beach Unit No. 2 A533B results (dashed curve for 0.14% Cu) appear to correlate well with those (two solid curves for 0.10 and 0.20% Cu) obtained from high flux test reactor studies.(7,31,35)

Based on the above results as well as those from other studies,(6,9,37) it appears that the constant A and the slope N, of the equation $\Delta NDTT = A(\phi t)^N$, are both functions of chemistry. With reference to the preparation of the ASTM IE Correlation Practice, Figure 1, and in addition to the inclusion of a thermal annealing term to account for possible saturation effects, it is concluded that such equations may have to include N as a function of Cu, P, etc.

In summary and in consideration of the application of ORR-PSF experimental data, test reactor and surveillance capsule irradiation effects data should not be combined to predict PV steel fracture toughness and embrittlement as

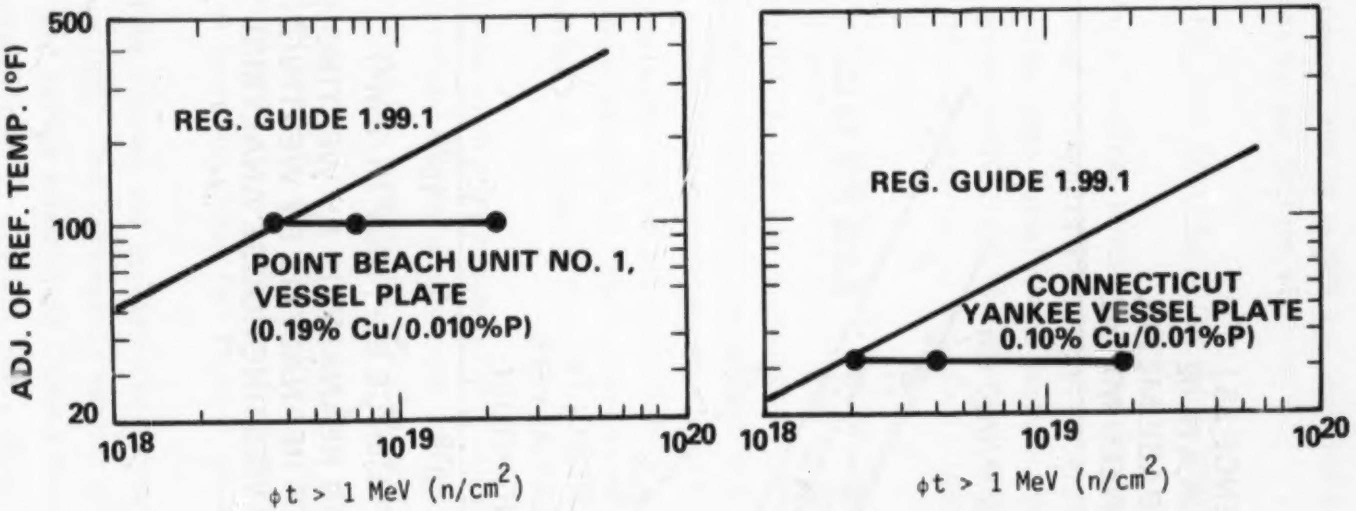

NOTE: THE VESSEL WELDPLATE AND A302B CORRELATION MATERIALS, NOT SHOWN HERE, ALSO SHOW APPARENT SATURATION.

HEDL 8009-054.2

FIGURE 7. Point Beach Unit No. 1 and Connecticut Yankee Trend Curve Results.

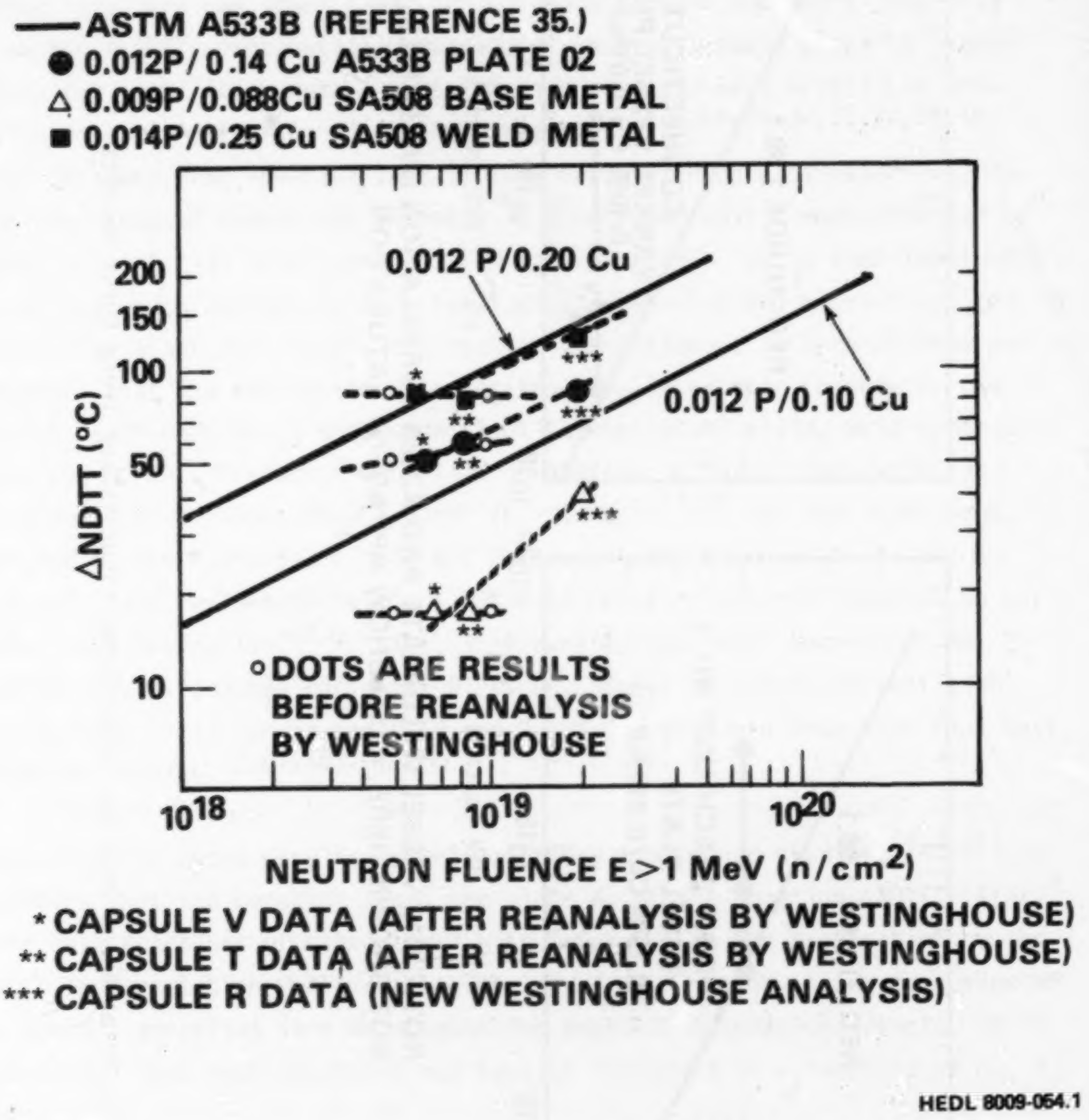

FIGURE 8. Point Beach Unit No. 2 Trend Curve Results.

a function of neutron exposure without having 1) more precisely defined and representative data bases, 2) a better understanding of the mechanisms causing damage, and 3) tested and verified exposure data and physical correlation models; see Section VI.

B. ORR-PSF Test Facility Irradiation Program Status

The LWR Metallurgical Pressure Vessel Benchmark Facility, shown in Figure 9, was completed in April 1980. It consists of three irradiation capsules--the first simulated surveillance capsule (SSC-1), the simulated pressure vessel capsule (SPVC), and the void box capsule (VBC). Capsule irradiation at ORR full power started in late April 1980.

The metallurgical assembly that is inserted into the surveillance capsule is shown in Figure 10. Three metallurgical assemblies located at the inside surface (SPV-0T), the quarter-thickness point (SPV-1/4T), and the half-thickness point (SPV-1/2T), are loaded into the simulated pressure vessel capsule. These assemblies are individually shown in Figures 11, 12, and 13. An exploded view of the SPVC, Figure 14, shows the positions of the metallurgical assemblies, the heater assemblies, and the cooler assemblies. A fifth assembly, shown in Figure 15, is inserted into the void box capsule.

It should be noted that the metallurgical specimens are all labeled, so that each participant in the program can identify the location of their specimens to correlate with temperature and flux profiles.(2)

As-built pictures of the metallurgical assemblies, designed at ORNL, are shown in Figures 16, 17, and 18. A second surveillance capsule, SSC-2, is currently being assembled for irradiation in FY-81.

Pre-startup testing and dosimetry measurements were completed in late 1979 and early 1980. The radiometric monitor (RM), solid state track recorder (SSTR), and helium acumulation fluence monitor (HAFM) dosimetry analysis is being accomplished by CEN/SCK, HEDL, ORNL, EG&G ORTEC, Harwell, and RI staff members.

FIGURE 9. The LWR Metallurgical Pressure Vessel Benchmark Facility. Neg 8010270-19

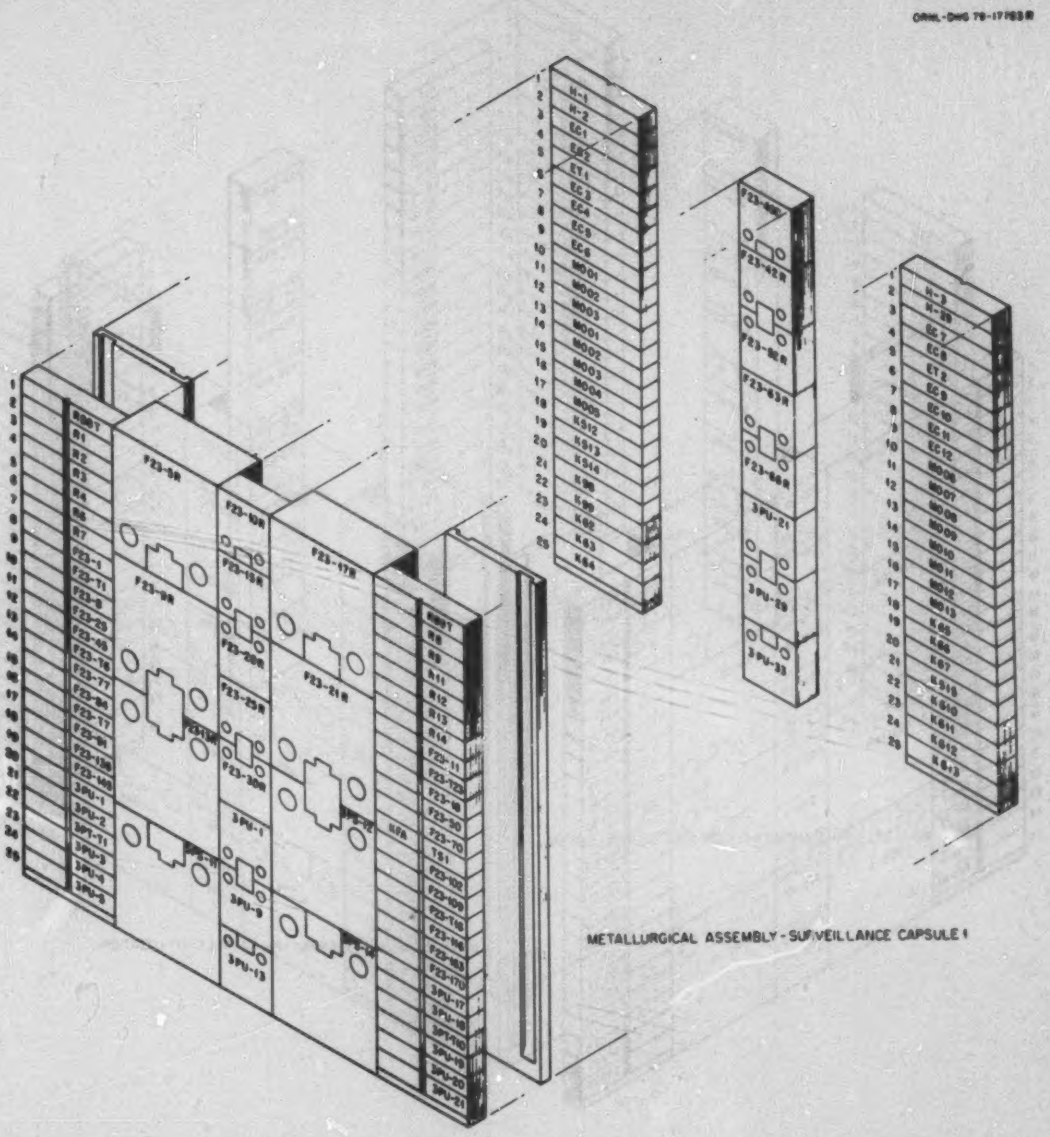
ORNL-DWG 79-17783R
H-1
H-2
EC1
EC2
ET1
EC3
EC4
EC5
EC6
MO01
MO02
MO03
MO01
MO02
MO03
MO04
MO05
KS12
KS13
KS14
K62
K63
K64
F23-42R
F23-62R
F23-63R
F23-66R
3PU-21
3PU-29
3PU-33
H-3
EC7
EC8
ET2
EC9
EC10
EC11
EC12
MO06
MO07
MO08
MO09
MO10
MO11
MO12
MO13
K65
K66
K67
KS15
KS10
KS11
KS12
KS13
R1
R2
R3
R4
R6
R7
F23-1
F23-T1
F23-8
F23-25
F23-45
F23-T6
F23-77
F23-84
F23-17
F23-91
F23-130
F23-140
3PU-1
3PU-2
3PT-T1
3PU-3
3PU-4
3PU-5
F23-5R
F23-9R
F23-10R
F23-15R
F23-20R
F23-25R
F23-30R
3PU-1
3PU-9
3PU-13
F23-17R
F23-21R
NFA
R8
R9
R11
R12
R13
R14
F23-11
F23-T23
F23-18
F23-50
F23-70
TS1
F23-102
F23-109
F23-T16
F23-116
F23-183
F23-170
3PU-17
3PU-18
3PT-T10
3PU-19
3PU-20
3PU-21
METALLURGICAL ASSEMBLY - SURVEILLANCE CAPSULE 1

FIGURE 10. The Metallurgical Assembly Located in the Surveillance Capsule.
Neg 8010270-10

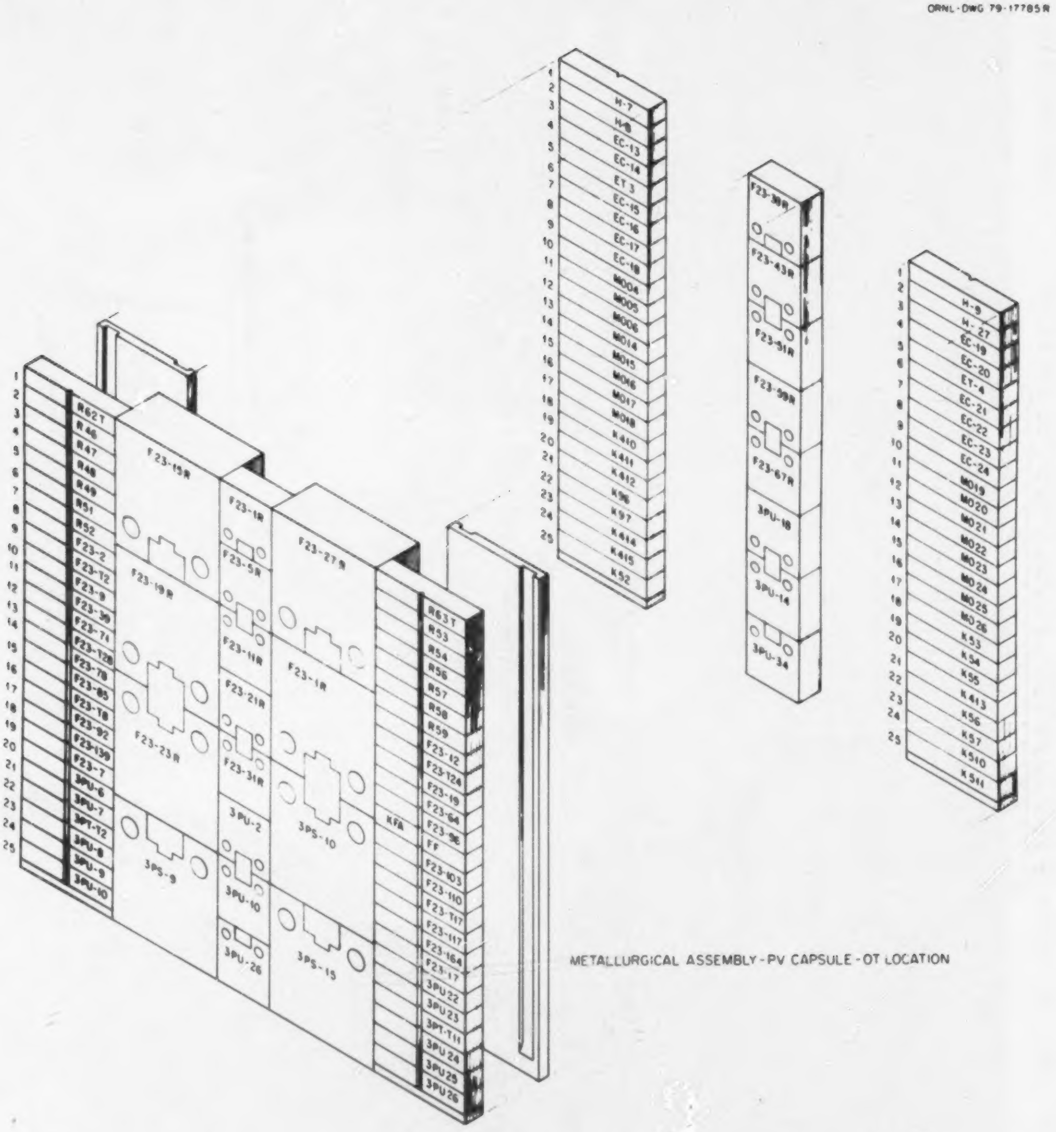
ORNL-DWG 79-17785R
1
2
3
4
5
6
7
8
9
10
11
12
13
14
15
16
17
18
19
20
21
22
23
24
25
H-7
H-8
EC-13
EC-14
ET 3
EC-15
EC-16
EC-17
EC-18
M004
M005
M006
M014
M015
M016
M017
M018
K410
K411
K412
K96
K97
K414
K415
K52
F23-30R
F23-43R
F23-51R
F23-59R
F23-67R
3PU-18
3PU-14
3PU-34
H-9
H-27
EC-19
EC-20
ET-4
EC-21
EC-22
EC-23
EC-24
MO19
MO20
MO21
MO22
MO23
MO24
MO25
MO26
K53
K54
K55
K413
K56
K57
K510
K511
R62T
R46
R47
R48
R49
R51
R52
F23-2
F23-T2
F23-9
F23-39
F23-74
F23-T28
F23-78
F23-85
F23-T8
F23-92
F23-139
F23-7
3PU-6
3PU-7
3PT-T2
3PU-8
3PU-9
3PU-10
F23-15R
F23-19R
F23-23R
3PS-9
F23-1R
F23-5R
F23-11R
F23-21R
F23-31R
3PU-2
3PU-10
3PU-26
F23-27R
F23-1R
3PS-10
3PS-15
KFA
R63T
R53
R54
R56
R57
R58
R59
F23-12
F23-T24
F23-19
F23-64
F23-96
FF
F23-103
F23-110
F23-T17
F23-117
F23-164
F23-17
3PU22
3PU23
3PT-T11
3PU24
3PU25
3PU26
METALLURGICAL ASSEMBLY-PV CAPSULE-OT LOCATION

FIGURE 11. The Metallurgical Assembly at the Inside Surface (Zero-Thickness Position, OT) of the Simulated Pressure Vessel Capsule. Neg 8010270-9

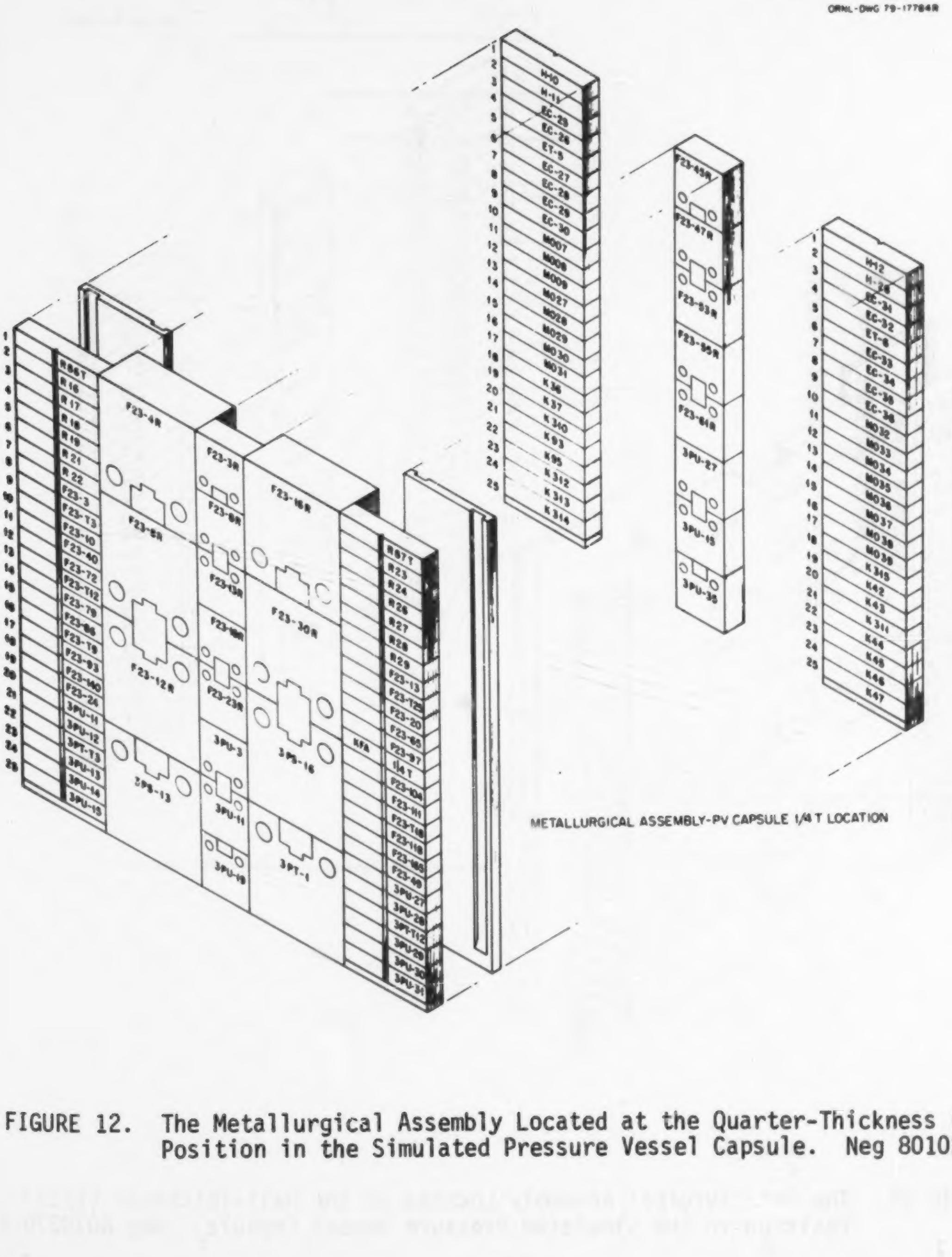
ORNL-DWG 79-17784R
1
2
3
4
5
6
7
8
9
10
11
12
13
14
15
16
17
18
19
20
21
22
23
24
25
H-10
H-11
EC-25
EC-26
ET-5
EC-27
EC-28
EC-29
EC-30
M007
M008
M009
M027
M028
M029
M030
M031
K36
K37
K340
K93
K95
K312
K313
K314
F23-43R
F23-47R
F23-53R
F23-55R
F23-61R
3PU-27
3PU-15
3PU-35
1
2
3
4
5
6
7
8
9
10
11
12
13
14
15
16
17
18
19
20
21
22
23
24
25
H12
H-26
EC-31
EC-32
ET-6
EC-33
EC-34
EC-35
EC-36
M032
M033
M034
M035
M036
M037
M038
M039
K315
K42
K43
K311
K44
K45
K46
K47
1
2
3
4
5
6
7
8
9
10
11
12
13
14
15
16
17
18
19
20
21
22
23
24
25
R66T
R16
R17
R18
R19
R21
R22
F23-3
F23-T3
F23-10
F23-40
F23-72
F23-T12
F23-79
F23-86
F23-T9
F23-93
F23-140
F23-24
3PU-11
3PU-12
3PT-T3
3PU-13
3PU-14
3PU-15
F23-4R
F23-5R
F23-12R
3PS-13
F23-3R
F23-6R
F23-13R
F23-19R
F23-23R
3PU-3
3PU-11
3PU-19
F23-16R
F23-30R
3PS-16
3PT-1
KFA
R67T
R23
R24
R26
R27
R28
R29
F23-13
F23-T25
F23-20
F23-65
F23-97
1/4T
F23-104
F23-111
F23-T18
F23-118
F23-185
F23-49
3PU-27
3PU-28
3PT-T12
3PU-29
3PU-30
3PU-31
METALLURGICAL ASSEMBLY-PV CAPSULE 1/4 T LOCATION

FIGURE 12. The Metallurgical Assembly Located at the Quarter-Thickness (1/4T) Position in the Simulated Pressure Vessel Capsule. Neg 8010270-8

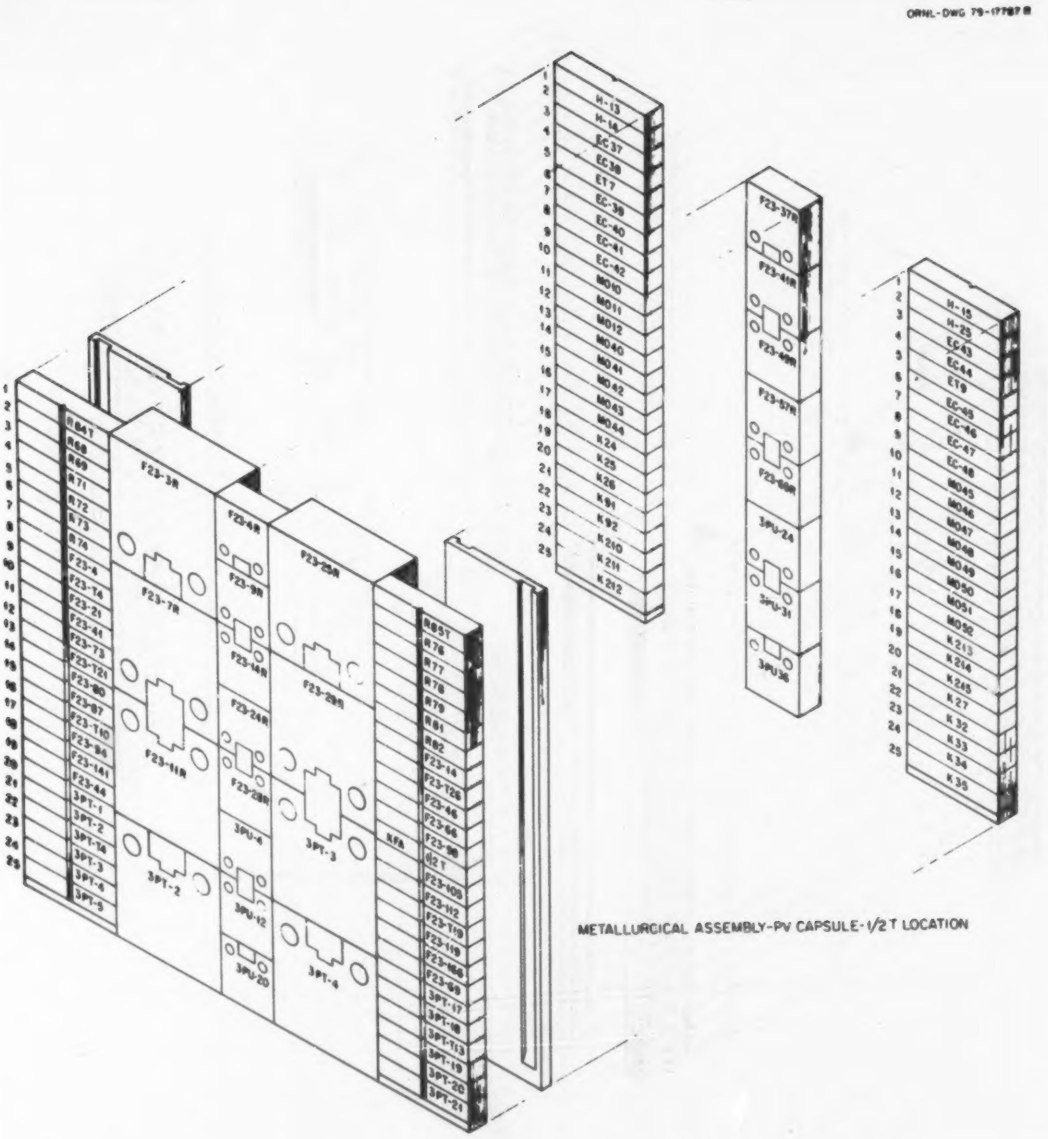
ORNL-DWG 79-17787 R
1
2
3
4
5
6
7
8
9
10
11
12
13
14
15
16
17
18
19
20
21
22
23
24
25
R84T
R68
R69
R71
R72
R73
R74
F23-4
F23-T4
F23-21
F23-41
F23-73
F23-T21
F23-80
F23-87
F23-T10
F23-94
F23-141
F23-44
3PT-1
3PT-2
3PT-T4
3PT-3
3PT-4
3PT-5
F23-3R
F23-7R
F23-11R
3PT-2
F23-4R
F23-9R
F23-14R
F23-24R
F23-28R
3PU-4
3PU-12
3PU-20
F23-25R
F23-29R
3PT-3
3PT-4
KFA
R85T
R76
R77
R78
R79
R81
R82
F23-14
F23-T26
F23-46
F23-66
F23-90
1/2 T
F23-105
F23-112
F23-T19
F23-119
F23-166
F23-69
3PT-17
3PT-18
3PT-T13
3PT-19
3PT-20
3PT-21
H-13
H-14
EC37
EC38
ET7
EC-39
EC-40
EC-41
EC-42
MO10
MO11
MO12
MO40
MO41
MO42
MO43
MO44
K24
K25
K26
K91
K92
K210
K211
K212
F23-37R
F23-41R
F23-48R
F23-57R
F23-68R
3PU-24
3PU-31
3PU36
H-15
H-25
EC43
EC44
ET9
EC-45
EC-46
EC-47
EC-48
MO45
MO46
MO47
MO48
MO49
MO50
MO51
MO52
K213
K214
K245
K27
K32
K33
K34
K35
METALLURGICAL ASSEMBLY-PV CAPSULE-1/2T LOCATION

FIGURE 13. The Metallurgical Assembly Located at the Half-Thickness (1/2T) Position in the Simulated Pressure Vessel Capsule. Neg 8010270-7

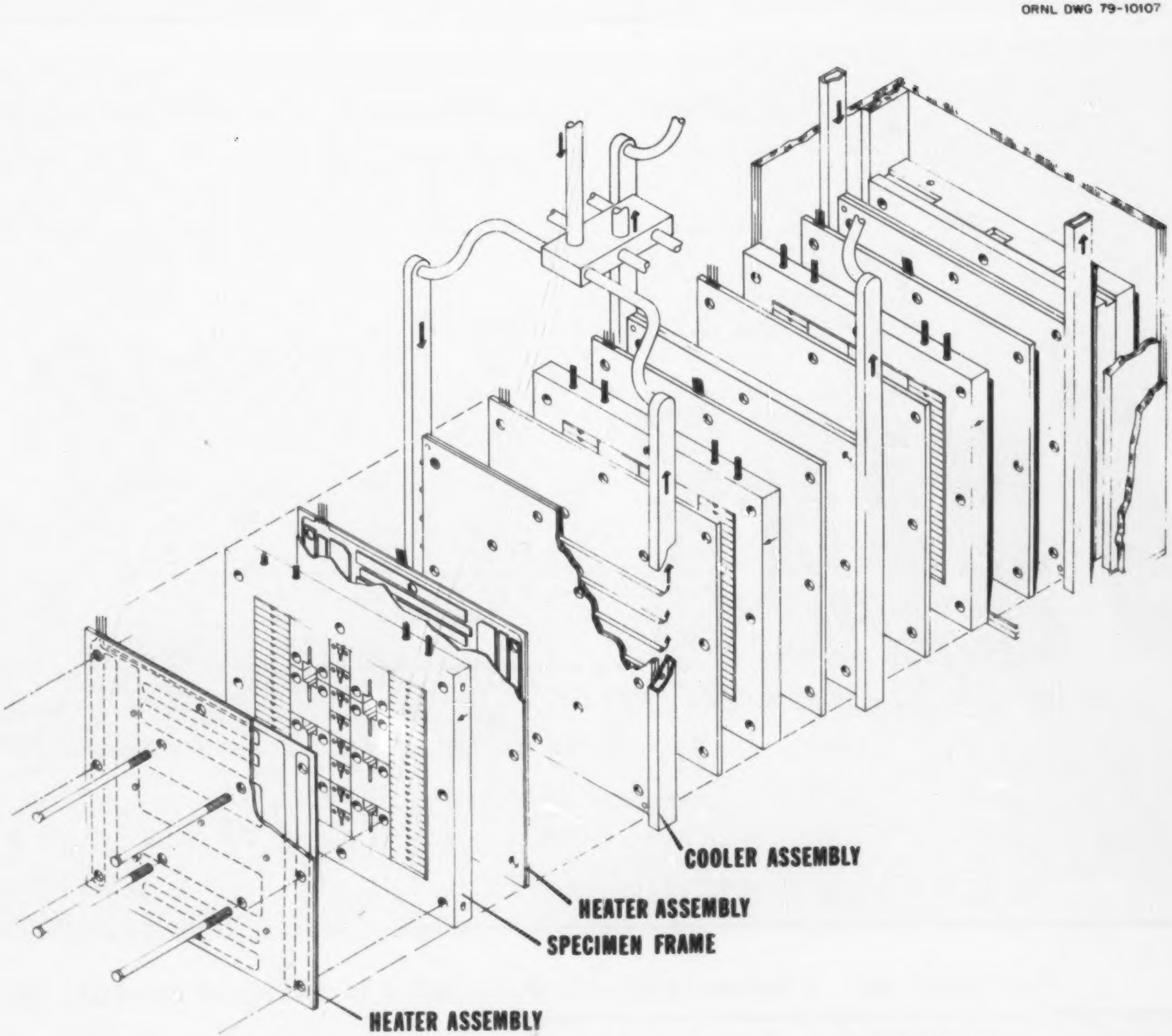
ORNL DWG 79-10107
COOLER ASSEMBLY
HEATER ASSEMBLY
SPECIMEN FRAME
HEATER ASSEMBLY

FIGURE 14. Exploded View of the Simulated Pressure Vessel Capsule. Neg 8010270-15

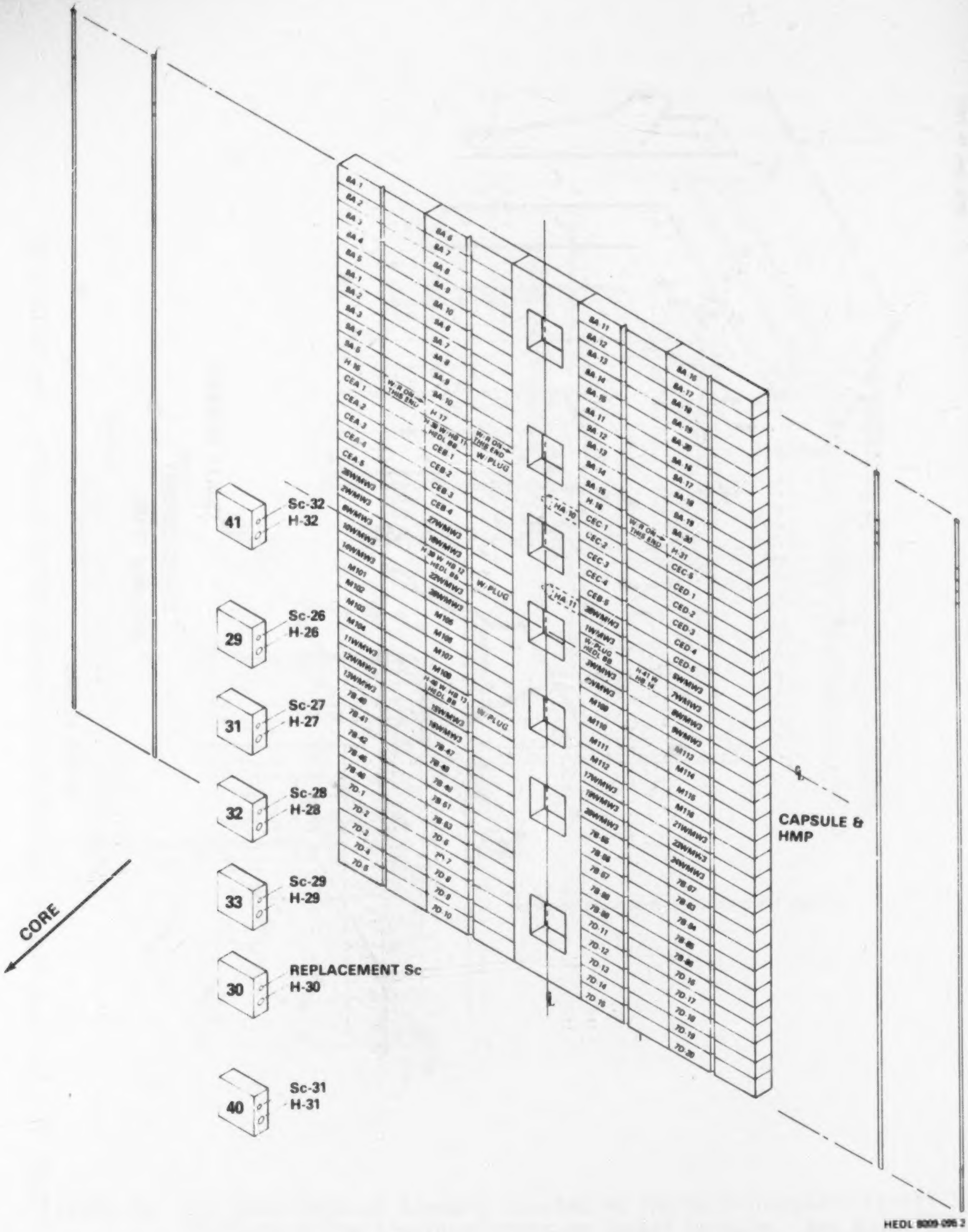
41
Sc-32
H-32
29
Sc-26
H-26
31
Sc-27
H-27
32
Sc-28
H-28
33
Sc-29
H-29
30
REPLACEMENT Sc
H-30
40
Sc-31
H-31
CORE
CAPSULE & HMP
HEDL 8009-095.2

FIGURE 15. The Metallurgical Assembly Contained in the Void Box Capsule (VBC).

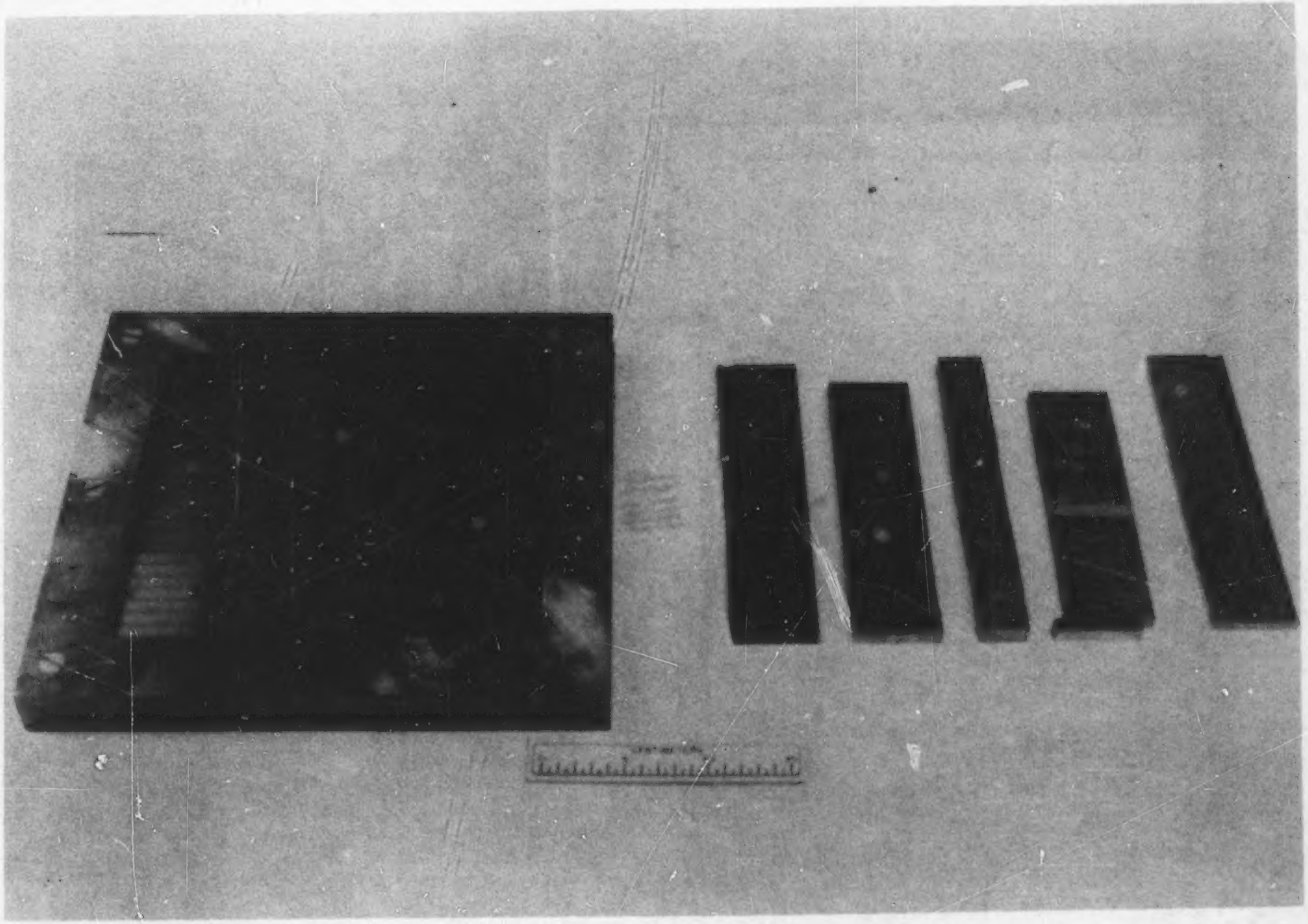

FIGURE 16. As-Built Photograph of a Typical Metallurgical Assembly. Neg 8010270-17

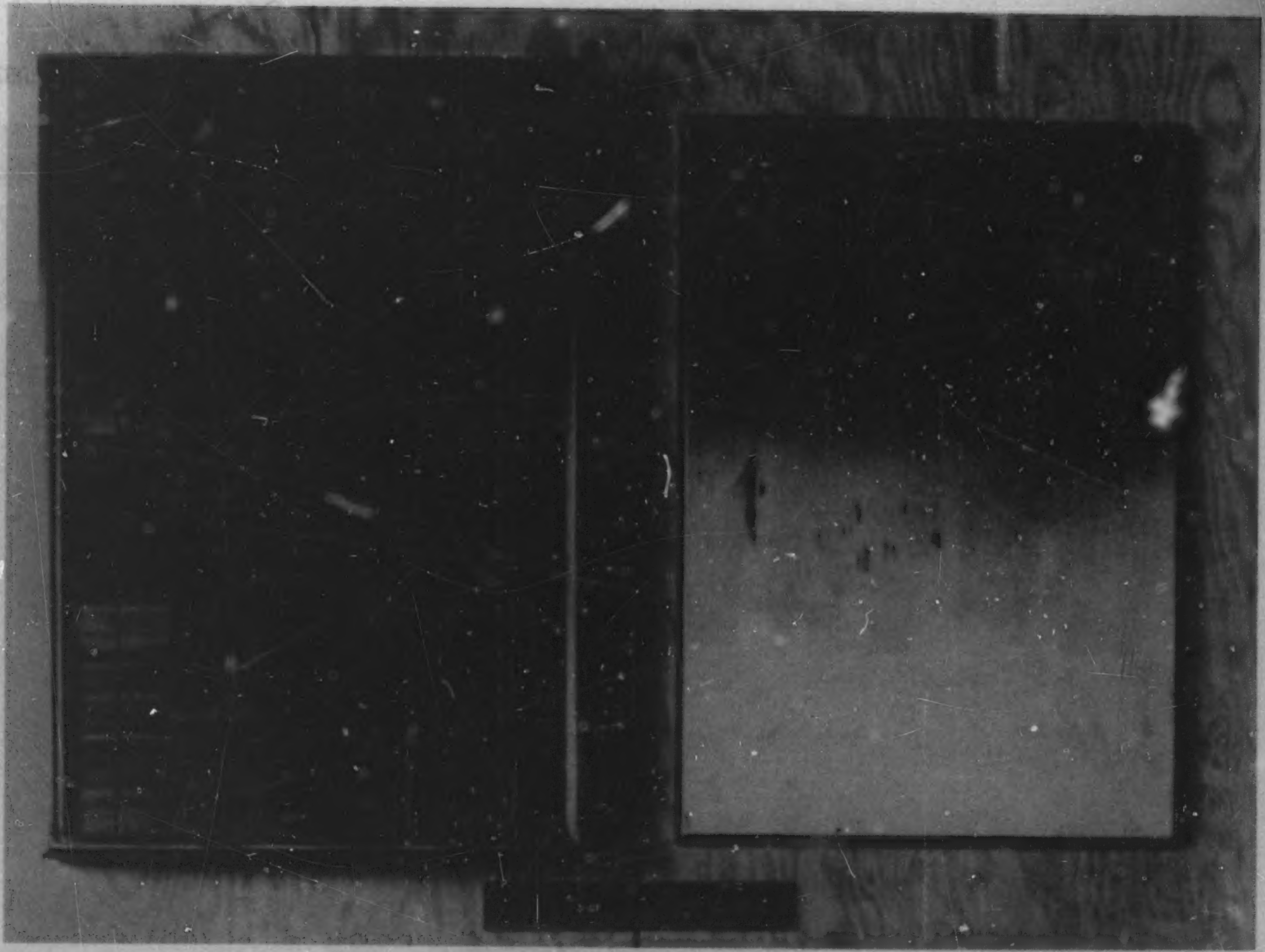

FIGURE 17. Rear View of the Void Box Metallurgical Assembly, Showing Iron Gradient Wires and Holder Tubes Positioned in Charpy Notches. Neg 8010270-18

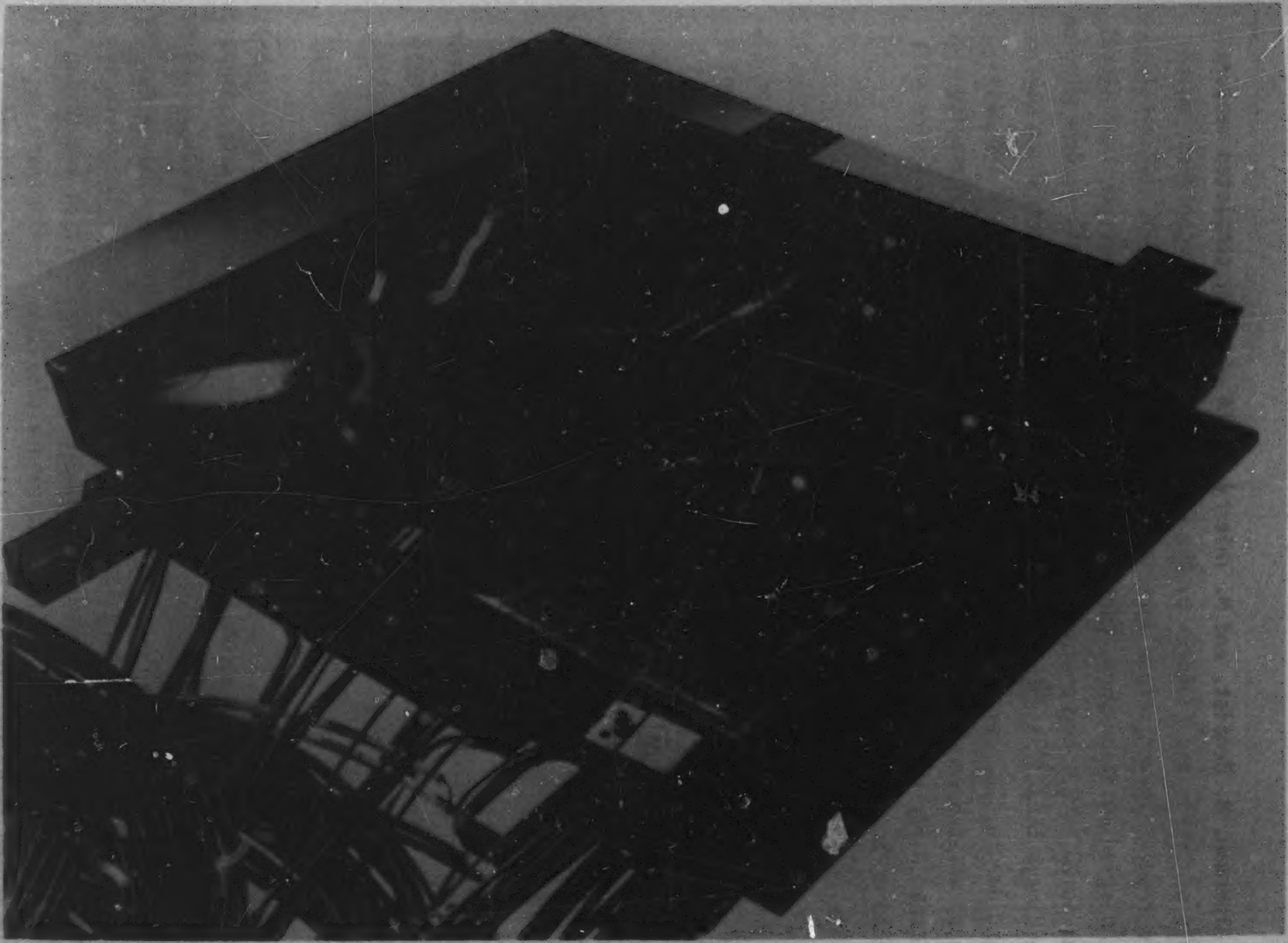

FIGURE 18. An Assembled Pressure Vessel Capsule, Showing Thermocouple Leads. Neg 8010270-21

A. Alberman, M. Benoist, and M. Thierry of CEN, Saclay, completed measurements of the damage fluences by the GAMIN and Tungstene techniques, which gave results in very close agreement. Evaluation of the SPV 1/4T steel irradiation position shows that the damage effectiveness per unit of nickel flux is 20 to 30% higher than at the SSC surveillance position, depending on the damage model. They concluded, therefore, that any effect which may exist due to flux level (a factor of 10 difference between the two positions) would predominate over the effect due to the 20 to 30% damaging spectral differences.(34) Certainly, the validity of this conclusion will depend on the chemistry and microstructure of the steels under study.(14-16,31,35-46)

The first surveillance capsule, SSC-1, was removed at 13:53 hours, June 23, 1980 after approximately 45 days of irradiation at 30 MW, and is presently in an ORNL hotcell awaiting decapsulation. The accumulated fluence of $\sim 2 \times 10^{19} n/cm^2$ ($E > 1$ MeV) will correspond to the fluence received at the SPV-1/4 T assembly after 570 days of irradiation. It is anticipated that SSC-1 metallurgical and dosimetry capsules will be shipped to program participants by September 1980.

The process control panel, which monitors, controls, and records the temperature profiles in the SSC-1 and SPVC is shown in Figure 19. The VBC contains no temperature monitors. The temperature profile data is currently being processed for the SSC-1, which has already acquired the designed neutron fluence.

Temperature control is accomplished through the use of coolant water and a mixture of neon and helium gas, which provide decoupling of the metallurgical assemblies in the SPVC, and electrical heaters. The gas mixture and the coolant water set temperature for fixed heating conditions. The heaters, controlled by Variac settings under computer supervision, then are turned on or off to maintain the specified temperature profiles. Preliminary data analysis indicates that temperatures will lie between 281°C and 293°C, with the bulk of the data at approximately 288°C.

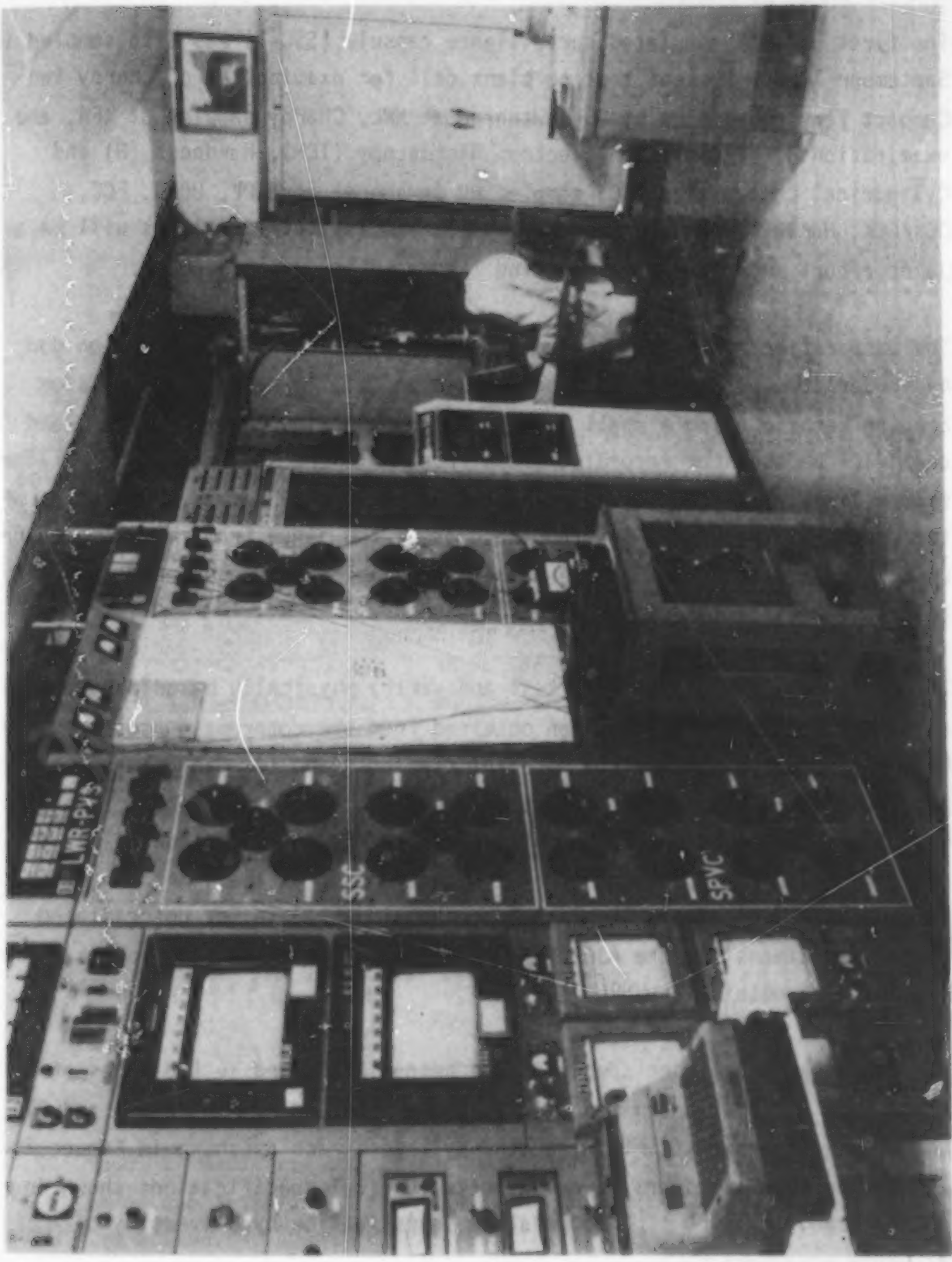
LWR-PVS
SSC
SPVC

FIGURE 19. The Process Control Panel for the Pressure Vessel Benchmark Facility. Neg 8010270-20

C. ORR-PSF Metallurgical Specimen Test Program

The first ORR-PSF simulated surveillance capsule (SSC-1) was disassembled in September 1980. Present testing plans call for examination of Charpy and Compact Tension samples by J. Hawthorne at NRL, Charpy samples at KFA, and examination of Transmission Electron Microscopy (TEM), Hardness (H) and Cylindrical Compression (CC) samples by personnel at HEDL, UCSB, FCC, CEN/SCK, Harwell, and elsewhere. Physics and dosimetry analysis will be a joint effort among the participating laboratories; see Figure 21.

The preparation for testing of compression cylinders at HEDL has been done by K. Carlson. The tests will be done in an "MTS" hydraulic compression testing machine using a small sub-press shown in Figure 20. The MTS load cell will be used for recording the stress while the strain will be obtained from a linear variable transformer attached to the sub-press. Operation of the equipment is planned for temperatures in the range from room temperature up to approximately 260°C. The number and types of compression samples to be tested are identified in Tables 7 and 8.

In addition to its use to help test and verify physically based damage correlation models, the information obtained from the compression tests on the NRC/NRL A302B and A533B plate material (Tables 9 and 10) can be used to help plan the distribution of test temperatures for Charpy specimens. This will optimize the ability of NRL to obtain an accurate determination of the 30 ft-lb and 50 ft-lb charpy-energy temperatures from the limited number of Charpy samples, Table 9. Charpy V-notch impact data for unirradiated control specimens for the A302B and A533B reference plate materials have already been obtained by NRL.

The compression cylinder specimens are being irradiated in two types of holders 1) transverse drilled blocks (e.g., block 38 of Figure 21) and 2) Charpy-sized carriers containing nine cylinders each as shown in Figure 22. The latter type specimens cover the metallurgical specifications shown in Table 10 and are part of a cooperative investigation by University of

[POSITION 1] SURVEILLANCE ($\sim 2.0 \times 10^{19}$)* [POSITION 1] SURVEILLANCE ($\sim 3.6 \times 10^{19}$)*, AND [POSITION 2] SURFACE ($\sim 3.6 \times 10^{19}$)* CAPSULES

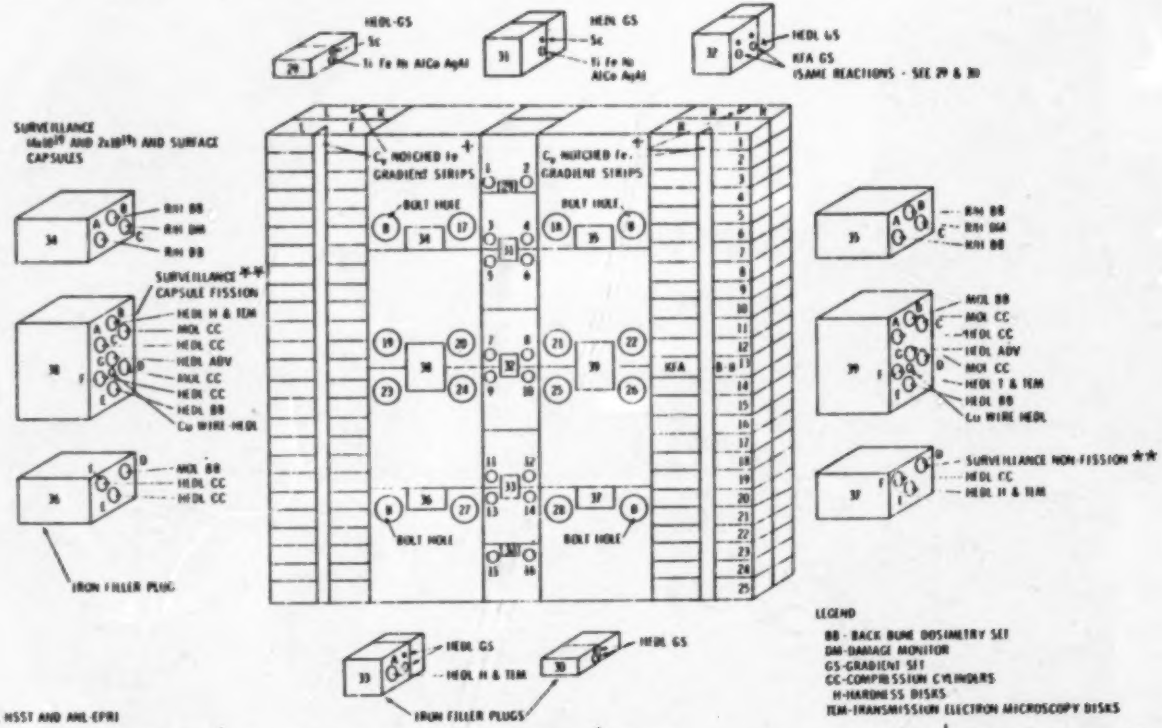
HEDL-GS
Sc
Ti Fe Ni AlCo AgAl
29
HEDL GS
Sc
Ti Fe Ni AlCo AgAl
31
HEDL GS
KFA GS
(SAME REACTIONS - SEE 29 & 30)
32
SURVEILLANCE (4x10^19 AND 2x10^19) AND SURFACE CAPSULES
34
A
B
C
RNI BB
RNI DM
RNI BB
SURVEILLANCE ** CAPSULE FISSION
38
HEDL H & TEM
MOL CC
HEDL CC
HEDL ADV
HUL CC
HEDL CC
HEDL BB
Cu WIRE-HEDL
36
MOL BB
HEDL CC
HEDL CC
IRON FILLER PLUG
Cv NOTCHED Fe + GRADIENT STRIPS
Cv NOTCHED Fe. + GRADIENT STRIPS
BOLT HOLE
BOLT HOLE
BOLT HOLE
BOLT HOLE
KFA
B-B
35
RNI BB
RNI DM
RNI BB
39
MOL BB
MOL CC
HEDL CC
HEDL ADV
MOL CC
HEDL T & TEM
HEDL BB
Cu WIRE HEDL
37
SURVEILLANCE NON FISSION **
HEDL CC
HEDL H & TEM
33
HEDL GS
HEDL H & TEM
30
HEDL GS
IRON FILLER PLUGS

LEGEND

BB - BACK BURN DOSIMETRY SET
DM-DAMAGE MONITOR
GS-GRADIENT SET
CC-COMPRESSION CYLINDERS
H-HARDNESS DISKS
TEM-TRANSMISSION ELECTRON MICROSCOPY DISKS

SHOULD INCLUDE ORNL HSST AND ANL-EPRI

PT#	HOLE	LAB	CONTENTS
17	RRA-	HARWELL	CC & TEM
18	"	"	"
19	AVAILABLE FOR UP TO THREE GE DOSIMETRY SETS		
20	" " " " "	CE "	"
21	" " " " "	WEST "	"
22	" " " " "	BW "	"
23	" " " " "	"OTHERS" "	"
24	4x10^19 SURV. AND SURFACE CAPS.	HEDL	EXPLORATORY SSTR-DM
25	"	"	"
26	AVAILABLE FOR UP TO THREE OTHERS DOSIMETRY SETS		
27		HEDL	H & TEM
28		"	"
29		HEDL	GS
30		"	"
31		"	"
32		HEDL & KFA	"
33		HEDL	(GS+H&TEM IN Al)
34	A	BRABIAR (RNI)	BB
	B	"	BB
	C	"	DM
35	A	"	BB
	B	"	BB
	C	"	DM
36	D	MOL	BB
36	E	HEDL	533 CC
	F	HEDL	533 CC
37	D	HEDL	NON FISSION
	E	HEDL	H&TEM
	F	HEDL	533 CC
38	A	HEDL	302 CC
	B	HEDL	FISSION
	C	MOL	CC
	D	MOL	CC
	E	HEDL	BB
	F	HEDL	302 CC
	G	HEDL	ADV DOS
39	A	HEDL	302 CC
	B	MOL	BB
	C	MOL	CC
	D	MOL	CC
	E	HEDL	BB
	F	HEDL	H&TEM
	G	HEDL	ADV DOS
CVRF-13		KFA	BB
CVIF Fe		NOTCHED A	
CVIR Fe		" "	
CVRI "		" "	
CVRR "		" "	

HEDL 7808-170.1

* FLUENCE (n/cm^2)

** Only in Position 1 Surveillance ($\sim 2.0 \times 10^{19}$) Capsule.

+ Fabricated by ORNL $\sim$0.010" Dia. Fe will be used instead of notched gradient strips.

FIGURE 21. Metallurgical Specimen Configuration.

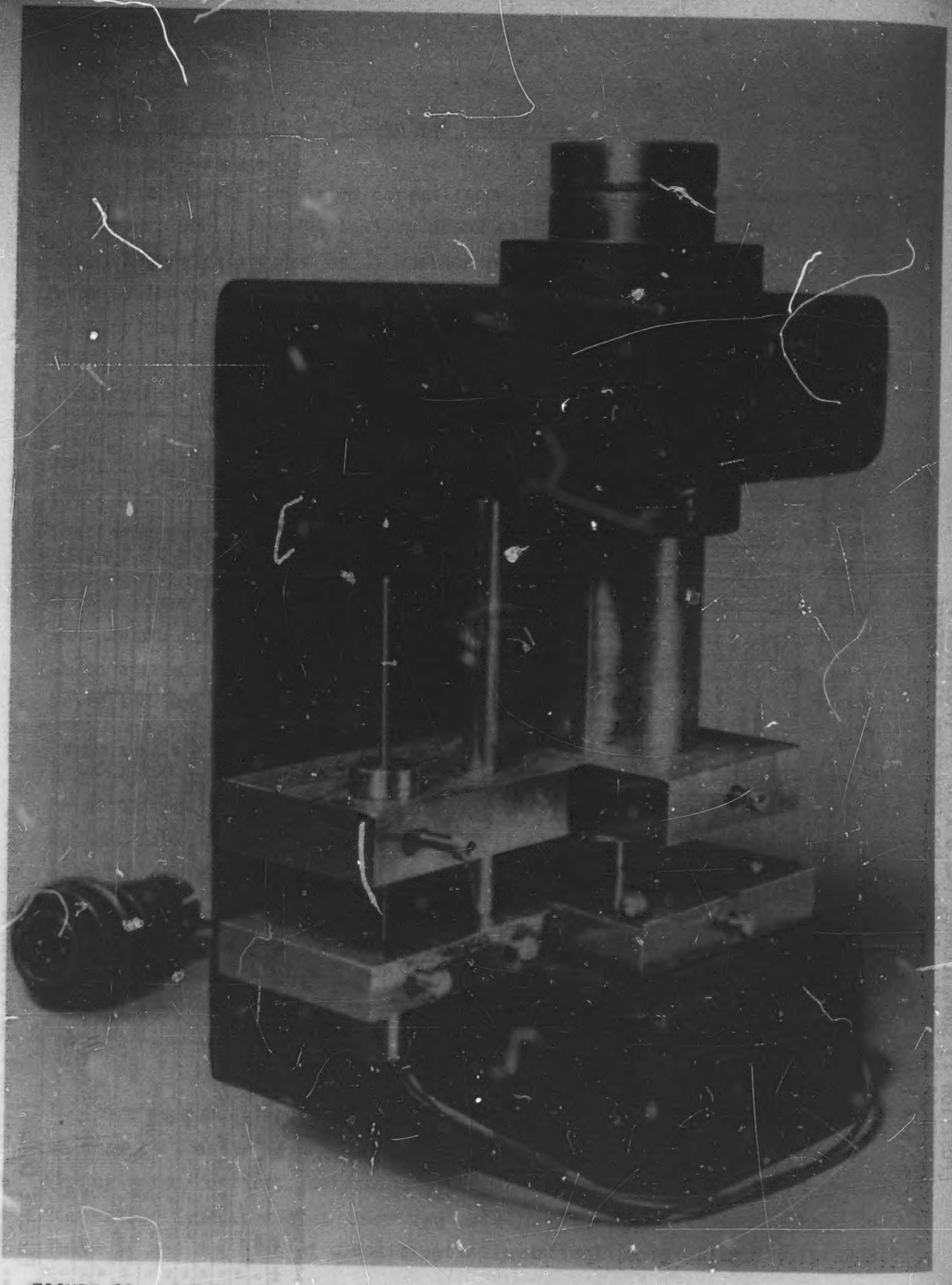

FIGURE 20. "MTS" Hydraulic Compression Testing Machine. Neg 8008646-3

TABLE 7

DESCRIPTION OF COMPRESSION CYLINDER SPECIMENS

HEDL Material Designation	Source and Source Code	Dimensions	Irradiation Locations	Material Description
27 N	NRL 27N	.157" diam. X .392" long cylinder	Located in Charpy carriers Fig (22) in LR1, LR2, and RR1 positions in SSC-1, SSC-2 1/4T, 1/2T and PVF capsules. Also in void box.	A533B plate material, cross rolled, .13% Cu, 1/4T position.
29 N	NRL 29N			A533B plate, cross rolled, .03 Cu, 1/4T position.
BG 1	EPRI 2bE			A508-2 Forging. 1/4T depth. EPRI received from B&W.
BG 2	EPRI EP24			Hi Cu-Hi Shelf. Linde 0091 weld on A533B-1 base. EPRI/West/NRL Source.
BG 3	EPRI 1bA			Originally from NRL. Surface Of HSST-02 plate. A533B.
BG 4	EPRI NP 933-1-150 Heat Code 1mQ			EPRI archive. E8018-03 electrode 1 mQMMA weld on an SA533B-1 base. Weld by Combustion Engineering. CE gave plate and weld to EPRI.
BG 5	EPRI 1bA			Originally from NRL. Broken halves of 1TCT specimens differ from BG 3 in that it is 1/4T location. HSST-02 A533B plate.
BG 6	EPRI 4bA			Originally from NRL. Broken halves of 1TCT specimens A302B ASTM heat, samples from 1/4T position.
BG 7	EPRI 7bB			A533-2 material went to EPRI from General Atomic, Manufactured by Lukens. Broken halves of 1TCT specimens.
3 PT	NRL-3PT	.250" diam. X .410" long cylinder	Located in block holes (Fig 21) 38A, 38F, 39A, 36F, 36E, 37F of SSC-1, SSC-2, 1/4T, 1/2T and and PVF capsules	HSST-03 plate of A533B. 1/4T location cut directly from plate.
F 23	NRL-F23			ASTM Reference heat 1/4T location cut directly from plate.

NOTE: Accumulation of above materials was done principally by Fracture Control Corp. (R. Wullaert)

TABLE 8

COMPRESSION CYLINDER CHEMISTRY (wt %)

HEDL Designation	C	Mn	P	S	Si	Ni	Cr	M_o	V	Cu	NDT	RTNDT	Upper Shelf
BG-1	.23	.73	.007	.009	.31	.65	.41	.59	.054	.04	-7°C	-7°C	182.J
BG-2*	.11	1.57	.007	.011	∿.23	.64	.02	.48	.005	.36	---	---	---
BG-3	.23	1.55	.009	.014	.2	.67	.04	.53	.003	.16	-30°C	-15°C	144.J
BG-4	.1	1.11	.007	.01	.4	1.06	.01	.34	.006	.02	-57°C	-57°C	212.J
BG-5	.23	1.55	.009	.014	.2	.67	.04	.53	.003	.16	---	---	---
BG-6	.23	1.47	.013	.024	.26	.17	.05	.52	.004	.2	-18°C	---	61.J
BG-7	.21	1.25	.007	.007	.170	.210	.250	.08	.005	.12	---	---	138.J
27 N	.18	1.29	.008	.008	.20	.56	.06	.51	---	.13	---	---	---
29 N	.18	1.27	.008	.007	.20	.55	.06	.52	---	.03	---	---	---
3 PT	.20	1.26	.011	.018	.25	.56	.10	.45	---	.10	---	---	---
F 23	.23	1.47	.013	.024	.26	.17	.05	.52	.004	.20	---	---	---

* Preliminary analysis

TABLE 9

CHARPY, TENSILE, AND CT SPECIMENS FOR EACH OF FIVE CAPSULES FOR PSF*

Metallurgical Material	Regular** Charpy V	Charpy** Sized Tensile Specimen	0.5TCT	1.0TCT
EPRI Weld Metal	12	2	0	0
NRC/NRL A302B Ref. Plate	18	5	10	5
NRC/NRL A553-03 Ref. Plate	10	2	6	3
KFA/22Ni Mo Cr37, KFA, Jülich, Germany	14	2	0	0
CEN-SCK/COCKERILL SA 508 CLASS-3 FORGING, CEN/SCK, Mol, Belgium	14	2	0	0
High Sensitivity SA Weld (.23 Cu) on an A533 Base, Rolls-Royce and Associates Limited, United Kingdom	12	2	0	0

*Specimens and materials for the void box position are not identified in this table.

**The accounting of Charpy positions is that 95 Charpy or Charpy equivalent spaces were allotted to participants and five such spaces were available for space compatible specimens, for utilization by assemblers for dosimeters, or for other uses.

TABLE 10

A. SPACE COMPATIBLE SPECIMEN MATERIALS FOR PSF (ENGINEERING MATERIALS)

Material	Heat Code	Source	Description
A302B Ref. Plate	F23	NRC/NRL	Table 8 Material
A533-03 Ref. Plate	3PT	NRC/NRL	Table 8 Material
A508	-	CEN/SCK, Mol, Belguim	Forging
A533B-1	1bA	EPRI Archive (HSST-02)	1/4T, 4-1T Compact Halves
A533B-1	1bA	EPRI Archive (HSST-02)	Surface, 6 1/2x10x2 1/4 Piece
A302B	4bA	EPRI Archive (ASTM-CM)	1/4T, 4-1T Compact Halves
SA Weld-Linde 0091 (A533B-1 base)	EP24	EPRI/West/NRL	Hi Cu, Hi Shelf
MMA Weld-E8018-C3 (A533B-1 base)	1mQ	EPRI Archive (CE)	11 x 13 x 6 Piece
A508-2	2bE	EPRI/Archive (B&W)	1/4T, 5 x 9 x 1 Piece
A537-2	7bB	EPRI/Archive (GA)	1/4T, 4-1T Compact Halves

B. SPACE COMPATIBLE SPECIMEN MATERIALS FOR PSF (MODEL MATERIALS)

Material	Heat Code	Source	Description
A533B-1 (0.03Cu)	N29	NRL/Hawthorne	1/4T, 3 pieces 1/2 x 1/2 x 1/4 in
A533B-1 (0.13Cu)	N27	NRL/Hawthorne	1/4T, 3 pieces 1/2 x 1/2 x 1/4 in
Pure Iron	Fe-6	NRL/Smidt	30 TEM Discs
Fe - 0.3at%V	Fe-2	NRL/Smidt	30 TEM Discs
Fe - 0.3at%Cu	Fe-4	NRL/Smidt	30 TEM Discs
Fe - .34wt%Cu	Alloy 1	West./Spitznagel	Misc. Pieces of Strip & Wire
Fe - 0.1wt%N	Alloy 2	West./Spitznagel	Misc. Pieces of Strip & Wire
Fe - .34wt%Cu - 0.1wt%N	Alloy 3	West./Spitznagel	Misc. Pieces of Strip & Wire

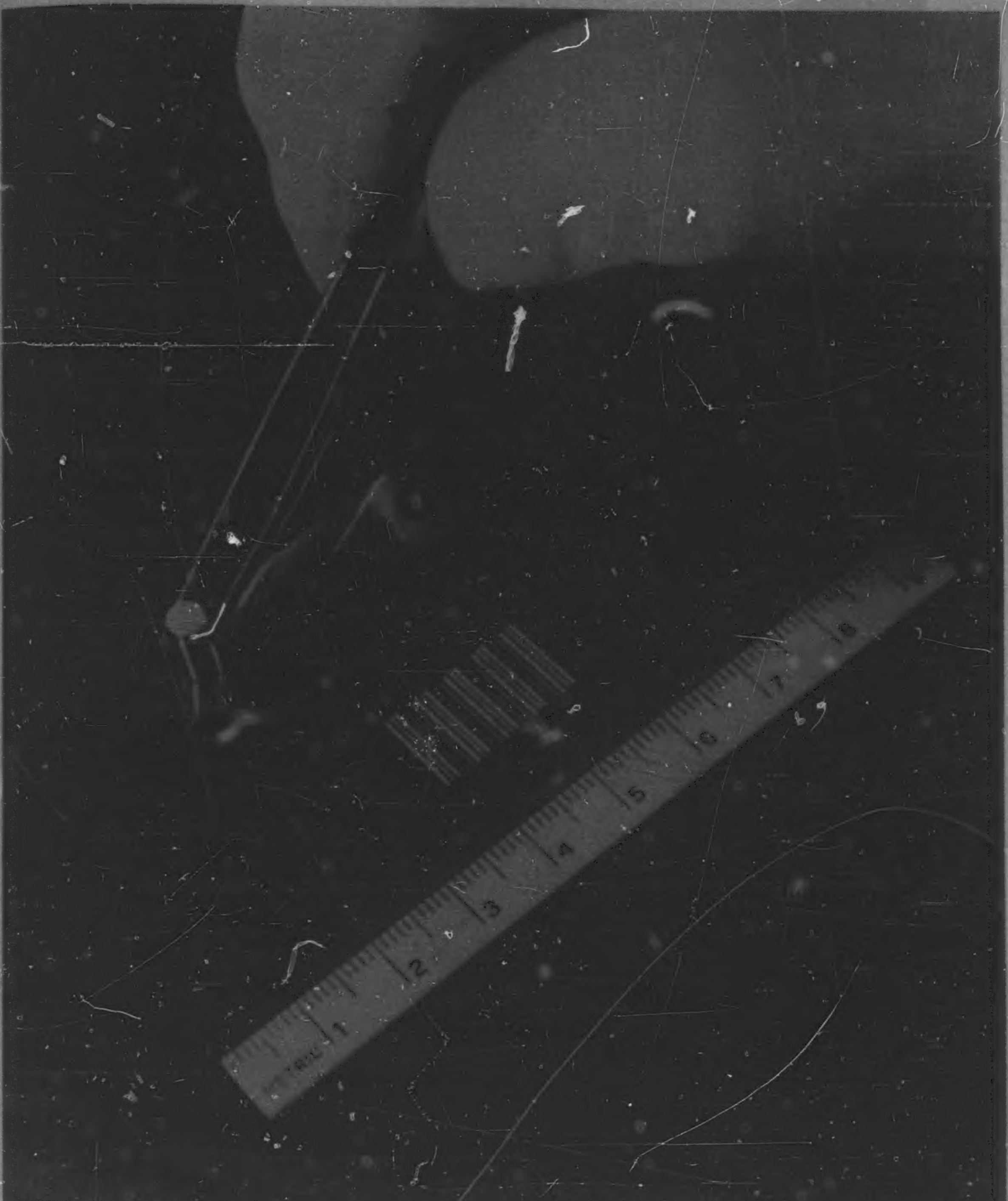

FIGURE 22. Space Compatible Compression Specimens. Neg 7906745-2cn

California at Santa Barbara, EPRI, Fracture Control Corporation and HEDL personnel using "engineering" and "model" materials obtained from a number of different sources identified in Table 10.

Two types of holders in each irradiation capsule contain small disks 0.003" to 0.004" thick and 3 mm diameter. These holders are 1) Charpy carriers (one in each irradiation capsule; at the surveillance, surface, 1/4T, and 1/2T locations as shown in Figure 23 and 2) small open cylindrical holders which fit in holes in the transverse drilled blocks (e.g., block 38F of Figure 21). These specimens can be used in TEM examinations and in hardness studies. Some preliminary work has been done by L. Thomas at HEDL to prepare for the TEM examinations.(26) The hardness examinations are expected to be conducted using commercial hardness test machines together with instrumented hardness test procedures and microhardness techniques under development by G. Odette and G. Lucas at the University of California at Santa Barbara.

The preliminary TEM studies mentioned above have been conducted as part of a joint KFA-HEDL study of samples of three alloy heats irradiated in West German test reactors. This study involves TEM examination and coordinated hardness studies of samples subjected to a series of isochronal anneals. The hardness data collected for this study are already quite extensive(39) but the TEM studies are in a preliminary stage. To date, the HEDL TEM part of the program has consisted of studies of methods of electropolishing the samples, as well as TEM examinations of unirradiated control specimens and irradiated specimens prior to initial isochronal anneals. A list of the joint HEDL-KFA specimens available for examination appears in Table 11.

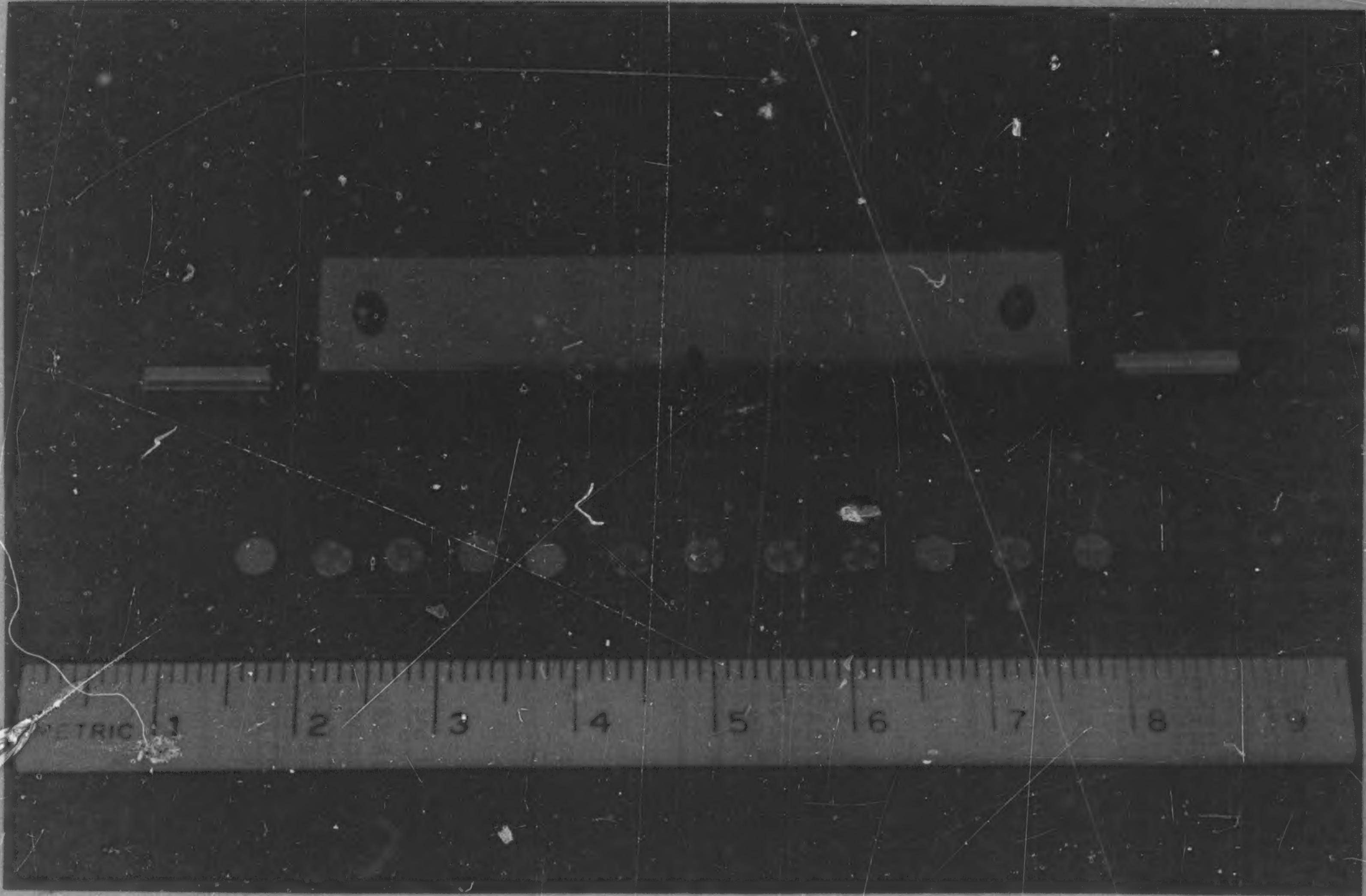

FIGURE 23. Space Compatible Hardness and TEM Specimens. Neg 7906745-6cn

TABLE 11

PROPOSAL FOR TEM ANNEALING HEAT TREATMENT TEMPERATURES FOR ISOCHROMAL ANNEALS

Material	A 533 B HSST 03 LF					A 533 B Modified					Weld
Chemical Analysis wt %	0.22 C 0.0005 B 0.25 Si 0.01 Co 1.44 Mn 0.12 Cr 0.012 P 0.12 Cu 0.015 S 0.51 Mo 0.023 N 0.63 Ni 0.023 Al 0.01 V					0.11 C 0.001 B 0.35 Si 0.013 Co 1.36 Mn 0.11 Cr 0.012 P 0.11 Cr 0.008 S 0.37 Mo 0.016 N 1.5 Ni 0.014 Al 0.015 V					0.06 C 0.0003 B 0.21 Si 0.023 Co 1.85 Mn 0.08 Cr 0.012 P 0.29 Cu 0.003 S 0.56 Mo 0.011 N 1.3 Ni 0.015 Al 0.02 V
Capsule No.	KFA 1	KFA 2	KFA 3	KFA 4	KFA 5	KFA 6	KFA 7	KFA 8	KFA 9	KFA 10	KFA 11
Neutron Fluence n/cm^2 E 1 MeV	$1.5x10^{18}$	$1.5x10^{19}$	$1.5x10^{19}$	$3x10^{19}$	$7x10^{19}$	$1.5x10^{18}$	$1.5x10^{19}$	$1.5x10^{19}$	$3x10^{19}$	$7x10^{19}$	$5x10^{19}$
Neutron Flux FRJ-1 n/cm^2 E 1 MeV	$3x10^{13}$	$3x10^{13}$	$6x10^{11}$	$3x10^{13}$	$3x10^{13}$	$3x10^{13}$	$3x10^{13}$	$6x10^{11}$	$3x10^{13}$	$3x10^{13}$	$3x10^{13}$
Transition Temp. TT 30 Ft-Lb=51 J/cm^2	60°C	145°C	150°C	145°C	187°C	24°C	110°C	105°C	114°C	168°C	--
Increase of Transition Temp. ΔTT	35°C	120°C	125°C	120°C	162°C	36°C	122°C	117°C	126°C	180°C	--
Vickers Hardness HV 10 N/mm^2	2200	2800	2700	2820	2980	2250	2800	2840	2930	3070	3440
Increase of Vickers Hardness	10%	40%	35%	41%	50%	23%	53%	55%	60%	68%	55%
Irradiation Temp.	150°C	150°C	150°C	150°C	150°C	150°C	150°C	150°C	150°C	150°C	150°C
Proposal for TEM 1)	A.R.	A.R.	A.R.	A.R.	A.R.	A.R.	A.R.	A.R.	A.R.	A.R.	A.R.
Annealing Heat 2)	330°C	260	280	260	270	310	270	290	270	270	290
Treatment 3)	400	310	330	310	310	400	330	330	330	330	330
Temperature for 4)		400	400	400	400	490	400	400	400	400	400
Isochronal 5)		490	490	490	490		490	490	490	490	500
Anneals 6)								600	600	600	

NOTE: A.R. = As Received, i.e., not yet annealed.

VI. Analysis and Interpretation of Research and Power Reactor Test and Surveillance Results

[Variables Studied: All those initially listed in the first paragraph of Section II.]

A primary objective of this multilaboratory supported program is to help in the development of statistically valid radiation embrittlement data bases (Reg. Guide 1.99, MPC, EPRI, and others) for use in the critical evaluation of the procedures used for predicting the fracture toughness and embrittlement of irradiated reactor pressure vessel and support structure steels.

Analysis of the existing and new additions to these data bases (from test and power reactors) has revealed that the variance of test data does not arise entirely from material variability. A substantial portion stems from lack of consistency in the application and/or shortcomings in test methods and control of important variables associated with the "reactor systems analysis," "dosimetry," "metallurgical," and "fracture mechanics" disciplines.

Summary information is presented in Sections VI-A, B, and C on the results of recent studies associated with metallurgical and physics-dosimetry data development and testing.

A. Surveillance Capsule Metallurgical Data Development and Testing

As part of the LWR Dosimetry Improvement Program, statistically based data correlation studies have been made by G. Guthrie, F. Berting, and R. Simons of existing metallurgical data banks in anticipation of the analysis of new embrittlement data from the ORR-PSF and other experiments.(1,2,6-9,25-27,44-47) Some of the available data collections are 1) the Charpy shift vs exposure data for welds and plates, as collected by Beimiller and Byrne,(42) and Varsik and Byrne,(43), 2) the Charpy shift vs exposure data collected by the MPC study(38), and 3) the data available in various reactor surveillance reports. The immediate purpose of such analyses is the application of the results to the preparation of the ASTM Standard Practice, IE, on "Damage Correlation" and the ASTM Standard Guide, IIF, on "Correlation of ΔNDTT with Fluence," Figures 1 and 2.

Nineteen surveillance capsule reports for Westinghouse reactors have been examined for inconsistencies in reported fluence values. Details of this work are discussed in Section VI-B-4 and summary results are presented in Table 16. Twelve of the 19 capsules analyzed contained Charpy specimens from the so-called ASTM A302B "reference heat." As a first approximation, it is possible to assume that the chemistry of these specimens is roughly identical. Therefore it is possible to use these data to check for the applicability of various forms of equations relating ΔNDTT and flux or fluence, while avoiding the complexities usually imposed by chemical variations.

Several formulas were used to relate ΔNDTT to flux or fluence. Of the expressions examined, it was found that a formula of the type

$$\Delta NDTT = A(\phi t)^N \qquad (1)$$

gave the best fit for the set of 12 Charpy shift data points. The 1σ standard deviation of the fit was 11.45°F with $A = 261$ and $N = 0.238$ when ΔNDTT is expressed in °F and ϕt is given in DPA.

Another satisfactory expression was

$$\Delta NDTT = A \cdot \left[\tau \cdot \Phi \cdot (1 - \exp(- \frac{t}{\tau})) \right]^N \qquad (2)$$

where ΔNDTT is given in °F, and the derived values were $A = 282$, $\tau = 2.73 \times 10^8$ sec, and $N = 0.248$, and t is given in seconds while Φ is expressed in DPA/sec. For this relation, $\sigma = 12.11°F$. It might be noted that τ is 8.66 years which would indicate the presence of a saturation process which would only become apparent with data from long term irradiations.

Simple theories relating resistance of dislocation flow to obstacle density would indicate that the exponent on the bracketed term of Eq (2) might well be set at the value 0.5. This would be in harmony with the point of view that the bracketed term is somehow associated with the number of remaining defects at any given time and the exponent relates the defects to the flow resistance. However, this also assumes a simple proportionality between flow resistance and ΔNDTT. The use of such a formula, with N set equal to 0.5 in Eq (2), however, did not give improved results. The value derived for sigma was 23.09°F.

Other formulas tested included

$$\Delta \mathrm{NDTT} = A \cdot [1 - \exp(-B \cdot \phi t)]^N \tag{3}$$

which gave a value of sigma of the order of 12°F, and

$$\Delta \mathrm{NDTT} = A \cdot \left[1 - \exp\left(- \frac{t}{\tau_1} \right) \right] + B \cdot \left[\phi \cdot \tau_2 \cdot \left(1 - \exp\left(- \frac{t}{\tau_2}\right)\right) \right]^{0.5} \tag{4}$$

This latter formula gave a sigma of approximately 18°F.

The use of a simple straight line relation,

$$\Delta \mathrm{NDTT} = A + B \cdot (\phi t) \tag{5}$$

gave a value of sigma of 12.22°F.

The statistical similarity of results with and without saturation effects, Eq (1) and Eq (2), indicates no apparent advantage for one equation over the other. However, when the two formulas are extrapolated to a 30-year end-of-life type irradiation, Eq (1) shows Charpy shifts approximately one third larger than those given by Eq (2).

The advantages to be found by removing inconsistencies from existing data banks are shown by taking the 12 data sets for the 12 capsules, both in the corrected and uncorrected forms, and applying a mathematical relationship of the type given by Eq (1). This results in a decrease in sigma of approximately 2.0°F in going from the uncorrected to the corrected values. The lack of any startling improvement is due to the fact that the error in the determination of the Charpy 30 ft-lb transition temperature is approximately 10°F, which places a lower limit on the value of sigma. Also, the data are all taken from one type of PWR plant where reasonably uniform calculational procedures, cross-section values, etc. have been used in the analysis of the data. Therefore the errors tend to be consistent and incorrect values show a bias rather than a scatter.

An analysis of the MPC data base was performed to detect features in the data which would be indicative of the presence of fluence reporting errors.(27) Such an analysis is possible because fluence errors tend to follow a log-normal distribution rather than a normal one. The results of the analysis showed that a reduction of 7°F in sigma can be expected if fluence errors are removed, but this does not take into account the additional benefits derived from the removal of the bias.

B. Surveillance Capsule Dosimetry Data Development and Testing

1. Program Status

In establishing improved metallurgical data bases, careful consideration must be given to the variables associated with the use and accuracy of neutron exposure units and values. The total fluence above 1.0 MeV is currently used as the critical spectral parameter for the prediction of LWR reactor material property change. This is a widely accepted practice, even though the mechanisms which effect the radiation-induced property change cannot be described in such simple terms. The use of the DPA as a more realistic exposure unit for the measurement of materials property change has been recommended and an ASTM Standard E693-79 is now available for its routine application,(49) Figure 1.

The effects of using different exposure units, of neutron spectrum changes from surveillance through ex-vessel positions, of photofission and surveillance capsule flux perturbations, and the impact of the selection of RM, SSTR, HAFM, and Damage Monitor (DM) dosimetry sets on the accuracy of derived exposure values (with and without "Benchmark Field Referencing"), are discussed in references 1, 2, 4, 5, 10, 11, 23, 28, 29, and 48. In this section of this report emphasis is placed on a discussion of the results of validation and calibration studies associated with current state-of-the-art LWR surveillance capsule dosimetry measurements and derived exposure values.

Table 12, taken from reference 2, provides the results of a previous study of individual and multiple foil reported exposure values for several PWR and one BWR power plant. The results were obtained from several surveillance capsule reports and showed the existence of serious discrepancies between fission and nonfission radiometric monitor results.(2) In a number of cases the fission foil fluence values were up to a factor of 1.5 to 2.7 higher than the nonfission foil results. In addition to data reduction and radiometric monitor measurement problems, these discrepancies are thought to be associated with surveillance capsule flux perturbation and photofission effects.(1,2,10,23,28,29,48)

2. ORR-PSF Dosimetry/Perturbation Experiment

For a Westinghouse surveillance capsule geometry for a 2-loop PWR power plant (at the center of an approximately 1" x 1" x 48" bar of steel located behind the thermal shield), S. Anderson has calculated perturbed $^{54}Fe(n,p)^{54}Mn$ reaction rates that are approximately 12 to 15% less and $^{237}Np(n,f)F.P.$ fission rates that are approximately 40 to 60% higher than the unperturbed values for 13°, 23°, and 33° azimuthal positions. Consequently, without correcting for these perturbation effects, the $^{54}Fe(n,p)^{54}Mn$ and $^{237}Np(n,f)F.P.$ reported values of flux greater than 1.0 MeV could appear to be discrepant by approximately 73%, 55%, and 64% for the 13°, 23°, and 33° azimuthal positions, respectively.(1,48)

TABLE 12

REPORTED SURVEILLANCE CAPSULES SINGLE FOIL FLUX/FLUENCE VALUES [$\emptyset_i$ > 1 MeV] - RELATIVE TO ^{54}Fe(n,p)

Reactor Name (Vendor-Type, Country, Operation Date)	Service Laboratory Report	SINGLE FOIL FLUX/FLUENCE >1MeV			
		$\emptyset_{^{58}\mathrm{Ni}(n,p)}$	$\emptyset_{^{63}\mathrm{Cu}(n,\alpha)}$	$\emptyset_{^{238}\mathrm{U}(n,f)}$(e)	$\emptyset_{^{237}\mathrm{Np}(n,f)}$(e)
Point Beach #1	BMI (1973)	1.09	1.63	1.61	2.17
(West. PWR, USA, 12/70)		[Reported Surveillance Value: 1.0(Fe)](d)			
Same (Angle A)	WEST.(1979) (a)	0.80	1.51(b)	1.03	1.25
Same (Angle A + 180°)	WEST.(1979) (a)	1.01	1.14(b)	1.13	1.01
		[Reported Surveillance Value: 1.0 (Fe)](d)			
Average Values For Seven WEST. Power Plants	WEST.(1979) (a)	0.97	1.25(b)	1.08	1.15
Humboldt Bay 3	GE (1967)	0.88	0.80	-	-
(GE BWR, USA, 8/63)		[Reported Surveillance Value: 1.0 (Fe)](d)			
San Onofre #1	SWRI(1971)	1.00	1.27	1.10	1.42
(West. PWR, USA, 1/68)					(BNW Spectrum 1)
(West. PWR, USA, 1/68)	SWRI(1971)	1.05	0.88	1.29	1.45 (BNW Spectrum 2)
		[Reported Surveillance Value: 0.85 (SAND II, multiple foils)](d)			
OCONEE #1	B&W (1975)	1.18	-	2.50	2.70
(B&W PWR, USA, 7/73)		[Reported Surviellance Value: $\frac{1.0 + 2.5}{2} = 1.76$ (Fe+U)](d)			
DOEL I	CEN/SCK (1979)	1.09	1.51(b)	-	2.41
Belgium-West. PWR Belgium 1/75)	CEN/SCK (1979)	1.09	1.06(c)	-	2.41
		[Reported Surveillance Value: ~ 1.09 (Ni)] (d)			

TABLE 12 FOOTNOTES

(a) Surveillance capsule flux perturbation corrections were calculated by Westinghouse to provide necessary correlations between the U, Np, Cu, Ni, and Fe results. None of the other results shown in the table have been corrected for perturbation effects.

(b) ENDF/B-IV $\sigma(E)$ for $^{63}Cu(n,\alpha)$

(c) Mann-Schenter $\sigma(E)$ for $^{63}Cu(n,\alpha)$

(d) These reported surveillance capsule measured fluence values are used for correlating the surveillance capsule metallurgical data with other test and power reactor data. They are also used for making localized predictions of expected pressure vessel lifetime neutron exposures and/or can be used to simply confirm the correctness of one, two, and three dimensional reactor physics computations.

(e) Based on ^{137}Cs analysis.

NOTE: The Ni, Fe, and Cu provide experimental fluence data for time periods up to about 1 year, 5 years, and 25 years with a knowledge of the surveillance capsule flux level time history, this information is not needed for a reliable interpretation of fission foil $^{137}Cs(t_{1/2} \sim 31$ years) results.

To provide experimental verification of these and other analytical predictions, a dosimetry perturbation experiment was irradiated in the PSF high-power LWR pressure vessel mockup facility. Two 1" x 1" x 12" long, carbon-steel mockup surveillance capsules, supplied by Westinghouse, were positioned in the PSF for a nine-day irradiation. Both capsules were exposed simultaneously to a maximum fluence of about 5 x 10^{18}n/cm^2 (E > 1 MeV). One capsule was located at the outer surface of the thermal shield, six inches to the right of center, and the other at the pressure vessel surface six inches to the left of center. The PSF is a 4/12 configuration. Radiometric monitors (RM), solid state track recorder (SSTR), and helium accumulation fluence monitors (HAFM) were positioned within the capsules by HEDL and CEN/SCK. Six replicate dosimeter sets were irradiated in nearly zero gradient configurations so that essentially identical dosimeters were supplied for independent analysis by four vendors (W, GE, CE, and B&W) and two services laboratories (SWRI and BMI). Analysis and "Benchmark Field Referencing" of these and other RM, SSTR, and HAFM monitor results is being accomplished by CEN/SCK, EG&G-ORTEC, HEDL, NBS, ORNL and RI. The six sets of dosimeters were recovered and shipped to HEDL for initial radiometric analyses. Subsequently, one complete set of dosimeters was sent to each of the six laboratories for counting; final counting and data analysis is in progress.

A preliminary analysis of laboratory-to-laboratory biases for the ORR-PSF Dosimetry/Perturbation Experiment for the radiometric monitors has been completed by L. Kellogg and A. Davis. The Table 13 evaluation shows the present laboratory-to-laboratory comparative status but also shows the improvements in the data comparisons as a result of interim evaluations and discussions with participants. All laboratories remain anonymous for these intercomparisons and are identified only as laboratories A, B, C, D, E, and F. With reference to Table 13, and for each reaction listed, the following information is provided:

READEX FICHE best copy available

TABLE 13

RANGE EVALUATION (MAXIMA/MINIMA) RADIOMETRIC RESULTS

	^{58}Ni(n,p)				^{46}Ti(n,p)				^{63}Cu(n,α)				^{54}Fe(n,p)			
	Ratio 1	Ratio 2	Ratio 3	Labs	Ratio 1	Ratio 2	Ratio 3	Labs	Ratio 1	Ratio 2	Ratio 3	Labs	Ratio 1	Ratio 2	Ratio 3	Labs
HNF - 1	1.14 C/B	1.10 D/B	1.06 D/C	6	1.39 C/B	1.16 C/B	1.04 C/E	6	1.11 F/B	------	1.11 F/E	6	1.38 C/B	1.11 C/B	1.04 C/E	6
- 3	1.28 C/B	1.05 A/C	1.05 A/C	6	1.48 C/B	1.21 C/B	1.07 C/E	6	1.05 C/E	1.06 C/F	------	6	1.27 C/B	1.10 C/B	1.04 C/F	6
- 2	1.25 C/B	1.13 F/B	1.06 F/E	6	1.42 C/B	1.19 A/B	1.08 A/E	6	1.06 C/E	1.09 C/E	------	6	1.46 C/B	1.12 C/B	1.07 C/E	6
- 4	1.28 C/B	1.14 F/B	1.06 F/E	6	1.41 C/B	1.17 C/B	1.10 C/E	6	1.08 C/E	1.07 C/E	------	6	1.43 C/B	1.15 C/B	1.09 C/F	6

	^{58}Fe(n,γ)			
	Ratio 1	Ratio 2	Ratio 3	Labs
HNF - 1	1.15 C/A	1.03 E/A	1.03 E/A	3*
- 3	1.02 C/E	1.02 A/E	1.02 A/E	3
- 2	1.23 C/A	1.04 E/A	1.04 E/A	3
- 4	1.12 C/E	1.01 A/E	1.01 A/E	3

	^{59}Co/Al(n,γ)			
	Ratio 1	Ratio 2	Ratio 3	Labs
HF - 3	1.15 C/B	1.09 C/B	1.06 C/F	6
- 5	1.15 C/B	1.11 C/B	1.04 C/A	6
- 4	1.06 F/B	1.10 C/B	1.05 C/D	6
- 6	1.23 C/B	1.17 C/B	1.07 C/E	6

	^{235}U(n,f)^{140}Ba				^{235}U(n,f)^{103}Ru				^{235}U(n,f)^{95}Zr				^{235}U(n,f)^{137}Cs			
	Ratio 1	Ratio 2	Ratio 3	Labs	Ratio 1	Ratio 2	Ratio 3	Labs	Ratio 1	Ratio 2	Ratio 3	Labs	Ratio 1	Ratio 2	Ratio 3	Labs
HF - 3	1.06 A/E	------	------	3	1.19 C/D	1.22 A/C	1.10 A/D	4	1.09 D/C	1.22 D/C	1.08 D/E	5	------	1.11 E/C	------	3
- 5	1.19 A/D	------	------	3	1.73 C/D	1.19 A/D	1.07 A/E	4	1.51 C/B	1.29 C/B	1.12 C/E	5	------	1.31 C/D	------	3
- 4	1.05 A/D	------	------	3	1.30 C/D	1.11 A/C	------	4	1.13 D/C	1.14 D/C	1.07 A/C	5	------	1.06 E/C	------	3
- 6	1.10 A/D	------	------	3	1.43 C/D	1.14 A/D	------	4	1.15 C/E	1.11 A/C	1.07 A/B	5	------	1.07 E/D	------	3

	^{237}Np(n,f)^{140}Ba				^{237}Np(n,f)^{103}Ru				^{237}Np(n,f)^{95}Zr				^{237}Np(n,f)^{137}Cs			
	Ratio 1	Ratio 2	Ratio 3	Labs	Ratio 1	Ratio 2	Ratio 3	Labs	Ratio 1	Ratio 2	Ratio 3	Labs	Ratio 1	Ratio 2	Ratio 3	Labs
HF - 1	1.10 D/F	------	------	4	1.37 C/F	1.11 A/F	------	5	1.16 A/E	1.21 A/C	1.16 A/E	6	------	1.09 D/C	------	4
- 2	1.13 A/E	------	------	4	1.27 C/F	1.12 A/F	------	5	1.14 D/F	------	------	6	------	1.14 F/D	------	4

	^{238}U(n,f)^{140}Ba				^{238}U(n,f)^{103}Ru				^{238}U(n,f)^{95}Zr				^{238}U(n,f)^{137}Cs			
	Ratio 1	Ratio 2	Ratio 3	Labs	Ratio 1	Ratio 2	Ratio 3	Labs	Ratio 1	Ratio 2	Ratio 3	Labs	Ratio 1	Ratio 2	Ratio 3	Labs
HF - 1	1.09 A/E	------	1.04 D/E	4	1.44 C/F	1.16 A/F	------	5	1.16 C/F	1.09 B/F	------	6	------	1.08 E/C	------	4
- 2	1.10 A/E	------	------	4	1.27 C/F	1.13 A/F	------	5	1.13 D/F	------	------	6	------	1.08 D/C	------	4

*Results for the ^{58}Fe(n,γ) reaction were not reported by one laboratory after preliminary recalibration of their counting systems.

a. Ratio 1 - The maxima/minima range (within set) of the reported results from the participating laboratories--after initial review of the data to eliminate obvious errors resulting from the handling of a large number of samples in a relatively short time period.

b. Ratio 2 - The maxima/minima range after preliminary recalibration of one laboratory.

c. Ratio 3 - Nonfission monitors--The maxima/minima range after eliminating the results from one laboratory that appears to be consistently biased low on the majority of the reported activitation products. (Investigation into this possible bias is being made by the participant). For fission monitors--the maxima/minima range after elimination of an apparent high or low result to indicate the general overall range.

d. Labs - The number of laboratories (A, B, C, D, E, and F) reporting results utilized in the determination of Ratios 1 and 2.

The maxima/minima ratios of Table 13 show the laboratory-to-laboratory biases that currently could be introduced into surveillance capsule reported values of fluence (E > 1 MeV) as a result of the measurement and data reduction of individual flux/fluence monitors by these six laboratories. For example, if laboratories C and B were both to have reported flux/fluence values based on the $^{54}Fe(n,p)^{54}Mn$ reaction, the laboratory C values would have been up to a factor of 1.46 higher than the laboratory B results. With "Benchmark Field Referencing," however, such large factors as 1.27 to 1.46 for the $^{54}Fe(n,p)^{54}Mn$ monitor, the Ratio 1 column, would be reduced to values of 1.15 and less, the Ratio 2 and 3 columns of Table 13.

3. Benchmark Field Referencing

The bases for benchmark field referencing are irradiations performed for the purpose of detector calibrations in a neutron field of known energy spectrum and intensity. In addition to benchmark referencing the exvessel cavity dosimetry being accomplished at the Arkansas Power and Light Company Unit #1 PWR, there are two additional benchmark efforts associated with the LWR-PV Surveillance Dosmietry Improvement Program.

One is to help provide accuracy limits on the experimental data that are the basis for comparison of calculated and measured neutron flux levels and the core power in the PCA/LWR pressure vessel mockup at ORNL. This standardization program includes special certified-fluence irradiations of dosimetry materials and detectors, as well as measurements with the NBS dual fission chambers in the pressure vessel mockup. Results of this effort are discussed in Section IV.

The other major benchmark referencing activity is attempting to establish interlaboratory consistency in measuring and evaluating fluence detectors. To accomplish this, NBS periodically issues counting standards internationally. Such standards are typical dosimetry materials made radioactive by an irradiation to a certified fluence. These are normally distributed as "blinds" and participating laboratories must deduce the fluence. The first such exercise for the LWR-PVS-Dosimetry Improvement Program is drawing to a close and some preliminary results follow.

Table 14 gives the logistics of the distribution of 26 nickel foils activated in the NBS U-235 standard fission spectrum. The radioactivity of interest is the 811-keV gamma radiation from the ^{58}Ni(n,p)^{58}Co reaction. A 76% laboratory response was achieved and the ratio of the reported results to the NBS values are summarized in Table 15. In general, the consistency level is fairly good, with 47% of the ratios within the range 0.980-1.020. The distribution is skewed in that 68% lie in the range 0.979-1.070. A detailed report of the intercomparison will be made after participants have been notified of results and several laboratores have been given the opportunity to evaluate a second nickel counting standard. All laboratories remain anonymous in these intercomparisons, as they do for the ORR-PSF Dosimetry Perturbation Experiment.

TABLE 14

LOGISTICS OF THE CERTIFIED FLUENCE IRRADIATIONS OF NICKEL FOILS IN THE NBS CAVITY FISSION (U-235) SPECTRUM

NICKEL FOIL IDENTIFICATION	DATES AND TIMES OF IRRADIATION START	END	TIME DURATION (SECONDS)
BV, BW, BX, BY	7/17/78 17:19 EDST	7/18/78 23:27 EDST	108480
CA, CB, CC, CD	8/1/78 17:35 EDST	8/2/78 23:10 EDST	106500
AP, AR, AS, AT, AU	8/21/78 20:51 EDST	8/22/78 17:53 EDST	75720
CF, CG, CH, CI	9/15/78 11:36 EDST	9/16/78 09:50 EDST	80040
CJ, CK, CL, CM	9/22/78 15:24 EDST	9/23/78 22:37 EDST	112380
BK, BL, BM, BN	1/13/79 14:55 EST	1/14/79 23:03 EST	115680

The foils were distributed to participants between 27 November 1978 and 3 February 1979. The percentage returned as a function of time after February 1979 is as follows:

ELAPSED TIME (months)	DATE	PERCENT RESPONSE
6	August 1979	41%
12	February 1980	69%
18	August 1980	76%

TABLE 15

COMPARISON OF RESULTS OF INTERLABORATORY CONSISTENCY IN MEASURING THE NICKEL CERTIFIED FLUENCE STANDARDS

Result Number	Ratios of Results To NBS Values
1	0.979
2	1.018
3	1.015
4	1.112
5	1.134
6	0.993
7	1.033
8	0.936
9	0.946
10	0.982
11	1.065
12	0.990
13	0.932
14	1.062
15	1.011
16	1.011
17	1.000
18	0.932
19	1.044

Overall average 1.0103 ± 0.0565 (±5.6%)

With reference to the Section VI-B-2 example (Table 13, results), if the ^{58}Ni(n,p)^{58}Co measured reaction rate had been used instead of the ^{54}Fe(n,p)^{54}Mn to obtain flux/fluence values for a surveillance capsule, the laboratory C values would have been up to a factor of 1.28 higher than the laboratory B results. Similarly, for the 19 laboratories, Table 15, the laboratory 5 values would have been a factor of 1.22 higher than the laboratory 13 and 18 results. Consequently, for the development of reliable metallurgical data bases, the range of laboratory-to-laboratory reported maxima/minima exposure values for a given irradiation experiment should be reduced and maintained at bounds that are well within a 5 to 15% (1σ) accuracy limit. In this regard, a pressure vessel benchmark facility for power reactor surveillance dosimetry validation and certification is being established at the Oak Ridge Bulk Shielding Reactor (BSR) facility. It will be identified as the BSR simulated dosimetry measurement facility (SDMF).

The information obtained from this BSR-SDMF facility will be applied to the investigation of results obtained from current surveillance capsules, so that the dosimetry methods currently applied by vendors and service laboratories can be:

1) Validated and certified;
2) Improved by development of supplementary experimental data; and
3) Evaluated in terms of actual uncertainties.

A preliminary design, shown in Figure 24 is currently being reviewed and evaluated by program participants. The facility support structure is being designed to accommodate a PVS and void box simulator, but only a thermal shield simulator is considered necessary for most applications. Initially, CEN/SCK, EG&G ORTEC, HEDL, NBS, and ORNL and a number of other program participants will cooperate in the design characterization and calibration of this facility.

ORNL-DWG 80-16371

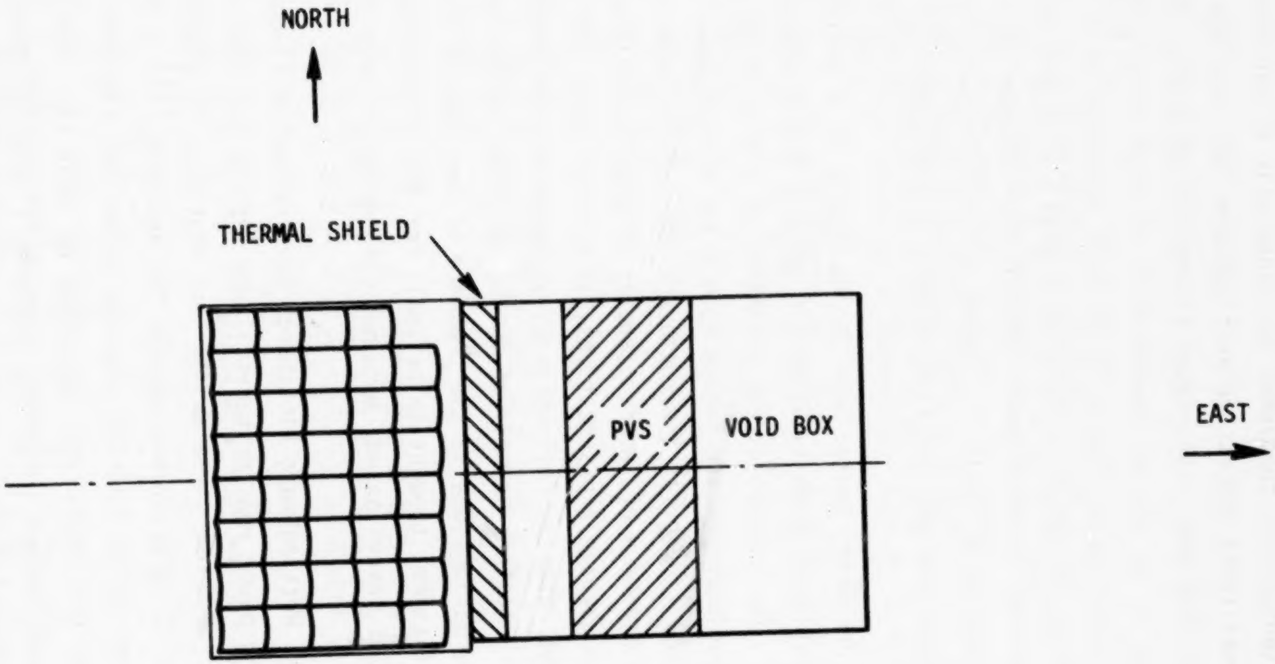
NORTH
THERMAL SHIELD
PVS
VOID BOX
EAST

FIGURE 24. Preliminary Design of the BSR-Simulated Dosimetry Measurement Facility (SDMF). Neg 8010270-14

4. Surveillance Capsule Exposure Units and Values

R. L. Simons has tentatively completed the reanalysis of exposure units and values for 19 surveillance reports on Westinghouse PWRs, and the results are shown in Table 16. The newly calculated fluence values differ from those originally reported by an average upward shift of about 1.42 (~40%) with individual variations ranging from a low of 1.08 to a high of 2.11. The extent of the changes continues to indicate a need for re-evaluation of fluence values reported in other power reactor surveillance reports. In addition, future studies of ΔNDTT vs fluence will also require a reanalysis of the fluence values reported for test reactor irradiations.(47)

This HEDL Reactor Dosimetry Center work is the result of a recheck of 19 power reactor surveillance reports which are part of the bibliography of the MPC data base.(38) The magnitudes and frequency of the observed changes indicate that inconsistencies are nonnegligible and widespread. The HEDL work recalculated the fluence at the center of the surveillance capsule and was a test for the presence of inconsistencies in physics calculations, in calculated spectrum average cross-sections, in nuclear data, and in improper decay adjustments of reported foil activity adjusted for the known power time history of the reactor, as well as inconsistencies in the calculation of local flux perturbations due to the presence of the capsule itself. Corrections for photofission, thought to be small for the 19 Westinghouse type surveillance capsules investigated, were not considered in this first study.

Recently, workers at Westinghouse Pittsburgh have rechecked fluence values reported in existing power reactor surveillance reports and have reached conclusions similar to those given above. For instance, as a part of the Point Beach Unit No. 2 surveillance capsule "R" analysis,(31) S. Anderson has re-evaluated previously reported exposure values for capsules "V" and "T." The results of this reanalysis are shown in Table 17. The relative swing in the reported (before and after) capsule "V" and "T" results was 1.56. This swing was related to changes in the manner of handling, interpreting, and applying reported data and was not associated with changes in

TABLE 16

RE-EVALUATED EXPOSURE VALUES FOR SURVEILLANCE CAPSULES

Reactor	Unit	Capsule	old ϕt >1	new ϕt > 1	Ratio new/old	dpa	Ratio dpa/ϕt new	D	A302B ΔTT Correlation Monitor (^{O}F)	time(sec)
Turkey Point	4	S	1.25+19	1.81+19	1.45	.032	1.77-21	2.96-10	115*	1.084+8
"	4	T	6.05+18	8.57+18	1.42	.0140	1.62-21	3.66-10	100	3.840+7
"	3	S	1.41+19	1.99+19	1.40	.0350	1.77-21	3.14-10	139	1.114+8
"	3	T	5.68+18	6.44+18	1.13	.0123	1.90-21	3.99-10	82	3.094+7
H. B. Robinson	2	S	3.2+18	5.09+18	1.59	.00936	1.83-21	2.14-10	80	4.385+7
"	2	V	4.51+18	7.76+18	1.72	.0137	1.77-21	1.29-10	105	1.061+8
Prairie Island	1	V	5.21+18	6.29+18	1.21	.0109	1.73-21	2.51-10	---	4.350+7
"	2	V	5.49+18	7.18+18	1.31	.0122	1.70-21	2.74-10	---	4.454+7
Point Beach	1	S	---	9.52+18	--	.0157	1.65-21	1.35-10	---	1.163+8
"	1	R	2.22+19	2.69+19	1.21	.0442	1.64-21	2.72-10	110	1.632+8
R. E. Ginnea	1	R	7.60+18	1.33+19	1.75	.0247	1.86-21	2.87-10	---	8.628+7
"	1	V	5.32+18	6.91+18	1.30	.0110	1.84-21	2.80-10	90	3.923+7
Kewaunee		V	5.59+18	7.23+18	1.29	.0123	1.71-21	2.96-10	---	4.167+7
San Onofre	1	A	1.20+19	1.48+19	1.23	.0310	2.04-21	5.30-10	115	5.846+7
"	1	D	2.36+19	4.98+19	2.11	.0887	1.78-21	9.95-10	150	8.914+7
Point Beach	2	T	9.45+18	1.02+19	1.08	.0170	1.67-21	1.55-10	105*	1.098+8
"	2	V	4.74+18	7.71+18	1.63	.0127	1.65-21	2.61-10	90*	4.859+7
Conn. Yank.		A	2.08+18	2.85+18	1.37	.00516	1.81-21	9.59-11	85	5.377+7
"		F	4.04+18	5.54+18	1.37	.00977	1.76-21	1.26.10	80	7.728+7
				Average	1.42					

*A533B Steel

TABLE 17

DOSIMETRY/PHYSICS RESULTS*

	CAPSULE $V^{(1)}$	CAPSULE $T^{(2)}$	CAPSULE $R^{(3)}$
BEFORE ANALYSIS:	$4.74 \times 10^{18} (n/cm^2 > MeV)$	9.45×10^{18}	20.1×10^{18}
AFTER REANALYSIS:	6.53×10^{18}	8.29×10^{18}	20.1×10^{18}
RATIO: AFTER/BEFORE	1.37	0.88	1.0
RELATIVE SWING	1.37/0.88 = 1.56		

E10.5 and E10.05.06 CONCLUSION: All surveillance reports and test reactor reports must be reanalyzed to improve exposure values!!!

1) Surveillance Capsule report, BMI, June 10, 1975
2) Surveillance Capsule report, West, August 1978
3) Surveillance Capsule Report, West, December 1979

---

*EPRI Report by Yanichko, Anderson, Shogan, Lott, December 1979, Analysis of Capsule R from Point Beach #2 the measured reaction rates. CEN/SCK, EG&G ORTEC, HEDL, and RI will assist Westinghouse/EPRI in rechecking of the measured reaction rates for the capsule "R" Co-Al alloy (bare and cadmium covered), $^{237}Np(n,f)$, $^{238}U(n,f)$, $^{54}Fe(n,p)^{54}Mn$, $^{58}Ni(n,p)^{58}Co$, and the $^{63}Cu(n,\alpha)^{60}Co$ monitors. The iron monitor material is obtained from Charpy specimens. It is planned to have RI analyze some of the nonfission monitors for total helium content to assist in the verification of the radiometric monitors results. Since time history corrections are not required, HAFM monitors give a direct measurement of the fluence. Of particular interest will be a comparison of the measured and calculated $Al(n,\alpha)$ and $Cu(n,\alpha)$ total helium and $^{63}Cu(n,\alpha)^{60}Co$ radiometric results.

The status of RI work related to the measurement of helium in pressure vessel steel chips to provide a direct means of obtaining three-dimensional information on the fast neutron fluence in operating PWR and BWR plants is discussed in the next section.

Based on the above studies, it is concluded that a rechecking of the fluence calculations in existing data bases would decrease the standard deviation in the statistically derived formulas giving Charpy-shift and other property changes as a function of fluence and chemistry. Further, the data bases should be improved by taking into account the different spectral shapes of the flux with the use of DPA as an exposure unit. This latter change will be most important when surveillance data and test reactor data are combined and subsequently used for ex-vessel structural component end-of-life predictions (see Table 3 of E706-80, reference 23).

5. Helium Accumulation Fluence Dosimetry for Reactor Vessel Surveillance

Several pieces of pressure vessel steel chips taken from a test specimen irradiated in the Belgian Reactor BR3 have been analyzed at Rockwell International for helium concentration. The purpose of the analysis was to see if the helium concentration could be used to provide a measurement of the fast neutron fluence received by the specimen. The test specimen was taken from the upper shell plate (Heat No. 19281) of the Yankee Rowe pressure vessel, and was irradiated about 15 years ago in a low flux surveillance position during the first BR3 core (so-called "first Westinghouse core"). The helium results from seven independent mass spectrometric analyses gave accurate results, despite the very low helium levels involved, providing a concentration of 0.692 ± 0.026 atomic parts per billion (6.92 x 10^{-10} atom fraction).

Recent calculations both at Rockwell and at the CEN/SCK Laboratories at Mol, Belgium, have attributed this helium concentration to the threshold Fe(n,α) reaction with high-energy fission neutrons, rather than to a thermal reaction with some possible boron impurity. If this is so, then helium measurements of BR3 pressure vessel scrapings would provide the fast fluence received by the BR3 vessel as a function of location of the scrapings. The same situation will apply to any vessel steels which have levels of boron sufficiently low that the thermal neutron (n,α) reactions with boron do not mask the fast neutron reactions with iron.

The next step in demonstrating if the helium accumulation technique can be used to retroactively determine the fast fluences received by existing pressure vessels is to determine the boron content of this and other pressure vessel steels. For the extremely low boron concentrations of interest here, this can only be accomplished by irradiating the steels in a highly thermalized flux (where only ^{10}B(n,α) reactions will occur) and subsequently measuring the helium by mass spectrometry.

C. OTHER REACTOR DATA DEVELOPMENT AND TESTING STUDIES

1. Spectral Effects Associated with the Extrapolation of TMI-2 PWR Surveillance Capsule Measurements

As part of the NRC DSI (Division of Systems Integration) Radiation Embrittlement Program, and in support of the Reactor Vessel Materials Toughness Task Force (A-11), a review of the techniques used to infer pressure vessel damage from surveillance capsule measurements has been performed by J. Carew. This review concerned the effect of neutron spectral shifts, between surveillance capsule and vessel locations, on estimates of pressure vessel damage and the principal results of this review are as follows:

The extrapolation of surveillance capsule measurements to the pressure vessel 1/4T and 3T/4 locations is generally performed using fluence lead and attenuation factors. Typically, in the determination of these factors the shift in spectrum between the capsule and vessel locations is neglected. This assumption has been evaluated for the TMI-2 vessel/downcomer/shield configuration and found to result in $\sim$40% under-prediction of ΔRT_{NDT} (change in reference nil ductility temperature) at the 3T/4 location for an accelerated surveillance capsule, and $\sim$10% and $\sim$50% under-prediction of ΔRT_{NDT} at the T/4 and 3T/4 locations, respectively, for a standard capsule.

2. Status of Exvessel Dosimetry in Arkansas Power and Light Company's Unit #1 PWR

The purpose of these exvessel experiments is to gain dosimetry and spectrum-unfolding experience in an RPV-related environment almost untouched by measurements. The previous (1979) annual report$^{(2)}$ provided analyses of dosimeters from the first irradiation, completed in February 1978. The following is a summary of the next three irradiations.

The second and third irradiation experiments were essentially a repeat of the first in an attempt to study reproducibility and the effects of different power histories, particularly during the last few days of irradiation, on dosimery results.

The fourth irradiation was the first time NP-237 dosimeters were included in the dosimetry sets. NP-237 is an extremely important dosimeter for flux in the 500 keV to 1 MeV energy range. The dosimery set containing the NP-237 was again at the reactor core centerline outside the pressure vessel. A second set of dosimeters was positioned in the cavity above core level in the vicinity of the nozzle penetration. This is believed to be the first time serious flux and spectrum measurements have been made on neutron leakage flux in this area of an operating PWR.

Dosimeters from the four experiments were counted in a cooperative program between the University of Arkansas (UA) and the Hanford Engineering and Development Laboratory. However, final analysis of the data has not yet been accomplished. The UA work is being supported by EPRI as well as the utility and more extensive cooperative measurements and analyses are planned.

3. Status of Metallurgical and Dosimetry Measurements in the Garigliano BWR, Rome, Italy

Charpy metallurgical specimens and associated radiometric neutron dosimeters were received at NBS from the Garigliano BWR Reactor in Rome, Italy. The metallurgy was shipped to R. Hawthorne, Naval Research Laboratory, for testing and the dosimeters will be sent to HEDL for analyses. Irradiation of this material ended August 8, 1979 after 129 equivalent full power days of operation. The materials were irradiated to approximately 4×10^{18} n/cm^2(E > 1 MeV) inside the pressure vessel of Garigliano.

The cooperative joint-research program with the Italian Atomic Power Authority (ENEL) in the area of reactor pressure vessel neutron dosimetry is conducted through F. Remondino, the ENEL representative in the USA, and with M. Galliani at the Garigliano Reactor, Rome, Italy. Improving and standardizing measurement methods for reactor pressure vessel dosimetry is now a recognized international activity and the early pilot efforts at Garigliano, at Unit #1 of Arkansas Power and Light, and at the BR-3 Reactor in Mol, Belgium have contributed significantly to this recognition.

4. Status of Dosimetry Measurements for the NRC HSST Program

Recommended values for the neutron flux (E>1 MeV) at various experimental locations within the dosimetry capsule simulating metallurgical capsules A and B are given in Tables 18 and 19. These results were obtained from the dosimetry experiment of the Fourth HSST Irradiation Series. The values are given for a BSR core power of 2 MW, and are estimated to be accurate to within ±5% (1σ) or better.

The measurements have been performed by means of the two transportable NaI(Tl) spectrometers calibrated at the CEN/SCK Mol, Cavity ^{235}U Thermal Fission Neutron Spectrum Standard Field. The methods and techniques are the same as applied to the neutron spectral characterization of the PCA Pressure Vessel Simulator. The good accuracy obtained stems largely from the use of this "Benchmark Field Referencing" approach. The directly observed experimental quantities, gathered in Tables 20 and 21, are the equivalent fission fluxes for each selected dosimetry reaction in capsules A and B.

It has been assumed that the neutron spectrum along the axis of a given vertical experimental channel does not change with the distance to the capsule top. As shown by Tables 22 and 23 this is true within experimental uncertainties, except very close to the edge (location 2.04 in. in center channel).

Figs. 25 and 26 are plots of the relative axial variation of the fast flux as a function of distance to the capsule top. Complete documentation of this work, including an analysis of the uncertainties, will be prepared for future HSST progress report dissemination.

Table 18. Neutron Fluxes (E>1 MeV) in BSR-HSST Capsule Mock-up "A", at a BSR Core Power of 2.0 MW. Data derived from equivalent fission flux measurements and transport theory calculations.

Experimental Location[a]	^{103}Rh(n,n')^{103m}Rh	^{115}In(n,n')^{115m}In	^{58}Ni(n,p)^{58}Co	^{27}Al(n,α)^{27}Na	Recommended (Average)
South Channel					
16.5	1.94(12)[b]	2.17(12)	2.09(12)	2.17(12)	2.09(12)
11.0	2.11	2.32	2.19	2.28	2.23
5.5	1.59	1.77	1.68	1.74	1.70
Center Channel					
13.04	1.12	1.25	1.23	1.25	1.21
7.54	.993	1.08	1.08	1.13	1.07
2.04	.601	.713	.661	.715	.673
East Channel					
16.5	.988	1.02	1.13	1.21	1.09
11.0	1.04	1.28	1.20	1.27	1.20
5.5	.812	.831	.907	.972	.881

[a] Locations are in inches, measured from the top of the dummy capsule.

[b] Read 1.94 × 10^{12} neutrons cm^{-2} s^{-1}.

Table 19. Neutron Fluxes (E>1 MeV) in BSR-HSST Capsule Mock-up "B", at a BSR Core Power of 2.0 MW. Data derived from equivalent fission flux measurements and transport theory calculations.

Experimental Location[a]	$^{103}Rh(n,n')^{103m}Rh$	$^{115}In(n,n')^{115m}In$	$^{58}Ni(n,p)^{58}Co$	$^{56}Fe(n,p)^{56}Mn$	$^{27}Al(n,\alpha)^{24}Na$	Recommended (Average)
South Channel						
16.5	1.63(12)[b]	1.84(12)	1.90(12)	2.21(12)	1.97(12)	1.91(12)
11.0	1.77	1.95	1.94	2.19	1.95	1.96
5.5	1.34	1.45	1.44	1.61	1.45	1.46
Center Channel						
16.5	.895	1.01	1.08	1.26	1.12	1.07
12.0	1.00	1.10	1.12	1.29	1.12	1.13
8.25	.884	.960	.966	1.10	.981	.978
4.5	.668	.730	.725	.857	.741	.744
2.375	.518	.549	.588	.657	.586	.580
0.25	.307	.336	.368	.458	.407	.375

---

[a] Locations are in inches, measured from the top of the dummy capsule.

[b] Read 1.63 × 10^{12} neutrons cm^{-2} s^{-1}.

Table 20. Experimental Equivalent Fission Fluxes in BSR-HSST Capsule Mock-up "A" at a BSR Core Power of 2.0 MW.

Experimental Location[a]	^{103}Rh(n,n')^{103m}Rh	^{115}In(n,n')^{115m}In	^{58}Ni(n,p)^{58}Co	^{27}Al(n,α)^{24}Na
South Channel				
16.5	3.56(12)[b]	2.80(12)[b]	1.67(12)[b]	1.53(12)[b]
11.0	3.86	3.00	1.75	1.61
5.5	2.92	2.28	1.34	1.23
Center Channel				
13.04	2.25	1.58	.839	.745
7.54	2.00	1.36	.737	.670
2.04	1.21	.901	.452	.425
East Channel				
16.5	1.97	1.29	.780	.733
11.0	2.08	1.62	.828	.772
5.5	1.62	1.05	.626	.589

---

[a] Locations are in inches, measured from the top of the dummy capsule.

[b] Read 3.56 × 10^{12} neutrons cm^{-2} s^{-1}; note, these four values would be the same only if the BSR-HSST capsule Mockup spectrum at the given location were the same as the ^{235}U fission spectrum.

Table 21. Experimental Equivalent Fission Fluxes in BSR-HSST Capsule Mock-up "B" at a BSR Core Power of 2.0 MW

Experimental Location[a]	$^{103}Rh(n,n')^{103m}Rh$	$^{115}In(n,n')^{115m}In$	$^{58}Ni(n,p)^{58}Co$	$^{56}Fe(n,p)^{56}Mn$	$^{27}Al(n,\alpha)^{24}Na$
South Channel					
16.5	2.84(12)[b]	2.34(12)[b]	1.57(12)[b]	1.60(12)[b]	1.47(12)[b]
11.0	3.08	2.48	1.60	1.59	1.46
5.5	2.34	1.85	1.19	1.17	1.08
Center Channel					
16.5	1.70	1.25	.757	.764	.711
12.0	1.90	1.36	.783	.781	.715
8.25	1.68	1.19	.677	.665	.624
4.5	1.27	.905	.508	.519	.471
2.375	.985	.681	.412	.398	.373
0.25	.584	.417	.258	.277	.259
East Channel					
11.0	1.54	1.12	.653	.659	.610
5.5	1.00	.846	.492	.494	.469

---

[a] Locations are in inches, measured from the top of the dummy capsule.

[b] Read 2.84 × 10^{12} neutrons cm^{-2} s^{-1}; note, these five values would be the same only if the BSR-HSST Capsule Mock-up spectrum at a given location were the same as the ^{235}U fission spectrum.

Table 22. Integral Spectral Indices in BSR-HSST Capsule Mock-up "A"

Experimental Location[a]	$\frac{^{103}\mathrm{Rh}(n,n')^{103m}\mathrm{Rh}}{^{27}\mathrm{Al}(n,\alpha)^{24}\mathrm{Na}}$[b]	$\frac{^{115}\mathrm{In}(n,n')^{115m}\mathrm{In}}{^{27}\mathrm{Al}(n,\alpha)^{24}\mathrm{Na}}$	$\frac{^{58}\mathrm{Ni}(n,p)^{58}\mathrm{Co}}{^{27}\mathrm{Al}(n,\alpha)^{24}\mathrm{Na}}$
South Channel			
16.5	2.33	1.83	1.09
11.0	2.40	1.86	1.09
5.5	2.37	1.85	1.09
Theory[c]	2.60	1.83	1.14
Theory[d]	2.32	1.71	1.10
Center Channel			
13.04	3.02	2.12	1.13
7.54	2.98	2.03	1.10
2.04	2.85	2.12	1.06
Theory[c]	3.36	2.11	1.14
Theory[d]	2.75	1.85	1.08

[a] Locations are in inches, measured from the top of the dummy capsule.

[b] Spectral index or equivalent fission flux ratio.

[c] Dosimetry capsule calculation.

[d] Metallurgical capsule calculation.

Table 23. Integral Spectral Indices in BSR-HSST Capsule Mock-up "B"

Experimental Location[a]	^{103}Rh(n,n')^{103m}Rh[b] / ^{27}Al(n,α)^{24}Na	^{115}In(n,n')^{115m}In / ^{27}Al(n,n')^{24}Na	^{58}Ni(n,p)^{58}Co / ^{27}Al(n,α)^{24}Na	^{56}Fe(n,p)^{56}Mn / ^{27}Al(n,α)^{24}Na
South Channel				
16.5	1.93	1.59	1.07	1.09
11.0	2.11	1.70	1.10	1.09
5.5	2.17	1.71	1.10	1.08
Theory[c]	2.33	1.70	1.10	0.97
Theory[d]	2.35	1.73	1.12	0.97
Center Channel				
16.5	2.39	1.76	1.06	1.07
12.0	2.66	1.90	1.10	1.09
8.25	2.69	1.91	1.08	1.07
4.5	2.70	1.92	1.08	1.10
2.375	2.64	1.83	1.10	1.07
0.25	2.25	1.61	1.00	1.07
Theory[c]	2.99	1.95	1.10	0.95
Theory[d]	2.78	1.86	1.09	0.95

[a] Locations are in inches, measured from the top of the dummy capsule.

[b] Spectral index or equivalent fission flux ratio.

[c] Dosimetry capsule calculation.

[d] Metallurgical capsule calculation.

ORNL-DWG 80-16268

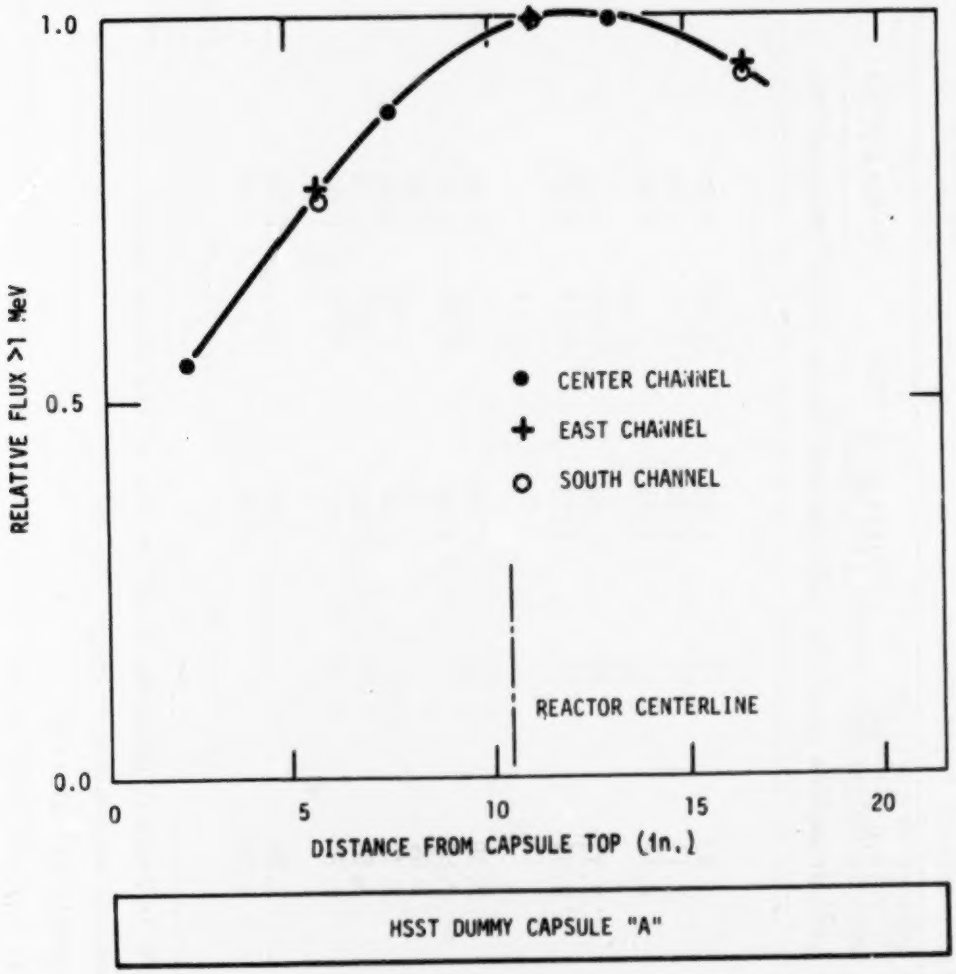

FIGURE 25. Relative Flux Distribution as a Function of the Distance from the Capsule Top, in the Dummy HSST Capsule at the BSR. Neg 8010270-13

ORNL-DWG 80-16269

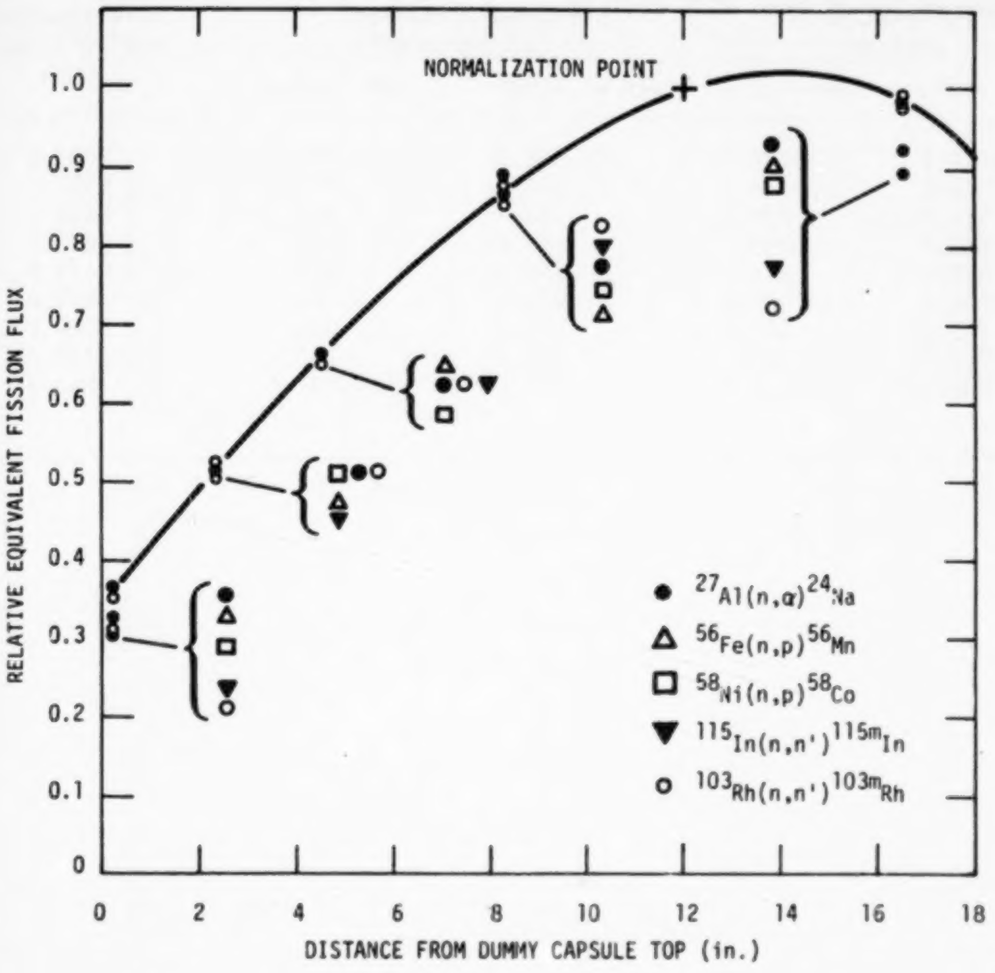

FIGURE 26. Relative Equivalent Fission Flux Along the Center Channel of the Dummy HSST Capsule, as a Function of the Distance from the Capsule Top. Neg 8010270-12

The results of the present measurements, after correction has been applied for the differences between the dosimetry mockup and the real metallurgical capsule, are given in Tables 24 and 25. These values can be combined with in-situ neutron fluence measurements to provide an improved neutronic characterization of this HSST capsule.

Table 24. Estimated Neutron Fluxes (E>1.0 MeV) in BSR-HSST Capsule "A", at a Core Power of 2 MW

Distance from Capsule Face (cm)	Dosimetry Capsule (Measurements)		Metallurgical Capsule (From Meas. and Calc.)	
	$\phi(E)>1$ MeV	$\phi(E)>.14$ MeV	$\phi(E)>1$ MeV	$\phi(E)>.14$ MeV
0.3908	2.594(12)[a]	8.382(12)	1.883(12)	5.479(12)
1.1723	2.279	7.811	1.651	5.087
1.9538	2.008	7.251	1.464	4.642
2.7354	1.767	6.707	1.285	4.283
3.5169	1.555	6.183	1.115	3.836
4.2985	1.367	5.679	9.726(11)	3.453
5.0800	1.200	5.193	8.342	3.033
5.8615	1.051	4.723	7.182	2.659
6.6431	9.182(11)	4.269	6.112	2.320

[a] Read 2.594 × 10^{12} neutrons cm^{-2} s^{-1}.

Table 25. Estimated Neutron Fluxes (E>1.0 MeV) in BSR-HSST Capsule "B", at a Core Power of 2 MW

Distance from Capsule Face (cm)	Dosimetry Capsule (Measurements)		Metallurgical Capsule (From Meas. and Calc.)	
	$\phi(E)>1$ MeV	$\phi(E)>.14$ MeV	$\phi(E)>1$ MeV	$\phi(E)>.14$ MeV
0.3908	2.371(12)[a]	6.886(12)	2.114(12)	6.007(12)
1.1723	2.094	6.439	1.842	5.589
1.9538	1.843	5.966	1.608	5.088
2.7354	1.622	5.516	1.402	4.604
3.5169	1.424	5.072	1.231	4.166
4.2984	1.249	4.650	1.057	3.726
5.0800	1.093	4.242	9.207(11)	3.327
5.8615	9.553(11)	3.855	7.849	2.888
6.6431	8.318	3.479	6.677	2.512

[a] Read 2.371×10^{12} neutrons cm^{-2} s^{-1}.

REFERENCES

1. W. N. McElroy, et al., "Development and Testing of Standardized Procedures and Reference Data for LWR Surveillance," HEDL-SA-1719, in Proceedings of an IAEA Specialists' Meeting on Irradiation Embrittlement, Thermal Annealing and Surveillance of Reactor Pressure Vessels, Vienna, Austria, February 26-March 1, 1979; IWG-RRPC-79/3, December 1979.

2. W. N. McElroy, et al., LWR Pressure Vessel Surveillance Dosimetry Improvement Program, NUREG/CR-1291, HEDL-SA 1949, October 1979.

3. T. U. Marston and K. E. Stahlkopf, "The Significance of Radiation Embrittlement on the Integrity and Operation of Light Water Reactor Pressure Vessels," Nuclear Safety, 1980, and T. U. Marston, "U.S. Nuclear Reactor Vessel Integrity Considerations," Proceedings of an IAEA Specialists' Meeting at Jülich, West Germany, September 24-27, 1979.

4. F. B. K. Kam, et al., PCA Blind Test Summary," Proceedings of the NRC 8th Safety Research Information Meeting, National Bureau of Standards, Gaithersburg, Maryland, October 27-31, 1980.

5. A. Fabry, et al., "PSF-HSST Neutron Characterization," Ibid.

6. Proceedings of the 3rd ASTM-Euratom International Symposium on Reactor Dosimetry, Ispra, Italy, October 1-5, 1979.

7. L. E. Steele and I. K. Terentiev, Proceedings of an IAEA Specialists' Meeting on Irradiation Embrittlement, Thermal Annealing and Surveillance of Reactor Pressure Vessels, Vienna, Austria, February 26-March 1, 1979; IWG-RRPC-79/3, December 1979.

8. L. Steele, "Review of the IAEA Specialists' Meeting on Irradiation Embrittlement, Thermal Annealing and Surveillance of Reactor Pressure Vessels," Proceedings of the 3rd ASTM-Euratom International Symposium on Reactor Dosimetry, Ispra, Italy, October 1-5, 1979.

9. W. Schneider, "Accuracies in Correlation Between Property Change and Exposure Data from Reactor Pressure Vessel Steel Irradiation," Proceedings of an IAEA Specialists' Meeting at Jülich, West Germany, September 24-27, 1979.

10. H. Till, "Neutron Radiometric and Calculation Benchmarking for LWR Pressure Vessel Radiation Effects," Proceedings of the 3rd ASTM-Euratom International Symposium on Reactor Dosimetry, Ispra, Italy, October 1-5, 1979.

11. A. Fabry and F. B. K. Kam, "Towards Adequate Evaluation of LWR Pressure Vessel Steel Irradiation Exposures," Proceedings of an IAEA Specialists' Meeting on Accuracies in Correlation Between Property Change and Exposure Data from Reactor Pressure Vessel Steel Irradiations, Jülich, West Germany, September 24-27, 1979.

REFERENCE (Cont'd)

12. ASME Boiler and Pressure Vessel Code, Section III, Nuclear Power Plant Components, Subsection NF.

13. W. C. Hopkins, "Suggested Approach for Fracture-Safe RPV Support Design in Neutron Environments," *ANS Transactions, 30,* 187, November 1978.

14. K. E. Stahlkopf and T. U. Marston, "A Comprehensive Approach to Radiation Embrittlement Analysis," in *Proceedings of an IAEA Specialists' Meeting on "Irradiation Embrittlement, Thermal Annealing and Surveillance of Reactor Pressure Vessels, Vienna, Austria, February 26-March 1, 1979.*

15. G. R. Odette, W. L. Server, W. Oldfield, R. O. Ritchie, and R. A. Wullaert, *Analysis of Radiation Embrittlement Reference Toughness Curves*, FCC 78-11, Fracture Control Corporation, November 14, 1978.

16. G. R. Odette, "Neutron Exposure Dependence of the Embrittlement of Reactor Pressure Vessel Steels: Correlation Models and Parameters," in *Proceedings of an IAEA Specialists' Meeting on Accuracies in Correlation Between Property Change and Exposure Data from Reactor Pressure Vessel Steel Irradiations, Jülich, West Germany, September 24-27, 1979.*

17. P. N. Randall, "Regulatory Aspects of Radiation Embrittlement of Reactor Vessel Steels," *Proceedings of an IAEA Specialists' Meeting on Irradiation Embrittlement, Thermal Annealing, and Surveillance of Reactor Pressure Vessels, Vienna, Austria, February 26-March 1, 1979.*

18. C. Z. Serpan, "Standardization of Dosimetry Related Procedures for the Prediction and Verification of Changes in LWR-PV Steel Fracture Toughness During a Reactor's Service Life: Status and Recommendations," *Proceedings of the 3rd ASTM-Euratom International Symposium on Reactor Dosimetry, Ispra, Italy, October 1-5, 1979.*

19. Code of Federal Regulations, Chapter 10, Part 50, Appendix G, "Fracture Toughness Requirements."

20. Code of Federal Regulations, Chapter 10, Part 50, Appendix H, "Reactor Vessel Materials Surveillance Program Requirements."

21. Regulatory Guide 1.99, Revision 1, "Effects of Residual Elements on Predicted Radiation Damage on Reactor Vessel Materials," U.S. Nuclear Regulatory Commission, April 1977.

22. *1980 Annual Book of ASTM Standards*, Part 4-Structural Steel, *Part 10-Metals, Part 11-Metallography*, and Part 45-Nuclear Standards, American Society for Testing and Materials, Philadelphia, Pa, 1980.

REFERENCE (Cont'd)

23. Master Matrix for LWR Pressure Vessel Surveillance Standards-Revision of E706-80, ASTM, Philadephia, Pa, 1980.

24. The Advisory Committee on Reactor Safeguards, Subcommittee on Metal Components, Transcribed Proceedings of January 24, 1980 Meeting, Washington, D.C.

25. LWR-PV Irradiation Surveillance Improvement Program Progress Report for October-December, 1979, HEDL-TME 80-3, NUREG/CR-1240, 1980.

26. LWR-PV Irradiation Surveillance Improvement Program Progress Report for January-March, 1980, HEDL-TME 80-4, NUREG/CR-1241, Vol. I, 1980.

27. LWR-PV Irradiation Surveillance Improvement Program Progress Report for April-June, 1980, HEDL-TME 80-5, NUREG/CR-1241, Vol. II, 1980.

28. G. L. Simmons, V. V. Verbinski, W. K. Hagan, and C. G. Cassapakis, Measurement and Analysis of Gamma Ray Induced Contamination of Neutron Dosimetry Procedures Used for Reactor Pressure Vessel Applications, EPRI NP-1056, April 1979.

29. G. C. Martin, Browns Ferry Unit 3 In-vessel Neutron Spectral Analysis, General Electric Company, NEDO-24793, August 1980.

30. K. E. Stahlkopf, G. R. Odette, and T. V. Marston, "Radiation Damage Saturation in Reactor Pressure Vessel Steel: Data and Preliminary Model," Proceedings of the 4th International Conference or Pressure Vessels and Pipings, London, England, 1980.

31. S. E. Yanichko, S. L. Anderson, R. P. Shogan, and R. G. Lott, Analysis of Capsule R from the Wisconsin Electric Power Company Point Beach Nuclear Plant Unit No. 2 Reactor Vessel Radiation Surveillance Program," Westinghouse Electric Corporation, WCAP-9635, EPRI Research Project 1021-3, December 1979.

32. C. Z. Serpan, "Overview of the USNRC Research into the Structural Integrity of Steel Reactor Pressure Vessels," Proceedings of the 5th International Conference on Structural Mechanics in Reactor Technology, Berlin, Germany, August 15, 1979.

33. R. L. Jones, T. V. Marston, S. T. Oldberg, and K. E. Stahlkopf, Pressure Boundary Technology Program: Progress 1974 through 1979, EPRI NP-1103-SR, Electric Power Research Institute, March 1979.

34. A. Alberman, M. Benoist, and M. Thierry, Dosimetry of Damage in the Simulated PWR Vessel of the ORNL Reactor, D. CEN/SPS/EAR/80/009, aa/cp, CEN, Saclay, France, January, 1980.

REFERENCE (Cont'd)

35. L. Steele, "Standards and Specifications for Selecting Optimum Nuclear Reactor Pressure Boundary Metals - A Review of U.S. Approaches and Needs," Nucl. Engr. Design, Vol. 27, 121, 1974.

36. S. E. Yanichko and J. N. Chirigos, "Assessment of the Validity of Trend Curves in Predicting Embritters of Reactor Pressure Vessels," NS-TMA-1843, 9th ASTM International Symposium on Effects of Radiation on Structural Materials, Richland, Washington, July 1978.

37. L. M. Davies, et al., "Irradiation Embrittlement of a Variety of RPV Steel Plates and Weldments," AERE-R 9385, January 1979 and T. J. Williams, "Interim Analysis of the Results to Date from A Materials Test Reactor (MTR) Irradiation Programme," RRA/N/3467, Rolls-Royce & Associates Limited, November 1979.

38. Metal Properties Council Subcommittee-6 on Nuclear Materials Report to ASTM Subcommittee E10.02 on Behavior and Use of Metallic Materials in Nuclear Systems, "Prediction of the Shift in the Brittle-Ductile Transition Temperature of LWR Pressure Vessel Materials," June 1980.

39. D. Pachur, "Apparent Embrittlement Saturation and Radiation Mechanisms of Reactor Pressure Vessel Steels," Proceedings of the 10th International Symposium on Effects of Radiation on Materials, Savannah, Georgia, June 3-5, 1980.

40. C. Guionnet, et al., "Radiation Embrittlement of PWR Pressure Vessel Steels SA 508 Cl 3, Effects of Impurity and Nickel Contents," Ibid.

41. M. Brumovsky, "Effects of Alloying Elements on Radiation Damage in Iron Alloys," Ibid.

42. E. C. Beinmiller and S. J. Byrne, "Evaluation of the Effect of Chemical Composition on the Irradiation Sensitivity of Reactor Vessel Weld Metal," ASTM STP 611, pp. 418-433, American Society of Testing and Materials, 1976.

43. J. D. Varsik and S. J. Byrne, "An Empirical Evaluation of the Irradiation Sensitivity of Reactor Pressure Vessel Materials", Proceedings of the Ninth International Symposium on "Effects of Radiation on Structural Materials," STP 683, p. 252, ASTM 1916 Race Street, Philadelphia, 1974.

44. G. L. Guthrie and F. M. Berting, "The Effect of Minor Elements on the Irradiation Sensitivity of Weld Metal," LWR-PV Irradiation Surveillance Improvement Program Progress Report for October-December 1977, HEDL-TME 78-5, NUREG/CR-0122, 1979.

REFERENCE (Cont'd)

45. G. L. Guthrie, "The Effect of Minor Elements on the Irradiation Embrittlement of Weld Metal II," LWR-PV Irradiation Surveillance Improvement Program Progress Report for April-June 1978, HEDL-TME 78-7, NUREG/CR-0550, 1979.

46. G. L. Guthrie, "Statistical Analysis of the Effects of Chemistry Variations on Charpy Test Results for Irradiated Reactor Pressure Vessel Steels," Proceedings of the 3rd ASTM-Euratom International Symposium on Reactor Dosimetry, Ispra, Italy, October 1-5, 1979.

47. R. L. Simons, "Re-evaluation of Damage Functions for Change in Ductile Brittle Transition Temperature in Ferritic Steels," Ibid.

48. S. Anderson, "Data Correlation Between Surveillance Measurements in the Predicted Vessel Neutron Exposure," Ibid and in Reference 9.

49. 1980 Annual Book of ASTM Standards, Part 45, Nuclear Standards, American Society for Testing and Materials, Philadelphia, PA, 1980.

REACTOR CALCULATION "BENCHMARK" PCA BLIND TEST RESULTS

F. B. K. Kam and F. W. Stallmann

Operations Division

Oak Ridge National Laboratory
Oak Ridge, Tennessee 37830

For presentation at the Eighth Water Reactor
Safety Research Information Meeting in
Gaithersburg, Maryland
October 27-31, 1980

By acceptance of this article, the publisher or recipient acknowledges the U.S. Government's right to retain a nonexclusive, royalty-free license in and to any copyright covering the article.

CONTRIBUTIONS

R. E. Maerker, L. F. Miller, J. F. Eastham, C. A. Baldwin
Oak Ridge National Laboratory
Oak Ridge, Tennessee

W. N. McElroy, L. Kellogg, R. Gold
Hanford Engineering Development Laboratory
Richland, Washington

E. D. McGarry, J. A. Grundl
National Bureau of Standards
Washington, DC

A. Fabry, G. DeLeeuw-Gierts, S. DeLeeuw, G. Minsart
CEN/SCK, Mol, Belgium

G. Cavanaugh
Combustion Engineering
Windsor, Connecticut

S. L. Anderson
Westinghouse Electric Company, Nuclear Power Division
Pittsburgh, Pennsylvania

G. Prillinger
IKE, University of Stuttgart
West Germany

U. Gröschel
Kraftwerk Union
West Germany

M. Austin
Rolls-Royce and Associates, Ltd.
Derby, England

K. Takeuchi
Ship Research Institute
Japan

C. Whitmarsh
Babcock and Wilcox
Lynchburg, Virginia

J. W. Rogers
EG&G Idaho, Inc.
Idaho Falls, Idaho

REACTOR CALCULATION "BENCHMARK" PCA BLIND TEST RESULTS*

F. B. K. Kam and F. W. Stallmann

1. SIGNIFICANCE

The code of Federal Regulations 10 CFR Part 50, App. G, requires the establishment of a surveillance program for all operating Light Water Reactors, with two major objectives;

1) To monitor changes in fracture toughness of ferritic materials in the pressure vessel beltline region, as a function of neutron exposure and vessel temperature; and
2) To determine the conditions under which the vessel can be utilized with adequate margins of safety against fracture throughout the reactor's service life.

2. SCOPE

1) To prepare an updated and improved set of ASTM dosimetry, damage correlation, and reactor analysis standards for LWR-PV Irradiation Surveillance Programs.
2) To determine and certify the accuracy of the experimental and analytical methods which are recommended in the standards.
    a) To determine how accurately transport theory calculations can predict neutron exposures in a LWR-PV benchmark field simulating steel-water configurations of commercial power reactors.

---

*Research sponsored by Division of Reactor Safety Research U.S. Nuclear Regulatory Commission under Interagency Agreement DOE 40-551-75 with the U.S. Department of Energy under contract W-7405-eng-26 with the Union Carbide Corporation.

b) To access the accuracy of the methodology used to translate damage and exposure data and the corresponding uncertainties obtained at designed surveillance locations to the pressure vessel beltline region.

3. SUMMARY OF RESULTS*

3.1 Discrete ordinates codes were used by all participants with the exception of one who used Monte Carlo. The Cartesian coordinate system was adopted by all calculators to model the geometry except one who used cylindrical coordinates (Table 4).

3.2 The primary source for experimental data for this investigation is integral measurements based on threshold reactions and fission chambers (Table 1). All instruments and sensors of integral measurements were calibrated by exposure to Standard Neutron Fields at NBS and Mol, Belgium. The measurements were validated through interlaboratory comparisons. Neutron spectroscopy measurements, ^{6}Li(n,α)t and gas proton recoil, are compared with calculations between 0.1-1.0 MeV.

The uncertainties in experiment data for the integral measurements are, in general, accurate to ±7% except for ^{237}Np and ^{238}U reactions which have not been corrected for photo-fission effects (Table 3).

3.3 There is a definite trend towards underestimation of the calculational values of the equivalent fission fluxes in the PV simulator (Figs. 1-3).

3.4 There is good agreement between calculated and measured results for the spectral indices of non-fission reactions (Figs. 4-6). The results of the ^{238}U(n,f) reaction and the ^{237}Np(n,f) (in water) reaction indicates that photo-fission effects requires investigation (Figs. 7-8).

---

*See Reference 3 for more complete evaluation.

3.5 Plots of the no-leakage correction cases for neutron exposure parameters, flux greater than 0.1 MeV and flux greater than 1.0 MeV indicate a spread of approximately 8% between the high and low values (Figs. 9-10).

3.6 Comparison of calculations and spectroscopy results shows a trend towards over-calculation of the neutrons in the energy range $0.111 < E < 1.05$ MeV (Fig. 11). This trend is also indicated by the somewhat higher calculated values for the ^{103}Rh/^{58}Ni spectral index. Spectral results, however, are not final at this time.

3.7 The spread between the high and low values of the calculated neutron exposure parameters, flux greater than 0.1 MeV, flux greater than 1.0 MeV, and dpa, ranges from 32-69% (Figs. 12-14). There seems to be no correlations between values at the core center and at other positions.

3.8 The "experimental" exposure parameters* were determined to be 12-30% for flux greater than 0.1 MeV, 7-12% for flux greater than 1.0 MeV, and 5-10% for dpa (Table 5). The uncertainties increase with increasing distance from the core because of the dissimilarity of the given spectrum from the reference fission spectrum.

3.9 The ratios between calculated and adjusted spectra normalized to the 1/4T position show an additional 5% discrepancy in scale factor** (Table 6).

---

*To compare calculated neutron exposure parameters with measurements, the "experimental" parameters were obtained with a logarithmic least squares adjustment method.

**A part of the adjustment procedure is a scaling of the input fluxes by a common factor applied to all energy groups. The scale factors are average ratios between the original and adjusted spectra.

4. CONCLUSIONS AND RECOMMENDATIONS

4.1 Further improvement in calculational procedures or a combination of calculations and measurements is necessary to attain 10-15% (1 σ) accuracy for neutron exposure parameters (flux greater than 0.1 MeV, flux greater than 1.0 MeV, and dpa).

4.2 The calculational modeling of power reactors should be benchmarked in an actual LWR plant to provide final uncertainty estimates for end-of-life predictions and limitations for plant operations.

5. RELATED REFERENCES

1. W. N. McElroy, et al, LWR Pressure Vessel Surveillance Dosimetry Improvement Program, HEDL-SA-2225 (to be published).

2. W. N. McElroy, et al, LWR Pressure Vessel Surveillance Dosimetry Improvement Program, 1979 Annual Report, NUREG/CR-1291 (February 1980).

3. F. W. Stallmann, J. F. Eastham, F. B. K. Kam, Evaluation of the NRC-PCA Calculational Blind Test Results, ORNL/TM-7565 (to be published).

4. F. B. K. Kam, et al, "Validation of Flux and Spectrum Predictions for a Pressure Vessel Wall Environment," NRC Seventh Water Reactor Safety Research Information Meeting, Gaithersburg, MD, Nov. 5-7, 1979.

5. J. J. Wagschal, R. E. Maerker, B. L. Broadhead, "LWR-PV Damage Estimate Methodology," Proceedings of the Advances in Reactor Physics and Shielding Technology Meeting, Sun Valley, Idaho, Sept. 15-18, 1980.

6. J. J. Wagschal, "Extrapolation of Surveillance Dosimetry Information to Predict Pressure Vessel Fluences," Proceedings of the American Nuclear Society, Las Vegas, Nevada, June 8-13, 1980.

7. F. W. Stallmann, F. B. K. Kam, "Neutron Characterization of the PCA-PV Benchmark Facility," Proceedings of the Third ASTM-EURATOM International Symposium on Reactor Dosimetry, Ispra, Italy, Oct. 1-5, 1979.

8. F. B. K. Kam, F. W. Stallmann, "Status Report on Activities of ASTM E10.05.01 Task Group on Uncertainty Analysis," Proceedings of the Third ASTM-EURATOM International Symposium on Reactor Dosimetry, Ispra, Italy, Oct. 1-5, 1979.

9. R. E. Maerker, "S_n Transport Calculations of the PCA Experiments With Some Estimated Uncertainties," Proceedings of the American Nuclear Society, Las Vegas, Nevada, June 8-13, 1980.

10. "Differential and Integral Nuclear Data Requirements for Shielding Calculations," Report IAEA 207, Proceedings of a Specialists' Meeting, Vienna, Oct. 12-15, 1976.

11. F. W. Stallmann, F. B. K. Kam, "Neutron Spectral Characterization of the BSR-HSST Dosimetry Tests," Proceedings of the Third ASTM-EURATOM International Symposium on Reactor Dosimetry, Ispra, Italy, Oct. 1-5, 1979.

12. F. B. K. Kam, et al, "Status of PSF Metallurgical Irradiation Program," Proceedings of the Third ASTM-EURATOM International Symposium on Reactor Dosimetry, Ispra, Italy, Oct. 1-5, 1979.

13. I. I. Siman-Tov, "Nuclear Heating in Thick Iron Slabs at the ORR Poolside Facility," Proceedings of the 1979 ANS Winter Meeting, San Francisco, Nov. 11-15, 1979.

14. I. I. Siman-Tov, LWR-PV Benchmark Facility Irradiation Capsules Heat Transfer Analysis, (to be published).

15. L. F. Miller, A Computerized Process Control System for the ORR-PSF Irradiation Experiment: Part 2: Mathematical Basis and Computer Implementation of the Temperature Control Algorithm, ORNL/NUREG/TM-405/P2 (to be published).

16. S. H. Merriman, A Computerized Process System for the ORR-PSF Irradiation Experiment: Part 1: Overall View of the Control System, ORNL/NUREG/TM-405/P1 (to be published).

17. F. B. K. Kam, A. Fabry, G. Minsart, F. Stallmann, J. H. Swanks, E. D. McGarry, W. N. McElroy, "The Core Power of the Critical Assembly Light Water Reactor Pressure Vessel Benchmark," Proceedings of the Third ASTM-EURATOM International Symposium on Reactor Dosimetry, Ispra, Italy, Oct. 1-5, 1979.

18. A. Fabry, G. DeLeeuw-Gierts, S. DeLeeuw, G. Minsart, "Progress Report on the Belgian Contribution to the USNRC Neutron Theory Blind Test in a LWR Pressure Vessel Benchmark," *Prepared for the NEA Committee on Reactor Physics*, NEACRP-A-   , September 1980.

19. E. D. McGarry, A. Fabry, "Dosimetry Characterization of a Reactor Pressure Vessel Simulator by Fission Chamber and Foil Activation Measurements," *Proceedings of the Third ASTM-EURATOM International Symposium on Reactor Dosimetry*, Ispra, Italy, Oct. 1-5, 1979.

20. A. Fabry, et al, "Reactor Dosimetry Integral Reaction Rate Data in LMFBR Benchmark and Standard Neutron Fields: Status, Accuracy and Implications," *Proceedings of the First ASTM-EURATOM Symposium on Reactor Dosimetry*, Petten (Holland), Sept. 22-26, 1975, Report EUR 5667 e/f Supplement.

21. S. DeLeeuw, R. Menil, H. Tourwé, A. Fabry, "New Trends and Progress in the Development of Reactor Damage Monitors for Light Water Reactor Pressure Vessel Surveillance Applications," *Proceedings of the Third ASTM-EURATOM International Symposium on Reactor Dosimetry*, Ispra, Italy, Oct. 1-5, 1979.

22. F. Ruddy, R. Gold, J. Roberts, "Solid State Track Recorder Measurements in the PCA," *Proceedings of the Third ASTM-EURATOM International Symposium on Reactor Dosimetry*, Ispra, Italy, Oct. 1-5, 1979.

23. G. DeLeeuw-Gierts, S. DeLeeuw, "Li-6 Neutron Spectrometry in the CEN/SCK Iron Shell Benchmark Fields at BR-1 and in the U.S. LWR-PV Simulator Mock-up at the Pool Critical Assembly," *Proceedings of the Third ASTM-EURATOM International Symposium on Reactor Dosimetry*, Ispra, Italy, Oct. 1-5, 1979.

24. J. W. Rogers, "Proton-Recoil Neutron Spectroscopy at the Pool Critical Assembly (PCA)," *Proceedings of the Third ASTM-EURATOM International Symposium on Reactor Dosimetry*, Ispra, Italy, Oct. 1-5, 1979.

25. R. Gold, B. J. Kaiser, "Reactor Gamma Spectrometry Status," *Proceedings of the Third ASTM-EURATOM International Symposium on Reactor Dosimetry*, Ispra, Italy, Oct. 1-5, 1979.

26. V. V. Verbinski, C. Cassapakis, W. K. Hagen, G. L. Simmons, "The Effect of Photo-fission and Other Photo-reactions on Neutron Dosimetry for Reactor Pressure Vessel Lifetime Studies," *Proceedings of the Third ASTM-EURATOM International Symposium on Reactor Dosimetry*, Ispra, Italy, Oct. 1-5, 1979.

ORNL-DWG-80-18091

Table 1. Measured Equivalent Fission Fluxes and Experimentally Derived Cross Sections.

Location	Distance from Core (cm)	^{237}Np(n,f)	^{103}Rh(n,n′)	^{115}In(n,n′)	^{238}U(n,f)	^{58}Ni(n,p)	^{27}Al(n,α)
			8/7 Configuration				
A1(TSF)	8.9	1.41(-5)[a]					
A3M(PVF)	20.7	1.65(-6)					
A4(1/4T)	30.4	5.74(-7)	4.63(-7)	3.37(-7)	3.39(-7)	2.40(-7)	3.57(-7)
A5(1/2T)	35.6	3.17(-7)	2.54(-7)	1.59(-7)	1.46(-7)	9.39(-8)	1.42(-7)
A6(3/4T)	41.0	1.68(-7)	1.29(-7)	7.09(-8)	6.13(-8)	3.41(-8)	5.20(-8)
A7(VB)	50.0		3.67(-8)	1.77(-8)			1.46(-8)
			12/13 Configuration				
A1(TSF)	12.8	6.54(-6)	5.42(-6)	5.50(-6)		5.86(-6)	7.80(-6)
A3M(PVF)	30.7	2.30(-7)	2.02(-7)	1.97(-7)		2.26(-7)	4.46(-7)
A4(1/4T)	40.4	9.18(-8)	7.65(-8)	5.81(-8)	6.27(-8)	5.18(-8)	1.02(-7)
A5(1/2T)	45.6	5.12(-8)	4.10(-8)	2.70(-8)	2.76(-8)	2.05(-8)	4.10(-8)
A6(3/4T)	51.0	2.67(-8)	2.08(-8)	1.17(-8)	1.14(-8)	7.29(-9)	1.53(-8)
A7(VB)	60.0	8.01(-9)					
Average ^{235}U Fission Spectrum Cross Section (mb)		1312 ±50	733 ±38	189 ±8	305 ±9	108.5 ±5.4	.705 ±.040

---

[a] Read as 1.41×10^{-5}

TSF: Thermal shield front; PVF: Pressure vessel front; VB: Void box.

ORNL-DWG-80-18092

Table 2. Dosimetry Experiments Performed in the PCA Benchmark Facility.

Dosimetry Technique	Laboratory	Type Method	Comments
Active fission chambers	NBS and MOL	Integral	
Radiometric (threshold foils) techniques	MOL	Integral	Confirmatory measurements made by HEDL and EG&G Ortec
Silicon damage monitors	MOL	Integral	
Solid state track recorders	HEDL	Integral	
^{6}Li(n,α)t neutron spectrometry	MOL	Differential	
Gas proton-recoil	EG&G Idaho	Differential	
Gamma spectrometry	HEDL	Differential	

Table 3. Summary of the Uncertainties in the Experimental Data.

1.	General experimental precision, including statistical spread, dead-time and background corrections, corrections for competing reactions, run-to-run monitoring, and uncertainty of positioning in experimental channel:	±0.5 to 1.5%
2.	Uncertainty in instrument calibration:	±3.5 to 4.0%
3.	Long-term maintenance of instrument performance:	±0.5 to 1.0%
4.	Neutron field instrumental perturbation. In water:	±3.0%
	In steel:	±0.5%
5.	Positioning of the experimental channels, relative to the reactor core:	±1.5%
6.	Normalization to core source strength, including core power measurement, correction, relationship of run-to-run monitor response with core power, and small mechanical variation of configuration between 1978 and 1979-1980 runs:	±4.3%

The data have not been corrected for gamma-ray-induced responses because no reliable estimates have been established so far; however, the influence is less than 1 to 1.5% except for ^{237}Np(n,f) in the water gaps and for ^{238}U(n,f) at all locations.

ORNL-DWG 80-17727

Table 4. Basic Features of the Blind Test Calculations for Various Participants.

Code	Program	Cross Section Library		Model	3-D Leakage	Purpose
		Descrip.	Groups			
A1.1	ANISN	DLC-41B VITAMIN-C	171	1D(y)	None	Collapse cross sections and obtain spectral data
A1.2	DOT 4.2 (S8, P3)	VITAMIN-C (Collapsed)	51	2D(y,x)	Space dependent buckling	Compare with experiment
A2.1	DOT 4.2 (S8,P3)	"	"	1D(y)	None	Obtain space dependent leakage correction factor
A2.2	DOT 4.2 (S8,P3)	"	"	2D(y,z)	None	" " "
A2.3	DOT 4.2 (S8,P3)	"	"	2D(y,x)	Synthesis based on ratio of A2.2 to A2.1	Compare with experiment
A3.1	MORSE	VITAMIN-E (Collapsed)	24	3D(y,x,z)	N/A	Obtain 3-D results to compare with experiment
A3.2	MORSE	"	"	2D(y,x)	None	Determine actual 3-D/2-D effects
A3.3	MORSE	"	"	2D(y,z)	None	Evaluate synthesis procedure
A3.4	MORSE	"	"	1D(y)	None	" " "
B1.1	ANISN (S8,P3)	DLC-41B/ VITAMIN-C	171	1D(y)	Space dependent buckling	Collapse cross sections
B1.2	DOT 3.5 (S8,P3)	VITAMIN-C (Collapsed)	17	2D(y,x)	Space dependent buckling	Compare with experiment
B2.1	ANISN (S8,P3)	DLC-41B VITAMIN-C	17	1D(y)	Fixed buckling based on x and z dimensions	Study leakage effects
B2.2	ANISN (S8,P3)	"	"	"	Fixed buckling on x; variable for z	" " "
B2.3	ANISN (S8,P3)	"	"	"	No buckling for x; variable for z	" " "
B2.4	ANISN (S8,P3)	"	"	"	Same as B2.3 except "D" based on Σ_{tot}	
B2.5	ANISN (S8,P3)	"	"	"	Doubled vertical buckling relative to B2.1	" " "
B2.6	ANISN (S8,P3)	"	"	"	Same as B2.1 except "D" based on Σ_{tot}	" " "
B2.7	ANISN (S8,P3)	"	"	"	Variable bucklings for x and z; B_x^2 based on DOT flux map	" " "
Z1.1	DOT 3.5 (S8,P3)	RSIC-37 EPR (Collapsed)	16	2D(x,y)	Synthesis based on ratio of Z1.2 to Z1.3	Compare with experiment
Z1.2	DOT 3.5 (S8,P3)	"	"	2D(x,z)	None	Obtain leakage correction for Z1.1
Z1.3	ANISN (S8,P3)	"	"	1D(x)	None	" " "

ORNL-DWG 80-17726

Table 4. Basic Features of the Blind Test Calculations for Various Participants (Cont'd).

Code	Program	Cross Section Library		Model	3-D Leakage	Purpose
		Descrip.	Groups			
C1.1	SN1D	EURLIB-110	100	1D(x)	Space denendent buckling	Collapse cross sections
C1.2	TWOTRAN	EURLIB-100 (Collapsed)	45	2D(x,y)	" " "	Generate buckling data for C1.3 and compare with experiment
C1.3	SN1D	DLC-41B/ VITAMIN-C	171	1D(x)	" " "	Compare with experiment
Q1.1	DOT-3 (S8,P3)	DLC-23E (Cask)	22	2D(x,y)	Synthesis based on ratio of Q1.3 to Q1.2	Compare with experiment
Q1.2	DOT-3 (S8,P3)	DLC-23E (Cask)	"	1D(x)	None	Obtain space dependent leakage correction factor
Q1.3	DOT-3 (S8,P3)	DLC-23E (Cask)	"	2D(x,z)	None	" " "
S1.1	ANISN (S8,P3)	EURLIB-4	100	1D(x)	Synthesis based on ratio $\frac{S1.2}{S1.1} \cdot \frac{S1.3}{S1.1}$	Compare with experiment
S1.2	DOT-3 (S4,P3)	EURLIB-4	"	2D(x,y)	None	Obtain leakage correction for S1.1
S1.3	DOT-3 (S4,P3)	EURLIB-4	"	2D(x,z)	None	" " "
U1.1	DOT (S6,P1)	ENDF/B-IV (Collapsed)	21	2D(x,y)	DB^2 from balance tables of U1.2	Compare with experiment
U1.2	DOT (S6,P1)	ENDF/B-IV (Collapsed)	21	2D(x,z)	None	Obtain leakage correction for U1.1
V1.1	MCBEND	EURLIB-100 (Collapsed)	40	3D(x,y,z)	N/A	Compare with experiment
Y1.1	DOT 3.5 (S8,P3)	DLC-23E/ Cask 22	22	2D(x,y)	Synthesis based on ratio of Y1.2 to Y1.3	Compare with experiment
Y1.2	ANISN (S8,P3)	"	"	1D(x)	Buckling in axial and horizontal transverse directions	Obtain leakage correction for U1.1
Y1.3	ANISN (S8,P3)	"	"	"	Buckling in the horizontal transverse direction	" " "
W1.1	DOT 4.2 (S8,P3)	DLC-41B/ VITAMIN-C (Collapsed)	12	2D(y,z)	None	Compare with experiment
W1.2	DOT 4.2 (S8,P3)	"	"	"	Fixed buckling from core dimensions	" " "
R1.1	PALLAS	ENDF/B-IV (Processed)	80	1D(r)	N/A	Compare with experiment
R1.2	PALLAS	"	40	2D(r,z)	N/A	" " "
K1.1	DOT 3.5 (S8,P1)	DLC-23E/Cask (Collapsed)	15	2D(x,y)	Unknown	Compare with experiment
K1.2	DOT 3.5 (S8,P1)	"	"	2D(x,z)	Unknown	" " "

ORNL-DWG-80-18093

Table 5. Calculated and Experimental Integral Parameters in the PCA 12/13 Configuration.

Code	Location						
	A0	A1	A2	A3	A4	A5	A6
				Flux Greater Than 0.1 MeV			
A	3.08(-4)	6.02(-6)[a]		2.14(-7)[b]	1.19(-7)	7.79(-8)	4.61(-8)
B2	3.00	5.87	7.25(-7)	1.94	1.05	6.80	4.01
C1	-	7.41	9.88	2.79	1.74	1.15(-7)	6.65
C2	2.98	6.73	9.08	2.55	1.62	1.07	6.22
K	2.11	7.76	9.80	2.06	1.27	8.61(-8)	5.11
Q	-	5.68	6.98	1.71	1.12	7.27	4.02
S	3.23	6.35	8.47	2.06	1.26	8.43	5.00
U	2.88	6.50	7.89	2.31	1.18	7.69	4.37
V	-	5.61	3.43	1.70	1.17	7.60	4.66
Y	3.13	6.08	8.16	2.28	1.42	9.39	5.38
Z	3.08	6.25	7.34	2.12	1.29	8.45	4.85
Exp. Values Standard Deviation		7.12 ±12%		2.55 ±12%[b]	1.43 ±17%	9.59 ±19%	5.71 ±20%
				Flux Greater Tnan 1.0 MeV			
A	1.68(-4)	3.39(-6)		1.21(-7)[b]	3.96(-8)	1.84(-8)	7.88(-9)
B2	1.61	3.29	3.57(-7)	1.09	3.43	1.58	6.87
C1	-	4.18	4.93	1.57	5.38	2.47	1.05(-8)
C2	1.60	3.82	4.53	1.42	5.27	2.49	1.08
K	1.13	4.25	5.17	1.09	4.01	1.92	8.53(-9)
Q	-	3.21	3.53	9.71(-8)	3.57	1.63	6.84
S	1.73	3.61	4.21	1.15(-7)	3.56	1.62	6.85
U	1.54	3.68	3.88	1.29	3.94	1.89	8.33
V	-	3.24	1.25	1.03	4.10	1.89	8.87
Y	1.72	3.50	4.13	1.29	4.39	2.03	8.65
Z	1.66	3.55	3.89	1.21	3.99	1.82	7.87
Exp. Values Standard Deviation		3.80 ±7%		1.36 ±7%	4.41 ±9%	2.12 ±11%	9.34 ±12%
				Displacements per Atom			
A	2.59(-1)	7.19(-3)		2.20(-4)[b]	6.54(-5)	3.58(-5)	1.86(-5)
B2	2.28	5.90	5.91(-4)	1.94	5.78	3.15	1.65
C1	-	7.88	8.75	3.02	8.97	4.88	2.49
C2	2.28	6.01	7.17	2.28	8.77	4.84	2.49
K	1.57	6.01	7.46	1.61	6.85	3.90	2.07
Q	-	4.82	5.44	1.51	6.07	3.30	1.64
S	2.44	5.86	5.81	1.93	6.29	3.49	1.83
U	2.19	7.56	7.18	2.65	6.47	3.57	1.81
V	-	4.39	2.48	1.46	6.56	3.47	1.92
Y	2.42	7.08	7.67	2.64	7.56	4.21	2.15
Z	2.34	6.35	6.21	2.14	7.00	3.86	2.00
Exp. Values Standard Deviation		5.44 ±5%		1.99 ±5%	7.70 ±8%	4.38 ±10%	2.32 ±12%

[a] Read as 6.020×10^{-6}.

[b] Data actually obtained at location A3M, which is 0.80 cm closer to the core than A3.

ORNL-DWG-80-18094

Table 6. PCA 12/13 Configuration, Ratios between Calculated and Adjusted Spectra from Logarithmic Least Squares Adjustment Procedure.

Code	TSF	1/4 T	1/2 T	3/4 T
	A1	A4	A5	A6
		Ratios		
A	0.86	0.85	0.82	0.80
B	0.85	0.77	0.73	0.72
C1	1.06	1.18	1.14	1.10
C2	0.98	1.18	1.15	1.15
K	1.10	0.92	0.92	0.93
Q	0.84	0.82	0.79	0.76
S	0.96	0.82	0.76	0.74
U	0.90	0.83	0.79	0.75
Y	0.88	1.00	0.98	0.96
V*	0.83	0.96	0.85	1.03
Z	0.94	0.91	0.86	0.84
		Ratios Normalized to 1/4 T Position		
A	1.01	1.00	0.96	0.94
B	1.11	1.00	0.95	0.94
C1	0.90	1.00	0.97	0.93
C2	0.83	1.00	0.98	0.98
K	1.19	1.00	0.99	1.00
Q	1.03	1.00	0.96	0.93
S	1.17	1.00	0.93	0.90
U	1.09	1.00	0.96	0.91
Y	0.88	1.00	0.98	0.96
V*	0.86	1.00	0.88	1.07
Z	1.03	1.00	0.94	0.92

*Monte Carlo calculation.

ORNL-DWG-80-18072

Fig. 1. PCA 12/13 C/E RATIOS FROM EQUIVALENT FISSION FLUXES

NP237 REACTION

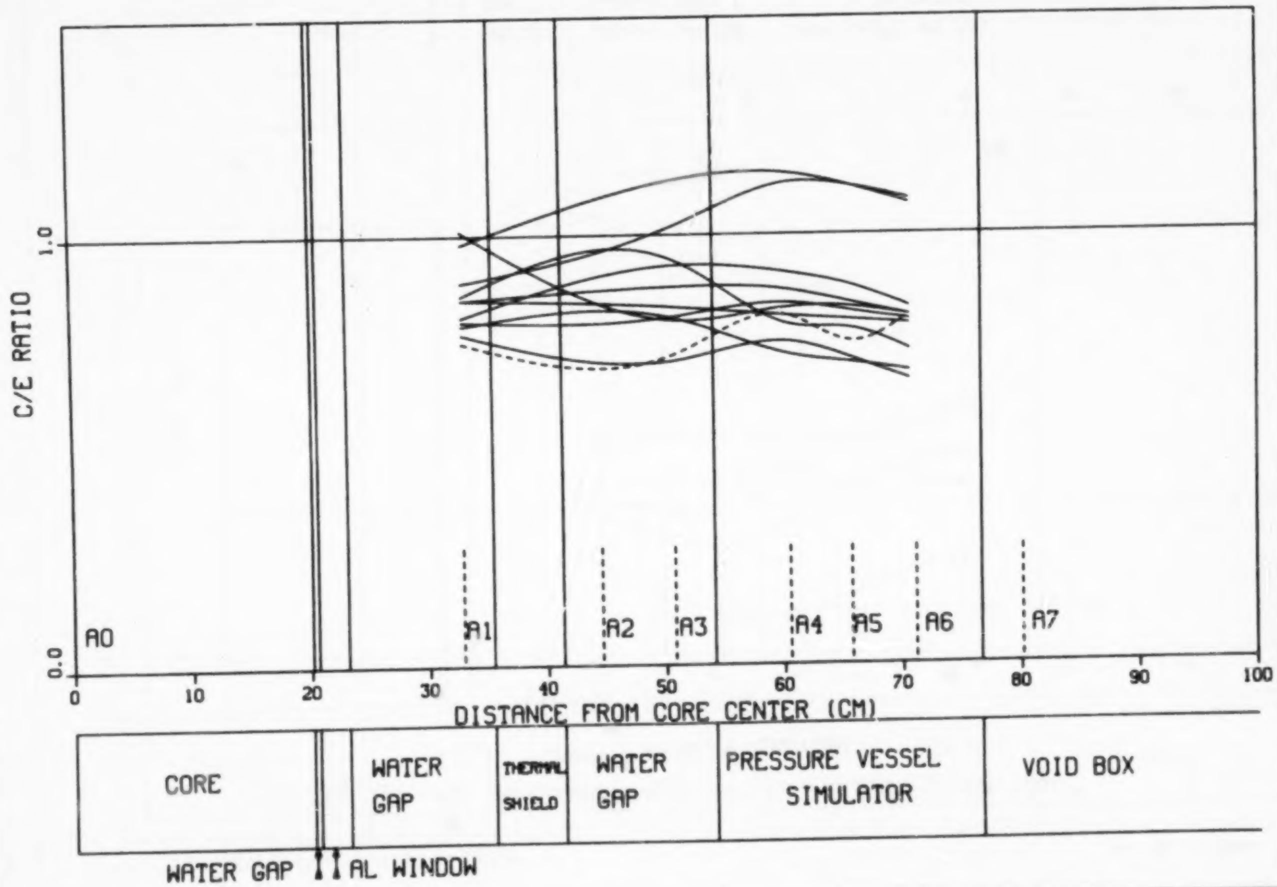

ORNL-DWG-80-18074

Fig. 2. PCA 12/13 C/E RATIOS FROM EQUIVALENT FISSION FLUXES

IN115 REACTION

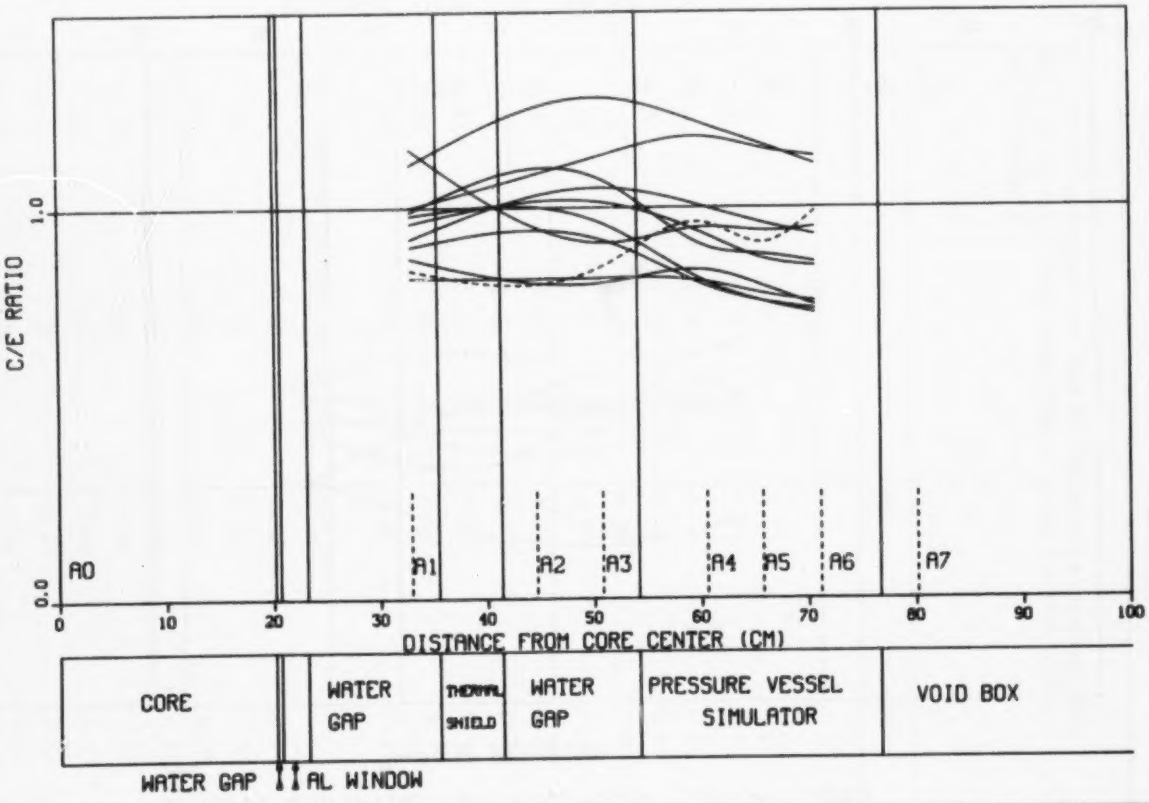

ORNL-DWG-80-18076

Fig. 3. PCA 12/13 C/E RATIOS FROM EQUIVALENT FISSION FLUXES

NI58 REACTION

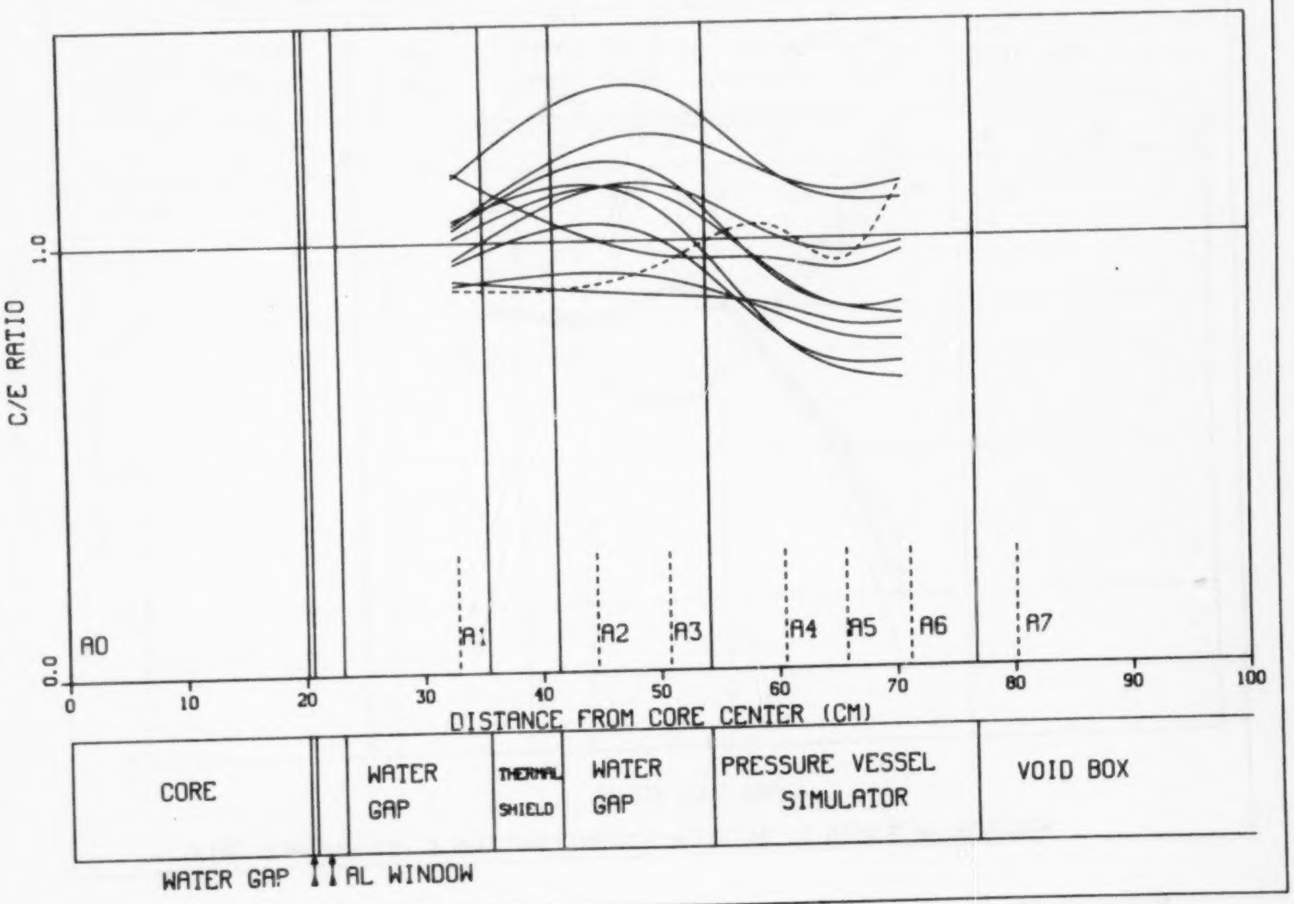

ORNL-DWG-80-18078

Fig. 4. PCA 12/13 SPECTRAL INDICES RELATIVE TO NI58(N,P) REACTION

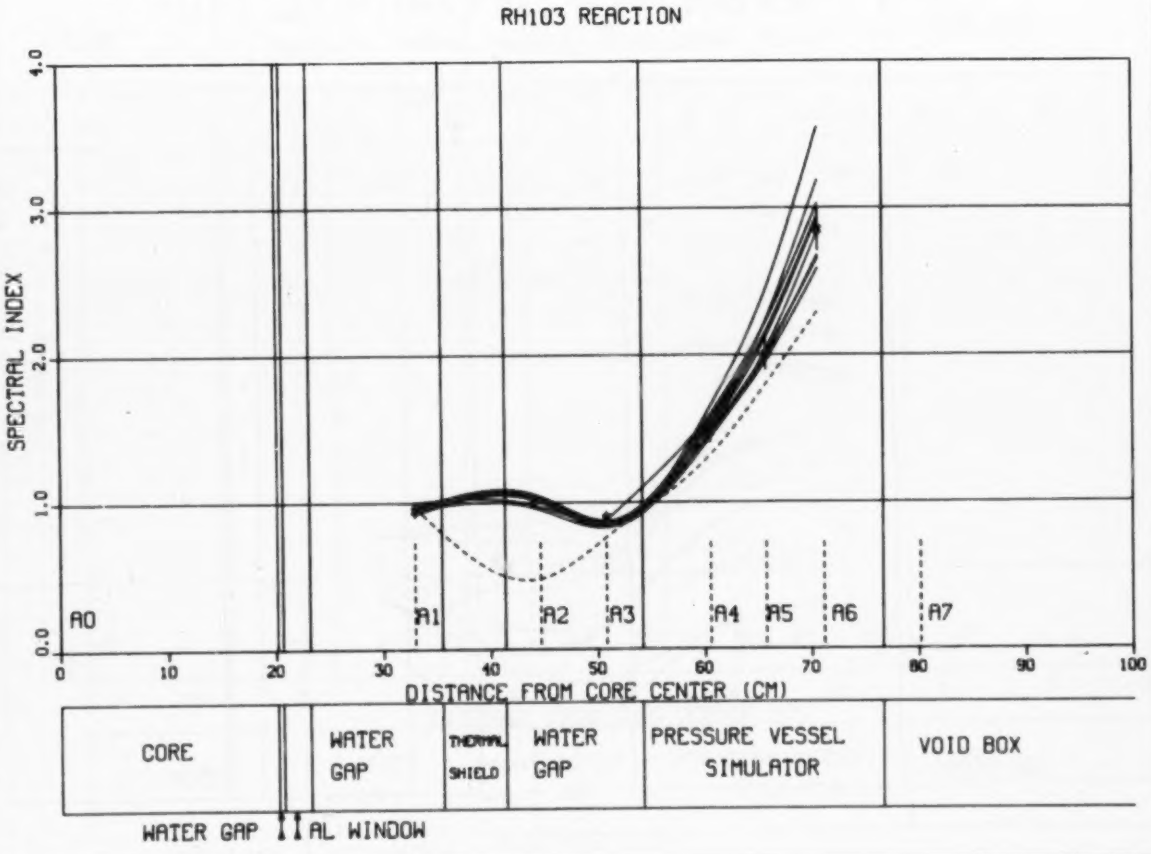

ORNL-DWG-80-18080

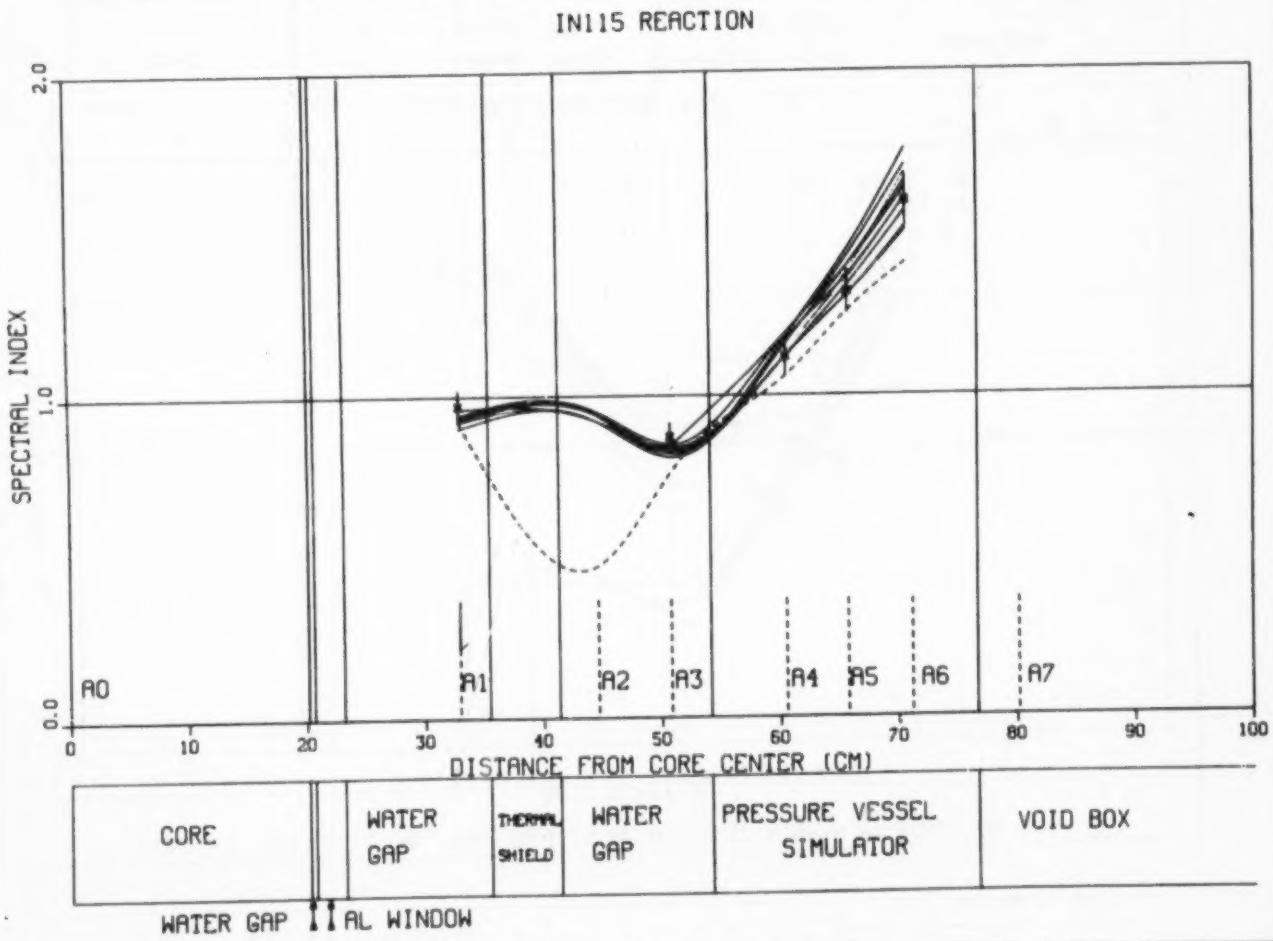

Fig. 5. PCA 12/13 SPECTRAL INDICES RELATIVE TO NI58(N,P) REACTION

ORNL-DWG-80-18082

Fig. 6. PCA 12/13 SPECTRAL INDICES RELATIVE TO NI58(N,P) REACTION

AL27 REACTION

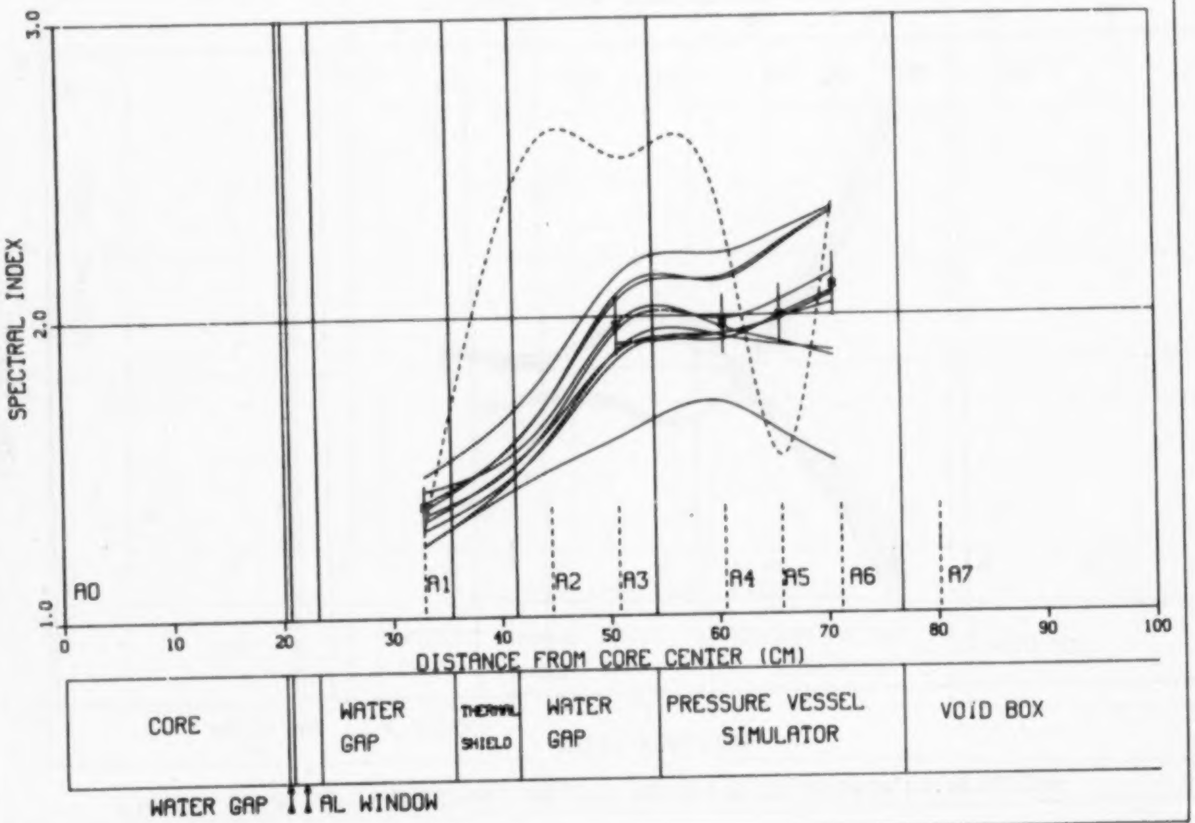

ORNL-DWG-80-18079

Fig. 7. PCA 12/13 SPECTRAL INDICES RELATIVE TO NI58(N,P) REACTION

NP237 REACTION

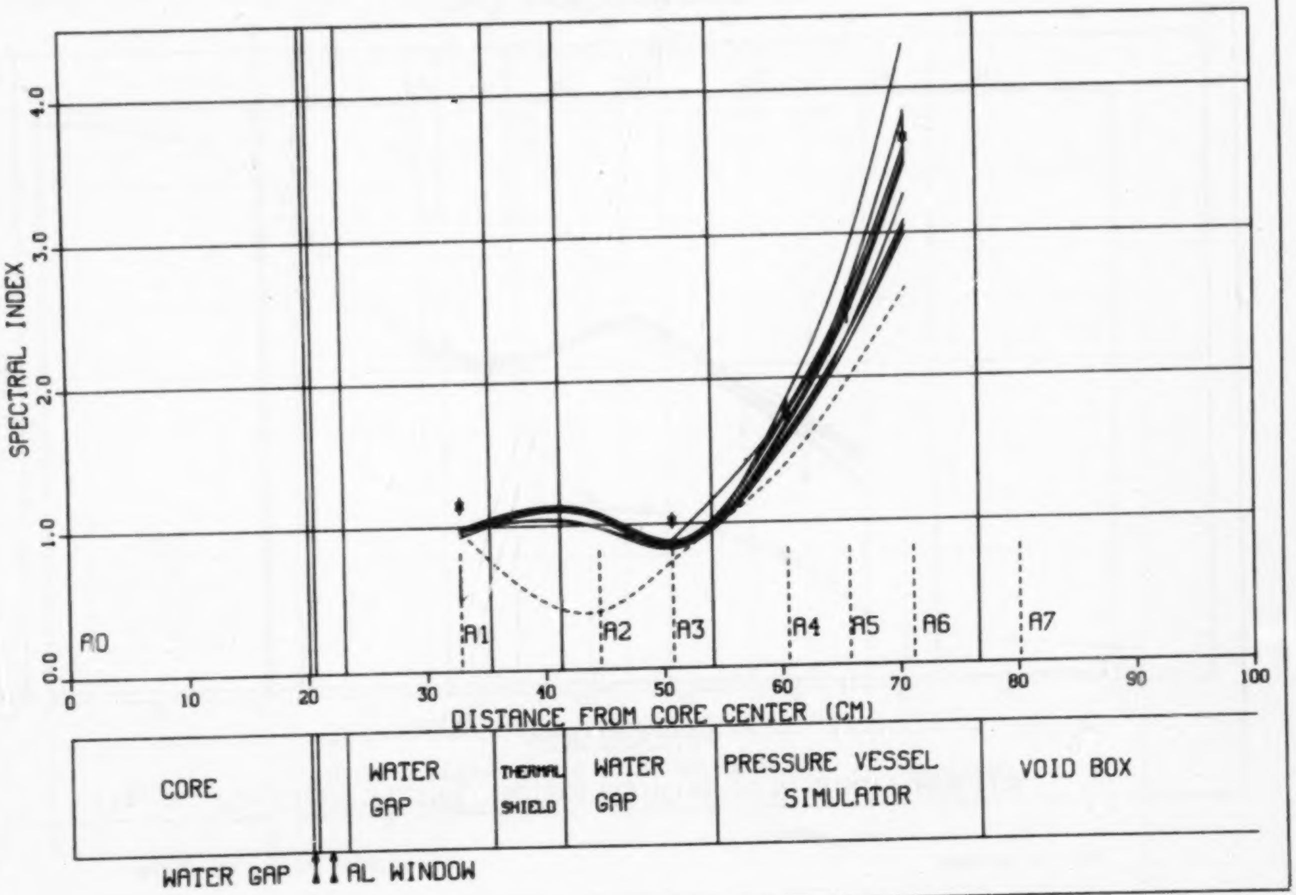

ORNL-DWG-80-18081

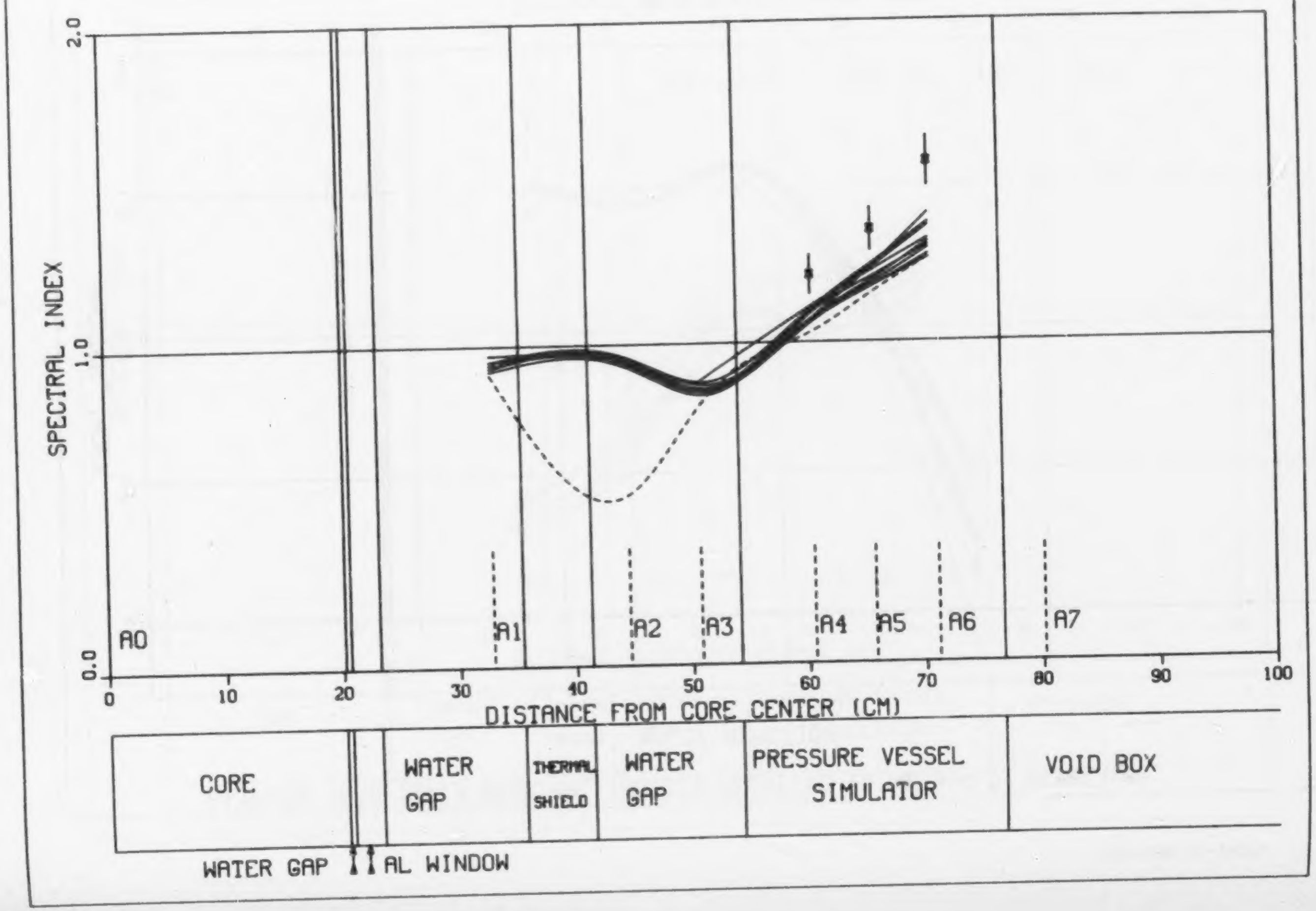
Fig. 8. PCA 12/13 SPECTRAL INDICES RELATIVE TO NI58(N,P) REACTION

U238 REACTION

ORNL-DWG-80-18083

Fig. 9. PCA 12/13 CONFIGURATION

FLUX >0.1 MEV., NO AXIAL LEAKAGE CORRECTION

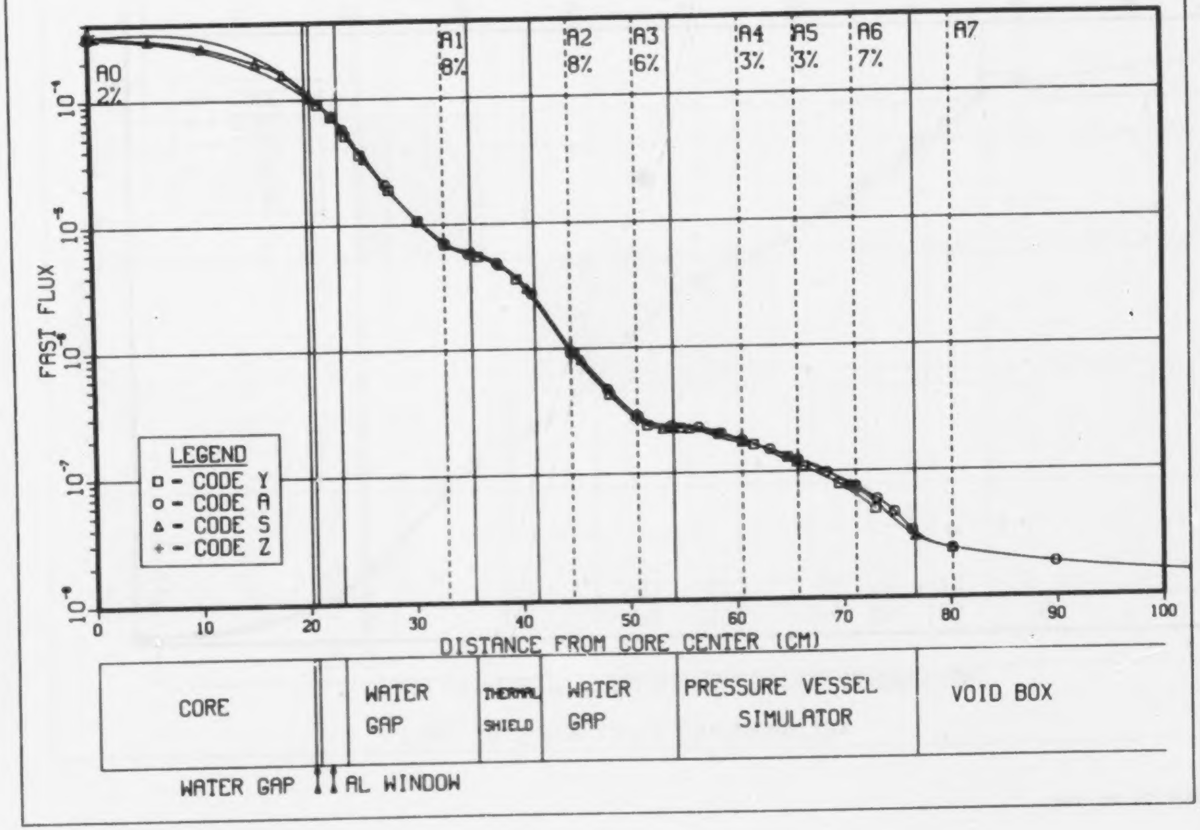

ORNL-DWG-80-18084

Fig. 10. PCA 12/13 CONFIGURATION

FLUX >1.0 MEV. NO AXIAL LEAKAGE CORRECTION

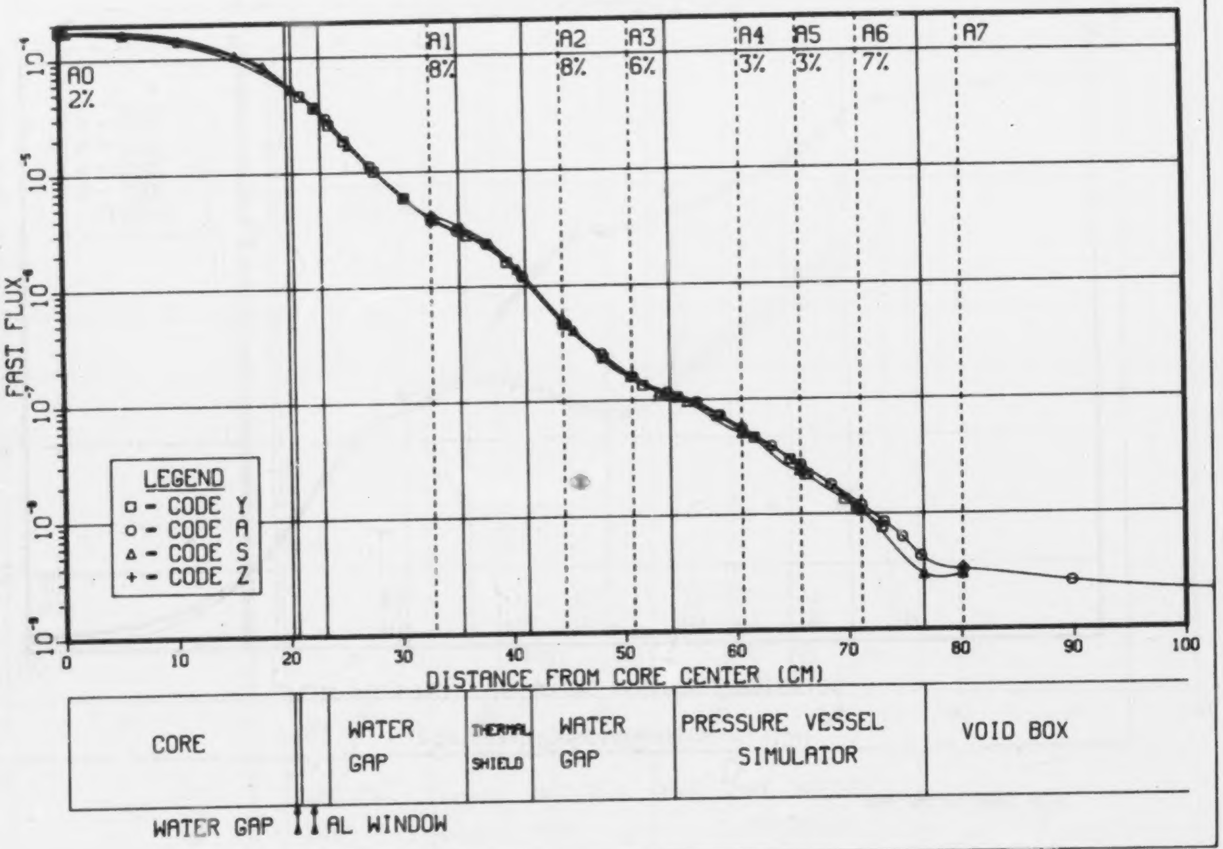

ORNL-DWG-80-18068

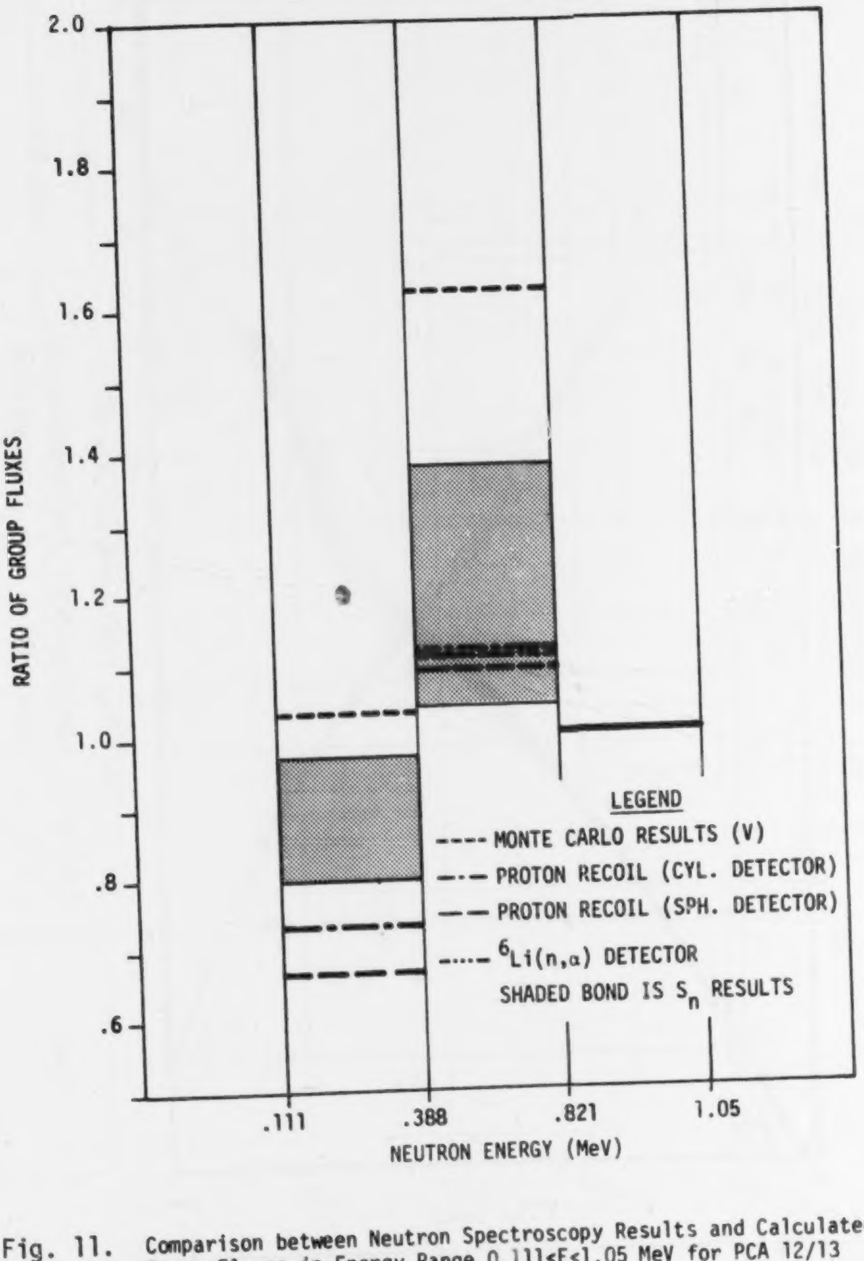

Fig. 11. Comparison between Neutron Spectroscopy Results and Calculated Group Fluxes in Energy Range 0.111<E<1.05 MeV for PCA 12/13 Configuration, 1/4 T Position.

ORNL-DWG-80-18085

Fig. 12. PCA 12/13 CONFIGURATION

FLUXES ABOVE 0.1 MEV.

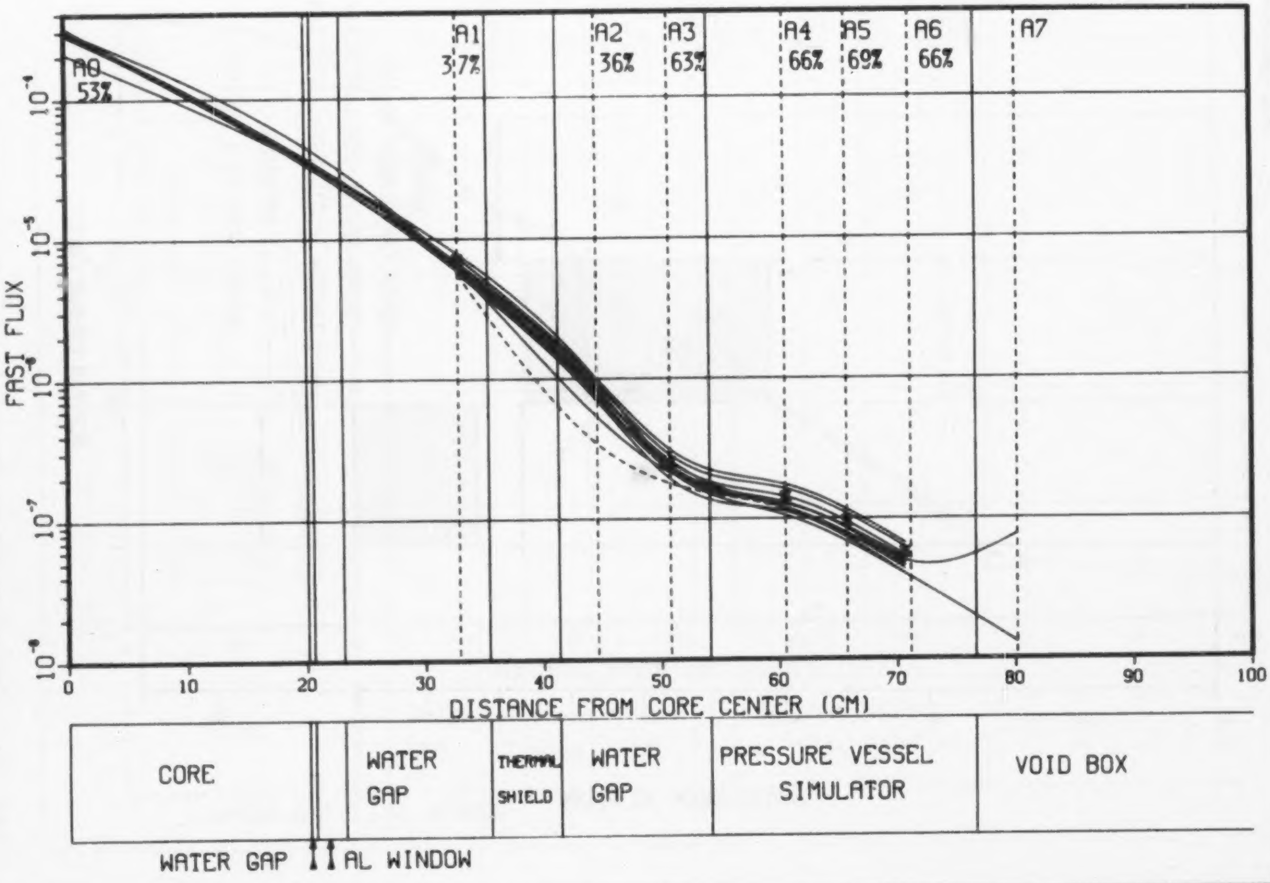

ORNL-DWG-80-18086

Fig. 13. PCA 12/13 CONFIGURATION

FLUXES ABOVE 1.0 MEV.

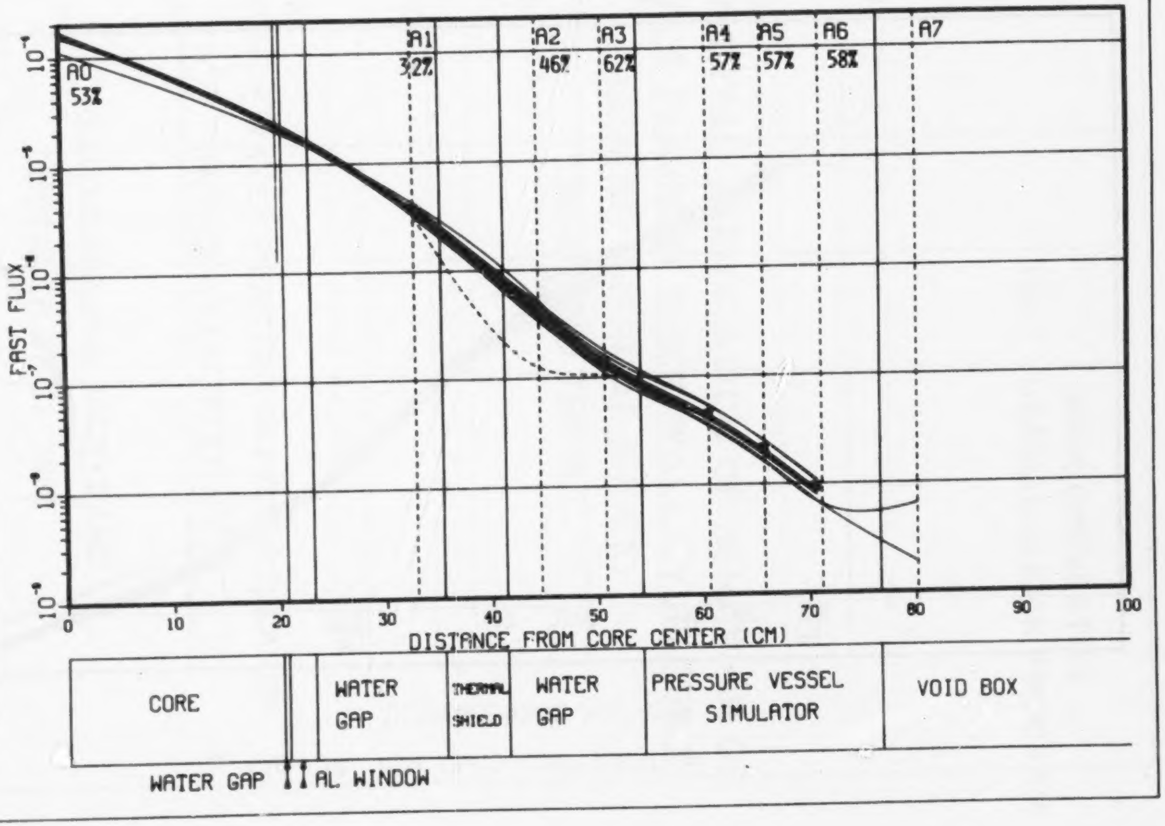

ORNL-DWG-80-18087

Fig. 14. PCA 12/13 CONFIGURATION

DISPLACEMENTS PER ATOM

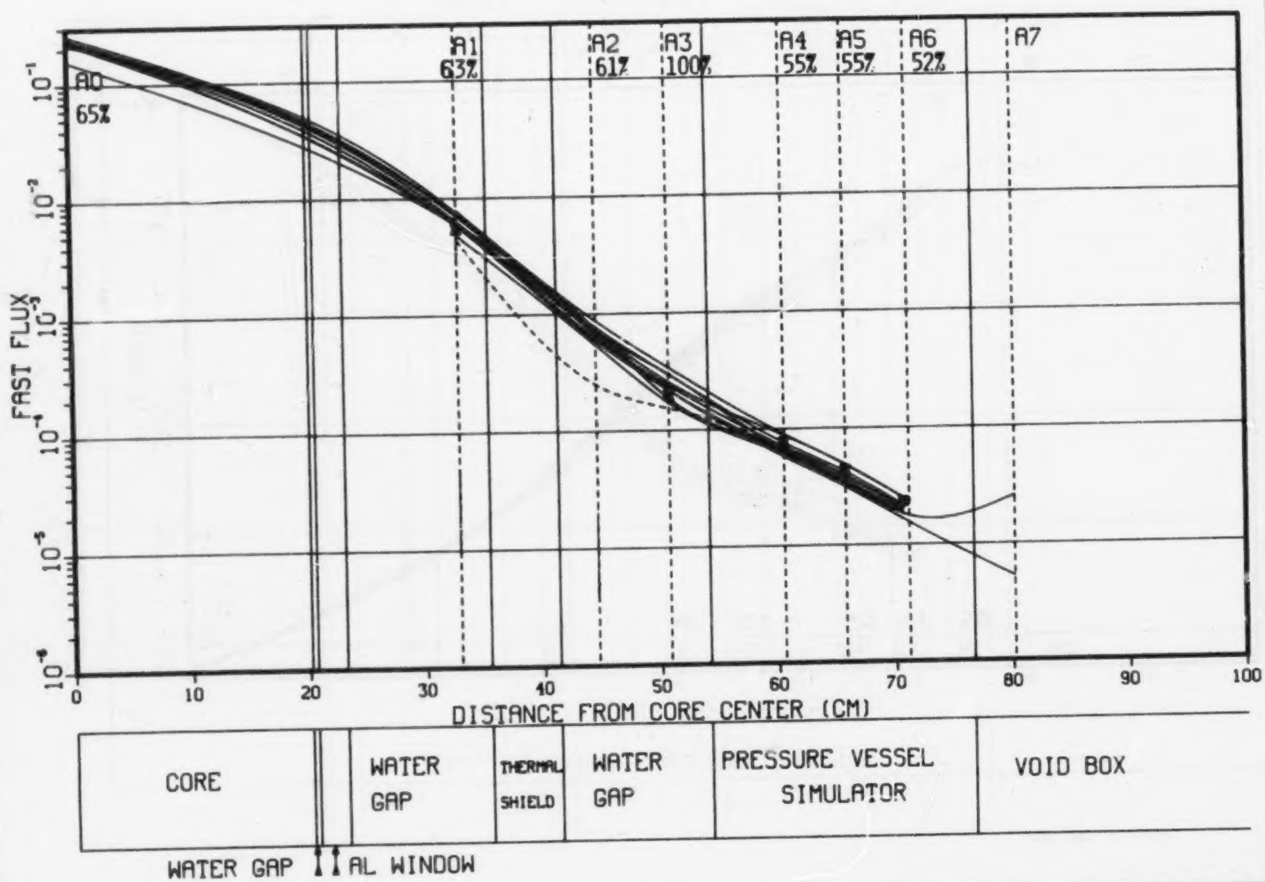

UNION CARBIDE
ORNL

DICK CHEVERTON
HSST THERMAL-SHOCK PROGRAM

EXPERIMENTAL VERIFICATION OF BEHAVIOR OF SURFACE FLAWS IN THICK-WALL CYLINDERS DURING THERMAL SHOCK: TSE-5 AND TSE-5A

EIGHTH WATER REACTOR SAFETY RESEARCH
INFORMATION MEETING

GAITHERSBURG, MARYLAND
OCTOBER 27–31, 1980

EXPERIMENTAL VERIFICATION OF THE BEHAVIOR OF SURFACE FLAWS IN THICK-WALLED STEEL CYLINDERS DURING SEVERE THERMAL SHOCK: TSE-5 AND TSE-5A*

R. D. Cheverton
Oak Ridge National Laboratory
Oak Ridge, Tennessee 37830

The behavior of inner-surface flaws in thick-wall vessels subjected to severe thermal-shock loadings has been under investigation at ORNL for several years. During this time six thermal-shock experiments have been conducted. The first four[1-4] were conducted with 533-mm-OD × 152-mm-wall × 914-mm-length steel cylinders (A508, class-2 chemistry, quench-only heat treatment). They demonstrated initiation and arrest of shallow flaws under severe thermal shock conditions and indicated that LEFM is valid for this particular situation.

Analysis of the PWR LOCA-ECC indicates that under some circumstances a preexisting flaw on the inner surface of the vessel could propagate deep into the wall, and that the extent of propagation would be influenced by the vessel diameter-to-thickness ratio and also by warm prestressing (WPS).[1,2] Neither of these effects could be investigated in the first four experiments because the test specimen diameter-to-thickness ratio was too small and because the toughness was too low. Thus, additional experiments were in order.

The purpose of the fifth experiment (TSE-5), which was conducted in August 1979, was to demonstrate initiation, arrest, WPS and arrest in a rising K_I field $[dK_I/d(a/w) > 0]$ during a severe thermal shock and under conditions that promote deep penetration prior to final arrest.[5]

Appropriate design conditions for TSE-5 included a 991-mm-OD × 152-mm-wall × 1220-mm-length cylinder with toughness properties similar to those for HSST plate 02, a test cylinder initial temperature of ∼93°C and a thermal

---

*Research sponsored by Office of Nuclear Regulatory Research, U.S. Nuclear Regulatory Commission, under Interagency Agreements 40-551-75 and 40-552-75 with the U.S. Department of Energy under contract W-7405-eng-26 with the Union Carbide Corporation.

By acceptance of this article, the publisher or recipient acknowledges the U.S. Government's right to retain a nonexclusive, royalty-free license in and to any copyright covering the article.

shock medium of liquid nitrogen (−197°C). To overcome film boiling associated with LN_2 quenching a special inner-surface coating was developed; and in an attempt to achieve the desired toughness characteristics for our existing A508 class-2-chemistry test cylinder, a toughness-vs-tempering-temperature study was conducted and subsequently a tempering temperature of 613°C specified. The initial flaw selected for TSE-5 was a sharp, 16-mm-deep, long (1220-mm) axial crack.

As reported at the 5th WRSR Information Meeting, the results of TSE-5 indicated that the fracture toughness of the test-cylinder material was substantially less than expected on the basis of the pretest material-characterization studies. Since the time of the information meeting and because of the apparent discrepancy in toughness an extensive post-test material-characterization study was conducted. The results indicated a large scatter (±50%) in fracture toughness (K_J) in the lower transition region. A comparison of these results with K_{Ic} values deduced from TSE-5 indicated that the long axial flaw in TSE-5 behaved in accordance with the lower bound of the laboratory data derived from 1T- and 2T-CT specimens.

When the lower-bound toughness curve was used in a post-test analysis of TSE-5, it became apparent that linear-elastic fracture mechanics (LEFM) was applicable for both shallow and deep flaws during severe thermal shock; that a long crack jump that took place during TSE-5 was due to a blunted crack tip ($K_I > K_{Ic}$ required for initiation); and that there were essentially no dynamic effects associated with the arrest of the long crack jump. Warm prestressing and arrest in a rising K_I field were not adequately demonstrated because of the unexpectedly low fracture toughness.

The sixth experiment, TSE-5A, was designed to achieve the intent of TSE-5, using the same type of test cylinder and the same liquid-nitrogen test facility. An extensive pretest material-characterization study was conducted to define an appropriate lower-bound fracture-toughness curve and a corresponding mean curve for K_{Ia}. The required tempering temperature was established after testing at least ten 1T-CT specimens at each of three testing temperatures for three different tempering temperatures. The tempering temperature finally specified was 679°C, and for this material ten 1T-CT specimens were eventually tested at each of five testing temperatures to obtain the final TSE-5A-K_{Ic} design curve. Relatively few 6 x 6 x 1-CT K_{Ia} specimens were tested to obtain the K_{Ia} design curve.

A post-test analysis of TSE-5A, using the design toughness curves and the measured temperature distributions in the wall, indicated (1) four initiation-arrest events should have taken place; (2) the final arrested fractional crack depth (a/w) should have been 0.54; and (3) WPS should have prevented a fifth initiation event even though late in the transient $(K_I/K_{Ic})_{max}$ for the final crack depth was well in excess of unity (∿2.0). The calculation also indicated that the first arrest, but not the others, should have taken place in a rising K_I field.

During TSE-5A, four initiation-arrest events did take place, the final fractional crack depth at midlength of the test cylinder was 0.53, and it appeared that WPS was effective and that the first arrest event took place in a rising K_I field. However, the events took place sooner than calculated, indicating that once again the material toughness was less than expected. Comparing the K_{Ic} and K_{Ia} values deduced from TSE-5A with the design curves indicated that a shift in the curves of ∿22K would result in very good agreement. A final post-test analysis using the shifted toughness curves indicated that the first arrest event took place in a rising K_I field, that WPS prevented a fifth initiation event, and that $(K_I/K_{Ic})_{max}$ for the final crack depth was 2.3; the corresponding crack-tip temperature was −46°C. Thus, WPS in a large structure subjected to severe thermal shock was demonstrated in a convincing manner and all objectives of TSE-5A were met. A summary of events for TSE-5A is presented in Table 1.

References

1. R. D. Cheverton, *Pressure Vessel Fracture Studies Pertaining to a PWR LOCA-ECC Thermal Shock: Experiments TSE-1 and TSE-2*, ORNL/NUREG/TM-31 (September 1976).

2. R. D. Cheverton and S. E. Bolt, *Pressure Vessel Fracture Studies Pertaining to a PWR-LOCA-ECC Thermal Shock: Experiments TSE-3 and TSE-4 and Update of TSE-1 and TSE-2 Analysis*, ORNL/NUREG-22 (December 1977).

3. R. D. Cheverton, S. K. Iskander, and S. E. Bolt, *Applicability of LEFM to the Analysis of PWR Vessels Under LOCA-ECC Thermal Shock Conditions*, NUREG/CR-0107, ORNL/NUREG-40 (October 1978).

4. R. D. Cheverton and S. K. Iskander, *Application of Static and Dynamic Crack Arrest Theory to Thermal Shock Experiment TSE-4*, NUREG/CR-0767, ORNL/NUREG-57 (June 1979).

5. R. D. Cheverton, "Thermal Shock Investigations," *HSST Program Quarterly Progress Report for July–September 1979*, NUREG/CR-1197, ORNL/NUREG/TM-370, pp. 52–80.

Table 1. Summary of events for TSE-5A

Event	Time (min.)	Crack depth (a/w)	K_I (MPa $m^{1/2}$)	Temperature (°C)	$(K_I/K_{Ic})_{max}$
Initiation					
1	1.31	0.076	70	−11	
2	1.51	0.138	85	12	
3	2.05	0.199	108	13	
4	3.08	0.316	135	21	
Arrest					
1	1.31	0.138	76	22	
2	1.51	0.199	86	38	
3	2.05	0.316	107	51	
4	3.08	0.535	130	67	
$(K_I/K_{Ic})_{max}$	~14	0.535	110	−46	2.3
Removal from LN_2	30				

THERMAL SHOCK MAY RESULT IN PROPAGATION OF INNER-SURFACE FLAWS

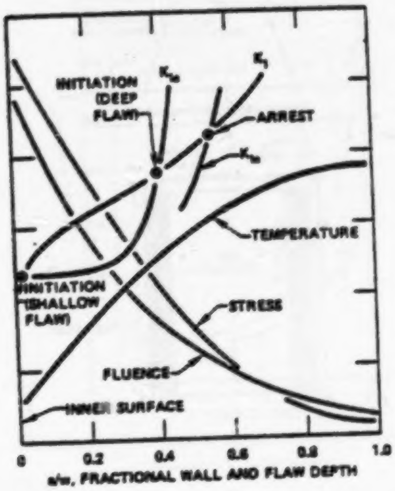

FLAWS WILL PROPAGATE IN SUCCESSIVE STEPS THAT ARE LIMITED BY WARM PRESTRESSING

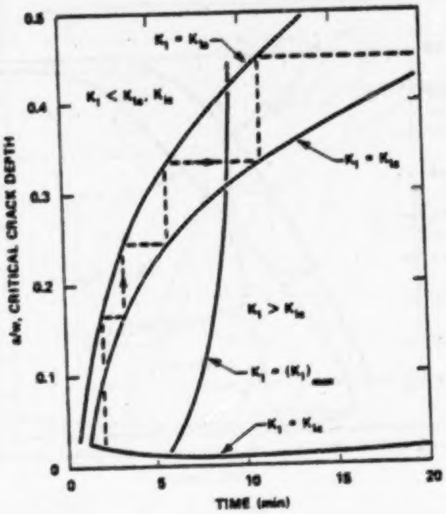

SCOPE OF EXPERIMENTAL PROGRAM DICTATED BY RESULTS OF PWR-LOCA ANALYSIS

- INITIATION AND ARREST OF SHALLOW AND DEEP FLAWS
- SERIES OF INITIATION-ARREST EVENTS
- LONG CRACK JUMPS
- ARREST IN RISING K_I FIELD
- WARM PRESTRESSING

FRACTURE-MECHANICS AND HEAT-TRANSFER CONSIDERATIONS DICTATED CERTAIN TEST CONDITIONS

- THICK-WALL STEEL CYLINDERS (TEST SPECIMENS)
- INNER-SURFACE FLAWS
- THERMAL SHOCK TO INNER SURFACE
- THERMAL SHOCK MORE SEVERE THAN FOR PWR-LOCA

TSE-5 AND TSE-5A DESIGNED FOR DEEP PENETRATION OF LONG AXIAL FLAW WITH SERIES OF EVENTS

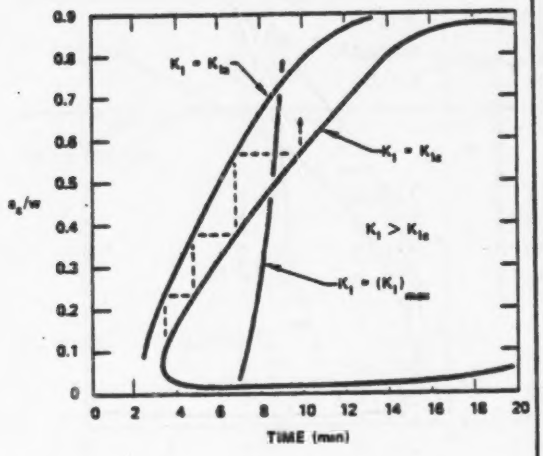

THERMAL SHOCK ACHIEVED BY EFFECTIVELY DUNKING TEST CYLINDER (100°C) IN LN_2 (−196°C)

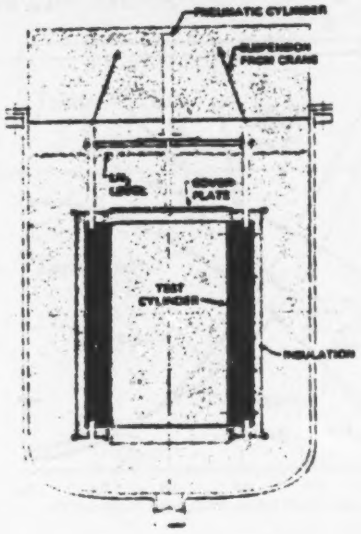

PNEUMATIC CYLINDER
SUSPENSION FROM CRANE
LN_2 LEVEL
COVER PLATE
TEST CYLINDER
INSULATION

ADDITIONAL STUDIES REVEALED LARGE SCATTER IN K_{Ic} (~ ± 50%) AND LOWER-BOUND CRACK BEHAVIOR

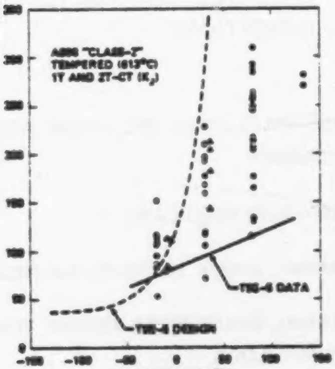

POSTTEST ANALYSIS WITH LOWER-BOUND K_{Ic} INDICATES

- LEFM VALID
- LONG JUMP DUE TO BLUNTED CRACK TIP
- NEGLIGIBLE DYNAMIC EFFECTS

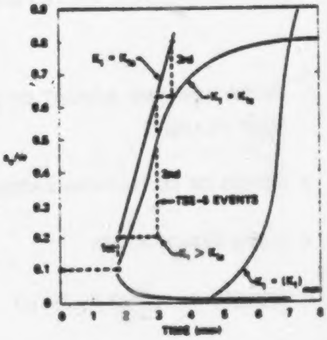

EXTENSIVE MATERIAL-CHARACTERIZATION STUDY CONDUCTED TO DETERMINE LOWER-BOUND K_{Ic} AND K_{Ia} FOR TSE-5A

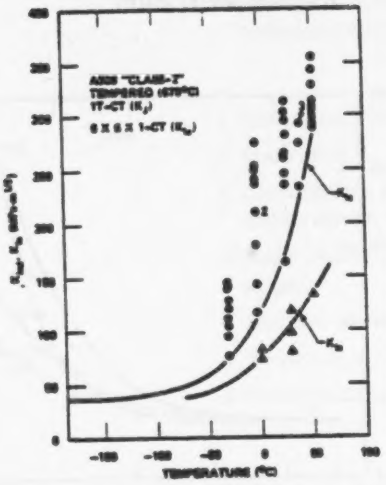

POSTTEST ANALYSIS OF TSE-~~6~~5A INDICATES:

- FOUR INITIATION-ARREST EVENTS
- WARM PRESTRESSING EFFECTIVE

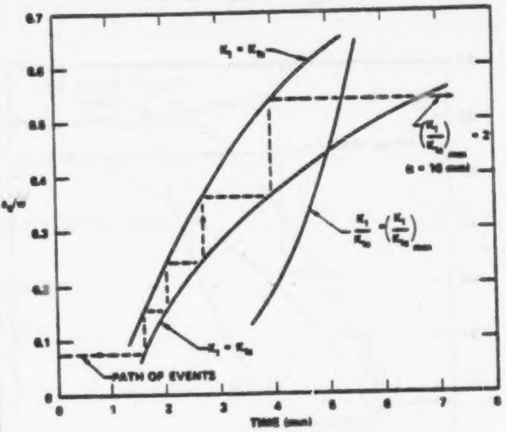

COD GAGES AND UT INSTRUMENTATION USED TO DETECT EVENTS AND DETERMINE CRACK DEPTH

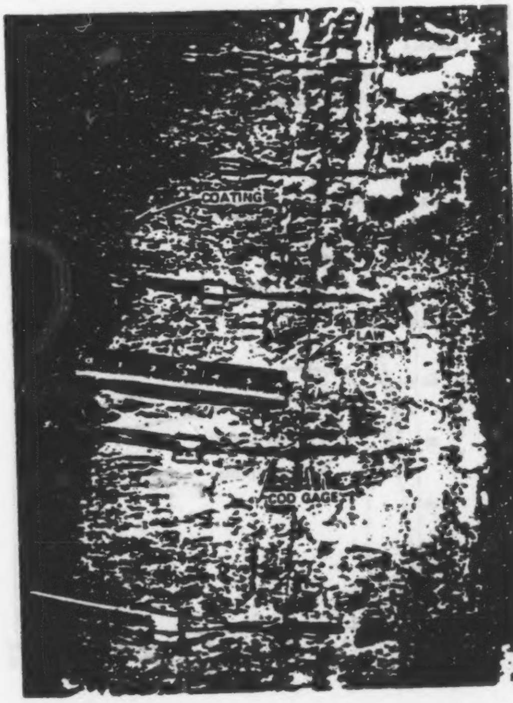

COD AND UT INSTRUMENTATION IDENTIFIED FOUR INITIATION-ARREST EVENTS

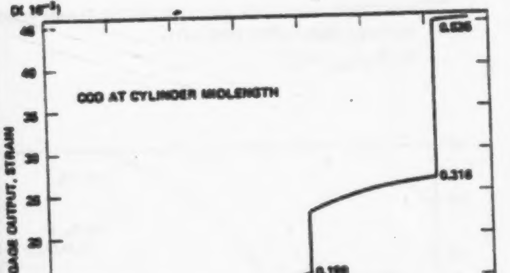

RESULTS OF TSE-5A INDICATE

- K_{Ic} < LAB LOWER BOUND
- K_{Ia} < LAB MEAN

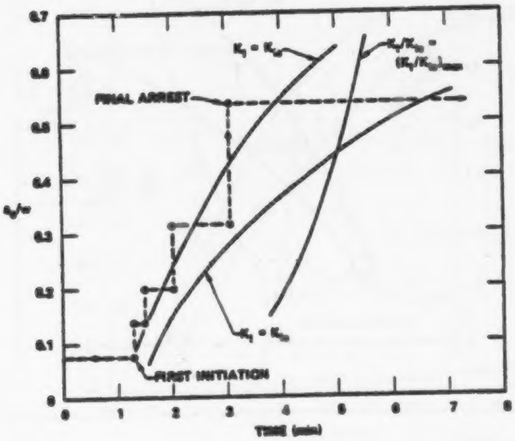

APPARENT DIFFERENCE IN TOUGHNESS ≅ + 22 K (40°F) SHIFT

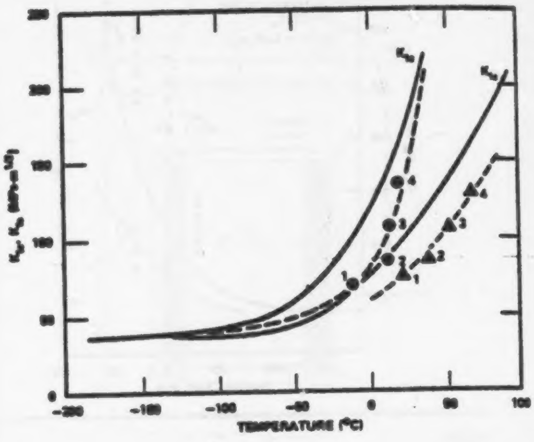

POSTTEST ANALYSIS USING SHIFTED TOUGHNESS CURVES INDICATES WPS WITH $(K_I/K_{Ic})_{max}$ = 2.3

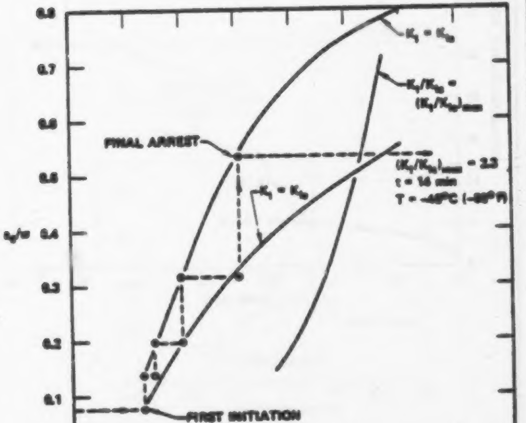

ARREST TOOK PLACE IN A RISING K_I FIELD DURING TSE-5A

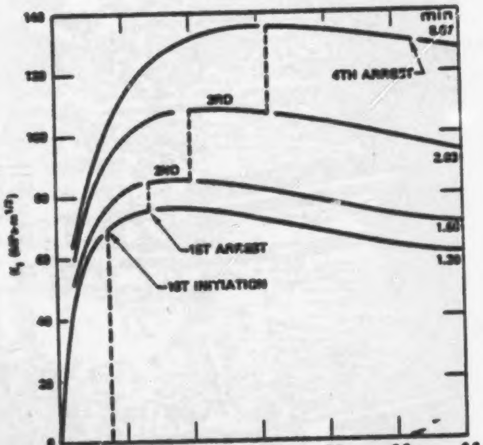

STUDIES ARE REVEALING BEHAVIOR OF SURFACE FLAWS DURING SEVERE THERMAL SHOCK

- LEFM VALID FOR SHALLOW AND DEEP FLAWS
- SCATTER IN K_{Ic} (±50% BASED ON J INTERGRAL)
- LONG CRACKS BEHAVE IN ACCORDANCE WITH LOWER-BOUND K_{Ic}
- SHORT FLAWS EFFECTIVELY BECOME LONG FLAWS
- DYNAMIC EFFECTS NEGLIGIBLE
- ARREST IN RISING K_I FIELD
- WPS EFFECTIVE

CRACK STABILITY ANALYSIS FOR VESSEL TESTS IN THE UPPER SHELF TEMPERATURE RANGE*

J. G. Merkle

Oak Ridge National Laboratory
Oak Ridge, Tennessee 37830

The upper shelf Charpy impact energy of some in-service vessel weldments may eventually decrease to less than the specified minimum value of 50 ft.lbs. due to irradiation. Procedures for determining safety margins based on load and flaw size that have been verified by experiment are needed for these vessels. The NRC Division of Safety Technology has organized a Technical Working Team to develop an approach to this problem, which is known as NRC Safety Issue A-11. The primary source of experimental data for analysis method verification is the series of Intermediate Pressure Vessel Tests conducted by the HSST Program, which is sponsored by the NRC Division of Reactor Safety Research. Methods of elastic-plastic fracture analysis that specifically consider stable crack growth have been used successfully to analyze three of the intermediate test vessels (ITV's) that were tested in the upper shelf temperature range. Analyses are currently being made in preparation for a forthcoming intermediate pressure vessel test (Vessel V-8A) in which a part-through surface crack will be

---

*Paper prepared for presentation at the NRC Eighth Water Reactor Safety Research Information Meeting, Gaithersburg, MD, October 27-31, 1980.

*Research sponsored by Office of Nuclear Reactor Regulation, U.S. Nuclear Regulatory Commission, under Interagency Agreements 40-544-75 and 40-545-75, and Office of Nuclear Regulatory Research under Interagency Agreements 40-551-75 and 40-552-75 with the U.S. Department of Energy under contract W-7405-eng-26 with the Union Carbide Corporation.

By acceptance of this article, the publisher or recipient acknowledges the U.S. Government's right to retain a nonexclusive, royalty-free license in and to any copyright covering the article.

located in a low upper shelf toughness weldment.

J Integral resistance curve data have been obtained by the U.S. Naval Research Laboratory (NRL) under the sponsorship of the Electric Power Research Institute (EPRI), for pressure vessel steels over a wide range of Charpy upper shelf impact energies. These data have facilitated the development of correlations between Charpy and tensile data and resistance curve parameters that form an important part of the analysis methods being used. The resistance curves obtained by NRL were generally nonlinear, suggesting an approximate representation by a simple power law. Consequently, a pair of correlations relating the power law parameters of an R curve to the Charpy upper shelf and tensile values for a pressure vessel steel were developed at ORNL, under the Fracture and Irradiation Effects Program, which is sponsored by the NRC Office of Standards Development. These correlations were used to estimate the resistance curves for the materials of the intermediate test vessels analyzed, because no resistance curves for these materials have yet been obtained experimentally.

The best agreement between analysis and experimental data was obtained by using correlations based on resistance curves obtained from 1T-Compact Specimens with 20 percent side grooving and with data corrections being made for plastic arm rotation and prior crack extension. The ITV analytical results showed that flaw shape variations during stable crack growth can significantly affect the calculated load for flaw instability. They also showed that local plastic instability and flaw instability due to stable crack growth can nearly coincide for fairly large flaws in pressure vessels constructed of high toughness materials.

REFERENCES

1. K. G. Hoge, "Evaluation of the Integrity of SEP Reactor Vessels," NUREG-0569, U.S. Nuclear Regulatory Commission, Washington, D.C., December 1979.

2. D. G. H. Latzko (ed.), "Post-Yield Fracture Mechanics," Applied Science Publishers Ltd., London, 1979.

3. P. C. Paris (ed.), "CSNI Specialists Meeting on Plastic Tearing Instability," NUREG/CP-0010, Proceedings of a meeting held at Washington University, St. Louis, Mo., Sept. 25-27, 1979; report dated January 1980.

4. J. R. Hawthorne (ed.), "The NRL-EPRI Research Program (RP886-2), Evaluation and Prediction of Neutron Embrittlement in Reactor Pressure Vessel Materials, Annual Progress Report for CY 1978," NRL Report 8327, U.S. Naval Research Laboratory, Washington, D.C., August 30, 1979.

5. R. W. Derby et al, "Test of 6-Inch-Thick Pressure Vessels. Series 1: Intermediate Test Vessels, V-1 and V-2," ORNL-4895, Oak Ridge National Laboratory, Oak Ridge, Tenn., February 1974.

6. R. H. Bryan et al, "Test of 6-Inch-Thick Pressure Vessels. Series 2: Intermediate Test Vessles V-3, V-4 and V-6," ORNL-5059, Oak Ridge National Laboratory, Oak Ridge, Tenn., November 1975.

7. J. G. Merkle, G. D. Whitman and R. H. Bryan, "An Evaluation of the HSST Program Intermediate Pressure Veysel Tests in Terms of Light Water-Reactor Pressure Vessel Safety," ORNL-TM-5090, Oak Ridge National Laboratory, Oak Ridge, Tenn., November 1975.

UNION CARBIDE
ORNL

NOTES FOR RSR INFORMATION MEETING

OCTOBER 30, 1980

J. G. MERKLE
OAK RIDGE NATIONAL LABORATORY

A. SUBJECT:

CRACK STABILITY ANALYSIS FOR VESSEL TESTS IN THE UPPER SHELF TEMPERATURE RANGE

B. SAFETY ISSUE:

THE UPPER SHELF CHARPY IMPACT ENERGY OF SOME IN-SERVICE VESSEL WELDMENTS MAY EVENTUALLY DECREASE TO LESS THAN THE SPECIFIED MINIMUM VALUE OF 50 ft-lb DUE TO IRRADIATION. VERIFIED PROCEDURES FOR DETERMINING SAFETY MARGINS BASED ON LOAD AND FLAW SIZE ARE NEEDED FOR THESE VESSELS

C. RESULTS:

1. THE NRC HAS FORMED A TECHNICAL TEAM TO RESOLVE THIS PROBLEM, WHICH IS KNOWN AS NRC SAFETY ISSUE A-11
2. HSST PROGRAM ITV TEST DATA AND ANALYSIS METHODS ARE BEING APPLIED TO THE PROGRAM
3. ANALYSES CONSIDERING STABLE CRACK GROWTH THAT AGREE WITH EXPERIMENTAL DATA HAVE BEEN MADE FOR THREE INTERMEDIATE TEST VESSELS
4. ANALYSES ARE CURRENTLY BEING MADE FOR A LOW SHELF ITV TEST SCHEDULED FOR FY 1982

D. PROBLEM ILLUSTRATION

1. REGULATORY REQUIREMENTS

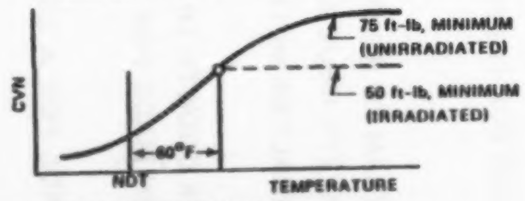

2. EXAMPLE CALCULATIONS

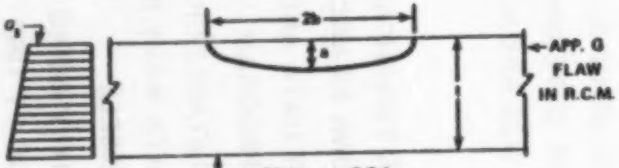

r_i = 98 in.; t = 8.5 in.;

$a = \frac{t}{4} = 2.125$ in.; $2b = 6a = 12.75$ in.;

$K_I = C\sigma_s\sqrt{\pi a}$

$K_I = C\left(\frac{\sigma_s}{p}\right)p\sqrt{\pi a}$

C = 1.081 (APP. G, SECT. III)

$\frac{\sigma_s}{p} = 9.641$

$K_I = 26.93\ p$

$p_f = \frac{K_{Ic}}{26.93}$

p_f IN ksi; K_{Ic} IN ksi$\sqrt{\text{in.}}$

LET

$$p_{all} = \frac{1}{2}p_f$$

THEN $\boxed{p_{all} = \frac{K_{Ic}}{53.86}}$

LET

$$\left(\frac{K_{Ic}}{\sigma_Y}\right)^2 = 5\left[\frac{CVN}{\sigma_Y} - 0.05\right]$$

ROLFE–NOVAK UPPER SHELF CORRELATION

VALUES OF K_{Ic} AND ALLOWABLE PRESSURE

CVN (ft-lb) → σ_Y (ksi) ↓	40	50	
50	K_{Ic} = 97 ksi$\sqrt{\text{in.}}$ p_{all} = 1800 psi	K_{Ic} = 109 ksi$\sqrt{\text{in.}}$ p_{all} = 2020 psi	p_d = 2515 psi
85	K_{Ic} = 123 ksi$\sqrt{\text{in.}}$ p_{all} = 2290 psi	K_{Ic} = 139 ksi$\sqrt{\text{in.}}$ p_{all} = 2590 psi	p_o = 2250 psi

3. DISCUSSION

(a) $\Delta\sigma_Y$ DUE TO IRRADIATION HAS TO BE CONSIDERED TO SATISFY CRITERIA OF APP. G, SECT. III

(b) NOT YET POSSIBLE TO REDUCE CVN_{min} TO 40 ft-lb

(c) ABILITY TO MEET CRITERIA FOR THERMAL SHOCK AND STEAM BREAK ON THIS BASIS IS DOUBTFUL,

(d) NEED TO RECOGNIZE INCREASE IN TOUGHNESS DUE TO STABLE CRACK GROWTH;

E. DEFINITION OF THE UPPER SHELF

1. MATERIAL BEHAVIOR (STRAIN RATE EFFECTS)

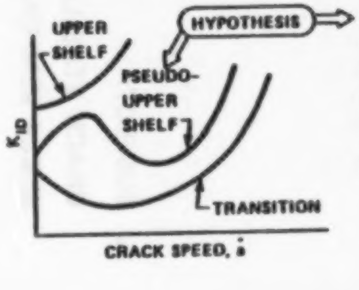

NOTE: IN THE PSEUDO-UPPER SHELF TEMPERATURE RANGE, CONVERSION TO CLEAVAGE IS POSSIBLE DUE TO CRACK ACCELERATION CAUSED BY PLASTIC OR TEARING INSTABILITY

2. IMPACT TEST CRITERIA
   - (a) 100 % SHEAR
   - (b) CVN_{max}
   - (c) NO "POPIN" LOAD DROPS (INSTRUMENTED TEST)

F. RESISTANCE CURVE MEASUREMENTS

1. SPECIMEN REQUIREMENTS
   - (a) SIZE: $B > 1$ in.
   - (b) SIDE GROOVING: 20%
2. ANALYSIS CORRECTIONS
   - (a) Δa CORRECTION TO J (SEE OCTOBER 1979 E24.08.04 DRAFT OF J_{Ic} TEST PROCEDURE)

$$J_o = \frac{\eta A}{B\,b_o}\ ;\ \eta = \frac{2(1+\alpha)}{(1+\alpha^2)}\ ;$$

$$J = J_o\left[1 - \frac{\left(\frac{3}{4}\eta - 1\right)}{b_o}\,\Delta a\right]$$

   - (b) ARM ROTATION CORRECTION TO UNLOADING COMPLIANCE (SEE NRL REPORT 8327, AUGUST 30, 1979)

$$\delta = 2V$$

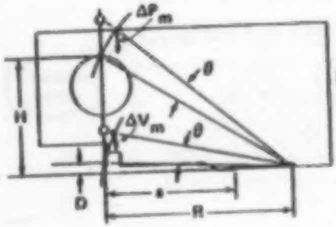

$$\left(\frac{\Delta\delta}{\Delta P}\right)_c = \frac{\left(\frac{\Delta\delta}{\Delta P}\right)_m}{\left(\cos\theta - \frac{D}{R}\sin\theta\right)\left(\cos\theta - \frac{H}{R}\sin\theta\right)}$$

ADJUSTS $\Delta\delta$ AND ΔP FOR THE FACT THAT THE INITIAL GEOMETRY IS DEFORMED DUE TO PRIOR YIELDING;

G. RESISTANCE CURVE DATA FOR HIGH AND LOW SHELF MATERIALS (NRL AND HEDL)

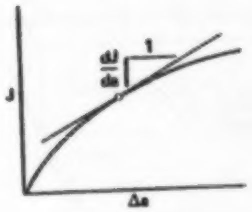

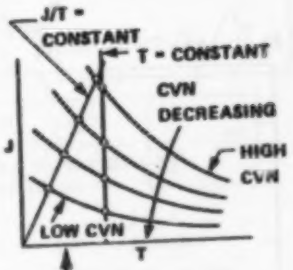

NOTE THAT THE Δa VALUES ARE NOT INCLUDED IN THE J VS T DIAGRAM

1. DEFINITION (PARIS):

$$T = \underbrace{\frac{dJ}{da}\cdot\frac{E}{\sigma_o^2}}_{\text{NONDIMENSIONAL}}$$

2. THE R CURVE IS GENERALLY NONLINEAR
3. THERE MAY BE NO PHYSICALLY DISTINCT J_{Ic}
4. A POWER LAW FIT APPEARS REASONABLE

$$J = J_1(\Delta a)^n$$

H. CORRELATIONS

1. J VS CVN AT J/T = 50
2. J VS CVN AT T = 20 } (PARIS)
3. POWER LAW PARAMETERS VS CVN AND σ_o

$$J = (1000)\,c\left(\frac{\Delta a}{1.0}\right)^n$$

c AND n ARE DIMENSIONLESS

UNION CARBIDE ORNL

CORRELATION OF c AND CVN USING NRL CORRECTED DATA

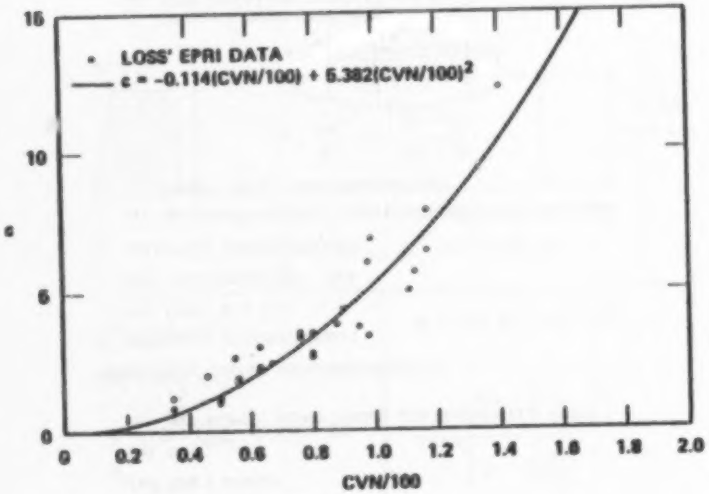

UNION CARBIDE ORNL

CORRELATION OF c, n AND f_s USING NRL CORRECTED DATA

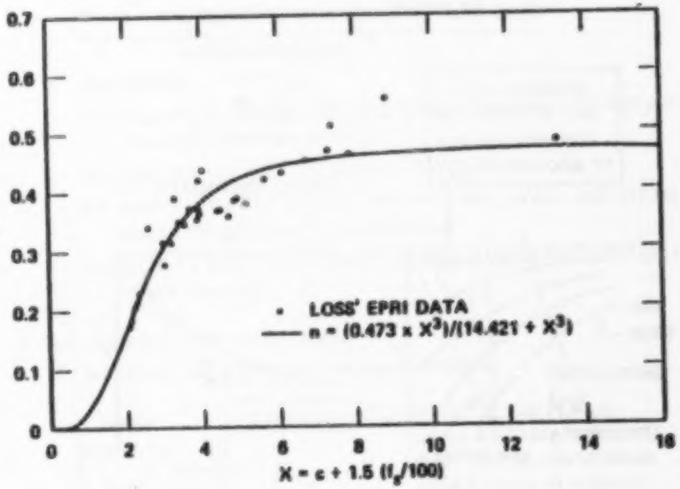

I. HSST PROGRAM INTERMEDIATE VESSEL CALCULATIONS

1. VESSELS ANALYZED

VESSEL NO.	TEMPERATURE (°F)	FLAW SIZE (in.)	MATERIAL TESTED	CVN (ft-lb)
1	130	2.58	A508-2	90
3	130	2.11	WELD	125
6	190	1.87	WELD	125

2. FLAW GEOMETRY ASSUMED FOR ANALYSIS

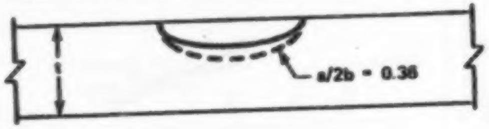

3. STABLE CRACK GROWTH

(a) CORRELATION

CVN AND σ_o ⟹ c AND n

(b) POWER LAW R-CURVE APPROXIMATION

$$J = (1000)\,c\left(\frac{\Delta a}{1.0}\right)^n$$

4. LOCAL PLASTIC INSTABILITY

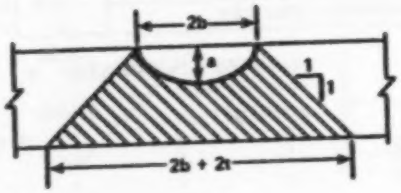

$$A_c = \frac{\pi ab}{2}$$

$$A = (2b + t)t$$

$$p_f = \frac{\sigma_o^*\left(1 - \frac{A_c}{A}\right)}{\left(\frac{r_i}{t}\right)}$$

J. SOLUTION PROCEDURE

1. ANALYTICAL BASIS

$$\boxed{J = \frac{K_T^2}{E_T} = \frac{K_\infty^2}{E}} \longrightarrow \boxed{K_\sigma K_\epsilon = K_t^2} \longrightarrow \boxed{d\epsilon\sqrt{\rho} = 2C\sqrt{a}\sqrt{\frac{E_g}{E_s}}\,d\lambda}$$

$$\boxed{\int d\epsilon\sqrt{\rho} = \epsilon_1\sqrt{\rho} = \left(\frac{2}{\sqrt{\pi}}\sqrt{\frac{E}{E_s}}\,\lambda_Y\right)\frac{K_c}{S_Y}} \quad ; \quad \boxed{K_c = \sqrt{EJ}}$$

2. STEPS

(a) ASSUME Δa; THEN CALCULATE a, a/2b AND J

(b) ESTIMATE THE TANGENT MODULUS, E_g, IN THE TRANSITION RANGE OF STRAIN (~0.24 TO 1.2%)

(c) SOLVE THE FLAW SIZE-STRAIN-TOUGHNESS RELATION FOR THE STRAIN CORRESPONDING TO THE CALCULATED VALUE OF J BASED ON Δa

(d) DETERMINE p FROM THE PRESSURE-STRAIN CURVE

(e) CALCULATE THE PRESSURE FOR LOCAL PLASTIC INSTABILITY FOR THE SAME CRACK SIZE

3. GRAPHICAL PRESENTATION

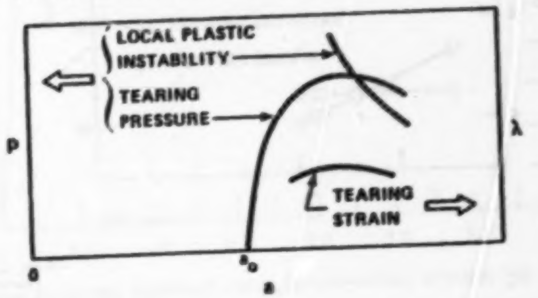

4. PREVIOUS ITV RESULTS

VESSEL	FAILURE CONDITIONS					
	ACTUAL		CALCULATED			
	p (ksi)	λ (%)	p (ksi)	λ (%)	J_i (in.-lb/in.^{2})	Δa (in.)
1	26.8	0.92	27.6	0.62	3409	0.60
3	31.0	1.47	30.2	1.61	7790	0.88
6	31.9	2.00	32.2	2.29	6717	0.64

(a) ITV-6

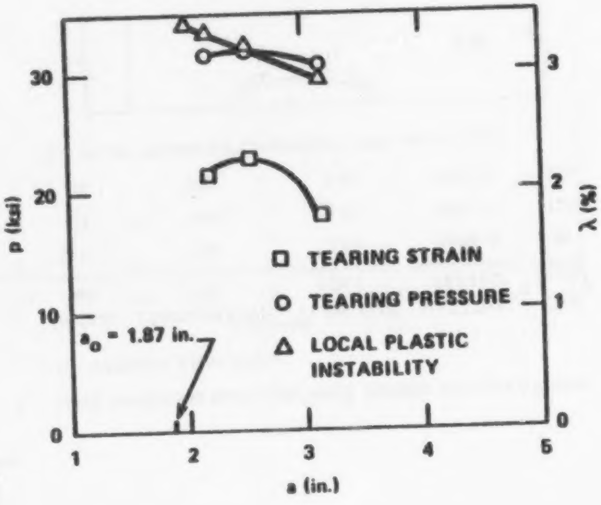

(b) ITV-1

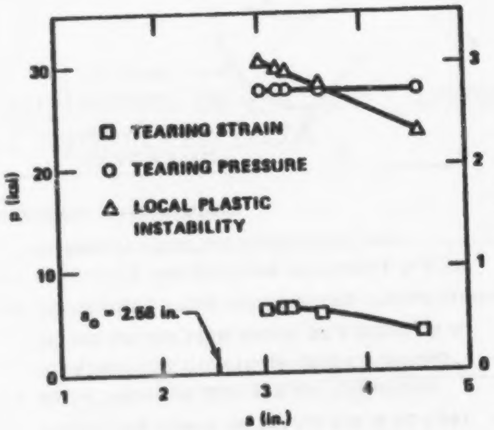

(c) ITV-3

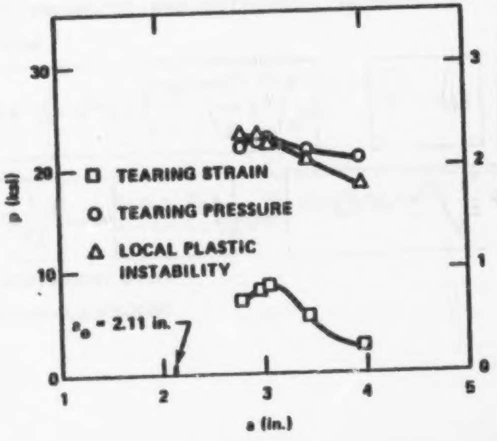

5. LOW-SHELF ITV ESTIMATE (V-8A)

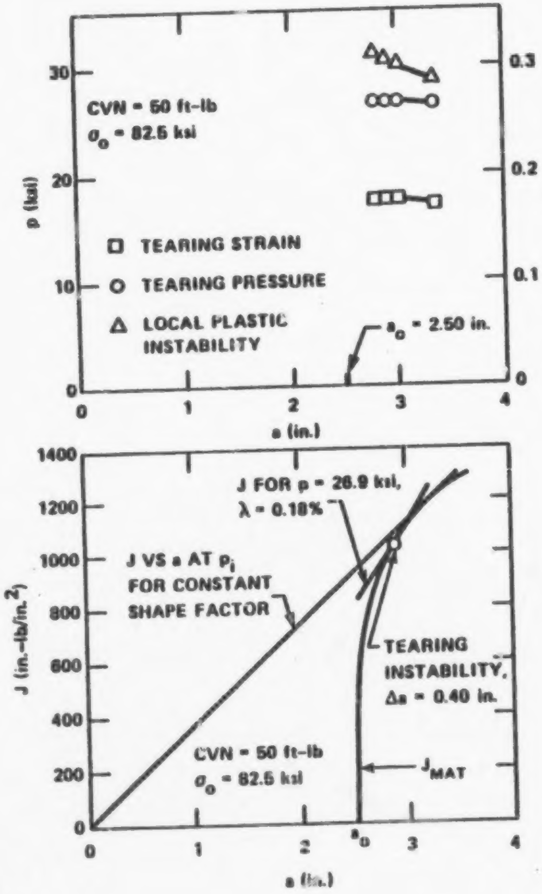

CALCULATED OUTSIDE SURFACE CIRCUMFERENTIAL PRESSURE-STRAIN CURVE FOR INTERMEDIATE TEST VESSELS

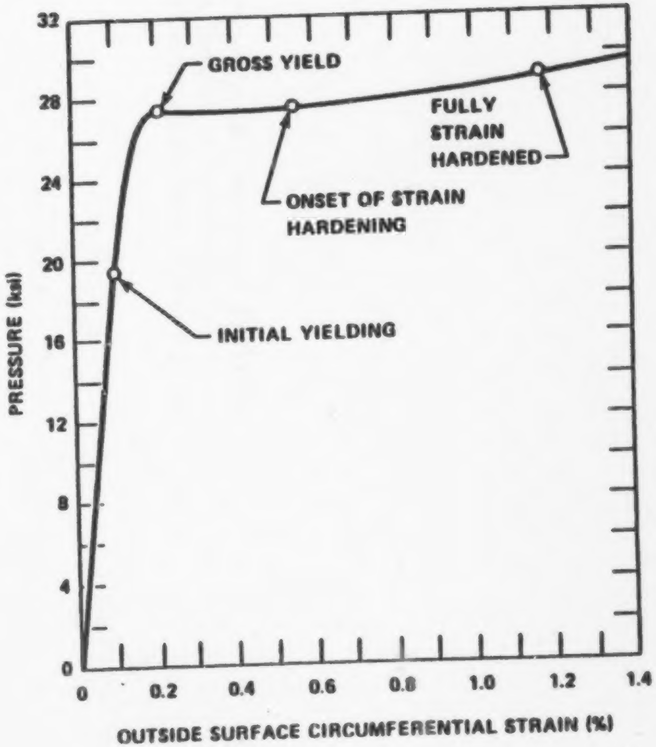

Application of Key Curve Analysis to Dynamic Elastic-Plastic Fracture Toughness Testing

by

Dr. J. A. Joyce

U. S. Naval Academy
Annapolis, Md. 21402

Application of Key Curve Analysis
to Dynamic Elastic-Plastic Fracture Toughness Testing

by

Dr. James A. Joyce

U. S. Naval Academy
Annapolis, Maryland 21402

Abstract

It has become quite common over the past few years to characterize the toughness of an elastic plastic material through the use of the J_{Ic} fracture parameter and the J_I-R curve. A test procedure for J_{Ic} is presently approaching a consensus standard of the American Society for Testing and Materials and a recommended procedure is in the draft stage for J-R curve testing. The methods used to date are, however, not readily adapted to rapid loading, though this type of loading would be expected in operating components.

This project has been directed toward the development of test procedures for the evaluation of J_{Ic} values and J-R curves at high loading rates. The basic method used here was first recommended by Ernst et.al[1] and called the "Key Curve Method" or "Calibration Function Method." It involves the experimental evaluation of a Key Curve Function which describes the behavior of a particular specimen geometry under load if no crack extension were to occur.

This type of function can be evaluated from small scale or blunt notched specimens of the identical material as shown by Joyce et.al[2] and Joyce[3]. Load displacement curves of larger specimens which do exhibit crack extension can be compared with the Key Curve Function and J and crack extension can be evaluated using the analysis of Ernst et.al[1]. All corrections for specimen rotation and crack extension are included in this J-R curve and do not have to be added to the result as is common for unloading compliance methods. More important is the fact that J-R curves can be obtained at any rate at which a good load-displacement record can be obtained for the specimen - which can be done today at loading rates in excess of 100 in/sec.

The major result of this work to date has been to show that the Key Curve Method does work for A533B HSST-02 steel compact tensile specimens at 300°F loaded statically and at load point rates in excess of 10 inches/second. The material was found to demonstrate an increased J_{Ic} toughness parameter in the high rate tests but similar tearing resistance.

References

1. Ernst, Hugo, Paris, P. C., Rossow, Mark, and Hutchinson, J. W., "Analysis of Load-Displacement Relationships to Determine J-R Curve and Tearing Instability Material Properties," Fracture Mechanics, ASTM STP 677, C. W. Smith, Ed., American Society for Testing and Materials, 1979, pp. 581-599.

2. Joyce, J. A., Ernst, Hugo, and Paris, P. C., "Direct Evaluation of J-Resistance Curves from Load Displacement Records," Fracture Mechanics: Twelfth Conference, ASTM STP 700, American Society for Testing and Materials, 1980, pp. 222-236.

3. Joyce, J. A., "Application of the Key Curve Method to Determine J-R Curves for A533B Steel," NUREG/CR-1290, U. S. Nuclear Regulatory Commission, Washington D.C., January 1980.

Objectives

1. Develop a Key Curve Function for A533B steel tested at 5 in/sec loading rates.
2. Utilize the Key Curve Function to develop J-R curves for A533B tested at similar high rates of loading.
3. Compare the J-R curve features with static J-R curves evaluated previously for this steel.
4. Evaluate the effect of loading rate and specimen geometry on the J-R curve of A533B steel.

TABLE 1. Chemical Composition of HSST-02 A533B Steel
Elements in Weight Percent

C	Mn	Ni	Mo	Si	S	P
.22	1.48	0.68	0.52	0.25	0.018	.012

TABLE 2. Tensile Mechanical Properties of
HSST-02 A533B Steel

.2% Yield Strength psi	Ultimate Tensile Strength psi	Total Elongation %
65,000	90,000	19

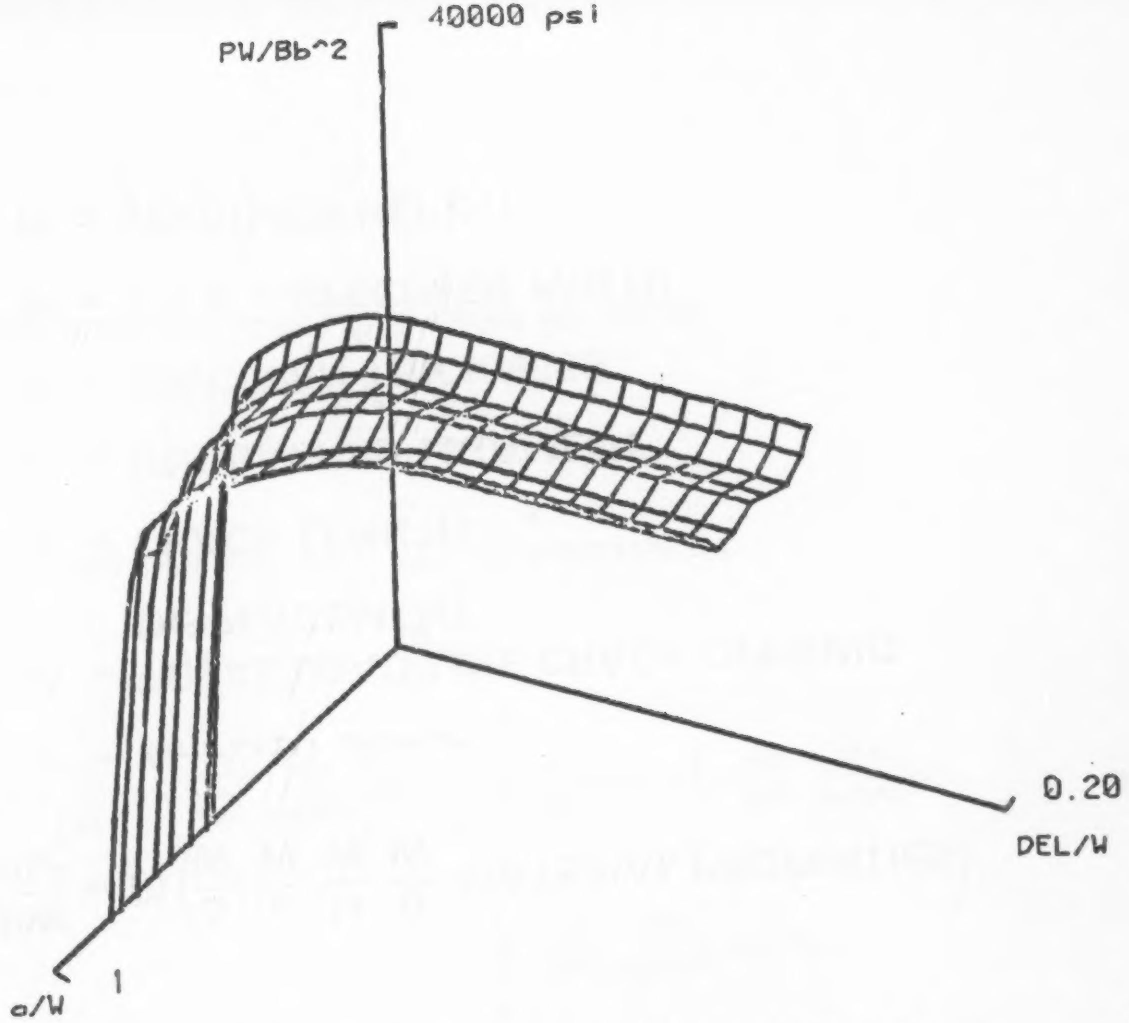

Figure 4. Experimental key curve function for the blunt notched specimens extended at the maximum F1 values of each individual curve.

$$\frac{PW}{Bb^2} = F1\left(\frac{\Delta}{W}, \frac{a}{W}, \frac{H}{W}, \frac{B}{W}, \text{MATERIAL PROPERTIES}\right)$$

WHERE: P = APPLIED LOAD

Δ = TOTAL LOAD LINE CRACK OPENING DISPLACEMENT

a = CRACK LENGTH

b = UNCRACKED LIGAMENT

B = SPECIMEN THICKNESS

$W = a + b$ = SPECIMEN WIDTH

H = SPECIMEN HEIGHT

$$J = \frac{-1}{W}\int_{o}^{\Delta}\left(\frac{\partial P}{\partial (a/W)}\right)_{\Delta} d\Delta$$

AND SUBSTITUTING FOR P FROM EQ. GIVES:

$$J = -\int_{o}^{\Delta}\left(\frac{b^2}{W^2}\,\frac{\partial F1}{\partial (a/W)} - \frac{2b}{W}F1\right) d\Delta.$$

THE DIFFERENTIAL OF J CAN BE WRITTEN AS

$$dJ = \frac{\partial J}{\partial \Delta} d\Delta + \frac{\partial J}{\partial a} da.$$

$$dJ = \left[\frac{2b}{W}F1 - \frac{b^2}{W^2}\,\frac{\partial F1}{\partial (a/W)}\right] d\Delta + \left[-\int_{o}^{\Delta}\frac{2}{W}F1 d\Delta + \int_{o}^{\Delta}\frac{4b}{W^2}\,\frac{\partial F1}{\partial (a/W)} d\Delta - \int_{o}^{\Delta}\frac{b^2}{W^3}\,\frac{\partial F1}{\partial (a/W)^2} d\Delta\right] da,$$

$$dP = \frac{\partial P}{\partial \Delta} d\Delta + \frac{\partial P}{\partial a} da.$$

EVALUATING THE COEFFICIENTS IN TERMS OF F1 GIVES

$$dP = \left[\frac{b^2}{W^2} \frac{\partial F1}{\partial(\Delta/W)}\right] d\Delta \quad \left[\frac{b}{W^2} \frac{\partial F1}{\partial(a/W)} - \frac{2b}{W} F1\right] da.$$

SOLVING FOR da GIVES

$$da = \frac{\dfrac{b^2}{W^2} \dfrac{\partial F1}{\partial(\Delta/W)} d\Delta - dP}{\dfrac{2b}{W} F1 - \dfrac{b^2}{W^2} \dfrac{\partial F1}{\partial\left(\frac{a}{W}\right)}}$$

$$\delta J_n = \left[\frac{2b}{W} F1_n - \frac{b^2}{W} \frac{\partial F1^*}{\partial (a/W)_n}\right] \delta\Delta_n$$

$$+ \left[-\frac{2}{W} \sum_{i=1}^{n} F1_i \, \delta\Delta_i + \frac{4b}{W^2} \sum_{i=1}^{n} \frac{\partial F1^*}{\partial (a/W)_i} \delta\Delta_i\right] \delta a_n$$

$$\delta a_n = \frac{\dfrac{b^2}{W^2} \dfrac{\partial F1^*}{\partial (\Delta/W)_n} \delta\Delta_n - \delta P_n}{\dfrac{2b}{W} F1_n - \dfrac{b^2}{W^2} \dfrac{\partial F1^*}{\partial (a/W)_n}}$$

AT EACH POINT ON THE LOAD DISPLACEMENT RECORD OF A SPECIMEN THE TOTAL J AND Δa ARE:

$$J = \sum_{n=1}^{m} \delta J_n$$

$$\Delta a = \sum_{n=1}^{m} \delta a_n$$

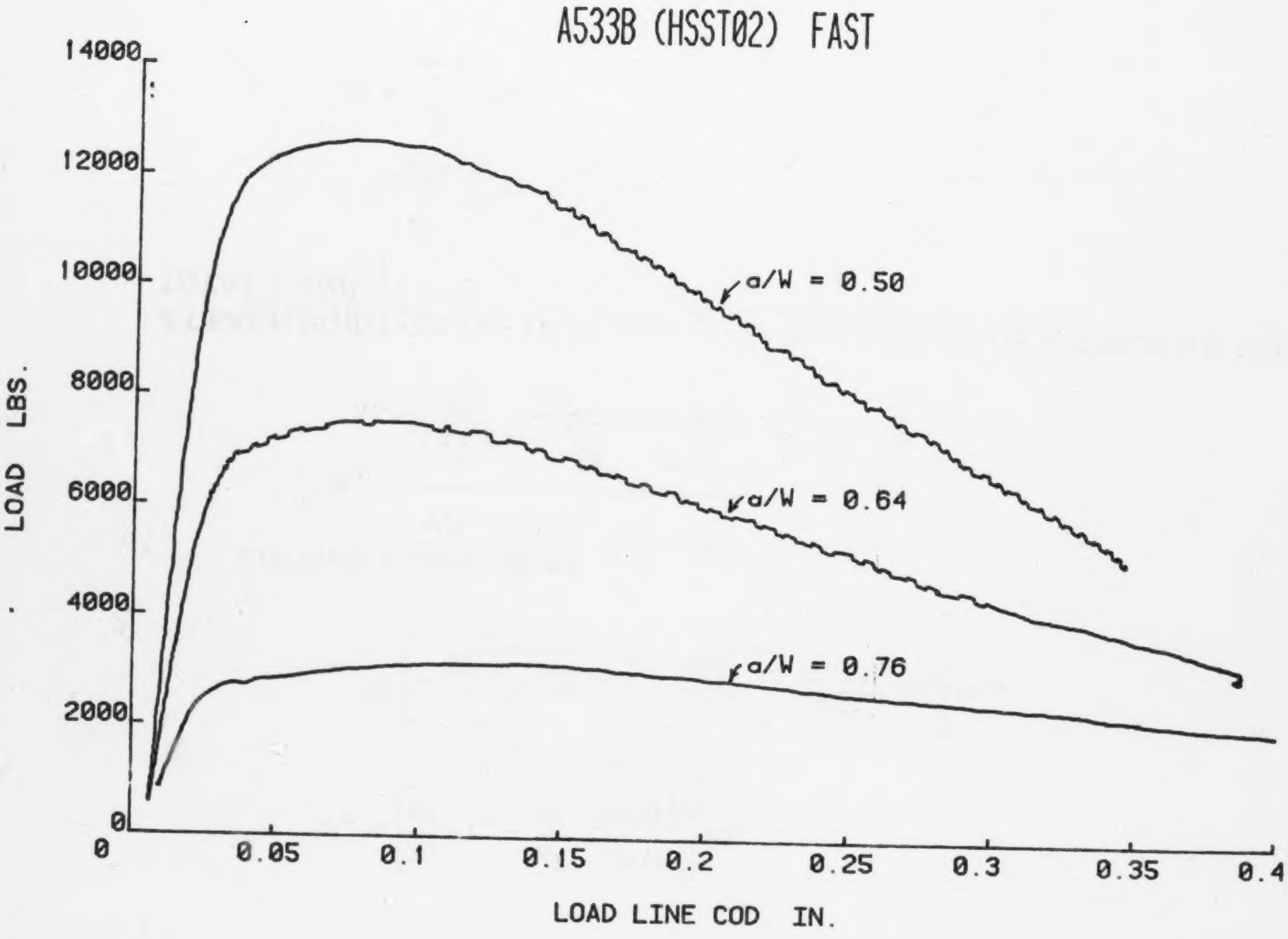

READEX FICHE best copy available

A533B (HSST-02) LOAD VS. COD CURVES

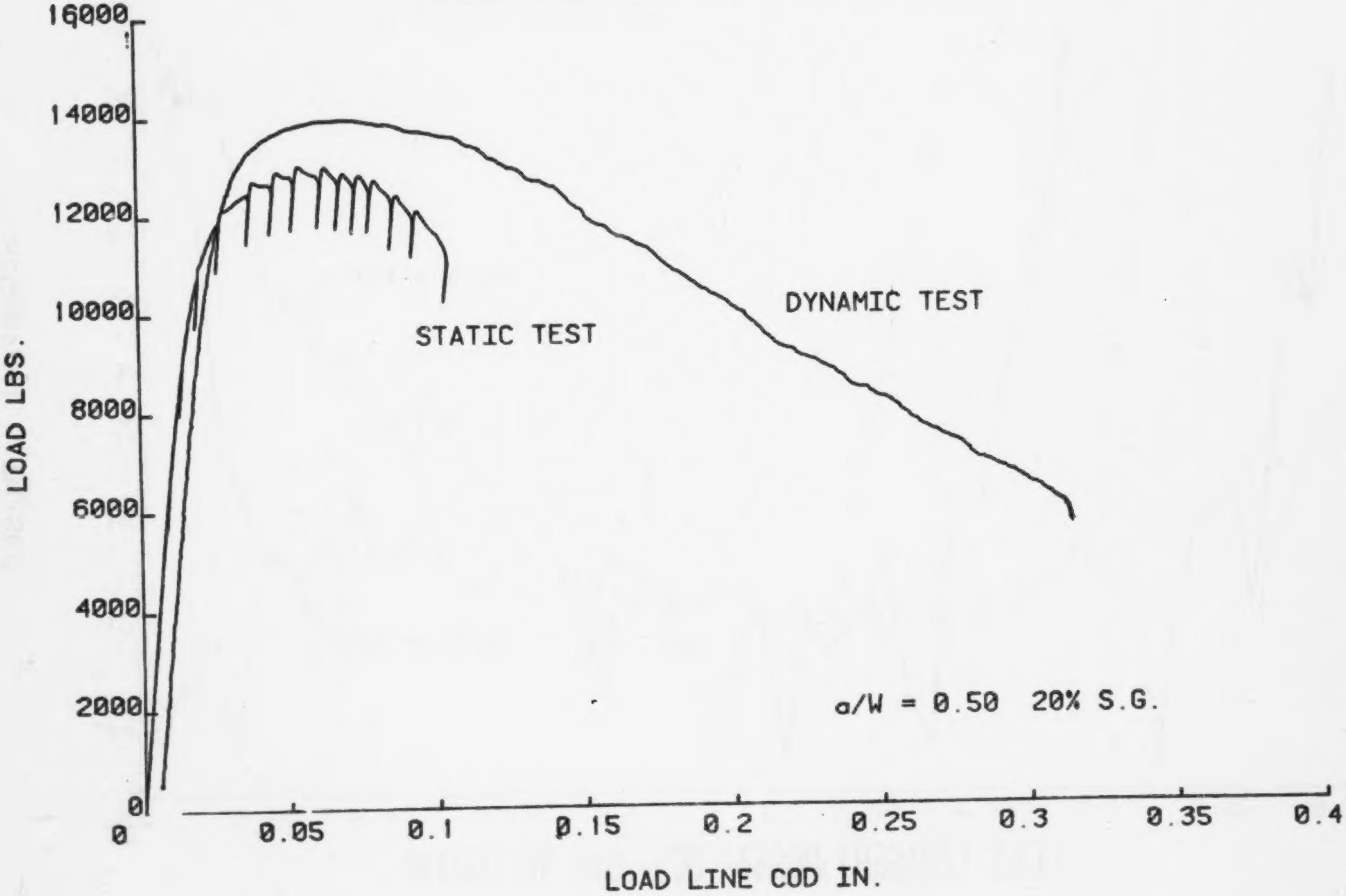

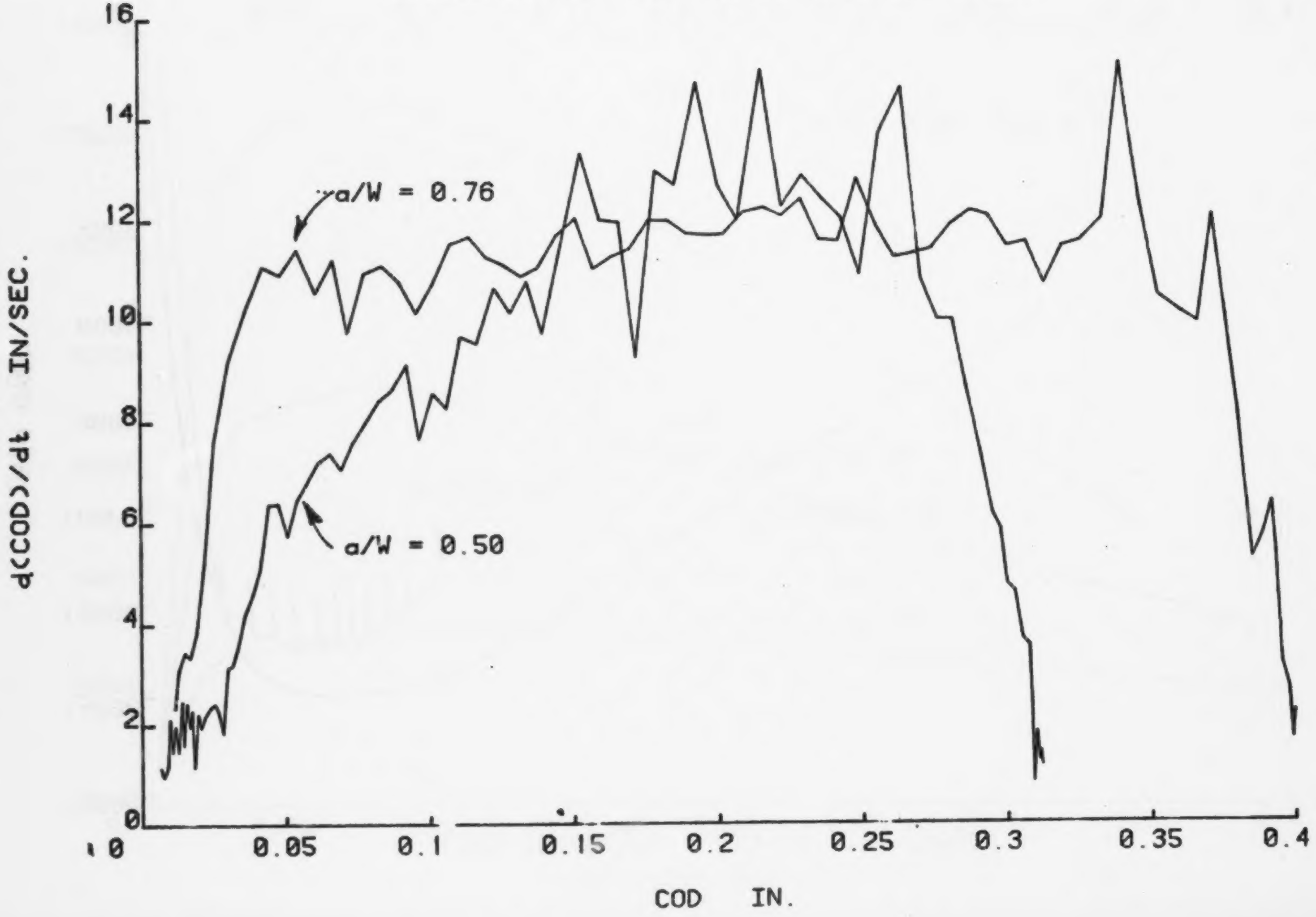

d(COD)/dt VS COD A533B (HST02) STEEL

da/dt VS CRACK EXTENSION A533B (HSST 02) STEEL

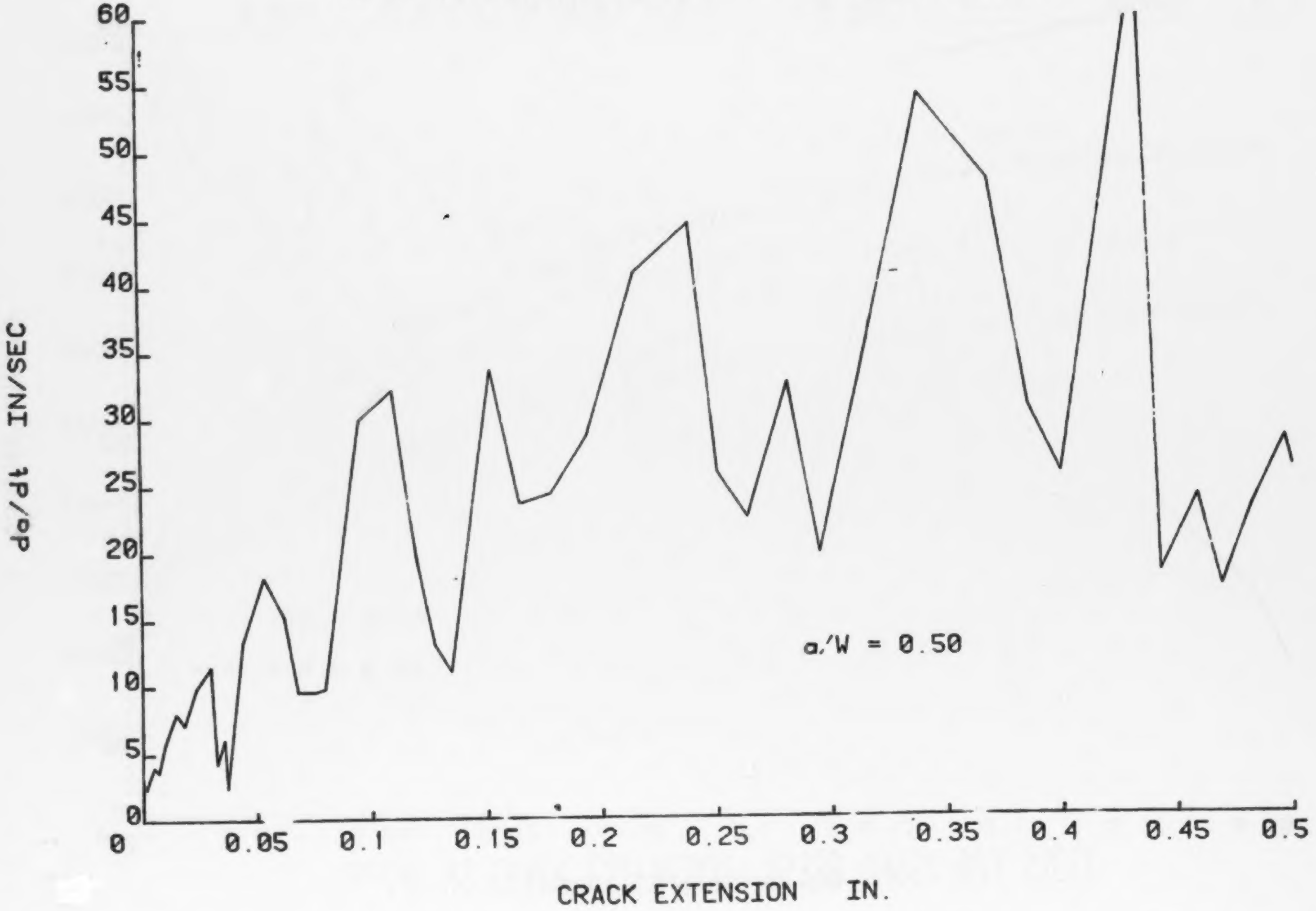

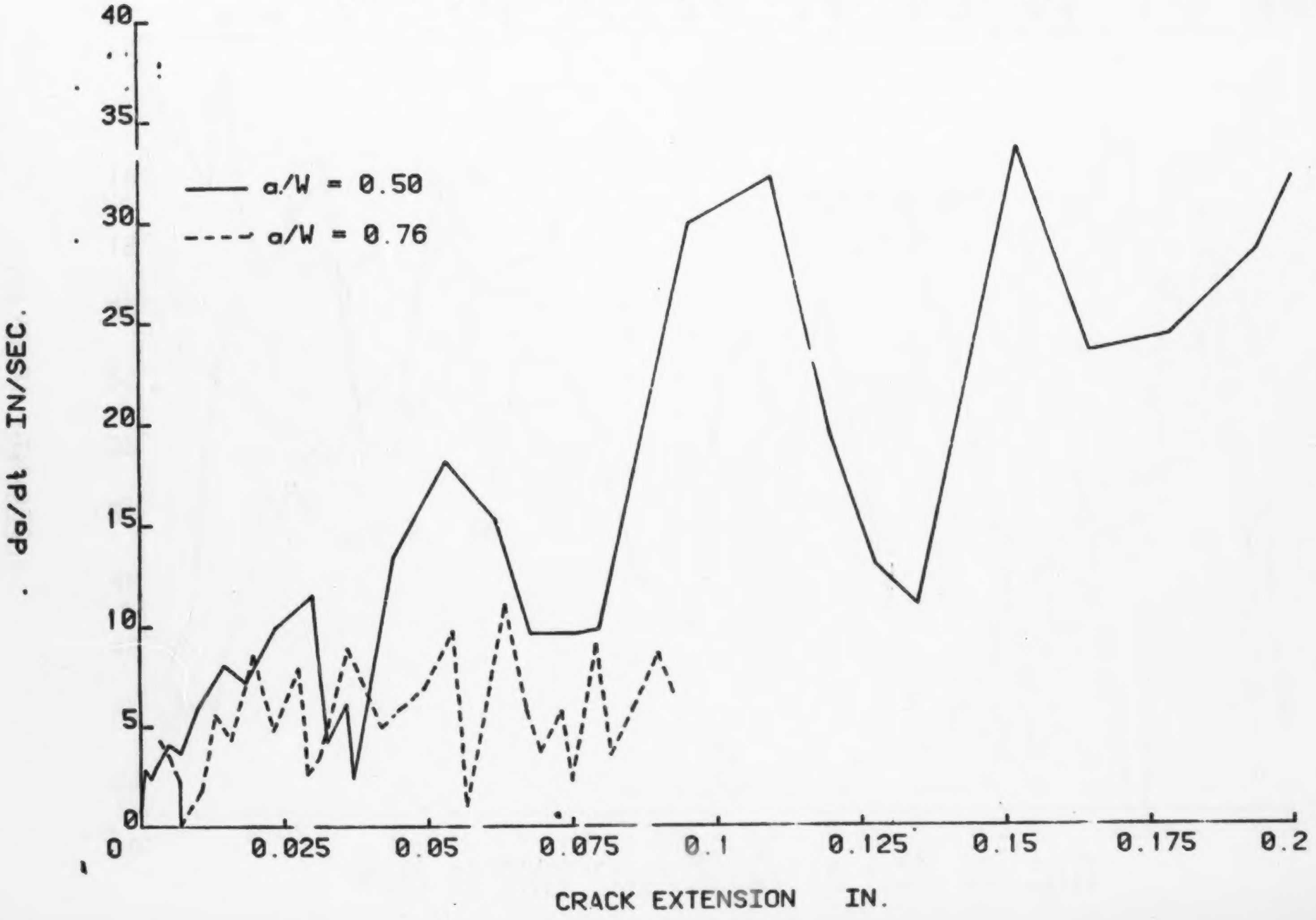

da/dt VS CRACK EXTENSION A533B (HSST 02) STEEL

A533B (HSST-02) FAST J-R CURVES

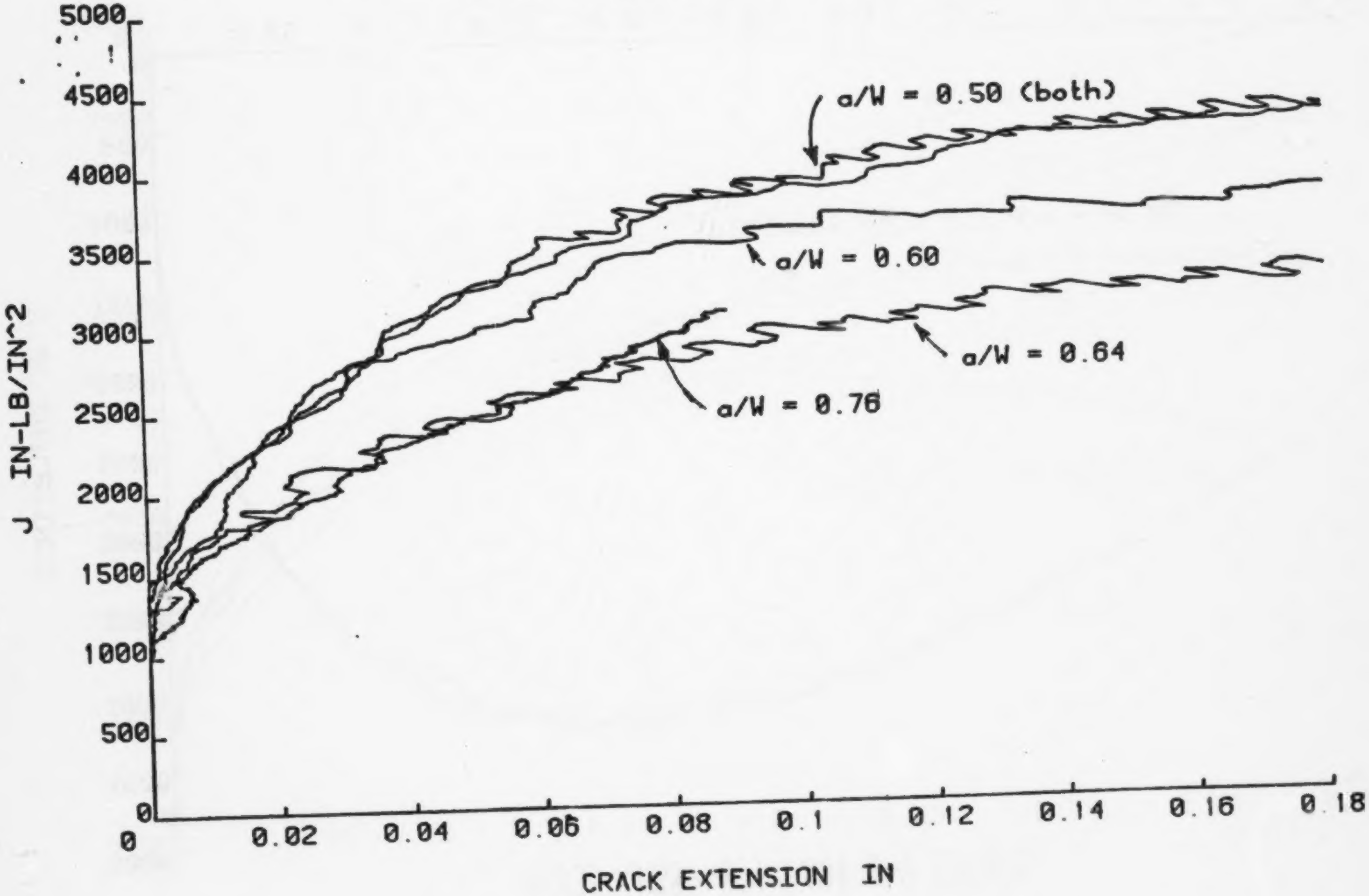

A533B (HSST-02) FAST J-R CURVES

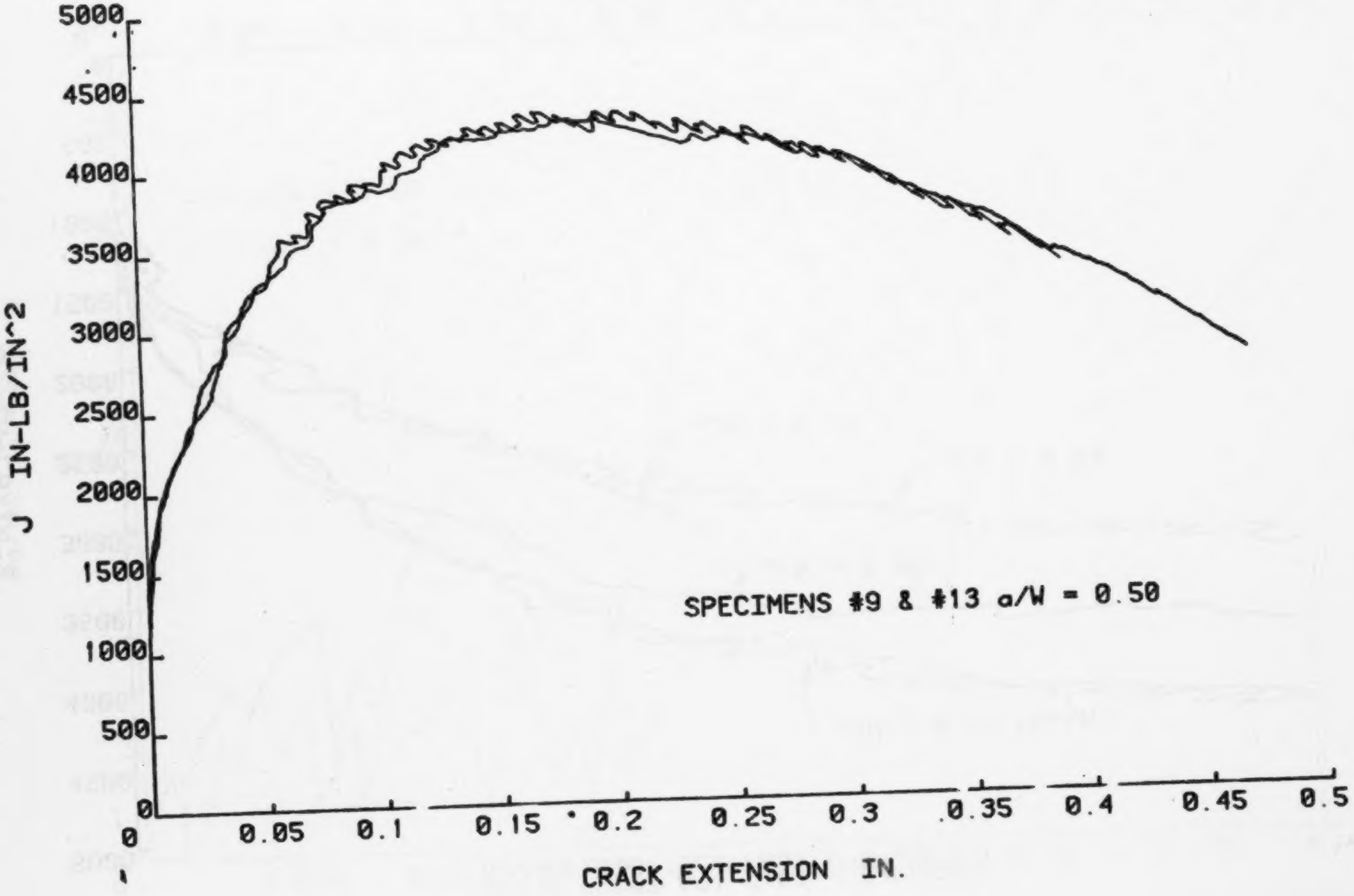

A533B (HSST-02) FAST J-R CURVES

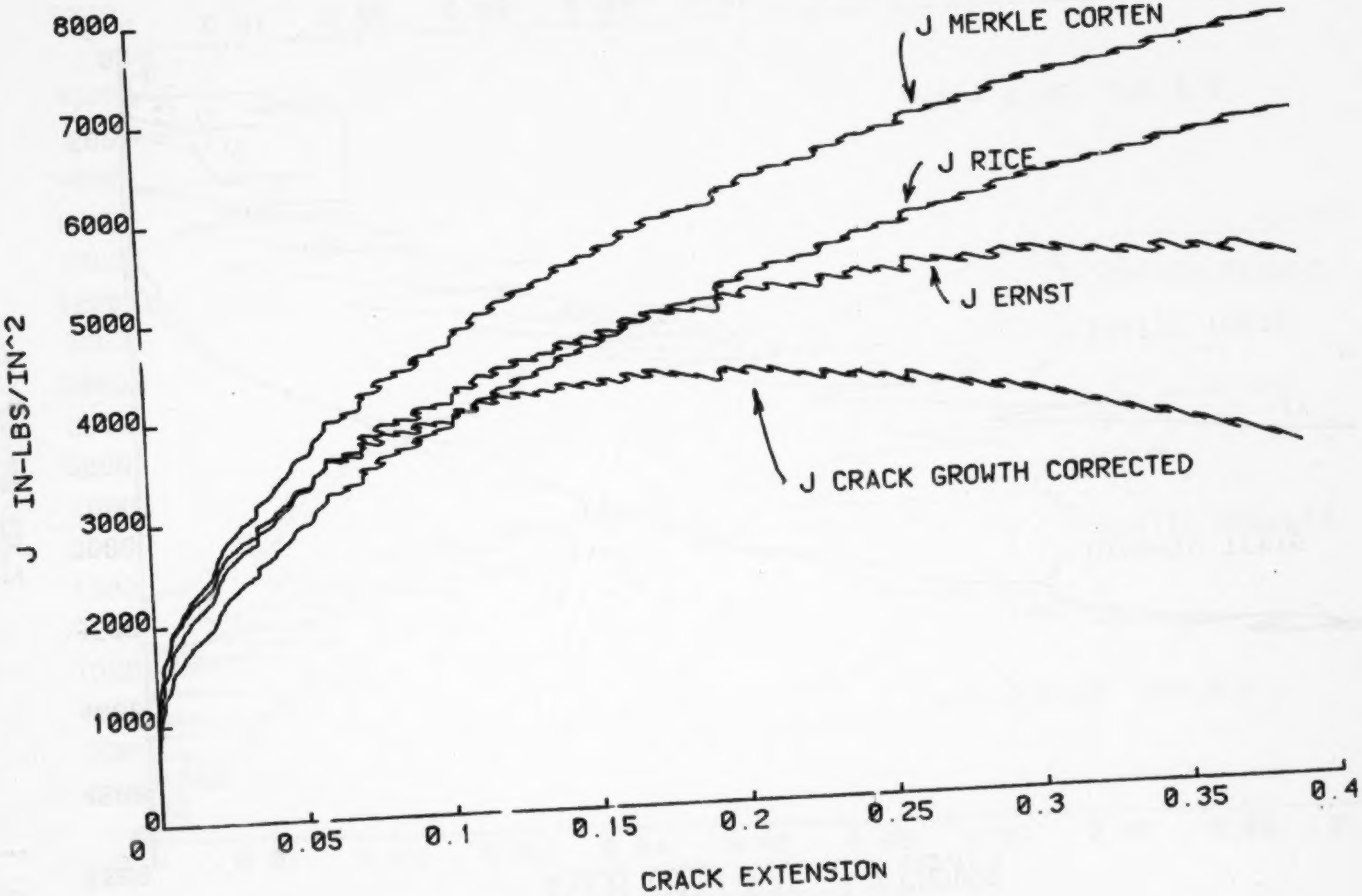

A533B (HSST-02) J-R CURVES

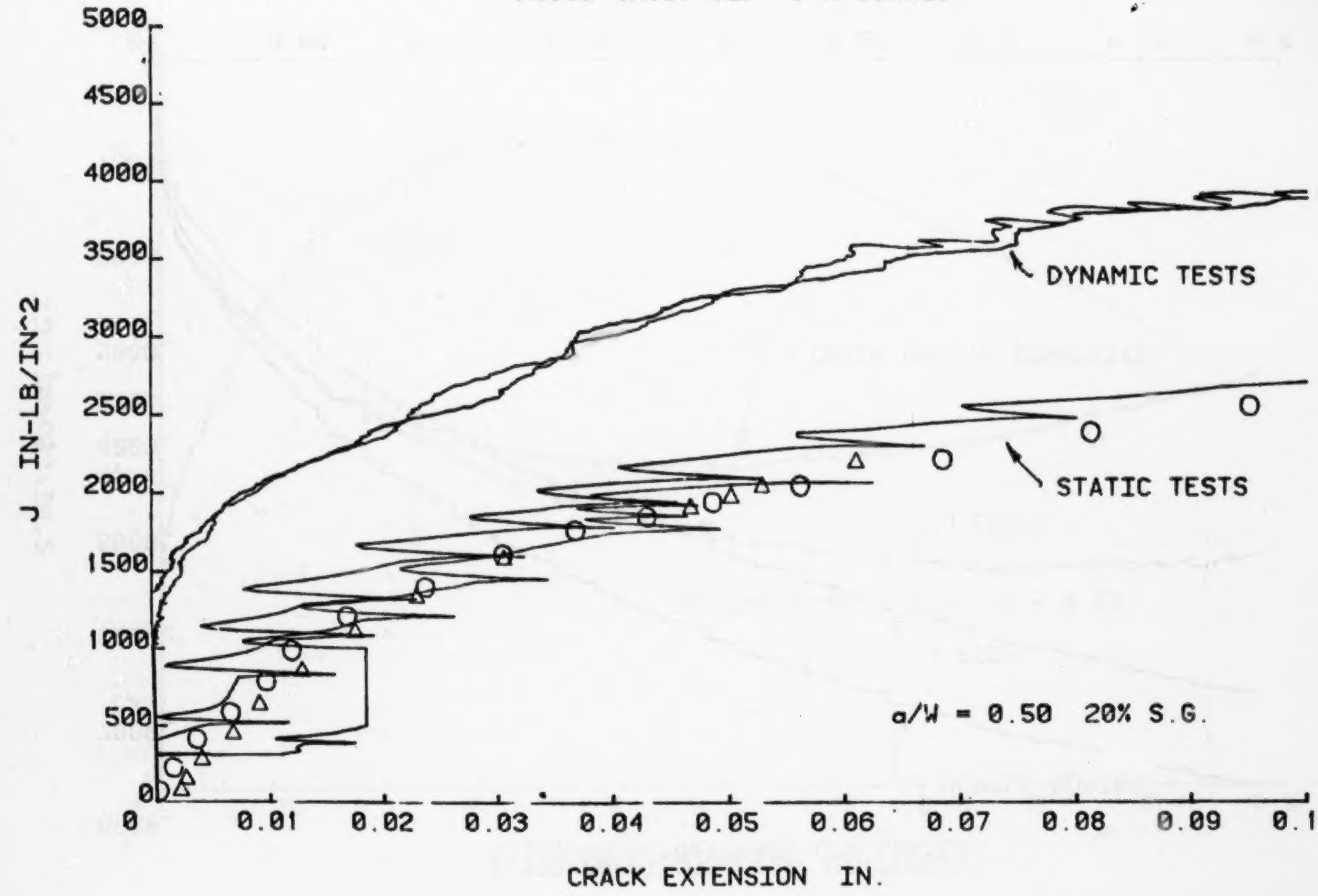

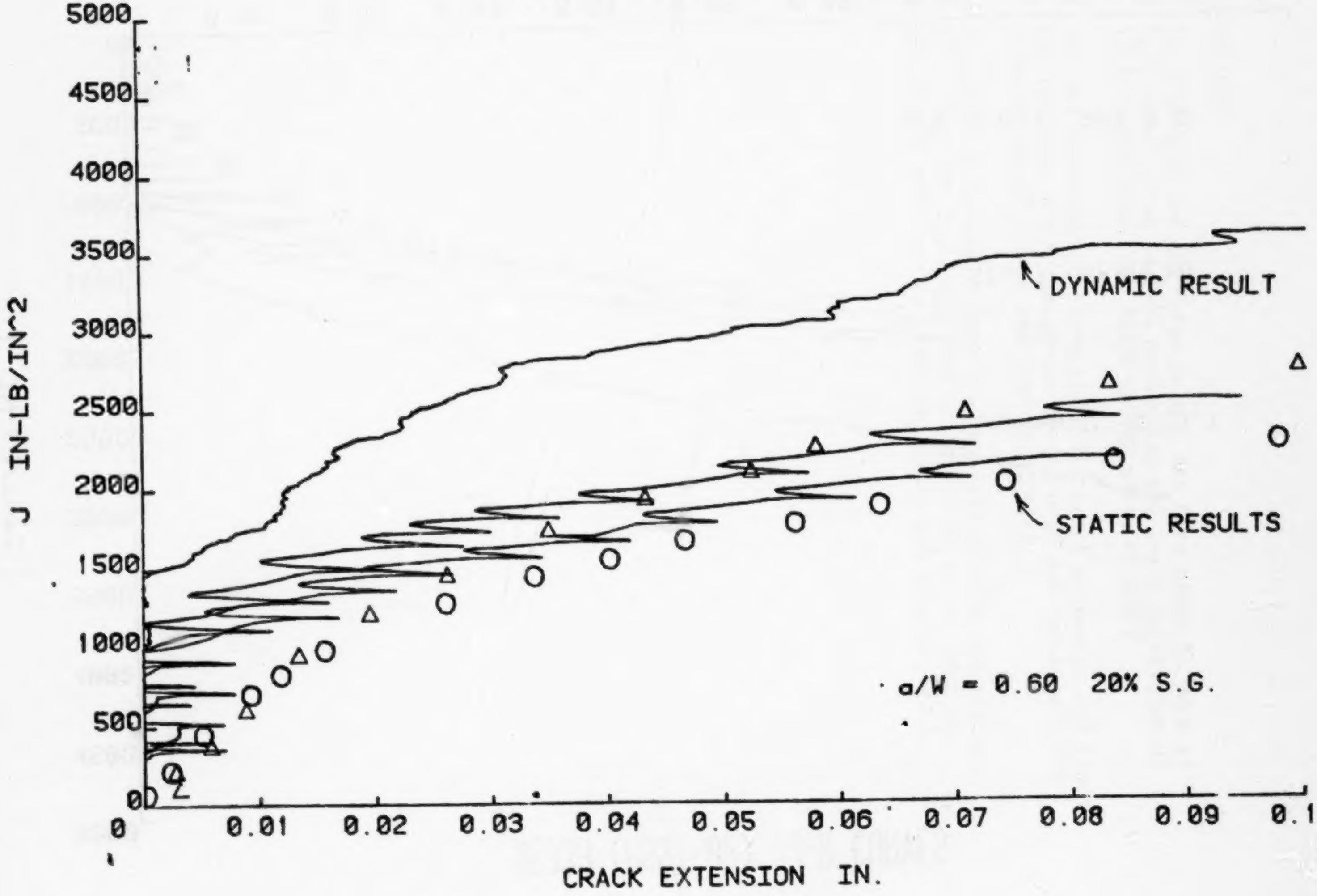
A533B (HSST-02) J-R CURVES

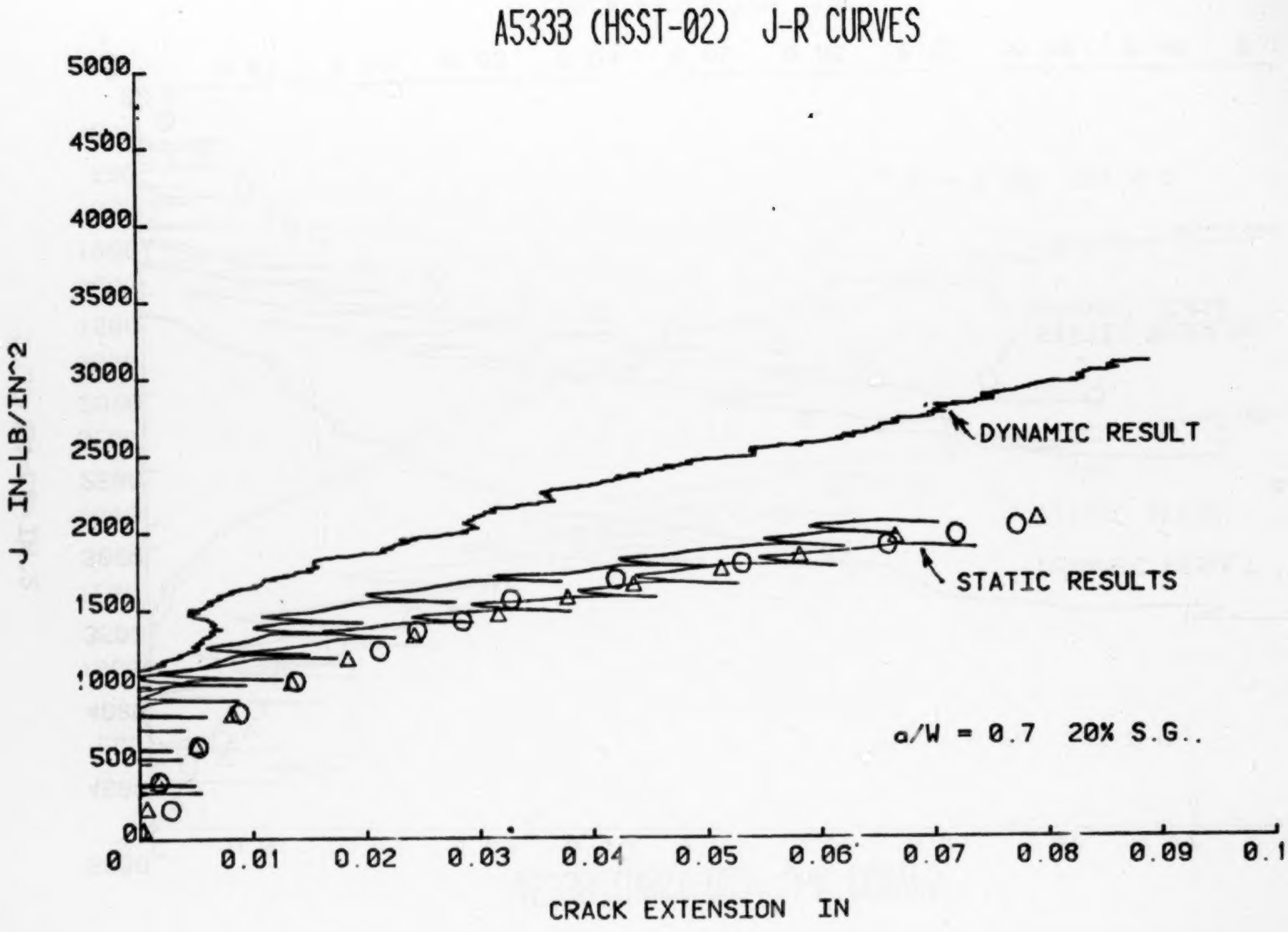
A533B (HSST-02) J-R CURVES
J IN-LB/IN^2
5000
4500
4000
3500
3000
2500
2000
1500
1000
500
0
0
0.01
0.02
0.03
0.04
0.05
0.06
0.07
0.08
0.09
0.1
CRACK EXTENSION IN
DYNAMIC RESULT
STATIC RESULTS
a/W = 0.7 20% S.G..

Conclusions

1. In this task the Key Curve method has been shown to work at test rates of up to 5-10 inches/sec and crack velocities of 10-20 inches/sec. for A533B HSST02 plate at 300°F.

2. The Key Curve method corrections for crack extension and specimen ratation allow evaluation of improved J-R curves showing clearly the effect of specimen constraint.

3. Dynamic J-R curves, to the loading rate of 5-10 inches/sec, show elevated J_{IC}'s compared to static tests but tearing slopes are similar for both the static and dynamic tests.

List of Related References

Joyce, J. A. and Gudas, J. P., "Computer Interactive J_{IC} Testing of Navy Alloys," Elastic-Plastic Fracture, ASTM STP 668, J. D. Landes, J. A. Begley, and G. A. Clarke, Eds., American Society for Testing and Materials, 1979, pp. 451-468.

Gudas, J. P., Joyce, J. A., and Davis, D. A., "Investigation of Specimen Geometry Modifications to Determine the Conservative J-R Curve Tearing Modulus Using the HY-130 Steel System," Fracture Mechanics, ASTM STP 677, C. C. Smith, Ed., American Society for Testing and Materials, 1979, pp. 474-485.

Joyce, J. A., "Application of the Key Curve Method to Determine J-R Curves for A533B Steel," NUREG/CR-1290, U. S. Nuclear Regulatory Commission, Washington, D.C., January 1980.

Joyce, J. A., Ernst, Hugo, and Paris, P. C., "Direct Evaluation of J-Resistance Curves from Load Displacement Records," Fracture Mechanics: Twelfth Conference, ASTM STP 700, American Society for Testing and Materials, 1980, pp. 222-236.

N. G. Vassilaros, J. A. Joyce, and J. P. Gudas, "Effects of Specimen Geometry on the J-R Curve for ASTM A533B Steel," Fracture Mechanics: Twelfth Conference, ASTM STP 700, American Society for Testing and Materials, 1980.

Joyce, J. A. and D. F. Hasson, "Characterization of Transition Temperature Behavior of HY130 Steel by the J_{IC} Fracture Toughness Parameter," Engin-ering Fracture Mechanics, Vol. 13 No. 3, 1981, pp. 417-430.

TOUGHNESS AND DUCTILE SHELF PROPERTIES OF IRRADIATED LOW-SHELF WELD METALS

F.J. Loss
Naval Research Laboratory
Washington, D.C. 20375

Presented at

8th Water Reactor Safety Research Information Meeting
National Bureau of Standards
Gaithersburg, MD
27-31 October 1980

TOUGHNESS AND DUCTILE SHELF PROPERTIES
OF IRRADIATED LOW-SHELF WELD METALS

F.J. Loss
Naval Research Laboratory
Washington, D.C. 20375

BACKGROUND

Previous studies have shown that A533-B submerged arc weld deposits of the type used in the beltline region of some commercial, light water reactors can exhibit low Charpy-V (C_v) upper shelf energy levels after irradiation, that is, energy levels which lie below 68J (50 ft-lb). In this event, Federal regulations (10 CFR Part 50) require, as one option, the performance of a fracture mechanics analysis which conservatively demonstrates the existence of adequate margins of safety for continued operation. To address this situation emphasis in research programs has been placed upon characterizing the fracture toughness of these steels in order to provide a quantitative basis to assess the safety margin. The objective of the current fracture toughness program is to develop J-R curve trends within the upper shelf regime. It is believed that these data could be used in conjunction with a tearing instability concept as defined by Paris [1] to assess the margin of safety against catastrophic fracture.

As part of the Heavy Section Steel Technology (HSST) Program seven A533-B submerged arc weld deposits (61W-67W) containing a high copper impurity level have been irradiated to provide a source of materials having low, upper shelf energy. Compact toughness (CT) specimens of various sizes, which include 0.5T-, 0.8T-, 1.6T-, and 4T-CT as well as C_v specimens were irradiated in this program to nominal fluence levels of 0.6 to 1.8×10^{19} n/cm^2 >1 MeV; postirradiation C_v upper shelf energy levels for these welds ranged from 54 to 81J (40 to 60 ft lb). Initial results from the testing of the 0.5T- and 1.6T-CT specimens are summarized here.

SUMMARY OF RESULTS

J-R curves have been obtained by means of the single specimen compliance (SSC) technique [2,3]. This method is capable of producing well-defined R curves having little scatter among the data points. In addition, it has been found that the crack extension must proceed uniformly throughout the specimen thickness in order to achieve an accurate correspondence between this quantity as predicted by the SSC technique and as measured optically after the specimen has been broken apart. Previous studies by the author have shown that side grooving of the specimen by 20% is required to achieve a straight crack-front extension in nuclear vessel steels. In this regard, the initial tests of irradiated 0.5T-CT specimens from the subject welds using 10% side grooves [4] showed that extensive crack-front tunneling resulted as the R curves were developed. Consequently, a side-groove depth of 20% was chosen for the 1.6T-CT tests of these same steels.

The first R curves from the 1.6T-CT HSST specimen irradiations are shown in Fig. 1. The test temperature of 200°C was chosen to be on the C_v upper shelf for both materials. The crack extension (Δa) was purposely taken to large values, e.g., 14 to 20 mm, because this had never before been accomplished for irradiated vessel steels. Even at this long crack extension the crack front profile remained straight (Fig 2) and the correspondence between measured and predicted values of final crack extension was excellent. However, this long crack extension may have caused the crack to outgrow the region of J dominance and thus possibly invalidate some of the computed values of J and tearing modulus T. Planned tests of larger (4T-CT) specimens of these welds will provide information to assess the utility of current results at large values of crack extension.

An expanded R curve for one of the specimens denoted in Fig. 1 is presented in Fig. 3. This curve highlights the power law behavior exhibited at small values of crack extension. The latter was first documented by the author in previous R curve studies of nuclear pressure vessel steels [3,5,6]. It has been found convenient to fit the initial portion of the R curve with the form:

$$J = C\,\Delta a^{n} \tag{1}$$

where C and n are fitted constants and Δa is the crack extension. This formulation is indicated in Fig. 3. Because of this curvature in the R curve, it is not possible to compute a unique value of tearing modulus for these materials. For comparison between different steels, however, we have defined an average value of tearing modulus (T_{AVG}) which characterizes the R curve for a limited crack extension increment of $0.15 < \Delta a < 1.5$ mm. It should be noted that the power law expression of the R curve cannot be extrapolated beyond the region shown in Fig.3. The flattening of the R curve at large crack extensions (Fig.1) precludes an accurate fit of the data by a power law formulation. In fact, the values of tearing modulus are essentially zero at the point where the test was terminated.

As explained in Ref. 3, the power law behavior led the author to devise a new definition of J_{Ic} which allows a small amount of crack extension. Specifically, J_{Ic} is computed from the power law fit at a point where the R curve crosses the 0.15 mm extension line. This definition of J_{Ic} is different from that of the proposed ASTM procedure for J_{Ic}. However, the ASTM procedure was designed for multiple specimen testing whereby the curvature in the R curve for nuclear vessel steels cannot be readily discerned. Consequently, J_{Ic} by the latter procedure is taken as the intersection of the least squares fit to the data between the exclusion lines in Fig. 3 and the blunting line. The agreement in J_{Ic} by these two procedures has been found to be within ±10% [3,6]. The results shown in Fig.1 indicate a range in J_{Ic} of 61 to 88 kJ/m^2 for the HSST welds; the latter is equivalent to K_{Jc} of 115 to 137 MPa$\sqrt{m}$.

Figure 4 compares R curves from weld 63W generated by two different size specimens, 0.5T- and 1.6T-CT. The irradiation conditions and test temperatures for both specimens were similar. The R curve for the 1.6T-CT specimen appears to project a lower trend from that for the 0.5T-CT specimen. It was expected that this difference would be even greater in view of the tunneled crack front which was exhibited by the 0.5T-CT specimen and not by the 1.6T-CT specimen. Previous studies have shown that for the same size specimen, crack-front tunneling produces an R curve which lies above that associated with a straight crack-front extension.

The power law behavior of the R curve has led to considerations of tearing instability in terms of a J vs T diagram (Fig 5). Use of this diagram requires knowledge of the applied values of T and J in a flawed structure as well as an accurate characterization of the R curve which describes the material behavior in geometrical configurations which are usually different from those of the test specimen. These areas are being explored in current research studies sponsored by NRC.

To support the new analysis procedures being considered, an R curve data base for nuclear pressure vessel steels has been evolved through studies at NRL. A generalization of the individual R curves implies a correlation with C_v upper shelf energy at a specific test temperature (Fig. 6). The possibility of a correlation between C_v energy and the R curve is encouraging and suggests that the C_v data obtained in surveillance programs may have additional application in fracture toughness assessments. Further evidence of a correlation between the R curve and C_v shelf energy is illustrated by the comparison of the latter with T_{AVG} (Fig 7).

In summary, the studies of nuclear pressure vessel steels have shown that it is possible to characterize the elastic plastic behavior of irradiated steels by means of a single specimen technique; this provides the means for judicious testing of valuable surveillance specimens. The first data base for irradiated vessel steel has been formulated. These data are essential to assess safety margins in terms of the tearing instability concept. Furthermore, it has been suggested that a correlation exists between the R curve and C_v shelf energy. A correlation of this type is expected to enhance the significance of C_v surveillance data. However, further studies are required to analyze the generality of such a correlation as well as its possible dependence upon specimen size and test temperature.

REFERENCES

1. P.C. Paris, H. Tada, A. Zahoor and H. Ernst, "Instability of the Tearing Mode of Elastic-Plastic Crack Growth," in Elastic-Plastic Fracture, ASTM STP 668, 1979, pp. 5-36.

2. F.J. Loss, Ed., "Structural Integrity of Water Reactor Pressure Boundary Components-Quarterly Progress Report, April-June 1979," NUREG/CR-0943, NRL Memorandum Report 4064, September 28, 1979.

3. F.J. Loss, Ed., "Structural Integrity of Water Reactor Pressure Boundary Components, Annual Report, Fiscal Year 1979," NUREG/CR-1128, NRL Memorandum Report 4122, 31 December 1979.

4. F.J. Loss, Ed., "Structural Integrity of Water Reactor Pressure Boundary Components-Quarterly Progress Report, October-December 1979," NUREG/-CR-
1268, NRL Memorandum Report 4174, March 20, 1980.

5. F.J. Loss, et al., "J-R Curve Characterization of A533-B Weld Metal With Irradiation and Postirradiation Annealing," in Proceedings, Symposium on Effects of Radiation on Materials, Savannah, Georgia, 3-5 June 1980, ASTM STP 725, 1981.

6. F.J. Loss and G. Angelino, "Elastic-Plastic Characterization of Nuclear Vessel Steels," Proceedings of Intn. Conference on Analytical and Experimental Fracture Mechanics, Rome, Italy, 23-27 June 1980.

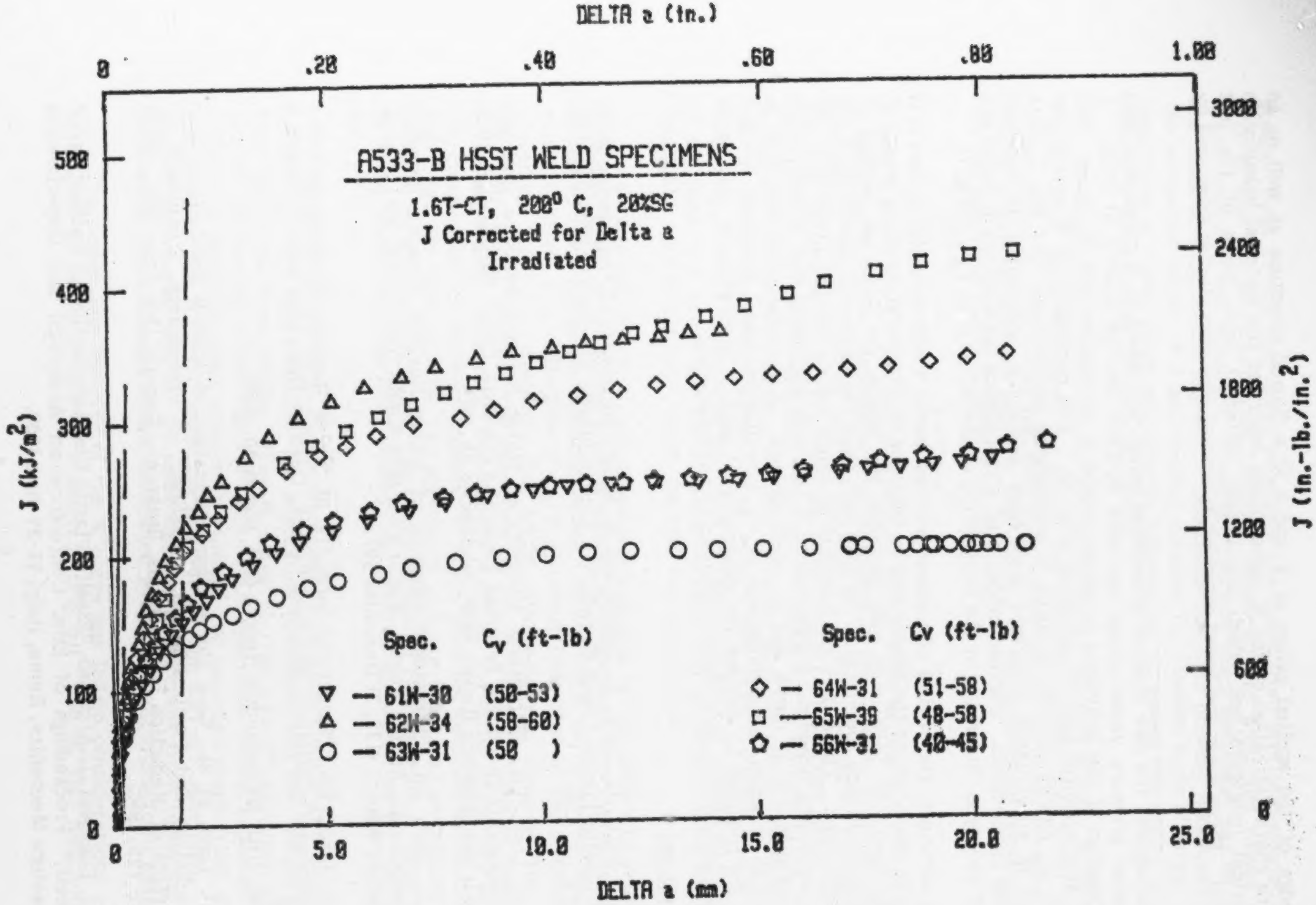

Fig. 1. J-R curves from 1.6T-CT HSST specimens tested in the upper shelf regime. Welds 61W, 62W, and 63W received a fluence of 12 to 16 x 10^{18} n/cm^2 >1 MeV while the fluence range for welds 64W, 65W, and 66W was 6.2 to 8.5 x 10^{18} n/cm^2 >1 MeV.

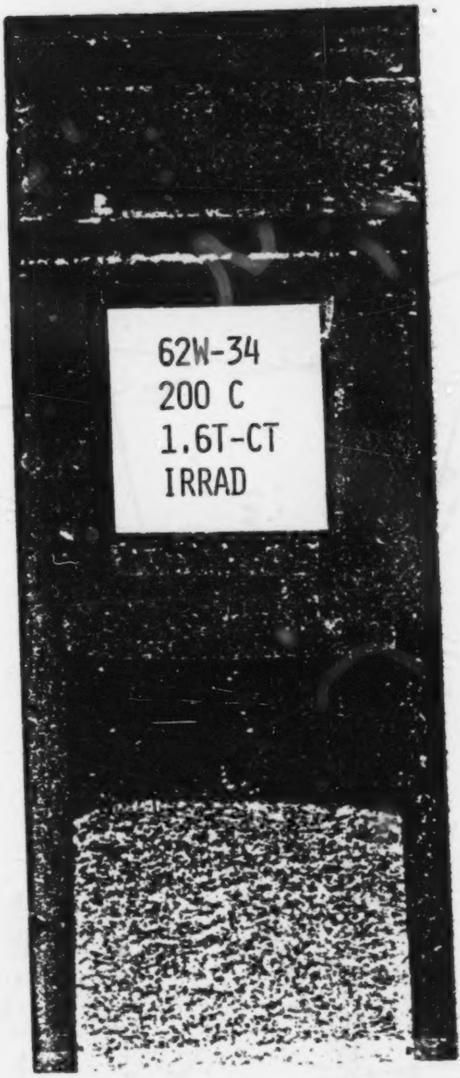
62W-34
200 C
1.6T-CT
IRRAD

Fig. 2. Fracture surface of a 1.6T-CT specimen illustrating the straight crack-front extension which has resulted from the 20% side grooves.

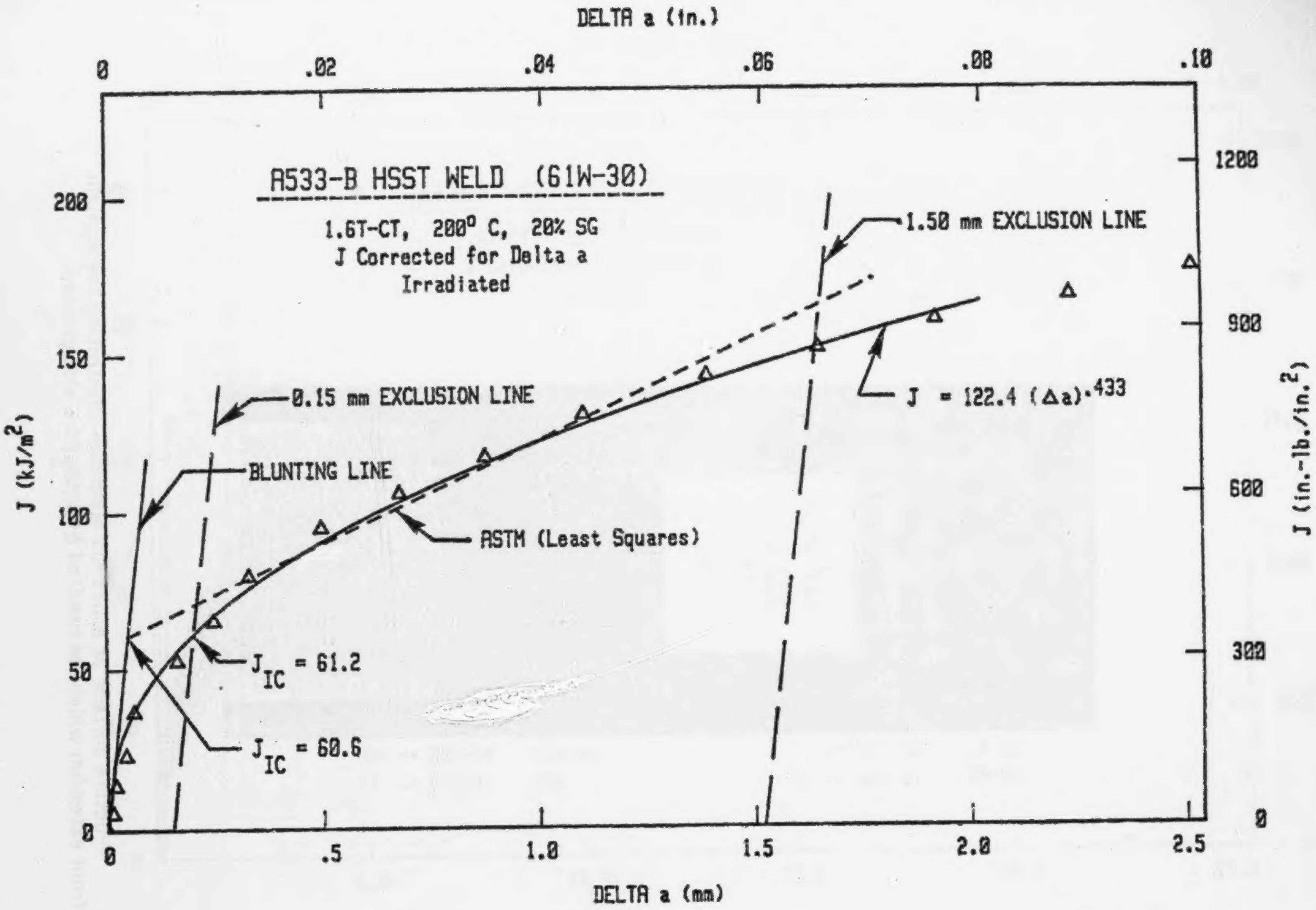

Fig. 3. Expanded R curve illustrating the power law behavior exhibited at small crack extension. With the NRL procedure, J_{Ic} is taken as that value where the R curve intersects the 0.15 mm exclusion line. Conversely, J_{Ic} is defined by the proposed ASTM standard as the intersection of the least squares fit of the data (between exclusion lines) with the blunting line.

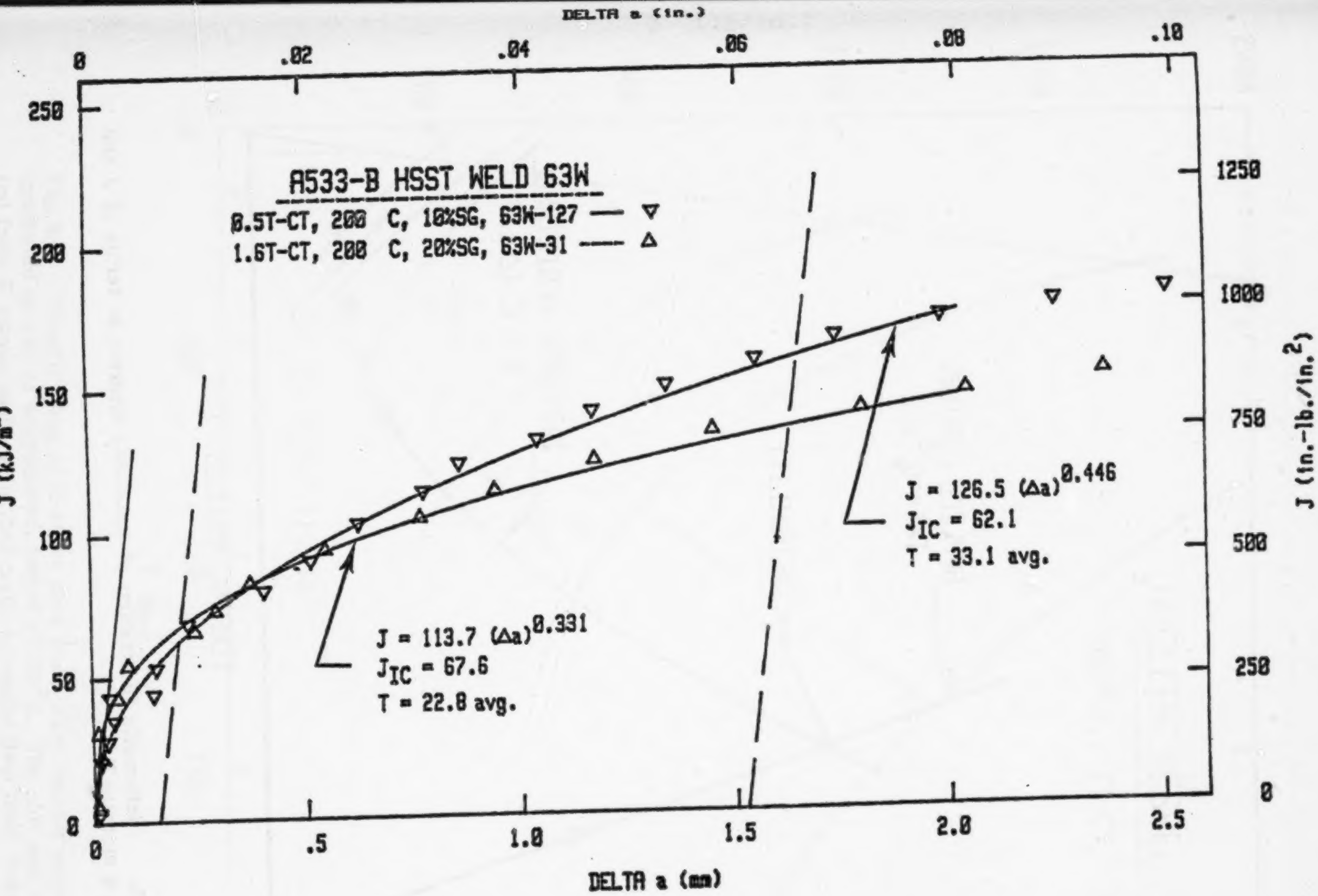

Fig. 4. Comparison of R curves obtained from two different size compact specimens. The fluences for the 0.5T- and 1.6T-CT specimens were 10 and 14 x 10^{18} n/cm^2 > 1 MeV, respectively.

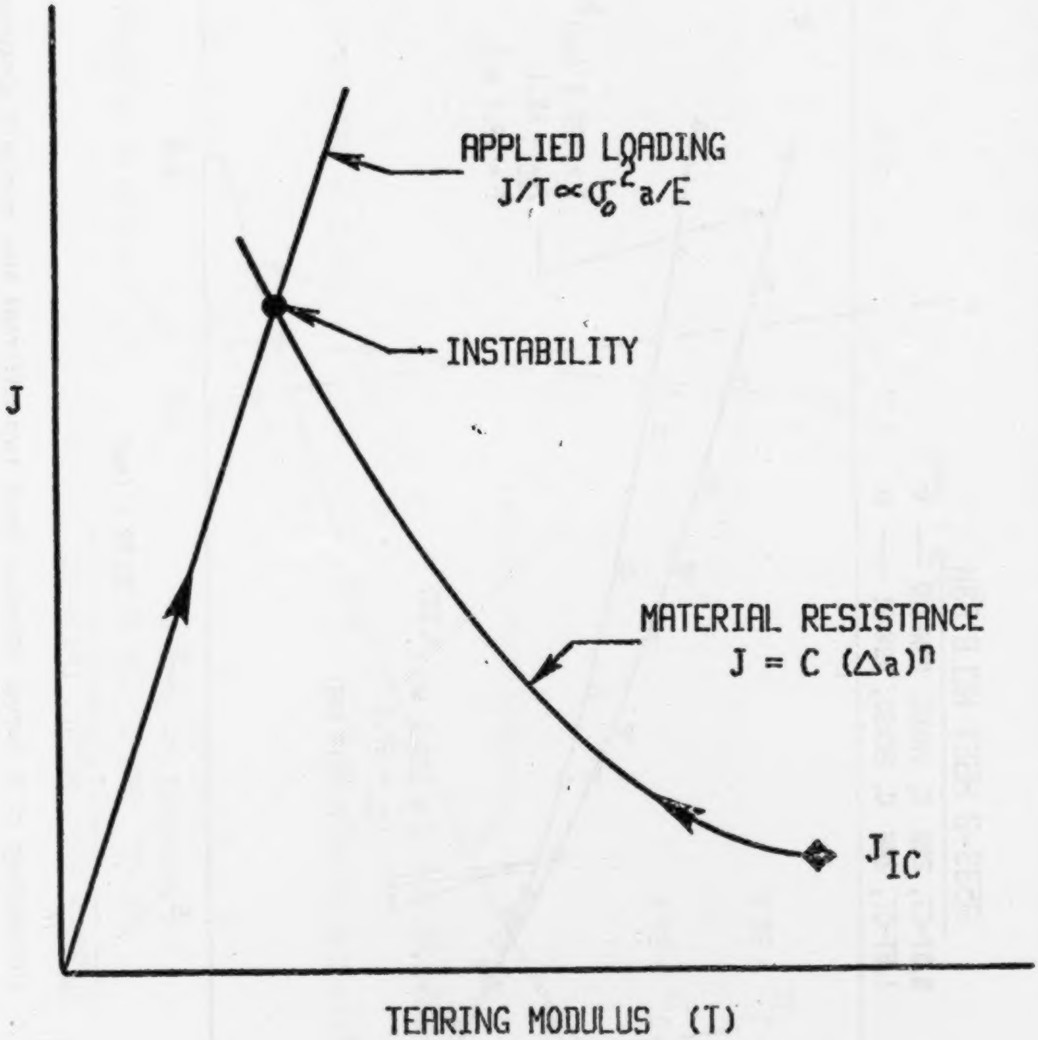
APPLIED LOADING
J/T ∝ σ₀² a/E
INSTABILITY
J
MATERIAL RESISTANCE
J = C (Δa)ⁿ
J_IC
TEARING MODULUS (T)

Fig. 5. Schematic illustration of instability diagram in terms of J and tearing modulus T.

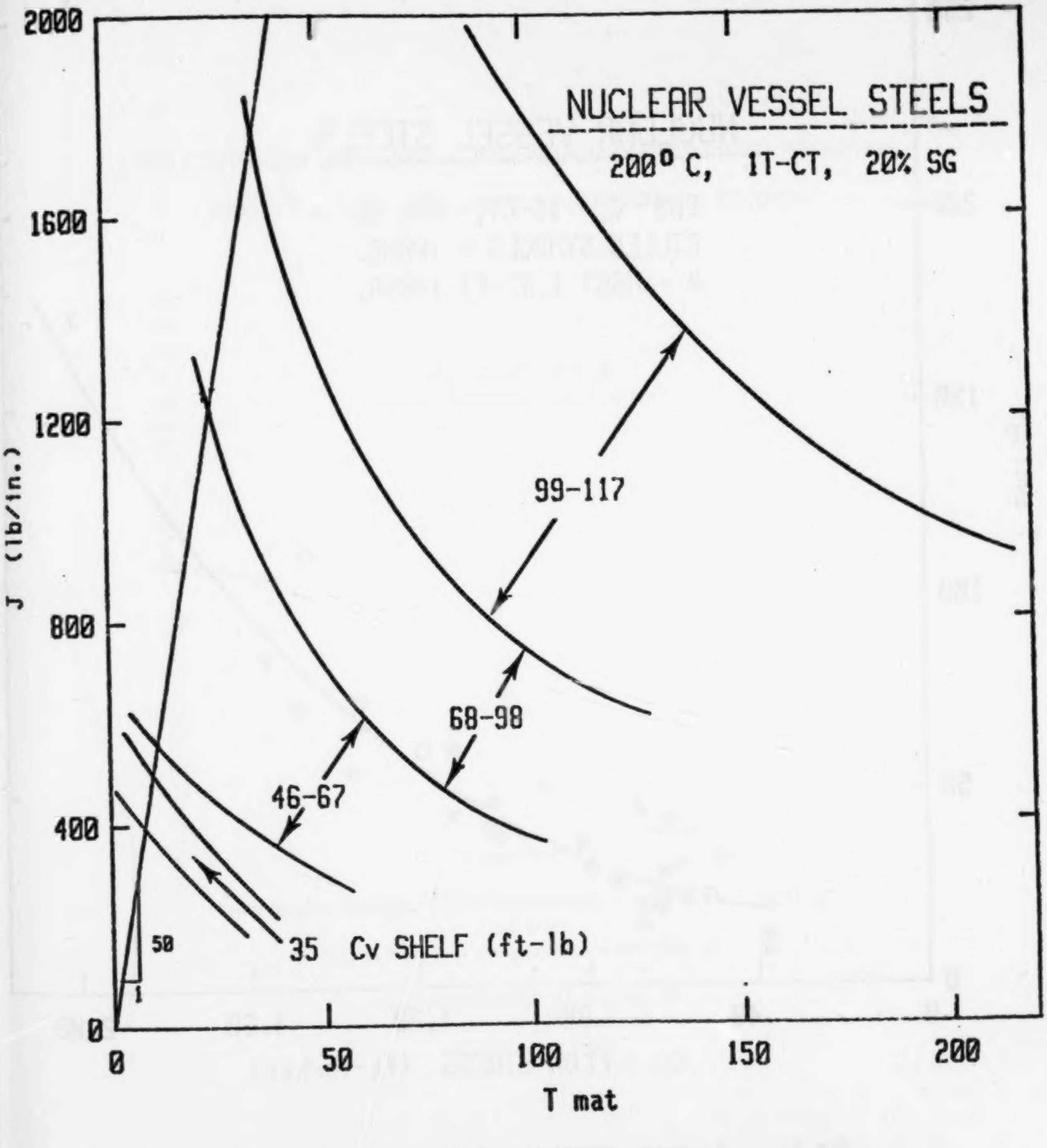

Fig. 6. General trend of R-curve data from many reactor vessel steels, irradiated as well as unirradiated, tested at 200°C. The plot was constructed from R curves having a limited crack extension (less than 2 mm) where a power law representation is valid.

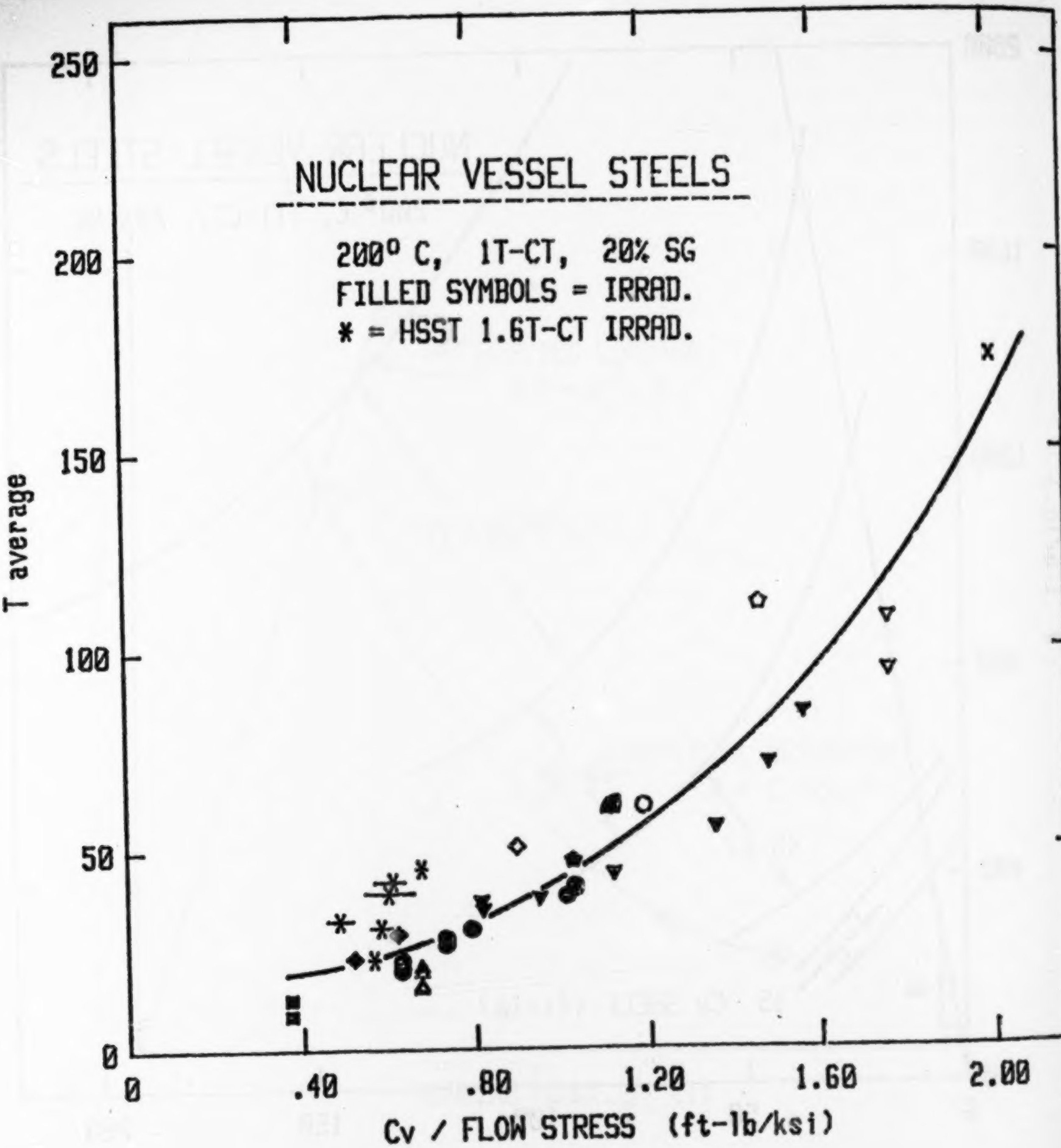

Fig. 7. Apparent correlation between $T_{Average}$ and C_v upper shelf energy at a given temperature. $T_{Average}$ was calculated from a least squares fit to the R curves within a crack extension increment of $0.15 < \Delta a < 1.5$ mm.

CYCLIC IRRADIATION-ANNEALING-REIRRADIATION (IAR) PROGRAM AND OTHER RPV IRRADIATION SENSITIVITY STUDIES

J. R. HAWTHORNE
Naval Research Laboratory

Presented to:

8th Water Reactor Safety Research Information Meeting
of the
U. S. Nuclear Regulatory Commission

National Bureau of Standards
Gaithersburg, Maryland
30 October 1980

SUMMARY

This report describes a study of Charpy-V (C_v) notch ductility and tensile properties behavior of two representative reactor vessel welds under cyclic 399°C postirradiation annealing and 288°C reirradiation. The welds were by the submerged arc process and were chosen for their high radiation sensitivity (high copper content) and for their difference in as-fabricated C_v upper shelf energy levels derived from different welding fluxes. Weld properties were determined at each phase of the anneal-reirradiation-reanneal-reirradiation sequence.

The study clearly demonstrates the capability of the annealing method for maintaining property changes of reactor steels, including C_v upper shelf reduction and transition temperature elevation, below prefixed limits. In addition, the study confirms a significantly greater rate of embrittlement by heat-treated material compared to nonheat-treated material. Pronounced dissimilarities between C_v upper shelf energy and transition temperature behavior were observed but show parallels, respectively, with tensile ductility and strength changes during annealing and reirradiation.

This report also describes a study in progress on the suspected interaction of nickel and copper content on radiation sensitivity development in low alloy steels and welds. Laboratory melts of A302-B steel prepared with nickel content, copper content, and nickel-to-copper ratio variations (split melt practice) have been prepared for studies of relative radiation resistance by Charpy-V notch ductility determinations.

Finally, the initial mechanical property test results developed by NRL for the NRC LWR-PVI Surveillance Dosimetry Improvement Program are reported. Irradiations are being conducted in the Oak Ridge Research Reactor (ORR) pool side facility (PSF) in an experimental assembly designed to simulate a reactor vessel wall and thermal shield. The initial test results are for the two reference steels exposed in surveillance specimen capsule No. 1 (SSC-1) and show good agreement with prior test reactor data at the 2×10^{19} n/cm^2 > 1 MeV estimated fluence levels.

SELECTED REFERENCES

J. R. Hawthorne, H. E. Watson, and F. J. Loss, "Experimental Investigation of Multicycle Irradiation and Annealing Effects on Notch Ductility of A533-B Weld Deposits," Proceedings, International Symposium on Effects of Radiation on Structural Materials, Savannah, Georgia, June 1980, ASTM STP 725, 1981.

F. J. Loss, B. H. Menke, R. A. Gray, Jr., J. R. Hawthorne, and H. E. Watson, "J-R Curve Characterization of A533-B Weld Metal with Irradiation and Postirradiation Annealing," Proceedings, International Symposium on Effects of Radiation on Structural Materials, Savannah, Georgia, June 1980, ASTM STP 725, 1981.

[illegible]

[illegible]

[illegible]

[illegible]

[illegible]

[illegible]

[illegible]

[illegible]

TOPICS

- IAR PROGRAM
- NICKEL + COPPER STUDIES
- LWR-PVI SURVEILLANCE DOSIMETRY IMPROVEMENT PROGRAM

IRRADIATION-ANNEAL-REIRRADIATION (IAR) PROGRAM

- MULTICYCLE IAR BEHAVIOR
- HIGH COPPER, SUBMERGED ARC WELDS
- Cv, TENSION, CT TEST METHODS
- 288C IRRADIATION
- 399C ANNEALING

PROGRESS

- PHASE 1 IAR STUDIES COMPLETED
- FINDINGS REPORTED (1980) ASTM SYMPOSIUM)
- PHASE 2 IAR STUDIES INITIATED

CYCLIC IRRADIATION-ANNEAL CONDITIONS

I	$\sim 1.2 \times 10^{19}$ AT 550F
IA	(I) + 750F-168h
IAR	(IA) + $\sim 0.7 \times 10^{19}$
IARA	(IAR) + 750F-168h
IARAR	(IARA) + $\sim 0.7 \times 10^{19}$

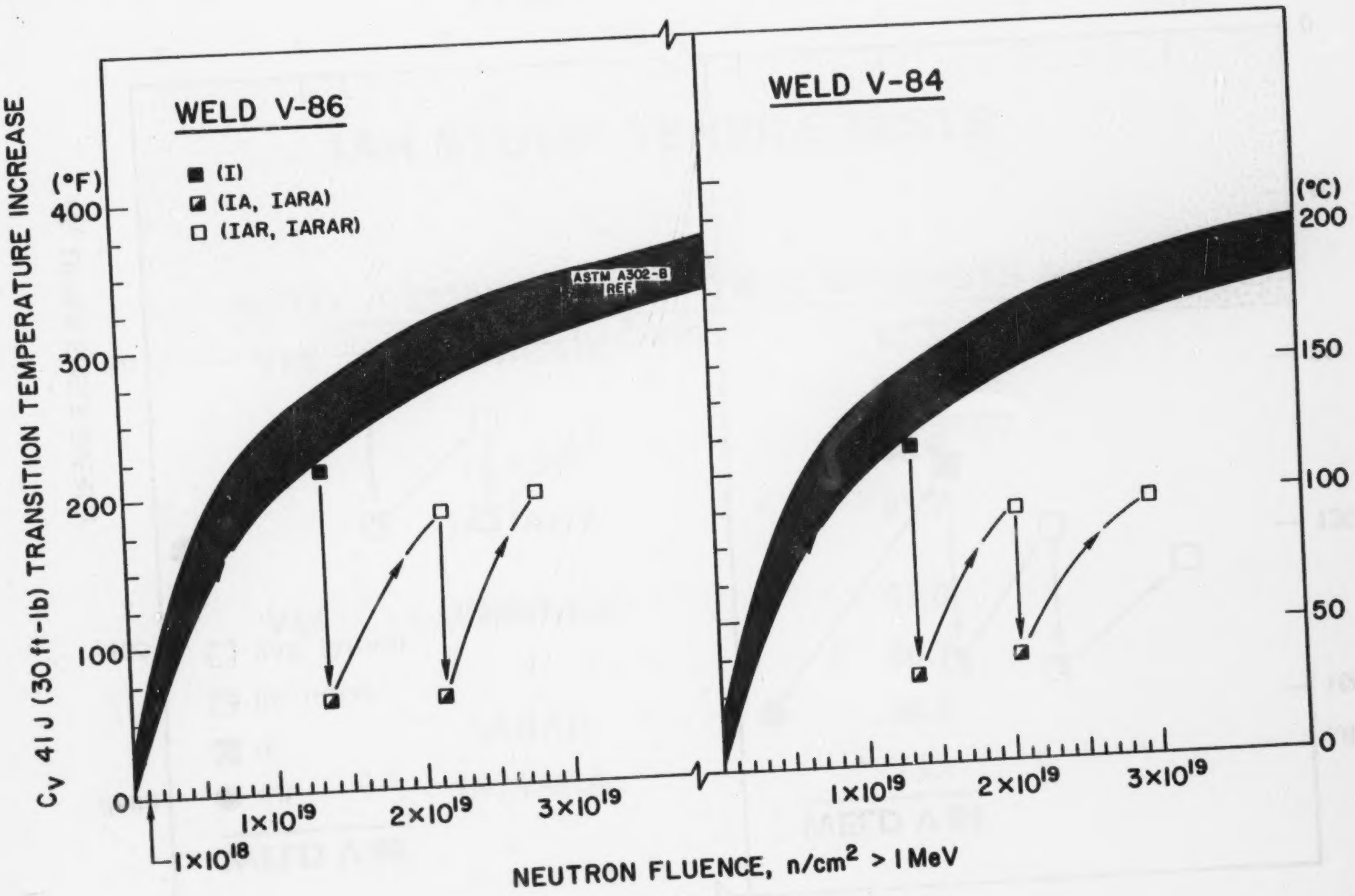
WELD V-86
(I)
(IA, IARA)
(IAR, IARAR)
ASTM A302-B REF.
WELD V-84
Cv 41 J (30 ft-lb) TRANSITION TEMPERATURE INCREASE
(°F)
400
300
200
100
0
(°C)
200
150
100
50
0
1×10^18
1×10^19
2×10^19
3×10^19
NEUTRON FLUENCE, n/cm^2 > 1 MeV

UPPER SHELF IAR TRENDS

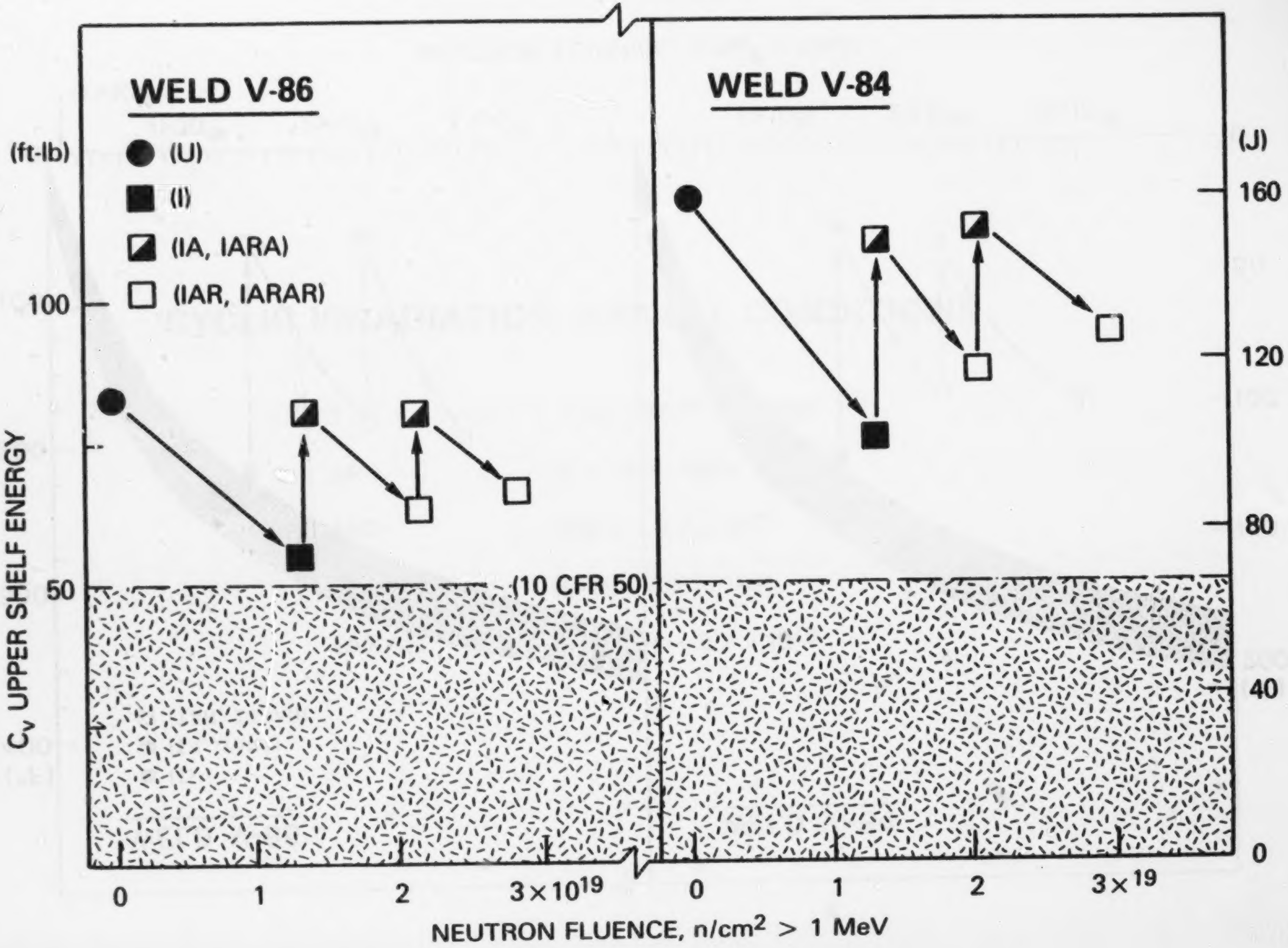

IAR STUDY–TENSILE TESTS

WELD	CONDITION	YIELD STRENGTH (ksi)
V86	UNIRRAD.	67.3
	I	91.5
	IARAR	86.6
	IA, IARA	81.7
V84	UNIRRAD.	67.0
	I	96.7
	IARAR	86.0
	IA, IARA	75.7

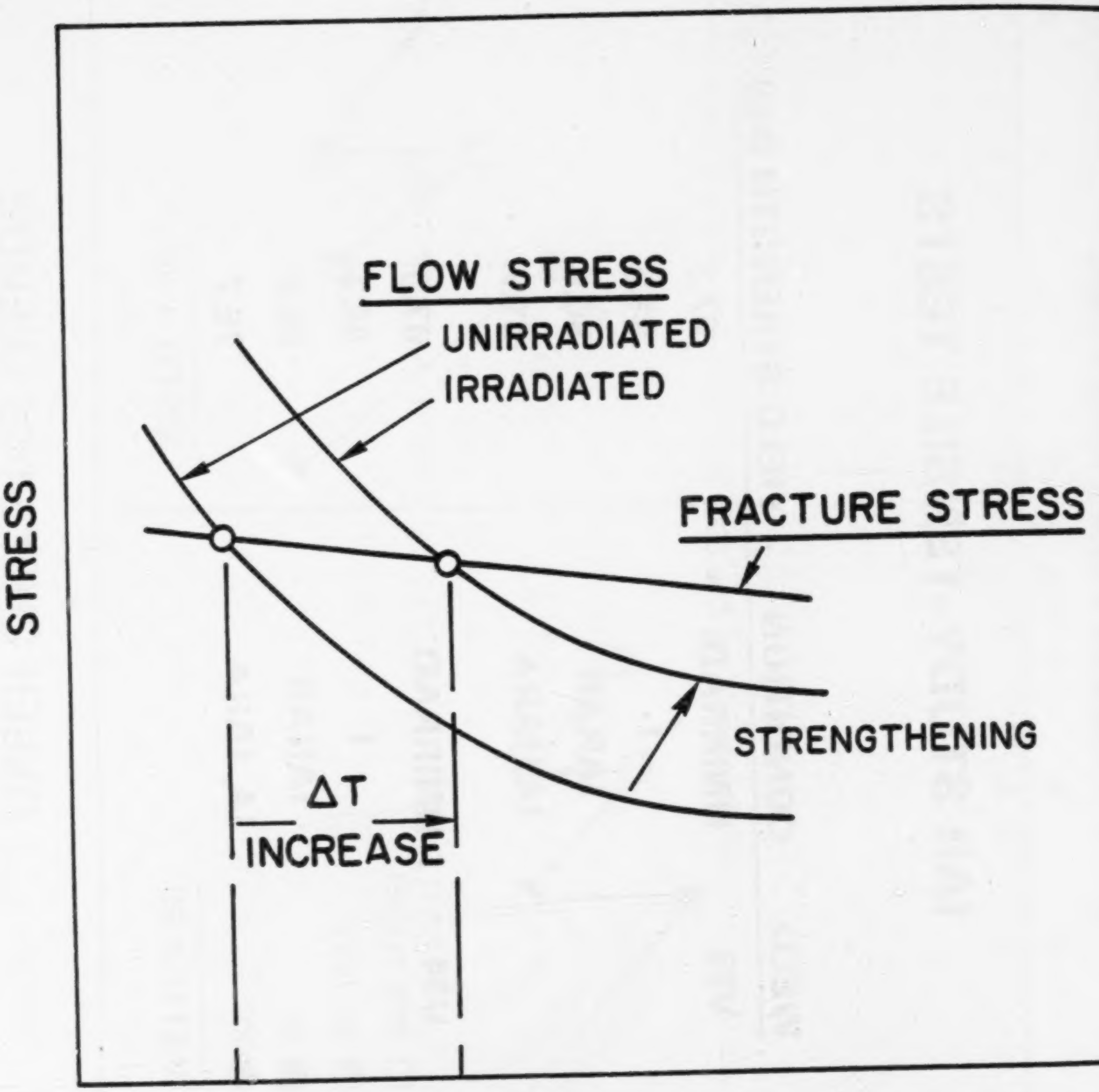
FLOW STRESS
UNIRRADIATED
IRRADIATED
FRACTURE STRESS
STRESS
STRENGTHENING
ΔT
INCREASE
T UNIRRAD.
T IRRAD.
TEMPERATURE, T

SUMMARY - IAR

- CAPABILITIES OF ANNEALING METHOD DEMONSTRATE
  (2 IAR CYCLES)
- RESTRICTION OF UPPER SHELF/TRANSITION CHANGES BELOW PREFIXED LIMITS POSSIBLE
- RATE OF EMBRITTLEMENT AFTER HEAT TREATMENT HIGHER THAN RATE WITHOUT HEAT TREATMENT
- IAR UPPER SHELF RECOVERY $\neq$ TRANSITION RECOVERY

RESEARCH NEEDS

- REEMBRITTLEMENT PATH
- EFFECT OF PRIOR FLUENCE/COMPOSITION
- Cv vs J-R CURVE

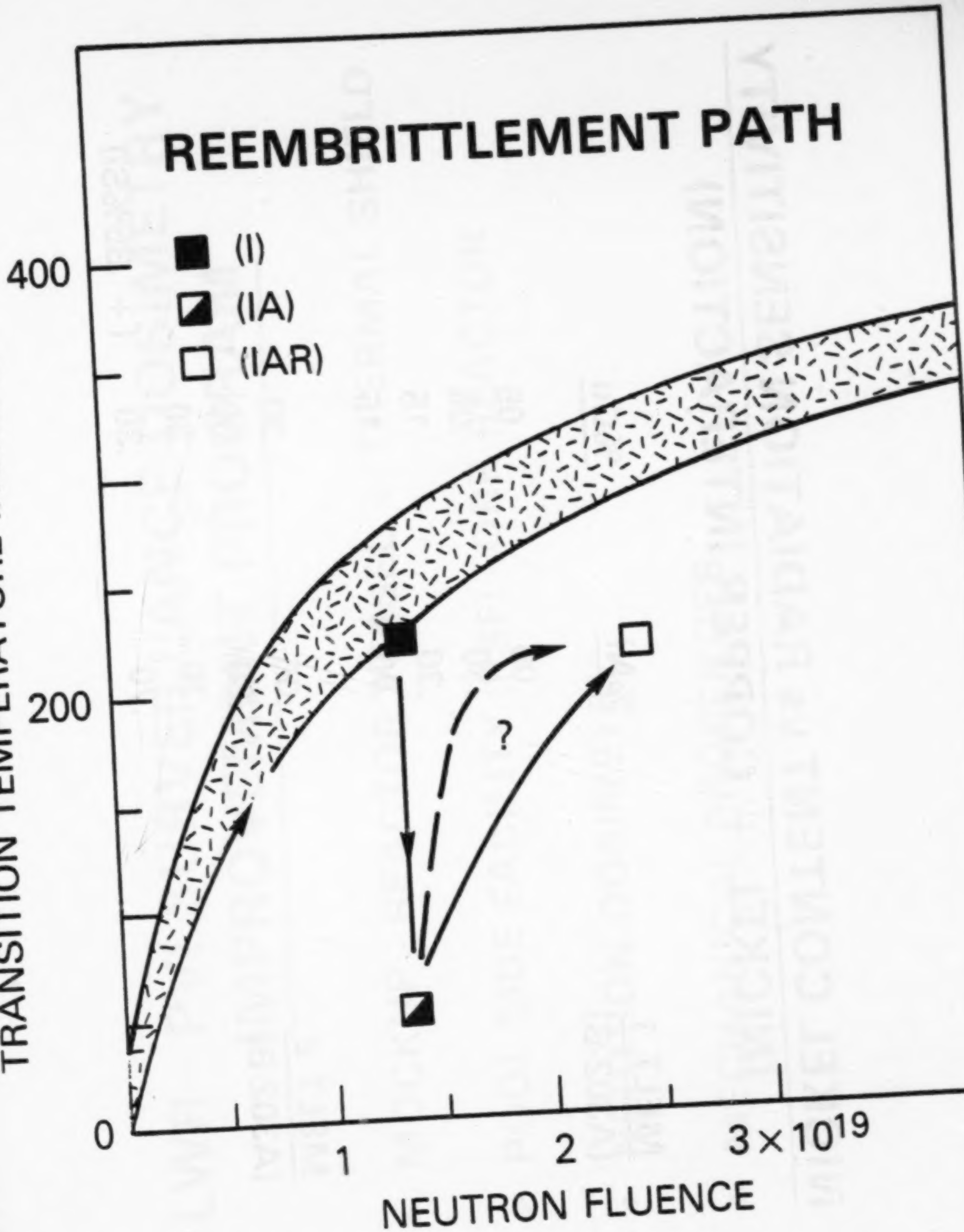

REEMBRITTLEMENT PATH
■ (I)
◪ (IA)
□ (IAR)
?
TRANSITION TEMPERATURE INCREASE
400
200
0
1
2
3×10¹⁹
NEUTRON FLUENCE

NICKEL CONTENT vs RADIATION SENSITIVITY
(NICKEL + COPPER INTERACTION)

	%Ni	%Cu	
MELT 1 (A302-B)			
	.05	.05	
	.30	.05	
	.30	.15	
	.70	.15	
MELT 2 (A302-B)	.05	.30	
	.30	.30	
	.70	.30	
	.70	.30	(+ .35%Si)

LWR - PVI SURVEILLANCE DOSIMETRY IMPROVEMENT PROGRAM

- MOCKUP - REACTOR VESSEL + THERMAL SHIELD
- POOL SIDE FACILITY (PSF) - ORR REACTOR
- NEUTRON DOSIMETRY
- MECHANICAL PROPERTIES

NRL RESPONSIBILITIES
(PSF IRRADIATIONS)

- REFERENCE MATERIALS
- MECHANICAL PROPERTIES
- PRE-POSTIRRADIATION TESTING
  (Cv, CT, TENSILE)

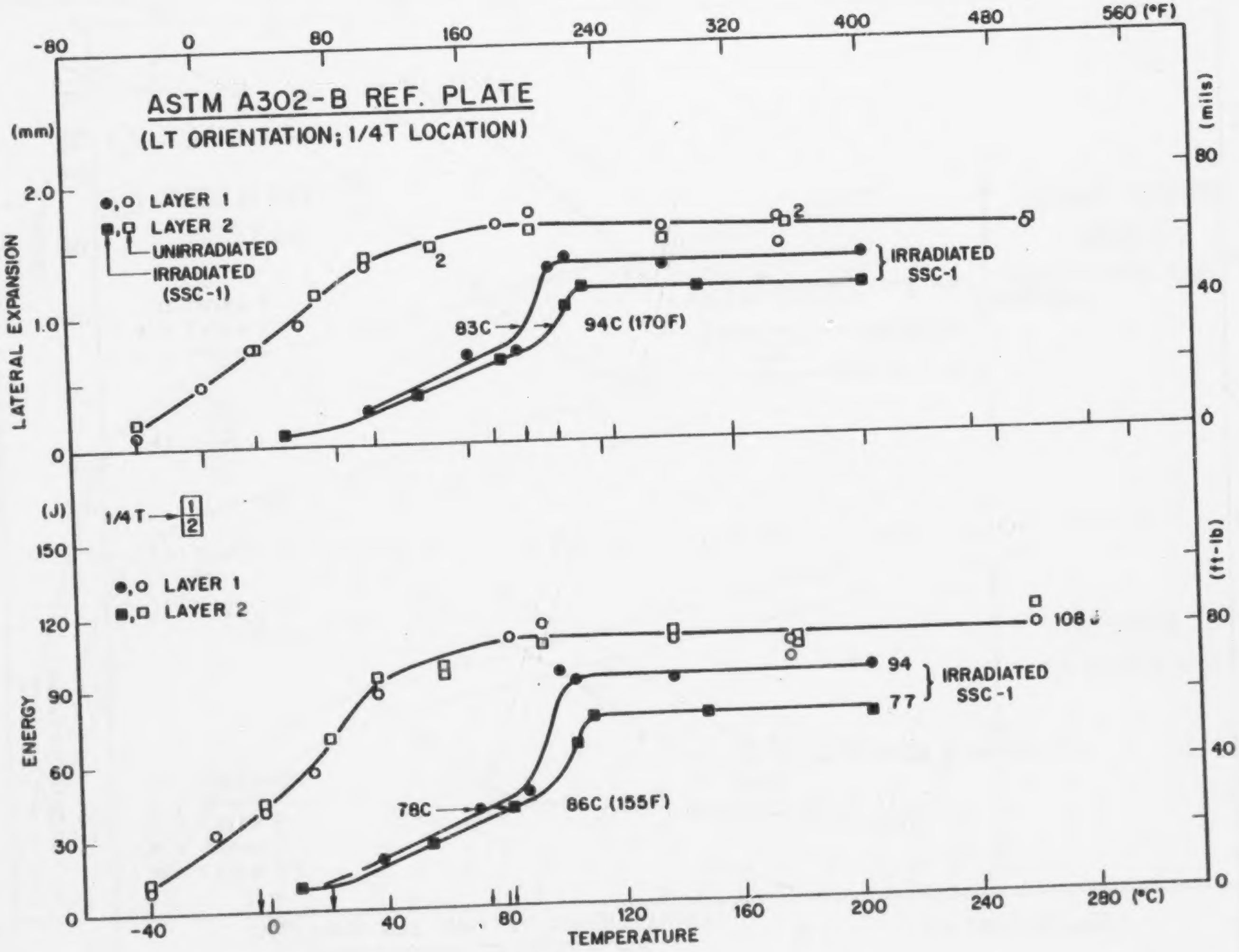
ASTM A302-B REF. PLATE
(LT ORIENTATION; 1/4T LOCATION)
●,○ LAYER 1
■,□ LAYER 2
UNIRRADIATED
IRRADIATED (SSC-1)
IRRADIATED SSC-1
83C
94C (170F)
LATERAL EXPANSION
(mm)
2.0
1.0
0
(mils)
80
40
0
-80
0
80
160
240
320
400
480
560 (°F)
1/4T
1
2
(J)
150
120
90
60
30
0
ENERGY
●,○ LAYER 1
■,□ LAYER 2
108 J
94
77
IRRADIATED SSC-1
78C
86C (155F)
(ft-lb)
80
40
0
-40
0
40
80
120
160
200
240
280 (°C)
TEMPERATURE

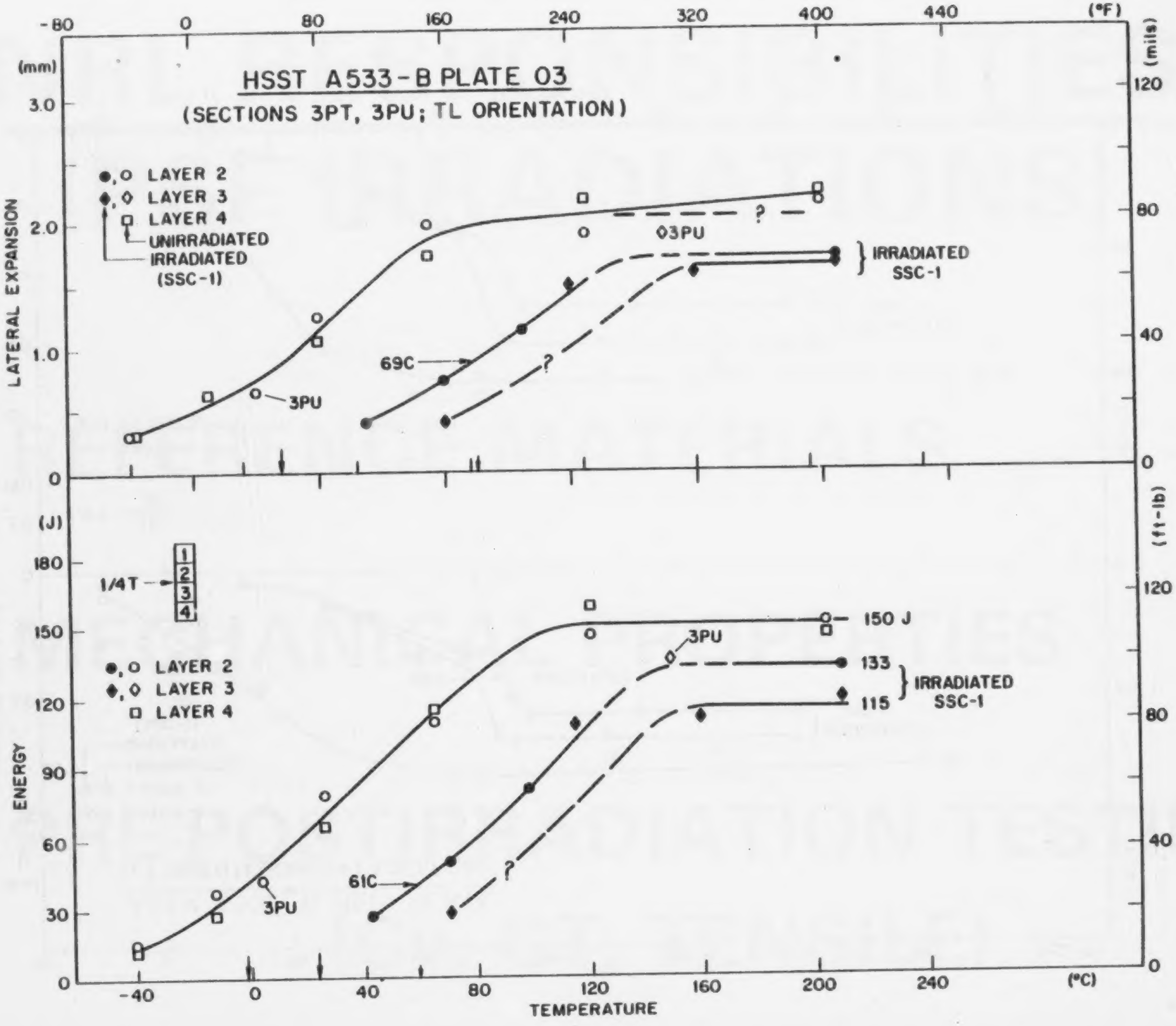
HSST A533-B PLATE 03

(SECTIONS 3PT, 3PU; TL ORIENTATION)

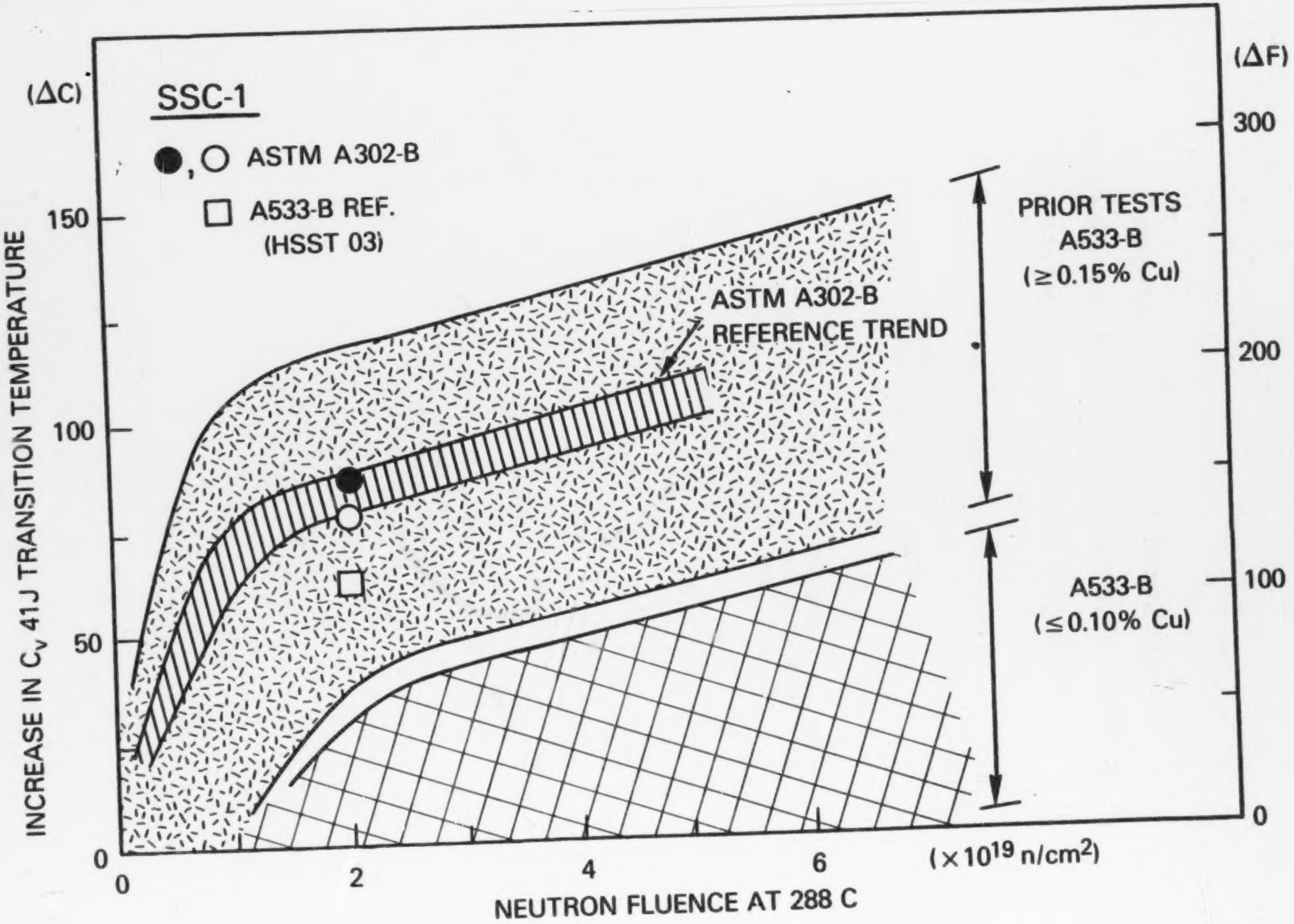
SSC-1
●, ○ ASTM A302-B
☐ A533-B REF. (HSST 03)
(ΔC)
150
100
50
0
INCREASE IN C_v 41J TRANSITION TEMPERATURE
(ΔF)
300
200
100
0
0
2
4
6
($\times 10^{19}$ n/cm^2)
NEUTRON FLUENCE AT 288 C
ASTM A302-B REFERENCE TREND
PRIOR TESTS A533-B (≥0.15% Cu)
A533-B (≤0.10% Cu)

INFLUENCE OF CRITICAL VARIABLES ON ENVIRONMENTALLY-ASSISTED CRACK GROWTH RATES OF PVP MATERIALS IN PWR COOLANT ENVIRONMENTS

W. H. Cullen, F. J. Loss and H. E. Watson
Code 6392
Naval Research Laboratory
Washington, D.C 20375

and

W. H. Bamford and L. J. Ceschini
Westinghouse Nuclear Energy Systems Division
Forest Hills Site, B-300
P. O. Box 855
Pittsburgh, PA 15230

Presented to:

8th Water Reactor Safety Information Meeting
National Bureau of Standards
Gaithersburg, Maryland
30 October 1980

SUMMARY

This research is directed toward the determination of the critical variables which influence environmentally assisted crack growth rates in pressure vessel and piping materials. Tests are conducted in high-temperature, pressurized, reactor-grade water. Progress on this program, carried out through the cooperative efforts of the Naval Research Laboratory and Westinghouse Nuclear Energy Systems Division, has been concentrated in three related areas:

a. Main Test Matrix (Unirradiated). Fatigue crack growth rate determination in unirradiated reactor pressure vessel materials. Testing according to this matrix has been nearly completed.

b. Main Test Matrix (Irradiated). The first fatigue crack growth rate tests of irradiated pressure vessel materials have been completed for three materials.

c. Stress Corrosion Cracking. The finding, in December 1979, that cracking occurred after about 1000 hours in the heat-affected zone of pressure vessel steels, and later, in some plate material, opened a new area of concern.

The results of research in these areas are discussed below.

DISCUSSION

Main Matrix Testing (Unirradiated)

The main test matrix was conceived to allow an evaluation of the majority of steels and welds used in United States reactor vessels. There were three primary welds and companion heat-affected zones investigated, those made with Linde 80, Linde 124, and Linde 0091 flux. The materials which have been studied are listed in Table 1, along with their chemistries There were a total of eight different materials, with multiple heats having been tested for one weld (Linde 0091) and both the plate and forging materials.

As may be seen in Table 2, two loading effects variables were investigated. The R ratio (minimum stress/maximum stress) is known to be the major factor influencing fatigue crack growth rates of these materials in water environments. The second loading variable investigated was the waveform, where the sinusoidal waveform was compared to a ramp/reset condition.

The construction of the matrix also allowed study of heat-to-heat variation within a given material type for the plate and forging material. It was found that these can be very important. The matrix, as it appears in Table 2, contains all test results available on the materials and conditions listed. In many cases these data were obtained in earlier years [1-4], but have been included to provide a more complete portrayal of the state of knowledge on these materials in a simulated PWR environment. There have been nearly 50 specimens completed thus far in the matrix; therefore, results of the tests have been separated by material type.

Results thus far indicate there are two factors, besides R ratio, which can strongly influence the susceptability of these steels to a given water environment. These are the loading form and the material chemistry. In most of the materials studied, a sinusodial loading form results in more accelerated crack growth than a similarly timed ramp-reset loading, or positive saw-tooth. Secondly, it appears that the sulfur content of the steel has a strong impact on its environmental sensitivity, with highest sulfur content resulting in more susceptibility. The sulfur effect and the R-ratio effect and, to a lesser extent, the waveform effect are the most important influences on water environment crack growth behavior observed thus far, and appear to overshadow material-to-material differences in the results obtained to date. The sulfur effect was first observed during the past year.

The best characterized material to date is SA533-B plate material for which seven heats have been tested. Results obtained for low R-ratio tests are summarized in Fig. 1, which contains the results of testing four heats under a sine wave loading. The results fall into two distinct patterns, which can be separated by the sulfur content. Three heats showed considerable environmental enhancement and were quite consistent. The sulfur contents of these heats "1HT," "IN," and "04A" were 0.012, 0.026 and 0.018 weight percent, respectively. The second set of results, for specimens TW-4 and W7-2C2, show very little environmental enhancement, and Table 1 shows that the sulfur content is only 0.004 weight percent. It appears that a certain level of sulfur is required for environmental enhancement, and beyond this level enhancement does not increase further. Comparison of specimens TW-4 and W7-2C2 further indicates that the sine wave loading is somewhat more damaging than the ramp-reset load form.

Figure 2 shows a summary of results obtained for A533-B plate at high R ratio. Note that both heats were high in sulfur and thus showed considerable environmental enhancement, although the result for specimen 04A-102 is slightly less severe.

The behavior shown for the plate was also typical of that obtained for the SA-508 Class 2 forging material and for the welds, where again the dominant effects were R ratio and material chemistry. The welds showed somewhat more scatter than the base metals and heat-affected zones, but, overall, the effects were the same. Figure 3 shows a comparison of results obtained at low R ratio for welds made with Linde 80 and Linde 0091 flux. The Linde 80 weld contained 0.014 weight percent sulfur, while the Linde 0091 weld contained only .008 weight percent sulfur. Another comparison is shown in Fig. 4, where a Linde 124 weld is compared with the same Linde 0091 results. As in Fig. 3, the high sulfur Linde 124 weld (0.012) shows more environmental enhancement.

It is interesting to note that the R-ratio effects show up consistently even in the low sulfur material which shows very little enhancement over air behavior at low R. Figure 5 shows an increase in growth rate with R ratio about equal to that obtained for all the other material, even though these two Linde 0091 welds were low in sulfur. Also note the comparison of loading form.

Main Matrix Testing (Irradiated)

Fatigue crack growth data for A533-B steel in both the irradiated and unirradiated condition is shown in Figs. 6a and b. Although the materials (Codes L83 and HT) are from different heats, and the initial ΔK for the HT-material tests is somewhat higher, the trend of the results is very similar. The 1 Hz tests produce results residing on or near the ASME air default line over the higher portion of the ΔK range which was tested. The 17 mHz results show a substantial increase in growth rate over the 1 Hz results, but since the increase is about the same for both irradiated and unirradiated materials, it appears to be a function of the environment and cyclic period, rather than irradiation. Irradiated specimen L83-1 was tested over a ΔK range which began with a value sufficiently low that the classical-three-region behavior of corrosion fatigue crack-growth rates can be seen [5]. Region I, or start-up behavior occurs at the lowest values of the ΔK range, with crack growth rates rising to a plateau termed Region II behavior, characterized by somewhat more ΔK-independent growth rates then for Regions I or III. Lastly, for the higher ΔK values, Region III behavior, the growth resumes a strong ΔK-dependence. A similar set of tests was conducted on A508-2 material, code Q71. These results are shown in Fig. 7. As for A533-B, there is a significant increase in growth rates for the 17 mHz waveform as opposed to the 1 Hz waveform, but this increase is nearly identical to the increase shown in Fig. 6a and b and, as before, is due to the influence of the environment during the longer period waveform. Since the test on Q71-9 was carried out to a longer final crack length, and hence higher ΔK value than L83-6, the onset and extent of Region II growth behavior is more clearly described in this case. Note that the increase in growth rates between the 1 Hz and 17 mHz results is about a factor of twenty, while the increase in cyclic period is about sixty. The relationship is not, therefore, one-to-one, and in fact, if irradiation has little or no effect, we can expect, on the basis of unirradiated results [6,7] that the 17 mHz waveform affords a saturation or maximization of the environmental effect, for PWR environments. Thus, the 17 mHz results of Figs. 6 and 7 represent the probable upper limits of fatigue crack growth for the $R = 0.2$ constant load-amplitude condition.

As shown in Fig. 8, testing of an irradiated sample of A508-2, code V82 material, produced crack growth rates nearly identical to the growth rates of an unirradiated specimen, indicating that irradiation damage did not further aggravate an already environmentally susceptible material (see Ref. 8, Fig. 9). The V82-1 results are from a 2T-CT specimen and mark the completion of the first test with an irradiated specimen of this size.

The overall result derived from this study, that irradiation does not enhance crack growth rates at low load ratio, for simulated nuclear coolant environment, is parallel to the earlier results for tests in high and low temperature air environments [8]. In those instances of irradiated specimen results for which the growth rates are depressed (A508, code Q71, 1 Hz tests), this may be due to the increased yield strength of the irradiated specimen. In those cases for which the irradiated results are slightly higher than for comparable tests of similar materials (17 mHz tests-all cases), the increase may be due to a synergistic effect of the environmental influence on the radiation damaged steel; however, the variability is well within a scatterband defined by previous growth rate evaluations for these materials. In the case of the A508-2 forging, code V82, which seems to be slightly more environmentally susceptible than the code Q71 material, irradiation did not provide any further detrimental effects. It is important to note that for the specific sets of conditions studied (1 Hz and 17 mHz sinusodial waveforms, $R = 0.2$, PWR conditions) none of the present results exceed the existing ASME default lines for aqueous environment fatigue crack growth.

A test of irradiated A508-2, code V82 material, using an R = 0.7 is underway and suitable (2T-CT) specimens of A533-B and submerged-arc weld metal (Linde 0091 flux) have been irradiated and are available for testing.

Stress-Corrosion Cracking

A number of bolt-loaded precracked K_{ISCC} specimens have been tested in the PWR environment in conjunction with the crack growth specimens for over five years now. Materials in testing included A533-B Class 1 plate (material 04A, A508 Class 2 forging (F) and a Linde 124 weld ("C"). During the past year, testing of two heat-affected zones was initiated, and static load cracking was observed in both the Linde 80 HAZ and the Linde 124 HAZ materials, after 1100 hours in the former case and 1500 hours in the environment for the latter. Further tests to study two other heat-affected zones have recently begun.

No cracking has been observed yet in either the weld or the forging material, after almost 50,000 hours of loading, 40,000 in the environment. Crack propagation has just recently occurred in the plate material, after nearly six years.

Values obtained thus far for the heat-affected zones have been as low as 45 to 50 ksi$\sqrt{\text{in.}}$ (49 to 55 Mpa$\sqrt{\text{in.}}$), although testing is continuing. The K_{ISCC} values obtained for the plate materials have been similar, but if further propagation occurs, the apparent K_{ISCC} number could go lower.

Examples of the crack propagation paths for the heat affected zone specimens are shown in Fig. 9a-c. Note that the paths are generally non-planar, and that once the crack begins it shows no preference for the heat-affected zone, weld, or base metal.

As noted above, testing on the above samples will continue, and many more specimens are being readied for testing. Specimens for heat affected zone testing are being irradiated at the present time; testing will commence in a few months.

REFERENCES

[1] W. H. Bamford, D. M. Moon, and L. J. Ceschini, "Effect of High-Temperature Primary Reactor Water on the Subcritical Crack Growth of Reactor Vessel Steels," in Heavy Section Steel Technology Program Quarterly Progress Report for July-September 1979, G. D. Whitman and R. H. Bryan (Eds.), NUREG/CR-1197, ORNL/NUREG/TM-370, April 1980.

[2] W. H. Bamford, D. M. Moon and L. J. Ceschini, "Cyclic Crack Growth Rate Studies Conducted by Westinghouse Nuclear Energy Systems Under NRL Contract," in Structural Integrity of Water Reactor Pressure Boundary Components, F. J. Loss (Ed.), NUREG/CR-1268, NRL Memorandum Report 4174, January 1980.

[3] W. H. Bamford and L. J. Ceschini, "Corrosion Fatigue Crack Behavior of Pressure Vessel Steels," in Structural Integrity of Water Reactor Pressure Boundary Components, F. J. Loss (Ed.), NUREG/CR-1472, NRL Memorandum Report 4254 (August 1980).

[4] W. H. Bamford and L. J. Ceschini, "Corrosion Fatigue Crack Growth Behavior of Pressure Vessel Steels," in Structural Integrity of Water Reactor Pressure Boundary Components, F. J. Loss (Ed.), NUREG/CR-1783, NRL Memorandum Report 4400 (pending publication).

[5] M. O. Speidel, et al., "Corrosion Fatigue and Stress Corrosion Crack Growth in High-Strength Aluminum Alloys, Magnesium Alloys and Titanium Alloys Exposed to Aqueous Solutions," in Corrosion Fatigue - Chemistry, Mechanics and Microstructure, NACE-2, National Association of Corrosion Engineers, 1972.

[6] W. H. Cullen, et al., "Fatigue Crack Growth of A508-2 Steel in High-Temperature, Pressurized Reactor-Grade Water," NUREG/CR-0969, NRL Memorandum Report 4063, Naval Research Laboratory, September 1979.

[7] W. H. Cullen, H. E. Watson, and V. Provenzano, "Results of Cyclic Crack Growth Rate Studies in Pressure Vessel and Piping Steels," in Structural Integrity of Water Reactor Pressure Boundary Components, Annual Report, Fiscal Year 1979," NUREG/CR-1128, NRL Memorandum Report 4122, 1979.

[8] W. H. Cullen, R. E. Taylor, H. E. Watson, and Wolfgang Rohrs, "Evaluation of Critical Factors in Crack Growth Rate Studies," in Structural Integrity of Water Reactor Pressure Boundary Complonents, F. J. Loss (Ed.), NUREG/CR-1472, NRL Memorandum Report 4254, August 1980.

SELECTED BIBLIOGRAPHY (FY-80)

W. H. Cullen, Jr. et al., "Evaluation of Factors in Cyclic Crack Growth Rate Studies" in Structural Integrity of Water Reactor Pressure Boundary Components, F. J. Loss (Ed.), NUREG/CR-1268, NRL Memorandum Report 4174, (Jan. 1980).

W. H. Bamford, D. M. Moon and L. J. Ceschini, "Cyclic Crack Growth Rate Studies Conducted by Westinghouse Nuclear Energy Systems Under NRL Contract" in Structural Integrity of Water Reactor Pressure Boundary Components, F. J. Loss (Ed.), NUREG/CR-1268, NRL Memorandum Report 4174, (Jan. 1980).

W. H. Cullen, Jr., R. E. Taylor, H. E. Watson, and Wolfgang Rohrs, "Evaluation of Critical Factors in Crack Growth Rate Studies" in Structural Integrity of Water Reactor Pressure Boundary Components, F. J. Loss (Ed.), NUREG/CR-1472, NRL Memorandum Report 4254, (Aug. 1980).

W. H. Bamford and L. J. Ceschini, "Corrosion Fatigue Crack Behavior of Pressure Vessel Steels" in Structural Integrity of Water Reactor Pressure Boundary Components, F. J. Loss (Ed.), NUREG/CR-1472, NRL Memorandum Report 4254, (Aug. 1980).

W. H. Cullen, Jr., R. E. Taylor, and H. E. Watson, "Evaluation of Critical Factors in Crack Growth Rate Studies," in Structural Integrity of Water Reactor Pressure Boundary Components, F. J. Loss (Ed.), NUREG/CR-1783, NRL Memorandum Report 4400 (pending publication).

W. H. Bamford and L. J. Ceschini, "Corrosion Fatigue Crack Growth Behavior of Pressure Vessel Steels" in Structural Integrity of Water Reactor Pressure Boundary Components, F. J. Loss (Ed.), NUREG/CR-1783, NRL Memorandum Report 4400 (pending publicaton).

W. H. Bamford and D. M. Moon, "Some Mechanistic Observations on the Crack Growth Characteristics of Pressure Vessel and Piping Steels in PWR Environment," Corrosion, Vol. 36, No. 6, June 1980.

W. H. Cullen, H. E. Watson, R. E. Taylor, and F. J. Loss, "Fatigue Crack Growth Rates of Irradiated Pressure Vessel Steels in Simulated Nuclear Coolant Environment," J. Nuclear Materials, Vol. 96 (1980).

W. H. Cullen and K. Torronen, "A Review of Fatigue Crack Growth of Pressure Vessel and Piping Steels in High-Temperature, Pressurized Reactor-Grade Water," NRL Memorandum Report 4298, Naval Research Laboratory, September 1980.

W. H. Bamford, "Technical Basis for Revised Reference Crack Growth Rate Curves for Pressure Boundary Steel in LWR Environment," ASME Trans., J. Pressure Vessel Technology, November 1980.

W. H. Cullen, H. E. Watson, R. E. Taylor, and K. Torronen, "Fatigue Crack Growth Rates of Irradiated Pressure Vessel Steels in Simulated Nuclear Coolant Environment," in Proceedings, International Conference on Effects of Radiation on Structural Materials, Savannah, Georgia, June 1980, ASTM STP 725, 1981.

W. H. Cullen, B. H. Menke, H. E. Watson, and F. J. Loss, "A Computerized Data Acquisition System for High-Temperature, Pressurized-Water, Fatigue Test Facility," in Computer Automation of Materials Testing, ASTP STP 710, pp. 127-140 (1980).

K. Torronen and W. H. Cullen, "The Effect of Light Water Reactor Environments on the Fatigue Crack Growth Rates in Reactor Pressure Vessel Steels," Proceedings, Symposium on Low Cycle Fatigue and Life Predictions, Firmany, France, 1980 (pending publication in ASTM STP).

D. Sturm, F. J. Loss, W. H. Cullen, "Autoclave for Fatigue Crack Growth Tests with Unirradiated and Irradiated Specimens," Materialprufungesanstalt, Vol 22, pp. 5-12 (1980).

W. H. Cullen, R. E. Taylor and H. E. Watson, "Operation of a High Temperature Pressurized Water Fatigue Crack Growth System," Closed Loop, MTS Corporation, Minneapolis, MN, pp. 3-14, October 1980.

V. Provenzano, K. Torronen, W. H. Cullen, and G. Gabetta, "Fractography and Mechanisms of Environment-Assisted Crack Growth in A508-2 Pressure Vessel Steel in Reactor-Grade Water," Proceedings, Int. Conference on Analytical and Experimental Fracture Mechanics, Rome, Italy, June 1980.

TABLE 1

Materials Chemistries

MATERIAL	C	Mn	P	S	Si	Ni	Cr	Mo	Cu	V	Co
Linde 124 Weld "C"	.085	1.32	.013	.012	.48	.91	.14	.49	.05	.005	-
Linde 124 Weld HAZ "C" (adjoining plate plate)	.23	1.33	.009	.014	.22	.58	-	.55	.12	-	-
Linde 80 Weld "C"	.14	1.36	.019	.014	.42	.54	.06	.37	.18	-	-
Linde 80 Weld "C" HAZ adjoining forging	.23	.58	.005	.008	.28	.72	.39	.60	.05	.03	.02
Linde 0091 Weld "D"	.14	1.06	.012	.008	.20	-	-	.48	.15	-	-
Linde 0091 Weld "D-HAZ	.25	1.37	.010	.020	.27	.61	-	.55	.13	-	-
A533B Cl 1 "L83"	.22	1.37	.008	.008	.22	.66	.15	.54	.18	-	-
"2D","02GB"	.22	1.45	.011	.019	.22	.69	.12	.53	-	-	-
"04A"	.23	1.29	.010	.018	.24	.60	.09	.50	.14	-	-
"1HT"	.19	1.28	.009	.013	.25	.61	.04	.55	.10	.005	-
"IN"	.21	1.26	.012	.026	.25	.47	-	.47	.19	-	-
"TW"	.21	1.38	.008	.004	.21	.67	-	.56	.08	-	-
"W7"	.23	1.40	.005	.004	.25	.70	-	.57	-	-	-
A508 Cl 2 "R","R2","R1"	.19	.64	.010	.009	.23	.69	.42	.60	-	-	-
"F","F1"	.19	.60	.010	.012	.26	.70	.33	.56	-	.02	.008
"V82"	.20	.60	.013	.012	.20	.73	.35	.56	-	-	-
"Q71"	.19	.69	.007	.009	.31	.82	.38	.62	.01	-	-

TABLE 2

TEST SPECIMENS COMPLETED

MATERIAL	Test Conditions			
	R = 0.2		R = 0.7	
	One Cycle Per Minute SINE	One Min-Ramp No Hold	One Cycle Per Minute SINE	One Min-Ramp No Hold
Linde 124 Weld (2TWOL)	C-2 C-3	C-7 C-9	C-1 C-6	C-8 C-10
Linde 124 Weld HAZ (In A533B Cl 1 Plate) (2TCT)		C-24-HAZ-1		C-23-HAZ-1
Linde 80 Weld (2TCT)	C-3-WLD C-6-WLD	C-1-WLD	C-4-WLD C-7-WLD	C-2-WLD
Linde 80 Weld HAZ (In A508 Cl 2 Forging) (2TCT)	C-3-HAZ	C-1-HAZ	C-4-HAZ	C-2-HAZ
Linde 0091 Weld (2TCT)	D-1-WLD D-3-WLD	Q342W2	D-2-WLD	Q342W1
Linde 0091 Weld HAZ (In A533B Cl 1 Plate) (2TCT)	D-1-HAZ			
A533B Cl 1 Plate	TW-4 04A-103 1HT20 IN4 2D3Q-6 2D3Q-5 2D3C-3 1HT16	W7-2C2	02GB-2 04A-102 2D1Q-2	
A508 Cl 2 Forging	R2-05 V82-8	R-8 F-10 V82-5 R2-16	F-1	

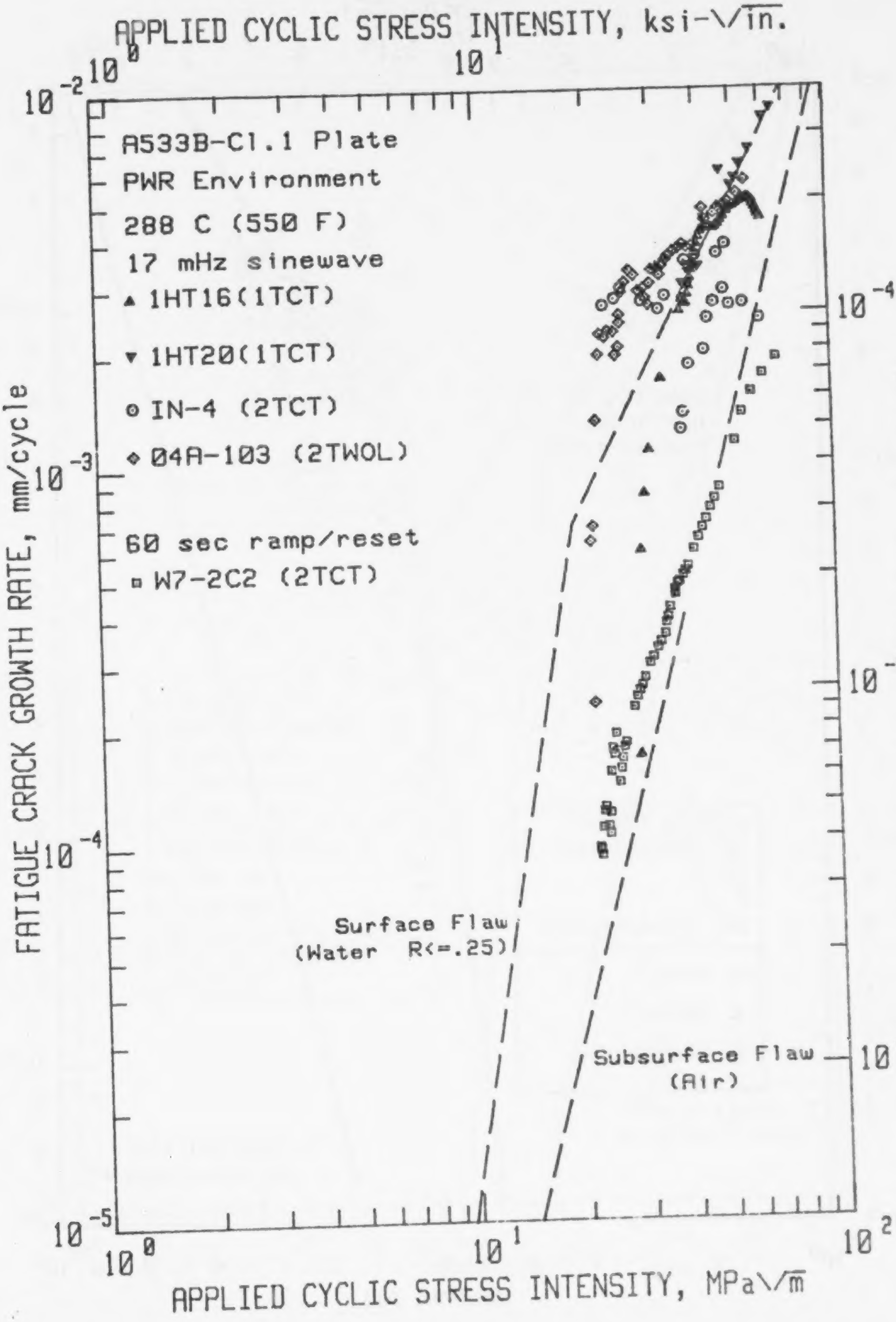

Fig. 1. Fatigue crack growth rates vs applied cyclic stress intensity factor for A533-B steel in simulated PWR environment.

17450-12

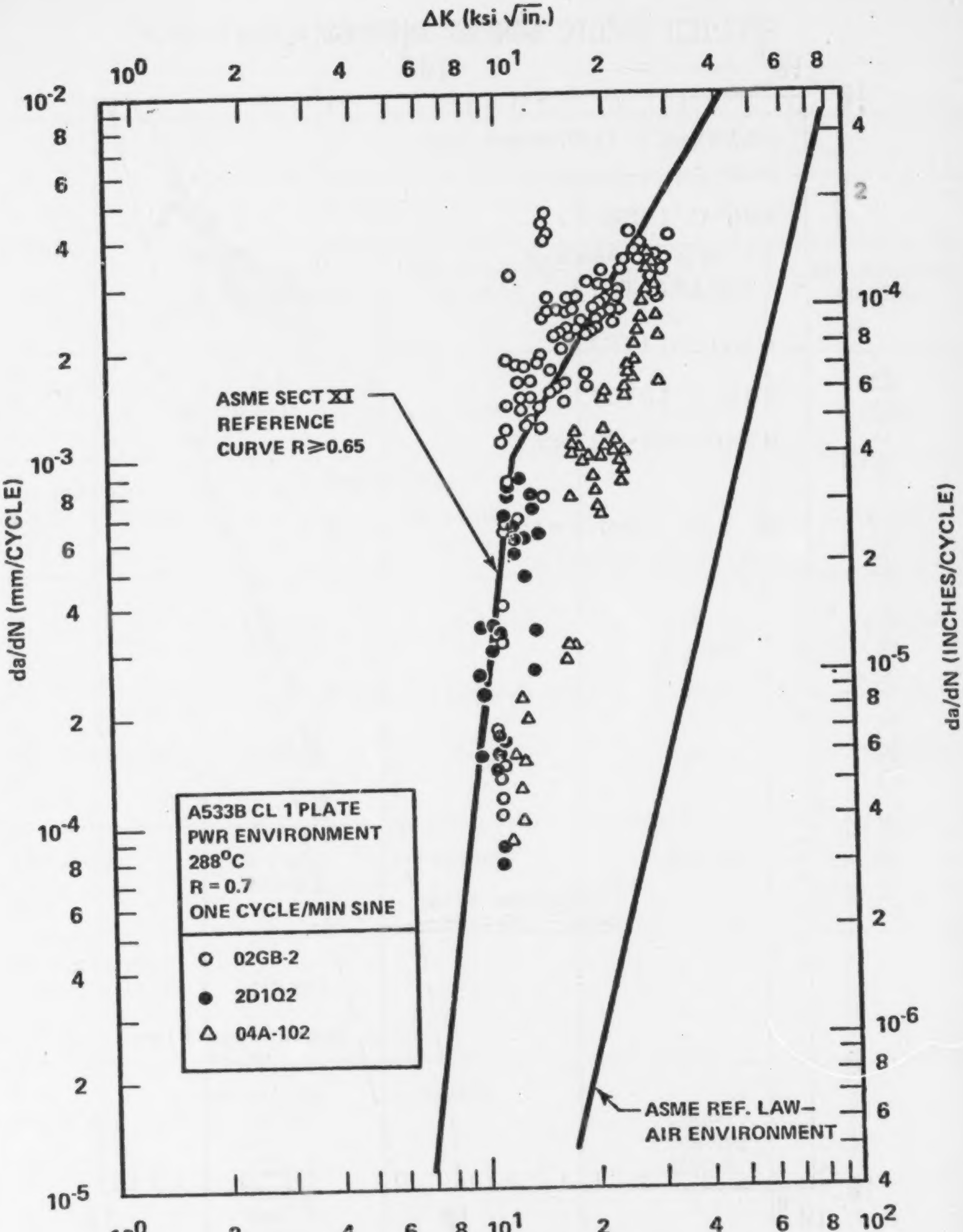

Fig. 2. Fatigue crack growth rates vs applied cyclic stress intensity factor for A533-B steel in simulated PWR environment.

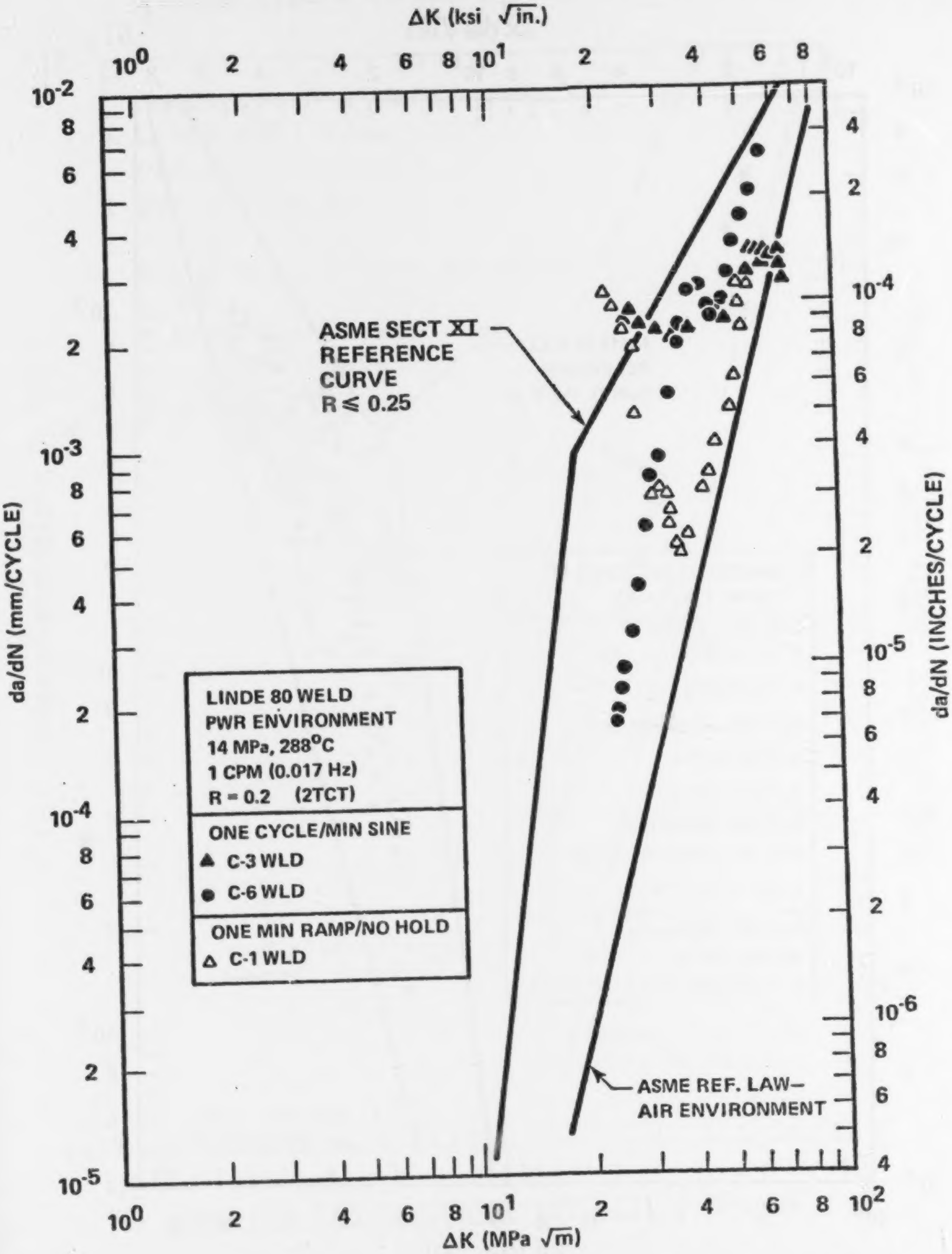

Fig. 3. Fatigue crack growth rates vs applied cyclic stress intensity factor for submerged arc welds with Linde 80 fluxes.

17450-1

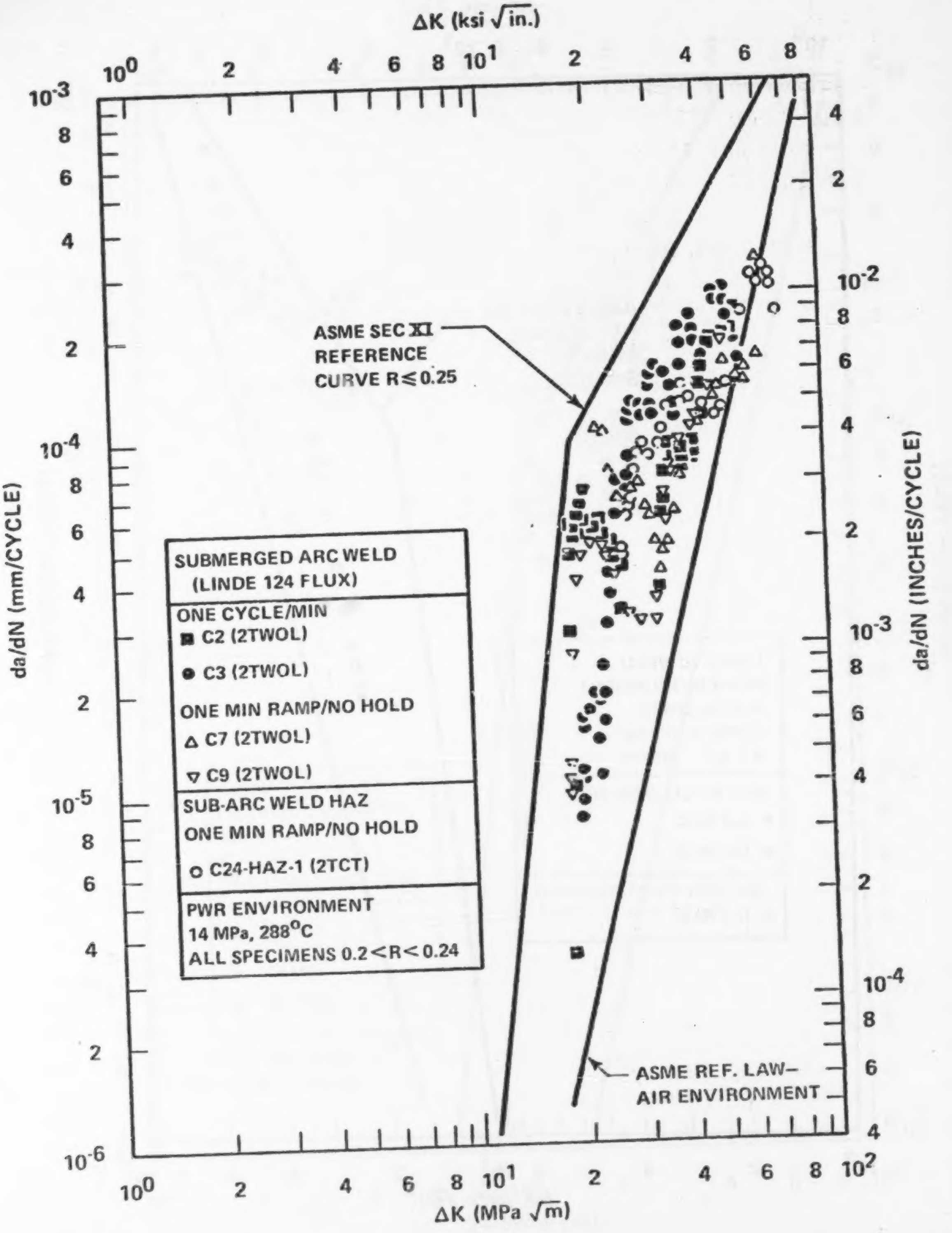

Fig. 4. Fatigue crack growth rates vs applied cyclic stress intensity factor for submerged arc welds with Linde 124 flux.

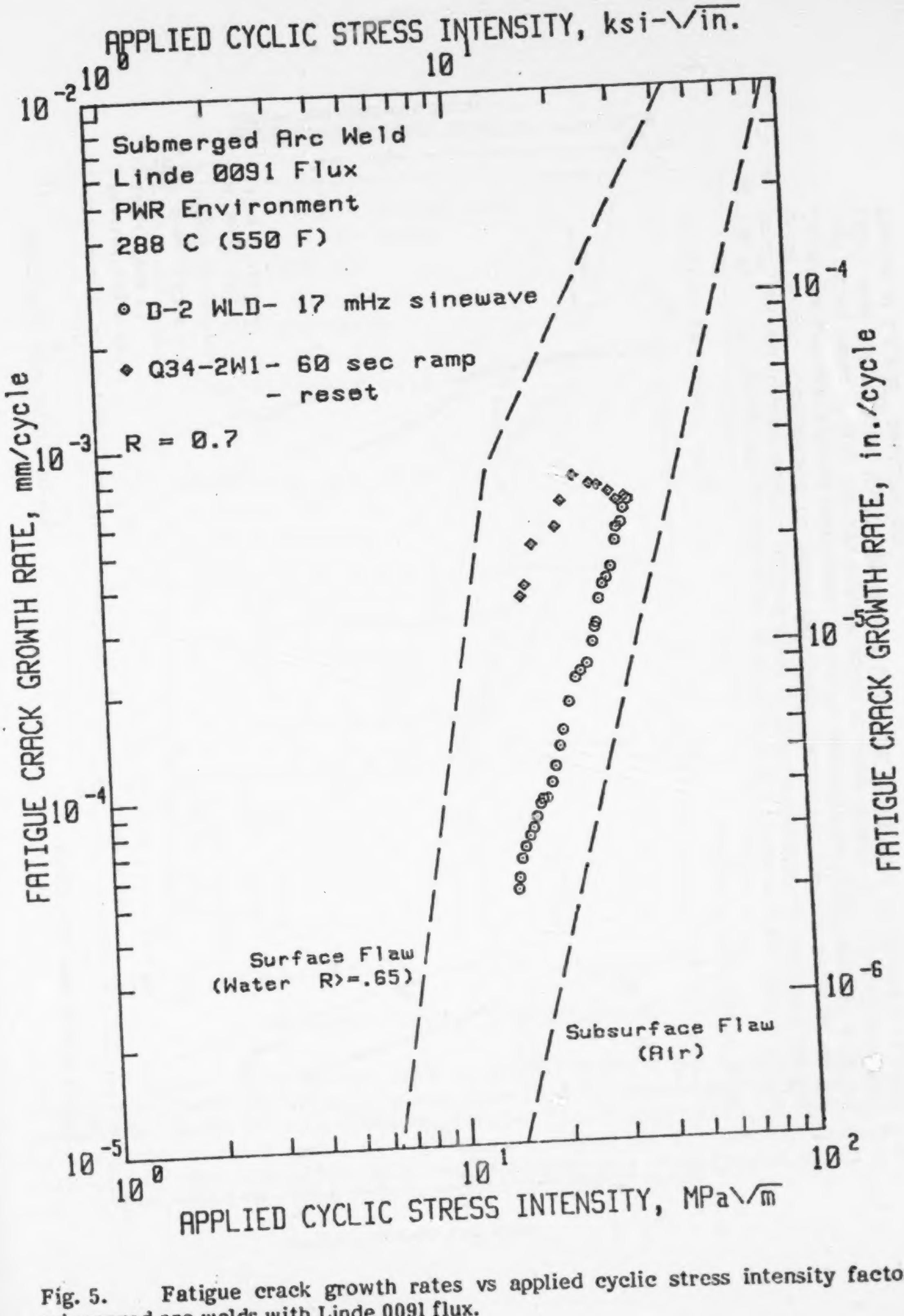

Fig. 5. Fatigue crack growth rates vs applied cyclic stress intensity factor for submerged arc welds with Linde 0091 flux.

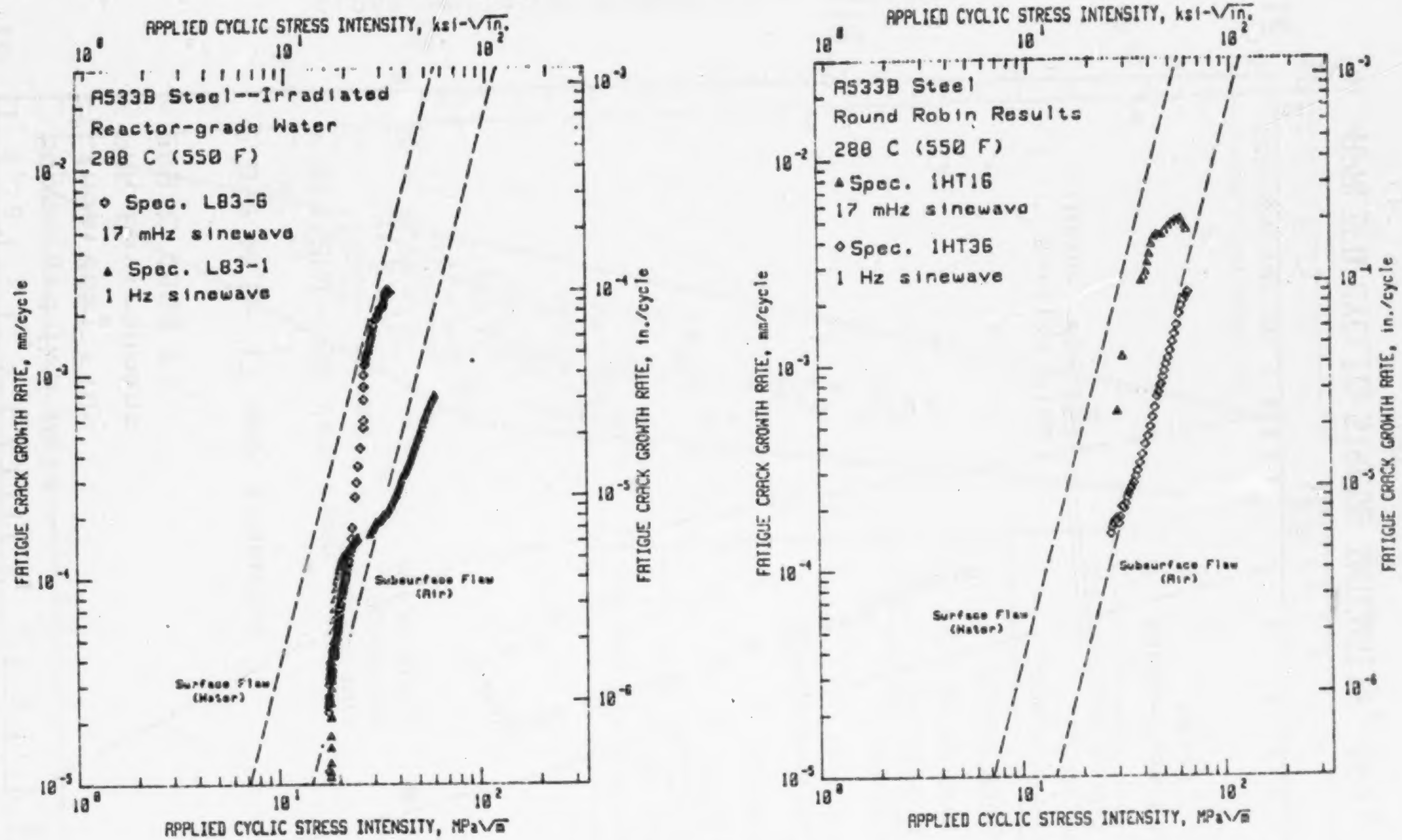

Fig. 6. Fatigue crack growth rates vs applied cyclic stress intensity factor for (a) irradiated and (b) unirradiated A533-B steel in high-temperature pressurized reactor grade water. Comparison of these two graphs shows the parallel behavior of the irradiated and unirradiated specimens. Since the unirradiated tests began at a rather high initial value of ΔK, the three-stage behavior, seen clearly in irradiated specimen L83-1, does not manifest itself. Specimens L83-1 and L83-6 were irradiated to a total fluence of 3.4 x 10^{19} neutrons/cm^2.

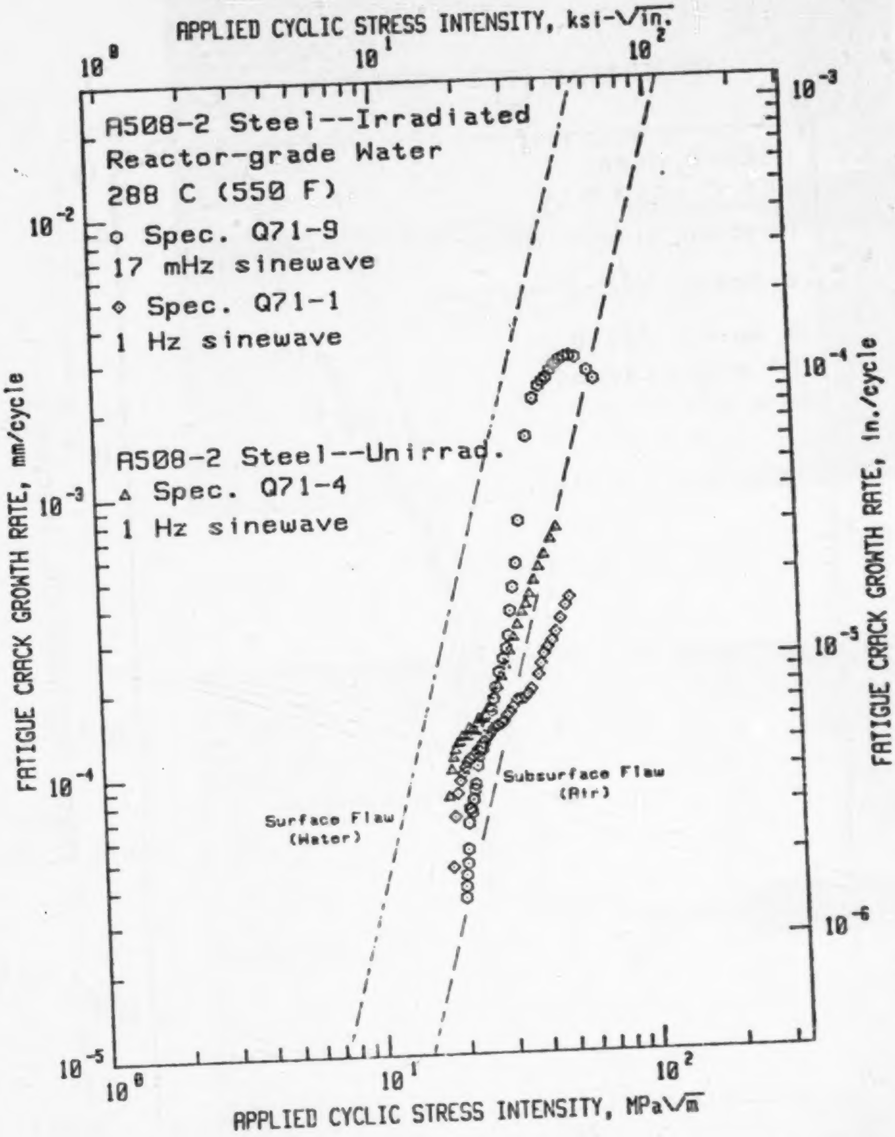

Fig. 7. Fatigue crack growth rates vs applied cyclic stress intensity factor for irradiated and unirradiated, but reactor time- and temperature-conditioned A508-2 steel. These results are very similar to those for A533-B shown in Fig. 6. In this case, the irradiated specimen tested at 1 Hz shows a slight, but measurable, decrease in crack growth rates. Specimen Q71-1 was irradiated to a total fluence of 3.4×10^{19} neutrons/cm^2, Q71-9 to a total fluence of 4.5×10^{19} neutrons/cm^2.

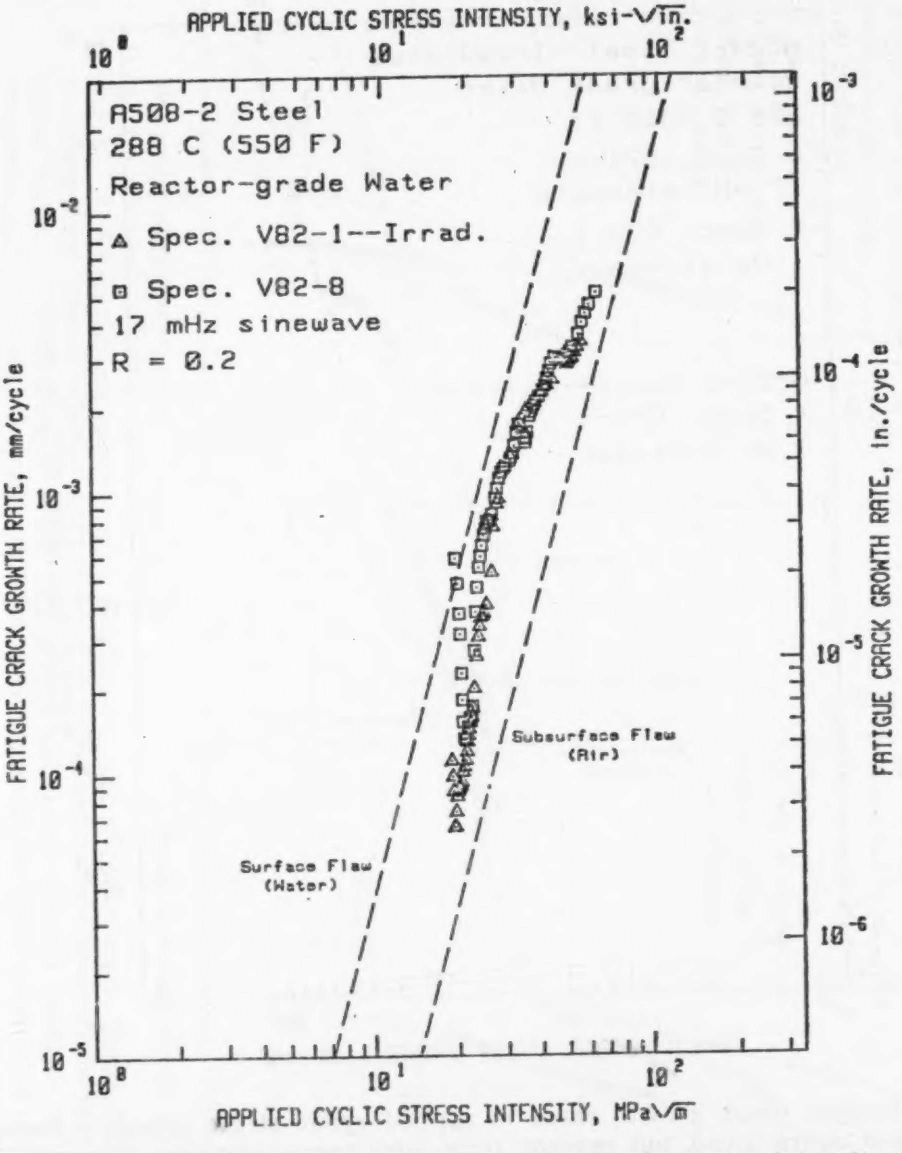

Fig. 8. Fatigue crack growth rates vs applied cyclic stress intensity factor for irradiated and unirradiated, as received A508-2 steel in high-temperature, pressurized reactor-grade water. There is no observable effect of irradiation from these initial data. Specimen V82-1 was irradiated to a total fluence of 2.46 x 10^{19} neutrons/cm^2.

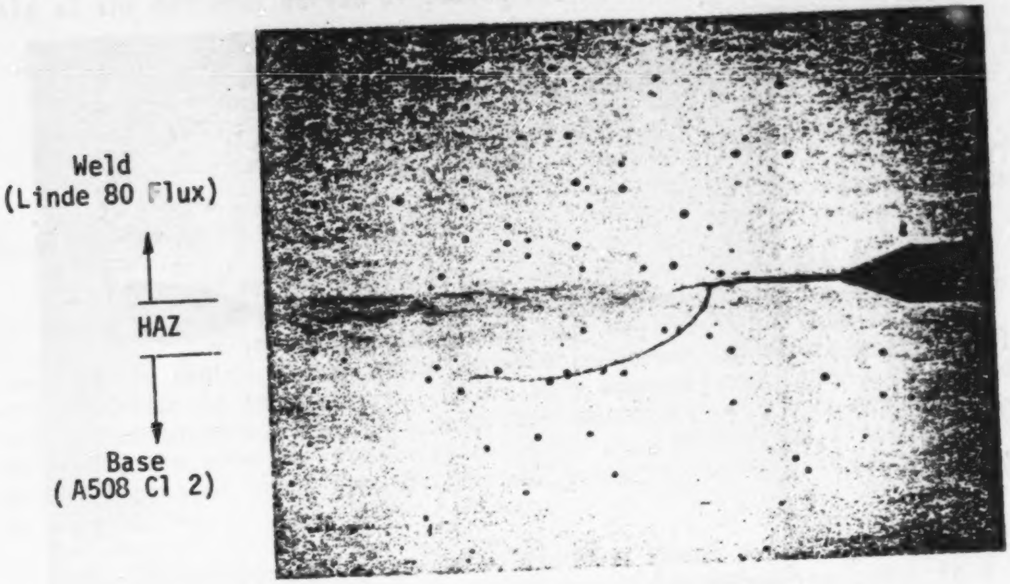
Weld
(Linde 80 Flux)
HAZ
Base
(A508 Cl 2)

SPECIMEN C-9

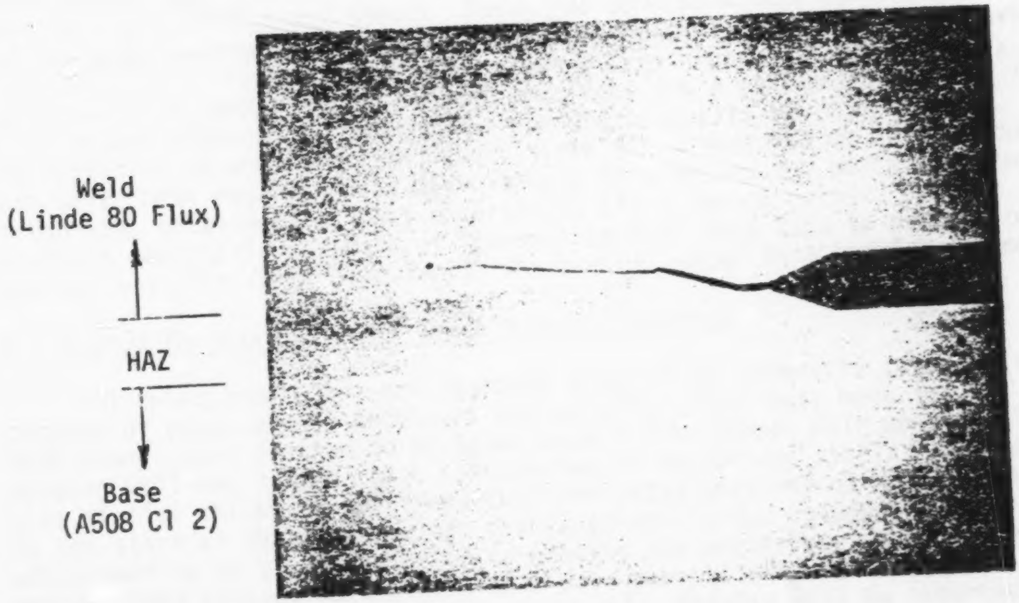
Weld
(Linde 80 Flux)
HAZ
Base
(A508 Cl 2)

Specimen C-10

Fig. 9. Macrograph of transverse sections of stress-corrosion cracks in the heat-affected zone of A508-2 steel near a submerged arc weld deposited with Linde 80 flux.

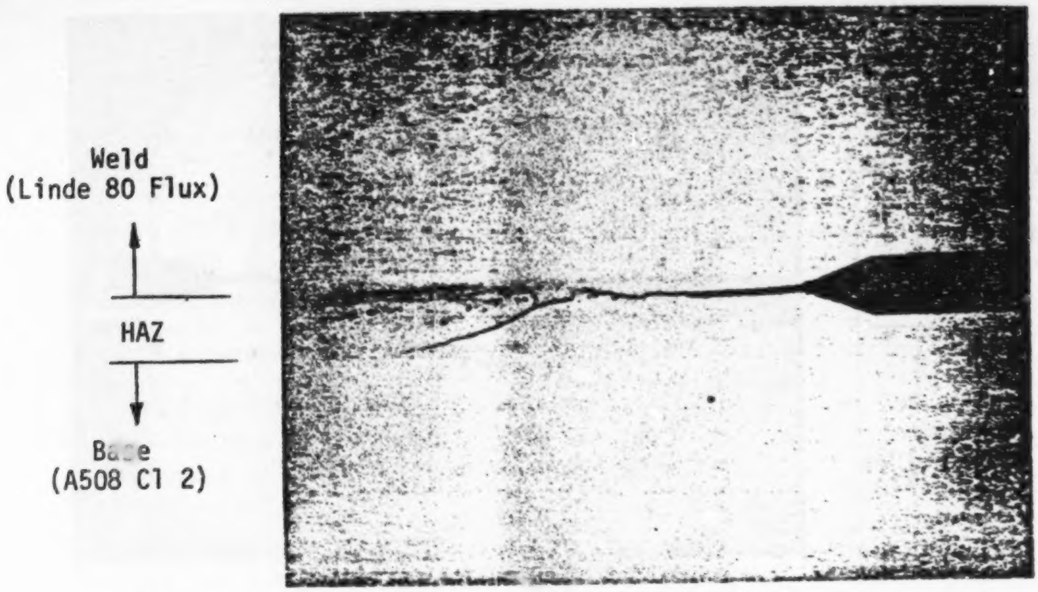
Weld
(Linde 80 Flux)
HAZ
Base
(A508 Cl 2)

SPECIMEN C-11

Picture of crack bolt-loaded specimen - Linde 80 weld HAZ

Presented at the Eighth Water Reactor Research Information Meeting
held at the National Bureau of Standards, Gaithersburg, MD. October, 1980.

Crack Arrest Technology

G.R. Irwin
University of Maryland

1. Perspective

With regard to RPV applications, the interest in crack arrest is restricted to the temperature region between the NDTT and a temperature high enough to eliminate dominant cleavage fracturing. This is the temperature region within which dynamic toughness increases most rapidly with increase of temperature. Below this temperature region, the rapid load initiation toughness, K_{Id}, is less than the crack arrest toughness, K_{Ia} [1]. Above it, the expected strain rate sensitivity of fibrous fracturing is small and estimates of crack propagation using tearing instability ideas should be serviceable.

The 1979 report on crack arrest to this group noted that evaluations of crack arrest toughness and estimates of K for a running crack in a component are separate tasks which are related quite differently to results from dynamic analysis computer programs. Secondly, it was noted that, both from theory and from direct experiments [2], the crack driving force increased monotonically with crack speed. These two considerations eliminated aspects of the crack arrest research program which could be regarded as controversial. For example, it is now clear that values of crack arrest toughness, K_{Ia}, obtained using wedge-loaded compact specimens and a static analysis of test results are acceptable. Whether or not these results are moderately conservative is uncertain. However, since a moderate degree of conservatism has never been regarded as a disadvantage in a method for measuring fracture toughness, settlement of this uncertainty has a low priority. Dynamic analysis computations remain of interest because they tend to predict the maximum possible crack jump length which might occur in a service component[3].

2. Method for Evaluation of Crack Arrest Toughness

Following completion and thorough study of an extensive cooperative program of crack arrest toughness evaluations, plans were made for an ASTM round robin program to be based upon a provisional ASTM method. This program will use 2 inch thick test plates of two bridge steels, A36 and A514, plus similar thickness specimens cut from heavy sections of A533. A delay in the start of this program has developed mainly due to uncertainties which need to be clarified prior to writing the provisional test method. Wedge-loaded compact specimens with a weld-embrittled notch root will be employed, as in the cooperative program [4]. Results will be reported on the basis of a static analysis. It has been agreed that precompression of the notch is not necessary and may be undesirable. The uncertainties which require settlement pertain mainly to loading procedure and to size requirements relative to plane-strain. A sequential loading method suggested recently by Battelle-Columbus is potentially advantageous and is receiving further study. A plan for judging degree of plane-strain from measurements of thickness reduction may assist settlement of the degree of plane-strain problem. The ASTM E-24 task group expects to start the round robin test program next January.

3. Dynamic Analysis of Running Cracks

A dynamic analysis computer program for a run-arrest segment of crack extension is sufficiently complex so that comparisons of results obtained from the BCL (Finite Difference) and University of Maryland (Finite Element) programs were desirable. It has now been established that these two programs provide only moderately different results when the same K versus crack speed input data are used [2]. These programs were specialized for use with the wedge-loaded compact specimens used in crack arrest toughness testing. Dynamic computer programs suitable for an axial crack in a cylinder during thermal shock testing are more complex. Comparisons between BCL and University of Maryland computations for that problem are also desirable and are the objective of the current work.

4. Cleavage-Fibrous Transition

Analysis of K values for running cracks obtained using high speed photography of isochromatic fringes have consistently indicated a substantial loss of energy by damping. In the case of steels, in the temperature range upward from the NDTT, among the possible causes for damping, the clearest mechanism is the yielding and impingement of late-breaking ligaments behind the main crack front. SEM stereo views of the cleavage fracture surface produced in the transition temperature range show numerous local regions in which separation occurred by hole-joining. A common example occurs where two non-coplanar cleavage cracks undercut leaving a ligament which breaks by a combination of shear and hole-joining after substantial bending. In such cases, the bending of the ligament, as well as the strain associated with hole-joining, causes final separation to occur well behind the front of the running cleavage crack. In structural steels, cleavage is a self-stimulating behaviour which cannot occur slowly and is therefore vulnerable to being quenched by a sufficient increase of interference to rapid spreading. Our fractographic studies are relatively incomplete but seem promising toward providing an improved understanding of cleavage-fibrous transition behaviours. Meanwhile, with regard to crack arrest predictions, the available facts suggest that, in the temperature range upward from the NDTT, dynamic influences will be considerably reduced by damping so that successful predictions of crack arrest using static analysis are likely as indicated by thermal shock fracture experiments at ORNL.

References

1. Irwin, G.R., "Comments on Dynamic Fracturing," Proc. Dynamic Fracture Testing Conference (London, 1975), British Welding Institute, 1975.
2. "Photoelastic Studies of Damping, Crack Propagation, and Crack Arrest," Dept. of Mech. Engg., Univ. of Maryland, NUREG/CR-1455, November 1979.
3. "Critical Experiments, Measurements, and Analyses to Establish a Crack Arrest Methodology for Nuclear Pressure-Vessel Steels," Battelle Columbus Laboratories, NUREG/CR-1601, July 1980.
4. Crosley, P.B. and Ripling, E.J., "Crack Arrest Studies," EPRI NP-1225, November 1979.

Table I Summary of Crack Jump Distances from Experiments and the University of Maryland (SAMCR) and BCL Computer Codes (from [2])

Test Number	Experimental Crack Jump	SAMCR Prediction	BCL Code Prediction
P-9	65.0 mm	77.5 mm (119.4%)	82.97 mm (125.0%)
P-7	79.5 mm	87.4 mm (109.8%)	91.44 mm (115.0%)
P-10	86.1 mm	100.6 mm (117.0%)	104.1 mm (121.9%)

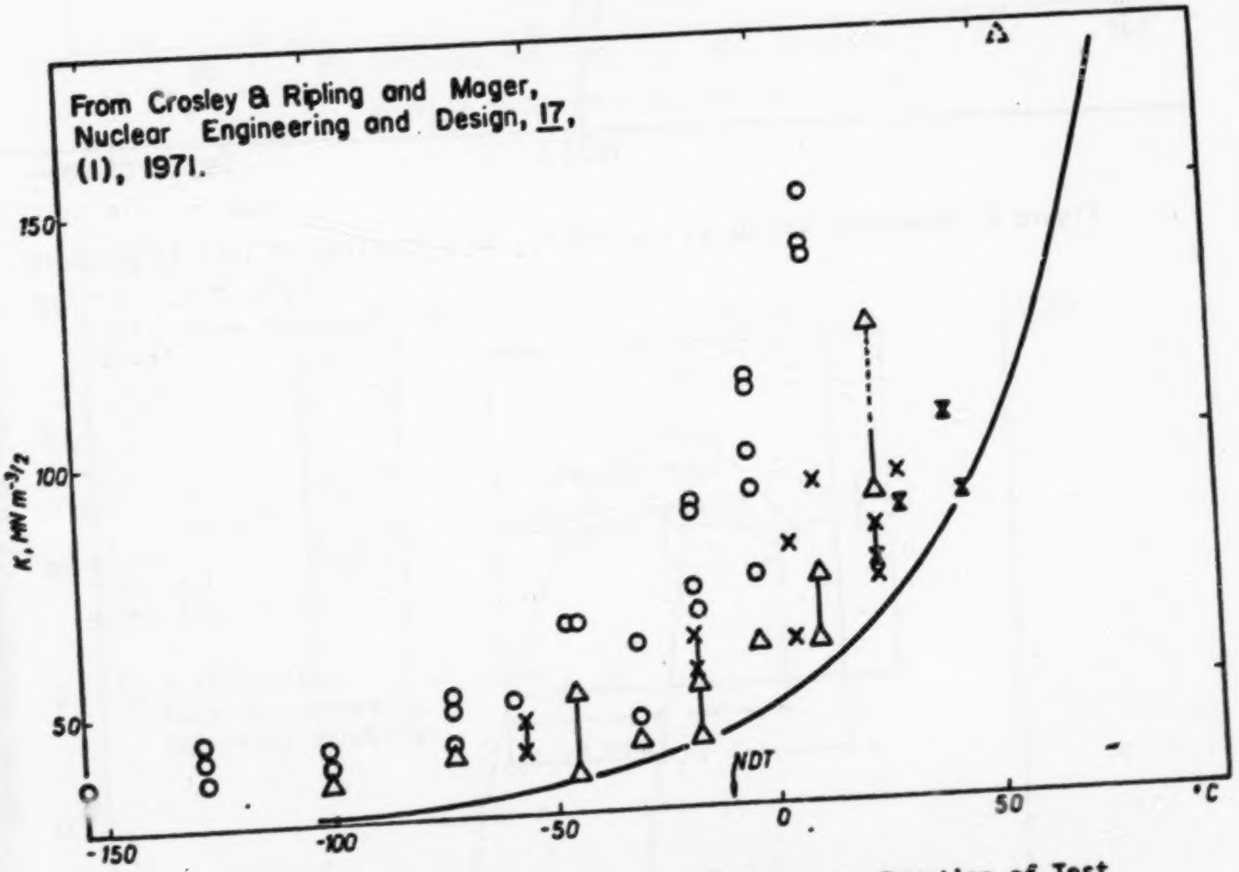
From Crosley & Ripling and Mager, Nuclear Engineering and Design, 17, (1), 1971.

Figure 1 Values of Slow and Rapid Load K_{Ic} Shown as a Function of Test Temperature for A533-B Class 1 Steel. Also shown are values of Crack Arrest K_{Ia}. Drawn curve shows K_{IR} (reference) values from ASME code for boilers and pressure vessels. o - slow, and Δ - rapid load K_{Ic}; x - crack arrest K_{Ia}; I - thermal gradient K_{Ia}.

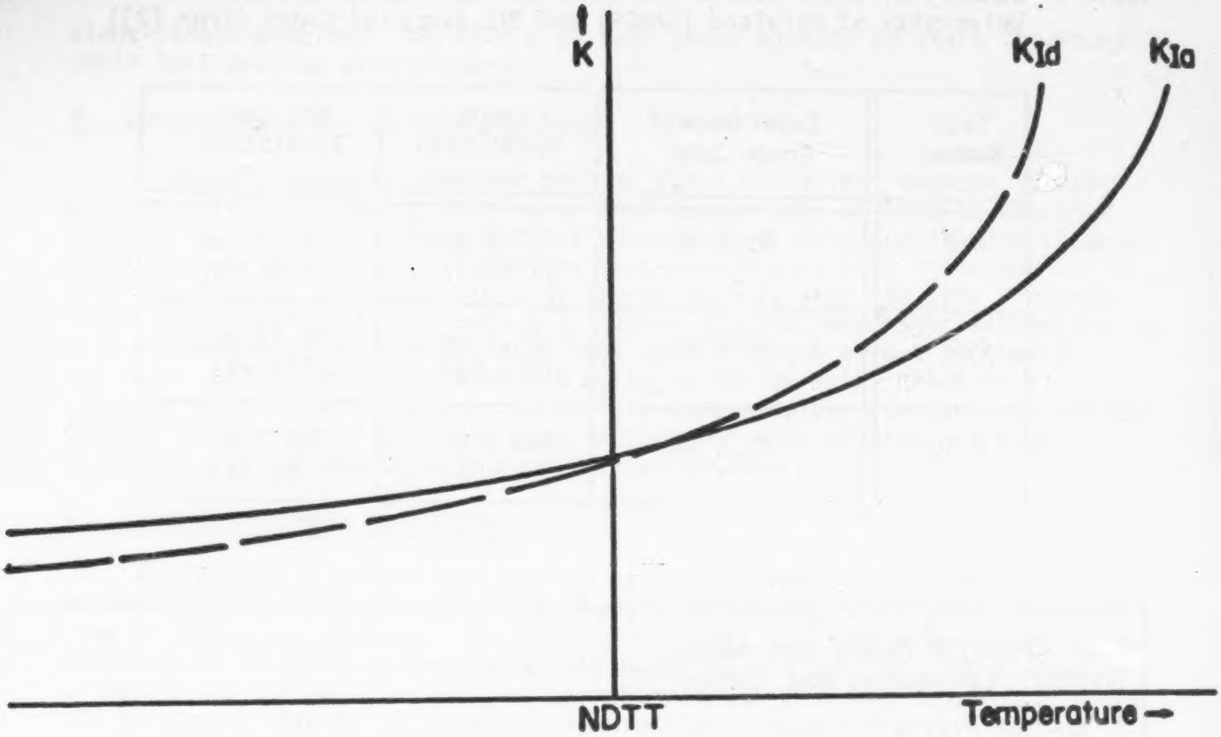

Figure 2 Schematic Trends of K_{Id} and K_{Ia} as a Function of Test Temperature.

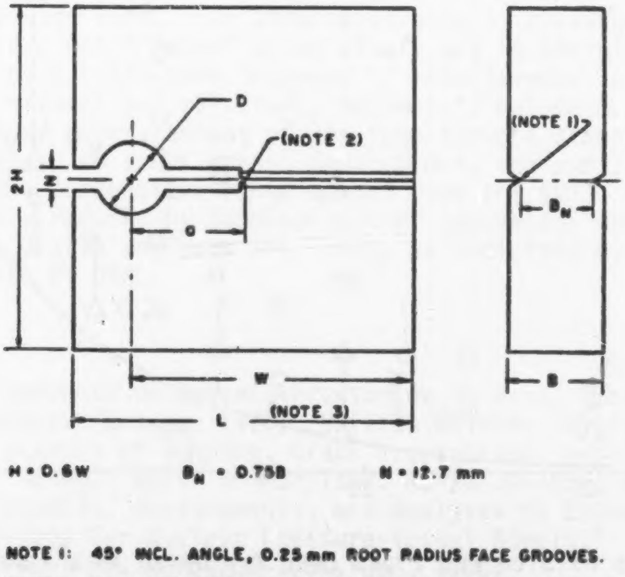
D
(NOTE 2)
(NOTE 1)
2H
N
a
W
L
(NOTE 3)
B_N
B
H = 0.6W
B_N = 0.75B
N = 12.7 mm

NOTE 1: 45° INCL. ANGLE, 0.25 mm ROOT RADIUS FACE GROOVES.

NOTE 2: MACHINED NOTCH IN BRITTLE WELD DEPOSIT APPROX. 2 mm DEEP, 0.25 mm ROOT RADIUS.

NOTE 3: DIMENSION MAY BE ADJUSTED SO THAT DISPLACEMENT GAGE CAN BE MOUNTED 0.25 W FROM LOAD LINE.

Figure 3 Geometry of the Wedge-Loaded Compact Specimen for Crack Arrest Studies

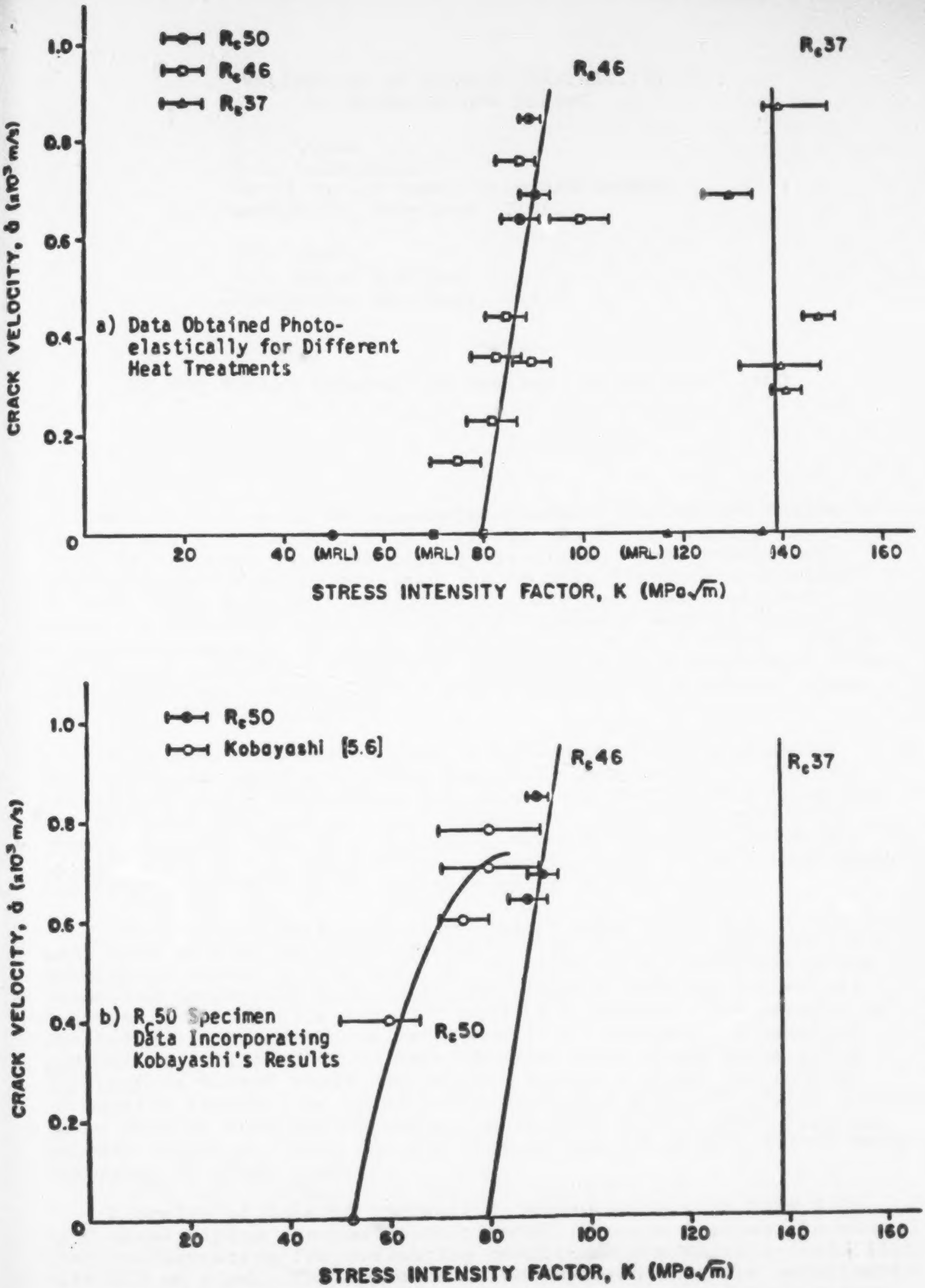

Figure 4 Stress Intensity Factor as a Function of Crack Velocity for 4340 Steel (from [2])

VALIDATION OF TEARING INSTABILITY ON DEGRADED LWR PIPING

J.P. Gudas
M.G. Vassilaros
David Taylor Naval Ship R&D Center
Annapolis, Maryland 21402

J.A. Joyce
U.S. Naval Academy
Annapolis, Maryland 21402

US NRC Public Information Meeting, 30 October, 1980

The objective of NRC-sponsored research at DTNSRDC during FY 1980 was to experimentally validate the Paris tearing instability concept with LWR piping materials. Experiments were initially performed to evaluate the ductile fracture properties of ASTM A106, ASTM A516 and centrifugally cast 304 stainless steel. J-Integral tests with ASTM A106 steels were performed to evaluate effects of crack orientation in pipe product. Table 1 presents results of J-Integräl characterization tests with ASTM A516 GR70 steel, while Table 2 presents results of simular tests with ASTM A106 Cl C steel.

With these results in hand, a series of J-Integral tests were performed with a variably compliant test machine. The objective of these experiments was to systematically vary $T_{APPLIED}$ and evaluate the type of crack extension. Tearing instability theory suggests that when $T_{MATERIAL}$ exceeds $T_{APPLIED}$, crack extension will be in a stable manner. When $T_{APPLIED}$ exceeds $T_{MATERIAL}$, the crack will grow in an unstable manner [1,2].

The tearing instability experiments were performed with compact specimens as shown in Figure 1. The variably compliant test machine is shown in Figure 2. Conventional computer-interactive unloading-compliance tests were performed to develop J-Integral R-Curves with ASTM A516 and ASTM A106 Cl C steels. The details of the tests are described in Reference [3]. Figures 3-5 describe typical digital load - COD data obtained with these tests where $T_{APPLIED}$ is varied about $T_{MATERIAL}$. Figure 6 shows the results of tearing instability experiments performed with LWR piping alloys. These results show that ductile instability occurs where $T_{APPLIED}$ exceeds $T_{MATERIAL}$, even for the case of the LWR piping alloys where $T_{MATERIAL}$ is quite high.

A series of tearing instability experiments with ASTM A106 Cl C steel piping are now being planned. Figure 7 shows the general test configuration for evaluating conditions for ductile instability with 200 mm pipe. The approach to be employed in these experiments is outlined in Figure 8. The tests will be performed in a manner similar to the compact specimen tests in that a variably compliant test machine will be employed to test pipe in four-point bending. Tests will be performed to evaluate the type and extent of crack growth. Further the instability observed in the tests will be related to J_I-R curves developed with compact specimens and pipe configurations.

REFERENCES

1. Paris, P.C., Tada, H., Zahoor, A., and H. Ernst, in ASTM STP 688, American Society for Testing and Materials, 1979, pp 5-36.
2. Paris, P.C., Tada, H., Ernst, H., and A. Zahoor, in ASTM STP 688, American Society for Testing Materials, 1979, pp 251-265.
3. Joyce, J.A. and M.G. Vassilaros, "An Experimental Evaluation of Tearing Instability Using the Compact Specimen, presented at the 13th National Symposium on Fracture Mechanics, ASTM, Philadelphia, PA, June 1980, to be published.

RECENT REPORTS AND PUBLICATIONS

1. Vassilaros, M.G., J.A. Joyce and Gudas, "Effects of Specimen Geometry on the J-R Curve for ASTM A533-B Steel", presented at 12th National Symposium on Fracture Mechanics, ASTM, St. Louis, MO, June 1979, to be published.
2. Joyce, J.A. and M.G. Vassilaros, "An Experimental Evaluation of Tearing Instability Using the Compact Specimen, presented at the 13th National Symposium on Fracture Mechanics, ASTM, Philadelphia, PA, June 1980, to be published.
3. Gudas, J.P., M.G. Vassilaros, J.A. Joyce, D.A.Davis and D.R. Anderson, "A Summary of Recent Investigations of Compact Specimen Geometry Effects on the J_I-R Curve of High Strength Steels", NUREG to be published.

DUCTILE FRACTURE DATA SUMMARY
ASTM A516 GR70 STEEL
1TCT SPECIMENS, 20% S.G.

SPECIMEN I.D.	CRACK ORIENTATION	TEST TEMP (°F)	J_{IC} (in-LB/in^2)	dJ/da (Lb/in^2)	T
FOJ-1	T-L	RT	882	12008	73
FOJ-11	T-L	RT	847	13433	82
FOJ-12	T-L	RT	780	13270	81
FOJ-2	T-L	300	740	9172	76
FOJ-3	T-L	300	747	6879	57
FOJ-10	T-L	300	883	9204	77
FOJ-13	T-L	300	764	9850	82
FOY-2	T-L	550	536	12477	144
FOY-7	T-L	550	637	11439	132

σy (RT) = 69 ksi
σy (300°F) = 59 ksi
σy (550°F) $\approx$ 50 ksi (est)

DTNSRDC

TABLE 1

DUCTILE FRACTURE DATA SUMMARY
ASTM A106 CI C STEEL
1TCT SPECIMENS, 20% S.G.

SPECIMEN I.D.	CRACK ORIENTATION	TEST TEMP (°F)	J_{IC} (in-Lb/in^2)	d J/da (Lb/in^2)	T	COMMENTS
FOP 505	L-C	RT	1254	40886	214	
FOP 512	L-C	RT	1493	33204	174	
FOP 516	L-C	RT	1618	25999	136	
FOP 515	L-C	300	518	8927	47	SLAG INCLUSION
FOP 520	L-C	300	1012	32976	172	
FOP 523	L-C	300	1226	31638	165	
FOP-B3	L-C	RT	1062	35762	187	
FOP-B5	L-C	RT	920	36920	193	
FOP-B7	L-C	RT	763	30296	158	
FOP-B4	L-C	300	893	16875	88	SECONDARY CRACKS
FOP-602	C-R	RT	1259	24334	127	
FOP-605	C-R	RT	1162	21955	115	
FOP-703	C-L	RT	855	20819	109	
FOP-704	C-L	RT	949	16394	86	
FOP-800	L-R	RT	2506	40975	214	
FOP-804	L-R	RT	1935	43107	225	

DTNSRDC

TABLE 2

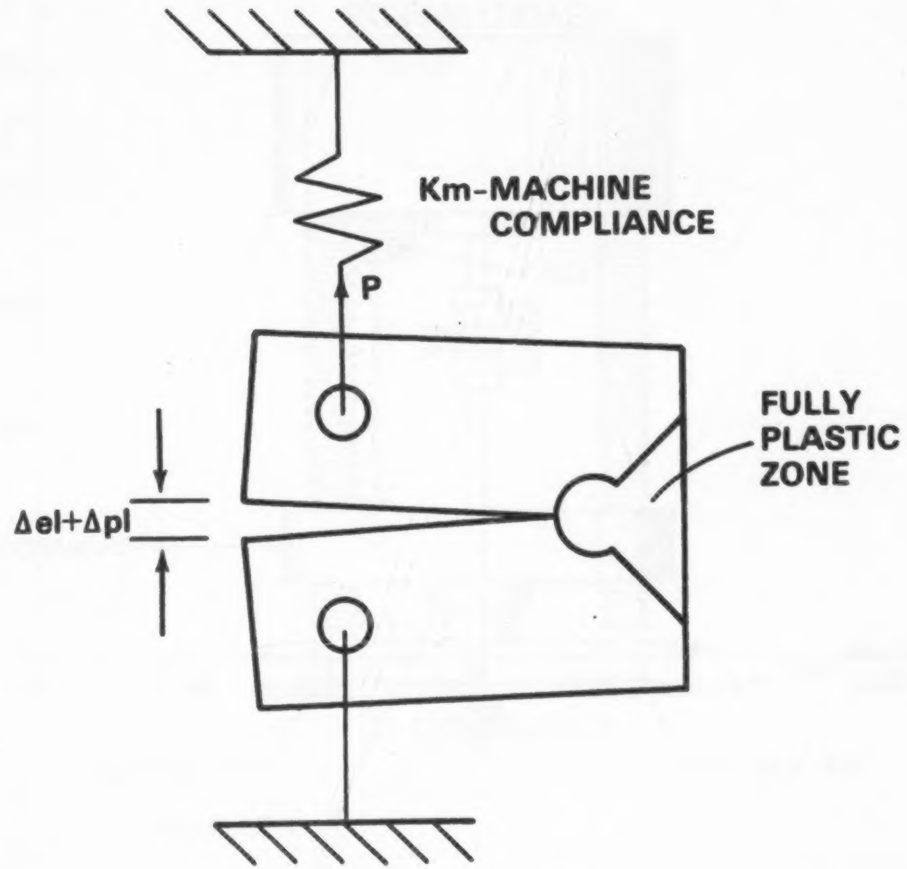
Km-MACHINE COMPLIANCE
P
FULLY PLASTIC ZONE
Δel+Δpl

FIGURE 1

TEST SETUP FOR TEARING INSTABILITY EXPERIMENTS

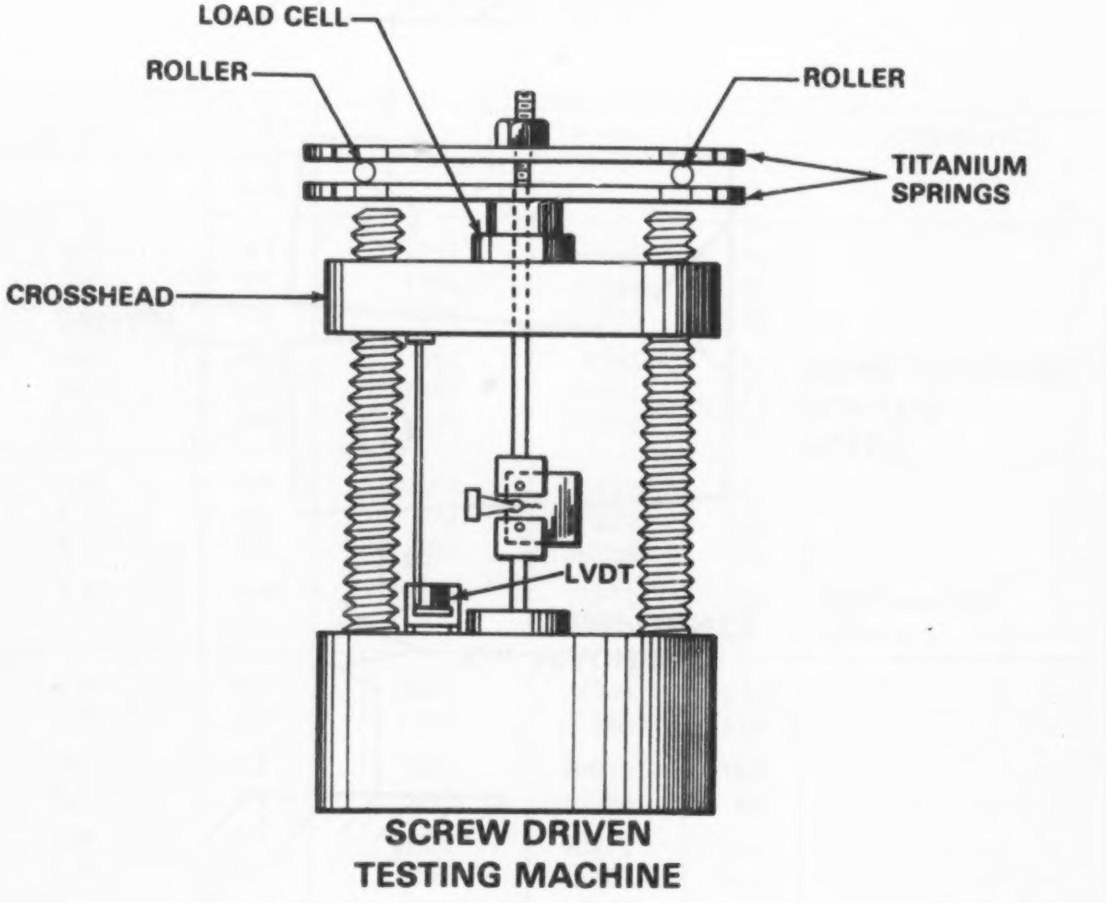
LOAD CELL
ROLLER
ROLLER
TITANIUM SPRINGS
CROSSHEAD
LVDT
SCREW DRIVEN TESTING MACHINE

FIGURE 2

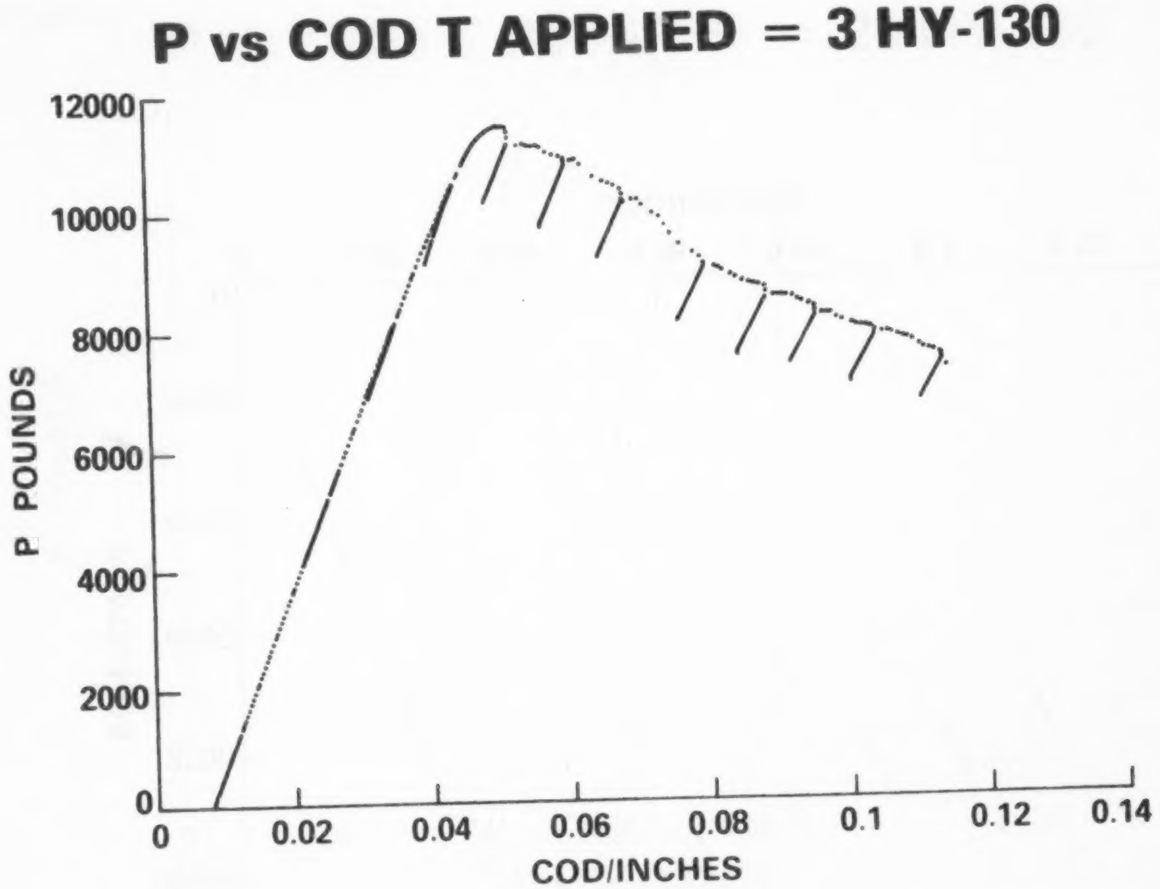
P vs COD T APPLIED = 3 HY-130
P POUNDS
12000
10000
8000
6000
4000
2000
0
0
0.02
0.04
0.06
0.08
0.1
0.12
0.14
COD/INCHES

FIGURE 3

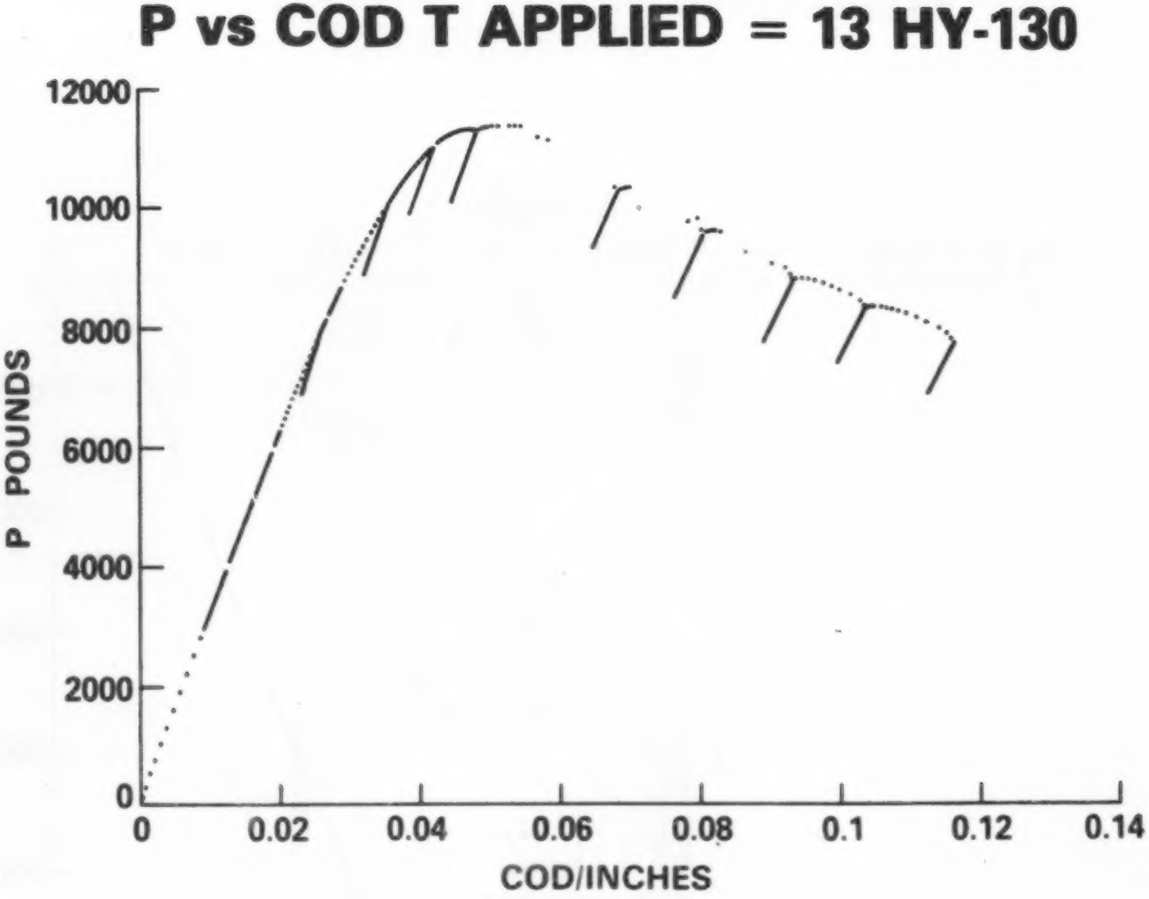
P vs COD T APPLIED = 13 HY-130
P POUNDS
12000
10000
8000
6000
4000
2000
0
0
0.02
0.04
0.06
0.08
0.1
0.12
0.14
COD/INCHES

FIGURE 4

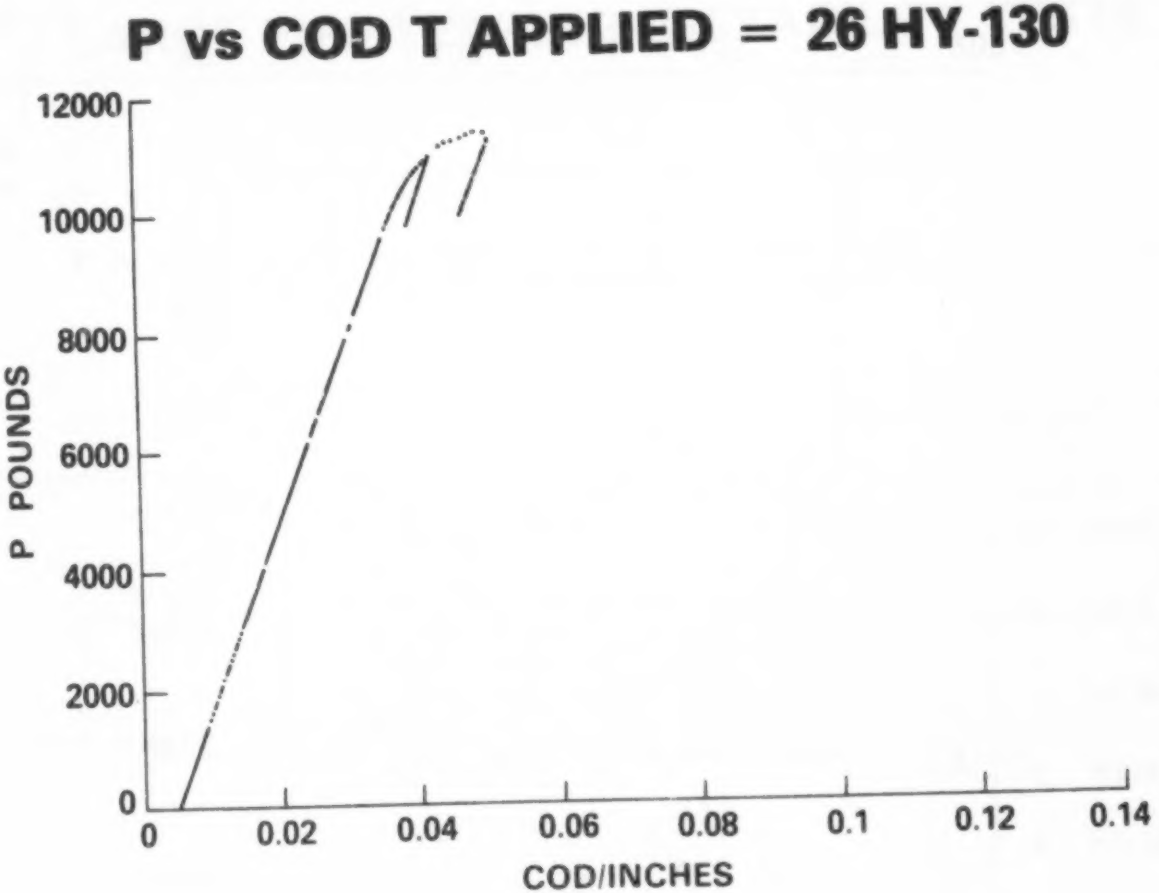

P vs COD T APPLIED = 26 HY-130

FIGURE 5

RESULTS OF TEARING INSTABILITY TESTS

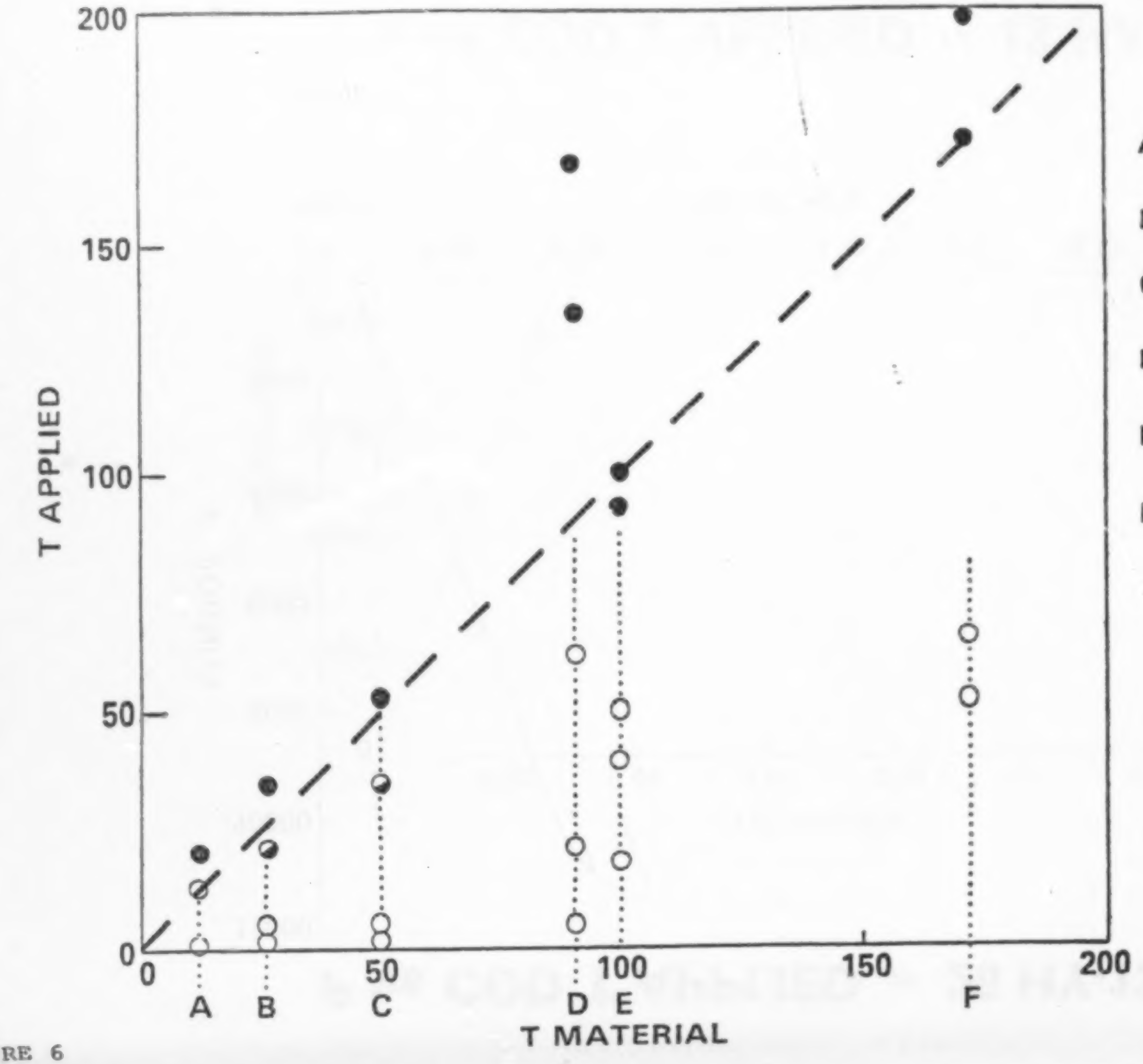

	MAT'L	a/W	%SG	TEMP
A	HY-130	0.8	20	RT
B	HY-130	0.8	0	RT
C	A516	0.65	20	RT
D	HY-80	0.65	0	RT
E	A516	0.65	0	300
F	A106	0.65	0	RT

DTNSRDC

FIGURE 6

SCHEMATIC OF TESTING APPARATUS FOR LARGE PIPE TEARING INSTABILITY TESTS

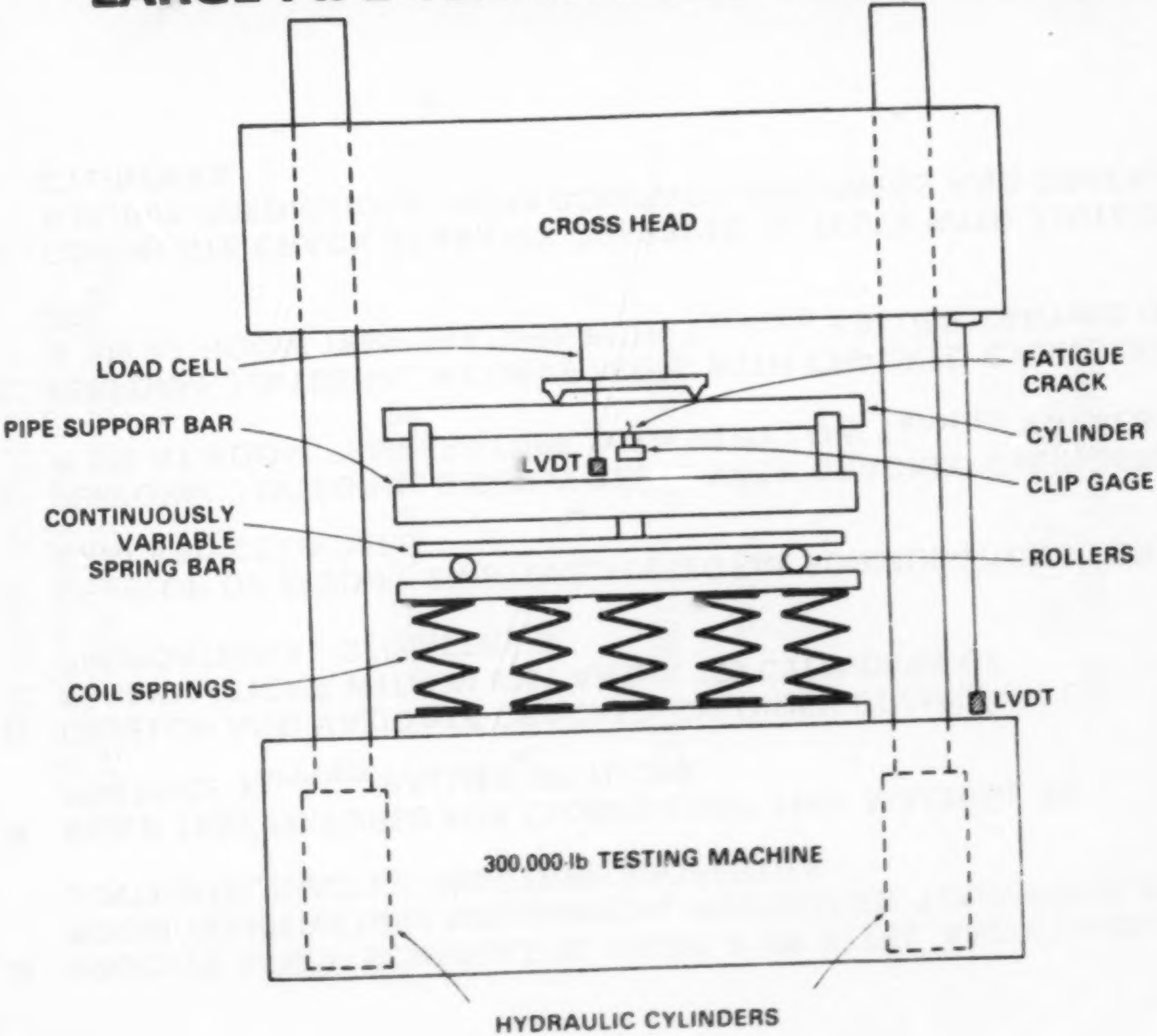
CROSS HEAD
LOAD CELL
FATIGUE CRACK
PIPE SUPPORT BAR
CYLINDER
LVDT
CLIP GAGE
CONTINUOUSLY VARIABLE SPRING BAR
ROLLERS
COIL SPRINGS
LVDT
300,000-lb TESTING MACHINE
HYDRAULIC CYLINDERS

DTNSRDC

FIGURE 7

APPROACH

A. PROCURE 8-INCH SCHEDULE 80, ASTM A 106 STEEL, AND CHARACTERIZE ROOM TEMPERATURE MECHANICAL PROPERTIES, TOUGHNESS AND J-INTEGRAL DUCTILE FRACTURE PROPERTIES;

B. BUILD TEST FIXTURES FOR CLOSED-LOOP TEST MACHINE TO PRODUCE $T_{APPLIED}$ VALUES UP TO 200;

C. DEVELOP AND VALIDATE CRACKED CYLINDER COMPLIANCE FORMULATIONS WITH Al 6061 AND A 106 CYLINDERS OF PROPORTIONAL GEOMETRIES;

D. DEVELOP OR MODIFY EXISTING J-INTEGRAL FORMULATIONS FOR CRACKED CYLINDERS;

E. PERFORM J-INTEGRAL R-CURVE TESTS WITH CRACKED CYLINDERS OF A 106 AT ROOM TEMPERATURE WITH VERY LOW $T_{APPLIED}$ VALUES:

F. PERFORM J-INTEGRAL R-CURVE TESTS WITH CRACKED CYLINDERS OF A 106 AT ROOM TEMPERATURE WITH $T_{APPLIED}$ VALUES VARYING UP TO 200;

G. CORRELATE CRACK STABILITY OBSERVED IN TESTS WITH J-INTEGRAL R-CURVE PREDICTIONS FROM COMPACT SPECIMENS AND CRACKED CYLINDERS.

DTNSRDC

FIGURE 8

PROBABILITY MODELS FOR PIPING FAILURE

D.O. HARRIS

SCIENCE APPLICATIONS, INC.

OCTOBER 31, 1980

PRESENTED AT EIGHTH WATER REACTOR
RESEARCH INFORMATION MEETING
GAITHERSBURG, MARYLAND

RC FORM 335
77)

U.S. NUCLEAR REGULATORY COMMISSION

BIBLIOGRAPHIC DATA SHEET

1. REPORT NUMBER *(Assigned by DDC)*
NUREG/CP-0023, Vol. 3

TITLE AND SUBTITLE *(Add Volume No., if appropriate)*
Eighth Water Reactor Safety Research Information Meeting

2. *(Leave blank)*

3. RECIPIENT'S ACCESSION NO.

AUTHOR(S)

5. DATE REPORT COMPLETED
MONTH | YEAR

PERFORMING ORGANIZATION NAME AND MAILING ADDRESS *(Include Zip Code)*

Office of Nuclear Regulatory Research
U.S. Nuclear Regulatory Commission
Washington, DC 20555

DATE REPORT ISSUED
MONTH March | YEAR 1982

6. *(Leave blank)*

8. *(Leave blank)*

2. SPONSORING ORGANIZATION NAME AND MAILING ADDRESS *(Include Zip Code)*

Same as 9, above.

10. PROJECT/TASK/WORK UNIT NO.

11. CONTRACT NO.

3. TYPE OF REPORT

PERIOD COVERED *(Inclusive dates)*

5. SUPPLEMENTARY NOTES

14. *(Leave blank)*

16. ABSTRACT *(200 words or less)*

This is a compilation of papers which were presented at the Eighth Water Reactor Safety Research Information meeting. It consists of four volumes.

17. KEY WORDS AND DOCUMENT ANALYSIS

17a. DESCRIPTORS

17b. IDENTIFIERS/OPEN-ENDED TERMS

18. AVAILABILITY STATEMENT
Unlimited

19. SECURITY CLASS *(This report)*
Unclassified

20. SECURITY CLASS *(This page)*
Unclassified

21 NO. OF PAGES

22 PRICE
$

NRC FORM 335 (7 77)

*U.S. GOVERNMENT PRINTING OFFICE: 1982-0-361-297/2025